

ACS SYMPOSIUM SERIES **542**

# **Biomarkers of Human Exposure to Pesticides**

**Mahmoud A. Saleh, EDITOR**

*Texas Southern University*

**Jerry N. Blancato, EDITOR**

*U.S. Environmental Protection Agency*

**Charles H. Nauman, EDITOR**

*U.S. Environmental Protection Agency*

Developed from a symposium sponsored  
by the Division of Agrochemicals  
at the 204th National Meeting  
of the American Chemical Society,  
Washington, DC,  
August 23–28, 1992



American Chemical Society, Washington, DC 1994



## Library of Congress Cataloging-in-Publication Data

Biomarkers of human exposure to pesticides: developed from a symposium sponsored by the Division of Agrochemicals at the 204th National Meeting of the American Chemical Society, Washington, DC, August 23–28, 1992 / [edited by] Mahmoud A. Saleh, Jerry N. Blancato, Charles H. Nauman.

p. cm.—(ACS symposium series, ISSN 0097–6156; 542)

Includes bibliographical references and index.

ISBN 0–8412–2738–1

1. Biological monitoring—Congresses. 2. Biochemical markers—Congresses. 3. Pesticides—Toxicology—Congresses.

I. American Chemical Society. Division of Agrochemicals.  
II. American Chemical Society. Meeting (204th: Washington, D.C.)  
III. Saleh, Mahmoud A. IV. Blancato, Jerry N. V. Nauman, C. H.  
(Charles H.) VI. Series.

[DNLM: 1. Biological Markers—congresses. 2. Environmental Monitoring—congresses. 3. Occupational Exposure—adverse effects—congresses. 4. Pesticides—poisoning—congresses. 5. Risk—congresses. WA 240 B6185 1992]

RA1223.B54B57 1993

615.9'07—dc20

DNLM/DLC

for Library of Congress

93–36410

CIP

The paper used in this publication meets the minimum requirements of American National Standard for Information Sciences—Permanence of Paper for Printed Library Materials, ANSI Z39.48–1984.



Copyright © 1994

American Chemical Society

All Rights Reserved. The appearance of the code at the bottom of the first page of each chapter in this volume indicates the copyright owner's consent that reprographic copies of the chapter may be made for personal or internal use or for the personal or internal use of specific clients. This consent is given on the condition, however, that the copier pay the stated per-copy fee through the Copyright Clearance Center, Inc., 27 Congress Street, Salem, MA 01970, for copying beyond that permitted by Sections 107 or 108 of the U.S. Copyright Law. This consent does not extend to copying or transmission by any means—graphic or electronic—for any other purpose, such as for general distribution, for advertising or promotional purposes, for creating a new collective work, for resale, or for information storage and retrieval systems. The copying fee for each chapter is indicated in the code at the bottom of the first page of the chapter.

The citation of trade names and/or names of manufacturers in this publication is not to be construed as an endorsement or as approval by ACS of the commercial products or services referenced herein; nor should the mere reference herein to any drawing, specification, chemical process, or other data be regarded as a license or as a conveyance of any right or permission to the holder, reader, or any other person or corporation, to manufacture, reproduce, use, or sell any patented invention or copyrighted work that may in any way be related thereto. Registered names, trademarks, etc., used in this publication, even without specific indication thereof, are not to be considered unprotected by law.

PRINTED IN THE UNITED STATES OF AMERICA

**American Chemical  
Society Library**  
1155 16th St., N.W.  
Washington, D.C. 20036

# 1993 Advisory Board

## ACS Symposium Series

M. Joan Comstock, *Series Editor*

**V. Dean Adams**  
University of Nevada—  
Reno

**Robert J. Alaimo**  
Procter & Gamble  
Pharmaceuticals, Inc.

**Mark Arnold**  
University of Iowa

**David Baker**  
University of Tennessee

**Arindam Bose**  
Pfizer Central Research

**Robert F. Brady, Jr.**  
Naval Research Laboratory

**Margaret A. Cavanaugh**  
National Science Foundation

**Dennis W. Hess**  
Lehigh University

**Hiroshi Ito**  
IBM Almaden Research Center

**Madeleine M. Joullie**  
University of Pennsylvania

**Gretchen S. Kohl**  
Dow-Corning Corporation

**Bonnie Lawlor**  
Institute for Scientific Information

**Douglas R. Lloyd**  
The University of Texas at Austin

**Robert McGorin**  
Kraft General Foods

**Julius J. Menn**  
Plant Sciences Institute,  
U.S. Department of Agriculture

**Vincent Pecoraro**  
University of Michigan

**Marshall Phillips**  
Delmont Laboratories

**George W. Roberts**  
North Carolina State University

**A. Truman Schwartz**  
Macalaster College

**John R. Shapley**  
University of Illinois  
at Urbana-Champaign

**L. Somasundaram**  
DuPont

**Peter Willett**  
University of Sheffield (England)

## Foreword

THE ACS SYMPOSIUM SERIES was first published in 1974 to provide a mechanism for publishing symposia quickly in book form. The purpose of this series is to publish comprehensive books developed from symposia, which are usually “snapshots in time” of the current research being done on a topic, plus some review material on the topic. For this reason, it is necessary that the papers be published as quickly as possible.

Before a symposium-based book is put under contract, the proposed table of contents is reviewed for appropriateness to the topic and for comprehensiveness of the collection. Some papers are excluded at this point, and others are added to round out the scope of the volume. In addition, a draft of each paper is peer-reviewed prior to final acceptance or rejection. This anonymous review process is supervised by the organizer(s) of the symposium, who become the editor(s) of the book. The authors then revise their papers according to the recommendations of both the reviewers and the editors, prepare camera-ready copy, and submit the final papers to the editors, who check that all necessary revisions have been made.

As a rule, only original research papers and original review papers are included in the volumes. Verbatim reproductions of previously published papers are not accepted.

*M. Joan Comstock*  
Series Editor

# Preface

**BIOMARKER DATA ARE BECOMING INCREASINGLY** important in evaluating the impact of human environmental and occupational exposure to pesticides. In this volume, we distinguish between two basic types of biomarkers: first, residue analysis (of parent compound or metabolites) in easily sampled matrices, and second, endpoints that represent interactions between the xenobiotic and endogenous components (e.g., enzyme inhibition, protein adducts, receptor complexes, antibody–antigen complexes, and mutation). Both types are used in biomonitoring studies to more fully assess exposure, and both are addressed in the chapters in this book.

Exposure assessment typically has been a weak link in the assessment of risk for all chemicals, including pesticides. Exposure biomarkers are important for two general reasons. These endpoints provide evidence that exposure has occurred, resulting in absorption by the body; also these endpoints provide the data that may be compared to exposure measurements and analyzed through pharmacokinetic modeling to estimate target tissue dose and risk. In addition, biomarkers provide a measure of integrated exposure, that is, exposure that occurs by all routes into the body. Our capabilities in effectively using biomarker data are in their infancy, but advancing. We now recognize that in most cases, biomonitoring data are not an end in themselves for estimating exposure, but they complement relevant environmental measurements. Biomonitoring data will be valuable in making associations with health effect and risk of adverse outcome.

The symposium on which this book is based focused on the range of activities needed to bring an exposure biomarker full circle in its usefulness. In this volume, the molecular basis for particular biomarker methods is characterized, including structure–activity relationships, to gain the basic understanding of the marker required before it can become tested in the field. Some of the biomarker measurement methods that are currently being addressed and applied by the research community are surveyed. Finally, methods for biomarker data analysis and the application of these methods to risk assessment are discussed.

We acknowledge the efforts of the contributing authors in providing insightful chapters in their areas of expertise. Also, we acknowledge the assistance and patience of our acquisitions editor, Anne Wilson, who guided three first-time ACS Symposium Series editors through the numerous hurdles of publication.

**MAHMOUD A. SALEH**

Environmental Chemistry and Toxicology Laboratory

Department of Chemistry

Texas Southern University

Houston, TX 77004

**JERRY N. BLANCATO**

Environmental Monitoring Systems Laboratory

U.S. Environmental Protection Agency

Las Vegas, NV 89193

**CHARLES H. NAUMAN**

Environmental Monitoring Systems Laboratory

U.S. Environmental Protection Agency

Las Vegas, NV 89193

**RECEIVED July 14, 1993**

## Chapter 1

# Biomonitoring for Pesticide Exposure

C. H. Nauman<sup>1</sup>, John A. Santolucito<sup>2</sup>, and Curtis C. Dary<sup>1</sup>

<sup>1</sup>Exposure Assessment Research Division, Environmental Monitoring Systems Laboratory, U.S. Environmental Protection Agency, P.O. Box 93478, Las Vegas, NV 89193-3478

<sup>2</sup>Harry Reid Center for Environmental Studies, University of Nevada, Las Vegas, NV 89154-4009

The biological monitoring of pesticide residues and metabolites is becoming increasingly important in the surveillance of occupationally and environmentally exposed individuals. Detection of these compounds in the body indicates that an exposure has occurred; that the pesticide is bioavailable, having been absorbed; and that a dose to critical tissues may have been incurred. Biomarker methods such as for adducted proteins or nucleic acids are being investigated for some pesticides. However, the chemical analyses of readily sampled matrices, such as urine and blood, for parent compound and/or metabolite(s) remain the standard tools of the trade. Methods are becoming more sensitive as advances are made in analytical instrumentation systems. Immunochemical methods are being developed and emphasized for screening purposes, as well as for an enhanced sensitivity and the potential to detect parent compound and multiple metabolites through selective cross-reactivity. When initiating the biomonitoring component of an exposure assessment for pesticides an array of decisions must be made, primarily based on what is known about the metabolism of the pesticide of interest. Detectability of pesticide exposure depends upon selecting the most appropriate biological matrix, the dominant analyte(s) in

0097-6156/94/0542-0001\$06.00/0  
© 1994 American Chemical Society

that matrix, and the timing of sample collection relative to exposure. Useful analytical results are dependent on proper handling and storage of biological samples, as well as the availability of sensitive analytical methods. These factors, currently known biomonitoring approaches, and the results of selected recent biomonitoring studies are presented.

Biological monitoring, the routine analysis of human tissues or excreta for direct or indirect evidence of exposure to chemical substances (1), increasingly is being employed for all classes of compounds, including pesticides. Biomonitoring data complement occupational and environmental monitoring data (e.g., personal exposure measurements, ambient and microenvironmental measurements, as well as human activity pattern information) in reducing the uncertainty inherent in any assessment of exposure or risk. The U.S. Environmental Protection Agency's Office of Research and Development, under the Human Exposure and other planning issues, currently is emphasizing the collection and use of biomonitoring data in field monitoring programs.

The critical piece of information provided by biomonitoring data for any pesticide (or other) exposure situation is that of the bioavailability of the compound of concern -- i.e., the completeness of absorption of a substance from environmental media (2). Bioavailability can be documented only if the index of exposure (parent compound, metabolite, adduct, enzyme, etc.) can be measured at a level that is significantly above any background level occurring in the body.

Background or reference levels of pesticides are known to be elevated in human tissues and fluids (3,4). This is especially true for pesticides to which exposure is continuous, such as pentachlorophenol (PCP), and for pesticides that bioaccumulate and are excreted slowly, e.g., hexachlorobenzene (HCB) and dichlorodiphenyltrichloroethane (DDT). The potential for bioaccumulation for a pesticide can be predicted from its  $\text{Log } K_{ow}$  value (5,6).

As with other classes of compounds that are ubiquitous in our environment, the distinction between occupational and environmental (nonoccupational) exposure to pesticides is being blurred: homeowners increasingly are using pesticides outside the home (7), and are being exposed to pesticides used inside the home for insect control (8). Other environmental sources may be more significant than previously imagined: numerous insecticides and herbicides have been detected in fog, and in the rain falling on both agricultural and urban locations (9, 10), indicating that significant volatilization of these compounds occurs following application. Recent studies with a variety of classes of common, high-use pesticides indicate that volatilization can be highly significant, and is dependent upon temperature and the type of tillage employed (11-13). Additionally, the general population is exposed, more or less, to pesticides used on home lawns and gardens, at public golf courses, from roadside applications to maintain utility line access, etc. Although environmental exposure to pesticides for the general population appears low relative to occupational exposures (14), multiple

sources are now known to contribute to background levels that may be measured in all humans. Data from the Second National Health and Nutrition Examination Survey (NHANES II; samples collected 1976-1980) indicate almost universal exposure of the general population to certain pesticides such as DDT, and that most people are not occupationally exposed (15).

In instances where reference levels are exceeded, and no other exposure data are available, biomonitoring data are useful in documenting only that (excess) exposure has taken place at some time. However, often pharmacokinetic (PK) modeling approaches can be used to analyze biomonitoring data. PK models potentially can be used to estimate what the exposure level has been, especially if the exposure regimen (e.g., continuous over a known time period) is known (6, 16, 17), or if the half-life in the body is known (18). Development of this capability is of critical importance, and will greatly enhance the value of biomonitoring data. Biomonitoring data also may be evaluated via PK models to estimate dose of the parent compound or metabolite in other tissues (19). If these are critical or target tissues, the data may be more closely associated with adverse effect, and thus useful in estimating health risk.

### Classification and Use of Pesticides

A classification of pesticides that represent past or present significant usage is presented in Table I. All major classes include pesticides that have been and/or are of interest for biomonitoring. This classification scheme is instructive as similar analytical procedures and protocols for the analysis of parent compound or metabolite tend to be applicable within various groupings of pesticides.

Uses of pesticides classified by this scheme are not indicated; however, useful generalizations can be made. Organophosphorus and organochlorine compounds tend to be insecticides; some organochlorines serve as fungicides. There are significant numbers of both insecticidal and herbicidal carbamates, with a few having use as fungicides. The chlorophenoxy and related acids all are herbicides. Among the miscellaneous pesticides listed in the table, most are herbicides (acetanilide, amide, bipyridyl, carboxylic acid, dinitroaniline, diphenyl ether, imidazolinone, phenylurea, phosphonic acid, sulfonylurea, triazine, triazole). Most benzonitriles also are herbicides, but one (chlorothalonil) is a fungicide. The pyrethroids, inorganic and organic fumigants, and formamidine are insecticides, while the organometallic and phthalimides are fungicides.

Some of those in the miscellaneous category represent the most heavily used compounds. For example, in recent years Atrazine and Alachlor have been the two most heavily used herbicides in the United States (20); herbicides are much more heavily used in the United States than either insecticides or fungicides (21).

Multianalyte methods are available for some of the classes indicated. For example, the organochlorines often can be picked up in a single GC run (22, 23), as can most of the dialkylphosphorus metabolites of the organophosphorus pesticides (24, 25). However, many compounds require individual efforts, and many of the recently recognized metabolites demand analysis via LC due to thermal instability.

Table I. General Classification of Pesticides

---

**Organophosphorus Compounds**

- Phosphate esters (P=O) -- e.g., Dicrotophos, Methamidophos, Mevinphos, Phosphamidon
- Phosphorothioate esters (P=S) -- e.g., Chlorpyrifos, Diazinon, Malathion, Terbufos

**Carbamates -- e.g., Carbaryl, Chlorpropham, Propoxur**

- Thiocarbamates -- e.g., Butylate, Thiobencarb
- Dithiocarbamates -- e.g., Metham-sodium, Thiram
- Ethylenebisdithiocarbamates -- e.g., Maneb, Metiram

**Organochlorines**

- Dichlorodiphenylethanes (and analogs) -- e.g., DDT, Dicofol, Chlorobenzilate, Methoxychlor
- Cycloienes -- e.g., Chlordane, Dieldrin, Endrin, Heptachlor, Toxaphene
- Chlorinated benzenes and cyclohexanes -- e.g., Hexachlorobenzene (HCB), Pentachlorophenol (PCP), Hexachlorocyclohexanes (HCHs)
- Caged structures -- e.g., Chlordecone, Mirex

**Chlorophenoxy Acids -- e.g., 2,4-D, Diclofop, MCPA, Silvex****Miscellaneous**

- Acetanilides -- e.g., Alachlor, Metolachlor
  - Amides -- e.g., Monalide, Propanil
  - Benzonitriles -- e.g., Bromoxynil, Chlorothalonil
  - Bipyridyls -- e.g., Diquat, Paraquat
  - Carboxylic acids -- e.g., Chlorthal, Dicamba
  - Dinitroanilines -- e.g., Pendimethalin, Trifluralin
  - Diphenyl ethers -- e.g., Bifenox, Diclofop
  - Formamidines -- e.g., Chlordimeform
  - Imidazolinones -- e.g., Imazethapyr
  - Inorganic fumigants -- e.g., Phosphine
  - Organic fumigants -- e.g., 1,3-Dichloropropene
  - Organometallics -- e.g., Agrosan
  - Phenylureas -- e.g., Diuron, Linuron
  - Phosphonic acid -- e.g., Glyphosate
  - Phthalimides -- e.g., Captan, Folpet
  - Pyrethroids -- e.g., Permethrin, Cypermethrin
  - Sulfonylureas -- e.g., Chlorsulfuron, Metsulfuron
  - Triazines -- e.g., Atrazine, Cyanazine
  - Triazoles -- e.g., Amitrole, Triadimefon
-

## General Biomonitoring Considerations

In planning the biomonitoring component of any pesticide study, decisions must be made regarding several pertinent options. These considerations are noted in Table II.

Table II. Biomonitoring Considerations

- 
1. Most appropriate biological matrix.
  2. Timing of sample collection relative to exposure.
  3. Most appropriate analyte(s).
  4. Sample handling and storage.
  5. Most appropriate analytical method(s).
- 

The first three of these considerations reflect the importance of an understanding of pesticide pharmacokinetics in planning any biomonitoring study. Initial planning also should include a full consideration of the quality assurance needed in all aspects of the anticipated study, which is reflected across the last two above considerations.

**Biological Matrix.** Urine and/or blood have been the media of choice in most field studies. Urine, of course, is the most easily obtained, although it must be refrigerated quickly after voiding to prevent biological and/or chemical degradation of analytes of interest, and it can impose matrix interference effects during analysis. Many studies have used grab samples of urine (e.g., first morning void), as a matter of convenience, and as a way of potentially obtaining the highest concentration of desired analyte. A complete twenty-four hour sample will provide more information concerning the amount of exposure encountered, and this type of information will be much more useful in any assessment of exposure or intake (dose), or risk that may be needed.

The choice of matrix may be influenced by the practicalities of when samples may be obtained, as discussed below. Blood is an excellent medium for monitoring the parent compound of (especially the lipophilic organochlorine) pesticides. Depending largely on the chemical class of pesticide, partitioning of analytes may be predominantly to plasma/serum, to formed elements, or both. Thus a decision is required regarding the handling of blood samples shortly after drawing the blood and prior to preservation and shipment to the analytical laboratory. In a practical sense, analysis of whole blood samples is problematic due to the interferences introduced by red cells. In practice, plasma or serum is almost always the medium of choice, although significant amounts of some lipophilic analytes are known to partition to red cells (26).

Adipose tissue is an appropriate matrix for lipophilic pesticides, although difficult to obtain except from cadavers. Many organochlorine compounds partition to the fat stores, and are released to the blood over time. In some cases we now know the kinetics of this process in humans. For example, the concentration of one representative organochlorine, chlordecone (mirex), in a controlled clinical study with

chemical workers who had been occupationally exposed, has been found consistently in blood at approximately one-seventh of its concentration in adipose tissue (27, 28). Studies with other organochlorines comparing blood and biopsy adipose samples from 25 patients indicate adipose/blood ratios that vary from 9 to greater than 800 (29).

Through the National Human Adipose Tissue Survey (NHATS), measures of concentrations of organochlorines have been made on samples taken in the late 1970s and early 1980s (30, 31). Many of these samples still are archived. Recent recommendations from the Committee on Monitoring of Human Tissues of the National Research Council (2) are that, at least for the purposes of determining levels of exposure of the general population, the NHATS be replaced with a blood monitoring program as the primary method of measuring toxic substances in human tissue. For this and other reasons it may be more advisable to concentrate on measurements in blood.

For the reasons discussed, blood and urine may remain the matrices of choice for definitive exposure monitoring studies. However, other matrices such as saliva, perspiration, and tears are more easily obtained and should be given continued consideration, particularly to screen for negative samples. These matrices will assume greater importance with continued development of more cost-effective immunoassay- and biosensor-based analytical methods.

**Timing of Sample Collection.** This consideration is critical for episodic exposure to pesticides that are rapidly eliminated from the body. For those compounds that are stored in adipose tissue and released slowly and continuously to the blood (e.g., many of the organochlorines), sampling time is not critical. However, if exposure is periodic or intermittent, sampling time is critical: all classes of pesticides tend to be cleared rapidly (within hours) from blood, either to the urine (with or without being metabolized) or through the feces.

In general, those pesticides and their metabolites that are not sequestered in fat are cleared from the blood within a few hours, often not being detectable after 12 hours or less. The analysis of blood samples taken after that time will be a waste of time and money. Exceptions may occur when exposure is predominantly dermal vs inhalation or ingestion, possibly delaying peak accumulation in blood by as many as 18 hr (e.g., see 32). Clearance of parent compound or metabolite from the urine usually peaks within 24-48 hr or less, depending on the analyte, and may be detectable for several more days (33, 34). Again, dermal exposure typically results in delayed urinary excretion relative to other exposure routes (33). Chances of detection beyond 5 days post exposure are diminishingly small, unless exposure to the pesticide is ongoing.

If the biomonitoring effort includes physiological or biochemical biomarkers, the expression of these may indicate a similar or a longer delay after exposure before sample collection. Biomarker endpoints such as the measurement of cholinesterase depression; an inducible enzyme such as one of the P-450's; a gene-tox endpoint such as sister chromatid exchange, micronucleus formation, chromosome aberration, or mutation; and nucleic acid or blood protein adduct, are examples of those that may be expressed optimally at later times.

**Appropriate Analytes.** Selection of appropriate analyte(s) requires a knowledge of the metabolism of the particular pesticide of interest. In most cases the parent compound is the predominant analyte encountered in blood. Metabolism of the parent compound occurs mostly in the liver with elimination through urine or feces, with no or very low levels of metabolites occurring in blood. In some cases the parent compound also is excreted unchanged in the urine (e.g., phenoxyacid herbicides), or in the feces (e.g., organochlorines), but for many pesticides metabolites are the predominant species encountered in the urine (e.g., alkyl phosphates from organophosphorus compounds, or mercapturates from acetanilides). Lipophilic pesticides such as the organochlorines are excreted largely through the feces. Naturally, the chances of documenting exposure through biomonitoring are enhanced if one is aware of the chemical species that will appear in highest concentration in the most appropriate biological medium, and is able to measure that compound.

**Sample Handling.** Urine samples should be quickly refrigerated after collection to prevent bacterial or chemical degradation of target analytes. Freezing of urine samples at minus 20° C prior to shipment to the analytical laboratory is preferred. Storage at minus 70-80° C at the laboratory is needed if significant time will elapse prior to analysis.

Blood is collected in tubes with or without anticoagulant. Handling of these tubes consistently should follow prescribed protocols, depending on which fractions (serum, plasma, red cells) are needed. Freezing usually is indicated prior to shipment. If whole blood is needed, as for the analysis of certain cytogenetic or biochemical endpoints, the whole blood should be refrigerated and shipped on ice.

Shipment should take place with frozen samples packed in enough ice or dry ice to ensure that all samples will arrive at the analytical laboratory at the starting temperature. Proper chain of custody practices and documentation should accompany any shipment. This is one aspect of quality assurance that is especially critical if data from the analyses will be used in litigation or in regulatory decision making. Appropriate chain of custody documentation ensures not only that samples were not compromised through tampering, but that their physical state has not been altered, thus precluding degradation of analytes.

Reduction of sample handling is important because the associated costs are high and because sample handling provides additional opportunity for the introduction of error. Consideration must be given to reducing sample handling by carrying out analytical procedures on site using methods which will provide results in real-time. Continued development of immunoassay- and biosensor-based methods will make this increasingly possible.

**Analytical Methods.** Few validated methods exist for pesticide analyses for biological media. Methods for environmental matrices have been adapted to the analysis of biological samples. Unless these methods are up and running in an analytical laboratory, an up-front developmental effort will be necessary so that the laboratory may validate the method for the target analytes in urine or blood.

Often some variation of the method of Shafik et al., 1973 (24) has been applied; for example, see Holler et al., 1989 (35). Depending on the structure of the target

analyte, this method may include hydrolysis, extraction, derivatization, cleanup and analysis via GC, with confirmation by mass spectrometry. The beauty of this procedure is that unanticipated metabolites can be picked up during the GC run and identified. Compounds not stable enough for the GC may require analysis via LC. Thermospray and electrospray mass spectroscopy are useful in the analysis of polar metabolites.

Immunoassay kits currently are available for a few pesticides and/or their metabolites. These kits have been developed for environmental matrices such as water; adapting them to the analysis of biological samples typically is not easy, requiring a substantial investment of time and financial resources. If the immunoassay incorporates polyclonal antibodies, the cross-reactivity incurred may prove advantageous in that both parent pesticide and metabolites are registered simultaneously. Immunoassays presently are viewed as being most useful as screening tools, although quantitation of analyte levels is possible. Incorporated in biosensor devices, they offer the potential for rapid and cost-effective analyses.

### Biomonitoring Methods

Perhaps the most notable recent review of currently available pesticide biomonitoring methods (analytes, analytical methods) that have been used by others is that of Coye et al., 1986 (36), although others have provided less extensive reviews (3, 30, 37). A review of the more recent literature, as well as selected older literature is included in Table III. As more analytes are identified, often through advances in chemical analytical methods, more pesticides are proving to be candidates for biomonitoring. General descriptions of some aspects of major pesticide groups follow.

**Organochlorines.** Organochlorine pesticides as a group are persistent in human fat stores of the general population. This was recognized early-on as evidenced by the publication about a decade ago of papers which analyzed the data on organochlorines in blood and urine samples collected in NHANES II (15, 31), and in adipose samples from NHATS (30). Papers have continued to be published in recent years which further analyze the NHANES II data for organochlorines (and other pesticides) in blood (99) and (primarily PCP) in urine (37). The literature regarding organochlorine pesticide levels measured in human adipose tissue has been summarized recently (100).

This early work has been followed in recent years by a continuing worldwide interest in documenting the body burdens of organochlorine residues in human adipose, milk, blood, and urine. Studies published in the past five years include those in Table IV.

One common theme throughout these studies is that concentrations of organochlorines increase in blood and adipose tissue with the age of individuals monitored (99, 106, 107, 112), reflecting accumulation over longer exposure periods. Comparison of these more recent biomonitoring results with blood, adipose, and milk measurements from older studies reveals that body burden concentrations are decreasing with time over the past 20 years (106, 110, 111, 113, 114), reflecting the controls that have been placed on usage of some organochlorine pesticides. However,

Table III. Biomonitoring Methods<sup>1</sup>

Class, Compound	Analyte	Matrix, (Species <sup>2</sup> )	Anal. Method	Ref.
<b>Acetanilides</b>				
Alachlor	DEA, HEEA	Urine	HPLC	38
	Alachlor mercap- turate	Urine (Monkey)	HPLC	39
	Alachlor mercap- turates (2)	Urine (Monkey)	HPLC	40
	Cysteinyl conjugate			
	Glucuronide			
	Thioacetic acid conjugate			
	DEA, Alachlor equivalents	Urine Urine	HPLC, ELISA	41
<b>Amides</b>				
Propanil	3,4-Dichloroaniline	Urine	LC	42
	3,4-Dichloroaniline	Urine	UNSP	43
<b>Bipyridyls</b>				
Paraquat	Paraquat	Urine	UNSP	44
<b>Carbamates</b>				
Benomyl	MBC, 4-OH MBC, 5-OH MBC	Urine	HPLC	45
Carbaryl	1-Naphthol	Urine	GLC	46, 47
Carbofuran	Carbofuran phenol, 3-Ketocarbofuran	Urine	UNSP	48 30
	Mercapturic acid, Cysteinyl conjugate	Urine	GLC	49
EPTC				
Maneb, Mancozeb	ETU	Urine	HPLC	50-52
Propoxur	2-Isopropoxyphenol	Urine	GLC	53
<b>Chlorophenoxy acids (&amp; related)</b>				
2,4-D	2,4-D	Plasma, Urine	GLC	54
	2,4-D	Urine	GLC	55
	2,4-D	Urine	RIA	56
	2,4,5-T	Urine	GLC	57
MCPA	MCPA	Urine	HPLC	58
	MCPA	Plasma, Urine	GLC	59
	MCPA	Urine	GLC	60
	Silvex	Urine	GLC	57
Dicamba	Dicamba	Urine	GLC	57
<b>Diazoles</b>				
Etridiazole	Mercapturic acid	Urine	GLC	61
<b>Diphenyl Ethers</b>				
Bifenox	Bifenox acid	Urine	GLC	45
Diclofop	Diclofop	Urine	GLC	62
<b>Formamidines</b>				
Chlordimeform	Chlordimeform,	Urine	GLC	63
	4-Chloro-o-toluidine			
	4-Chloro-o-toluidine	Urine	HPLC	64

*Continued on next page*

Table III. Biomonitoring Methods (Continued)

Class, Compound	Analyte	Matrix, (Species <sup>a</sup> )	Anal. Method	Ref.
<b>Organic Fumigants</b>				
1,3-dichloropropene	Mercapturic acids	Urine	GLC	65-67 68 69, 70
<b>Organochlorines</b>				
Aldrin	Dieldrin	Serum	GLC	31
Chlorbenzilate	4,4-Dichlorobenzo- phenone	Urine	GLC	71 72
Chlordane	Heptachlor	Serum	GLC	31
DDT	DDT	Serum	GLC	73
		Blood	GLC	74
	DDE	Serum	GLC	73
		Serum	GLC	75
		Blood	GLC	74
	DDA	Urine	GLC	73
		Urine	GLC	76
		Urine	GLC	77
p-Dichlorobenzene	2,5-Dichlorophenol	Urine	GLC	78
m-Dichlorobenzene	2,4-Dichlorophenol	Urine	GLC	78
HCB	HCB	Plasma	GLC	79
Heptachlor	Trans-nonachlor, Oxychlordane, Heptachlor epoxide	Serum	GLC	31
Lindane	Lindane	Plasma	GLC	80
PCP	Trichlorophenols	Urine	GLC	
	PCP	Urine	GLC	24 22
<b>Organophosphorus Compounds</b>				
Any OP containing these molecules	Dialkyl-phosphorus, -thiophosphorus, or -dithiophosphorus	Urine	GLC	36 81
Acephate	Acephate	Urine	GLC	82
Chlorpyrifos	3,5,6-Trichloro-2- pyridinol	Urine	GLC	83 84
Ethion	Ethion	Saliva	GLC	85
Malathion	Malathion DCA Malathion MCA	Urine	GLC	86 87 37
Parathion	p-Nitrophenol	Urine	GLC	48
EPN	p-Nitrophenol	Urine	GLC	88
<b>Phenyl Ureas</b>				
Diuron	3,4-Dichloroaniline	Urine	HPLC	42
Linuron	3,4-Dichloroaniline	Urine	HPLC	42
<b>Phthalimides</b>				
Captan	THPI	Urine	GLC	89
	THPI	Urine	GLC	90
	TTCA	Urine	HPLC	90
<b>Propanoates</b>				
Haloxypop	Haloxypop-methyl	Urine	GLC	91
<b>Pyrethroids</b>				
Cypermethrin	cis & trans-DCVA	Urine	GLC	92-94
	3PBA, 4OH3PBA	Urine	GLC	94
$\alpha$ -Cypermethrin	cis-DCVA	Urine	GLC	93
Deltamethrin	Deltamethrin	Urine	GLC	95
Fenvalerate	Fenvalerate	Urine	GLC	95

Table III. Biomonitoring Methods (Continued)

Class, Compound	Analyte	Matrix (Species <sup>2</sup> )	Anal. Method	Ref.
<b>Triazines</b>				
Atrazine	Desisopropyl atrazine	Urine	GLC	96
	Didesalkyl atrazine			
	Atrazine	Urine	GLC	97
	Desethyl atrazine	Urine	ELISA	98
	Desisopropyl atrazine			
	Atrazine mercapturate			
<b>Triazoles</b>				
Triadimefon	p-Chlorophenol	Urine	UNSP	43
Bitertanol	p-Phenylphenol	Urine	UNSP	43

<sup>1</sup>Abbreviations: HPLC, high performance liquid chromatography; DEA, 2,6-diethyl-aniline; HEEA, 2-(1-hydroxyethyl)-6-ethylaniline; ELISA, enzyme linked imm-unosorbent assay; LC, liquid chromatography; UNSP, unspecified; GLC, gas-liquid chromatography; MBC, methyl 2-benzimidazolecarbamate; 4-OH MBC, 4-hydroxy MBC; 5-OH MBC, 5-hydroxy MBC; EPTC, S-ethyl dipropylthiocarbamate; ETU, ethylenethiourea; 2,4-D, 2,4-dichlorophenoxyacetic acid; 2,4,5-T; 2,4,5-trichlorophenoxyacetic acid; MCPA, 2-methyl-4-chlorophenoxyacetic acid; RIA, radioimmunoassay; DDT, dichlorodiphenyltrichloroethane; DDD, tetrachloro-diphenylethane; DDE, dichlorodiphenyldichloroethylene; DDA, dichlorodiphenyl-acetic acid; HCB, hexachlaorobenzene; PCP, pentachlorophenol; DCA, dicarbox-yllic acid; MCA, monocarboxylic acid; EPN, ethyl p-nitrophenylthionobenzene-phosphonate; THPI, tetrahydrophthalimide; TTCA, thiazolidine-2-thione-4-carboxylic acid; DCVA, 3-(2,2-dichlorovinyl)-2,2-dimethylcyclopropane carbox-yllic acid; 3PBA, 3-phenoxybenzoic acid; 4OH3PBA, 4-hydroxy-3-phenoxybenzoic acid

<sup>2</sup>If other than human.

Table IV. Recent Studies Documenting Worldwide Occurrence of Organochlorine Pesticides in Tissues and Fluids from the General Population

Tissue	Number of		Nation	Year Publ	Ref
	Samples Analyzed	Analytes Detected			
Urine	197	7	USA	1989	78
Blood	34	1	USA	1989	101
Urine	143	1			
Milk	29	3	Yugoslavia	1990	102
Blood	52	4	Finland	1991	103
Fat	23	13	USA	1991	104
Milk	8	8	Kenya	1992	105
Blood <sup>1</sup>	11	8			
Blood <sup>2</sup>	11	8			
Fat	11	8			
Fat	168	3	Spain	1992	106
Blood	135	3	Germany	1992	107
Blood	31	14	India	1992	108
Blood	52	9	India	1992	109
Urine	52	9			
Blood	25	20	Canada	1992	29
Blood	90	1	USA	1992	110
Milk	20	13	France	1993	111
Blood	383	3	Japan	1993	112
Milk	51	11	Spain	1993	113
Blood	97	5	Croatia	1993	114
Milk	41	2	New Guinea	1993	115
Milk	128	5	Australia	1993	116
Blood <sup>1</sup>	31	3			
Blood <sup>2</sup>	31	3			
Fat	128	5			

<sup>1</sup> Maternal blood<sup>2</sup> Umbilical cord blood

body burdens may be increasing in or near developing countries where usage continues (105).

**Organophosphorus Compounds.** The organophosphorus (OP) pesticides are phosphate or phosphorothioate esters that do not accumulate in the body, but rather are quickly metabolized through the action of esterases to their respective dialkyl phosphorus metabolites, which are detectable in urine. Due to the rapid metabolism and clearance of OPs, the parent compound is not readily detectable in blood unless a massive dose has been received. Analytical methods for detecting dialkyl metabolites are rather tedious, requiring derivatization. However, methods recently have been developed for these metabolites that are more rapid (25).

Cholinesterase (ChE) depression has been used for years as a means to document exposure to organophosphorus compounds and insecticidal carbamates. Since there are considerable interindividual differences in ChE levels, one or more preexposure values should be determined for each person being monitored; these are the values to which comparison of postexposure measurements are made. ChE depression is most useful as a measure of acute exposure; it is a less sensitive indicator of chronic exposure than dialkylphosphorus metabolites in urine (81), which often are detectable at exposure levels that will not depress ChE (117). ChE continues to find use as an indicator of higher level occupational exposures, as evidenced by continuing and recent usage (118-120.)

**Herbicides.** Biomonitoring of humans for herbicide exposure is a rapidly advancing area. Studies distributed in time produce results that are complementary, and at times can appear contradictory. Atrazine is an interesting example of this phenomenon.

Early animal studies indicated that N-dealkylation accounts for the sum of metabolites produced following exposure to triazine herbicides (121). Later human studies showed that two metabolites (the didealkylated atrazine, 2-chloro-4,6-diamino-s-triazine, and desisopropyl atrazine, 2-chloro-4-amino-6-(ethylamino)-s-triazine) predominated and appeared in equal amounts in urine shortly after exposure of workers spraying atrazine from a railway car (96). Unchanged parent atrazine has been found in workers exposed during the manufacture and packaging of atrazine in a production plant (97). The authors of this study acknowledge that unchanged compound accounts for only a very minor part of the total absorbed dose. Parent atrazine in urine thus is not a good biomarker for exposure, potentially being detectable only in samples from highly exposed workers.

Later studies utilizing an ELISA assay indicate that while the above noted metabolites are detectable in human urine, the major human urinary metabolite is the mercapturate conjugate of atrazine (98). This mercapturate was found in concentrations at least ten times that of any of the N-dealkylated products or the parent compound from workers applying atrazine. In this assay, over 80% of immunoreactive material in urine was mercapturate of atrazine, while the parent compound accounted for less than 1% of the response; the parent and N-dealkylated compounds accounted for about 10% of the immunoreactive response.

A similar interest has developed for the heavily-used herbicide, alachlor. Recent studies with mice, rats, and monkeys have indicated substantial interspecies

differences in pertinent pharmacokinetic parameters of alachlor; these species excreted  $^{14}\text{C}$  alachlor metabolites in urine and feces in the ratios of 1:2 (mice), 1:1 (rats), and 10:1 (monkeys) (40). Initial human studies (38) monitored diethyl aniline (DEA) and a hydroxyethyl-ethyl aniline (HEEA) following base-pressure hydrolysis of alachlor metabolites. Only DEA was found in human urine. Both anilines were found in monkey urine (in a DEA:HEEA ratio of 4:1), as were mercapturates and other conjugates (40).

Most recently, diethylaniline-yielding metabolites have been detected in human urine (as DEA) by HPLC and compared to values (alachlor equivalents) determined via the adaptation of an ELISA kit designed for the analysis of alachlor in water (41). This ELISA technique for alachlor was at least 50 times more sensitive than the HPLC method; this sensitivity is speculated to be due to cross-reactivity of the anti-alachlor antibodies with putative thioether metabolites in human urine. Work remains to definitively identify these human metabolites; however, this technique has the potential of being particularly valuable for human screening, especially if human excretion kinetics for alachlor parallel those of the monkey.

### Conclusions / Use of Biomonitoring Data

Biomonitoring methods are becoming available for a greater variety and number of pesticides. Data generated through measurements of pesticides or their metabolites in biological matrices now are regarded as complementary to environmental measurement data in the assessment of exposure and risk, and in regulatory decision making (e.g., see Lunchick et al., 1989 (122)). Environmental exposure data such as ambient monitoring, personal monitoring, microenvironmental measurements, and questionnaire information provide clues to the sources of exposure -- while biomonitoring measurements integrate exposure (as dose) to the human receptor, the compound of concern having traveled through all environmental pathways (air, water, soil, food) and passed into the body through all portals of entry (lung, gut, skin).

Biomonitoring data are being used to validate questionnaires as meaningful indicators of exposure, and are useful in reducing exposure misclassification in epidemiology studies. However, biomonitoring data are difficult to interpret, and currently there are no guidelines for their interpretation. The lack of human pharmacokinetic data for many pesticides impedes efforts to estimate external exposure or target organ dose. The relationship between internal exposure and health effect most often is unknown, thus frustrating health practitioners who would like to be able to more effectively use exposure and early effect biomonitoring and biomarker data in a preventive context. These factors notwithstanding, biomonitoring data are an increasingly important component of exposure assessment, and as these limitations are overcome will become more important in the assessment of exposure and health impacts.

### Acknowledgments

The information in this document has been funded by the United States Environmental Protection Agency. It has been subjected to Agency review and approved for publication.

## Literature Cited

1. Miller, S. *Environ. Sci. Technol.* 1984, 18, 188A-190A.
2. National Research Council. *Monitoring Human Tissues for Toxic Substances*; National Academy Press: Washington, DC, 1991; pp 6-18.
3. Fatiadi, A.J. *Environ. Int.* 1984, 10, 175-205.
4. Wagner, S.L.; Durand, L.R.; Inman, R.D.; Kiigemagi, U.; Deinzer, M.L. *Arch. Environ. Contam. Toxicol.* 1991, 21, 596-606.
5. Geyer, J.J.; Scheunert, I.; Korte, F. *Chemosphere* 1987a, 16, 239-252.
6. Geyer, J.J.; Scheunert, I.; Korte, F. *Chemosphere* 1987b, 16, 887-899.
7. Davis, J.R.; Brownson, R.C.; Garcia, R. *Arch. Environ. Contam. Toxicol.* 1992, 22, 260-266.
8. Kamble, S.T.; Ogg, C.L.; Gold, R.E.; Vance, A.D. *Arch. Environ. Contam. Toxicol.* 1992, 22, 253-259.
9. Glotfelty, D.E.; Majewski, M.S.; Seiber, J.N. *Environ. Sci. Technol.* 1990, 24, 353-357.
10. Nations, B.K.; Hallberg, G.R. *J. Environ. Qual.* 1992, 21, 486-492.
11. Whang, J.M.; Schomburg, C.J.; Glotfelty, D.E.; Taylor, A.W. *J. Environ. Qual.* 1993, 22, 173-180.
12. Wienhold, B.J.; Sadeghi, A.M.; Gish, T.J. *J. Environ. Qual.* 1993, 22, 162-166.
13. Zabik, J.M.; Seiber, J.N. *J. Environ. Qual.* 1993, 22, 80-90.
14. Wilkinson, C.F. In *The Health Effects of Pesticides on Human Health*; Baker, S.R.; Wilkinson, C.F., Eds.; Advances in Modern Environmental Toxicology, Vol. 18; Princeton, NJ, 1990; pp 5-33.
15. Murphy, R.; Harvey, C. *Environ. Hlth. Perspect.* 1985, 60, 115-120.
16. Hattemer-Frey, H.A.; Travis, C.C. *Arch. Environ. Contam. Toxicol.* 1989, 18, 482-489.
17. Coad, S.; Newhook, R.C. *J. Expo. Anal. Environ. Epidemiol.* 1992, 2, 391-413.
18. Johnson, E.S.; Parsons, W.; Weinberg, C.R.; Shore, D.L.; Mathews, J.; Patterson, D.G., Jr.; Needham, L.L. *J. Natl. Cancer Inst.* 1992, 84, 1648-1653.
19. Blancato, J.N. *Ann. Ist. Super. Sanità* 1991, 27, 601-608.
20. Gianessi, L.P.; Puffer, C. *Herbicide Use in the United States: National Summary Report*; Resources for the Future: Washington, DC, 1991; pp 1-9.
21. Baum, R.M. *Chem. Engr. News* 1993, 71 (March 8), 38-41.
22. Edgerton, T.R.; Moseman, R.F.; Lindner, R.E.; Wright, L.H. *J. Chromatogr.* 1979, 170, 331-342.
23. Sherma, J. *Anal. Chem.* 1987, 59, 18R-31R.
24. Shafik, T.M.; Sullivan, H.C.; Enos, H.R. *J. Agr. Food. Chem.* 1973, 21, 295-298.
25. Weisskopf, C.P.; Seiber, J.N. In *Biological Monitoring for Pesticide Exposure*; Wang, R.G.M.; Franklin, C.A.; Honeycutt, R.C.; Reinert, J.C., Eds.; ACS Symposium Series 382; American Chemical Society: Washington, D.C., 1989; pp 206-214.
26. Needham, L.L.; Burse, V.W.; Head, S.L.; Korver, M.P.; McClure, P.C.; Andrews, J.S., Jr.; Rowley, D.L.; Sung, J.; Kahn, S.E. *Chemosphere* 1990, 20, 975-980.

In Biomarkers of Human Exposure to Pesticides; Saleh, M., et al.;

ACS Symposium Series; American Chemical Society: Washington, DC, 1993.

27. Cohn, W.J.; Boylan, J.J.; Blanke, R.V.; Fariss, M.W.; Howell, J.R.; Guzelian, P.S. *N. Engl. J. Med.* 1979, 298, 243-248.
28. Guzelian, P.S. *Toxicol. Lett.* 1992, 64/65, 589-596.
29. Mes, J. *Bull. Environ. Contam. Toxicol.* 1992, 48, 815-820.
30. Kutz, F.W. *Residue Rev.* 1983, 85, 277-292.
31. Murphy, R.S.; Kutz, F.W.; Strassman, S.C. *Environ. Hlth. Perspect.* 1983, 48, 81-86.
32. Nolan, R.J.; Freshour, N.L.; Kastel, P.E.; Saunders, J.H. *Toxicol. Appl. Pharmacol.* 1984, 76, 264-269.
33. Feldmann, R.J.; Maibach, H.I. *Toxicol. Appl. Pharmacol.* 1974, 28, 126-132.
34. Harris, S.A.; Solomon, K.R. *J. Toxicol. Environ. Hlth.* 1992, 36, 233-240.
35. Holler, J.S.; Fast, D.M.; Hill, R.H. Jr.; Cardinali, F.L.; Todd, G.D.; McCraw, J.M.; Bailey, S.L.; Needham, L.L. *J. Anal. Toxicol.* 1989, 13, 152-157.
36. Coye, M.J.; Lowe, J.A.; Maddy, K.J. *J. Occup. Med.* 1986, 28, 628-636.
37. Kutz, F.W.; Cook, B.T.; Carter-Pokras, O.D.; Brody, D.; Murphy, R. *J. Toxicol. Environ. Toxicol.* 1992, 37, 277-291.
38. Cowell, J.E.; Danhaus, R.G.; Kunstman, J.L.; Hackett, A.G.; Oppenhuizen, M.E.; Steinmetz, J.R. *Arch. Environ. Contam. Toxicol.* 1987, 16, 327-332.
39. Feng, P.C.C.; Patanella, J.E. *Pest. Biochem. Physiol.* 1988, 31, 84-90.
40. Sharp, D.B. In *Herbicides: Chemistry, Degradation and Mode of Action*; Kearny, P.C.; Kaufman, D.D., Eds.; Marcel Dekker: New York, NY, 1988, Vol.3; pp 301-333.
41. Biagini, R.E.; Tolos, W.; Henningsen, G.M.; MacKenzie, B.; Sanderson, W.T.; Ringenburg, V. *J. Agric. Food Chem.* (Submitted) 1993.
42. Lores, M.; Meekins, F.C.; Moseman, R.F. *J. Chromatogr.* 1980, 188, 412-416.
43. Lewalter, J.; Korallus, U. *Toxicol. Lett.* 1986, 33, 153-165.
44. Wojeck, G.A.; Price, F.J.; Nigg, H.N.; Stamper, J.H. *Arch. Environ. Contam. Toxicol.* 1983, 12, 65-70.
45. Lavy, T.L.; Mattice, J.D.; Massey, J.H.; Skulman, B.W. *Arch. Environ. Contam. Toxicol.* 1993, 24, 123-144.
46. Shafik, T.M.; Sullivan, H.C.; Enos, H.R. *Bull. Environ. Contam. Toxicol.* 1971, 6, 34-39.
47. De Bernardinis, M. Jr.; Wargin, W.A. *J. Chromatogr.* 1982, 246, 89-94.
48. Kutz, F.W.; Murphy, R.S.; Strassman, S.C. In *Pentachlorophenol: Chemistry, Pharmacology, and Environmental Toxicology*; Rao, K.R., Ed.; Environmental Science Research; Plenum Press: New York, NY, 1978, Vol. 12; pp 363-369.
49. Knaak, J.B.; Al-Bayati, M.A.; Raabe, O.G.; Wiedmann, J.L.; Pensyl, J.W.; Ross, J.H.; Leber, A.; Jones, P. In *Biological Monitoring for Pesticide Exposure*; Wang, R.G.M.; Franklin, C.A.; Honeycutt, R.C.; Reinert, J.C., Eds.; ACS Symposium Series 382; American Chemical Society: Washington, D.C., 1989; pp 288-303.
50. Savolainen, K.; Kurttio, P.; Vertiainen, T.; Kangas, J. *Arch. Toxicol.* 1989, 13, Suppl. 120-123.
51. Kurttio, P.; Savolainen, K. *Scand. J. Work Environ. Hlth.* 1990, 16, 203-207.
52. Kurttio, P.; Vartiainen, T.; Savolainen, K. *Brit. J. Ind. Med.* 1990, 47, 203-206.

53. Leenheers, L.H.; Van Breugel, D.C.; Ravensberg, J.C.; Meuling, W.K.A.; Jongen, M.J.M. *J. Chromatogr.* 1992, *578*, 189-194.
54. Kohli, J.D.; Khanna, R.N.; Gupta, B.N.; Dhar, M.M.; Tandon, J.S.; Sircar, K.P. *Xenobiotica* 1974, *2*, 97-100.
55. Frank, R.; Campbell, R.A.; Sirons, G.J. *Arch. Environ. Contam. Toxicol.* 1985, *14*, 427-435.
56. Knopp, D.; Glass, S. *Int. Arch. Occup. Environ. Hlth.* 1991, *63*, 329-333.
57. Draper, W.M. *J. Agric. Food Chem.* 1982, *30*, 227-231.
58. Fjeldstad, P.; Wannag, A. *Scand. J. Work. Environ. Hlth.* 1977, *3*, 100-103.
59. Kolmodin-Hedman, B.; Erne, K. *Arch. Toxicol.* 1980, *Suppl. 4*, 318-321.
60. De Felip, E.; Di Domenico, A.; Tancredi, F.; Volpi, F.; Bagnasco, G. *Ecotoxicol. Environ. Safety* 1988, *16*, 170-175.
61. Van Welie, R.T.H.; Mensert, R.; Van Duyn, P.; Vermeulen, N.P.E. *Arch. Toxicol.* 1991, *65*, 625-632.
62. Cessna, A.J.; Grover, R. *J. Chromatogr.* 1992, *600*, 327-332.
63. Folland, D.S.; Kimbrough, R.D.; Cline, R.E.; Swiggart, R.C.; Schaffner, W. *JAMA*, 1978, *239*, 1052-1055.
64. Cheung, M.W.; Kahrs, R.A.; Nixon, W.B.; Ross, J.A.; Tweedy, B.G. In *Biological Monitoring for Pesticide Exposure*; Wang, R.G.M.; Franklin, C.A.; Honeycutt, R.C.; Reinert, J.C., Eds.; ACS Symposium Series 382; American Chemical Society: Washington, D.C., 1989; pp 231-239.
65. Osterloh, J.D.; Cohen, B.S.; Popendorf, W.; Pond, S.M. *Arch. Environ. Hlth.* 1984, *39*, 271-275.
66. Osterloh, J.D.; Wang, R.; O'Connell, L.; Jacob, P., III; Maddy, K.T. In *Biological Monitoring for Pesticide Exposure*; Wang, R.G.M.; Franklin, C.A.; Honeycutt, R.C.; Reinert, J.C., Eds.; ACS Symposium Series 382; American Chemical Society: Washington, D.C., 1989; pp 215-230.
67. Osterloh, J.D.; Wang, R.; Schneikder, F.; Maddy, K. *Arch. Environ. Hlth.* 1989, *44*, 207-213.
68. Van Sittert, N.J. *Arch. Toxicol.* 1989, *13* (Suppl.), 91-100.
69. Van Welie, R.T.H.; Van Duyn, P.; Vermeulen, N.P.E. *J. Chromatogr.* 1989, *496*, 463-471.
70. Van Welie, R.T.H.; Van Duyn, P.; Vermeulen, N.P.E. *Int. Arch. Occup. Environ. Hlth.* 1991, *63*, 169-173.
71. Brady, S.C.; Enos, H.F.; Levy, K.A. *Bull. Environ. Contam. Toxicol.* 1980, *24*, 813-815.
72. Griffith, J.; Duncan, R.C. *Bull. Environ. Contam. Toxicol.* 1985, *35*, 496-499.
73. Laws, E.R. Jr.; Curley, A.; Biros, F.J. *Arch. Environ. Hlth.* 1967, *15*, 766-775.
74. Violante, F.S.; Gennari, P.; Raffi, G.B.; Coltelli, E.; Lev, D.; Minak, G.; Tiraferri, S. *Arch. Environ. Hlth.* 1986, *41*, 117-119.
75. Edmundson, W.F.; Davies, J.E.; Cranmer, M. *Public Hlth. Rpt.* 1970, *85*, 457-463.
76. Cranmer, J.F.; Carroll, J.J.; Copeland, M.F. *Bull. Environ. Contam. Toxicol.* 1969, *4*, 214-223.
77. Roan, C.; Morgan, D.; Paschel, E.H. *Arch. Environ. Hlth.* 1971, *22*, 309-315.

78. Hill, R.H., Jr.; To, T.; Holler, J.S.; Fast, D.M.; Smith, S.J.; Needham, L.L.; Binder, S. *Arch. Environ. Contam. Toxicol.* 1989, 18, 469-474.
79. Ando, M.; Hirano, S.; Itoh, Y. *Arch. Toxicol.* 1985, 56, 195-200.
80. Drummond, L.; Gillanders, E.M.; Wilson, H.K. *Brit. J. Ind. Med.* 1988, 45, 493-497.
81. Drevenkar, V.; Radić, Z.; Vasilčić, Ž.; Reiner, E. *Arch. Environ. Contam. Toxicol.* 1991, 20, 417-422.
82. Maroni, M.; Catenacci, G.; Galli, D.; Cavallo, D.; Ravazzani, G. *Arch. Environ. Contam. Toxicol.* 1990, 19, 782-788.
83. Nolan, R.J.; Rick, D.L.; Freshour, N.L.; Saunders, J.H. *Toxicol. Appl. Pharmacol.* 1984, 73, 8-15.
84. Fenske, R.A.; Elkner, K.P. *Toxicol. Industr. Hlth.* 1990, 6, 349-371.
85. Nigg, H.N.; Stamper, J.H.; Mallory, L.L. *Chemosphere*, 1993, 26, 897-906.
86. Fenske, R.A.; Leffingwell, J.T. *J. Agric. Food Chem.* 1989, 37, 995-998.
87. Draper, W.M.; Wijekoon, D.; Stephens, R.D. *J. Agric. Food Chem.* 1991, 39, 1796-1801.
88. Dillon, H.K.; Ho, M.H. In *Biological Monitoring of Exposure to Chemicals: Organic Compounds*; Ho, M.H.; Dillon, H.K., Eds.; John Wiley & Sons: New York, NY, 1987; pp 227-287.
89. Winterlin, W.L.; Kilgore, W.W.; Mourer, C.R.; Schoen, S.R. *J. Agric. Food Chem.* 1984, 32, 664-672.
90. Krieger, R.I.; Thongsinthusak, T. *Drug Chem. Toxicol.* 1993, 16, 207-225.
91. Campbell, R.A.; Kastl, P.E.; Kropscott, B.E.; Bartels, M.J. In *Biological Monitoring for Pesticide Exposure*; Wang, R.G.M.; Franklin, C.A.; Honeycutt, R.C.; Reinert, J.C., Eds.; ACS Symposium Series 382; American Chemical Society: Washington, D.C., 1989; pp 251-261.
92. Eadsforth, C.V.; Baldwin, M.K. *Xenobiotica*, 1983, 13, 67-72.
93. Eadsforth, C.V.; Bragt, P.C.; van Sittert, N.J. *Xenobiotica*, 1988, 18, 603-614.
94. Woollen, B.H.; Marsh, J.R.; Chester, G. In *Prediction of Percutaneous Penetration: Methods, Measurements, Modelling*; Scott, R.C., Ed.; IBC Technical Services, Ltd: London, 1991; pp 20-25.
95. Zhang, Z.; Sun, J.; Chen, S.; Wu, Y.; He, F. *Brit. J. Ind. Med.* 1991, 48, 82-86.
96. Ikonen, R.; Kangas, J.; Savolainen, H. *Toxicol. Lett.* 1988, 44, 109-112.
97. Catenacci, G.; Maroni, M.; Cottica, D.; Pozzoli, L. *Bull. Environ. Contam. Toxicol.* 1990, 44, 1-7.
98. Lucas, A.D.; Jones, A.D.; Goodrow, M.H.; Saiz, S.G.; Blewett, C.; Seiber, J.N.; Hammock, B.D. *Chem. Res. Toxicol.* 1993, 6, 107-116.
99. Stehr-Green, P.A. *J. Toxicol. Environ. Hlth.* 1989, 27, 405-421.
100. Kutz, F.W.; Wood, P.H.; Bottimore, D.P. *Rev. Environ. Contam. Toxicol.* 1991, 120, 1-82.
101. Cline, R.E.; Hill, R.H., Jr.; Phillips, D.L.; Needham, L.L. *Arch. Environ. Contam. Toxicol.* 1989, 18, 475-481.
102. Galetin-Smith, R.; Pavkov, S.; Roncevic, N. *Bull. Environ. Contam. Toxicol.* 1990, 45, 811-818.
103. Mussalo-Rauhamaa, H.; Pyysalo, H.; Antervo, K. *Arch. Environ. Hlth.* 1991, 46, 340-346.

104. Dearth, M.A.; Hites, R.A. *Environ. Sci. Technol.* 1991, 25, 1279-1285.
105. Kanja, L.W.; Skaare, J.U.; Ojwang, S.B.O.; Maitai, C.K. *Arch. Environ. Contam. Toxicol.* 1992, 22, 21-24.
106. Ferrer, A.; Bona, M.A.; Castellano, M.; To-Figueras, J.; Brunet, M. *Bull. Environ. Contam. Toxicol.* 1992, 48, 561-566.
107. Lommel, A.; Kruse, H.; Müller, E.; Wassermann, O. *Arch. Environ. Contam. Toxicol.* 1992, 22, 14-20.
108. Bhatnagar, V.K.; Patel, J.S.; Variya, M.R.; Venkaiah, K.; Shah, M.P.; Kashyap, S.K. *Bull. Environ. Contam. Toxicol.* 1992, 48, 302-307.
109. Chandra, H.; Pangtey, B.S.; Modak, D.P.; Singh, K.P.; Gupta, B.N.; Bharti, R.S.; Srivastava, S.P. *Bull. Environ. Contam. Toxicol.* 1992, 48, 295-301.
110. Hovinga, M.E.; Sowers, M.F.; Humphrey, H.E.B. *Arch. Environ. Contam. Toxicol.* 1992, 22, 362-366.
111. Bordet, F.; Mallet, J.; Maurice, L.; Borrel, S.; Venant, A. *Bull. Environ. Contam. Toxicol.* 1993, 50, 425-432.
112. Hirai, Y.; Tomokuni, K. *Bull. Environ. Contam. Toxicol.* 1993, 50, 316-324.
113. Hernández, L.M.; Fernández, M.A.; Hoyas, E.; González, M.J.; Garcia, J.F. *Bull. Environ. Contam. Toxicol.* 1993, 50, 308-315.
114. Krauthacker, B. *Bull. Environ. Contam. Toxicol.* 1993, 50, 8-11.
115. Spicer, P.E.; Kereu, R.K. *Bull. Environ. Contam. Toxicol.* 1993, 50, 540-546.
116. Stevens, M.F.; Ebell, G.F.; Psailasavona, P. *Med. J. Australia* 1993, 158, 238-241.
117. Franklin, C.A.; Fenske, R.A.; Greenhalgh, R.; Mathieu, L.; Denley, H.V.; Leffingwell, J.T.; Spear, R.C. *J. Toxicol. Environ. Hlth.* 1981, 7, 715-731.
118. Jauhainen, A.; Kangas, J.; Laitinen, S.; Savolainen, K. *Bull. Environ. Contam. Toxicol.* 1992, 49, 37-43.
119. Karr, C.; Demers, P.; Costa, L.G.; Daniell, W.E.; Barnhart, S.; Miller, M.; Gallagher, G.; Horstman, S.W.; Eaton, D.; Rosenstock, L. *Environ. Res.* 1992, 59, 229-237.
120. Vasilic, Z.; Drevenkar, V.; Rumenjak, V.; Stengl, B.; Fröbe, Z. *Arch. Environ. Contam. Toxicol.* 1992, 22, 351-357.
121. Bradway, D.E.; Moseman, R.F. *J. Agric. Food Chem.* 1982, 30, 244-247.
122. Lunchick, C.; Burin, G.; Reinert, J.C.; Warkentien, K.E. In *Biological Monitoring for Pesticide Exposure*; Wang, R.G.M.; Franklin, C.A.; Honeycutt, R.C.; Reinert, J.C., Eds.; ACS Symposium Series 382; American Chemical Society: Washington, D.C., 1989; pp 327-337.

RECEIVED August 4, 1993

## Chapter 2

# Modeling Cytochrome P-450 Mediated Acute Nitrile Toxicity Using Theoretical Linear Solvation Energy Relationships

George R. Famini<sup>1</sup>, Leland Y. Wilson<sup>2</sup>, and Stephen C. DeVito<sup>3,4</sup>

<sup>1</sup>Development and Engineering Center, U.S. Army Chemical Research, Aberdeen Proving Ground, Aberdeen, MD 21010

<sup>2</sup>Department of Chemistry, La Sierra University, Riverside, CA 92515

<sup>3</sup>Office of Pollution Prevention and Toxics (TS-779), U.S. Environmental Protection Agency, Washington, DC 20460

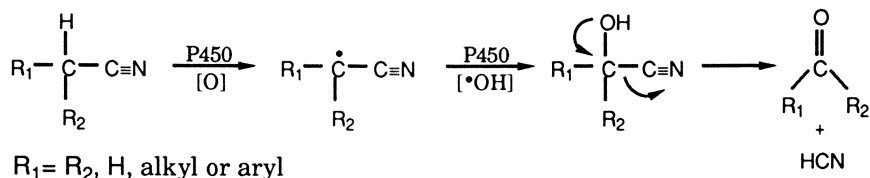
A theoretical linear solvation energy relationship (TLSER) model for predicting acute nitrile toxicity was developed using molecular volume, dipolarity/polarizability, hydrogen bond (molecular orbital) acidity, and electrostatic basicity terms as descriptors. It was observed that molecular orbital acidity was the most important descriptor in the model, followed by molecular volume. The predictive quality of the TLSER model appears to be equal to that of a recently reported model that uses octanol-water partition coefficients and estimated rates of  $\alpha$ -hydrogen atom abstraction as descriptors. Previously reported TLSER models of toxicity have largely been confined to predicting non-specific toxicity. The results of this study suggest that TLSER models may be useful in predicting specific (mechanism-based) toxicity.

## Biochemical Basis of Cyanide Release from Nitriles

Nitriles represent a large class of compounds which have wide industrial application as solvents and chemical intermediates. Studies have shown that exposure of humans (1, 2) and experimental animals (3-11) to certain nitriles has resulted in cyanide release and subsequent acute toxicity. Ohkawa et al. (5) suggested that cyanide release from nitriles results from cytochrome P450 catalyzed hydroxylation of the  $\alpha$ -carbon to form a cyanohydrin intermediate, which undergoes rapid nonenzymatic decomposition to the carbonyl derivative with the

<sup>4</sup>Corresponding author

simultaneous release of cyanide. Other investigators have since demonstrated the role of cytochrome P450 oxidation in the release of cyanide from various nitriles (6-15). It is now known that cytochrome P450 catalyzed hydroxylation includes substrate binding, oxygen activation, hydrogen atom abstraction, recombination of the resulting hydroxy radical equivalent with substrate, and dissociation of the hydroxylated product. The overall reaction sequence of cytochrome P450 mediated hydroxylation of nitriles is illustrated in Scheme I.



**Scheme I. Cytochrome P450-Mediated Cyanide Release From Nitriles**

**Structure-Toxicity Relationships of Nitriles.** Several investigators have reported similar structure-toxicity relationships for the acute toxicity of a variety of nitriles (6-14). Tanii and Hashimoto (9) observed a parabolic relationship in mice between acute toxicity and hydrophobicity, expressed as  $\log P$ , for phenylalkyl nitriles and primary and secondary nitriles containing chloro- or unsubstituted alkyl groups of three carbons or less ( $r = 0.96$ ,  $n = 13$ ). They concluded that acute toxicity of these nitriles is largely a function of hydrophobicity with respect to susceptibility to hepatic biotransformation to release cyanide. However, nitriles containing alkyl substituents of four carbons or larger follow a linear relationship with  $\log P$  (9). Release of cyanide from these nitriles is much slower and hence their acute toxicity is not believed to be due to cyanide release, but rather the parent compounds (9, 10). They later reported that dinitriles do not follow any relationship with  $\log P$ , and they attributed the acute toxicity of dinitriles to a combination of cyanide release and the parent compound (11).

In a recent retrospective analysis of nitrile acute toxicity ( $\text{LD}_{50}$ ) data, DeVito and Pearlman pointed out that many nitriles have the same hydrophobicity but differ greatly in acute toxicity, and that use of  $\log P$  alone as a descriptor in predicting acute toxicity of nitriles may not always be sufficient. They hypothesized that the acute toxicity of nitriles depends largely on the relative stability of the  $\alpha$ -carbon radical formed from cytochrome P450  $\alpha$ -hydrogen atom abstraction (16). Nitriles that form tertiary or benzylic radicals on the  $\alpha$ -carbon atom are generally much more acutely toxic than nitriles that form secondary radicals, which are more toxic than nitriles that form primary radicals.

**Mechanism-Based Model for Predicting Nitrile Toxicity.** Using the hypothesis of DeVito and Pearlman (16), a mechanism-based model for quantitative prediction of acute nitrile toxicity was developed by Grogan et al. using octanol-water partition coefficients ( $\log P$ ) and estimated relative rates of  $\alpha$ -hydrogen atom abstraction ( $k_{\alpha\text{corr}}$ ) as descriptors of hydrophobicity (lipophilicity) and cyanohydrin formation (oxidation), respectively (17). This model (equation 1) is very useful for estimating the acute toxicity of structurally diverse nitriles, including amino-substituted nitriles, dinitriles, and nitriles containing long and short alkyl substituents;

$$\log(1/\text{LD}_{50}) = \underset{(0.05)}{-0.16(\log P)^2} + \underset{(0.10)}{0.22(\log P)} + \underset{(0.20)}{0.11(\ln k_{\alpha\text{corr}})} + 5.67$$

$$n = 26 \quad r = 0.85 \quad (1)$$

The number of nitriles used is represented by  $n$ ,  $r$  is the correlation coefficient, and the numbers in parentheses are the standard errors of the coefficients (95% confidence level). The relative rates of  $\alpha$ -hydrogen atom abstraction were calculated from electronic considerations only, and did not include steric effects involving enzyme-substrate association (17). It was assumed, however, that since the nitriles used in the study are relatively small molecules, differences in rates arising from steric considerations may be less important. The octanol-water partition coefficient ( $\log P$ ) is a measure of relative solubility in lipid/aqueous phases (hydrophobicity), and as such is often used as a descriptor of a compound's ability to penetrate biological membranes in modeling biological response (18, 19). Removal of the  $\log P$  term from equation 1 moderately reduced the predictive quality of the model;  $r = 0.76$  (17).

### Linear Solvation Energy Relationships

We were interested in identifying other approaches to model acute nitrile toxicity, by investigating the usefulness of established methods used for quantitative correlation of structure-property and structure-activity relationships. A very successful approach for structure-property/activity estimation is the Linear Solvation Energy Relationship (LSER) model of Kamlet, Abboud and Taft (20). The basic tenet of the LSER model is that a given property can often be defined by a linear relationship of three different types of terms which describe steric, polarizability/dipolarity and hydrogen bonding effects. The generalized LSER model is shown in equation 2.

$$\log \text{property} = \text{steric} + \text{polarizability/dipolarity} + \text{hydrogen bonding} \quad (2)$$

Kamlet, Abboud and Taft (20, 21), and later Park and co-workers (22), developed a series of empirically developed parameters describing each of the terms in equation 2. These terms were originally denoted the solvatochromic parameters because Kamlet and Taft developed them from UV-visible spectral shifts, however similar scales have been

developed through gas chromatography measurements (22). Using the LSER model, Kamlet, Taft and co-workers demonstrated that many types of chemical properties depend on solute-solvent interactions. Octanol-water partitioning (23-26), aqueous solubility (27-31), solubility in and partitioning between blood and body organs (32-36), and non-specific toxicity (37-39) are examples of some of these properties. The versatility of the LSER approach for structure-property and structure-activity estimation is evident by the successful correlation of more than 200 biological and physical properties (40, 41).

A major limitation of the LSER approach, however, is that it requires empirical (measured) values for each descriptor term. Although LSER descriptor values for many chemical substances (or predictive relationships for their estimation) are available, LSER values for complex molecules are not easily obtainable. Hence the difficulty in obtaining LSER values has greatly discouraged the application of the LSER model for use in quantitative structure-property/activity relationships. However methods for estimating LSER descriptor values for complex molecules have recently been reported (42-44), and may make use of the LSER model more feasible.

**Theoretical Linear Solvation Energy Relationships (TLSEs).** In the past theoretical chemistry has been used to provide descriptors for quantifying structure-property and structure-activity relationships. Representative work in this area is described by Loew and co-workers (45), Pedersen (46), and Chastrette and co-workers (47). Lewis has compiled an extensive summary on molecular orbital calculations applied to quantifying structure-activity relationships (the so called MO-QSAR) for a variety of biological properties (42). Other examples of theoretical descriptors, in addition to classical molecular orbital descriptors, include the molecular connectivity index of Kier and Hall (48). Ford and Livingstone point out the advantages of computationally derived descriptors over extra-thermodynamic parameters (49). They are typically not restricted to closely related compounds as is often the case with group theoretical and topological descriptors. In addition, the theoretical parameters describe clearly defined molecular properties, and are mutually orthogonal.

In an effort to combine the successful LSER approach with theoretical chemistry methods, the LSER approach has been extended to utilize descriptor values obtained solely from computational (theoretical) methods, and as such is known as the Theoretical Linear Solvation Energy Relationship (TLSE) model (50, 51). A primary advantage of the TLSE model over the LSER model is that the TLSE model does not require empirically determined descriptor values, TLSE descriptor values for complex molecules are obtained using theoretical methods.

**Basis for Using the TLSE Model in Predicting Nitrile Toxicity.** We were interested in testing the usefulness of the TLSE model in predicting the acute toxicity of nitriles. Several considerations suggested the feasibility of using the TLSE model for this purpose.

First, recent advances in computational power have enabled rapid and accurate calculation of the TLSEr descriptors (50). Second, the TLSEr descriptors have been successfully employed to predict  $\log P$  (51), an important parameter of nitrile toxicity. Third, excellent relationships have been observed in correlating the TLSEr descriptors to non-specific (52) and specific (53, 54) toxicities. Because of the high degree of correlation of the TLSEr descriptors with  $\log P$ , the high correlation to non-specific toxicities is expected. However, the TLSEr descriptors describe fundamental attributes of a molecule, and good correlation with specific (receptor-based) biological responses should also result as long as the specific activity is related to one or more of the TLSEr terms (55). In the present study, we have evaluated the usefulness of the TLSEr descriptors in predicting the acute toxicity of 26 structurally diverse nitriles.

## Methods

The nitriles used in this investigation were identical to those used in a previous study (17). Mouse oral acute toxicity ( $LD_{50}$ ) data obtained from the literature (1, 9, 11, 56) were used.  $\log P$  data and relative rates of  $\alpha$ -hydrogen atom abstraction statistically corrected for oxidation at other positions ( $k_{\alpha\text{corr}}$ ) were obtained from a previous study (17).

All geometries were optimized using the MNDO algorithm (57) as contained within MOPAC v6.0 (58). All calculations were carried out on a Kubota Pacific Titan superworkstation. Structure entry and visualization were performed using the in-house developed Molecular Modeling Analysis and Display System (MMADS) molecular modeling package (59). Multiple linear regressions were computed, using the Minitab statistical package (60).

**Calculation of the TLSEr Descriptors.** The TLSEr descriptors for each nitrile were taken directly from the MNDO calculations. These descriptors consist of six molecular parameters that attempt to describe the important features involved in solute-solvent interactions (equation 2). The steric term is represented by molecular volume ( $V_{\text{mc}}$ ), and was calculated using the method of Hopfinger (61). The polarizability/dipolarity term is the polarization volume, and was calculated using the procedure of Dewar and Stewart (62) but divided by the  $V_{\text{mc}}$  to remove any cross-correlation between these two terms. The resulting polarizability index ( $\pi_i$ ) is a volume independent measure of the ability of the electrons to move (or be polarized) throughout the molecule. The hydrogen bonding interactions are represented by four terms, two defining hydrogen bond basicity and two defining hydrogen bond acidity. The two hydrogen bonding basicity terms are represented by a molecular orbital term,  $\epsilon_\beta$  (the magnitude of the difference between the highest occupied molecular orbital (HOMO) of the substrate and the lowest unoccupied molecular orbital (LUMO) of water), and a electrostatic basicity term,  $q$ , (the absolute value of the formal charge of

the most negative site in the substrate). Analogously, the hydrogen bond acidity is represented by a molecular orbital acidity term,  $\epsilon_\alpha$  (the magnitude of the difference between the LUMO of the substrate and the HOMO of water), and an electrostatic acidity term,  $qH^+$  (the formal charge of the most positive hydrogen in the molecule). Because of how the  $\epsilon_\alpha$  and  $\epsilon_\beta$  terms are defined, acidity or basicity is inversely related to  $\epsilon_\alpha$  or  $\epsilon_\beta$ , respectively. In typical correlations, some of these descriptors will have little bearing on the relationship and are dropped from the equation (based on the  $t$  score at the 95% confidence level). The overall TLSER equation is described in its general form in equation 3;

$$\log \text{ property} = C_1 (V_{mc}/100) + C_2(\pi_i \cdot 10) + C_3(\epsilon_\beta) + C_4(q.) + C_5(\epsilon_\alpha/10) + C_6(qH^+) + C_7 \quad (3)$$

where  $C_1$ - $C_6$  are regression coefficients which reflect the relative contribution of each parameter to the property, and  $C_7$  is the intercept.

## Results

The mouse acute toxicity data of the nitriles in Table I were initially correlated with the entire set of TLSER descriptors in equation 3. Descriptors  $\epsilon_\beta$  and  $qH^+$  were found to have no usefulness, and were removed from further regression analyses. The numerical values of the molecular volume ( $V_{mc}$ ), polarizability ( $\pi_i$ ), molecular orbital acidity ( $\epsilon_\alpha$ ) and electrostatic basicity ( $q.$ ) terms are given in Table I, and were used to predict  $LD_{50}$  values for the 26 nitriles in Table I. The correlation is shown in equation 4;

$$\log(1/LD_{50}) = -0.66(V_{mc}/100) - 12.37(\pi_i \cdot 10) - 0.38(\epsilon_\alpha/10) - 3.81(q.) + 7.34$$
$$n = 26, \quad r = 0.78, \quad s = 0.437, \quad F = 8.04 \quad (4)$$

where  $n$  is the number of compounds used,  $r$  is the correlation coefficient,  $s$  is the standard deviation (95 % confidence level), and  $F$  is the Fisher-test for significance of the equation. Three compounds, 2-methylbutyronitrile, **11**, chloroacetonitrile, **17**, and 3-hydroxypropionitrile, **26**, had residuals greater than two standard deviations. Inclusion of the estimated corrected rate constant of  $\alpha$ -hydrogen atom abstraction ( $k_{\alpha\text{corr}}$ ) descriptor in the regression moderately improved the correlation (equation 5), although compounds **17**, and **26** still had residuals greater than two standard deviations.

Table I. log *P*, TLSER Descriptors, Theoretical Reaction Rate Constants, and Acute Toxicity Data of Nitriles 1-26

name	compound no.	structure	log <i>P</i> <sup>a</sup>	TLSER descriptors				<i>k</i> <sub>acorr</sub> <sup>f</sup>	exp	log(1/LD <sub>50</sub> g)		resid <sup>i</sup>
				<i>V</i> <sub>mc</sub> <sup>b</sup>	<i>π</i> <sub>s</sub> <sup>c</sup>	<i>ε</i> <sub>α</sub> <sup>d</sup>	<i>q</i> <sup>e</sup>			calcd <sup>h</sup>	exp <sup>j</sup>	
acetonitrile	1	CH <sub>3</sub> CN	-0.39	44.20	0.164	13.779	0.115	4.0	-0.816 <sup>j</sup>	-0.873	-0.816 <sup>j</sup>	0.057
propionitrile	2	CH <sub>3</sub> CH <sub>2</sub> CN	0.14	61.46	0.100	13.804	0.106	251.0	0.187 <sup>j</sup>	0.211	0.187 <sup>j</sup>	-0.024
butyronitrile	3	CH <sub>3</sub> CH <sub>2</sub> CH <sub>2</sub> CN	0.66	78.73	0.103	13.818	0.106	58.4	0.244 <sup>j</sup>	-0.025	0.244 <sup>j</sup>	0.269
valeronitrile	4	CH <sub>3</sub> (CH <sub>2</sub> ) <sub>3</sub> CN	1.19	96.47	0.103	13.836	0.106	24.7	-0.362 <sup>j</sup>	-0.235	-0.362 <sup>j</sup>	-0.127
capronitrile	5	CH <sub>3</sub> (CH <sub>2</sub> ) <sub>4</sub> CN	1.72	115.00	0.103	13.815	0.105	16.9	-0.679 <sup>j</sup>	-0.409	-0.679 <sup>j</sup>	-0.270
caprylonitrile	6	CH <sub>3</sub> (CH <sub>2</sub> ) <sub>6</sub> CN	2.78	150.97	0.104	13.835	0.106	8.1	-1.149 <sup>j</sup>	-0.822	-1.149 <sup>j</sup>	-0.327
pelargonitrile	7	CH <sub>3</sub> (CH <sub>2</sub> ) <sub>7</sub> CN	3.31	168.56	0.104	13.822	0.106	5.5	-1.170 <sup>j</sup>	-1.009	-1.170 <sup>j</sup>	-0.161
isobutyronitrile	8	(CH <sub>3</sub> ) <sub>2</sub> CHCN	0.44	78.63	0.102	13.849	0.099	8288.5	0.432 <sup>j</sup>	-0.013	0.432 <sup>j</sup>	0.445
3-methylbutyronitrile	9	(CH <sub>3</sub> ) <sub>2</sub> CHCH <sub>2</sub> CN	1.06	96.38	0.103	13.816	0.107	0.98	-0.447 <sup>j</sup>	-0.221	-0.447 <sup>j</sup>	-0.226
4-methylvaleronitrile	10	(CH <sub>3</sub> ) <sub>2</sub> CH(CH <sub>2</sub> ) <sub>2</sub> CN	1.59	130.64	0.105	13.820	0.106	6.6	-0.701 <sup>j</sup>	-0.624	-0.701 <sup>j</sup>	-0.077
2-methylbutyronitrile	11	CH <sub>3</sub> CH <sub>2</sub> CH(CH <sub>3</sub> )CN	0.97	97.85	0.102	13.848	0.100	4288.2	0.538 <sup>j</sup>	-0.208	0.538 <sup>j</sup>	0.746
malononitrile	12	NCCH <sub>2</sub> CN	-1.20	51.12	0.126	13.102	0.115	5.4	-0.255 <sup>h</sup>	0.147	-0.255 <sup>h</sup>	-0.402
succinonitrile	13	NC(CH <sub>2</sub> ) <sub>2</sub> CN	-0.82	76.98	0.104	13.713	0.115	28.9	-0.210 <sup>h</sup>	-0.015	-0.210 <sup>h</sup>	-0.195
glutaronitrile	14	NC(CH <sub>2</sub> ) <sub>3</sub> CN	-0.96	94.45	0.103	13.611	0.118	41.7	-0.452 <sup>h</sup>	-0.134	-0.452 <sup>h</sup>	-0.318
adiponitrile	15	NC(CH <sub>2</sub> ) <sub>4</sub> CN	-0.43	111.83	0.106	13.571	0.110	113.5	-0.201 <sup>h</sup>	-0.323	-0.201 <sup>h</sup>	0.122
pimelonitrile	16	NC(CH <sub>2</sub> ) <sub>5</sub> CN	0.11	128.83	0.107	13.661	0.109	202.1	-0.013 <sup>h</sup>	-0.562	-0.013 <sup>h</sup>	0.549
chloroacetonitrile	17	ClCH <sub>2</sub> CN	0.22	58.94	0.105	12.084	0.172	107.0	-0.265 <sup>j</sup>	-	-0.265 <sup>j</sup>	-
3-chloropropionitrile	18	Cl(CH <sub>2</sub> ) <sub>2</sub> CN	0.20	76.25	0.106	12.587	0.196	4.9	0.244 <sup>j</sup>	0.314	0.244 <sup>j</sup>	-0.070
4-chlorobutyronitrile	19	Cl(CH <sub>2</sub> ) <sub>3</sub> CN	0.38	93.98	0.107	12.730	0.202	16.2	0.284 <sup>j</sup>	0.030	0.284 <sup>j</sup>	0.254
propionitrile, 3-(dimethylamino)-	20	(CH <sub>3</sub> ) <sub>2</sub> N(CH <sub>2</sub> ) <sub>2</sub> CN	-0.24	109.37	0.106	13.846	0.449	500.2	-1.185 <sup>m</sup>	-1.400	-1.185 <sup>m</sup>	0.215
3-(isopropylamino)-	21	(CH <sub>3</sub> ) <sub>2</sub> CHNH(CH <sub>2</sub> ) <sub>2</sub> CN	0.12	127.19	0.105	13.822	0.344	0.005	-1.288 <sup>m</sup>	-1.264	-1.288 <sup>m</sup>	-0.024
3,3'-iminodi-	22	HN(CH <sub>2</sub> CH <sub>2</sub> CN) <sub>2</sub>	-0.92	124.04	0.108	13.638	0.343	0.041	-1.439 <sup>n</sup>	-1.183	-1.439 <sup>n</sup>	-0.256
3-butenitrile	23	CH <sub>2</sub> =CHCH <sub>2</sub> CN	0.12	72.41	0.107	12.842	0.135	12703.4	0.000 <sup>j</sup>	0.380	0.000 <sup>j</sup>	-0.380
phenylacetoneitrile	24	C <sub>6</sub> H <sub>5</sub> CH <sub>2</sub> CN	1.56	115.44	0.140	11.230	0.103	34808.9	0.409 <sup>j</sup>	0.204	0.409 <sup>j</sup>	0.205
3-phenylpropionitrile	25	C <sub>6</sub> H <sub>5</sub> CH <sub>2</sub> CH <sub>2</sub> CN	1.55	133.89	0.134	11.362	0.103	3.3	0.051 <sup>j</sup>	0.057	0.051 <sup>j</sup>	-0.006
3-hydroxypropionitrile	26	HO(CH <sub>2</sub> ) <sub>2</sub> CN	-1.10	68.69	0.099	13.655	0.319	0.82	-1.688 <sup>j</sup>	-	-1.688 <sup>j</sup>	-

<sup>a</sup> Logarithm of the octanol/water partition coefficient; obtained from ref 18. <sup>b</sup> Molecular volume. <sup>c</sup> Polarizability index. <sup>d</sup> Molecular orbital acidity. <sup>e</sup> Electrostatic basicity. <sup>f</sup> Theoretical reaction rate constants statistically corrected for metabolism at other positions; obtained from ref 18. <sup>g</sup> Acute median oral lethal dose in mice, mmol/kg. <sup>h</sup> Calculated using equation 6. <sup>i</sup> Residual; exp minus calcd log(1/LD<sub>50</sub>) values. <sup>j</sup> Obtained from ref 9. <sup>k</sup> Obtained from ref 11. <sup>l</sup> Not determined; see text for details. <sup>m</sup> Obtained from ref 1. <sup>n</sup> Obtained from ref 50.

$$\log(1/LD_{50}) = -0.50(V_{mc}/100) - 9.02(\pi_i \cdot 10) - 2.98(\epsilon_\alpha/10) - 2.86(q.) + 6.41(\ln k_{\alpha corr}/100) + 5.32$$

$$n = 26, \quad r = 0.84, \quad s = 0.387, \quad F = 9.51 \quad (5)$$

Compounds **17** and **26** were removed from the data set because, in addition to being statistical outliers, the acute toxicity of these compounds is not believed to be due to cyanide release (9, 10). Equation 6 is the correlation of the nitrile LD<sub>50</sub> values with the TLSEr descriptors only, excluding compounds **17** and **26**. The *t* scores of the coefficients of equation 6 are represented in parentheses directly under the coefficients. Table I shows the experimental, predicted and residual values of log(1/LD<sub>50</sub>) for the nitriles used in equation 6. The graphical output of the best fit of individual compounds to the equation is depicted in Figure 1. The bisecting line of the graph represents an ideal fit to the equation. Using the log *P*, *k*<sub>αcorr</sub> model for these same nitriles gave essentially the same regression (equation 7; *r* = 0.86) as equation 6.

$$\log(1/LD_{50}) = -1.05(V_{mc}/100) - 1.97(\pi_i \cdot 10) - 5.22(\epsilon_\alpha/10) - 2.83(q.) + 10.35$$

$$(4.45) \qquad (3.58) \qquad (4.81) \qquad (3.77)$$

$$n = 24, \quad r = 0.87, \quad s = 0.332, \quad F = 14.2 \quad (6)$$

$$\log(1/LD_{50}) = -0.13(\log P)^2 + 0.14(\log P) + 0.11(\ln k_{\alpha corr}) + 5.65$$

$$n = 24, \quad r = 0.86 \quad (7)$$

Inclusion of the corrected rate constant (*k*<sub>αcorr</sub>) descriptor into equation 6 resulted in a minor improvement in the model (equation 8).

$$\log(1/LD_{50}) = -0.89(V_{mc}/100) - 1.64(\pi_i \cdot 10) - 4.43(\epsilon_\alpha/10) - 2.22(q.) + 0.05(\ln k_{\alpha corr}/100) + 8.50$$

$$n = 24, \quad r = 0.90, \quad s = 0.293, \quad F = 15.9 \quad (8)$$

Removal of compound **11** from equation 6 marginally improved the correlation (equation 9).

$$\log(1/LD_{50}) = -1.04(V_{mc}/100) - 1.86(\pi_i \cdot 10) - 5.41(\epsilon_\alpha/10) - 2.56(q.) + 10.38$$

$$n = 23, \quad r = 0.90, \quad s = 0.288, \quad F = 18.3 \quad (9)$$

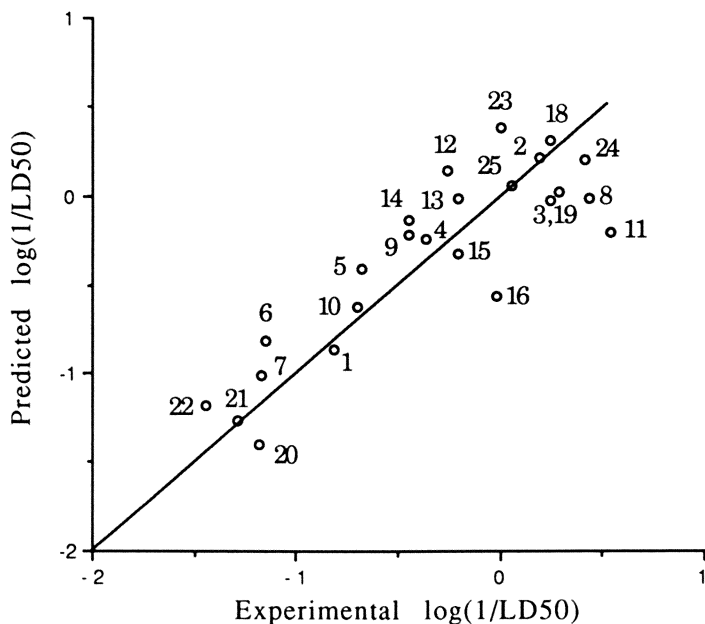


**Figure 1.** Experimental versus predicted  $\log(1/\text{LD}_{50})$  for nitriles in Table I (without **17** and **26**), obtained from multiple regression of  $V_{\text{mc}}$ ,  $\pi_i$ ,  $\epsilon_\alpha$ , and  $q$  with  $\text{LD}_{50}$  data. See equation 6 for regression coefficients.

## Discussion

Tanii and Hashimoto reported that, with the exception of dinitriles, the acute toxicity of nitriles is largely a function of hydrophobicity ( $\log P$ ) with respect to susceptibility to hepatic biotransformation to release cyanide (9,10,11). Using Tanii and Hashimoto's data sets, DeVito and Pearlman reported a correlation coefficient of 0.59 in a model that used only  $\log P$  as a descriptor of acute toxicity for nitriles **1-26** (16). DeVito and Pearlman hypothesized that the propensity of nitriles to release cyanide as a result of cytochrome P450 metabolism is also a function of relative ease of  $\alpha$ -hydrogen atom abstraction (16). That is, nitriles which form more stable  $\alpha$ -carbon radicals tend to be more acutely toxic than nitriles which form less stable radicals. In collaboration with other investigators, DeVito and Pearlman later reported a mechanism-based

model (equation 1) for prediction of acute toxicity for nitriles **1-26** that was developed using  $\log P$  and statistically corrected rates of  $\alpha$ -hydrogen atom abstraction, expressed as  $k_{\alpha\text{corr}}$ , as descriptors (17). The  $k_{\alpha\text{corr}}$  descriptor considers rates of oxidation at multiple sites with respect to oxidation at the  $\alpha$ -carbon, and, as such, describes the influence of cytochrome P450 oxidation at other carbon atoms on the rate of oxidation at the  $\alpha$ -carbon atom. The  $k_{\alpha\text{corr}}$  descriptor is based on electronic considerations only, and does not take steric interactions into account. Removal of either the  $\log P$  or  $k_{\alpha\text{corr}}$  descriptors from equation 1 reduced the predictive quality of the model (17).

Our original intent in this research was to investigate the usefulness of applying the TLSEr model in predicting the acute toxicity of structurally diverse nitriles. Initial application of the TLSEr descriptors in correlating the LD<sub>50</sub> values of nitriles **1-26** resulted in a model (equation 4) that predicts acute nitrile toxicity almost as well as the model that uses  $\log P$  and  $k_{\alpha\text{corr}}$  as descriptors (equation 1) for the same nitriles. The moderate improvement in the predictive quality of the model following inclusion of the  $k_{\alpha\text{corr}}$  term (equation 5) appears to be due to consideration of hydrogen atom abstraction from the  $\alpha$ -carbon. It is interesting to note that the predictive quality of the TLSEr model represented by equation 4 is very similar to that of the model reported by Grogan et al. (17) that uses only  $k_{\alpha\text{corr}}$  as a descriptor ( $r = 0.76$ ) in predicting acute toxicity for the same nitrile data set. Although the  $k_{\alpha\text{corr}}$  term is directly representative of cytochrome P450 oxidation of the  $\alpha$ -carbon (while taking into account oxidation at other positions), the relative closeness in the predictive qualities of equations 4 and 5 suggests that the TLSEr descriptors may be considering overall cytochrome P450 oxidation as well.

In addition to being statistical outliers, there may be biochemical reasons that justify removal of chloroacetonitrile (**17**) and 3-hydroxypropionitrile (**26**) from the data set. Administration of **17** to mice pretreated with CCl<sub>4</sub> (which attenuates cytochrome P450 activity) results in decreased cyanide liberation, but the acute toxicity of this compound *increases* (9,10). These observations suggest that normal hepatic metabolism of **17** is a detoxifying process, and that the acute toxicity of this compound is not cyanide-dependent. 3-Hydroxypropionitrile (**26**) can be excluded on the basis of the premise that nitriles hydroxylated at positions other than the  $\alpha$ -carbon are not metabolized by cytochrome P450 enzymes to release cyanide but are eliminated (63). Removal of compounds **17** and **26** from the data set moderately improved the TLSEr model (equation 6). 2-Methylbutyronitrile (**11**) is also a statistical outlier, and removal of this compound from the TLSEr model represented by equation 6 slightly improved the correlation (equation 9). However removal of **11** from the data set solely for statistical reasons may not be valid since the acute toxicity of this compound is known to be due to cytochrome P450-mediated cyanide release (9,10).

The apparently equal ability of the TLSER model represented by equation 6 to that of the  $\log P$ ,  $k_{\alpha\text{corr}}$  model (equation 7) for predicting the acute toxicity of the same nitriles implies that the TLSER model is taking into account both hydrophobicity and  $\alpha$ -hydrogen atom abstraction. This is supported by the observation that inclusion of the  $k_{\alpha\text{corr}}$  term into the TLSER model (equation 8) results in only a slight improvement over that of the TLSER model itself (equation 6). Hydrophobicity can be viewed as the combined effects of a number of other molecular properties following the interaction of a solute with its environment. The TLSER terms, molecular volume ( $V_{\text{mc}}$ ), dipolarity/polarizability ( $\pi_i$ ), hydrogen bond acidity ( $\epsilon_\alpha$  and  $\text{qH}^+$ ) and hydrogen bond basicity ( $\epsilon_\beta$  and  $\text{q}_\cdot$ ) are very useful for defining intermolecular interactions of solute molecules with other molecules, and are known to be important descriptors in modeling hydrophobicity and biologic response (50-55).

Unlike hydrophobicity, explaining any direct relationship between  $k_{\alpha\text{corr}}$  and the TLSER terms is a more difficult task since the TLSER terms describe steric, polarizability/dipolarity and hydrogen bonding properties of a given molecule and not of a particular atom within the molecule. However the coefficients, signs and  $t$  scores of each of the TLSER terms reflect their relative importance to nitrile toxicity, and, as such, may offer insight with respect to their importance in predicting cytochrome P450-mediated oxidation of nitriles. For equation 6, the  $t$  scores indicate that molecular orbital acidity ( $\epsilon_\alpha$ ) is the single most significant descriptor. The sign and coefficient of  $\epsilon_\alpha$  indicate that greater toxicity is directly related to greater acidity (smaller values of  $\epsilon_\alpha$  indicate higher acidity). This result also reinforces the regression model represented by equation 1, which is based largely on the hypothesis that increased ease of  $\alpha$ -hydrogen atom abstraction is consistent with greater toxicity (16,17). While the TLSER does not specifically include a term that can be related directly to radical formation, it is well known that substituents which stabilize anions following deprotonation also stabilize radicals following hydrogen atom abstraction. This may explain the importance of the  $\epsilon_\alpha$  descriptor in equation 6 analogously to the importance of the  $k_{\alpha\text{corr}}$  descriptor to equation 1, and why the TLSER models that include the  $k_{\alpha\text{corr}}$  descriptor (equations 5 and 8) do not greatly increase predictability over the TLSER models themselves (equations 4 and 6, respectively).

It is noteworthy however that the acute toxicity of individual nitriles cannot be qualitatively estimated from their  $\epsilon_\alpha$  values alone, as is possible with their  $k_{\alpha\text{corr}}$  values. Compounds **6**, **8**, and **11** for example have very similar  $\epsilon_\alpha$  values, but **6** (which has the lowest  $\epsilon_\alpha$  value of the three and hence is the most acidic) is less toxic than **8** or **11** by

approximately two orders of magnitude. However, comparison of the  $k_{\alpha\text{corr}}$  values of **6**, **8**, and **11** shows a very clear relationship between the magnitude of the  $k_{\alpha\text{corr}}$  term and toxicity (the larger the  $k_{\alpha\text{corr}}$  value the more toxic the compound). Similar examples can be seen in comparing  $\epsilon_{\alpha}$  or  $k_{\alpha\text{corr}}$  values of other nitriles in Table I.

The volume term,  $V_{\text{mc}}$ , appears to be the second most important term of the TLSEr with respect to nitrile toxicity (equation 6). The negative value of the coefficient for  $V_{\text{mc}}$  indicates that smaller nitriles are generally more toxic, implying that smaller sized nitriles are sterically more favorable for cytochrome P450 oxidation than larger nitriles. This is consistent with Tanii and Hashimoto's findings that cyanide release from nitriles **4-7**, **9**, and **10** (the larger nitriles) is much slower and as a group these nitriles are considerably less toxic (**9,10**).

Although the TLSEr descriptors are not specific to a particular chemical class or biologic mechanism, it appears from this study that the TLSEr model may be useful in supporting proposed toxicologic mechanisms of specific classes of compounds through analysis of the presence (or absence) of descriptors, and their relative significance to the regression model. While correlation of non-specific toxicity is fairly common with many different descriptor sets, the correlation with receptor-based or mechanism specific toxicity has been less studied. The fact that the TLSEr model, which has no information containing specific mechanisms, is able to generate a correlation for acute nitrile toxicity as efficiently as a regression model which contains a descriptor unique to the mechanism of nitrile toxicity provides an example of the usefulness of the TLSEr in modeling specific toxicity.

### Acknowledgment

S.C.D. thanks Drs. Roger L. Garrett and Joseph Breen for their support and encouragement. The research described in this paper has been reviewed by the Office of Pollution Prevention and Toxics, U.S. Environmental Protection Agency, and approved for publication. Approval does not signify that the contents necessarily reflect the views and policies of the Agency nor does mention of commercial products constitute endorsement or recommendation for use.

### Literature Cited

- (1) Zeller, Von H.; Hofmann, H. Th.; Theiss, A.M.; Hey, W. *Zentralbl. Arbeitsschutz* **1969**, *19*, pp 225-238.
- (2) Hartung, R. *Patty's Industrial Hygiene and Toxicology*, 3rd Revised Edition; Wiley-Interscience: New York, NY, 1982; pp 4845-4900.
- (3) Lang, S. *Arch. Exp. Path. Pharmacol* **1894**, *34*, pp 247-258.
- (4) Stern, J.; Weil-Malherbe, H.; Green, R.H. *Biochem. J.* **1952**, *52*, pp 114-125.

- (5) Ohkawa, H.; Ohkawa, R.; Yamamoto, I.; Casida, J.E. *Pest. Biochem. Physiol.* **1972**, *2*, pp 95-112.
- (6) Willhite, C.C.; Smith, R.P. *Toxicol Appl. Pharmacol.* **1981**, *59*, pp 589-602.
- (7) Silver, E.H.; Kuttub, S.H.; Hasan, T.; Hassan, M. *Drug Metab. Disp.* **1982**, *10*, pp 495-498.
- (8) Ahmed, A.A.; Farooqui, M.Y.H. *Toxicol. Lett.* **1982**, *12*, pp 157-163.
- (9) Tanii, H.; Hashimoto, K. *Arch. Toxicol.* **1984**, *55*, pp 47-54.
- (10) Tanii, H.; Hashimoto, K. *Toxicol. Lett.* **1984**, *22*, pp 267-272.
- (11) Tanii, H.; Hashimoto, K. *Arch. Toxicol.* **1985**, *57*, pp 88-93.
- (12) Johannsen, F.R.; Levinskas, G.J. *Fundam. Appl. Toxicol.* **1986**, *7*, pp 690-697.
- (13) Yoshikawa, H. *Med. Biol.* **1968**, *77*, pp 1-4.
- (14) Davis, R.H. In *Cyanide in Biology*; Vennesland, B., Conn, E.E., Knowles, C.J., Westley, J., Wissing, F., Eds.; Academic Press: London, 1981; pp 51-60.
- (15) Froines, J.R.; Postlethwait, E.M.; LaFuentes, E.J.; Liu, W.C.V. *J. Toxicol. Environ. Health* **1985**, *16*, pp 449-460.
- (16) DeVito, S.C.; Pearlman, R.S. *Med. Chem. Res.* **1991**, *1*, pp 461-465.
- (17) Grogan, J.; DeVito, S.C.; Pearlman, R.S.; Korzekwa, K.R. *Chem. Res. Toxicol.* **1992**, *5*, pp 548-552.
- (18) Hansch, C.; Dunn, W.J. *J. Pharm. Sci.* **1972**, *61*, pp 1-19.
- (19) Hansch, C.; Clayton, J.M. *J. Pharm. Sci.* **1973**, *62*, pp 1-21.
- (20) Kamlet, M.J.; Abboud, J.L.M.; Taft, R.W. *Prog. Phys. Org. Chem.* **1981**, *13*, pp 485-630.
- (21) Kamlet, M.J.; Taft, R.W. *J. Chem. Soc., Perkin Trans.* **1979**, *2*, pp 349-356.
- (22) Park, J.H.; Carr, P.W.; Abraham, M.H.; Taft, R.W.; Doherty, R. M.; Kamlet, M.J. *Chromatographia* **1988**, *25*, pp 373-381.
- (23) Kamlet, M.J.; Abraham, M.H.; Doherty, R.M.; Taft, R.W. *J. Am. Chem. Soc.* **1984**, *106*, pp 464-466.
- (24) Taft, R.W.; Abraham, M.H.; Famini, G.R.; Doherty, R. *J. Pharm. Sci.* **1985**, *74*, pp 807-814.
- (25) Kamlet, M.J.; Doherty, R.M.; Carr, P.W.; Mackay, D.; Abraham, M.H.; Taft, R.W. *Environ. Sci. Technol.* **1988**, *22*, pp 503-509.
- (26) Kamlet, M.J.; Doherty, R.M.; Abraham, M.H.; Marcus, Y.; Taft, R.W. *J. Phys. Chem.* **1988**, *92*, pp 5244-5255.
- (27) Taft, R.W.; Abraham, M.H.; Doherty, R.M.; Kamlet, M.J. *Nature (London)* **1985**, *313*, pp 384-386.
- (28) Kamlet, M.J.; Doherty, R.M.; Abboud, J.L.M.; Abraham, M.H.; Taft, R.W. *J. Pharm. Sci.* **1986**, *75*, pp 338-349.
- (29) Kamlet, M.J.; Doherty, R.M.; Abboud, J.L.M.; Abraham, M.H.; Taft, R.W. *CHEMTECH* **1986**, *16*, pp 566-576.
- (30) Kamlet, M.J.; Doherty, R.M.; Abraham, M.H.; Carr, P.W.; Doherty, R.F.; Taft, R.W. *J. Phys. Chem.* **1987**, *91*, pp 1996-2004.
- (31) Fuchs, R.; Abraham, M.H.; Kamlet, M.J.; Taft, R.W. *J. Phys. Org. Chem.* **1989**, *2*, pp 559-564.

- (32) Kamlet, M.J.; Doherty, R.M.; Taft, R.W.; Abraham, M.H.; Koros, W.J. *J. Am. Chem. Soc.* **1984**, *106*, pp 1205-1212.
- (33) Kamlet, M.J.; Abraham, M.H.; Carr, P.W.; Doherty, R.M.; Taft, R.W. *J. Chem. Soc., Perkin Trans.* **1988**, *2*, pp 2087-2092.
- (34) Kamlet, M.J.; Abraham, D.J.; Doherty, R.M.; Taft, R.W.; Abraham, M.H. *J. Pharm. Sci.* **1986**, *75*, pp 350-355.
- (35) Kamlet, M.J.; Doherty, R.M.; Fiserova-Bergerova, V.; Carr, P.W.; Abraham, M.H.; Taft, R.W. *J. Pharm. Sci.* **1987**, *76*, pp 14-17.
- (36) Abraham, M.H.; Grellier, P.L.; McGill, R.A.; Doherty, R.M.; Kamlet, M.J.; Hall, T.N.; Taft, R.W.; Carr, P.W.; Koros, W.J. *Polymer* **1987**, *28*, pp 1363-1369.
- (37) Kamlet, M.J.; Doherty, R.M.; Veith, G.D.; Taft, R.W.; Abraham, M.H. *Environ. Sci. Technol.* **1986**, *20*, pp 690-695.
- (38) Kamlet, M.J.; Doherty, R.M.; Abraham, M.H.; Veith, G.D.; Abraham, D.J.; Taft, R.W. *Environ. Sci. Technol.* **1987**, *21*, pp 149-155.
- (39) Kamlet, M.J.; Doherty, R.M.; Abraham, M.H.; Taft, R.W. *Quant. Struct.-Act. Relat.* **1988**, *7*, pp 71-78.
- (40) Kamlet, M.J.; Abboud, J.L.M.; Abraham, M.J.; Taft, R.W. *J. Org. Chem.* **1983**, *48*, pp 2877-2887.
- (41) Kamlet, M.J.; Doherty, R.M.; Famini, G.R.; Taft, R.W. *Acta Chem. Scand.* **1987**, *B41*, pp 589-598.
- (42) Lewis, D.F.V. *Prog. Drug Metab.* **1990**, *12*, pp 205-255.
- (43) Politzer, P.; Murray, J.S.; Brinck, T.; Lane, P. (1992) *Ab-Initio Quantum Chemical Investigation of Solute-Solvent Interactions*. Proceedings of the Second Meeting of Solute-Solvent Interactions, U.S. Army Chemical Research, Development & Engineering Center: Aberdeen Proving Ground, MD 21010. Held May 27-29, 1992.
- (44) Hickey, J.P.; Passino-Reader, D.R. *Environ. Sci. Technol.* **1991**, *25*, pp 1753-1760.
- (45) Loew, G.H.; Poulsen, M.; Kirkjian, E.; Ferrell, J.; Sudhindra, B.S.; Rebagliati, M. *Environ. Health Perspect.* **1985**, *61*, 69-96.
- (46) Pedersen, L. *Environ. Health Perspect.* **1985**, *61*, pp 185-190.
- (47) Chastrette, M.; Rajzmann, M.; Chanon, M.; Purcell, K.F. *J. Am. Chem. Soc.* **1985**, *107*, pp 1-11.
- (48) Kier, L.B.; Hall, L.H. In *Molecular Connectivity in Chemistry and Drug Research*; deStevens, G., Ed.; Medicinal Chemistry; Academic Press: New York, NY, 1976, Vol. 14; pp 1-257.
- (49) Ford, M.G.; Livingstone, D.J. *Quant. Struct.-Act. Relat.* **1990**, *9*, pp 107-114.
- (50) Famini, G.R. *Using Theoretical Descriptors in Structural Activity Relationships, IV. Molecular Orbital Basicity and Electrostatic Basicity*: CRDEC-TR-88013, U.S. Army Chemical Research, Development and Engineering Center, Aberdeen Proving Ground, MD, November 1988.
- (51) Famini, G.R.; Penski, C.E.; Wilson, L.Y. *J. Phys. Org. Chem.* **1992**, *5*, pp 395-408.

- (52) Wilson, L.Y.; Famini, G.R. *J. Med. Chem.* **1991**, *34*, pp 1668-1674.
- (53) Famini, G.R., Wilson, L.Y. (1992) Using theoretical descriptors in quantitative structure activity relationships: acetylcholinesterase inhibition by organophosphorous compounds. Manuscript in preparation.
- (54) Famini, G.R.; Wilson, L.Y. In *Biomedical Health Perspectives: Proceedings of the 12th Annual International Conference of the IEEE Engineering in Medicine and Biology Society*, **1990**, pp 1608-1609.
- (55) Famini, G.R.; Ashman, W.P.; Mickiewicz, A.P.; Wilson L.Y. *Quant. Struct.-Act. Relat.* **1992**, *11*, pp 162-170.
- (56) EPA Document 8(e) HQ-0988-0754, U.S. Environmental Protection Agency, Washington, DC, USA.
- (57) Dewar, M.J.S.; Thiel, W. *J. Am. Chem. Soc.* **1977**, *99*, pp 4899-4907.
- (58) Stewart, J.J.P. *MOPAC Manual (Sixth Edition)*, FJSRL-TR-90-0004, U.S. Air Force Academy, Colorado Springs, CO, November 1990. Available through the National Technical Information Service (NTIS), # AD-A233 489.
- (59) Leonard, J.M.; Famini, G.R. *A User's Guide to the Molecular Modeling Analysis and Display System*; CRDEC-TR-030, U.S. Army Chemical Research, Development and Engineering Center: Aberdeen Proving Ground, MD. January 1989. Available through the National Technical Information Service, # AD-A204 003.
- (60) Minitab is marketed by Minitab, Inc., 3081 Enterprise Drive, Stat College, PA 16801.
- (61) Hopfinger, A.J. *J. Am. Chem. Soc.* **1980**, *102*, pp 7196-7206.
- (62) Dewar, M.J.S.; Stewart, J.J.P. *Chem. Phys. Lett.* **1984**, *111*, pp 416-420.
- (63) Korshunov, N. *Gig. Primen. Toksikol. Pestits. Klin. Otravlenii* **1970**, *8*, pp 398-403. (See Chemical Abstracts # 77(19):122773q).

RECEIVED September 17, 1993

## Chapter 3

# Changes in Biochemical and Molecular Biological Parameters Induced by Exposure to Dioxin-Type Chemicals

Alan Blankenship and Fumio Matsumura

Department of Environmental Toxicology and Environmental Health Sciences Center, University of California, Davis, CA 95616-8588

The XB cell hyperkeratinization assay was further developed as an *in vitro* bioassay tool that can be utilized for estimating 2,3,7,8-tetrachlorodibenzo-*p*-dioxin (TCDD) equivalents (TEQ) in a complex mixture of halogenated aromatic hydrocarbons. A spectrophotometric method was developed to quantitate hyperkeratinization. The hyperkeratinization response was found to be dose-dependent for 2,3,7,8-TCDD and 3,4,3',4'-tetrachlorobiphenyl (TCB), a toxic congener with dioxin-type activity; however, 2,5,2',5'-TCB, a relatively non-toxic congener, failed to cause hyperkeratinization. Our results indicate that this bioassay can be used to screen complex mixtures for dioxin-type activity and act as an important complement to chemical analysis. To facilitate future developments of bioassay approaches and eventually "biomarker" technologies, various biochemical changes occurring as specific lesions of dioxin-type chemicals were examined in our laboratory. A few of these biochemical changes may be viewed as potential indicators of the specific effects of dioxin-type chemicals. Particularly promising are the changes that we have observed in glucose transporter titers in adipose tissue which appear to be sensitive, unique, reproducible, and reliable, indicating their group specific toxic action.

Halogenated aromatic hydrocarbons (HAHs) contain several distinct groups of toxic chemicals which are known to act through a very similar toxic action mechanism (1). They are chemically classified as polychlorinated dibenzo-*p*-dioxins (PCDDs), dibenzofurans (PCDFs), naphthalenes (PCNs), biphenyls (PCBs), azo- and azoxybenzenes, etc. (2). From an analytical point of view, these groups of chemicals present a tough challenge, since each group consists of many isomers, derivatives, and homologous compounds (i.e., congeners) as well as contaminants (3). From a toxicological viewpoint, they are even more problematic in terms of assessing their hazards, as toxicological potencies of those congeners vary greatly even within one group. Furthermore, their toxic manifestations are affected by the presence of other congeners, some acting as antagonists, some as inducers of metabolic systems, and some as

0097-6156/94/0542-0037\$06.00/0

© 1994 American Chemical Society

synergists. For instance, within the group of PCBs alone, several components have been identified that induce one type of cytochrome P450 (phenobarbital type), whereas others induce another type of cytochrome P450 (3-methylcholanthrene type) and clearly act as dioxin-type chemicals. Still other PCBs have been identified that block the action of 2,3,7,8-TCDD, the most toxic congener of the polychlorinated dibenzo-p-dioxin family, probably because these PCBs act as weak agonists for the Ah receptor, the cytosolic receptor to which dioxin-type chemicals bind (4).

Presently, the most sensitive and specific indicator of overexposure to TCDD-type chemicals in humans is chloracne (1), a skin condition characterized by epidermal hyperkeratinization. Chloracne has been observed in connection with the manufacture of several pesticides: 2,4,5-trichlorophenol (5), 2,4,5-T (6,7), pentachlorophenol (8), methazole (9), hexachlorobenzene (10), and technical hexachlorocyclohexanes (11). In these cases, chloracne probably resulted from exposure to complex mixtures of PCDDs, PCDFs, as well as to chlorinated azo- and azoxy-benzenes that were present as by-products in the synthesis of these pesticides.

### Past Attempts to Assess Dioxin-Type Toxic Expression

The assessment of environmental effects of these chemicals is further complicated by their differences in persistence, transport, bioaccumulation, etc. Yet there is a great need for assessing toxicological significance of these chemicals as they are ubiquitously present in various biota. One important source of input of this type of chemical to the environment is incineration, particularly those involving municipal wastes (3). In the past, various congeners of polychlorinated dibenzo-p-dioxins and dibenzofurans have been identified, but recently polychlorinated naphthalenes as well as other HAHs have also been found in some samples. The major problem is that even under controlled experimental conditions of the composition and the rate of incineration, formation of these HAHs vary greatly from one run to another.

Over the past several years, various scientists have made attempts to assess the toxicity of industrially formed and artificially created mixtures, extracts, and naturally present forms (4). The emerging consensus for the best way to approach the problem has been to (a) use 2,3,7,8-TCDD (TCDD) as the prototype and standard unit, (b) adopt a biochemical or toxicological parameter which distinctly represents a "dioxin-type" effect qualitatively, and (c) select a most sensitive parameter or parameters which can be readily tested and validated in the laboratory under controlled conditions. When adopting TCDD as the standard, the toxic potency of a mixture is usually expressed in terms of "TCDD-equivalent" (TEQ), meaning that the toxicity of a mixture is presumed to be equal to the sum of TCDD equivalencies of individual components of the mixture (12-14).

The biochemical parameters most frequently selected have been induction of cytochrome P4501A1 and P4501A2 hemoproteins and their associated microsomal monooxygenases, which include aryl hydrocarbon hydroxylase (AHH) and ethoxyresorufin O-deethylase (EROD) activities. Such an approach is a wise choice, since there is no question about its uniqueness and high sensitivity to dioxin-type chemicals and, furthermore, by using an appropriate substrate, the titer of this enzyme component may be assessed with relative ease (4). On the other hand, the main problems of this approach are (a) the induction phenomenon is reversible, (b) high backgrounds are often

encountered, and (c) while P450 induction is undeniably a sensitive response to TCDD exposure, P450 induction by itself has not been shown to be related to the direct toxic effects of TCDD, except in the cases where other chemicals might be converted by these enzymes to reactive metabolites (15). Moreover, there is a lack of correlation between induction of certain cytochrome P450-mediated enzyme activities and toxicity *in vivo* in different species (15). For example, the ED<sub>50</sub> for AHH induction is similar in rats, mice, and hamsters, even though their LD<sub>50</sub>s are very different (16). Guinea pigs, the most susceptible species to TCDD toxicity, show little or no induction of many enzymes and proteins, including cytochrome P450s, that are normally induced by TCDD in other species (17). On the other hand, hyperkeratinization of XB cells is an irreversible phenomenon, backgrounds are usually low because these cells do not spontaneously hyperkeratinize, and the assay is a good model for chloracne, a well-known toxic effect of TCDD in humans.

### Use of Hyperkeratinization of Epithelial Cells as Indicators of Dioxin-Type Actions

In view of the pressing need to develop a reliable assay system which accurately indicates the toxic potential of unknown mixtures of polycyclic aromatic hydrocarbons (PAHs), we have selected keratinizing epithelial cells as the potential indicators of dioxin-type toxic actions. The major reasons for such a decision are (a) in humans, skin lesions ("chloracne") are the only acknowledged toxic manifestation very specific to this group of chemicals, (b) hyperkeratinization is a phenomenon associated with cell differentiation in these cells and, therefore, an irreversible parameter, (c) hyperkeratinization signals are clearly distinguishable from those for cell proliferation (e.g. phorbol esters cause only the latter phenomenon while TCDD and epidermal growth factor (EGF) cause the former changes (18-20)), (d) these cells are very sensitive to TCDD and other HAHs, and (e) hyperkeratinization is very easy to measure, is stable, and under *in vitro* conditions variations are minimal.

Other scientists have already made valuable contributions to ascertain the usefulness of keratinizing epithelial cells for mechanism of toxic action studies and estimation of toxic equivalency factors (18-21). The uniqueness of this paper is the better quantitation of the assay. Our intention here is to make further efforts to use these cells for a bioassay system designed specifically to assess the toxic potential of mixtures of chemicals from a viewpoint of dioxin-type toxic expressions.

### Description of XB Cells

As indicated above, in humans the most consistent response to HAHs is chloracne, a severe skin disorder that can last for years and is characterized by epidermal hyperkeratinization. Poland and Knutson (1, 19, 20) were the first researchers to utilize the XB/3T3 cell culture system originally developed by Rheinwald and Green (22) as an *in vitro* model of 2,3,7,8-TCDD-induced hyperkeratinization. Kawamoto *et al.* (18) used the XB/3T3 cell culture system to study the biochemical mechanism of action of 2,3,7,8-TCDD and found that hyperkeratinization is preceded by a rapid increase in protein tyrosine kinase activity followed by down-regulation of epidermal growth factor (EGF) receptors. These workers have also demonstrated that XB cells are extremely sensitive to TCDD, with hyperkeratinization observed in XB cells treated with as low as 10<sup>-13</sup> to 10<sup>-9</sup> M of 2,3,7,8-TCDD. Furthermore, these cells were capable of distinguishing the effect of TCDD from that of 12-O-

tetradecanoylphorbol-13-acetate (TPA), a well known phorbol ester capable of stimulating skin cell proliferation and a skin cancer promoter, as the latter causes only cell proliferation and increase in colony formation without inducing hyperkeratotic cellular responses.

### Description of Experimental Approaches

**Materials.** 2,3,7,8-TCDD was a gift from the Dow Chemical Company, Midland, MI, and was >99% pure (by gas liquid chromatograph). 3,4,3',4'-tetrachlorobiphenyl (TCB) and 2,5,2',5'-TCB were generous gifts from Dr. Stephen Safe (College of Veterinary Medicine, Texas A&M University, College Station, TX). Other materials were obtained from the following sources: all cell culture reagents from GIBCO (Grand Island, NY); XB-2 and NIH 3T3 cell lines from American Type Culture Collection (ATCC); 60 mm diameter tissue culture dishes from Falcon Plastics (Oxnard, CA); 12-O-tetradecanoylphorbol-13-acetate (TPA), rhodamine B, and Nile blue from Sigma; and *p*-dioxane from Fisher Scientific.

**Cell Culture.** All cultures were grown in Dulbecco's modified Eagle's medium (DMEM) containing 100 µg/ml penicillin and 100 µg/ml streptomycin. The medium was supplemented with 20% fetal bovine serum for the XB cells and 10% calf serum for the NIH 3T3 cells. The cells were cultured at 37°C in a humidified atmosphere with 5% CO<sub>2</sub>. The medium was renewed twice weekly.

Confluent cultures of NIH 3T3 cells were lethally irradiated with 6000 rads from a cesium source. The cultures were trypsinized and replated together at  $3 \times 10^5$  XB cells per 60 mm dish. As noted by others (18, 21), the XB phenotype changes under conditions of cell passage, resulting in a decline in magnitude, but not the sensitivity, of the keratinization response to 2,3,7,8-TCDD. To overcome this problem, the phenotype was monitored continuously and "standard" XB cells were removed from liquid nitrogen and placed into culture as necessary.

**Addition of Chemicals to Cell Cultures.** Stock solutions of chemicals used in this study were prepared in *p*-dioxane. A Hamilton syringe was used to add chemicals directly to cell cultures immediately after each media change, starting with the third day after replating the cells. Subsequent studies showed that only one treatment of cells, on the third day after replating the cells, was necessary for eliciting hyperkeratinization. The volume of media was 4 mL and the final solvent concentration was 0.1%.

**Staining and Quantitation.** Cultures were rinsed with phosphate buffered saline (PBS) without CaCl<sub>2</sub> and MgCl<sub>2</sub>, fixed in 10% isotonic formalin for 30-45 minutes, stained with a 1:1 mixture of 1.5% rhodamine B and 1.5% Nile blue (i.e., rhodanile blue) for 30 minutes, and destained with water for 2 minutes. After completely drying, the stained cell culture dishes were analyzed with a Varian series 634 spectrophotometer. Two stands were constructed to hold dishes in place, one for the reference beam and one for the sample beam. A solvent-control cell culture dish was placed in the reference beam and used as a reference for all other dishes within each experiment. A spectral scan showed that maximal absorption of hyperkeratinized cultures stained with rhodanile blue occurs at 560 nm. For each dish, the absorbance at 560 nm was determined by rotating each dish 90 degrees between each reading and taking

the average of 4 readings. These 90 degree rotations increased the surface area analyzed on each dish, thereby minimizing dish-to-dish variations.

#### Calculation of 2,3,7,8-TCDD Equivalent (TEQ) Concentrations.

The method of calculating TEQ concentrations is essentially as described by Eadon *et al.* (12). In brief, serial dilutions of test agents were tested for their hyperkeratinizing ability and compared to 2,3,7,8-TCDD standards run simultaneously. The concentration of test agent that produced between half-maximal and maximal hyperkeratinization was taken as a reference concentration and set equal to the concentration of 2,3,7,8-TCDD that caused the same response. From this concentration, the original concentration of the test agent in terms of TEQ can be calculated by the following equation:

$$\text{TEQ} = \frac{\text{ED}_{50} \text{ for 2,3,7,8-TCDD } (\mu\text{g/mL})}{\text{ED}_{50} \text{ for test agent } (\mu\text{g/mL})}$$

#### Results of Hyperkeratinization Assay

Figures 1a and 1b show the results of a typical experiment in which the XB hyperkeratinization response was quantitated over a 10,000-fold range of TCDD concentrations. The dose-response relationship is clearly evident with half-maximal hyperkeratinization between  $10^{-10}$  and  $10^{-11}$  M for 2,3,7,8-TCDD. The  $\text{OD}_{560}$  values are obtained by using a control dish in the reference beam as described under Description of Experimental Approaches. Hyperkeratinization can be detected by rhodanile blue staining by day 4 after treatment and becomes maximal by day 12. For the experiments presented in this paper, hyperkeratinization was measured 8 days after single treatment because control dishes showed some increase in rhodanile blue staining at later time points (data not shown).

Figure 2 shows that XB cells hyperkeratinize in response to  $10^{-7}$  M 3,4,3',4'-tetrachlorobiphenyl (TCB), a toxic congener with dioxin-type activity, but fail to respond to  $10^{-7}$  M 2,5,2',5'-TCB, a relatively non-toxic congener. XB cells also fail to hyperkeratinize in response to  $10^{-6}$  M TPA. Using the hyperkeratinization assay, the calculated 2,3,7,8-TCDD-equivalent (TEQ) for 3,4,3',4'-TCB is 0.001 which agrees well with results from other investigators using EROD-induction in H-4IIE cells (13, 23).

#### Discussion of Hyperkeratinization Assay Using XB Cells

The experimental results above indicate that it is possible to develop the XB hyperkeratinization assay for measuring 2,3,7,8-TCDD equivalents (TEQ) in complex mixtures of halogenated aromatic hydrocarbons. The assay is simple, inexpensive, reproducible, specific, and quantifiable.

As for the question of reliability and specificity, we have clearly shown that 2,3,7,8-TCDD produces hyperkeratinization in XB cells in a dose-dependent manner with an  $\text{ED}_{50}$  between  $10^{-10}$  and  $10^{-11}$  M, which matches the observations made by Knutson and Poland (19). The high consistency between the results of two independent laboratories further supports the reproducibility of this assay. We have also demonstrated the specificity of this

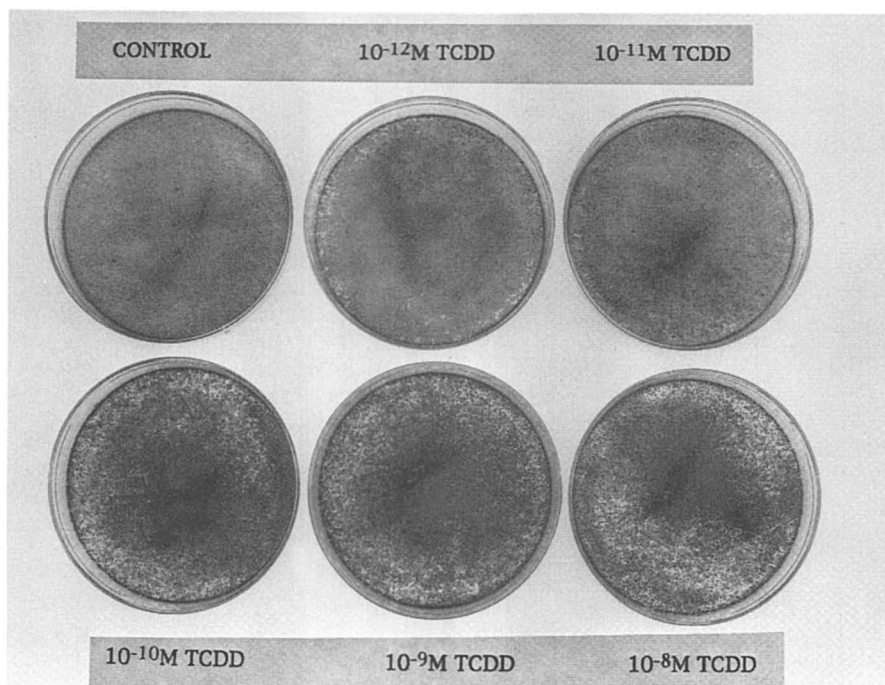


Figure 1a. Hyperkeratinization of XB cells in response to 2,3,7,8-TCDD. Photograph taken with a green filter.

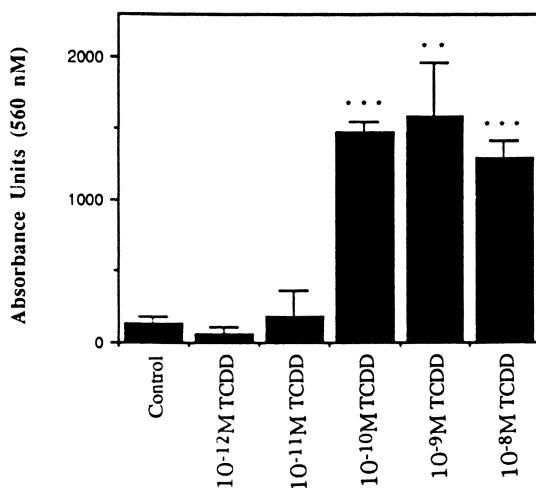


Figure 1b. Hyperkeratinization of XB cells in response to 2,3,7,8-TCDD. Each value represents the average absorbance at 560 nm  $\pm$  standard deviation from 4 dishes per treatment. Statistical significance was determined by the Student's *t* test (two-tailed). \* $p < 0.05$ , \*\* $p < 0.01$ , \*\*\* $p < 0.005$ .

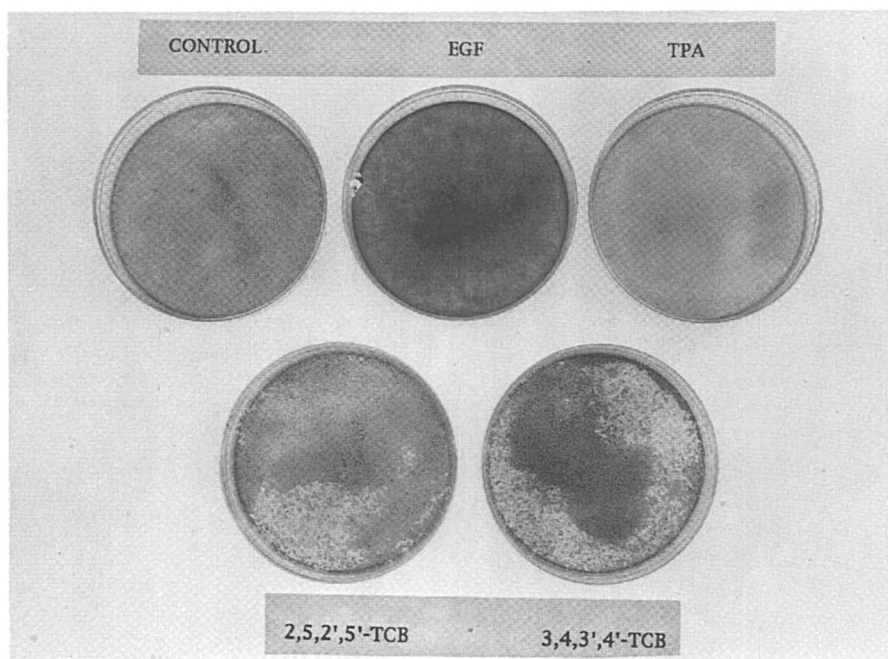


Figure 2a. Hyperkeratinization of XB cells in response to  $10^{-6}$ M TPA and  $10^{-7}$ M of two different congeners of tetrachlorobiphenyl (TCB). Photograph taken with a green filter. Epidermal growth factor (EGF) was used at a concentration of 25 ng/mL as a positive control for hyperkeratinization.

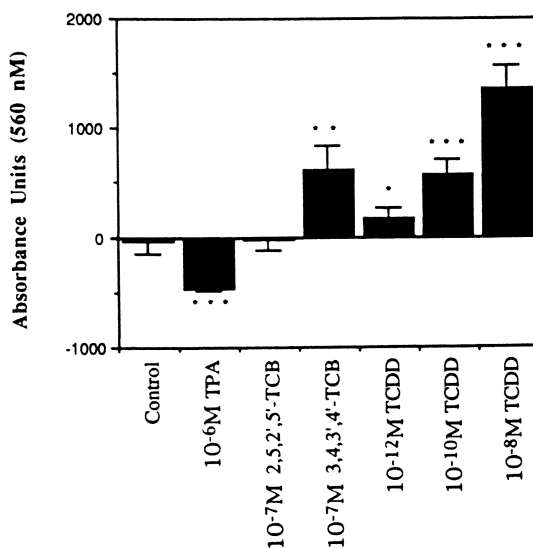


Figure 2b. Hyperkeratinization of XB cells in response to  $10^{-6}$ M TPA and  $10^{-7}$ M of two different congeners of tetrachlorobiphenyl (TCB). The absorbance values for TPA are less than zero because the values are relative to a control dish that is in the reference beam. Each value represents the mean  $\pm$  standard deviation from 4 cultures. Statistical significance was determined by the Student's t test (two-tailed). \* $p < 0.05$ , \*\* $p < 0.01$ , \*\*\* $p < 0.005$ .

assay by showing that 3,4,3',4'-TCB, a toxic inactive congener, causes hyperkeratinization, whereas 2,5,2',5'-TCB, a relatively non-toxic congener, and TPA, a potent tumor promoter that does not cause chloracne, both failed to cause hyperkeratinization. In addition, good structure-activity relationships have been observed with other chlorinated dibenzo-p-dioxins, dibenzofurans, biphenyls, and azo(xy)benzenes, while many other agents have failed to produce hyperkeratinization, including direct alkylating agents, inhibitors of nucleic acid synthesis, kepone, and 2,6-dichlorobenzonitrile, an acnegen which does not bind to the Ah receptor (19,20).

The main contribution of this report to the development of the XB hyperkeratinization assay is the ability to quantify the results. Previous reports involving the hyperkeratinization assay were primarily qualitative, in which cell culture dishes were visually examined and compounds were scored as the lowest concentration which caused red staining with rhodanile blue equivalent to the maximum staining produced by 2,3,7,8-TCDD. Quantifying the hyperkeratinization response with a simple spectrophotometric method offers the advantage of increased sensitivity detecting responses below that of maximal response by 2,3,7,8-TCDD.

Initial analysis of plastic pyrolysis and combustion samples indicates the usefulness of the XB hyperkeratinization assay to monitor for dioxin-type activity in complex environmental samples (unpublished data from this laboratory). Gierthy *et al.* (21) utilized the XB hyperkeratinization assay to monitor dioxin-type activity in extracts of soot from a fire involving a transformer containing PCBs. They observed a good correlation between relative keratinization activity and total PCDF concentrations.

As with other *in vitro* assays for calculating TEQ, caution should be used in extrapolating *in vitro* results to *in vivo* toxicity, because some of the polycyclic aromatic hydrocarbons (PAHs) and other inducers of P450 enzymes show dioxin-type activity *in vitro* but fail to do so *in vivo*. One possible explanation is rapid metabolism of these compounds to inactive species *in vivo* (24). Ideally, complex environmental mixtures should be subjected to a battery of bioassays, both *in vivo* and *in vitro*, that select for a variety of significant biological endpoints.

### Other Biochemical Changes Specific to Dioxin-Type Chemicals

There are several TCDD-induced biochemical changes that are potentially useful indicators of the action of dioxin-type chemicals. One that has been extensively studied by our research group in the past is the phenomenon of "down-regulation" of epidermal growth factor receptors (EGF-R) (25). This parameter is measured by using  $^{125}\text{I}$ -labeled EGF and intact cultured cells *in vitro* or plasma membrane rich fractions from tissue homogenates from TCDD treated animals *in vivo*. An example of the former case is the study of TCDD's action on the cell surface membrane receptor of C3H 10T $\frac{1}{2}$  cells (26). The ED $_{50}$  of 2,3,7,8-TCDD on  $^{125}\text{I}$ -EGF receptor down-regulation was in the order of  $3 \times 10^{-11}\text{M}$ . The same phenomenon was observed to occur when 2,3,7,8-TCDD was substituted by 3-methylchloroanthrene or benzo(a)pyrene, two known chemicals belonging to the same group of inducers except that their ED $_{50}$  values were much higher ( $3 \times 10^{-7}$  and  $2 \times 10^{-6}\text{M}$ , respectively). Thus the

sensitivity of this parameter in C3H 10T $\frac{1}{2}$  cells to 2,3,7,8-TCDD is the same order of magnitude as the hyperkeratinization phenomenon in XB cells. The former phenomenon, however, occurs at a slower pace than the latter, ED<sub>50</sub> value being in the order of over 70 hours, though the phenomenon of down-regulation itself becomes noticeable within 5 hours from the time of treatment. In the case of *in vivo* studies, a positive correlation between the susceptibility (in terms of mortality) of various animal species and strains to 2,3,7,8-TCDD and the sensitivity of down-regulation of EGF-R has been pointed out (25, 27). There is also a good correlation between *in vivo* toxicity of various HAH congeners to rats and their potencies in terms of causing down-regulation of EGF-R (27).

The shortcomings of the EGF-R assay from the viewpoint of obtaining TEQ are relative technical difficulties of this assay method, the changing nature of EGF-R (strongly affected by serum factors, etc.), and a less specific nature of EGF-R responses (e.g., TPA and other chemicals known to influence protein phosphorylation activities could cause the same phenomenon). The slowness of the development of this phenomenon could be a problem in some cases.

Another TCDD-sensitive biochemical parameter worthy of consideration in the same line of thought is *c-ras* expression (28, 29). This family of cellular oncogenes has been shown to respond very quickly to 2,3,7,8-TCDD (within 15 min *in vitro* and 1 hr *in vivo*), and yet its expressional changes are mediated by Ah receptor (29). The increase in *c-ras* expression is always accompanied by a rise in protein tyrosine kinase activities. These early changes clearly precede the occurrence of EGF-R down-regulation and the hyperkeratinization phenomenon. Thus an elevated expression of either *c-ras* gene or one of the protein tyrosine kinases such as *c-src* (30) could serve as an early indicator of action of dioxin-type chemicals. The probable shortcomings of the *ras* assay approach are (a) the ephemeral nature of *ras* expression, (b) complication of other factors affecting *ras* (e.g., GAP, protein kinase C, etc.), (c) a lack of fundamental baseline data, and (d) relative methodological difficulties of assay methods, though the last problem is becoming less formidable due to the commercial availability of probes, antibodies and hybridization kits. Nevertheless, this assay approach has the unique merit of being able to assess directly the important cellular oncogene signals which have the potential of indicating a fundamental change in cellular programming (31). Indeed, Jankun *et al.* (28) showed that the TCDD-induced activation of N-*ras* in NIH 3T3 fibroblast cells results not only in a reduction in <sup>125</sup>I-EGF binding, but also in promoting "anchorage independent growth" of these cells, indicating that excessive activation of *ras* expression by TCDD (or any other chemicals for that matter) in some cases could lead to precarcinogenic transformation of the cells involved.

Finally, we would like to introduce one more biochemical parameter which we have discovered recently (32,33). This parameter, readily and specifically altered by dioxin-type compounds, is the titer of glucose transporter proteins (34). The glucose transporter proteins are known to play the important role of transporting glucose available in blood into glucose utilizing cells. They are synthesized or destroyed quickly in response to hormones and other nutritionally regulating factors (34). We have found that 2,3,7,8-TCDD at doses as low as 0.03 µg/kg (single i.p. dosing) causes a profound reduction of glucose uptake by male guinea pig adipose tissue,

American Chemical  
Society Library

pancreas, and brain. In the case of adipose tissue, the decrease begins within 6 hours of single i.p. treatment and persists until the end of the experiment, 28 days later. Among dioxin-type compounds tested, 2,3,7,8-TCDD was the most active congener, as expected. Only the toxic congeners of PCBs were found to influence glucose transport in this manner under this test condition (32).

The most pertinent aspect of this finding is that such an observation likely provides the clue to the mystery of "wasting syndrome," which this group of chemicals is known to cause (1). The term "wasting syndrome" has been coined to describe the very characteristic toxic manifestation of dioxin-type chemicals to cause gradual and steady loss of body weight which occurs in most sensitive animal species (1, 2). The animals thus affected show drastic loss of adipose tissue and skeletal muscle, even if they were fed exactly the same amount of food (pair feeding) and despite the fact that all known biochemical processes involved in metabolism of glucose, amino acids, and lipids are operating normally (35). Originally, it was assumed that dioxins cause malabsorption of nutrients through the intestine, which later was shown to be functioning normally. Thus, our discovery that 2,3,7,8-TCDD causes a drastic reduction of glucose transporter titer on the plasma membrane of adipocytes and other types of glucose utilizing cells offers an interesting future possibility of adopting this parameter as a specific bioassay tool or even developing it as a biomarker of exposure to dioxin-type chemicals in the future.

In summary, we have determined that the XB hyperkeratinization assay is a potentially very promising approach to developing "biomarkers" of exposure to dioxin-type chemicals. This *in vitro* assay method is simple, very specific, economical, reliable, and quantifiable by a simple spectrophotometric method. Current experiments in our laboratory show that this assay is indeed a very useful tool for estimating TEQ in complex mixtures, such as combustion by-products from the incineration of chlorinated hydrocarbons and plastics (manuscript in preparation; 36). The most important aspect of this biochemical parameter is that hyperkeratinization itself is an irreversible change, representing the commitment by the cells to differentiate. Therefore, unlike other more ephemeral biochemical changes, hyperkeratinization represents a long lasting response to exposure to dioxin-type chemicals. Certainly in the future, the relative merits of this bioassay approach to other better studied assay methods, such as induction of cytochrome P4501A1, must be carefully evaluated. We understand that cytochrome P4501A1 induction, for instance, is a very sensitive and specific method to monitor relative effects of these chemicals. However, we also know that it has a number of drawbacks, the most important one being that it is an unsuitable indicator of the lethal effect of dioxin-type chemicals among various animal species. Furthermore, these chemicals are known to cause a variety of symptoms in different tissues and, therefore, we do need additional bioassay methods on sensitive types of cells expressing specific lesions that are unrelated to cytochrome P450s.

### Acknowledgments

This study was supported by ES03575, ES02533 and ES04699 from the National Institute of Environmental Health Sciences, Research Triangle Park, North Carolina. We thank Dr. Essam Enan and Mr. Phillip C.C. Liu at this laboratory for letting us cite their data on glucose transporters in this paper.

## Literature Cited

1. Poland, A.; Knutson, J.C. *Ann. Rev. Pharmacol. Toxicol.* **1982**, *22*, 517-554.
2. Moore, J.A. (ed.) *Environ. Health Perspect.* **1973**, *5*, 1-313.
3. Marklund, S.; Kjeller, L.-O.; Hansson, M.; Tysklind, M.; Rappe, C.; Ryan, C.; Collazo, H.; Dougherty, R. In *Chlorinated Dioxins and Dibenzofurans in Perspective*; Rappe, C., Choudhary, G., Keith, L.H., Eds.; Lewis Publishers, Inc.: Chelsea, MI, 1986; pp. 79-92.
4. Safe, S. *Toxicology* **1990**, *21*, 51-88.
5. Jensen, N.E. *Proc. R. Soc. Med.* **1972**, *65*, 687-688.
6. Jirasek, L.; Kalensky, J.; Kubec, K.; Pazderova, J.; Lukas, E. *Cesk. Dermatol.* **1974**, *49*, 145-157.
7. Ahling, B.; Lindskog, A.; Jansson, B.; Sunstrom, G. *Chemosphere* **1977**, *8*, 461-466.
8. Cole, G.W.; Stone, O.; Gates, D.; Culver, D. *Contact Dermatitis* **1986**, *15*, 164-168.
9. Taylor, J.S.; Wuthrich, R.D.; Lloyd, K.M.; Poland, A. *Arch. Dermatol.* **1977**, *113*, 616-619.
10. Villanueva, E.C.; Jennings, R.W.; Burse, V.W.; Kimborough, R.D. *J. Agric. Food Chem.* **1974**, *22*, 916-919.
11. Scholz, B.; Engler, M. *Chemosphere* **1987**, *16*, 1829-1835.
12. Eadon, G.; Kaminsky, L.; Silkworth, J.; Aldous, K.; Hilker, D.; O'Keefe, P.; Smith, R.; Gierthy, J.; Hawley, J.; Kim, N.; Decaprio, A. *Environ. Health Perspect.* **1986**, *70*, 221-227.
13. Hanbert, A.; Waern, F.; Asplund, L.; Hagland, E.; Safe, S. *Chemosphere* **1990**, *20*, 1161-1164.
14. Hanberg, A.; Stahlberg, M.; Georgellis, A.; de Wit, C.; Ahlborg, U. *Pharmacol. Toxicol.* **1991**, *69*, 442-449.
15. Gasiewicz, T.A. In *Handbook of Pesticide Toxicology*; Hayes, W.J., Laws, E.R., Eds.; Academic Press, Inc.: San Diego, CA, 1991; pp. 1191-1270.
16. Gasiewicz, T.A.; Rucci, G.; Henry, E.C.; Baggs, R. *Biochem. Pharmacol.* **1986**, *35*, 2737-2742.
17. Beatty, P.W.; Neal, R.A. *Biochem. Pharmacol.* **1978**, *27*, 505-510.
18. Kawamoto, T.; Madhukar, B.V.; Matsumura, F.; Bombick, D.W. *J. Biochem. Toxicol.* **1989**, *4*, 173-182.
19. Knutson, J.C.; Poland, A. *Cell* **1980**, *22*, 27-36.
20. Knutson, J.C.; Poland, A. *J. Cell. Physiol.* **1984**, *121*, 143-151.
21. Gierthy, J.F.; Crane, D.; Frenkel, G.D. *Fund. Appl. Toxicol.* **1984**, *4*, 1036-1041.
22. Rheinwald, J.G.; Green, H. *Cell* **1975**, *6*, 317-330.
23. Sawyer, T.; Safe, S. *Toxicol. Lett.* **1982**, *13*, 87-94.
24. Leece, B.; Denomme, M.A.; Towner, R.; Li, S.M.A.; Safe, S. *J. Toxicol. Env. Health* **1985**, *16*, 379-388.
25. Matsumura, F.; Brewster, D.W.; Madhukar, B.V.; Bombick, D.W. *Arch. Environ. Contam. Toxicol.* **1984**, *13*, 509-515.
26. Moriya, M.; Matsumura, F.; Kalimi, G.H. *J. Biochem. Toxicol.* **1986**, *1*, 45-54.
27. Madhukar, B.V.; Brewster, D.W.; Matsumura, F. *Proc. Natl. Acad. Sci. USA* **1984**, *81*, 7407-7411.
28. Jankun, J.; Matsumura, F.; Kaneko, H.; Trosko, J.E.; Mellicer, A.; Greenberg, A.H. *J. Molec. Toxicol.* **1989**, *2*, 177-186.
29. Tullis, K.; Olsen, H.; Bombick, D.W.; Matsumura, F.; Jankun, J. *J. Biochem. Toxicol.* **1992**, *7*, 107-116.

30. Bombick, D.W.; Matsumura, F. *J. Biochem. Toxicol.* **1987**, *2*, 141-154.
31. Barbacid, M. *Ann. Rev. Biochem.* **1987**, *56*, 779-827.
32. Enan, E.; Liu, P.C.C.; Matsumura, F. *J. Biol. Chem.* **1992**, *267*, 19785-19791.
33. Enan, E.; Liu, P.C.C.; Matsumura, F. *J. Environ. Sci. Health* **1992**, *B27(5)*, 495-510.
34. Unger, R.H. *Science* **1991**, *251*, 1200-1205.
35. Seefeld, M.D.; Corbett, S.W.; Keesey, R.E.; Peterson, R.E. *Toxicol. Appl. Pharmacol.* **1984**, *73*, 311-322.
36. Blankenship, A.L.; Chang, D.P.Y.; Jones, A.D.; Kelly, P.; Kennedy, I.M.; Matsumura, F.; Pasek, R.; Yang, G.S. (manuscript in preparation) **1993**.

RECEIVED May 28, 1993

## Chapter 4

# Regulation of Muscarine Receptors as Biomarkers of Exposure to Insecticides

Amira T. Eldefrawi, David A. Jett<sup>1</sup>, and John C. Fernando

Department of Pharmacology and Experimental Therapeutics, University  
of Maryland School of Medicine, Baltimore, MD 21201

Anticholinesterase organophosphate (OP) insecticides affect muscarinic receptors (mAChRs) indirectly as a consequence of their acetylcholinesterase (AChE) inhibition and directly by binding to mAChRs, with paraoxon being more selective for M<sub>2</sub>, M<sub>3</sub> and M<sub>4</sub> mAChR subtypes than the M<sub>1</sub>. Dietary exposure of adult male *Peromyscus* mice to parathion for 14 days reduced brain AChE and mAChR concentrations without changing receptor affinity. There was partial recovery of both in 7 days after discontinuing exposure. The M<sub>3</sub> receptor, its mRNA and AChE in submaxillary glands were also reduced by chronic parathion. The data suggest that down-regulation of mAChRs results mostly from reduced receptor synthesis due to reduced mRNA transcription. The feasibility of using erythrocyte, neutrophil and lymphocyte mAChRs as biomarkers can be assessed once their subtypes are identified and regulation determined.

Several neurotransmitter receptors are direct targets for insecticides such as the nicotinic acetylcholine (ACh) receptor for nicotine and nitromethylenes and the  $\gamma$ -aminobutyric acid receptor for cyclodienes, lindane and avermectins. These receptors play vital roles in insects as well as humans, other mammals, birds and fish, and interference with their functions produces acute toxicities and death. Neurotransmitter receptors such as muscarinic and nicotinic receptors are also indirect targets for insecticides. They are activated and subsequently desensitized by the excess ACh that accumulates when AChE is inhibited with OP or carbamate insecticides. In fact, death from poisoning by these anticholinesterases is by asphyxiation as a result of paralysis of diaphragm and

<sup>1</sup>Current address: Department of Environmental Health, School of Public Health, Johns Hopkins University, Baltimore, MD 21287

intercostal muscles (resulting from desensitization and inhibition of their nicotinic receptors), bronchial smooth muscle contraction, increased bronchial secretions and lowered heart rate and blood pressure (resulting from excessive activation of their mAChRs) and inhibition of the respiratory center in the brain.

Not only are neurotransmitter receptors primary and secondary targets for the acute toxicity of insecticides, they are also targets for their subacute and chronic toxicities. The most prominent effect is on the regulation of receptor concentrations. Cells respond to persistent activation of a receptor by decreasing its numbers (i.e. down-regulation). This regulation protects the cells and provides the postmitotic neurons in the brain with tremendous plasticity.

Reductions in mAChRs, measured by their specific high-affinity binding of [ $^3$ H]quinuclidinyl benzilate ([ $^3$ H]QNB), have been detected in rodent brains that have been exposed to OPs (24, 34). The significance of such a change even if temporary, is that if it occurs at periods during fetal and/or neonatal development when critical neuronal connections are being formed, it can still produce permanent deficits. mAChRs have been shown to play roles in memory and learning (23). Antagonists of mAChRs have been shown to impair learning/retention in rats (28) and the spatial memory of rats exposed daily to diisopropylfluorophosphate (DFP) or disulfoton (24). Also, rats given repeated low DFP doses, that did not produce visible cholinergic signs or weight loss, had progressively impaired working memory (6). More importantly is the persistent loss in memory of humans reported after acute or repeated exposure to low OP levels (10, 31). Also, occupational exposure to fenthion was reported to produce cognitive deficits, headache and psychiatric episodes (25, 26).

The following presentation is not an exhaustive review of OP toxicities nor mAChR structure and function. The focus is three-fold: 1. present evidence for the role of mAChRs as direct targets of OP anticholinesterase insecticides and its relevance to their toxicities. 2. present evidence of changes that occur in mAChR concentrations upon subchronic exposure to OPs. 3. discuss the possibility of mAChRs acting as biomarkers of human exposure to insecticides.

### Muscarinic Receptors

Five genes for mAChRs have been identified ( $m_1$ ,  $m_2$ ,  $m_3$ ,  $m_4$ ,  $m_5$ ), whose products are the subtypes  $M_1$ ,  $M_2$ ,  $M_3$ ,  $M_4$  and  $M_5$  (4). Generally, activation of the  $M_1$ ,  $M_3$  and  $M_5$  subtypes by ACh or agonists leads to a change in receptor conformation to one that binds G protein which activates phospholipase C, leading to increased phosphoinositide hydrolysis. On the other hand, the  $M_2$  and  $M_4$  preferentially couple to a  $G_i$  protein and their activation inhibits adenylyl cyclase. mAChRs also couple to other effectors such as the stimulation of  $M_1$  and  $M_3$  subtypes, which leads to activation of guanylyl cyclase and can also lead to arachidonic acid release, activation of  $K^+$  and  $Cl^-$  channels and inhibition of special neuronal  $K^+$  channel (15). The  $M_2$  cardiac mAChRs are also coupled to  $K^+$  channels via a  $G_k$  protein and receptor stimulation increases  $K^+$  levels, which

works with decreased cAMP to inhibit cardiac muscle activity. The mAChR protein is a membrane-bound glycoprotein that is made of a single subunit of  $\approx 80,000$  daltons and is composed of seven transmembrane segments with an extracellular amino terminal and an intracellular carboxy terminal (Fig. 1). The receptor has two binding domains: an extracellular binding domain where ACh and different drugs bind and an intracellular domain where the G-protein binds, largely in the first 20 amino acid of the protein's third cytoplasmic loop, with other points of interaction that contribute to both (5).

### Direct Actions of Organophosphates on Muscarinic Receptors

The strongest evidence for the direct binding of OP anticholinesterases to mAChRs is their inhibition of binding of specific radioligands to these receptors (3, 13, 21, 35). The competitive inhibition by paraoxon of binding of the agonist [ $^3\text{H}$ ]cis-methyl-dioxolane ([ $^3\text{H}$ ]CD), which binds selectively to a high-affinity subpopulation of  $M_2$  receptors in rat brain, suggested that OPs bind to the same site as ACh and the  $M_2$  receptor was probably a most sensitive subtype to OPs (3). The effective inhibition of the non-subtype selective antagonist [ $^3\text{H}$ ]QNB to brain mAChRs by paraoxon at  $< 1$  nM and the protection of this inhibition by the  $M_2$ -selective (AF-DX 116) and  $M_3$ -selective (4-DAMP) antagonists, but not the  $M_1$ -selective antagonist piperenzepine (21), pointed to the sensitivity of the  $M_2$  and  $M_3$  subtypes but not the  $M_1$  subtype, to the direct action of OP anti-AChEs.

Because most mAChRs in cardiac muscle are of the  $M_2$  subtype, it was an ideal tissue to study the direct effect of paraoxon and other OPs. Again, binding of [ $^3\text{H}$ ]CD was inhibited competitively by paraoxon with a  $K_i$  of  $< 1$   $\mu\text{M}$  (Fig. 2) (29). Paraoxon also inhibited [ $^3\text{H}$ ]CD binding to mAChRs in rat brain striatum, which is believed to be an  $M_4$  subtype (30). The  $K_{0.5}$  for the bioactive paraoxon was 80 nM, while its parent thio-compound the insecticide parathion (which is also a poor inhibitor of AChE) had a  $K_{0.5}$  of 7  $\mu\text{M}$  (Fig. 3). In order to determine whether paraoxon acts as an agonist or antagonist of this receptor, its effect on receptor function was determined (20). Both the agonist carbachol and paraoxon inhibited the forskolin-activated [ $^3\text{H}$ ]cAMP synthesis and their effects were totally blocked with atropine (Fig. 4). At low concentrations, the effects of carbachol and paraoxon were additive, but not at high saturating concentrations of either drug. The data suggest that paraoxon acts like the agonist carbachol.

Since almost all mAChRs in rat submaxillary gland cells are of the  $M_3$  subtype, we studied the effect of paraoxon on this receptor binding and function in these cells (1). Binding of [ $^3\text{H}$ ]QNB and [ $^3\text{H}$ ]4-DAMP was inhibited non-competitively by paraoxon with  $K_{0.5}$  nM. The receptor couples preferentially to phospholipase C than to adenylyl cyclase; thus carbachol activates the former with a  $K_D$  of 1  $\mu\text{M}$  and the latter with a  $K_D$  of  $> 1$  mM. Like carbachol, paraoxon inhibited the forskolin-activated [ $^3\text{H}$ ]cAMP synthesis with a  $K_D$  of 200 nM, without affecting phosphoinositide metabolism. However, the effect of paraoxon on [ $^3\text{H}$ ]cAMP synthesis was unlike that of carbachol; it was not inhibited by atropine; which suggested that this paraoxon effect was not via binding to the

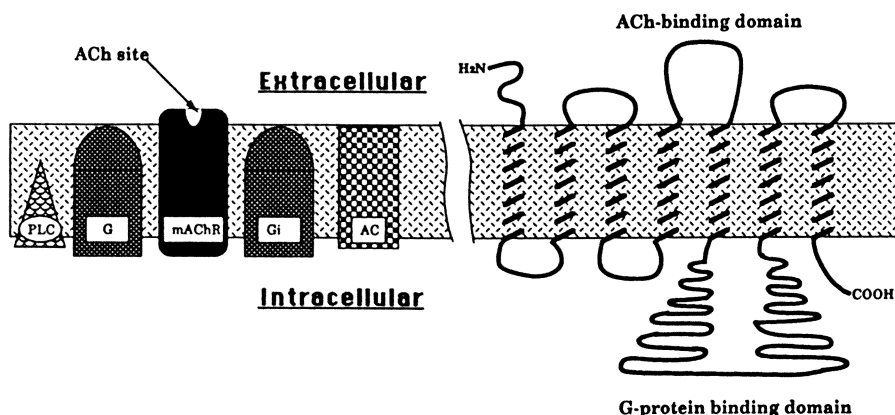


Figure 1. Schematic presentation of a mAChR and its relationship to the second messenger systems and cell membrane. Left: The mAChR, G or G<sub>i</sub> proteins that it may couple to and associated enzymes, phospholipase C (PLC) and adenylyl cyclase (AC). Right: Diagram of a typical mAChR protein with its amino and carboxy terminals, seven transmembrane regions and binding domains.

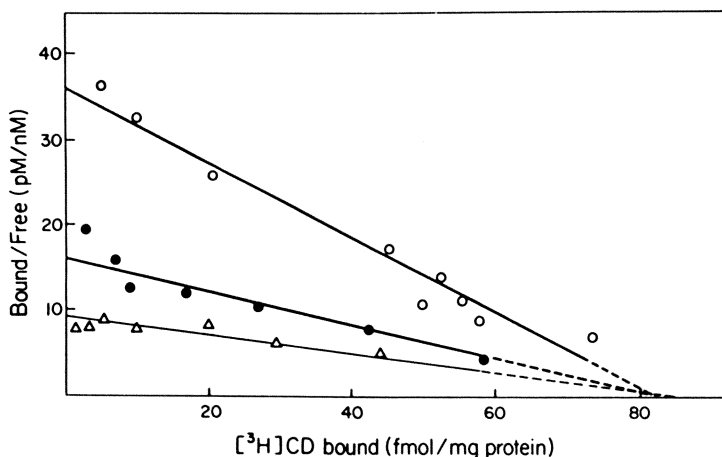


Figure 2. Scatchard plot of  $[^3\text{H}]\text{CD}$  binding to rat cardiac  $M_2$  receptors alone (○) and in presence of 20 nM of the OP nerve gas sarin (●) or 200 nM paraoxon (Δ). The common intercept on the X-axis suggests competitive inhibition. (Reproduced with permission from ref. 29).

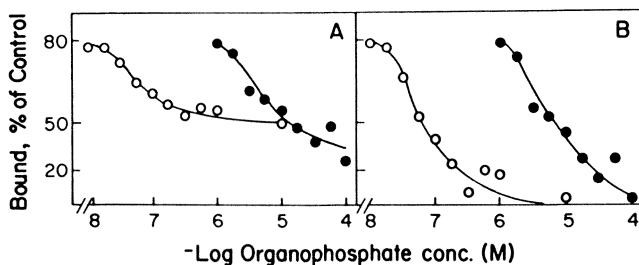


Figure 3. Displacement of  $[^3\text{H}]\text{CD}$  binding to rat brain striatal synaptic membranes by paraoxon (○) and parathion (●). (A) Experimental data obtained. (B) Data replotted after elimination of paraoxon-insensitive  $[^3\text{H}]\text{CD}$  binding. Symbols represent means of two experiments done in triplicate (N = 6). Standard error bars are smaller than symbols used. (Reproduced with permission from ref. 20).

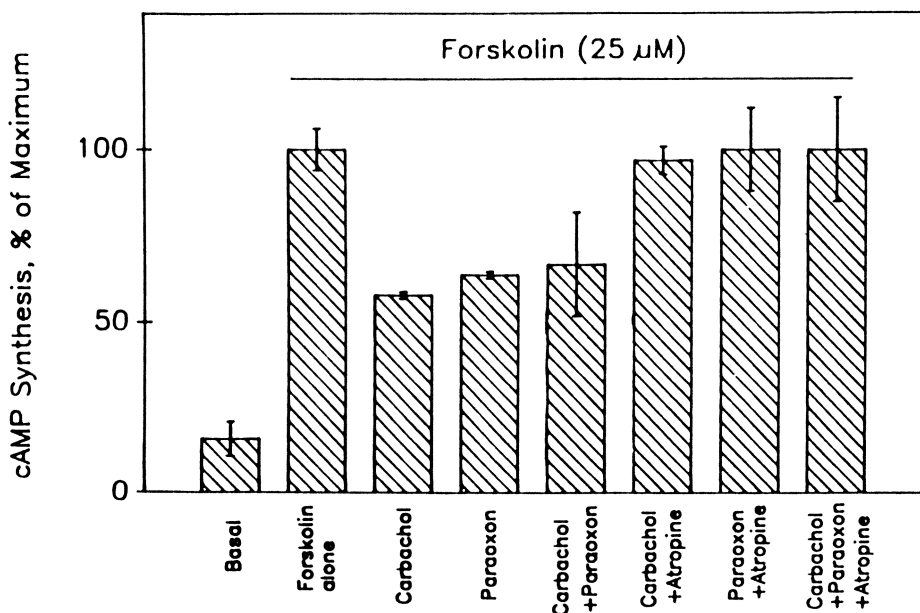


Figure 4. Inhibition of forskolin-activated adenylyl cyclase activity in rat brain striatum-dissociated cells by 100  $\mu\text{M}$  carbachol or 1  $\mu\text{M}$  paraoxon, with or without 10  $\mu\text{M}$  atropine (added prior to activation with forskolin when applicable). Synthesis of  $[^3\text{H}]\text{cAMP}$  in the presence of forskolin alone was considered maximal activity and basal  $[^3\text{H}]\text{cAMP}$  synthesis was in absence of forskolin. All measurements were run in triplicate and bars represent SEM. (Reproduced with permission from ref. 20).

mAChR. The data suggested that paraoxon bound to different sites: an allosteric site on the  $M_3$  receptor and another on the  $G_i$  protein-adenylyl cyclase system.

The significance of the direct effects of paraoxon on mAChRs to its acute toxicity, even though it is reversible, is its much higher binding affinity ( $K_D$  of  $< 1 \mu\text{M}$ ) compared to parathion's  $K_s$  for AChE (of  $\approx 1 \text{ mM}$ ) to form the intermediate complex (AChE-parathion) before AChE is phosphorylated irreversibly (12). Most of the reports on paraoxon effects on mAChRs have been on  $M_2$ ,  $M_3$  and  $M_4$  receptors. On the postsynaptic cardiac muscle  $M_2$  mAChRs, the reversible receptor activation by paraoxon would exaggerate its excessive activation by ACh that accumulates in the synaptic gap when AChE is inhibited by the OP. This effect would have considerable impact on OP toxicity, especially at the early stages of exposure, when only a small proportion of AChE is inhibited. The postsynaptic mAChRs would be activated by the excess ACh as well as by the OP directly. It may explain the particular therapeutic value of the mAChR inhibitor atropine on the heart during OP intoxication. On the other hand, activation of the presynaptic  $M_2$  mAChRs on neurons innervating the heart and the predominant presynaptic  $M_2$  and possibly  $M_4$  receptors in the brain, would reduce ACh release, thereby counteracting in part the toxicity that results from AChE inhibition. Adding to the complexity of OP actions is that mAChR activation of protein kinase C induces *c-fos* and *c-jun* oncogenes (17, 33).

### Effect of Subchronic Parathion on Muscarinic Receptors

Subchronic exposure to parathion is expected to chronically increase ACh at cholinergic synapses, thereby activating mAChRs and also paraoxon would directly activate certain mAChR subtypes. We studied the effect of *ad libitum* dietary exposure to parathion for 14 days on mAChR subtypes in brains and submaxillary glands of adult white-footed mice (*Peromyscus leucopus*) (19). The mAChR concentrations were monitored using the subtype-nonselective antagonists [ $^3\text{H}$ ]QNB and [ $^3\text{H}$ ]N-methylscopolamine ([ $^3\text{H}$ ]NMS) and the relatively selective antagonist of the  $M_3$  subtype ([ $^3\text{H}$ ]4-DAMP), which also binds with slightly less affinity to the  $M_1$  and  $M_4$  subtypes (36). Because of the variability in parathion concentrations in the food with length of exposure, consumption rates, mouse weight changes as well as parathion metabolism and pharmacokinetics, % AChE inhibition in brain and submaxillary gland membranes was used as a biomarker of exposure for *in situ* paraoxon concentrations. Accordingly, the binding parameters were presented in relation to AChE inhibition observed in each mouse at the time of sacrifice, rather than the concentration of parathion in the food.

At parathion concentrations, which were sufficiently high to cause AChE inhibition by up to  $\approx 90\%$ , brain mAChRs were reduced significantly by up to 58%, as judged by the reductions in maximal binding ( $B_{\text{max}}$ ) of [ $^3\text{H}$ ]QNB, [ $^3\text{H}$ ]NMS and [ $^3\text{H}$ ]4-DAMP (Fig. 5A-C), without significant changes in their affinities (Fig. 6A-C). The reductions in maximal [ $^3\text{H}$ ]QNB and [ $^3\text{H}$ ]4-DAMP binding were significant only at higher AChE inhibition (Fig. 4A and C). On the other hand, [ $^3\text{H}$ ]NMS binding was unique in that maximal reduction was reached with lower parathion concentrations that produced little ( $\approx 10\%$ ) inhibition of

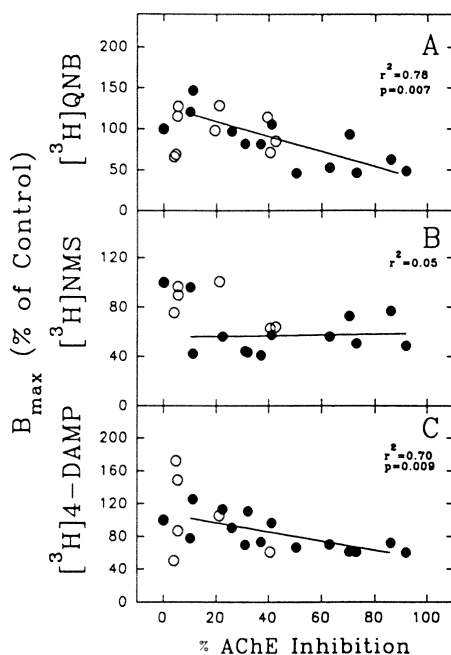


Figure 5. The relationship in *Peromyscus* whole brain membranes of maximal binding capacity ( $B_{\max}$ ) of [ $^3\text{H}$ ]QNB (A), [ $^3\text{H}$ ]NMS (B), and [ $^3\text{H}$ ]4-DAMP (C) to AChE inhibition in surviving adult males receiving parathion in corn oil in their diets. Each symbol represents a  $B_{\max}$  (obtained from a Scatchard plot of 10 radioligand concentrations from a single mouse brain) and AChE inhibition in the same brain, expressed as a percent of the mean ( $N = 13$ ) in control mice receiving corn oil only. Mice given parathion-treated feed for 14 days prior to sacrifice (●) or were given another 7 days of recovery on untreated feed before sacrifice (○). Regression analyses were performed only on the data obtained from mice that were not allowed a recovery period after parathion exposure. Control values (at 0% AChE inhibition) were not included in the regression. (Reproduced with permission from ref. 19).

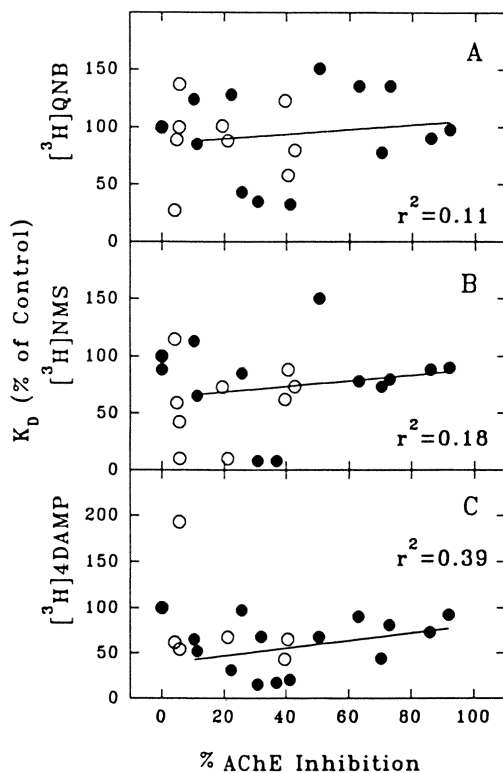


Figure 6. The relationship in *Peromyscus* whole brain membranes of the equilibrium dissociation constants ( $K_D$ ) of  $[^3H]QNB$  (A),  $[^3H]NMS$  (B), and  $[^3H]4-DAMP$  (C) to AChE inhibition in surviving adult males receiving parathion in corn oil in their diets. Each symbol represents a  $K_D$  (obtained from the same Scatchard plot as in Fig. 4) and AChE inhibition values in the brain, expressed as a percent of the mean ( $N = 13$ ) in control mice receiving corn oil only. Mice given parathion-treated feed for 14 days prior to sacrifice (●) or were given another 7 days of recovery on untreated feed before sacrifice (○). Regression analyses as in Fig. 4. (Reproduced with permission from ref. 19).

AChE, without further reduction at higher AChE inhibition (Fig. 4B). This is similar to the observed 33% decrease in  $B_{\max}$  of [ $^3\text{H}$ ]NMS in mice 24 h after a single dose of DFP without changes in [ $^3\text{H}$ ]QNB or [ $^3\text{H}$ ]4-DAMP binding (7). It is consistent with the hydrophilicity of NMS and thus its inability to detect the desensitized mAChRs, unlike the lipophilic QNB or 4-DAMP, since activation of mAChRs is followed by temporary removal of the receptor from the outer cell surface and its penetration into the lipid membrane.

Brains of parathion exposed mice, that were allowed a 7 day recovery period, had AChE that was inhibited by <40% and most were back to control levels. The  $B_{\max}$  values for mAChR antagonists were also generally reduced in the few mice with higher AChE inhibition, back to the levels of mice with lower AChE inhibition that were not allowed a recovery period (Fig. 5). Thus, despite the variabilities and few animals studied, there does appear to be significant partial recovery in 7 days in both AChE activity and mAChR concentration. In order to inquire into the mechanism for reduction in submaxillary mAChR concentration that results from dietary exposure to parathion,  $M_3$  subtype-selective rat cDNA probe (5) (kindly provided by Dr. Tom Bonner) was used to assess the receptor's mRNA levels in *Peromyscus* submaxillary glands. In mice exposed to dietary parathion for 14 days, AChE was significantly reduced, and so was [ $^3\text{H}$ ]QNB binding ( $r^2=0.66$ ,  $p=0.05$ ) without significant change in its  $K_D$  ( $r^2=0.25$ ) (Fig. 7). There was also a highly significant reduction in mRNA of the  $M_3$  receptors (Fig. 8). It suggests that the observed down-regulation of mAChRs in submaxillary glands, and most likely brain mAChRs, results mostly from their reduced synthesis as a result of reduced mRNA transcription. This supports the recent findings on the effect of agonists on  $m1$ ,  $m2$  and  $m3$  receptors (38) and DFP on the  $m2$  receptor (40). The degree of down-regulation of brain mAChRs (up to 50-58%), which is close to that in the  $M_3$  subtype in submaxillary glands (up to  $\approx 42\%$ ), does not reveal whether there is subtype-selective down-regulation in the brain. Utilization of subtype-specific antibodies (kindly provided by Dr. Barry Wolf), which are highly subtype-selective (37) compared to the "specific" radioligands used, revealed the cortical abundance of the subtypes was similar to the rat's:  $M_1 > M_4 > M_2 > M_3 > M_5$  (19). It is feasible to reveal if the different receptor subtypes in the brain are differentially regulated by subchronic parathion. There was a greater loss of  $M_3$  receptors compared to  $M_1$  receptors in submucosal gland cells of swine trachea after subacute exposure to DFP (39).

Receptors are constantly being synthesized and degraded with a certain half life that differs between various receptors and their locations amongst other factors. Agonists most likely down-regulate mRNA levels by regulating the rate of gene transcription. It is important to note that regulation of mAChR mRNA expression does not occur only as a result of persistent activation of mAChRs, but may also result from activation of other G-coupled receptors. Incubation of chicken heart cells with agonists for the  $A_1$  adenosine receptor (which inhibits adenylyl cyclase in chicken heart) has resulted in decreased mAChR numbers and its mRNA levels; albeit to a smaller degree than those seen with direct activation of mAChRs (18). However, the apparent higher reduction in

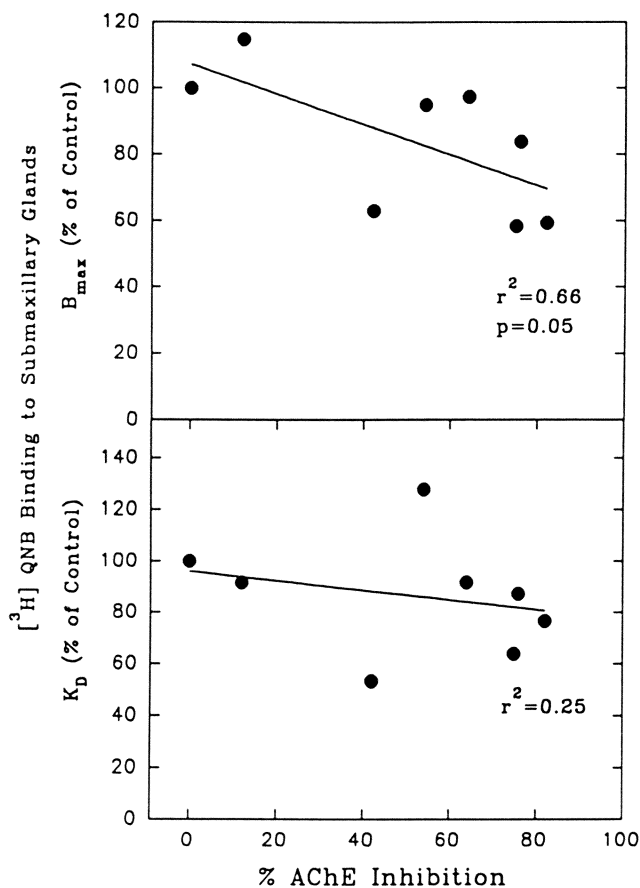


Figure 7. The relationship in *Peromyscus* submaxillary glands of mRNA to AChE inhibition in surviving adult males receiving parathion in corn oil. Each symbol represents a mouse given treated feed for 14 days. The mRNA levels were measured as the optical density of individual bands determined after autoradiography of Northern blots using radiolabeled rat m3 probe. Both mRNA levels and AChE inhibition are expressed as a percent of the mean ( $N = 4$ ) determined in control mice receiving corn oil only. (Reproduced with permission from ref. 19).

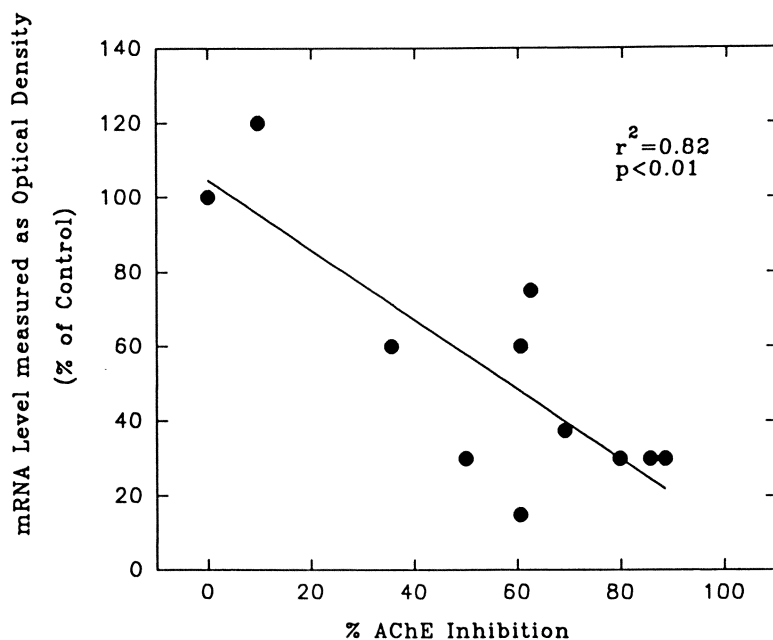


Figure 8. The relationship in *Peromyscus* submaxillary glands of  $B_{\max}$  and  $K_D$  of [ $^3\text{H}$ ]QNB to AChE inhibition in surviving adult males receiving parathion in corn oil. Each symbol represents a mouse given treated feed for 14 days.  $B_{\max}$  and  $K_D$  (obtained from a Scatchard plot of 10 radioligand concentrations) and AChE inhibition are expressed as a percent of the mean ( $N = 4$ ) in control mice receiving corn oil only. (Reproduced with permission from ref. 19).

submaxillary gland  $M_3$  mRNA (up to  $\approx 80\%$ ) (Fig. 8) than  $M_3$  receptor concentration (up to  $\approx 42\%$ ) (Fig. 7), suggests that there may be other changes in posttranscriptional processing that act in the opposite direction. Among possible explanations are increased translational efficiency or incorporation of receptor from premade pools, activation of previously inactive receptors and decreased receptor degradation. The present findings are consistent with previous data on the effects of sublethal repeated exposure of animals to OPs and the development of tolerance, which is believed to be due in part to a reduction in mAChRs (8, 9).

### Muscarinic Receptors in Blood Cells

The regulation of mAChRs in brain and submaxillary glands by OPs cannot possibly be utilized as a biomarker of exposure, since the sampling method is highly invasive. On the other hand, several blood cells have been found to have mAChRs. The presence of mAChRs in neuronal and innervated cells has long been widely documented by electrophysiological, biochemical and pharmacological techniques. However, there was no reason to search for these receptors in non-neuronal and noninnervated cells, since it could not be imagined why a receptor would be there and what the source of its transmitter would be. Using radioligand binding assays, mAChRs were identified in the outer surface membranes of human erythrocytes (2) and neutrophils (11) as well as in mouse lymphocytes (B and T) (16). There are suggestions of functional roles for these receptors, such as in altering cell deformability, osmotic fragility and membrane structure and possibly some mAChRs may be remnants from the stem cell stage, and play roles in cell differentiation. In searching for biomarkers of exposure, receptor density is an important determinant of detection sensitivity, while the life span of the cell is important for stability of the biomarker. Whereas the average life of a human erythrocytes is 4 months, that of a T lymphocyte is a few days, while for a B lymphocyte it is years. The concentrations of mAChRs also vary greatly between these blood cells. In erythrocytes, 2 (32), 3.6 (22) and 23 (2) fmol of mAChRs/mg protein have been reported, depending in part on the degree of membrane purification in the assays used. In mouse lymphocytes and human neutrophils, 200 (16) and 50,000 (11) sites per cell, respectively, were reported. The number of cells in the blood are also a factor that affects the sensitivity of the assay for mAChRs. There is an average of 2,000 lymphocytes, 5,000 neutrophils and 5 million erythrocytes per  $\text{mm}^3$  of blood.

The identity of the mAChR subtypes in these blood cells has not been determined, nor has any study been conducted on the effect of chronic exposure to muscarinic agonists, antagonists or OP anti-AChEs on mAChRs. Cytotoxic T lymphocytes and natural killer cells as well as monocytes play an important role in the elimination of virus-injected cells and provide immune surveillance for premalignant cells. Serine esterases in these cells are inhibited by very low concentrations of OPs (27). It is not known whether monocytes have mAChRs or whether they are regulated by exposure to OPs. Until such knowledge is available, there is no way of assessing the feasibility of using blood cell mAChRs

as biomarkers of human exposure to OP pesticides. The information would also reveal possible immunotoxic impact of chronic exposure to OPs.

### Acknowledgements

The research described herein was financed in part by NIH grant No. ES02594. The authors are indebted to Dr. Tom Bonner of NIH for donating the rat cDNA probe of the m3 receptor.

### Literature Cited

1. Abdallah, E.A.M.; Jett, D.A.; Eldefrawi, M.E.; Eldefrawi, A.T. *Arch. Insect Biochem. Physiol.* 1992, 7, 125-132.
2. Aronstam, R.S.; Abood, L.G.; MacNeil, M.K. *Life Sci.* 1977, 20, 1175-1180.
3. Bakry, N.M.S.; El-Rashidy, A.H.; Eldefrawi, A.T.; Eldefrawi, M.E. *J. Biochem. Toxicol.* 1988, 3, 235-259.
4. Bonner, T.I. *Trends Pharm. Sci.* 1992, 13, 48-50.
5. Bonner, T.I.; Buckley, N.J.; Young, A.; Brann, M.R. *Science* 1987, 257-532.
6. Bushnell, P.J.; Padilla, S.S.; Ward, T.; Pope, C.N.; Olszyk, V.B. *J. Pharm. Exp. Therap.* 1991, 256, 741-750.
7. Cioffi, C.L.; El-Fakahany, E.E. *Eur. J. Pharmacol.* 1988, 156, 35-45.
8. Costa, L.G.; Schwab, B.H.; Hand, H.; Murphy, S.D. *Toxicol. Appl. Pharmacol.* 1981, 60, 441-450.
9. Costa, L.G.; Schwab, B.H.; Murphy, S.D.; *Toxicology* 1982, 35, 79-97.
10. Duffy, F.H.; Burchfield, J.L.; Barlets, P.H.; Gaon, M.; Sim, V.M. *Tox. Appl. Pharmacol.* 47, 161-176.
11. Dulis, B.H.; Gordon, G.A.; Wilson, I.B.; *Mol. Pharmacol.* 1979, 15, 28-34.
12. Eldefrawi, A.T. In *Comprehensive Insect Physiology, Biochemistry and Pharmacology. Insect Control*; Editors, Kerkut, G.A.; Gilbert, L.I.; Pergamon Press, Oxford 1985, pp. 102-124.
13. Eldefrawi, A.T.; Jett, D.; Eldefrawi, M.E. In *Organophosphates: Chemistry, Fate, and Effects*; Editors, Chambers, J.E.; Levi, P., Academic Press, New York 1992, pp. 257-270.
14. Fukamauchi, F.; Hough, C.; Chuang C.-M. *J. Neurochem.* 1991, 56, 716-720.
15. Fukuda, K.; Higashida, H.; Kuba, T.; Maeda, A.; Akiba, I.; Bujo, H.; Mishina, M.; Numa, S. *Nature* 1988, 335, 355-358.
16. Gordon, M.A.; Cohen, J.J.; Wilson, I.B. *Proc. Natl. Acad. Sci. USA* 1978, 75, 2902-2904.
17. Gutkind, J.S.; Novotony, E.A.; Braun, M.R.; Robbins, K.C. *Proc. Natl. Acad. Sci. USA* 1991, 88, 4703-4707.
18. Habecker, B.A.; Nathanson, N.M. *Proc. Natl. Acad. Sci. USA* 1992, 89, 5035-5038.

19. Jett, D.A.; Hill E. F.; Fernando, J.C.; Eldefrawi M.E.; Eldefrawi, A.T. *Toxicol. Environ. Health* 1993, in press.
20. Jett, D.A.; Abdallah, E.A.M.; El-Fakahany, E.E.; Eldefrawi, M.E.; Eldefrawi, A.T. *Pestic. Biochem. Physiol.* 1991, *39*, 149-157.
21. Katz, L.S.; Marquis, J.K. *Toxicol. Appl. Pharmacol.* 1989, *101*, 114-123.
22. Mantione, C.R.; Hanin, I. *Mol. Pharmacol.* 1980, *18*, 28-32.
23. Matthies, H.; *Ann. Rev. Psychol.* 1989, *40*, 381-404.
24. McDonald, B.E.; Costa, L.G.; Murphy, S.D. *Toxicol. Lett.* 1988, *40*, 47-56.
25. Metcalf, R.L.; Branch, C.E.; Swift, T.R.; Sikes, R.K. *L. Georgia MMWR* 1985, *34*, 402-403.
26. Misra, U.K.; Nag, D.; Bushand, V.; Ray, P.K. *Toxicol. Lett.* 1985, *24*, 187-193.
27. Newcombe, D.S. *The Lancet* 1992, *339*, 539-541.
28. Riekkinen, P.J.; Sirvio, J.; Aaltonen, M.; Riekkinen, P. *Pharm. Biochem. Behav.* 1990, *37*, 405-410.
29. Silveira, C.L.P.; Eldefrawi, A.T.; Eldefrawi, M.E. *Tox. Appl. Pharmacol.* 1990, *103*, 474-481.
30. Surichamorn, W.; Amrhein, C.L.; Forray, C.; El-Fakahany, E.E. *Brain Res.* 1989, *493*, 320-325.
31. Tabershaw, I.R.; Cooper, W.C. *J. Occup. Med.* 1966, *8*, 5-10.
32. Tang, L.C. *Gen. Pharmac.* 1986, *17*, 281-285.
33. Trejo, J.; Brown, J.H. *J. Biol. Chem.* 1991, *266*, 7876-7882.
34. Veronesi, B.; Pope, C. *Neurotoxicol.* 1990, *11*, 609-626.
35. Volpe, L.S.; Biagioni, T.M.; Marquis, J.K. *Tox. Appl. Pharmacol.* 1985, *78*, 226-234.
36. Waelbroek, M.; Camus, J.; Tastenoy, M.; Christophe B. *J. Pharmacol.* 1992, 97-102.
37. Wall, S.T.; Yasuda, R.P.; Li, M.; Ciesla, W.; Wolf, B.B., J. *Pharmacol. Exp. Therap.*, 1992, *262*, 584-588.
38. Wang, S.Z.; Hu, J.; Long, R.M.; Pou, W.S.; Forray, C.; El-Fakahany, E.E. *FEBS Lett.* 1990, *276*, 185-188.
39. Yang, C.M.; Mohan, M.P.; Dwyer, T.M.; Farley, J.M. *J. Auton. Pharmacol.* 1988, *8*, 79-91.
40. Zhu, S.Z.; Wang, S.Z.; Abdallah, E.A.M.; El-Fakahany, E.E. *Life Sci.* 1991, *48*, 2579-2584.

RECEIVED August 4, 1993

## Chapter 5

# Correlations of Molecular Connectivity Indices with Toxicities of Organic Nitriles

Gordon G. Cash

Office of Pollution Prevention and Toxics (TS-798), U.S. Environmental Protection Agency, Washington, DC 20460

This investigation attempted, with partial success, to improve upon results of published quantitative structure activity relationships for 26 organic nitriles. Specifically, molecular connectivity indices and principal component scores derived from them were used in place of more difficultly computed parameters to predict acute toxicities. Many good correlations were discovered for subsets of the data, but a predictive equation generally applicable to the gamut of organic nitriles was not found.

The United States Environmental Protection Agency's (USEPA) Office of Pollution Prevention and Toxics (OPPT) has a longstanding interest in predicting biological activities of compounds through quantitative structure-activity relationships. A previous study (1) demonstrated some success in predicting the LD<sub>50</sub> of a variety of organic nitriles from a combination of log *P* and a parameter *k<sub>a</sub>* derived from quantum mechanical calculation of relative heats of formation. In the present work, the author sought to apply the much more easily calculated molecular connectivity indices (2-6) to the same task.

### Methodology

Molecular connectivity indices, <sup>n</sup>χ, and valence molecular connectivity indices, <sup>n</sup>χ<sup>v</sup>, here collectively called MCIs, were generated for paths (P), clusters (C), paths/clusters (P/C), and chains (CH) were generated through order six, comprising 38 indices in all. This paper refers to the resulting indices as P<sub>n</sub>, C<sub>n</sub>, P/C<sub>n</sub>, CH<sub>n</sub>, P<sub>n</sub>v, etc. (Most authors refer to the path/cluster indices as PC<sub>n</sub>, but P/C<sub>n</sub> is used here to avoid confusion with principal component scores.) For the set of 26 compounds from ref. 1, twelve indices, namely, CH<sub>3</sub>, CH<sub>4</sub>, CH<sub>5</sub>, CH<sub>4</sub>v, CH<sub>5</sub>v, CH<sub>6</sub>v, C<sub>4</sub>, C<sub>5</sub>, C<sub>6</sub>, C<sub>4</sub>v, C<sub>5</sub>v, and C<sub>6</sub>v, were all zero. Therefore, only the 26 for which there were some non-zero values were considered.

This chapter not subject to U.S. copyright  
Published 1994 American Chemical Society

Principal component analysis (PCA) was also performed on the sets of MCIs generated for the study compounds. Principal components may be derived from either the covariance matrix or the correlation matrix, the difference being that use of the correlation matrix has the effect of giving each of the underlying variables equal weight. In the present study, no compelling argument could be made for excluding either approach, so both were used.

Because comparisons are being made among correlations involving both different numbers of observations and different numbers of predictor variables, the author feels it more appropriate to compare adjusted  $R^2$  than multivariate  $R$ . The relationship of adjusted  $R^2$  to multivariate  $R$  is given by equation 1 (7)

$$\text{adjusted } R^2 = 1 - \left( \frac{n-1}{n-(p+1)} \right) (1-R^2) \quad (1)$$

(Note that adjusted  $R^2$  does not reduce to univariate  $R^2$  in the univariate case.)

The dependent variable addressed in ref. 1 was  $(-\log \text{LD}_{50})$ . Our multiple regression software was unable to find any relationships between this variable and the MCIs. Using a technique which has been somewhat successful with other datasets, the transform  $(-\log \text{LD}_{50})^n$  was adjusted to optimize the Kolmogorov-Smirnov score for normal distribution. (The Kolmogorov-Smirnov score for  $(-\log \text{LD}_{50})$  was well above the critical value.) In the present case, the optimum value of  $n$  was  $-0.5$ . All of the present studies were performed using the transformed variable,  $(-\log \text{LD}_{50})^{-0.5}$ . Using a transformed variable for regression analyses creates a problem in comparing standard errors of the estimates because the estimate will be for the error in the transformed variable. The equation relating the error in a function to the errors in its variables is equation 2:

$$s_F = \sqrt{\sum s_i^2 \left( \frac{\partial F}{\partial x_i} \right)^2} \quad (2)$$

For a case in only one variable, this reduces to equation 3:

$$s_F = \left| s_x \left( \frac{dF}{dx} \right) \right| \quad (3)$$

In the present study, the software estimates the error in  $(-\log \text{LD}_{50})^{-0.5}$ , and one wants to know the error in  $(-\log \text{LD}_{50})$ . Therefore, for the purpose of using equation 3,  $x$  is  $(-\log \text{LD}_{50})^{-0.5}$ ,  $F(x)$  is  $x^2$ , and  $dF/dx$  is  $-2x^{-3}$ . At the mean value of  $(-\log \text{LD}_{50})^{-0.5}$ ,  $0.8517$ ,  $-2x^{-3} = 3.24$ .

For similar reasons, one of the results reported below involves a transformation of an independent variable from ref. 1,  $\ln k_{a \text{ corr}}$  into  $(\ln k_{a \text{ corr}} + 5.5)^{1.3}$ .

The software package, SCOUT, used in this study to calculate the transformations and their Kolmogorov-Smirnov scores, as well as to find coplanar subsets of data in various 3-spaces, deserves special mention because those operations would have been prohibitively tedious without it. SCOUT is a

multivariate statistics package that runs under DOS, does not require expanded memory, a math coprocessor, or a mouse, reads ASCII input files, and writes its graphics to disk in PCX format. Of particular note, SCOUT is available in the public domain. Executable files may be obtained by sending a 5¼" (H.D. only) or 3½" (either density) floppy diskette to Mr. Jack Teuschler, U. S. Environmental Protection Agency, Center for Environmental Research Information (CERI), 26 Martin Luther King Drive, Cincinnati, OH 45268; (513) 569-7314. For additional technical information, contact Dr. George Flatman, U. S. Environmental Protection Agency, Environmental Monitoring and Systems Laboratory, P. O. Box 93478, Las Vegas, NV 89193-3478; (702) 798-2628. SCOUT also performed the principal component analyses (PCA) reported here, but it does not perform any sort of regression.

## Results and Discussion

It is a general principle of quantitative structure activity relationship (QSAR) studies that the relationships work best within a closely analogous group of compounds. Use of several such groups within the same study usually results in a description of the differences among the groups rather than among the compounds within the groups. The set of alkyl nitriles in Table I seemed a good choice for a QSAR study for the reasons given in ref. 1. As stated above, the approach taken in ref. 1 was computationally intensive, and one goal of the present study was to achieve comparable results with more easily accessible parameters. The parameters chosen were the MCIs described above and principal component scores derived from them.

**Table I. Compounds Examined in This Study and in Ref. 1**

Obs. #	Type <sup>a</sup>	R	Obs. #	Type <sup>a</sup>	R
1	mono	CH <sub>3</sub>	14	di	(CH <sub>2</sub> ) <sub>3</sub>
2	mono	CH <sub>3</sub> CH <sub>2</sub>	15	di	(CH <sub>2</sub> ) <sub>4</sub>
3	mono	CH <sub>3</sub> (CH <sub>2</sub> ) <sub>2</sub>	16	di	(CH <sub>2</sub> ) <sub>5</sub>
4	mono	CH <sub>3</sub> (CH <sub>2</sub> ) <sub>3</sub>	17	mono	ClCH <sub>2</sub>
5	mono	CH <sub>3</sub> (CH <sub>2</sub> ) <sub>4</sub>	18	mono	Cl(CH <sub>2</sub> ) <sub>2</sub>
6	mono	CH <sub>3</sub> (CH <sub>2</sub> ) <sub>6</sub>	19	mono	Cl(CH <sub>2</sub> ) <sub>3</sub>
7	mono	CH <sub>3</sub> (CH <sub>2</sub> ) <sub>7</sub>	20	mono	(CH <sub>3</sub> ) <sub>2</sub> N(CH <sub>2</sub> ) <sub>2</sub>
8	mono	(CH <sub>3</sub> ) <sub>2</sub> CH	21	mono	(CH <sub>3</sub> ) <sub>2</sub> CHNH(CH <sub>2</sub> ) <sub>2</sub>
9	mono	(CH <sub>3</sub> ) <sub>2</sub> CHCH <sub>2</sub>	22	di	(CH <sub>2</sub> ) <sub>2</sub> NH(CH <sub>2</sub> ) <sub>2</sub>
10	mono	(CH <sub>3</sub> ) <sub>2</sub> CH(CH <sub>2</sub> ) <sub>2</sub>	23	mono	CH <sub>2</sub> =CHCH <sub>2</sub>
11	mono	CH <sub>3</sub> CH <sub>2</sub> CH(CH <sub>3</sub> )	24	mono	φCH <sub>2</sub>
12	di	CH <sub>2</sub>	25	mono	φ(CH <sub>2</sub> ) <sub>2</sub>
13	di	(CH <sub>2</sub> ) <sub>2</sub>	26	mono	HO(CH <sub>2</sub> ) <sub>3</sub>

<sup>a</sup> Mononitrile, R-C≡N, or dinitrile, N≡C-R-C≡N.

The dependent variable taken from ref. 1 was  $\log(1/\text{LD}_{50})$ , which this study expresses as  $-\log \text{LD}_{50}$ , where  $\text{LD}_{50}$  was the acute median lethal dose in mice and was obtained from various published sources. Stepwise multiple regression techniques were unable to find any correlations between the set of 26 MCIs and  $-\log \text{LD}_{50}$ . Using the methodology described above, a transformed dependent variable,  $(-\log \text{LD}_{50})^{-0.5}$ , was chosen for trial. This transformation depends entirely on the distribution of  $-\log \text{LD}_{50}$  and utilizes no knowledge of the predictor variables.

Table II summarizes the results of all the regression analyses run with  $(-\log \text{LD}_{50})^{-0.5}$  as the dependent variable. Use of all 26 observations with  $F = 3$  to add and to remove a variable gave an adjusted  $R^2$  of only 0.5359 (Entry 1). Setting  $F\text{-to-add} = 1$  (Entry 5) added another predictor variable and improved adjusted  $R^2$  slightly. Equation 4 represents the best result obtained in the present study with all 26 compounds.

$$-2.5926 C3 + 5.7211 P/C4 + 0.3387 P2v - 4.4500 P6v - 5.7322 P/C4v + 0.5586$$

$$n = 26; s = 0.3337; \text{adj}R^2 = 0.5527; F = 7.177 \quad (4)$$

Because of mechanistic considerations, ref. 1 also looked at a subset ( $n = 21$ ) of the data (Entry 33). Table III shows which subsets of compounds correspond to the entries in Table II. With this subset, the MCI correlations (Entry 4) came somewhat closer to matching ref. 1 in adjusted  $R^2$ , resulting in Equation 5.

$$1.8821 P3 - 1.9983 P4 - 1.9081 P5 - 1.0890 P/C4 + 0.4752$$

$$n = 21; s = 0.2728; \text{adj}R^2 = 0.7044; F = 12.914 \quad (5)$$

Once again, however, as stated above, the standard error in Equation 5 is actually much larger than the one from ref. 1 because the former is the error in the transformed variable.

Using a technique described more fully below, a visual search was made for correlations between the dependent variable and various sets of two MCIs. Table II, Entry 6, is the most successful of these attempts, and with  $n = 15$  and adjusted  $R^2 = 0.6353$ , even that is not outstanding.

**Principal Component Analyses.** In a few words, principal component analysis (PCA) redefines an  $n$ -space in terms of  $n$  mutually orthogonal axes. Each axis is a linear combination of the underlying  $n$  variable axes. The coefficients, or loadings, of the  $n$  variable axes are normalized so that the sum of the squares of the loadings is 1 for each principal component axis. In addition, the origin in principal component space is placed at that point on the first principal component axis such that the mean of the first principal component scores is zero. Thus, PCA does not alter the constellation of data points, but merely describes the data in terms of a different set of axes. The main advantage of PCA is that it often concentrates the variability of the dataset into the first few principal components, thus reducing the effective dimensionality of any subsequent analysis. In the present case, the first four principal components accounted for >99% (covariance

Table II. Results of regression analyses

Entry	<i>n</i>	Predictors <sup>a</sup>	Adjusted <i>R</i> <sup>2</sup>	RMSE <sup>b</sup>	Equation #
1	26	C3, P/C4, P6v, P/C4v	.5359	.3400	
2	25	C3, P/C4, P6v, P/C4v	.6071	.3072	
3	24	P/C4, P0v, P3v, P/C4v	.6633	.2854	
4	21	P3, P4, P5, P/C4	.7044	.2728	5
5	26	C3, P/C4, P2v, P6v, P/C4v	.5527	.3337	4
6	15	P1, P2v	.6353	.1754	
7	26	PCV1, PCV2, PCV3, PCV4	.0922	.4754	
8	19	PCV1, PCV2, PCV3, PCV4	.6759	.2355	
9	13	PCV1, PCV2	.7723	.2170	
10	11	PCV1, PCV2	.7019	.1064	
11	12	PCV3, PCV4	.5394	.1801	
12	14	PCV3, PCV4	.9024	.1436	7
13	26	PCR1, PCR2, PCR3, PCR4	.0808	.4784	
14	19	PCR1, PCR2, PCR3, PCR4	.6529	.2437	
15	17	PCR1, PCR2	.6607	.2817	
16	6	PCR1, PCR2	.5621	.1103	
17	20	PCR1, PCR3	.4985	.3129	
18	20	PCR1, PCR4	.5537	.2952	
19	17	PCR1, PCR3	.6207	.2280	
20	17	PCR1, PCR4	.6322	.2246	
21	16	PCR1, PCR3	.6632	.2213	
22	16	PCR1, PCR4	.6958	.2103	
23	18	PCR2, PCR4	.7066	.2694	
24	15	PCR2, PCR4	.8842	.1848	8
25	12	PCR3, PCR4	.8468	.1636	
26	11	PCR3, PCR4	.9340	.1124	
27	10	PCR3, PCR4	.9707	.0798	9
28	15	PCR3, PCR4	.8517	.1908	
29	9	PCR3, PCR4	.9934	.0412	
30	7	PCR3, PCR4	.9983	.0217	
31	15	(ln $k_{\alpha \text{ corr}}$ + 5.5) <sup>1,3</sup>	.9273	.1349	10
32 <sup>c</sup>	26	(log <i>P</i> ) <sup>2</sup> , log <i>P</i> , ln $k_{\alpha \text{ corr}}$	.685	.35 <sup>d</sup>	
33 <sup>c</sup>	21	(log <i>P</i> ) <sup>2</sup> , log <i>P</i> , ln $k_{\alpha \text{ corr}}$	.776	.29 <sup>d</sup>	

<sup>a</sup> PCV = principal components derived from covariance matrix; PCR = principal components derived from correlation matrix. <sup>b</sup> Root mean standard error of the estimate of (-log LD<sub>50</sub>)<sup>-0.5</sup>. <sup>c</sup> from ref. 1. <sup>d</sup> Root mean standard error of the estimate of -log LD<sub>50</sub>.

Table III. Observations used in regression analyses

Entry	1	2	3	4	5	6	7	8	9	10	11	12	13	14	15	16	17	18	19	20	21	22	23	24	25	26
<i>Observation</i>																										
2	✓	✓	✓	✓	✓	✓	✓	✓	✓	✓	✓	✓	✓	✓	✓	✓	✓	✓	✓	✓	✓	✓	✓	✓	✓	✓
3		✓	✓	✓	✓	✓	✓	✓	✓	✓	✓	✓	✓	✓	✓	✓	✓	✓	✓	✓	✓	✓	✓	✓	✓	✓
4,33	✓	✓	✓	✓	✓	✓	✓	✓	✓	✓	✓	✓	✓	✓	✓	✓	✓	✓	✓	✓	✓	✓	✓	✓	✓	✓
6		✓	✓	✓	✓	✓	✓	✓	✓	✓	✓	✓	✓	✓	✓	✓	✓	✓	✓	✓	✓	✓	✓	✓	✓	✓
8,14		✓	✓	✓	✓	✓	✓	✓	✓	✓	✓	✓	✓	✓	✓	✓	✓	✓	✓	✓	✓	✓	✓	✓	✓	✓
9		✓	✓	✓	✓	✓	✓	✓	✓	✓	✓	✓	✓	✓	✓	✓	✓	✓	✓	✓	✓	✓	✓	✓	✓	✓
10				✓	✓	✓	✓	✓	✓	✓	✓	✓	✓	✓	✓	✓	✓	✓	✓	✓	✓	✓	✓	✓	✓	✓
11				✓	✓	✓	✓	✓	✓	✓	✓	✓	✓	✓	✓	✓	✓	✓	✓	✓	✓	✓	✓	✓	✓	✓
12		✓	✓					✓		✓	✓	✓	✓	✓	✓	✓	✓	✓	✓	✓	✓	✓	✓	✓	✓	✓
15		✓	✓	✓	✓	✓	✓	✓	✓	✓	✓	✓	✓	✓	✓	✓	✓	✓	✓	✓	✓	✓	✓	✓	✓	✓
16	✓								✓	✓										✓						✓
17,18		✓	✓	✓	✓	✓	✓	✓	✓	✓		✓	✓	✓	✓	✓	✓	✓	✓	✓	✓	✓	✓	✓	✓	✓
19,20		✓	✓	✓	✓	✓	✓	✓	✓	✓		✓	✓	✓	✓	✓	✓	✓	✓	✓	✓	✓	✓	✓	✓	✓
21,22		✓	✓	✓	✓	✓	✓	✓	✓	✓		✓	✓	✓	✓	✓	✓	✓	✓	✓	✓	✓	✓	✓	✓	✓
23		✓	✓	✓	✓	✓	✓	✓			✓	✓	✓	✓	✓	✓	✓	✓	✓	✓	✓	✓	✓	✓	✓	✓
24		✓	✓	✓	✓	✓	✓	✓			✓	✓	✓	✓	✓	✓	✓	✓	✓	✓	✓	✓	✓	✓	✓	✓
25		✓	✓	✓	✓	✓	✓	✓				✓	✓	✓	✓	✓	✓	✓	✓	✓	✓	✓	✓	✓	✓	✓
26		✓	✓	✓	✓	✓	✓	✓				✓	✓	✓	✓	✓	✓	✓	✓	✓	✓	✓	✓	✓	✓	✓
27		✓		✓		✓	✓						✓	✓	✓	✓	✓	✓	✓	✓	✓	✓	✓	✓	✓	✓
28			✓					✓	✓	✓			✓	✓	✓	✓	✓	✓	✓	✓	✓	✓	✓	✓	✓	✓
29			✓					✓	✓	✓			✓	✓	✓	✓	✓	✓	✓	✓	✓	✓	✓	✓	✓	✓
30			✓						✓	✓			✓	✓	✓	✓	✓	✓	✓	✓	✓	✓	✓	✓	✓	✓
31	✓	✓		✓	✓	✓	✓	✓	✓	✓	✓		✓	✓	✓	✓	✓	✓	✓	✓	✓	✓	✓	✓	✓	✓

matrix) or >97% (correlation matrix) of the variability in the data. The loadings for these principal components are listed in Table IV. Thus, the dimensionality of this problem was effectively reduced from 26 to 4. For this reason, no attempt was made to run stepwise multiple regression with the entire set of principal components. An effect of the difference between the two approaches in weighting the underlying variables is apparent by inspection of the higher-order MCI entries. MCIs numbered higher than 3 make little contribution to any of the PCV axes, but contribute substantially to PCR1-3.

Table IV. Principal component loadings

MCI	PCV1	PCV2	PCV3	PCV4	PCR1	PCR2	PCR3	PCR4
P0	.5097	-.0226	-.2106	.5603	.2118	-.1809	.1276	-.3227
P1	.3719	-.2025	-.3242	.1459	.2191	-.1807	.0466	-.3096
P2	.2903	-.216	.3168	.24	.2336	-.069	.1337	-.2595
P3	.219	-.3516	.0398	-.1265	.2379	-.0707	-.0062	-.1924
P4	.1723	-.4024	-.0393	-.2045	.2369	-.0581	-.0925	-.2719
P5	.1304	-.3471	.0063	-.2533	.2374	-.032	-.1174	-.1642
P6	.0635	-.1258	-.0748	-.0946	.2217	-.1204	-.1177	-.0073
C3	.0132	.0156	.3762	.1581	.0773	.2607	.39	.0456
P/C4	.0201	-.0843	.3801	.0305	.1258	.292	.2251	.2105
P/C5	.0317	-.1993	.2739	-.111	.1886	.2644	-.008	.0284
P/C6	.0367	-.2636	.1922	-.182	.2004	.2134	-.1517	-.0343
CH6	.0045	-.04	.0158	-.0341	.1915	.1821	-.2574	.0626
CH7	.0032	-.0282	.0111	-.0241	.1915	.1821	-.2574	.0626
P0v	.4678	.431	.1437	-.1439	.2039	-.1847	.1993	-.0166
P1v	.3185	.309	-.1067	-.3839	.1998	-.2181	.148	.068
P2v	.2334	.2694	.3641	-.0917	.2017	-.1266	.2654	.0934
P3v	.1597	.0598	-.0214	-.3139	.2145	-.1798	.1006	.1564
P4v	.1045	-.0165	-.0816	-.2512	.2184	-.1916	.0091	.1779
P5v	.0607	-.0367	-.0568	-.1816	.2186	-.1758	-.0448	.332
P6v	.0263	.0056	-.0492	-.086	.1822	-.2379	-.0307	.5864
C3v	.0088	.0348	.3073	.1401	.059	.2435	.419	.0126
P/C4v	.0125	-.0252	.2308	.0431	.119	.2818	.3074	.0517
P/C5v	.0135	-.0667	.1205	-.0236	.1871	.2609	.0666	-.0524
P/C6v	.0112	-.0741	.0583	-.049	.2015	.209	-.1296	-.0342
CH6v	.0014	-.0125	.005	-.0107	.1915	.1821	-.2574	.0626
CH7v	.001	-.009	.0036	-.0077	.1915	.1821	-.2574	.0626

Not unexpectedly, there was no good correlation between  $(-\log LD_{50})^{0.5}$  and any single principal component. Contrary to expectations, however, the first four principal components together were poor predictors of the dependent

variable (Table II, Entries 7 and 13), notably less successful than the underlying MCIs. An approach taken in ref. 1 to improve correlation was to work with only a subset of the compounds. The present study also utilized that approach, but where ref. 1 defined the subset first and then looked at correlations, here well-correlated subsets of data points were found without prior reference to structural or mechanistic considerations.

**Correlations with two principal components.** The existence of a set of nearly coplanar points in 3-space implies a least-squares Equation 6:

$$aX + bY + cZ + d = 0 \quad (6)$$

The three-dimensional, on-screen graphics capabilities of SCOUT make it very easy to rotate a cloud of data points to search for such planes visually. It is further possible with SCOUT to color to enumerate the relevant observations and delete the remainder from the graph. An example is shown in Figure 1.

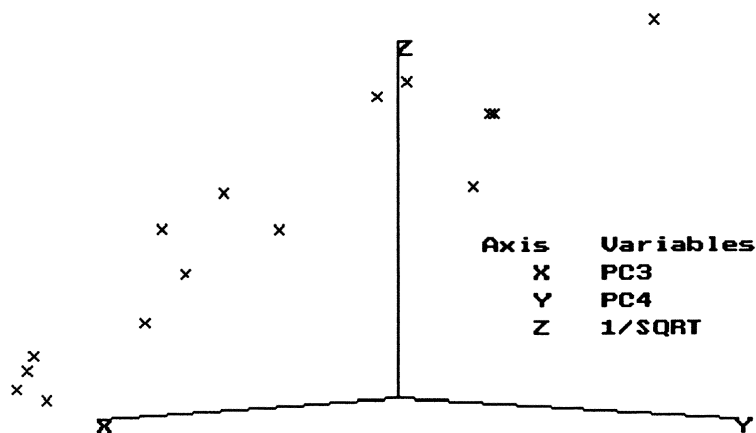


Figure 1. 3-D plot from SCOUT.  $1/\text{SQRT}$  is  $(-\log LD_{50})^{-0.5}$

In the present study, because of intercorrelations, one needed also to be aware that many planes exist parallel to the dependent variable axis  $Z$ , a situation corresponding to  $c = 0$  in Equation 6. These planes contain no information about the dependent variable.

Many subsets were found to exhibit correlation with two principal components, and the results are shown in Table II. Of particular note are Entries 12, 24, and 27. The compounds making up the subsets may be found in Table III. Comparisons among the data in Tables II and III reiterate the point that adjusted  $R^2$  does not necessarily increase when the ratio of the number of predictor

variables to the number of observations increases. Table II, Entry 12, resulted in Equation 7,

$$0.8172 \text{ PCV3} - 0.6625 \text{ PCV4} + 2.7122$$

$$n = 14; s = 0.1436; \text{adj}R^2 = 0.9024; F = 61.123 \quad (7)$$

Entry 24 in Equation 8,

$$0.2036 \text{ PCR2} - 0.2852 \text{ PCR4} + 1.0045$$

$$n = 15; s = 0.1848; \text{adj}R^2 = 0.8842; F = 54.475 \quad (8)$$

and Entry 27 in Equation 9:

$$- 0.4245 \text{ PCR3} + 0.1713 \text{ PCR4} + 0.4509$$

$$n = 10; s = 0.0789; \text{adj}R^2 = 0.9707; F = 150.343 \quad (9)$$

In the cases of Equations 7 and 8, more than half of the compounds are represented. Table III shows that these two cases are by no means the same subset. With only two predictor variables, these correlations are 7 - 7.5 times overdetermined. Similarly, while Equation 9 represents fewer compounds, the error of the estimate is about half that of Equations 7 and 8, and adjusted  $R^2$  is much nearer 1.0. (The Equation 9 compounds are a subset of those in Equation 8.) Keeping in mind that two sets of four principal components were derived entirely from structural considerations involving all 26 compounds, it stretches this author's imagination to believe that the correlations represented by these last three equations are chance occurrences. On the other hand, comparison of Tables I and III does not suggest any obvious structural features that distinguish the compounds that are represented in the correlations from those that are not.

It is also curious that the best correlations in Table II seem not to involve a first principal component axis. This phenomenon may be coincidental, although the author has submitted for publication elsewhere another study, involving different graph theoretical parameters, differently functionalized compounds, and a different target organism, in which the same phenomenon was observed.

**Transformation of  $\log P$  and  $\ln k_{a \text{ corr}}$**  Following the success with transforming the dependent variable, the question arose whether transforming the independent variables from ref. 1 would lead to better correlations. Power transformations of  $\log P$ , which of course includes  $(\log P)^2$ , did not produce any apparent improvements. The Kolmogorov-Smirnov value for  $(\ln k_{a \text{ corr}})^n$ , however, optimized at  $n = 1.3$ , and this transformed variable showed an obvious correlation with a subset of the compounds (Table II, Entry 31). The actual transformation used was  $(\ln k_{a \text{ corr}} + 5.5)^{1.3}$  because the power transformation demands that all values be  $\geq 0$ . The resulting correlation for 15 compounds is shown in Figure 2. The observations made above for the principal component correlations apply here as well.

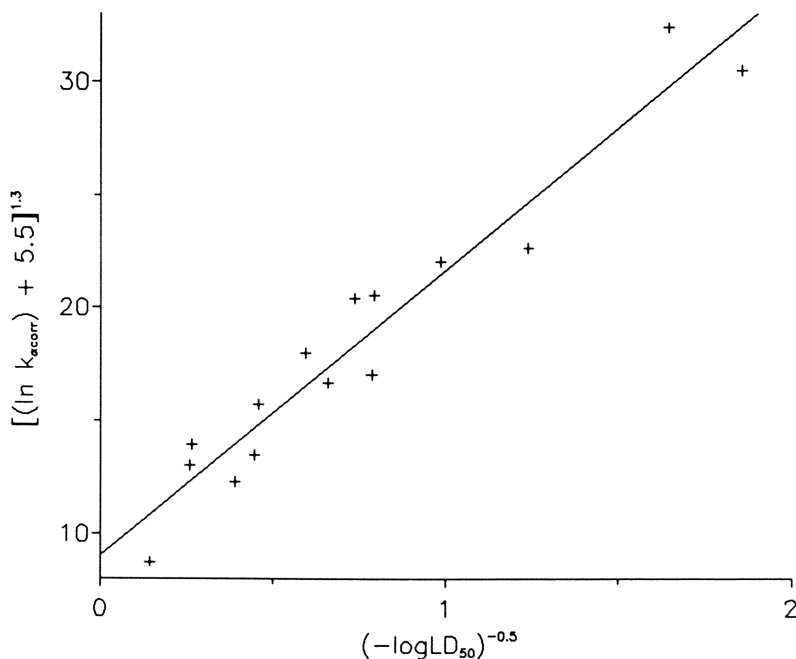


Figure 2. Univariate correlation of transformed variables.

The equation illustrated in Figure 2 is Equation 10:

$$0.0139 (\ln k_{\alpha \text{corr}} + 5.5)^{1.3} - 0.6162$$

$$n = 15; s = 0.1349; \text{adj}R^2 = 0.9273; F = 179.700 \quad (10)$$

## Conclusions

Transformation of both dependent and independent variables according to the Kolmogorov-Smirnov optimization procedure, even with a dataset of modest size ( $n = 26$ ), revealed correlations that would otherwise have been missed. Predictions made by the best correlations are listed in Table V. With software readily available to perform that optimization, the technique may find further use in QSAR studies. Visual searching for well-correlated subsets of data offers some advantage over simply removing sequentially the data points with the largest residuals, since the former technique in some cases revealed two correlation planes with a large dihedral angle in the same space. On the other hand, the visual technique is limited to 3-space. This study uncovered several good correlations within the principal component spaces derived from MCI space, but no correlation equation was applicable to either the entire dataset or a structurally distinct subset.

It is the author's belief that this study clearly indicates that graph theoretical parameters contain information capable of predicting acute toxicity, but much work remains to be done to define precisely where that information resides and what restrictions might apply to its use.

**Table V. Observed and Predicted Values of (-log LD<sub>50</sub>)**

Obs. #	Exp. <sup>a</sup>	Eqn. 4	Eqn. 5	Eqn. 7	Eqn. 8	Eqn. 9	Eqn. 10
1	6.55	2.49	4.43				11.81
2	0.65	1.87	0.50	0.58	0.57	0.77	0.90
3	0.57	1.33	0.83	0.62	0.93		
4	2.30	1.03	1.56		1.66	2.70	2.64
5	4.77	1.36	1.93		2.84	4.02	3.35
6	14.09	8.91	4.40		7.98	8.81	5.83
7	14.79	251.95	7.89		18.26	15.02	8.35
8	0.37	0.43	0.41	0.37	0.37		0.32
9	2.80	2.97	2.46				
10	5.02	23.56	11.49				7.00
11	0.29	0.28	0.28	0.33	0.37		0.37
12	1.80	1.90	0.83	1.52	0.87		
13	1.62	1.43	1.56	1.71	1.60	1.82	2.41
14	2.83	1.31	1.93	1.91	3.51	3.26	1.97
15	1.59	1.47	2.81	2.07			1.23
16	1.03	2.39	4.40	2.23			0.97
17	1.84	1.79					1.26
18	0.57	1.27	0.83	0.55	0.94		
19	0.52	0.98	1.56	0.55			
20	15.30	4.94	11.49				
21	19.40	6.96	8.86				
22	27.50	2.03	4.40	6.47	92.46	14.57	
23	1.00	1.65		1.00	0.89	1.13	
24	0.39	0.45		0.32	0.33	0.34	
25	0.89	0.76					
26	48.72	1.67					1111.11

<sup>a</sup> From ref. 1.**Literature Cited**

1. Grogan, J.; DeVito, S. C.; Pearlman, R. S.; Korzekwa, K. R. *Chem. Res. Toxicol.* **1992**, *5*, 548-552.
2. Kubinyi, H. *Progr. Drug Res.* **1979**, *23*, 97-198.
3. Randić, M. *J. Amer. Chem. Soc.* **1975**, *97*, 6609.
4. Kier, L. B.; Hall, L. H. *Molecular Connectivity in Chemistry and Drug Research*; Academic Press: New York, NY, 1976.
5. Kier, L. B.; Hall, L. H. *Eur. J. Med. Chem.* **1975**, *64*, 307.
6. Kier, L. B.; Hall, L. H. *J. Pharm. Sci.* **1976**, *65*, 1806.
7. Neter, J.; Wasserman, W. *Applied Linear Statistical Models*; Richard C. Irwin, Inc.: Homewood, IL, 1974, p. 229.

RECEIVED September 17, 1993

## Chapter 6

# Computer-Aided Molecular Modeling for Development of Biomarkers for Human Exposure to Pesticides

Mahmoud A. Saleh<sup>1</sup>, Cecil Wallace, Jr.<sup>1</sup>, and Jerry N. Blancato<sup>2</sup>

<sup>1</sup>Environmental Chemistry and Toxicology Laboratory, Department  
of Chemistry, Texas Southern University, Houston, TX 77004

<sup>2</sup>Exposure Assessment Research Division, Environmental Monitoring  
Systems Laboratory, U.S. Environmental Protection Agency, P.O. Box  
93478, Las Vegas, NV 89193-3478

A molecular modeling and computer graphics study has been conducted on a group of insecticides including 50 bicycloorthocarboxylates, 12 bicyclophosphorus esters and 20 chlorinated insecticides which are known to have a common mode of action, i.e., binding to the gamma-aminobutyric acid chloride channel receptor. Three-dimensional steric and electrostatic fields were correlated with each compound's toxicological properties using comparative molecular field analysis. Toxicological potencies were strongly influenced by the nature and orientation of the substituent groups, molecular volume and dipole moment. Also described are models for predicting binding affinity to the receptor and for predicting acute mammalian toxicity. These chemicals may serve as useful probes for elucidation of the topography of the binding sites of the receptor and provide leads in the design of new compounds with more potent insecticidal activity and selectivity.

Development of biomarkers for human exposure to insecticides which are both sensitive and selective is needed. This goal may be more efficiently realized when more in-depth knowledge of the mode of action at the molecular level and the essential structural characteristics of the biomarker and toxic chemical are realized. It has been demonstrated on many occasions that the molecular interactions of a chemical, e.g., a drug or insecticide, with the effector (receptor, enzyme, membrane, RNA, DNA etc.) are not dependent upon covalent bonding. Rather, they are primarily shape-dependent; therefore, only steric and electrostatic forces may account for a great variety of observed biological and toxicological properties (1-3). Thus, models that provide suitable sampling of the steric and electrostatic fields surrounding a set of ligand (insecticide) molecules might provide the necessary information for understanding the binding requirement of the chemical

to the active site of the receptor. Recently a large group of chemicals of diverse chemical structures were shown to have high affinity for the GABA receptor-ionophore complex (4-6). This group consisted of three major chemical categories: bicycloorthocarboxylates, bicyclopophosphorus esters, and some chlorinated hydrocarbon insecticides. Their toxicological properties and binding affinity for the GABA receptor were studied extensively (4,5,7-11). These studies provide a basis for developing models correlating shape and size of molecules to receptor binding and toxicity.

In the present study, the concept of comparative molecular field analysis (CoMFA) was used to correlate receptor binding and mammalian toxicity of the three groups to their steric and electrostatic forces using the QSAR molecular modeling program of SYBYL (Tripos Associate). Except in a few cases, the comparative molecular rigidity of the group of compounds allows the conformational variable about bond rotations to be neglected. Also evaluated was the ability of the constructed molecular model to predict the receptor binding constants and thus predict *in vivo* mammalian toxicity. A second approach to the prediction of receptor binding and mammalian toxicity also was used. Ordinary least squares regression and cross-validation techniques were employed to find how receptor binding and mammalian toxicity might be related to functions of molecular volume, molecular surface area, dipole moments, and strain energy.

## Material and Methods

**Compounds** The compounds included in this study, selected to reflect the great diversity in their structures and biological activities, represent three major classes of chemical structures. The first group contains the 2,6,7-trioxabicyclo[2.2.2]octane moiety as the basic common structure, with substituents at positions 1 and 4 of various steric and electronic properties (Figure 1, compounds 1-50). The second group contains either bicyclopophosphorothionate or bicyclopophosphate with different substituents at the four positions (Figure 1, compounds 51-62). The third group includes chlorinated insecticides of the cyclodienes, hexachlorocyclohexanes and three of the toxaphene isomers (Figure 2). Toxicological data on the selected chemicals were reported as mice LD<sub>50</sub> (mg/kg) and as their potency for inhibiting [<sup>35</sup>S]t-butyl-bicyclopophosphorothionate ([<sup>35</sup>S]TBPS) binding to the human brain receptor (IC<sub>50</sub>) were collected from the published literature (5,8,11).

**Molecular Modeling** All molecules used in this investigation were constructed using the SYBYL molecular modeling software of Tripos Associates, Inc. (St. Louis, MO) version 5.5 run on a Evans & Sutherland Unix Workstation. Building of molecules was carried out from standard molecular fragments followed by minimizing energy using minimum cleanup procedures. Charges on each individual atom of each molecule were calculated using the topological method of Gasteiger and Marsili (12). Because of the relative rigidity of all the molecules in this investigation, each compound was represented by a single conformer except hexachlorocyclohexane isomers. Conformation analysis was performed, and the

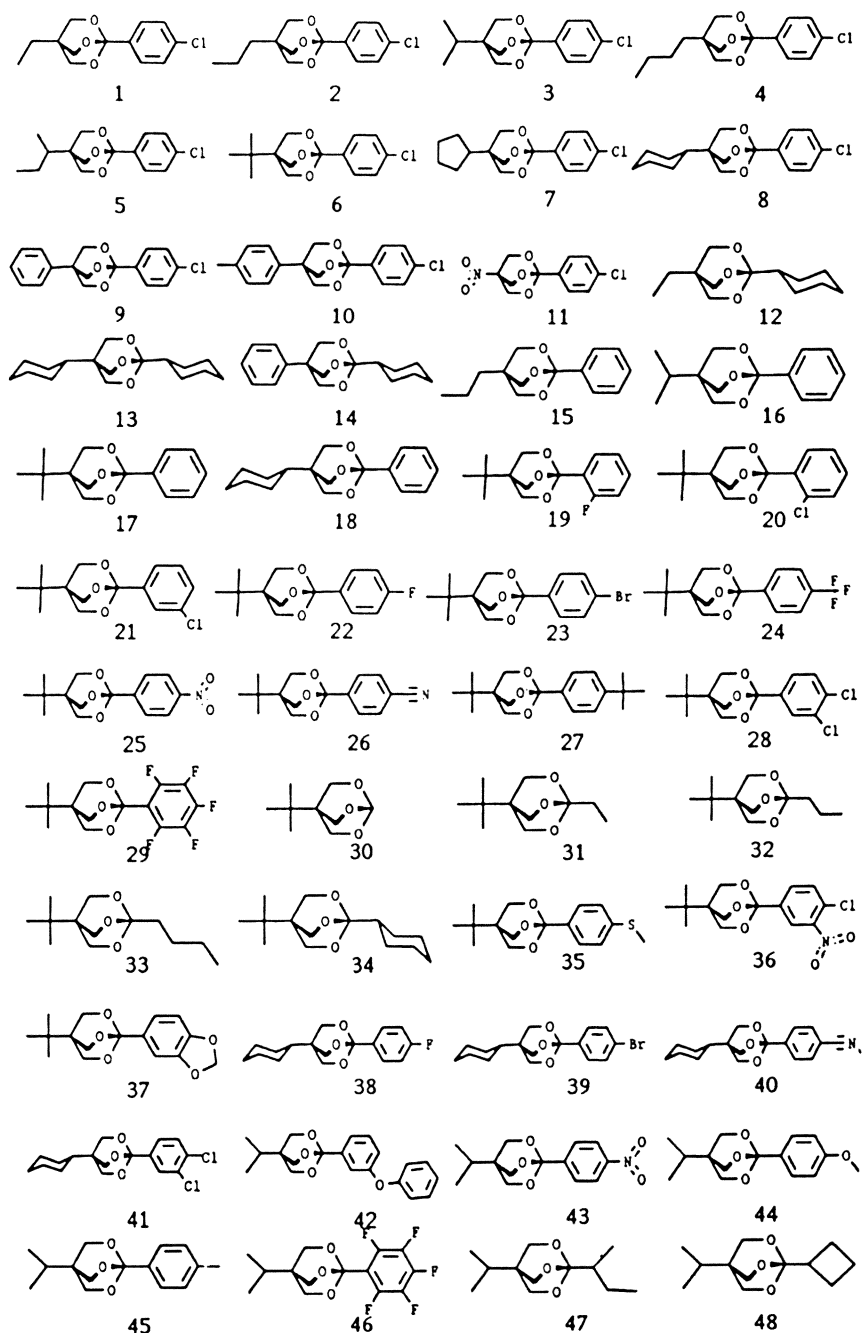


Figure 1. Bicycloorthocarboxylate and bicyclopophosphorus ester structures used to derive the CoMFA/QSARs.

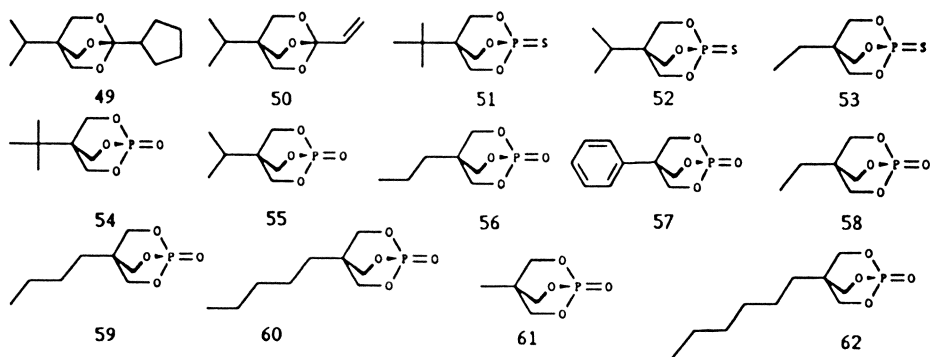


Figure 1. Continued.

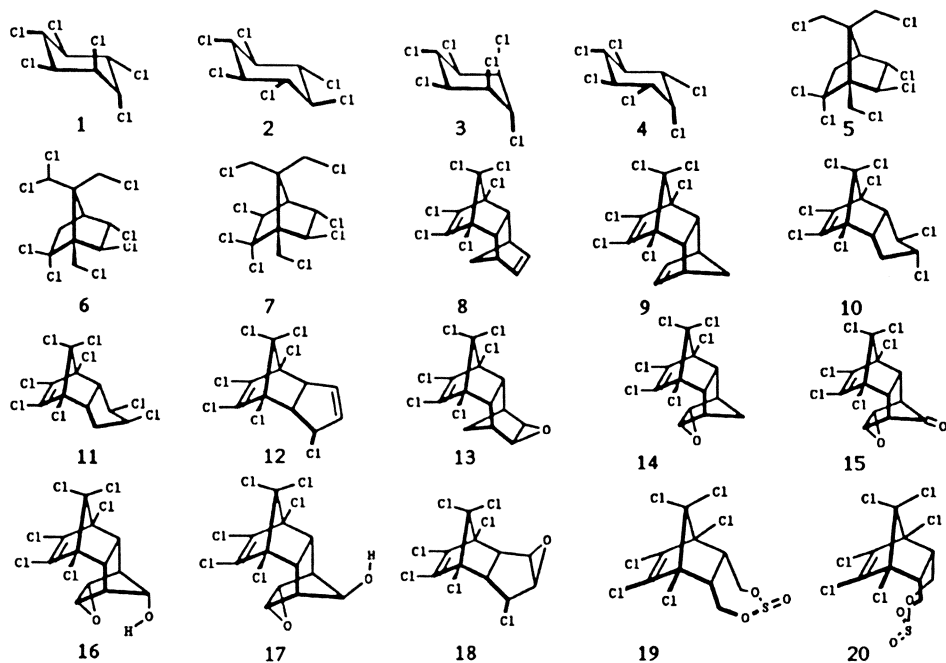


Figure 2. Chlorinated insecticide structures used to derive the CoMFA/QSARs.

most stable conformer was chosen for each isomer. In order to clearly study the effect of the shape and size of molecules on their biological activity, the basic structural unit of each group was fixed to a common orientation, and substituents were constructed consistently while retaining the orientation of the basic subunit.

**Energy Minimization and Calculation of Total Strain** All constructed molecules were subjected to energy minimization using the Maximin-2 molecular mechanics method within the SYBYL program and allowing bond length and valance angle to be adjusted simultaneously with variations of the torsional angles to achieve a minimum energy geometry. Total strain energy is then given for the most stable arrangement as described in the equation:

$$E = \sum E_{\text{str}} + \sum E_{\text{bend}} + \sum E_{\text{oop}} + \sum E_{\text{tors}} + \sum E_{\text{vdw}} + \sum E_{\text{ele}}$$

where the sums extend over all bonds, bond angles, torsion angles, and non-bonded interaction between atoms not bound to each other or to a common atom (i.e., 1,4-interactions and higher).

$E_{\text{str}}$  is the energy of bond stretched or compressed from its natural length.

$E_{\text{bend}}$  is the energy of bending bond angles from their natural values.

$E_{\text{oop}}$  is the energy of bending planar atoms out of the plane.

$E_{\text{tors}}$  is the torsional energy due to twisting about bonds.

$E_{\text{vdw}}$  is the energy due to Van der Waals non-bonded interactions.

$E_{\text{ele}}$  is the energy due to electrostatic interactions.

**Conformation Analysis** Conformation analysis of hexachlorocyclohexane isomers was performed using the search option for ring system which searches for allowed conformations from a steric point of view by screening Van der Waals' constant distances. Conformations are rejected if they contain interatomic distances shorter than the sum of the respective Van der Waals radii. Subsequently, energy calculations were performed for the valid search conformations using Maximin-2, and the most stable conformer of each isomer was chosen.

**Molecular Volume, Surface area and Dipole Moment** Volumes and surface areas of each individual molecule were calculated using mvolume and dots surface programs of advanced SYBYL, respectively. Dipole moments were calculated as total dipole moment and as its individual X, Y and Z components using the QSAR program of Sybyl.

**Molecular Alignment** The positioning of a molecular model within the fixed lattice is the most important input variable for comparing activities of different molecules due to the fact that relative interaction energies depend strongly on relative molecular orientation. Therefore, field fit was used to assure co-alignment of all molecules in each group of compounds. This was done using the root-mean squares fitting method (12). The bicycloorthocarboxylate group was aligned by fitting the 2,6,7-trioxabicyclo[2.2.2]octane unit and the first atom of the 1- and 4-substituents. The bicyclopophosphate group was aligned by fitting the bicyclopophosphate unit and the first atom of the 4-substituent. Cyclodiene insecticides were aligned by fitting the hexachlorobicycloheptane unit. Toxaphene and lindane isomers were best fitted manually.

**Comparative Molecular Field Analysis and Quantitative Structure Activity Relationship** The comparative molecular field analysis (CoMFA) method described by Cramer *et al.* (14) was performed for each group of the studied compounds using the logarithms of  $IC_{50}$  and  $LD_{50}$  as the bioactive variables. This procedure automatically calculates steric energy and electrostatic energy between the compound of interest and a "probe atom" placed at the various intersections of a regular three-dimensional lattice large enough to surround all the compounds in the series (14). The method of partial least-squares (PLS) regression (15,16) was used to extract the QSAR results. In a second approach to the development of quantitative structure activity relationships, ordinary least square regression and cross-validation procedures were employed to estimate prediction equations for log ( $IC_{50}$ ) and log ( $LD_{50}$ ). In this case, the predictor variables used were the non-CoMFA molecular properties: molecular volume, molecular surface area, dipole moments, and strain energy.

## Results and Discussion

**Structure, Energy and Orientation** Structural fit and alignment orientation of all molecules from the three groups was carried out prior to any analysis. This fit orientation allowed the structures to be locked in some relative orientation and vary the size and the physicochemical properties of substituents varied at one fixed point; i.e., relative to the basic structural unit in each group. The bicycloorthocarboxylates and bicyclophosphorus esters were fit to the bicyclooctane framework, while hexachlorobicycloheptane was used to fit cyclodiene insecticides. Molecular volume, dipole moment, strain energy and biological activities are shown in Table 1 for bicycloorthocarboxylates and bicyclophosphorus esters and in Table 2 for chlorinated insecticides. Total strain energy is expressed by the sum of bond distortions, torsional energy, and Van der Waals' interaction. By examining the individual components of energy, it was found that bonding distortion and torsional energy were the most important factors in increasing the total energy of the compound. Hydrogen bonding in the *syn*-12-hydroxyendrin lowered the energy of the molecule by about 2.2 k cal/mole relative to the *anti* isomer in which intramolecular hydrogen bonding is not possible. Conformation analysis of the hexachlorocyclohexane isomers revealed that the half boat conformation is the most stable conformation for the  $\gamma$ -isomer (lindane). Other isomers ( $\alpha$ ,  $\beta$ , and  $\delta$ ) were most stable in the chair form (Figure 3). Since the  $\gamma$ -isomer is the most toxic, this difference in molecular conformation may play a role in its toxicity and therefore its binding to the receptor.

**Predictivity of Structure-Activity Relationship** The most important finding in this study is the ability of the model to predict the activity of unknown compound as expressed by the predictive or cross-validated  $r^2$  shown in Tables 3 and 4 for both  $IC_{50}$  and  $LD_{50}$  of each group. The "crossvalidated  $r^2$ " or "predictive  $r^2$ " is defined as:

Table 1. PHYSIOCHEMICAL PROPERTIES AND BIOLOGICAL ACTIVITIES OF BICYCLOORTHOXYCARBOXYLATES AND BICYCLOPHOSPHATES

Compound Number	Volume ( $\text{\AA}^3$ )	Surface Area	Dipole Moments				Strain Energy (k cal/mole)	LD <sub>50</sub> (mg/kg)	IC <sub>50</sub> (nM)
			X	Y	Z	D <sup>a</sup>			
1	204.2	2789	-1.54	-3.82	1.58	4.41	15.579	13	413
2	221.1	3016	-1.54	-3.83	1.55	4.41	16.110	9.1	176
3	220.4	3024	-1.70	-3.74	1.61	4.42	17.347	2.3	45
4	237.5	3240	-1.55	-3.82	1.56	4.40	16.330	50	200
5	237.1	3258	-1.76	-3.70	1.60	4.40	19.176	2.5	6
6	237.2	3266	-1.59	-3.71	1.73	4.39	20.225	1.1	7
7	243.3	3282	-1.58	-3.47	2.08	4.34	25.771	6.1	21
8	259.6	3485	-1.33	-3.73	1.88	4.38	18.613	52	13
9	236.4	3189	-1.50	-3.63	1.69	4.27	16.656	54	100
10	252.7	3418	-1.54	-3.73	1.73	4.39	16.991	1000	100000
11	188.9	2627	-0.65	-1.45	0.54	1.67	15.562	150	100000
12	213.9	2915	-1.07	-2.55	1.16	3.00	14.696	170	100000
13	269.2	3602	-0.83	-2.78	-0.97	3.06	18.192	42	217
14	246.0	3310	-0.78	-2.68	-0.88	2.93	16.929	150	3500
15	209.0	2838	-1.14	-2.83	1.08	3.23	16.538	10	1500
16	208.3	2846	-1.31	-2.74	1.14	3.24	17.778	5.9	692
17	225.0	3087	-1.20	-2.70	1.26	3.21	20.659	1.3	49
18	247.4	3307	-0.93	-2.72	1.41	3.2	19.043	5.6	41
19	227.2	3136	-2.41	-1.20	1.18	2.94	20.550	0.7	16
20	236.0	3237	-1.93	-1.80	1.24	2.92	21.758	12	95
21	236.6	3267	-2.30	-2.78	1.68	3.98	20.201	1.6	13
22	227.2	3153	-1.83	-4.36	2.04	5.15	20.368	0.77	42
23	242.4	3337	-1.49	-3.46	1.62	4.10	20.207	1.2	10
24	248.8	3511	-1.91	-4.52	2.13	5.35	20.323	38	92
25	242.3	3368	-2.03	-4.86	2.27	5.73	22.525	2.9	55

<sup>a</sup> D =  $(X^2 + Y^2 + Z^2)^{0.5}$  = total dipole moment

Table 1. Continued

Compound Number	Volume (Å <sup>3</sup> )	Surface Area	Dipole Moments				Strain Energy (k cal/mole)	LD <sub>50</sub> (mg/kg)	IC <sub>50</sub> (nM)
			X	Y	Z	D <sup>a</sup>			
26	240.4	3329	-1.91	-4.55	2.13	5.38	20.315	0.06	5
27	289.8	3994	-1.10	-2.46	1.24	2.97	23.102	84	2200
28	248.7	3437	-2.68	-3.78	2.15	5.11	19.805	0.88	10
29	229.6	3401	-1.87	-4.41	2.06	5.21	19.334	1.1	8
30	158.9	2912	-1.13	-2.48	1.16	3.41	20.085	9.5	7200
31	191.6	2680	-1.09	-2.51	1.15	2.97	22.971	145	100000
32	208.4	3142	-1.14	-2.46	1.18	2.96	23.443	13	1150
33	224.9	3368	-1.13	-2.55	1.26	2.96	23.628	1.4	118
34	247.4	3254	-3.86	-3.91	2.44	3.06	19.332	25	970
35	241.2	3316	-1.69	-2.68	2.14	3.82	17.323	200	10000
36	237.7	3372	-1.59	-4.37	2.18	6.01	19.766	9.0	45
37	229.0	3101	-1.67	-3.23	2.22	4.26	30.005	200	2660
38	249.6	3372	-1.59	-4.37	2.18	5.14	18.758	3.5	21
39	264.6	3994	-1.67	-4.57	2.27	4.09	18.594	4.8	19
40	262.7	3653	-2.43	-3.79	2.28	5.37	18.701	0.6	10
41	271.0	3803	-2.21	-1.36	1.46	5.04	18.184	39	50
42	280.5	3803	-2.21	-1.36	1.46	2.98	21.579	200	1100
43	225.7	3126	-2.14	-4.87	2.15	5.74	19.788	8.5	255
44	232.0	3210	-2.77	-2.67	1.86	4.27	20.030	25	706
45	224.5	3070	-1.27	-2.64	1.09	3.12	18.257	25	684
46	219.7	3161	-1.96	-4.38	1.98	5.19	16.540	3.5	26
47	209.1	2915	-1.17	-2.48	1.00	2.92	20.666	500	100000
48	198.4	2736	-1.20	-2.60	1.15	3.08	49.550	375	100000
49	214.7	2912	-1.28	-2.58	1.11	3.09	26.531	150	10000
50	167.9	2357	-1.26	-2.76	1.16	3.25	17.750	150	100000
51	171.5	2365	3.78	0.84	-0.87	3.97	18.113	0.05	20

<sup>a</sup> D = (X<sup>2</sup> + Y<sup>2</sup> + Z<sup>2</sup>)<sup>0.5</sup> = total dipole moment*Continued on next page*

Table 1. Continued

Compound Number	Volume (Å <sup>3</sup> )	Surface Area	Dipole Moments				Strain Energy (k cal/mole)	LD <sub>50</sub> (mg/kg)	IC <sub>50</sub> (nM)
			X	Y	Z	D <sup>a</sup>			
52	155.3	2168	3.69	0.93	-0.66	3.86	16.421	0.26	400
53	138.8	1949	3.62	0.69	-0.63	3.74	15.033	1.28	2000
54	167.6	2316	5.56	1.23	-1.27	5.84	18.925	0.035	200
55	151.4	2113	5.50	1.00	-1.25	5.72	17.219	0.2	600
56	151.0	2113	5.53	1.00	-0.86	5.69	16.395	0.45	1000
57	166.3	2288	5.32	1.10	-1.21	5.57	17.354	1.90	2000
58	135.1	1895	5.39	1.09	-1.04	5.60	15.824	1	6500
59	167.2	2343	5.42	1.09	-1.05	5.63	16.413	1.9	6500
60	183.8	2568	5.43	1.09	-1.05	5.63	16.640	15	90000
61	117.9	1667	5.21	1.16	-1.20	5.47	14.594	30	90000
62	200.1	2789	5.45	1.08	-1.01	5.64	16.715	350	90000

<sup>a</sup> D = (X<sup>2</sup> + Y<sup>2</sup> + Z<sup>2</sup>)<sup>0.5</sup> = total dipole moment

Table 2. PHYSIOCHEMICAL PROPERTIES AND BIOLOGICAL ACTIVITIES OF  
SELECTED CHLORINATED INSECTICIDES

Compound Number	Volume (Å <sup>3</sup> )	Surface Area	Dipole Moments				Strain Energy (k cal/mole)	LD <sub>50</sub> (mg/kg)	IC <sub>50</sub> (nM)
			X	Y	Z	D <sup>a</sup>			
1	169.9	2409	-0.23	-1.42	0.77	1.87	-2.513	200	10000
2	170.5	2416	-0.02	-0.01	-0.01	0.02	-2.879	200	10000
3	169.4	2386	1.42	0.10	0.82	1.64	6.037	40	1700
4	170.2	2406	1.15	-1.63	-0.31	1.99	-2.635	200	10000
5	237.9	3244	1.15	1.25	0.29	1.73	28.085	75	170
6	248.1	3342	2.22	2.08	-0.56	3.09	41.331	3.3	240
7	249.0	3362	0.17	1.64	0.77	1.82	28.701	100	3600
8	222.6	3001	-1.74	-1.42	0.66	2.34	43.259	49	8700
9	223.0	2962	-2.16	-1.39	0.72	2.66	41.850	14	1400
10	231.3	3194	-2.11	-0.91	0.22	2.31	27.860	1100	2600
11	231.4	3177	-0.63	0.19	-0.31	0.72	25.428	600	1800
12	211.3	2948	-0.92	-0.95	-0.18	1.33	21.187	130	7500
13	228.0	3190	-1.40	-1.63	0.00	1.76	153.259	47	1400
14	229.0	3094	-1.96	0.91	0.18	2.17	157.101	2.0	220
15	228.1	3091	0.52	1.93	-0.52	2.06	158.413	0.9	36
16	234.3	3149	-0.71	1.85	-0.27	2.00	157.836	3	43
17	235.4	3206	-0.46	1.28	-0.23	1.38	160.049	16	4400
18	218.4	3047	1.20	0.11	-0.34	1.25	138.918	60	980
19	226.1	3151	1.24	0.64	-0.43	1.47	24.728	76	100
20	226.4	3094	-5.22	0.49	0.98	5.33	23.603	240	1500

<sup>a</sup> D = (X<sup>2</sup> + Y<sup>2</sup> + Z<sup>2</sup>)<sup>0.5</sup> = total dipole moment

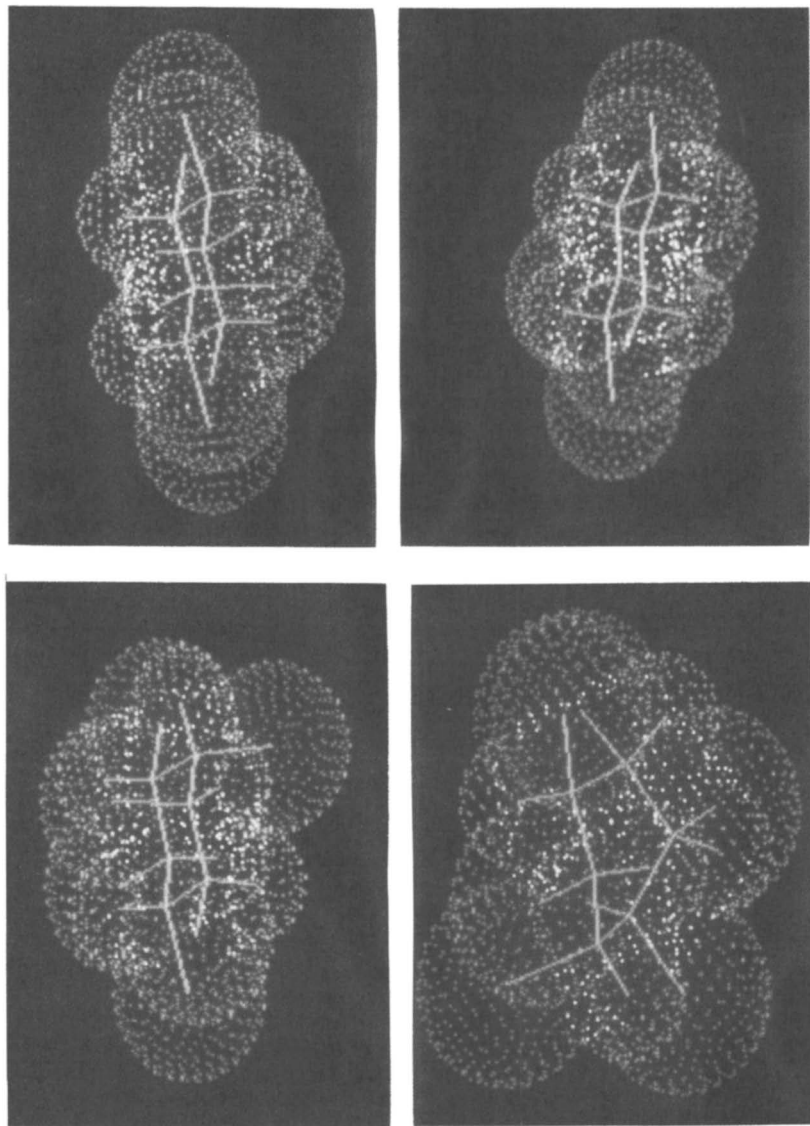


Figure 3. The low energy conformations of hexachlorohexane isomers. Arranged from left to right  $\alpha$ ,  $\beta$  (top),  $\gamma$ ,  $\delta$  (bottom).

Table 3. RESULTS FROM REGRESSIONS OF LOG(LD<sub>50</sub>) AND LOG(IC<sub>50</sub>) VALUES ON NON-CoMFA DATA

Group	Dependent	No. of Molecules	No. of Predictor	<u>Cross-validated</u>		<u>Conventional</u>	
	Variable			in Group	Variables	r <sup>2</sup>	s
<b>Bicycloorthocarboxylates</b>							
	Log(LD <sub>50</sub> )	36	8	0.479	0.500	0.592	0.442
	Log(IC <sub>50</sub> )	37	4	0.394	0.613	0.502	0.555
<b>Bicyclophosphates</b>							
	Log(LD <sub>50</sub> )	12	6	0.925	0.470	0.991	0.167
	Log(IC <sub>50</sub> )	12	4	0.852	0.552	0.936	0.362
<b>Chlorinated Insecticides</b>							
	Log(LD <sub>50</sub> )	14	5	0.872	0.346	0.975	0.152
	Log(IC <sub>50</sub> )	13	2	0.595	0.457	0.730	0.374

Table 4. RESULTS FROM PLS REGRESSIONS OF LOG(LD<sub>50</sub>) AND LOG(IC<sub>50</sub>) VALUES ON CoMFA DATA

Group	Dependent	No. of Molecules	No. of CoMFA	<u>Cross-validated</u>		<u>Conventional</u>	
	Variable			in Group	Components	r <sup>2</sup>	s
<b>Bicycloorthocarboxylates</b>							
	Log(LD <sub>50</sub> )	36	1	-0.110	0.650	0.224	0.543
	Log(IC <sub>50</sub> )	37	5	0.337	0.651	0.853	0.307
<b>Bicyclophosphates</b>							
	Log(LD <sub>50</sub> )	12	5	0.799	0.736	0.998	0.068
	Log(IC <sub>50</sub> )	12	7	0.864	0.700	0.996	0.126
<b>Chlorinated Insecticides</b>							
	Log(LD <sub>50</sub> )	14	4	0.406	0.658	0.883	0.292
	Log(IC <sub>50</sub> )	13	3	0.273	0.646	0.821	0.320

$$\text{Cross-Validated } r^2 = (\text{SD} - \text{press})/\text{SD},$$

where SD is the sum of squared deviations of each biological property value from the mean, and the "press" is the sum of squared deviations of the cross-validation predicted values from observed values. The maximum possible value for the coefficient of determination,  $r^2$  is 1. Cross-validation evaluates a model not by how well it fits data (as expressed by the conventional coefficient of determination,  $r^2$ , in least-squares regression analysis), but by how well it predicts data. For bicycophosphates and chlorinated insecticides, cross-validation was performed by predicting the LD<sub>50</sub>, or IC<sub>50</sub>, value for each molecule through the use of a regression equation derived from the data on the other (n-1) molecules in the same grouping. For the group of bicycloorthocarboxylates, cross validation was performed by predicting the LD<sub>50</sub>, or IC<sub>50</sub>, values for the molecules in each of six subsets of the molecules from a regression equation based on data on the molecules in the other five subsets. In this latter case, the molecules were randomly assigned to the subsets and each subset contained either 6 or 7 molecules. In standard least squares regression analysis, the estimate  $s$  of the standard deviation of a measurement is obtained by dividing the sum of squares of the residuals by the degrees of freedom for error and then taking the square root of the quotient. The cross-validation  $s$  given in the tables is obtained in the same way, only the residuals are now the differences between the cross-validation predicted values and the observed values. The cross validation  $s$  does not have the same statistical properties as the regression  $s$ , but does indicate how well on average the LD<sub>50</sub>, or IC<sub>50</sub>, of new molecules might be predicted. It is necessary to consider both  $s$  and  $r^2$  in determining how well a given model fits the data. One wants a high value for  $r^2$  (near one) and a low value for  $s$ . It is possible to have a low value for  $s$  and a low value for  $r^2$  if the observed values of the dependent variable are within a narrow range and the predictor variables are virtually unrelated to the dependent variable. On the other hand, one may obtain both a high value of  $r^2$  and a high value of  $s$  when the data falls into two widely separated groups and the regression is essentially fitting a fine between the two groups and at the same time giving a poor fit of each individual group.

Two types of predictive models were generated. The first type is based on molecular volume, molecular surface area, dipole moments, and strain energy. The second is based on steric energy and electrostatic energy values (i.e., CoMFA values) at each point on the lattice. The parameter values for the first type of predictive model were estimated by least squares regression. For the second type, the partial least square (PLS) subroutine in the SYBYL program was employed to estimate parameter values because of the large number of explanatory variables involved.

The development of the first type (for non-CoMFA variables) of predictive models was based on regression analyses followed by cross validation. The development of these models required a choice of the molecules from each group, a choice of functions of the non-CoMFA variables, and decisions as to which terms in the preliminary versions of the models should eventually be dropped. This development will first be discussed for the log (LD<sub>50</sub>) dependent variable. The

group of 50 bicycloorthocarboxylate molecules (the first 50 molecules listed in Table 1) was used as a training set. After only a visual inspection of the LD<sub>50</sub> values for these molecules, a decision was made to remove fourteen molecules prior to fitting the log (LD<sub>50</sub>) variable because the observed LD<sub>50</sub> values for the molecules were considered either too large (> 54 mg/kg) or too small (< 0.6 mg/kg) or too poorly defined (e.g., > 200 mg/kg). It is thought that the reported extreme values were probably not of the same level of accuracy as those in the middle range. In addition, outlying values can have excessive influence on regression results. (However, it should be noted that in limiting the range of values of LD<sub>50</sub> in the estimation process, one is also placing a similar restriction on the range of values that may be reasonably predicted with a resulting prediction model). A model containing all linear and quadratic terms in the three variables, volume, total dipole moment, and strain energy, and also containing linear terms in surface area and the three directional dipole moments was fit to the logarithms of the LD<sub>50</sub> values. Nonsignificant terms were eliminated to leave the model equation shown in Table 5. These nonsignificant terms were eliminated so as to obtain substantially lower estimates of *s* while only marginally reducing *r*<sup>2</sup>.

Owing to the small number (12) of molecules in the bicyclopophosphate group, a decision was made not to remove any molecules from the analysis. Now, by using a procedure similar to that described above, a regression of the log (LD<sub>50</sub>) values of the 12 bicyclopophosphate molecules on the non-CoMFA variables yielded the equation given in Table 5, for which *r*<sup>2</sup> = 0.991 and *s* = 0.167. Cross validation for this model gave a cross-validation *r*<sup>2</sup> of 0.925 and a cross validation *s* of 0.470. Following the same procedure for the chlorinated insecticides after removing six molecules with LD<sub>50</sub> values larger than 130, we obtained a regression equation with *r*<sup>2</sup> = 0.883 and *s* = 0.292. However, cross validation with this model gave a cross-validation *r*<sup>2</sup> of only 0.406. while one must expect that the cross-validation *r*<sup>2</sup> will be smaller than the conventional regression *r*<sup>2</sup>, this large difference between regression and cross-validation *r*<sup>2</sup> values indicates that the model is over fitting the data. Three terms (V, VS, and DS) that had nonsignificant *t*-values in the regression were removed from the model equation and the regression and cross validations were rerun. This time the regression and cross-validation *r*<sup>2</sup> values were 0.852 and 0.733, respectively, and the corresponding values were 0.7185 and 0.964. These results and corresponding results for IC<sub>50</sub> are summarized in Tables 3, 4, and 5..

The only change in approach for the IC<sub>50</sub> data occurred in analyzing the bicycloorthocarboxylate data. Here, upon inspection of the IC<sub>50</sub> data, we decided to keep in the analysis the 39 molecules with IC<sub>50</sub> not greater than 4400 nM. However, after fitting large regression models and finding very large residuals for the two modules with largest IC<sub>50</sub> values, it was decided to drop these two molecules also and thereby only include the 37 molecules with IC<sub>50</sub> less than or equal to 1500 nM.

The second type of model analysis for COMFA descriptor variables was performed with the same molecules from each group that were employed in fitting each of the two dependent variables in the above non-CoMFA model regression analyses. The first step in the COMFA model analyses was to run a cross-validation partial least

Table 5. RESULTS FROM THE REGRESSION OF LOG(LD<sub>50</sub>) AND LOG(IC<sub>50</sub>) ON NON-CoMFA VARIABLES (NORMALIZED REGRESSION COEFFICIENTS)

**Bicycloorthocarboxylates LD50 (N=36, all molecules with 0.6 ≤ LD50 ≤ 54)**

$$\widehat{\text{Log(LD}_{50})} = 1.002 + 0.907 V - 2.503 D - 0.139 S + 0.245 V^2 + 0.200 S^2 - 0.664 A - 1.146 X - 1.967 Y$$

Std. Errors: (0.236) (0.769) (0.080) (0.086) (0.085) (0.253) (0.339) (0.616)

$$\{V = [\text{Mol. vol.} - 230] / 21.1; D = [\text{Tot. dipole moment} - 4] / 0.942;$$

$$S = [\text{Str. energy} - 20] / 2.205; V^2 = [\text{Mol. vol.} - 230]^2 / 904.2;$$

$$S^2 = [\text{Str. energy} - 20]^2 / 7.285; VS = [\text{Mol. vol.} - 230][\text{Str. Energy} - 20] / 39.8;$$

$$A = [\text{Surface area} - 3000] / 2.965; X = [X \text{ dipole moment} + 2] / 0.6025;$$

$$Y = [Y \text{ dipole moment} + 3] / 0.876\}$$

**Bicycloorthocarboxylates IC50 (N=37, all molecules with IC50 ≤ 1500)**

$$\widehat{\text{Log(IC}_{50})} = 1.609 - 0.469 V_1 - 0.331 D_1 + 0.424 V_1^2 + 0.200 D_1^2$$

Std. Errors: (0.131) (0.115) (0.132) (0.109)

$$\{V_1 = [\text{Mol. vol.} - 230] / 18.2; D_1 = [\text{Tot. dipole moment} - 4] / 0.959;$$

$$V_1^2 = [\text{Mol. vol.} - 230]^2 / 566.38; D_1^2 = [\text{Tot. dipole moment} - 4]^2 / 0.932\}$$

**Bicyclopophosphates (N = 12, all molecules)**

$$\widehat{\text{Log(LD}_{50})} = -0.330 + 0.0359 V_2 + 0.132 D_2 - 0.0519 S_2 - 1.793 S_2^2 + 1.464 V_2 S_2 + 0.485 D_2 S_2$$

Std. Errors: (0.198) (0.081) (0.288) (0.375) (0.235) (0.119)

$$\widehat{\text{Log(IC}_{50})} = 3.500 + 0.864 V_2 + 0.633 D_2 - 1.592 S_2 + 0.393 S_2^2$$

Std. Errors: (0.165) (0.111) (0.228) (0.181)

$$\{V_2 = [\text{Molecular volume} - 150] / 22.3; D_2 = [\text{Total dipole moment} - 5] / 0.814;$$

$$S_2 = [\text{strain energy} - 16] / 1.20; S_2^2 = [\text{strain energy} - 16]^2 / 2.49;$$

$$V_2 S_2 = [\text{Mol. vol.} - 150][\text{str. energy} - 16] / 19.3; \text{ and}$$

$$D_2 S_2 = [\text{Tot. dipole moment} - 5][\text{str. energy} - 16] / 1.125 \}$$

Table 5. Continued

**Chlorinated Insecticides (N = 14, all molecules with LD50 ≤ 130)**

$$\widehat{\text{Log(LD}_{50})} = 1.163 - 0.449 D_3 - 0.287 S_3 + 0.234 X_3 - 0.437 Y_3 + 0.228 Z_3$$

$$\text{Std. Errors:} \quad (0.046) \quad (0.066) \quad (0.076) \quad (0.067) \quad (0.064)$$

$$\{D_3 = [\text{Tot. dipole moment} - 2] / 0.528; S_3 = [\text{str. energy} - 100] / 64.98;$$

$$X_3 = X \text{ dipole moment} / 1.43; Y_3 = Y \text{ dipole moment} / 1.34;$$

$$Z_3 = Z \text{ dipole moment} / 0.505\}$$

**Chlorinated Insecticides (N = 13, all molecules with IC50 ≤ 2600)**

$$\widehat{\text{Log(IC}_{50})} = 2.505 - 0.471 Y_4 - 0.219 S_4$$

$$\text{Std. Errors:} \quad (0.107) \quad (0.110)$$

$$\{Y_4 = [Y \text{ dipole moment} - 6] / 1.18; S_4 = [\text{Str. energy} - 100] / 64.9\}$$

squares fit of each dependent variable (individually) on the first ten components (COMFA latent variables). The number of cross validation groups was equal to the number of molecules in the analysis for the bicycophosphates and the chlorinated insecticides, but was six for the large bicycloorthocarboxylate group. This cross-validation partial least squares procedure (i.e., SYBYL) gives an  $r^2$  value for fitting the first  $k$  components for each  $k$  ( $k = 1, \dots, 10$ ). The number,  $k$ , of components for which the maximum cross-validation  $r^2$  was observed was determined to be the optimum number of components for that dependent variable and molecule grouping. The cross validation procedure was rerun with the optimum number of components and the resulting cross-validation  $s$  value was obtained. Finally, the (conventional) regression of the dependent variable on the optimum number of components was performed to obtain the "conventional" estimates  $s$  and  $r^2$  for a prediction equation based on all the data in the group. The results of these analyses are shown in Table 4.

Tables 6-17 give the observed values, cross-validation predicted values, and cross-validation residuals for each of the analyses summarized in Tables 3 and 4. Figure 4 gives scatter plots of cross-validation predicted values versus observed values of  $\text{Log}(\text{LD}_{50})$  and  $\text{Log}(\text{IC}_{50})$ . We chose to plot the cross-validated predictions rather than the more commonly used regression estimates of expected values because we believe this gives a truer picture of how well one can expect the obtained models to predict  $\text{LD}_{50}$ , and  $\text{IC}_{50}$  for new molecules.

A sizable part of the deviations of predicted values from observed values of  $\text{LD}_{50}$  and  $\text{IC}_{50}$  in Tables 6-17 may be caused by errors in the observed values. Reported values of  $\text{LD}_{50}$  and  $\text{IC}_{50}$  of a compound often cover a wide range. For example,  $\text{IC}_{50}$  values in the range 16-91 nM were reported for toxicant A of toxaphene (compound #6 in Table 2); an  $\text{IC}_{50}$  range of 8-22 nM was reported for  $\alpha$ -endosulfan (Compound 19, Table 2); and a range of 4-90 nM for endrin. In some cases, experimental values were reported as greater than or greater than or equal to some values. Values of  $\text{LD}_{50}$  and  $\text{IC}_{50}$  used in our calculations were the averages of reported values. It is also possible that conformation differences of the chemical may be the cause of a substantial part of a residual. Reported  $\text{LD}_{50}$  values were generally more precisely measured than the  $\text{IC}_{50}$  values. It could be that the better predictability of  $\text{LD}_{50}$  may be owing to other factors in the biological *in vivo* system such as bioactivation or synergistic factors that are absent in the *in vitro* measurements of the  $\text{LD}_{50}$ .

The results given in Tables 3 and 4 indicate that the models based on non-CoMFA explanatory variables are better in predicting  $\log(\text{LD}_{50})$  and  $\log(\text{IC}_{50})$  values than are the models based on the COMFA components. The best fitting models were obtained for  $\log(\text{LD}_{50})$  and  $\log(\text{IC}_{50})$  for the bicycophosphate group and for  $\log(\text{LD}_{50})$  in the chlorinated insecticides group. There was little success in developing a good predictor model for either  $\log(\text{LD}_{50})$  or  $\log(\text{IC}_{50})$  in the bicycloorthocarboxylate group, but molecular volume and dipole moments appear to be related to both dependent variables for this group. Molecular volume and/or dipole moments are also strongly related to  $\log(\text{LD}_{50})$  and  $\log(\text{IC}_{50})$  for the other two groups. In a future study, we plan to investigate models with explanatory variables that are components made up of orthogonal linear combinations of both the COMFA and non-CoMFA variables.

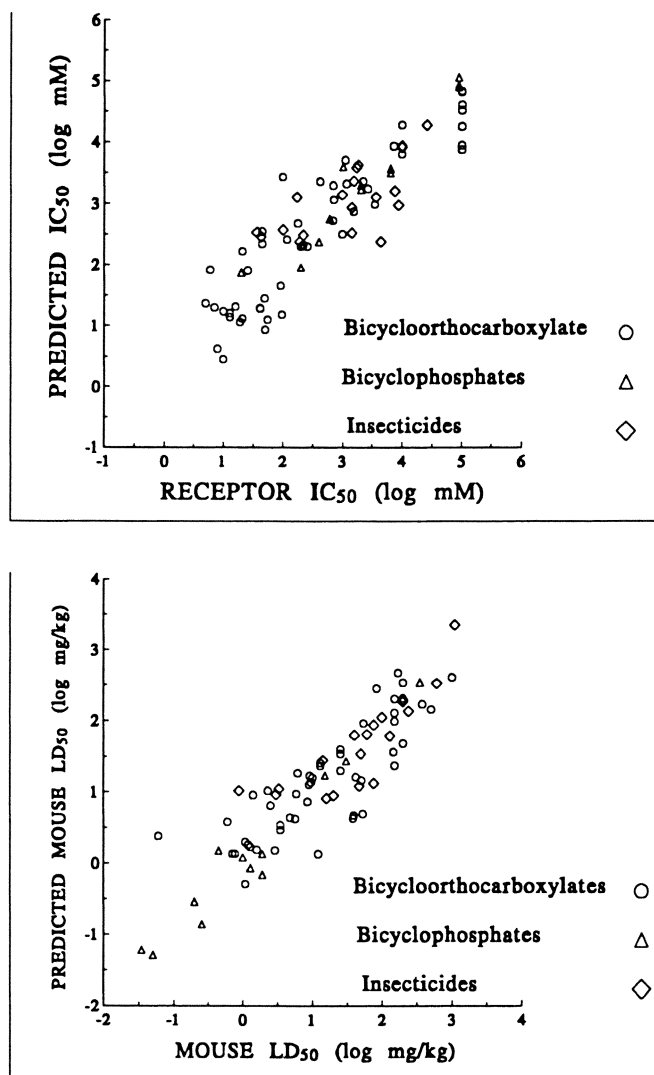


Figure 4. Scatterplot of cross-validation predicted and observed log (LD<sub>50</sub>) and log (IC<sub>50</sub>) values of bicycloorthocarboxylates, bicycrophosphorus esters and chlorinated insecticides.

Table 6. OBSERVED, PREDICTED, AND RESIDUAL  $\text{Log}(\text{LD}_{50})$  VALUES FOR BICYCLOORTHOCARBOXYLATES IN THE CROSS-VALIDATION OF THE REGRESSION ON NON-CoMFA PREDICTORS

Compound	$\text{LD}_{50}$	$\text{Log}(\text{LD}_{50})$	$\text{Log}(\text{LD}_{50})$	$\text{Log}(\text{LD}_{50})$
Number <sup>a</sup>	(mg/kg)	Observed	Predicted	Residual
1	13	1.1139	1.2495	-0.1356
2	9.1	0.9590	1.2523	-0.2932
3	2.3	0.3617	0.9504	-0.5887
4	50	1.6990	1.4212	0.2777
5	2.5	0.3979	0.8773	-0.4793
6	1.1	0.0414	0.4689	-0.4275
7	6.1	0.7853	1.0520	-0.2667
8	52	1.7160	0.7749	0.9411
9	54	1.7324	1.1028	0.6296
13	42	1.6232	1.6089	0.0143
15	10	1	1.1385	-0.1385
16	5.9	0.7709	0.9655	-0.1946
17	1.3	0.1139	0.3916	-0.2776
18	5.6	0.7482	0.7176	0.0306
19	0.7	-0.1549	0.3180	-0.4729
20	12	1.0792	0.8470	0.2322
21	1.6	0.2041	0.7381	-0.5340
22	0.77	-0.1135	0.1075	-0.2210
23	1.2	0.0792	0.6120	-0.5328

Table 6. Continued

Compound	LD <sub>50</sub>	Log (LD <sub>50</sub> )	Log (LD <sub>50</sub> )	Log (LD <sub>50</sub> )
Number <sup>a</sup>	(mg/kg)	Observed	Predicted	Residual
24	38	1.5798	1.2765	0.3033
25	2.9	0.4624	0.3859	0.0765
28	0.88	-0.0555	-0.1135	0.0580
29	1.1	0.0414	-0.2430	0.2844
30	9.5	0.9777	0.4746	0.5031
32	13	1.1139	0.2901	0.8238
33	1.4	0.1461	0.5641	-0.4180
34	25	1.3979	0.8376	0.5603
36	9	0.9542	1.2151	-0.2609
38	3.5	0.5441	0.4455	0.0986
39	4.8	0.6812	1.1538	-0.4726
40	0.6	-0.2218	-0.4269	0.2051
41	39	1.5911	1.8240	-0.2329
43	8.5	0.9294	0.2652	0.6642
44	25	1.3979	0.5364	0.8615
45	25	1.3979	0.9128	0.4851
46	3.5	0.5441	0.5810	-0.0369

<sup>a</sup> Numbers of molecules from Table 1 and Figure 1

Table 7. OBSERVED, PREDICTED, AND RESIDUAL  $\text{Log}(\text{IC}_{50})$  VALUES FOR BICYCLOORTHOCARBOXYLATES IN THE CROSS-VALIDATION OF THE REGRESSION ON NON-CoMFA PREDICTORS

Compound Number <sup>a</sup>	$\text{IC}_{50}$ (nM)	$\text{Log}(\text{IC}_{50})$ Observed	$\text{Log}(\text{IC}_{50})$ Predicted	$\text{Log}(\text{IC}_{50})$ Residual
1	413	2.6160	2.5061	0.1099
2	176	2.2455	1.8321	0.4134
3	45	1.6532	1.8513	-0.1981
4	200	2.3010	1.3330	0.9680
5	6	0.7782	1.4287	-0.6505
6	7	0.8451	1.4295	-0.5844
7	21	1.3222	1.2055	0.1167
8	13	1.1139	1.4773	-0.3634
9	100	2	1.4372	0.5628
13	217	2.3365	2.2929	0.0436
15	1500	3.1761	2.7835	0.3926
16	692	2.8401	2.9719	-0.1318
17	49	1.6902	2.2404	-0.5502
18	41	1.6128	1.8643	--0.2515
19	16	1.2041	2.4412	-1.2370
20	95	1.9777	2.0967	-0.1190
21	13	1.1139	1.5062	-0.3922
22	42	1.6232	1.5863	0.0369
23	10	1	1.4143	-0.4143

Table 7. Continued

Compound	IC <sub>50</sub>	Log (IC <sub>50</sub> )	Log (IC <sub>50</sub> )	Log (IC <sub>50</sub> )
Number <sup>a</sup>	(nM)	Observed	Predicted	Residual
24	92	1.9638	1.3012	0.6626
25	55	1.7404	1.4478	0.2926
26	5	0.6990	1.4159	-0.7170
28	10	1	1.2273	-0.2273
29	8	0.9031	1.4753	-0.5722
32	1150	3.0607	3.0636	-0.0029
33	118	2.0719	2.1985	-0.1266
34	970	2.9868	1.6770	1.3098
36	45	1.6532	1.6342	0.0190
38	21	1.3222	1.2922	0.0301
39	19	1.2788	1.6663	-0.3875
40	10	1	1.5173	-0.5173
41	50	1.6990	1.6344	0.0646
42	1100	3.0414	2.5364	0.5050
43	255	2.4065	1.7592	0.6474
44	706	2.8488	1.3642	1.4846
45	684	2.8351	2.1918	0.6432
46	26	1.4150	2.0088	-0.5939

<sup>a</sup> Numbers of molecules from Table 1 and Figure 1

Table 8. OBSERVED, PREDICTED, AND RESIDUAL LOG(LD<sub>50</sub>) VALUES FOR BICYCLOPHOSPHATES IN THE CROSS-VALIDATION OF THE REGRESSION ON NON-CoMFA PREDICTORS

Compound	LD <sub>50</sub>	Log (LD <sub>50</sub> )	Log (LD <sub>50</sub> )	Log (LD <sub>50</sub> )
Number <sup>a</sup>	(mg/kg)	Observed	Predicted	Residual
51	0.05	-1.3010	-0.9415	-0.3596
52	0.26	-0.5850	-0.7685	0.1835
53	1.28	0.1072	0.4329	-0.3257
54	0.035	-1.4559	-1.9244	0.4685
55	0.2	-0.6990	-0.8956	0.1967
56	0.45	-0.3468	-0.1409	-0.2059
57	1.9	0.2788	0.7471	-0.4684
58	1	0	-0.1721	0.1721
59	1.9	0.2788	0.3345	-0.0557
60	15	1.1761	1.3781	-0.2021
61	30	1.4771	1.4105	0.0667
62	350	2.5441	2.0568	0.4873

<sup>a</sup> Numbers of molecules from Table 1 and Figure 1

Table 9. OBSERVED, PREDICTED, AND RESIDUAL LOG(IC<sub>50</sub>) VALUES FOR BICYCLOPHOSPHATES IN THE CROSS-VALIDATION OF THE REGRESSION ON NON-CoMFA PREDICTORS

Compound Number <sup>a</sup>	IC <sub>50</sub> (nM)	Log (IC <sub>50</sub> ) Observed	Log (IC <sub>50</sub> ) Predicted	Log (IC <sub>50</sub> ) Residual
51	20	1.3010	1.5673	-0.2663
52	400	2.6021	2.0652	0.5369
53	2000	3.3010	3.7668	-0.4658
54	200	2.3010	2.3252	-0.0241
55	600	2.7782	2.7093	0.0689
56	1000	3	3.7366	-0.7366
57	2000	3.3010	3.0235	0.2775
58	6500	3.8129	3.5508	0.2621
59	6500	3.8129	4.1971	-0.3842
60	90000	4.9542	4.3432	0.6111
61	90000	4.9542	4.4523	0.5019
62	90000	4.9542	5.2560	-0.3018

<sup>a</sup> Numbers of molecules from Table 1 and Figure 1

Table 10. OBSERVED, PREDICTED, AND RESIDUAL  $\text{LOG}(\text{LD}_{50})$  VALUES FOR CHLORINATED INSECTICIDES IN THE CROSS-VALIDATION OF THE REGRESSION ON NON-CoMFA PREDICTORS

Compound Number <sup>a</sup>	$\text{LD}_{50}$ (mg/kg)	$\text{Log}(\text{LD}_{50})$ Observed	$\text{Log}(\text{LD}_{50})$ Predicted	$\text{Log}(\text{LD}_{50})$ Residual
3	40	1.6021	1.2602	0.3419
5	75	1.8751	2.0138	-0.1388
6	3.3	0.5185	-0.0782	0.5967
7	100	2	1.9684	0.0316
8	49	1.6902	1.5589	0.1313
9	14	1.1461	1.2945	-0.1484
12	130	2.1139	2.0156	0.0984
13	47	1.6721	1.7569	-0.0848
14	2.0	0.3010	0.4023	-0.1013
15	0.9	-0.0458	0.3258	-0.3716
16	3	0.4771	0.1828	0.2944
17	16	1.2041	1.0928	0.1113
18	60	1.7782	1.6285	0.1496
19	76	1.8808	2.0163	-0.1355

<sup>a</sup> Numbers of molecules from Table 2 and Figure 2

Table 11. OBSERVED, PREDICTED, AND RESIDUAL LOG(IC<sub>50</sub>) VALUES FOR CHLORINATED INSECTICIDES IN THE CROSS-VALIDATION OF THE REGRESSION ON NON-CoMFA PREDICTORS

Compound Number <sup>a</sup>	IC <sub>50</sub> (nM)	Log (IC <sub>50</sub> ) Observed	Log (IC <sub>50</sub> ) Predicted	Log (IC <sub>50</sub> ) Residual
3	1700	3.2304	2.9774	0.2530
5	170	2.2304	2.5434	-0.3130
6	240	2.3802	2.0077	0.3726
9	1400	3.1461	3.6274	-0.4813
10	2600	3.4150	3.3351	0.0799
11	1800	3.2553	2.8713	0.3840
13	1400	3.1461	3.2882	-0.1420
14	220	2.3424	2.1474	0.1951
15	36	1.5563	1.8741	-0.3178
16	43	1.6335	1.8843	-0.2508
18	980	2.9912	2.4818	0.5094
19	100	2	2.8609	-0.8609
20	1500	3.1761	2.7496	0.4265

<sup>a</sup> Numbers of molecules from Table 2 and Figure 2

Table 12. OBSERVED, PREDICTED, AND RESIDUAL  $\text{Log}(\text{LD}_{50})$  VALUES FOR BICYCLOORTHOCARBOXYLATES IN THE CROSS-VALIDATION OF THE PLS REGRESSION ON CoMFA PREDICTORS

Compound	$\text{LD}_{50}$	$\text{Log}(\text{LD}_{50})$	$\text{Log}(\text{LD}_{50})$	$\text{Log}(\text{LD}_{50})$
Number <sup>a</sup>	(mg/kg)	Observed	Predicted	Residual
1	13	1.114	0.792	0.322
2	9.1	0.959	1.321	-0.362
3	2.3	0.362	0.703	-0.341
4	50	1.699	1.177	0.522
5	2.5	0.398	1.030	-0.632
6	1.1	0.041	0.379	-0.338
7	6.1	0.785	0.686	0.099
8	52	1.716	0.761	0.955
9	54	1.732	0.711	1.021
13	42	1.623	0.965	0.658
15	10	1	1.155	-0.155
16	5.9	0.771	0.697	0.074
17	1.3	0.114	0.584	-0.471
18	5.6	0.748	1.245	-0.497
19	0.7	-0.155	0.581	-0.735
20	12	1.079	0.418	0.661
21	1.6	0.204	0.553	-0.349
22	0.77	-0.114	0.564	-0.678
23	1.2	0.079	0.488	-0.409

Table 12. Continued

Compound	LD <sub>50</sub>	Log (LD <sub>50</sub> )	Log (LD <sub>50</sub> )	Log (LD <sub>50</sub> )
Number <sup>a</sup>	(mg/kg)	Observed	Predicted	Residual
24	38	1.580	0.504	1.076
25	2.9	0.462	0.631	-0.169
28	0.88	-0.056	0.501	-0.557
29	1.1	0.041	0.580	-0.538
30	9.5	0.978	0.590	0.388
32	13	1.114	0.361	0.753
33	1.4	0.146	0.637	-0.491
34	25	1.398	0.495	0.903
36	9	0.954	1.084	-0.129
38	3.5	0.544	0.747	-0.203
39	4.8	0.681	1.285	-0.603
40	0.6	-0.222	1.302	-1.524
41	39	1.591	0.570	1.021
43	8.5	0.929	0.593	0.336
44	25	1.398	0.781	0.617
45	25	1.398	0.522	0.875
46	3.5	0.544	0.590	-0.046

<sup>a</sup> Numbers of molecules from Table 1 and Figure 1

Table 13. OBSERVED, PREDICTED, AND RESIDUAL LOG(IC<sub>50</sub>) VALUES FOR BICYCLOORTHO-CARBOXYLATES IN THE CROSS-VALIDATION OF THE PLS REGRESSION ON CoMFA PREDICTORS

Compound Number <sup>a</sup>	IC <sub>50</sub> (nM)	Log (IC <sub>50</sub> ) Observed	Log (IC <sub>50</sub> ) Predicted	Log (IC <sub>50</sub> ) Residual
1	413	2.616	3.396	-0.780
2	176	2.246	1.937	0.309
3	45	1.653	2.246	-0.592
4	200	2.301	1.831	0.470
5	6	0.778	1.784	-1.006
6	7	0.845	1.270	-0.425
7	21	1.322	0.746	0.576
8	13	1.114	1.213	-0.099
9	100	2	1.930	0.070
13	217	2.336	2.883	-0.547
15	1500	3.176	2.722	0.454
16	692	2.840	2.328	0.512
17	49	1.690	1.678	0.012
18	41	1.613	2.000	-0.387
19	16	1.204	1.629	-0.425
20	95	1.978	1.606	0.371
21	13	1.114	1.604	-0.490
22	42	1.623	0.955	0.668
23	10	1	1.322	-0.322

Table 13. Continued

Compound	IC <sub>50</sub>	Log (IC <sub>50</sub> )	Log (IC <sub>50</sub> )	Log (IC <sub>50</sub> )
Number <sup>a</sup>	(nM)	Observed	Predicted	Residual
24	92	1.964	1.149	0.815
25	55	1.740	1.155	0.585
26	5	0.699	1.328	-0.629
28	10	1	1.051	-0.051
29	8	0.903	0.617	0.286
32	1150	3.061	2.284	0.776
33	118	2.072	2.965	-0.893
34	970	2.987	2.395	0.592
36	45	1.653	2.227	-0.574
38	21	1.322	1.218	0.104
39	19	1.279	1.194	0.084
40	10	1	1.317	-0.317
41	50	1.699	0.640	1.059
42	1100	3.041	2.116	0.925
43	255	2.406	1.828	0.578
44	706	2.849	1.931	0.918
45	684	2.835	1.650	1.185
46	26	1.415	1.669	-0.254

<sup>a</sup> Numbers of molecules from Table 1 and Figure 1

Table 14. OBSERVED, PREDICTED, AND RESIDUAL LOG(LD<sub>50</sub>) VALUES FOR BICYCLOPHOSPHATES IN THE CROSS-VALIDATION OF THE PLS REGRESSION ON CoMFA PREDICTORS

Compound	LD <sub>50</sub>	Log (LD <sub>50</sub> )	Log (LD <sub>50</sub> )	Log (LD <sub>50</sub> )
Number <sup>a</sup>	(mg/kg)	Observed	Predicted	Residual
51	0.05	-1.301	-1.335	0.034
52	0.26	-0.585	-0.779	0.194
53	1.28	0.107	0.124	-0.017
54	0.035	-1.456	-1.234	-0.222
55	0.2	-0.699	-0.872	-0.173
56	0.45	-0.347	-0.080	-0.266
57	1.9	0.279	-0.028	0.307
58	1	0	0.154	-0.154
59	1.9	0.279	0.346	-0.068
60	15	1.176	1.537	-0.361
61	30	1.477	0.379	1.098
62	350	2.544	1.279	1.265

<sup>a</sup> Numbers of molecules from Table 1 and Figure 1

Table 15. OBSERVED, PREDICTED, AND RESIDUAL LOG(IC<sub>50</sub>) VALUES FOR BICYCLOPHOSPHATES IN THE CROSS-VALIDATION OF THE PLS REGRESSION ON CoMFA PREDICTORS

Compound Number <sup>a</sup>	IC <sub>50</sub> (nM)	Log (IC <sub>50</sub> ) Observed	Log (IC <sub>50</sub> ) Predicted	Log (IC <sub>50</sub> ) Residual
51	20	1.3010	1.909	-0.608
52	400	2.6021	2.298	0.304
53	2000	3.3010	3.050	0.251
54	200	2.3010	1.819	0.482
55	600	2.7782	2.683	0.095
56	1000	3	3.513	-0.513
57	2000	3.3010	2.902	0.399
58	6500	3.8129	4.052	-0.239
59	6500	3.8129	4.026	-0.213
60	90000	4.9542	4.469	0.485
61	90000	4.9542	4.299	0.655
62	90000	4.9542	5.033	-0.079

<sup>a</sup> Numbers of molecules from Table 1 and Figure 1

Table 16. OBSERVED, PREDICTED, AND RESIDUAL LOG(LD<sub>50</sub>) VALUES FOR CHLORINATED INSECTICIDES IN THE CROSS-VALIDATION OF THE PLS REGRESSION ON CoMFA PREDICTORS

Compound Number <sup>a</sup>	LD <sub>50</sub> (mg/kg)	Log (LD <sub>50</sub> ) Observed	Log (LD <sub>50</sub> ) Predicted	Log (LD <sub>50</sub> ) Residual
3	40	1.602	1.613	-0.011
5	75	1.875	1.402	0.473
6	3.3	0.518	1.394	-0.876
7	100	2	1.966	-0.034
8	49	1.690	1.433	0.257
9	14	1.146	0.693	0.453
12	130	2.114	1.690	0.424
13	47	1.672	1.419	0.253
14	2.0	0.301	0.666	-0.365
15	0.9	-0.045	0.952	-0.997
16	3	0.477	1.017	-0.540
17	16	1.204	0.288	0.916
18	60	1.778	1.811	-0.033
19	76	1.881	1.526	0.355

<sup>a</sup> Numbers of molecules from Table 2 and Figure 2

As mentioned above, molecular volume and dipole moments show strong relationships with the toxicological properties of the compounds when expressed as their acute mammalian toxicity (mouse LD<sub>50</sub>) and as their ability to inhibit binding of t-butylbicyclopophosphorothionate (TBPS) to the receptor (IC<sub>50</sub>). The correlation of the biological activity and molecular volume, total surface area, and dipole moment may be further examined by mapping the electrostatic and steric functions of the individual molecules as shown in Figure 5. Examples of highly active compounds are shown in the left column (in order, compound numbers 51 and 6 from Table 1, and 14 and 3 from Table 2), and examples of the least active compounds are shown in the right column (in order, compound numbers 27, 50, and 37 of Table 1, and 2 of Table 2) of the figure. All the active compounds showed the presence of a sterically bulky group and an electronegative group on the other end. Less active groups may lack the bulk group or the electronegative group, or both, or they may be less active if the electronegative group is masked by another group as in the case of  $\beta$ -lindane (compound number 2 of Table 2) where the electronegative end was totally masked by neutral cloud (Figure 5). The requirement of an electronegative group and sterically bulky group also was reported for bridged bicyclic insecticides (6).

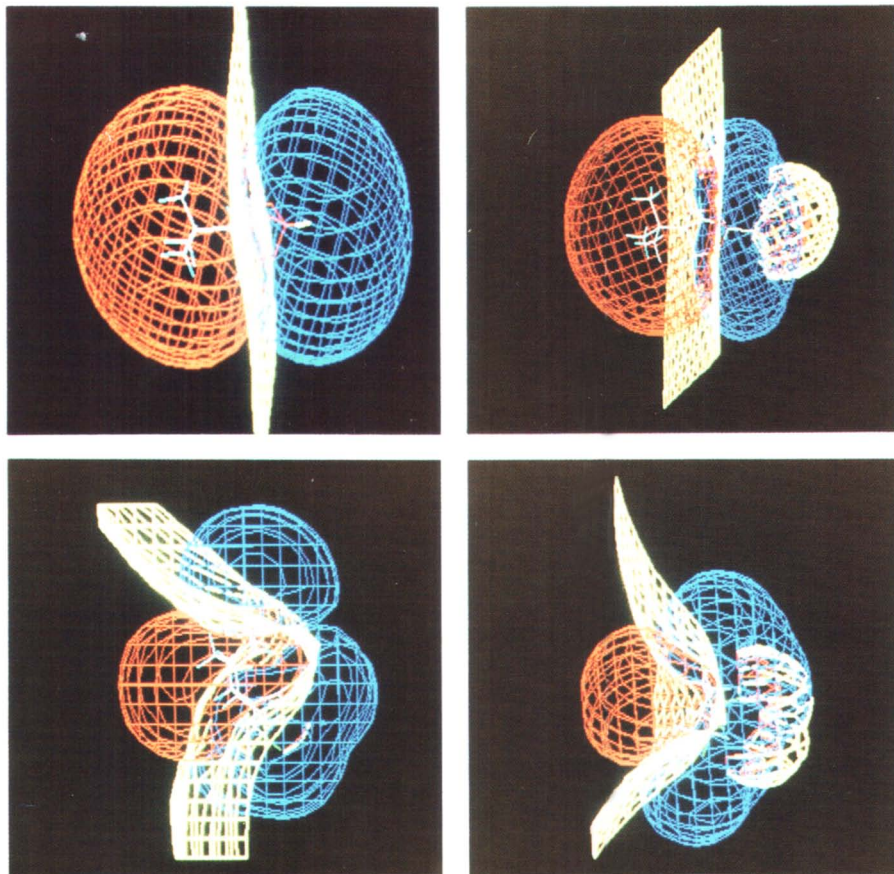


Figure 5. Electrostatic and volume mapping of two selected active compounds (left column): compound numbers 51 and 6 from Table 1 and two selected less-active compounds (right column): compound numbers 27 and 50 from Table 1. Continued on next page.

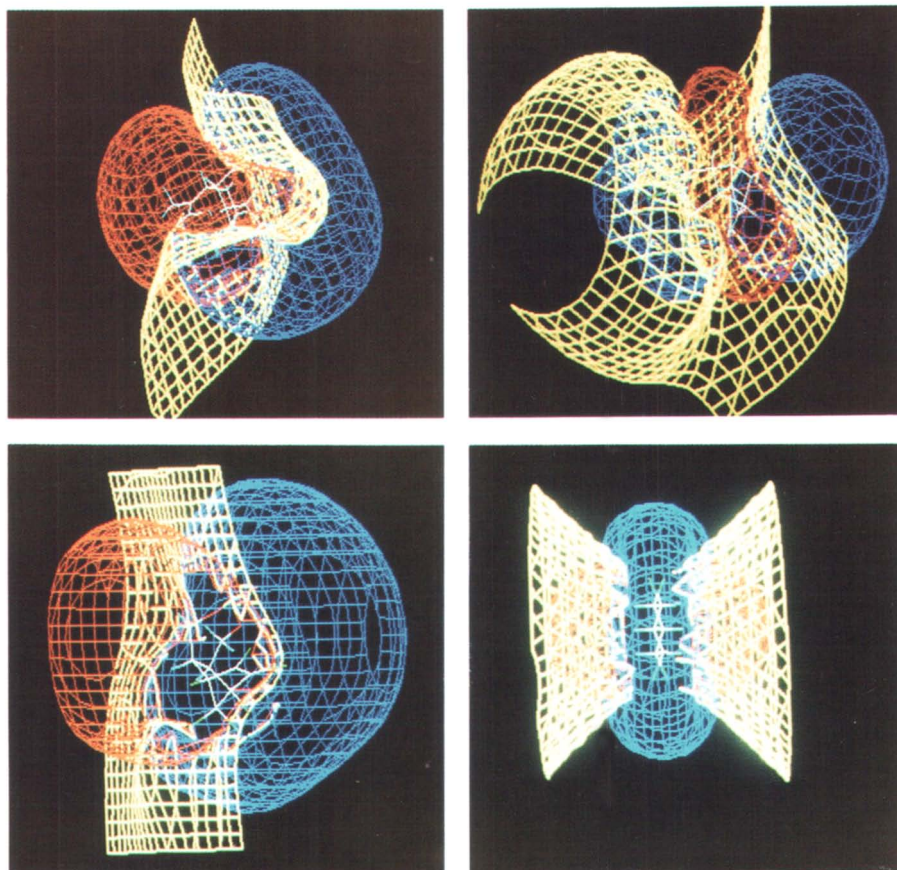


Figure 5. Continued. Electrostatic and volume mapping of two selected active compounds (left column): compound numbers 14 and 3 from Table 2 and two selected less-active compounds (right column): compound number 37 from Table 1 and number 2 from Table 2.

Table 17. OBSERVED, PREDICTED, AND RESIDUAL LOG(IC<sub>50</sub>) VALUES FOR CHLORINATED INSECTICIDES IN THE CROSS-VALIDATION OF THE PLS REGRESSION ON CoMFA PREDICTORS

Compound Number <sup>a</sup>	IC <sub>50</sub> (nM)	Log (IC <sub>50</sub> ) Observed	Log (IC <sub>50</sub> ) Predicted	Log (IC <sub>50</sub> ) Residual
3	1700	3.230	3.293	-0.063
5	170	2.230	2.154	0.076
6	240	2.380	2.085	0.295
9	1400	3.146	2.213	0.933
10	2600	3.415	3.439	-0.024
11	1800	3.255	2.631	0.624
13	1400	3.146	2.287	0.859
14	220	2.342	2.219	0.123
15	36	1.556	2.455	-0.898
16	43	1.634	2.333	-0.700
18	980	2.991	2.806	0.185
19	100	2	2.499	-0.499
20	1500	3.176	3.506	-0.330

<sup>a</sup> Numbers of molecules from Table 2 and Figure 2

It is clearly shown here that molecular modeling could be useful for predicting toxicity and receptor binding and, therefore, may provide a tool for theoretical bioassay measurements that may substantially reduce the use of experimental animals. The model may also provide information about the distances and electrostatic requirements for chemical receptor binding. This will be helpful in designing synthetic receptors for measurement methods utilizing receptor affinity.

### Acknowledgements

Although the research described in this article has been supported by the U.S. EPA, it has not been subjected to Agency review and, therefore, does not necessarily reflect the view of the Agency, and no official endorsement should be inferred.

### Literature Cited

1. Meyer, A.Y. *Chem. Soc. Rev.* **1986**, *15*,449.
2. Dual, W.L.; Griffin, J.F.; SmG.D. Stezowski, J.J., Huang, J.L., Shao, M. weds.) *Molecular Structure: Chemical Reactivity and Biological Activity.* Oxford University Press, Oxford,ith, **1988**, pp. 1-21.
3. Charifson, P.S.; Bowen, J.P.; Work, S.D.; Hoffman, M; Cory, A.J.; McPhail, T.; Mailman, B. *J. Med. Chem.* **1989**, *32*, 2050.
4. Palmer, C.J.; Casida, J.E.J. *Agric. Food Chem.* **1989**, *37*, 213.
5. Casida, J.E.; Palmer, C.J.; Cole, L.M. *Mol. Pharmacol.* **1985**, *28*:246.
6. Matsumura, F.; Tanaka , Y., K.;Ozoe, Y.; Hollingworth, R.M.,Green, M.B. weds.) *Sites of Action for Neurotoxic Pesticides.* American Chemical Society, Washington, D.C., **1987**, pp. 44-70.
7. Lawrence, L.J.; Casida, J.E.*Science* **1983**, *221*,1399-1401.
8. Casida, J.E.; Lawrence, L.J. *Environ. Health Perspect.* **1985**, *61*,123.
9. Lawrence, L.J.; Palmer, C.J.; Gee, K.W.; Wang, X.; Yamamura, H.I.; Casida, J.E. *J. Neurochem.* **1985**, *45*, 798.
10. Squires, R.F.; Casida, J.E.; Richardson, M.; Saederup, E. *Mol. Pharmacol.* **1983**, *23*, 326.
11. Lawrence, L.J.; Casida, J.E. *Life Sci.* **1984**, *35*, 171.
12. Gasteiger, J.; Marsili, M. *Tetrahedron* **1980**, *36*, 3219.
13. Labanowski, J.; Motoc, I.; Naylor, C.B.; Mayer, D.; Dammkoehler, J.L. Quint. Strut. Act. Relit. **1986**, *5*, 138.
14. Cramer, R.D.; Patterson, D.E.; Bunce, J.D. *J. Amer. Chem. Soc.* **1988**, *110*,5959.
15. Geladi, P.; Kowalski, B.R. *Analytica Chemica Acta* **1986**, *185*, 1.
16. Hell, I.S. *Commune. Statist.-Simula.*, **1988**, *17*,581.

RECEIVED September 17, 1993

## Chapter 7

# A Biosensor for Monitoring Blood Cholinesterases as a Biomarker of Exposure to Organophosphorus Anticholinesterase Pesticides

Mohyee E. Eldefrawi<sup>1</sup>, Kim R. Rogers<sup>2</sup>, Nabil A. Anis<sup>1</sup>, Roy Thompson<sup>3</sup>, and J. J. Valdes<sup>3</sup>

<sup>1</sup>Department of Pharmacology and Experimental Therapeutics, University of Maryland School of Medicine, Baltimore, MD 21201

<sup>2</sup>Exposure Assessment Research Division, Environmental Monitoring Systems Laboratory, U.S. Environmental Protection Agency, P.O. Box 93478, Las Vegas, NV 89193-3478

<sup>3</sup>Biotechnology Division, U.S. Army Research Development and Engineering Center, Edgewood, MD 21010

A fiber optic evanescent fluorosensor was developed for the rapid detection of anticholinesterases (AntiChEs) and was modified to measure cholinesterase (ChE) activities in whole blood. Quartz fibers coated with fluorescein isothiocyanate (FITC)-tagged acetylcholinesterase (AChE), detected AntiChEs by their reduction of quenching of fluorescence that was produced by protons generated during acetylcholine (ACh) hydrolysis. Blood ChE activity was detected by quenching the fluorescence of FITC bovine serum albumin immobilized on the quartz fiber. High ChE activity in blood samples produced strong fluorescence quenching and exposure to antiChEs reduced quenching. Fluorometric measurements were made in seconds to minutes by evanescent waveguide fluorometer on 200  $\mu$ l blood samples. A 2-minute rinse in Krebs buffer was sufficient to prepare the fiber for another measurement.

Biosensors have captured the imagination of the world's scientific and commercial communities by combining interdisciplinary skills of biologists, physicists, chemists and engineers to provide innovative solutions to analytical problems. Biosensors are applicable to clinical diagnostics, food analysis, cell culture monitoring, environmental pollutants and should also be applicable to detection of drug residues in milk and animal tissues and drugs of abuse and metabolites in urine, blood and sweat.

Biosensors are analytical devices made of biological recognition materials (e.g. enzymes, receptors or antibodies) coupled to transduction elements that

range from glass electrodes to silicon chips and optic fibers (Wise, 1989). The high specificities of the binding sites of these proteins for certain drugs, toxicants and toxins is the basis for their use in detection. Biosensors are possible successors to a wide range of analytical techniques in process control, clinical laboratories, veterinary health care and in food industry (McCann, 1987; Robinson, 1991). Although the functions of complex proteins are typically affected by pH, ionic strength, detergents, and denaturants, biosensors can function within a wide range of conditions. Receptors, enzymes and antibodies bind their specific ligands, substrates and antigens, respectively with high affinities in cellular and extracellular media in presence of ions, lipids and other proteins.

### Enzyme-, Receptor- and Immuno-Sensors

Enzyme (by far the most widely used biological recognition material tested) biosensors have led the developments in the field (Guilbault, 1981; Clark, 1987). A good example is glucose oxidase, which is used to construct glucose sensitive electrodes (Fortier et al., 1990), fiber optic biosensors (Mansouri and Schultz, 1984) and chemical field effect transistor sensors (Murakami et al., 1986). Another example is acetylcholinesterase (AChE), which has been used to construct enzyme electrodes (Baum and Ward, 1971; Durand et al., 1984), fiber optic biosensors (Rogers et al., 1991a; Hobel and Polster, 1992) and potentiometric biosensors (Rogers et al., 1991b) for detecting anticholinesterases (antiChEs). The approach used in the fiber optic biosensor is to label AChE with the pH-sensitive fluorescein-labeled-isothiocyanate and immobilize them on optic fibers. Hydrolysis of ACh by AChE releases acetate, which changes the pH thereby quenching the fluorescence. AntiChE values obtained with this biosensor were in good agreement with those obtained by the Ellman et al. (1961) spectrophotometric method using soluble AChE. Even though the biosensor is fast with results obtainable in seconds to minutes, a disadvantage is that many antiChEs require bioactivation and thus the less active parent compounds are detectable only at high concentrations. Since the antiChE-inhibited biosensor can be reactivated by oximes the biosensor can be used repeatedly. Also, inactivation of the biosensor by unrelated denaturants such as Hg can be determined.

The use of neurotransmitter or hormone receptors to construct biosensors has been utilized mostly with the nicotinic ACh receptor (Gotoh et al., 1987; Eldefrawi et al., 1988; Taylor et al., 1988; Rogers et al., 1989). The ACh receptor fiber optic evanescent fluorosensor has a wide detection range, and shows excellent sensitivity and pharmacological specificity (Rogers et al., 1991c).

Immunosensors utilize antibodies for the detection of specific antigens. In contrast to a receptor or enzyme, an antibody is specific for a single epitope or antigen. As a consequence, immunosensors are well suited for detecting a specific compound in relatively complex media, which may contain structurally related chemicals. Antibodies have been used as sensing elements in surface plasmon resonance (Morgan and Taylor, 1992), piezoelectric (Guilbault et al., 1992), capacitive and ISFET biosensors (Gotoh et al., 1987; Eldefrawi et al., 1988). Optical immunosensors, which utilize antibodies (Ab) for the detection of specific antigens, are under intensive investigation, in a number of laboratories (Robinson, 1991). Evanescent excitation with collection of the fluorescence that

In Biomarkers of Human Exposure to Pesticides; Saleh, M., et al.;

ACS Symposium Series; American Chemical Society: Washington, DC, 1993.

tunnels back into trapped modes of the waveguide was described by Hirschfeld and Block (1984) and Andrade et al. (1985). Fiber optic evanescent waveguide fluorosensors are superior in sensitivity to distal end sensors and have been used successfully (Rogers et al., 1989, 1991a, b; Anis et al., 1992).

### AChE-Biosensor for Detection of Anticholinesterases

The fiber-optic evanescent fluorosensor instrument, designed and built by ORD, Inc. (North Salem, NH), is a portable fluorometer that is adaptable to field work. Components of this instrument which were described in detail by Glass et al. (1987) include a 10-W Welch Allyn quartz halogen lamp, a Hamamatsu S-1087 silicon detector, an Ismatec fixed speed peristaltic pump, a Pharmacia strip chart recorder, and bandpass filters and lenses as indicated in Fig. 1. The quartz fibers are 1 mm in diameter and 6 cm long with polished ends. The fiber-optic evanescent fluorosensor makes use of the evanescent wave effect by exciting a fluorophore just outside the waveguide boundary (excitation wavelength = 485/20 nm; the latter number representing full width at half maximum). A portion of the resultant fluorophore emission then becomes trapped in the waveguide and is transmitted back up the fiber. This is detected after transmission through 510 nm LP and 530/30 nm filters. The flow cell allows the center 47 mm of a 60-mm-long fiber to be immersed in 46  $\mu$ l, which was exchanged every 14 sec.

An optical biosensor for antiChEs was constructed by immobilizing fluorescein isothiocyanate (FITC)-tagged AChE from electric eel on the quartz fiber and monitoring its activity in presence of the substrate ACh and in presence or absence of antiChEs. Fluorescence emission by the pH-sensitive dye, fluorescein, was reduced in presence of ACh that was hydrolyzed to choline and acetate and the latter reduced the pH of the medium significantly. A fairly low molarity (0.1 mM) phosphate-buffered Krebs was used to increase sensitivity. The fluorescent signal generated by the FITC-AChE immobilized on the fiber in the evanescent zone was extremely stable and showed little drift for several hours. Addition of the substrate ACh to buffer perfusion medium resulted in a readjustment of the steady-state fluorescence. The enzyme activity was assayed by interrupting the flow of the perfusate and measuring the percent decrease in the baseline fluorescence during a 2 min period. The magnitude of signal reduction was dependent on buffer capacity, and the biosensor function was dependent on the presence of the substrate ACh. In its presence (Fig. 2A), interruption of the buffer flow by turning the pump off, allowed the local pH in the vicinity of the FITC-labeled enzyme to drop resulting in fluorescence quenching (Fig. 2B). Resuming the buffer flow allowed the equilibrium to be reestablished. The assay was very stable and could be repeated numerous times on the same fiber without loss in enzyme activity (Fig. 2C).

Several factors most likely influenced the rate of fluorescence decrease upon interruption of the buffer flow. These include the decrease in substrate and increase in product in the local environment of AChE, the effect of local pH changes on the turnover number, and the nonlinear relationship between proton concentration and quantum yield of FITC. Kinetic analysis of ACh hydrolysis by the immobilized FITC-AChE, yielded an apparent  $K_m$  (i.e.,  $K_{app}$ ) value of 0.42 mM and a  $V_{max}$  of 400 mV/2 min assay. By comparison, the immobilized and

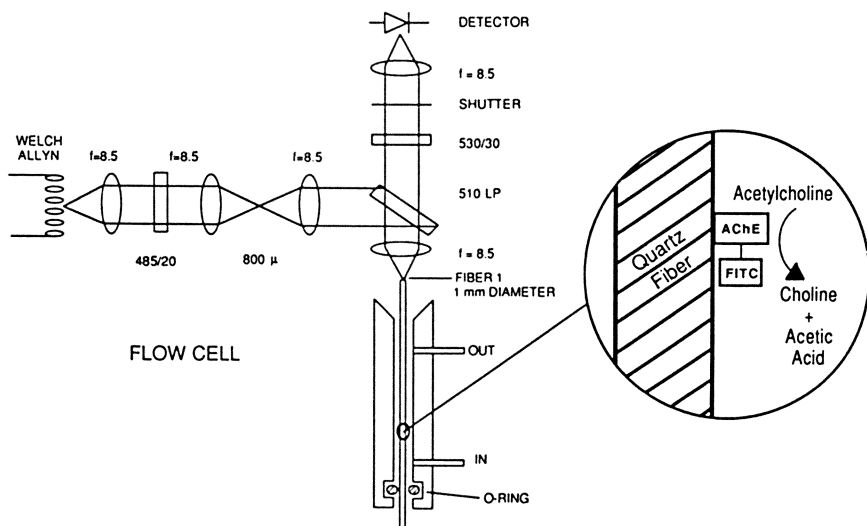


Figure 1. Schematic presentation of the optical system used to measure fluorescein. Fiber inset illustrates biochemical model for AChE biosensor used for detection of antiChEs.  $f$ , focal length. (Reproduced with permission from ref. 22).

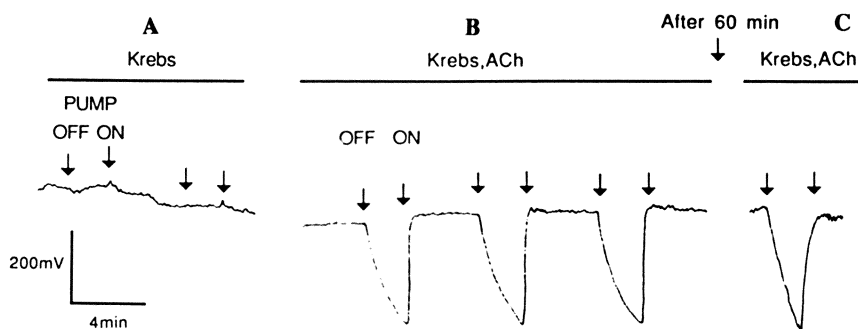


Figure 2. The change in total internal reflection fluorescence as a result of AChE activity. (A) Steady-state fluorescence in the absence of ACh was unaffected by interruption in the buffer flow. (B) In the presence of 1 mM ACh, fluorescence was quenched when the pump was turned off and protons accumulated. The baseline fluorescence was quickly reestablished when the pump was turned on and the excess protons were removed by the perfusing substrate solution. (C) Enzyme activity was measured by the amplitude of signal quenching after 2 min. This response was stable after 2 h. (Reproduced with permission from ref. 22).

soluble FITC-AChE yielded respective  $K_m$  values of 80 and 50  $\mu\text{M}$  for hydrolysis of acetylthiocholine measured by the method of Ellman et al. (1961). The specific activity of the soluble FITC-AChE was 680  $\mu\text{mol min}^{-1} \text{mg}^{-1}$  for hydrolysis of ACh. Assuming that the specific activity of FITC-AChE did not change upon immobilization, assay of the immobilized enzyme by the method of Ellman et al. (1961) yielded a value of 0.48 pmol catalytic sites immobilized per fiber.

The biosensor showed excellent substrate specificity (Table I) for several of the substrates used by Adams (1949) for characterization of human erythrocyte AChE. The differences in hydrolysis rate of butyrylcholine and *n*-butylacetate may be due to differences between erythrocyte AChE used by Adams and eel AChE, which was used in this study.

The addition of 0.1 mM of the reversible AntiChE, edrophonium, to the substrate-Krebs solution resulted in a 79% reduction in enzyme activity (Fig. 3B). Quenching of the fluorescent signal was stable for as long as edrophonium remained in the perfusion solution. However, upon removal of edrophonium by switching to edrophonium-free Krebs solution, the signal recovered totally within 2 min of wash.

Table I. Effect of AChE Substrates on the Response of the AChE Fiber-Optic Biosensor (Reproduced with permission from ref. 22)

Substrate	Relative rate of hydrolysis	
	Fiber-optic sensor <sup>a</sup>	Manometric (Warburg) <sup>b</sup>
Acetylcholine	100 $\pm$ 0	100 (0.006 M)
Acetyl- $\beta$ -methylcholine	63 $\pm$ 11	50 (0.03 M)
Benzyl acetate	22 $\pm$ 7	34 (0.03 M)
Butyrylcholine	21 $\pm$ 6	3 (0.03 M)
Benzoylcholine	< 1	< 1
<i>n</i> -Butyl acetate	< 1	24
Carbamylcholine	< 1	NA

<sup>a</sup>The AChE biosensor response expressed as relative to that of ACh hydrolysis rate. The concentration of substances was 1 mM.

<sup>b</sup>Rate of hydrolysis of substrates by red blood cell cholinesterase expressed as % of that of ACh. Concentration of substrates was 0.1 M unless otherwise indicated in parentheses (Adams, 1949).

The therapeutic organophosphorus echothiophate, an AntiChE that is an ester of diethoxythiophosphate of choline, at 0.1 mM inhibited AChE activity almost totally after 10 min exposure. The enzyme activity, did not recover upon perfusion of the treated fiber with 1 mM ACh in buffered Krebs for 30 min. However, perfusion for 10 min with 1 mM 2-pralidoxime (2-PAM) in the buffer resulted in 85% recovery of the phosphorylated AChE activity (Fig. 4). Thus,

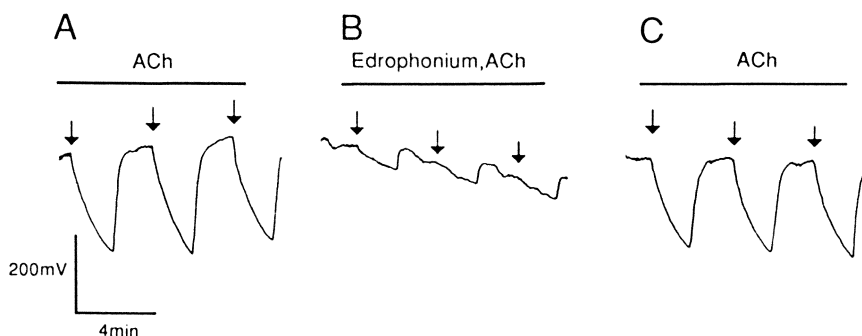


Figure 3. Reversible inhibition of the fluorescent signal generated by the biosensor in presence of 1 mM ACh (A), after 2 min perfusion with 0.1 mM edrophonium + 1 mM ACh (B). After removal of edrophonium and perfusion with 1 mM ACh again (C) the signal was restored. Arrows indicate times when the pump was turned off. The pump was turned on again after 2 min in each case. Three measurements 2 min apart were recorded for each condition. (Reproduced with permission from ref. 22).

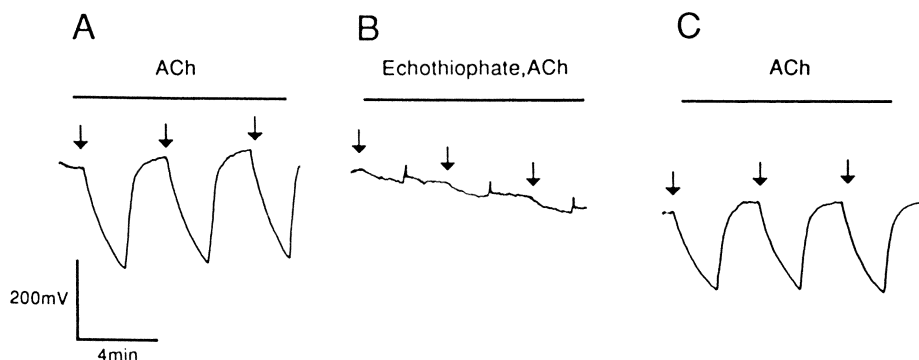


Figure 4. Inhibition of the AChE biosensor by echothiophate. (A) Control responses of the biosensor to ACh (1 mM). Echothiophate (0.1 mM) was then added to the ACh-Krebs solution and after a 10 min perfusion in the biosensor signal was recorded (B). Echothiophate was replaced with 1 mM 2-PAM in the ACh-Krebs solution and after a 10 min perfusion 2-PAM was removed and the biosensor response was recorded (C). (Reproduced with permission from ref. 22).

AChE immobilization and tagging with FITC did not interfere with the enzyme's catalytic activity (Fig. 6), nor was its substrate specificity (Table I) or inhibition by various antiChEs altered (Table II). This biosensor is highly stable, rapid and is reusable for multiple measurements without deterioration of enzyme activity.

Table II. Comparative Inhibition of Immobilized and Soluble AChE as Assayed by the Fiber-Optic Biosensor and Colorimetric Assays (Reproduced with permission from ref. 22)

Compound	Fiber-optic biosensor assay <sup>a</sup> IC <sub>50</sub> (M)	Colorimetric assay <sup>b</sup> IC <sub>50</sub> (M)
Echothiophate	$3.8 \times 10^{-8}$	$3.5 \times 10^{-8}$
Paraoxon	$3.7 \times 10^{-7}$	$4.0 \times 10^{-7}$
Bendiocarb	$2.2 \times 10^{-6}$	$6.4 \times 10^{-6}$
Methomyl	$9.0 \times 10^{-6}$	$1.5 \times 10^{-5}$
Dicrotophos	$3.3 \times 10^{-4}$	$1.1 \times 10^{-4}$

<sup>a</sup>AChE biosensor was incubated in the presence of each compound for 10 min prior to introduction of ACh (1 mM) and subsequent assay of activity in the presence of inhibitor.

<sup>b</sup>Soluble AChE was incubated in the presence of each compound for 10 min and then assayed using the method of Ellman et al. (1961).

### Biosensor for Detection of Cholinesterases

The above results made it abundantly clear that the optic fiber is simply converted into a pH sensor by immobilizing the FITC-AChE on it. It was then reasoned that any FITC-tagged protein would serve the purpose detecting activities of AChE and other cholinesterases (ChE) in the sample. Since our previous research with this optic fiber system indicated that the quartz fibers bind bovine serum albumin (BSA) avidly (Rogers et al., 1989, 1991a), we decided to use FITC-BSA to construct a pH sensitive fiber to utilize for detection of AChE or ChE in samples. Perfusion of this fiber with citrate buffer (pH 3) reduced fluorescence and perfusion with carbonate buffer (pH 9) increased it (Fig. 5). Because the flow cell accommodates a small volume of sample (46  $\mu$ l), it was reasoned that this fluorescent biosensor could monitor ChE activity in serum or blood if ACh were added to the sample. Blood samples were donated by the experimenters and either whole blood or serum ( $\approx 0.5$  ml) was used in testing. Perfusing the FITC-BSA coated fiber with human blood produced no change in fluorescence. However, when 10 mM ACh was added to the blood immediately before perfusion, there was a precipitous time-dependent decrease in fluorescence (Fig. 6). Inhibition of serum ChE by pretreatment with 1  $\mu$ M paraoxon for 60 min inhibited the serum-induced reduction in fluorescence. Different concentrations of serum gave concentration-dependent responses,

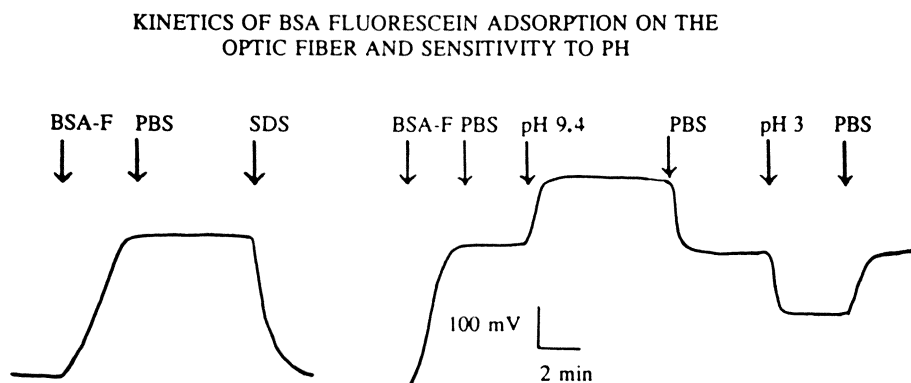


**Figure 5.** pH-induced changes in total internal reflection fluorescence of a BSA-FITC-coated quartz fiber. Phosphate (10 mM) buffered saline, pH 7.4 (PBS); carbonate (10 mM) buffered saline (pH 9.0); citrate (10 mM) buffered saline (pH 3.0). 1% SDS was used to desorb the BSA-FITC off the fiber.

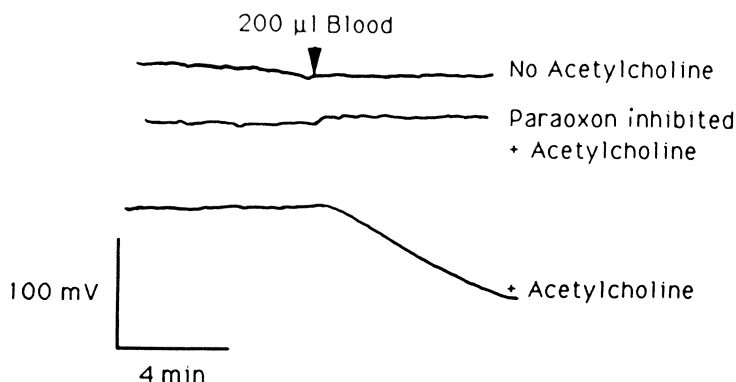


**Figure 6.** Changes in total internal reflection fluorescence upon perfusion of the fiber with whole blood and 1 mM ACh. No change in fluorescence was observed if ACh was not added or if 1  $\mu$ M paraoxon was added to the blood 10 min prior to assay.

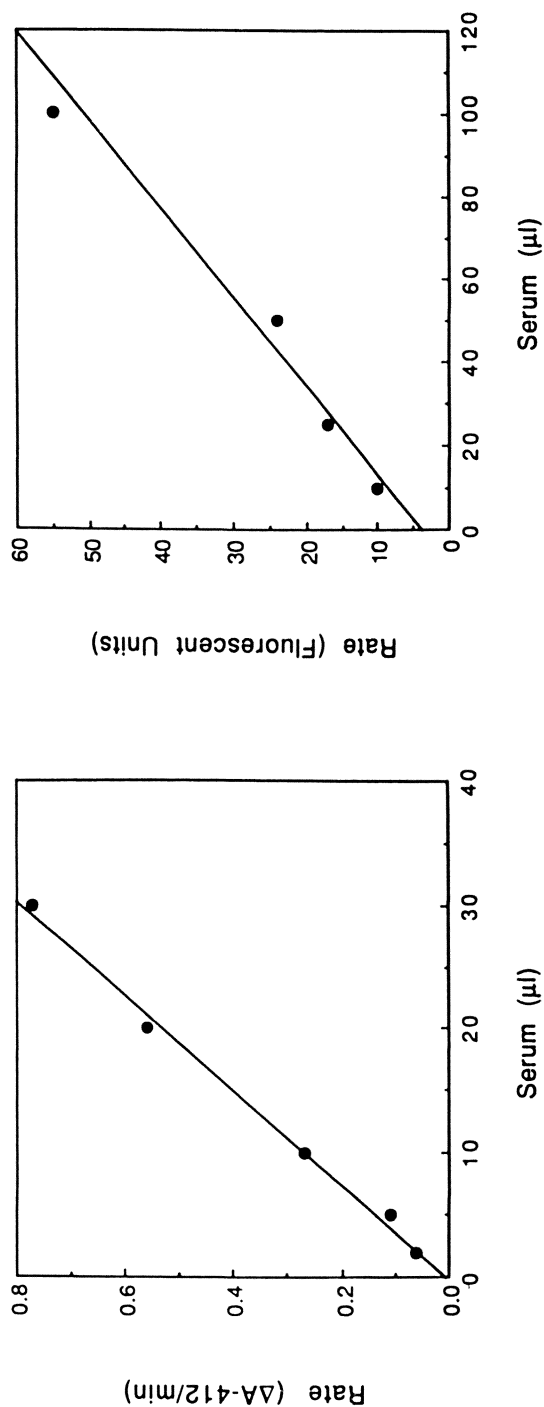


Figure 7. Cholinesterase activity of human serum measured by the Ellman spectrophotometric method (Left) or the Optic fiber fluorescence (Right).

confirming the conclusion that the change in fluorescence was dependent on the concentration of ChEs introduced into the assay (Fig. 6).

Although the results indicated that the optic fiber biosensor can be used to detect ChEs, the sensitivity of the method was slightly less than the spectrophotometric Ellman method (Fig. 7). On the other hand, an advantage for the biosensor is speed and the ability to measure ChE activity in whole blood samples without sample preparation, while hemoglobin in the blood interferes with the spectrophotometric analysis and must be corrected for or eliminated. We believe that the lower sensitivity of the fiber optic method is due mainly to the high buffering capacity of the blood or serum. Use of low capacity buffer in detecting antiChEs (Rogers et al., 1991a) was a major reason for its high sensitivity.

### Acknowledgements

The research described herein was financed in part by U.S. Army contract No. DAAA-15-89-C-0007.

### Literature Cited

1. Adams, D.H. *Biochim. Biophys. Acta* 1949, 3, 1-14.
2. Andrade, J.D.; Van Wagenen, R.A.; Gregonis, D.E.; Newby, K.; Lin, J.N. *IEEE Trans. Electron. Dev.* 1985 ED-32, 1175-1179.
3. Anis, N.A.; Wright, J.; Rogers, K.R.; Thompson, R.G.; Valdes, J.J.; Eldefrawi, M.E. *Analyt. Lett.* 1992, 25, 627-635.
4. Baum, G.; Ward, F.B. *Analyt. Biochem.* 1971, 42, 487-493.
5. Clark, L.C. In *"Biosensors: Fundamentals and Application"* (Turner, A.F.; Karube, I. and Wilson, G.S., eds) Oxford Sci. Publ. 1987, 3-12.
6. Durand, P.; Nicaud, J.M.; Mallevialle, J.J. *Analyt. Toxicol.* 1984, 8, 112-117.
7. Eldefrawi, M.E.; Eldefrawi, A.T.; Rogers, K.R.; Valdes, J.J. In *"Immunochemical Assays and Biosensor Technology for the 1990s"* (Nakamura, R.M.; Kasahara, Y.; Rechnitz, G.A., eds) Am. Soc. for Microbiology, Washington D.C. 1992, 391-406.
8. Eldefrawi, M.E.; Sherby, S.M.; Andreou, A.G.; Mansour, N.A.; Annau, Z.; Blum, N.A.; Valdes, J.J. *Analyt. Lett.* 1988, 21, 1665-1680.
9. Ellman, G.L.; Courtney, K.D.; Andres, V. Jr.; Featherstone, R.M. *Biochem. Pharmacol.* 1961, 7, 88-95.
10. Fortier, G.; Brassard, E.; Belanger, D. *Biosensors & Bioelectronics* 1990, 5, 473-490.
11. Gotoh, M.; Tamiya, E.; Monoi, M.; Kagawa, Y.; Karube, I. *Analyt. Lett.* 1987, 20, 857-870.
12. Glass, T.R.; Lackie, S.; Hirschfeld, T. *Appl. Optics* 1987, 26, 2181-2187.
13. Guilbault, G.G. *Ann. N.Y. Acad. Sci.* 1981, 369, 285-294.
14. Guilbault, G.G.; Hock, B.; Schmid, R. *Biosensors & Bioelectronics* 1992, 7, 411-419.

15. Hobel, W.; Polster, J. *Fresenius J. Analyt. Chem.* 1992, **343**, 101-102.
16. Hirschfeld, T.B.; Block, M.J. *U.S. Patent*, 1984, 4,447,546.
17. Mansuri, S.; Schultz, J.S. *Biotechnol.* 1984, **2**, 885-891.
18. McCann, J. In *"Biosensors: Fundamentals and Application"* (Turner, A.; Karub, I. and Wilson, G.S., eds) Oxford Sci. Publ. 1987, 3-12.
19. Morgan, H.; Taylor, D.M. *Biosensors & Bioelectronics* 1992, **7**, 405-410.
20. Murakami, T.; Nakamoto, J.; Kimura, T.; Kuriyama, T.; Karube, I. *Analyt. Lett.* 1986, **19**, 1973-1979.
21. Robinson, G.A. *Biosensors & Bioelectronics* 1991, **6**, 183-191.
22. Rogers, K.R.; Cao, C.J.; Valdes, J.J.; Eldefrawi, A.T.; Eldefrawi, M.E. *Fund. Appl. Toxicol.* 1991a, **16**, 810-820.
23. Rogers, K.R.; Eldefrawi, M.E.; Menking, D.E.; Thompson, R.G.; Valdes, J.J. *Biosensors & Bioelectronics* 1991c, **6**, 507-516.
24. Rogers, K.R.; Foley, M.; Alter, S.; Koja, P.; Eldefrawi, M.E. *Analyt. Lett.* 1991b, **24**, 191-198.
25. Rogers, K.R.; Valdes, J.J.; Eldefrawi, M.E. *Analyt. Biochem.* 1989, **182**, 353-359.
26. Taylor, R.F.; Marenchic, I.G.; Cook, E.J. *Analyt. Chimica Acta* 1988, **213**, 131-138.
27. Wise, D.L. *Applied Biosensors*. Butterworths Stroveham MA USP 1989, pp. 354.

RECEIVED September 17, 1993

## Chapter 8

# Hair as a Target Tissue for Developing a Biological Marker for Precursors to 2,5-Hexanedione

Deadre J. Johnson, Leon Lack, and Mohamed B. Abou-Donia<sup>1</sup>

Department of Pharmacology, P.O. Box 3813, Duke University Medical  
Center, Durham, NC 27710

This preliminary study was carried out to examine hair as a biomarker for exposure of male Sprague-Dawley rats to 2,5-hexanedione (2,5-HD). Rats were injected i.p. 50mg/kg/day with 2,5-HD for 45 days. Only hair samples from these animals stained positively with the Ehrlich's pyrrole reagent. This pyrrole response persisted during the entire period of administration and in samples taken 25 days post dosing. The extent of staining of vibrissae progressed linearly with progressing days of treatment. Our findings underscore the potential for utilizing hair to develop biomarkers for assessing exposure to neurotoxicants that form 2,5-HD. Hair should provide additional utility in other such investigations involving material with liabilities similar to that of pyrroles.

In 1857, a report by Hoppe-Seyler described the detection of arsenic in the hair of a body that was exhumed after eleven years, which yielded evidence that the metal was incorporated prior to death. See Moeller (*1*) for citations of this early history. A hundred years later Goldblum and co-workers described an ultraviolet method for the detection of barbiturates in guinea pig hair. With the development of more modern means of chemical analysis, a vast literature has emerged documenting the fact that many foreign substances such as drugs, heavy metals, and environmental toxicants can be incorporated into hair during their elaboration and growth. This has led to widespread applications in the fields of forensic sciences, environmental sciences, and toxicology.

Additional characteristics of the pilary system contribute to its usefulness in such endeavors: 1) The material is readily accessible and affords no difficulty in providing the requisite amounts for analysis. 2) The biological turnover of its cell contents is minimal. Most of the proteins and DNA of finally formed hair are

<sup>1</sup>Corresponding author

not degraded, and the hair can be used as a record of varying metabolic and toxicological states of the individual. 3) With hair, one can distinguish early biological signals from later ones. 4) Our experience shows that mature hair fibers have another property that, under certain situations, offer unique advantages not afforded by other tissues. The intracellular milieu is characterized by low water content, large concentrations of proteins, some of which are particularly high in sulfur content, and the absence of intracellular metabolism. It would be plausible to expect that such a milieu would not be conducive to autoxidation of any foreign substances that would be present there. This is particularly true for such substances as pyrroles (2), which are quite vulnerable to the action of oxygen and oxygen-derived free radicals including those normally arising from metabolic events.

Recently, we initiated feasibility studies employing the pilary system that were directed toward the development of a biological marker which would enable the detection of chronic exposure to *n*-hexane and methyl-*n*-butyl ketone. These are industrial solvents known to cause neurotoxicity in humans who have been subjected to chronic exposure (3). Our preliminary findings, which are encouraging, are described in part below and also serve to illustrate those above cited properties of the pilary apparatus that allow for such experimental initiatives.

It is believed that the neurotoxicity of *n*-hexane and methyl-*n*-butyl ketone is caused by their common metabolite 2,5-hexanedione (2,5-HD) (3-9). 2,5-Hexanedione is capable of forming N-substituted pyrroles by reacting with primary amines. This would include amino acids as well as the epsilon amino groups of lysine moieties of polypeptides (10-12). In addition, DeCaprio and co-workers in their mechanism studies of this neuropathy demonstrated that protein-bound pyrroles were formed *in vivo* in chickens that were treated daily with 2,5-HD (13). In their study, animals were treated 55 days with a toxic dose and 135 days with the subtoxic dose. Tissues that showed alterations included neural tissue, serum, liver, and kidneys. A notable finding made by these workers was the biphasic nature of the appearance of these pyrrole derivatives during the course of 2,5-HD administration. Peak levels of pyrroles were detected at 20 days (high dose) and 30 days (low dose) followed by dramatic declines of concentration values. This phenomenon could be attributed to two factors: 1) The well known labilities of the pyrrole substances, i.e., their autoxidation and polymerization to substances that cannot be detected by the Ehrlich's reagent for pyrroles (2), and 2) Their suggestion (13) of "a clearance mechanism capable of removing the altered proteins during the administration of 2,5-HD." Their finding of pyrroles was strongly suggestive of the possibility of utilizing *in vivo* pyrrole formation in tissues as a basis for developing a biological marker for chronic exposure to the industrial neurotoxicants. However, the biphasic nature of the above described pyrrole response precluded the possibility of correlating time of exposure to the neurotoxicant with pyrrole concentrations in any of those tissues studied (which would include serum).

Our interests in developing such biomarkers prompted us to examine whether hair could serve this purpose. It was anticipated that the intracellular milieu is one that would, to some extent, be protective against the autoxidation of the pyrrole substituents referred to above. Furthermore, because mature hair fibers

are not served by any blood supply, presumably any intracellular proteins, modified or otherwise, would remain within the hair structures until the hair is shed. The following which is a report of our preliminary findings, supports the above hypothesis and underscores the possibility of such biomarkers.

### Experimental Approach

Our initial approach consisted of three objectives: 1) To ascertain whether systemically administered 2,5-HD to rats results in its uptake by the hair-forming bulb cells resulting in pyrrole derivatives within the cells of the mature hair that would be detected with the Ehrlich colorimetric test for pyrrole substances. 2) To determine whether this discernable response persists during the entire period of administration. In addition, to investigate if such a signal remained manifest for a significant time after cessation of the 2,5-HD administration. 3) To examine the longer hairs (i.e., vibrissae) to see if the regions staining positively for pyrroles, progressively increase with the number of daily doses.

### Materials and Methods

2,5-Hexanedione and *p*-*N,N*-dimethylaminobenzaldehyde (DMAB, Ehrlich's reagent) were obtained from Aldrich Chemical Company (Milwaukee, WI). *N*-Ethylmaleimide (NEM) was obtained from Sigma Chemical Company (St. Louis, MO). 2,5-Hexanedione was redistilled *in vacuo*, made up in single use aliquots, and stored at -20°C. DMAB was stored in separate amber bottles under argon in accordance with the suppliers instructions. Male Sprague-Dawley rats were supplied by Charles River Laboratories (Raleigh, NC). Initial weights ranged between 280 and 320 g. Animals were housed in individual metabolic cages, a product of Nalge Company, catalog number 650, which allowed for timed fluid collections. Food and water was allowed *ad libitum*. Diurnal lighting was maintained at 12 hr cycles. Rats were injected i.p. with 50mg/kg 2,5-HD in 0.5ml saline. Daily injections were made at 5:00 p.m.

**Analyses of Rat Hair.** Samples of body hair, as well as individual vibrissa, were plucked from the animals while they were anesthetized with diethyl ether. The sites of hair removal, dorsal region and flanks, were distant from the sites of injection. Body hair was placed in test tubes to which were added: 1ml methanol containing 50mg NEM, 2ml of 1% sodium dodecyl sulfate (SDS) in water, and 2ml of 2.7% DMAB in 50% alcohol water containing 1% conc. HCl. Samples were allowed to sit overnight at room temperature away from light (in stoppered test tubes). After 15-18 hrs, the fluid was removed and the samples were washed as follows: twice with 50% methanol-water with 1% conc. HCl; twice with methanol; thrice with chloroform; once with methanol, and once with ethanol. Samples were then allowed to air dry at room temperature in the absence of light.

The vibrissae were allowed to react overnight while submerged in a solution

of 2.7% DMAB in 50% ethanol-water containing 1% conc. HCL. Fluid was removed and the vibrissae washed as follows: twice with 50% methanol-water containing 1% conc. HCL, twice with methanol, once with chloroform, and twice with ethanol. The samples were allowed to air dry in the absence of light.

## Results

Figure 1 depicts the colors developed by the Ehrlich's (DMAB) reagent in samples of body hair taken from four control animals and four animals treated with a daily i.p. dose of 50mg/kg/day 2,5-HD for 45 days. Also shown are the DMAB-treated body hair samples taken from the treated animals 25 days after they stopped receiving the diketone (i.e., Day 70).

Figure 2A shows the vibrissae from a representative animal that received daily i.p. doses of 50mg/kg 2,5-HD. Vibrissae were taken on day 0 and at 2, 3, and 4 weeks. The progressive increase in the regions that stained positively for pyrrole adducts suggests a causal relationship between the length of the stained area and the number of days the animals received the neurotoxicant. Initiation of the stained areas took place at the follicle end of the hair shafts. Also shown, Figure 2B, are magnifications (1.5X) of the regions adjacent to the follicle end of the hairs which were depicted in 2A. This allows for a better discernment of the colors elicited by DMAB. The yellow color characteristic of untreated tissue (8) is evident in the top hair, while the red regions are in the lower hairs--which is indicative of the presence of pyrroles.

This demonstration with single hairs merely shows the ongoing temporal nature of the DMAB response to chronic administration of 2,5-HD. Actual assessment of chronic exposure will require that each analysis consist of a representative number of hairs. The reasons for this requirement for a number of hairs resides in the patterns of growth that characterizes the hair cycles (see Discussion below).

## Discussion

The findings described in the Results section demonstrate certain advantages that could be important for developing biological markers to detect chronic exposure of individuals to foreign substances. The plan to develop biomarkers to assess chronic exposure to those neurotoxicants that give rise to 2,5-HD and in turn form pyrrole adducts with intracellular primary amines is a logical approach based on known sensitivity and degree of specificity of the Ehrlich's reagent. It is also consistent with previous reports (13) that administration of 2,5-HD to chickens did indeed give rise to protein-bound pyrroles. However, what appeared to be a serious complication was the transitory expression of these pyrrole adducts in various tissues during the course of 2,5-HD administration. This would put a limitation on the maximum time that exposure was detectable. In addition, the biphasic nature of the formation and subsequent decline would frustrate any attempts to correlate tissue levels or serum levels with the time of exposure. Equal values for pyrrole would be found on the ascending and descending phases of a

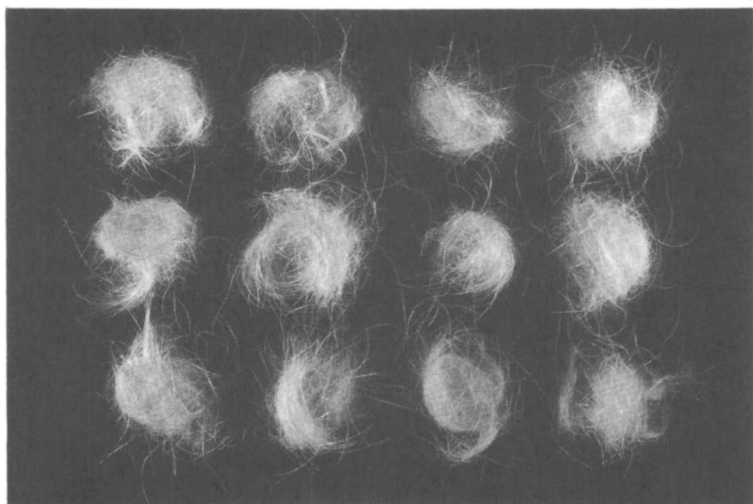


Figure 1. DMAB-treated body hair samples from four control rats and four experimental rats treated with 50 mg/day 2,5-HD for 45 days. From top to bottom, control animals, experimental animals treated for 45 days with 2,5-HD, and same experimental animals 25 days after 2,5-HD administration was stopped.

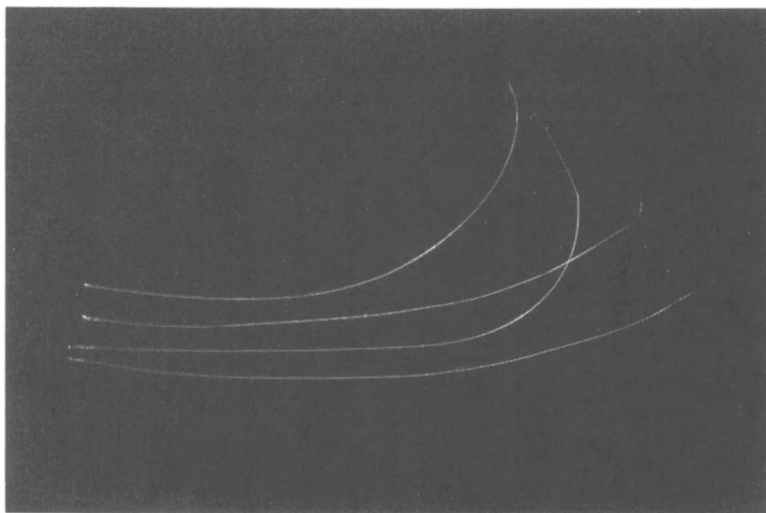


Figure 2A. Vibrissae taken from a 2,5-HD treated rat. From top to bottom, 0 week, 2 weeks, 3 weeks, and 4 weeks. Entire hair shown; magnification 1 X.

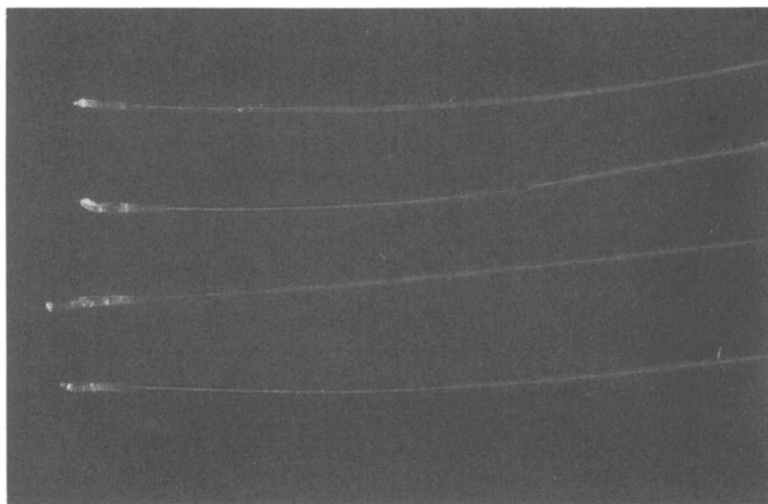


Figure 2B. Same as 2A, except that the region adjacent to the follicle end is depicted; magnification 1.5 X.

graph plotting concentration against time and such a value would have to be assigned to two time points.

We initiated these exploratory studies primarily to see if the detectable period of 2,5-HD-derived pyrroles is significantly greater in hair than that reported for serum and internal organs. The second objective was to see if the hair model could allow for a reasonable assessment of the duration of the exposure. The reason for this is that time of exposure would not logically correlate with concentration but rather with the maximum distance from the follicle end where pyrroles were detected when this distance is factored by the known rate of growth of hair. These rates of growth are characteristic of different species but tend to be fairly constant; see the Ebling *et al.* study, (14) particularly for the discussion of human hair.

Reference to the results of our studies reported above indicate that body hair shows longer time periods for the presence of pyrrole when compared with the published values for tissues. Furthermore, the pyrrole response persists even after 2,5-HD administration was terminated. The data with the longer hair (vibrissae), presented in Figures 2A and 2B, demonstrate the potential for correlating the length of the pyrrole positive portion of the hair with time of exposure.

An understanding of how this may be accomplished requires consideration of the cyclical nature of hair growth (15). The root of the hair, located in the follicle, has its lower portion expanded into the hair bulb. Growth of the hair results from the proliferating cells of the hair bulbs with commensurate elongation of the hair shafts. This is not a continual process--but undergoes cyclic activity. The active period of growth is termed the anagen phase. This active period is followed by cessation of growth or the catagen phase. This is characterized by an involution of the bulb; the hair now detached from the bulb is called a club hair and can remain anchored in place for extended periods before shedding. The catagen phase of the follicle is followed by the telogen phase at which time there occurs regrowth of germinal tissue in preparation for a new cycle of growth. At any one time, a plucked hair may be found to be in the growing phase (follicles in anagen) or in the nongrowing phase (follicles in catagen).

A final point must be considered. These preliminary studies were performed with white rats which allowed for direct visualization of the stained hair. Any practical application would have to deal with subjects bearing pigmented hair. We have found that hair proteins isolated from washed rat hair by the general method of Gillespie (16) from the 2,5-HD treated animals responded positively to the Ehrlich's reaction. This was in contrast to the negative reaction encountered with hair from control animals. Spectral analysis demonstrated that the absorbance maximum of the red chromophore was at 530 nanometers, which is characteristic of the absorbance range shown by pyrroles (data not shown). In addition, we have found that solubilized hair pigments do not interfere with the Ehrlich's test.

It is anticipated that the procedure to determine exposure to 2,5-HD will be as follows. A quantity of hair, sufficient to be representative of hairs in all phases of growth will be plucked at the skin surface and bundled to preserve the original tip-follicle orientation. Segments of bundled hair of known length will be assayed for pyrrole-bound protein following their solubilization. The distance of the

segment most distal to the follicle which shows a positive reaction when factored by the known rate of hair growth will provide an estimate of the duration of exposure.

### Acknowledgments

This work was supported by a NIOSH Grant No. OH00823. The authors wish to acknowledge Susan Embry and Steven Conlon for their skillful preparation of the photomicrographs and Shirley Faulkner for her excellent secretarial assistance.

### Literature Cited

- 1) Moeller, M.R.; *J. Chromatography* **1992**, *580*, 125-134.
- 2) Jones, R.A.; Bean, G.P. In *Organic Chemistry*; Blomquist, A.T. and Wasserman, H.H., Ed.; Academic Press: New York, NY and London, 1977, Vol. 34; 209-247.
- 3) Spencer, P.S.; Schaumburg, H.H.; Raleigh, R.L.; Terhaar, C.J. *Arch. Neurol.* **1975**, *32*, 219-222.
- 4) Abou-Donia, M.B.; Makkawy, H.M.; Graham, D.G. *Toxicol. Appl. Pharmacol.* **1982**, *62*, 369-389.
- 5) Abou-Donia, M.B.; Lapadula, D.M.; Campbell, G.M.; Abdo, K.M. *Toxicol. Appl. Pharmacol.* **1985**, *79*, 69-82.
- 6) Abou-Donia, M.B.; Makkawy, H.M.; Campbell, G.M. *J. Toxicol. Environ. Health* **1985**, *16*, 85-100.
- 7) Lapadula, D.M.; Suwita, E.; Abou-Donia, M.B. *Brain Res.* **1988**, *458*, 123-131.
- 8) Lapadula, D.M.; Habig, C.; Gupta, R.P.; Abou-Donia, M.B. *Biochem. Pharmacol.* **1991**, *41*, 877-883.
- 9) Abou-Donia, M.B.; Hu, Z.; Lapadula, D.M.; Gupta, R.P. *J. Pharmacol. Exper. Ther.* **1991**, *257*, 282-289.
- 10) Decaprio, A.P. *Mol. Pharmacol.* **1986**, *30*, 452-458.
- 11) Decaprio, A.P.; Olajos, E.J.; Weber, P. *Toxicol. Appl. Pharmacol.* **1982**, *65*, 440-450.
- 12) Graham, D.G.; Anthony, D.C.; Boekelheide, K., Maschmann, N.A., Richards, R.G., Wolfram, W.W., and Shaw, B.R. *Toxicol. Appl. Pharmacol.* **1982**, *64*, 415-422.
- 13) Decaprio, A.P.; Strominger, N.L.; Weber, P. *Toxicol. Appl. Pharmacol.* **1983**, *68*, 297-307.
- 14) Ebling, F.J.G.; Hale, P.A.; Randall, V.A. In *Physiology, Biochemistry, and Molecular Biology of the Skin*, Goldsmith, L.A., Ed; Oxford University Press: New York, NY, **1991**, Vol. 1, 660-696.
- 15) Montagna, W.; Parakkal, P.R. In *The Structure and Function of Skin*, Academic Press: New York, NY, **1974**, 172-258.
- 16) Gillespie, J.M. In *Physiology, Biochemistry, and Molecular Biology of the Skin*; Goldsmith, L.A., Ed.; Oxford University Press; New York, NY, **1991**, Vol 1; 625-659.

RECEIVED August 18, 1993

## Chapter 9

# Hemoglobin Adducts of Pesticides

Frank C. Schnell

Lockheed Environmental Systems and Technologies, 980 Kelly Johnson  
Drive, Las Vegas, NV 89119

The indirect analysis of protein adducts has long been utilized to monitor exposure to organophosphates via the assay of plasma pseudocholinesterase and erythrocyte cholinesterase activities. It may now be possible to monitor exposure to other classes of pesticides using direct measurements of protein adducts, particularly those of hemoglobin. Stable hemoglobin adducts tend to accumulate in a dose-related manner and persist for the life of the protein, during which time they integrate intermittent as well as continuous chemical exposures from all sources and by all routes of entry. A survey of the literature indicates that more than 30 different pesticides may form adducts with hemoglobin, and that many of these adducts have been used as biomarkers of exposure in animals and/or humans. Most promising so far are the acid/base labile sulfinic acid amide adducts formed *in vivo* between the  $\beta$ -93 cysteine of hemoglobin and the aromatic amine metabolites of certain N-aryl pesticides. Levels of these adducts reflect acetylation phenotype (which is associated with susceptibility to arylamine-induced bladder cancer), and tend to be more sensitive indicators of exposure than are methemoglobin levels. Several pesticides of other types reportedly bind to hemoglobin or erythrocytes *in vivo*. However, many of the resulting adducts have been identified only as "erythrocyte conjugates" and require further characterization.

The probability of human exposure to a pollutant will be determined by the distribution as well as the abundance of that pollutant in the environment, and will be affected by numerous chemodynamic factors including volatility, water solubility, and soil adsorption, as well as rates of photolysis, hydrolysis and biodegradation.

0097-6156/94/0542-0133\$07.25/0  
© 1994 American Chemical Society

Similarly, the consequence of human exposure will depend on the dose of the xenobiotic or its metabolites to a specific target tissue of the exposed individual. This tissue dose will be affected not only by the xenobiotic's concentration in the environment, but by various toxicokinetic factors including absorption, distribution, metabolism, and excretion, each of which exhibits some degree of interindividual variation. Consequently, different individuals subjected to similar levels of environmental exposure may exhibit significantly different tissue doses, and express the associated health effects to widely varying degrees. Clearly, the more direct the measurement of tissue dose, the greater the accuracy and reliability of the exposure assessment. The relationship between environmental exposure, biologically effective dose, and health effects is schematically depicted in Figure 1, using chemical carcinogenesis as an example health effect. Also shown are the sampling points for environmental and biological monitoring.

The exposure biomarkers most commonly monitored, i.e., the parent compound or its metabolites in blood or urine, typically reflect only those exposures occurring during the last 24-48 hrs. Less recent exposures may be detectable as reaction products of xenobiotics (or their metabolites) and macromolecules such as DNA and protein. Recently, where cancer has been the health effect of interest, such macromolecular adducts have received a great deal of attention as potential tools in molecular dosimetry (1-2). Due to the existence of efficient repair systems, DNA adducts levels tend to be extremely low and exhibit greater interindividual variability than do protein adducts. As a result, DNA adducts have less potential as practical biomarkers of exposure than they do as biomarkers of effect (i.e., of genotoxicity). The reverse is generally true of protein adducts, which tend to accumulate rather than be repaired but typically bear little or no relevance to the mechanism of carcinogenesis. (It should be noted, however, that a protein adduct would be a valid surrogate biomarker of genotoxicity if a corresponding DNA adduct were formed in proportional amounts by the same reactive metabolite.) Stable protein adducts integrate exposure from all sources via all portals of entry over the life of the protein, and reflect interindividual variation in absorption, metabolism and, in some cases, susceptibility. Exposure to compounds other than known or suspected carcinogens may also be monitored using protein adducts, provided only that the parent compound or one of its metabolites is sufficiently electrophilic and long-lived to form adducts with a readily-accessible protein.

One such readily-accessible protein is hemoglobin (Hb), which is among the best characterized of all proteins (3-4). It is a tetramer (approx. M.W. = 64,450) consisting of 2 identical  $\alpha$ - and 2 identical  $\beta$ -chains. Large quantities (0.5-1.5 grams) are available in a 5-10 mL sample of human blood. Over the life span of Hb, which averages about 60 days in rats and 4 months in humans, stable adducts tend to accumulate in a dose-dependent manner at various nucleophilic sites. The

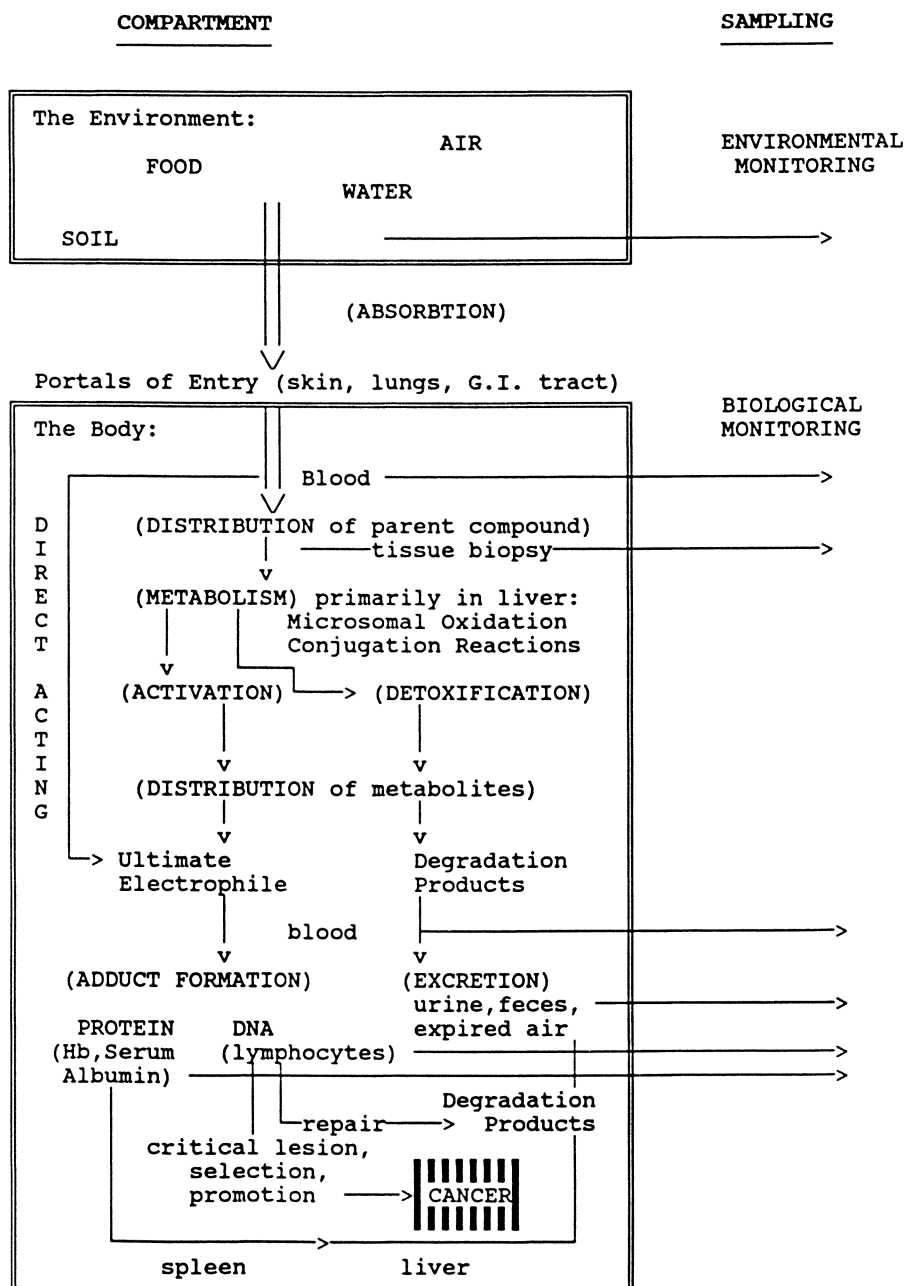


*Figure 1. Environmental vs. biological monitoring data. Schematic diagram illustrating relationship between an exposure marker's proximity to the target of effect and its relevance to health risk.*

sites at which adducts form most often in Hb include the sulfhydryl group of cysteine, the ring nitrogens of histidine and the N-terminal amino nitrogen of valine. In human Hb, the only reactive cysteine residues are those at position 93 in the  $\beta$ -chains.

The kinetics of adduct-formation in Hb make this protein an almost ideal dosimeter of human exposure to xenobiotics in the environment. In most single-dose experiments, Hb adduct-formation (and elimination) is a linear function of the administered dose, often over several orders of magnitude (5-6). When nonlinearities are observed in animal studies, they most often reflect saturation kinetics, a situation which will seldom be encountered in humans exposed to environmental levels of pollutants. Under conditions of chronic exposure, stable Hb adducts accumulate with time, ideally reaching a steady state level after an interval of time ( $t_{\alpha}$ ) equivalent to the mean life span of the erythrocyte (2). The degree of alkylation at steady state will be approximately equal to the daily increment in adducts times one half the life span of the erythrocyte. The resultant multiplier ( $0.5t_{\alpha}$ ) will therefore be about 30 in rats and 60 in humans. Upon termination of exposure, stable Hb adducts are generally eliminated at a rate that is consistent with the life span of the erythrocyte.

In addition to the usual expressions (e.g., nanomoles or picograms adduct/gm Hb), three measures of Hb-binding are commonly used in the literature. The so-called hemoglobin binding index (7), or HBI, is expressed in units of mmol adduct/mol Hb/mmol dose/kg body weight. (A similar index, the ABI, can be defined for binding to serum albumin.) The Covalent Binding Index (5), or CBI, is expressed in units of pmol/g Hb/ $\mu$ mol dose/kg and is 15.5 times larger than the equivalent HBI. The third measure of Hb-binding, the percentage of dose bound, takes into account the species-specific content of Hb per kg of animal. In rats, for example, the molar content of Hb is about 147  $\mu$ mol Hb/kg body weight (8), and the percent of dose bound would be calculated as  $100 \times 0.000147 \times \text{HBI}$ .

A survey of the literature reveals that more than 30 different pesticides have been reported to form adducts with Hb or unspecified erythrocyte proteins (Table 1), and that several of these adducts have been used as biomarkers of exposure in animals or humans. Several arylamine-based pesticides form well characterized arylamine-Hb adducts that may have potential as molecular dosimeters of exposure in humans, but most have so far been studied only in animals. Many other pesticides form extractable erythrocyte adducts *in vivo*, which have yet to be fully characterized or even positively identified as Hb adducts. Hydrolyzable Hb adducts or erythrocyte conjugates have been used to monitor human exposure to a few pesticides, including Diuron (a phenylurea herbicide), Propoxur (a carbamate insecticide), Amitrole (a triazole herbicide), Triadimefon and Bitertanol (triazole fungicides). Incomplete as it is, the available information on Hb adducts of pesticides is presented here with the hope of stimulating more interest in and research on this promising new biomonitoring tool.

TABLE 1. PESTICIDES REPORTED TO FORM HEMOGLOBIN ADDUCTS

CLASS	COMPOUND <sup>a</sup>	REFERENCE
ARYLAMINE DERIVATIVES:	2-Acetylaminofluorene	5,7,12,15
	Alachlor	26
	Chlordimeform	20
	Chloropropham	20
	Diuron	20,23
	Linuron	20
	Monuron	20
	Monolinuron	20
	Propanil	22
	Propham	20
ORGANO- PHOSPHATES:	Demeton-S-methyl	23
	Dichlorvos	38
	Omethoate	23
	Phoxim	23
CARBAMATES:	Carbofuran	23
	Eptam	31
	Methiocarb	23
	Molinate	31
	Propoxur	23
TRIAZOLES:	Amitrole	23
	Bitertanol	23
	Triadimefon	23
TRIAZINES:	Anilazine	23
	Atrazine	35
	Cyanatrin	31
	Metamitron	23
	Simetryn	32
PHENOLICS:	<i>p</i> -Nitrophenol	23
	Pentachlorophenol <sup>b</sup>	45
ORGANOMETALS:	Propineb	23
	Azocyclotin	23
PYRETHROIDS:	Fenfluthrin	23
OTHERS:	Ethylene dibromide <sup>b</sup>	40
	Fuberidazole	23
	Monochloroacetic acid <sup>b</sup>	43
	Naphthalene	5
	Tolylfluanid	23
	Trichloroacetonitrile	44

<sup>a</sup> Those compounds cited only by (23) form erythrocyte conjugates which may or may not be true hemoglobin adducts.

<sup>b</sup> Compound binds to protein, but reports do not specify hemoglobin.

### Arylamine-Based Pesticides

Of all the pesticides listed in Table 1, those which are, or may be metabolized to, aromatic amines show the greatest potential for protein adduct-based biomonitoring. This potential derives from the singular mechanism by which aromatic amines in general form Hb adducts. This mechanism, which was originally proposed by Green et al. (6), is illustrated in Figure 2 using aniline as an example. First, the aromatic amine is oxidized by cytochrome P-450 in the liver to the corresponding N-hydroxy-arylamine which migrates into the bloodstream. In the erythrocyte, the N-hydroxyarylamine is cooxidized with the heme iron of Hb to produce met-Hb and a nitrosoarene. Production of the latter is enhanced by the possibility of recycling, i.e., both the nitrosoarene and met-Hb may be reduced by NADPH-dependent reactions only to undergo another round of cooxidation. Alternatively, the nitrosoarene may react with the nearby sulfhydryl group of the  $\beta$ -93 cysteine residue (the only reactive cysteine residue in Hb) to form a sulfinic acid amide adduct which is stable at physiological pH, but labile to treatment with mild acid or base *in vitro*. In animals treated with aromatic amines,  $\beta$ -93 cysteine sulfinamide adducts may account for as much as 90% of the Hb-bound material and represent 5% or more of the administered dose (6).

In the method originally developed for the detection of 4-aminobiphenyl (4-ABP) adducts in rats (6,9), the hydrolyzed adducts were extracted with hexane and analyzed using GC with electron capture detection. The detection limit was 50-100 pg of 4-ABP/10 mL blood. Base-catalyzed hydrolysis was found to yield a much cleaner chromatogram than acid-catalyzed hydrolysis. The method has since been refined for the detection of cysteine sulfinamides in humans (10-13). By coupling GC to negative-ion chemical ionization mass spectrometry (NICI-MS) in the selective ion mode, selectivity has been enhanced and sensitivity has been increased to less than 10 pg or 50 fmole of 4-ABP/10 mL of human blood.

Pesticides known to form arylamine-Hb adducts include: Chlordimeform; Protham; Chlorprotham; Monuron; Monolinuron; Propanil; Linuron; Diuron; and Alachlor. These compounds are commonly used herbicides or insecticides that may be metabolized in mammals to the parent amine by both cytosolic and microsomal amidases. The aromatic amine 2-acetylaminofluorene (2-AAF) was originally developed as a pesticide but was never marketed because of its demonstrated carcinogenicity in mice, male rats, and dogs (14). Instead, it became a useful tool in cancer research, and was used in some of the earliest studies of protein adducts as biomarkers of exposure (5,15).

These early studies established the linear dose-dependence of Hb-binding over a wide range of dose, but total binding to Hb in rodents was greatly underestimated. At that time, globin was routinely isolated by precipitation in acidic acetone (16), and a high percentage of the sulfinamide adducts were apparently discarded with the supernatant. It was later demonstrated that 75-90%

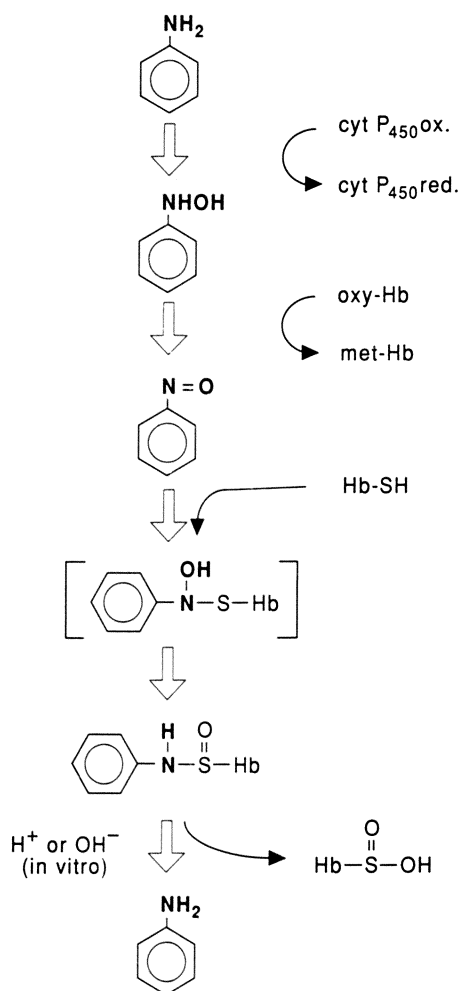


**Figure 2.** Mechanism of the *in vivo* formation of arylamine-hemoglobin adducts and their release *in vitro*.

of Hb-bound aromatic amines, including 2-AAF, could be removed under moderately acidic conditions (7). 2-AAF was also shown to bind with serum albumin, but these adducts were considerably less abundant and shorter-lived than were Hb-adducts (12). It is now clear that the greater abundance of arylamine adducts in Hb is due to the presence of the catalytic heme group. The slower elimination of the Hb adducts reflects the relatively long life span of rat Hb (ca. 60 days) compared to the short half-life of rat serum albumin ( $t_{1/2}$  = ca. 2.7 days) (17-18).

Over the last 5-10 years, acid/base-released cysteine adducts in Hb have been used to monitor exposure to numerous aromatic amines in both experimental animals and humans. For example, in a study of female Wistar rats receiving single oral doses (19), HBI values were determined for several monocyclic aromatic amines, including aniline, 4-chloro-aniline, 3,4-dichloro-aniline, and 4-chloro-*o*-toluidine. Most recently (20), it has been demonstrated that these same arylamines, among others, may be formed as metabolites in rats dosed orally with certain urea and carbamate pesticides. The amide bond of these and other arylamine-based pesticides can be hydrolyzed by certain nonspecific amidases present in mammalian tissues to yield the corresponding parent aromatic amines (20-22). Thus, the formamidine insecticide Chlordimeform may be hydrolyzed *in vivo* to form 4-chloro-*ortho*-toluidine, while the carbamate herbicides Protham and Chlorprotham yield aniline and 3-chloroaniline, respectively (Figure 3). Similarly, the acylamidase-catalyzed hydrolysis of the phenylurea herbicides Monuron and Monolinuron yields 4-chloroaniline (Figure 4), while that of Linuron and Diuron yields 3,4-dichloroaniline (Figure 5).

All these pesticides formed the expected base-labile, minor Hb-adducts in female Wistar rats dosed orally with up to 1 mmol/kg b.w. (20). The metabolic yield of the parent amine was 7-10% for all but Chlorprotham and Diuron which yielded 24% and 50%, respectively. When these different rates of conversion are taken into account, Hb-binding of *N*-aryl pesticides in rats correlates with the HBI of the parent amine metabolites just as one would expect (Table 2). Thus, among those pesticides with similar conversion rates (i.e., 10% or less), the highest binding occurred with those yielding 4-chloroaniline (HBI=569), and the lowest binding occurred with those yielding 3,4-dichloroaniline (HBI=9). Calculations by Sabbioni and Neumann (20) suggest that adducts of most of these pesticides should be detectable in humans exposed via residues in food. One cautionary note must be sounded, however, regarding potential confounding exposures. The amide hydrolysis product of protham is also the most abundant aromatic amine present in cigarette smoke. Concentrations of 364 and 10,800 ng aniline/cigarette have been reported in mainstream and sidestream cigarette smoke, respectively (11). Thus, in any effort to monitor human exposure to protham using Hb adducts, it would be imperative to carefully classify the subjects according to smoking status.

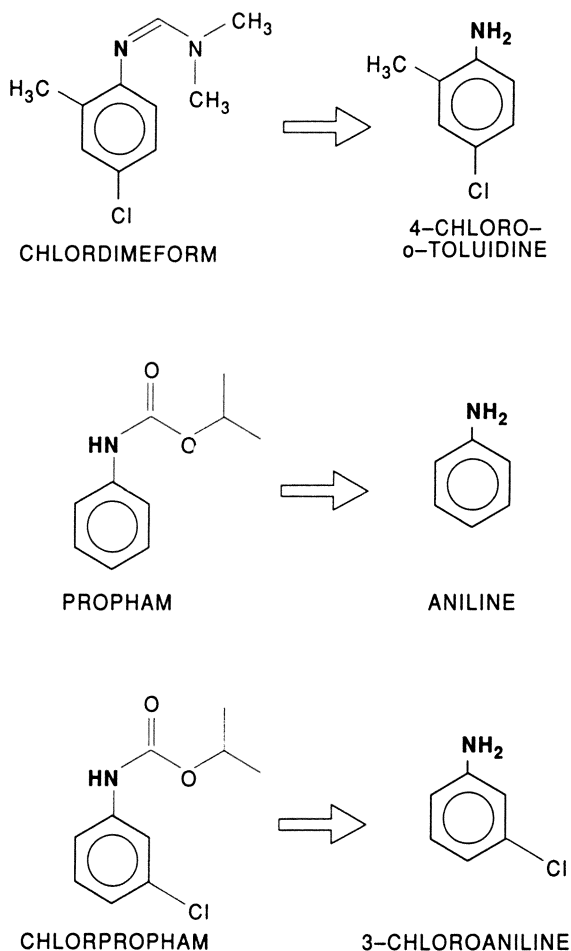


**Figure 3.** *Metabolism of the formamidine insecticide Chlordimeform and the carbamate herbicides Protham and Chlorprotham to Hb-binding hydroxylamines.*

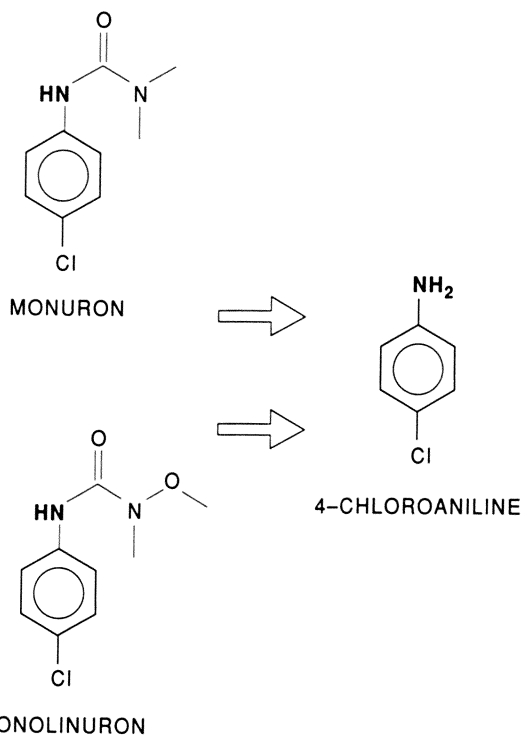


*Figure 4. Metabolism of the phenylurea herbicides Monuron and Monolinuron to 4-chloroaniline.*

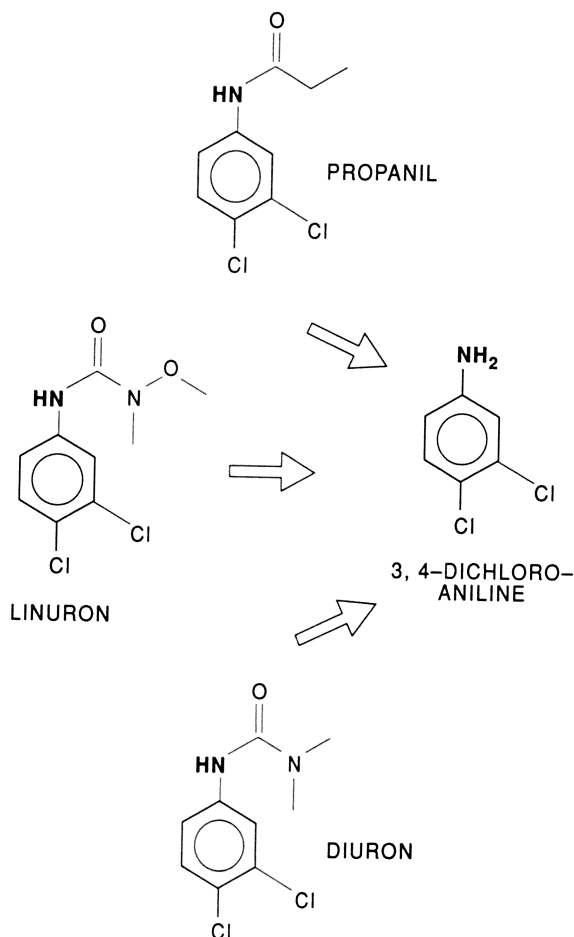


*Figure 5. Metabolism of the arylamide herbicide Propanil and the phenylurea herbicides Linuron and Diuron to 3,4-dichloroaniline.*

The arylamide herbicide Propanil, like Linuron and Diuron, may be metabolized to 3,4-dichloroaniline (Figure 5) by acylamidase-catalyzed hydrolysis (21). In male Sprague-Dawley rats given 30, 100, and 300 mg Propanil/kg i.p., maximum Hb-binding (measured as base-labile sulfinic acid amide adducts) was 10, 50, and 450 pmol/mg, respectively (22). By contrast, methemoglobin levels were measurable only at the two highest doses, reaching maximum levels of 5% and 24%. These results suggest that Hb-adducts may be better biomarkers of exposure to N-aryl pesticides than are the methemoglobin levels typically monitored in occupational settings. (Propanil was not included on Table 2 because, without knowing the percent absorption from the rat gut, it was not possible to normalize the results obtained with ip-dosed rats for comparison with the data obtained from orally-dosed rats.)

Human exposure to one of the N-aryl pesticides has already been successfully monitored using hydrolyzable, aromatic amine-Hb adducts. Monitoring Diuron exposure in German workers, Lewalter and Korallus (23) found a good correlation between the concentrations of 3,4-DCA in urine and in erythrocytes (Table 3). Furthermore, 3,4-DCA levels in both biological media reflected the acetylation status of the workers. Slow acetylators, which represent approximately 40% of the population in N. America and Europe and are known to be at higher risk for arylamine-induced cancer, form higher levels of Hb adducts than do fast acetylators. Thus, arylamine-Hb adducts may reflect susceptibility as well as exposure. The authors conclude that 100  $\mu\text{g/L}$  represents a safe level roughly equivalent to the 5% met-Hb standard currently used by industrial hygienists (23). The choice of 100  $\mu\text{g/L}$  probably reflects the fact that, in Germany, a new biological tolerance level for aniline based on the release from acidified Hb of 0.1 mg aniline/L blood is thought to provide better exposure control than the old equivalent tolerance levels based on a methemoglobin level of 5% or urinary levels of free aniline  $\leq 1 \text{ mg/L}$  (24).

At least one other arylamine-based pesticide has some potential to form cysteine sulfinamide adducts in Hb, but the available data is little more than suggestive. As shown in Figure 6, the chloroacetanilide herbicide Alachlor is metabolized *in vitro* by rat liver preparations to at least two potentially adduct-forming compounds (25-26). The activity of both amidases and peroxidases leads to the formation of the metabolite 2,6-diethylaniline (DEA), an aromatic amine which has the potential, at least, to form cysteine sulfinamide adducts in Hb. Alternatively, DEA may be further oxidized to the electrophilic compound 3,5-diethyl-benzoquinone-4-imine, which might also form Hb adducts. The formation *in vivo* of uncharacterized adducts of DNA and Hb has been demonstrated in mice exposed to Alachlor labeled in either the [ $^{14}\text{C}$ ]methoxy or [ $^{14}\text{C}$ ]phenyl positions (26). However, the highest degree of labeling of mouse DNA and Hb was from the methoxy group of Alachlor which may have been liberated as formaldehyde by O-demethylation. If, in fact, formaldehyde is a metabolite of alachlor, it would

**TABLE 2. HEMOGLOBIN BINDING OF SOME N-ARYL PESTICIDES AND THEIR AROMATIC AMINE METABOLITES<sup>a</sup>**

COMPOUND	HBI <sup>b</sup>	% DOSE <sup>c</sup>	METABOLITE	HBI <sup>d</sup>
Chloropropham	2.9	0.043	3-CA	12 <sup>f</sup>
Propham	2.4	0.035	Aniline	22
Chlordimeform <sup>e</sup>	2.4	0.036	4-Cl-o-T	28
Monuron	38.9	0.56	4-CA	569
Monolinuron	54.8	0.806	4-CA	569
Linuron	0.8	0.012	3,4-DCA	9
Diuron	4.5	0.067	3,4-DCA	9

<sup>a</sup> Unless otherwise indicated, data are from (20) Sabbioni and Neumann, 1990. In all cases, female Wister rats were dosed by gavage with 0.47 to 1.0 mmole/kg pesticide or aromatic amine and sacrificed 24 hours later. After hydrolysis of Hb in base (1N NaOH), amine was extracted with hexane for GC analysis.

<sup>b</sup> Hemoglobin Binding Index of pesticide, mmol amine/mol Hb/mmol dose/kg body weight. Dose = 1 mmole/kg pesticide (except for Chlordimefon).

<sup>c</sup> % Dose = percentage of total dose bound to total Hb as the hydrolyzable amine. 100% binding corresponds to an HBI of 6800.

<sup>d</sup> Hemoglobin Binding Index of parent aromatic amine as the hydrolyzable amine, mmol amine/mol Hb/mmol dose/kg body weight. Except for 3-CA, data are from (19) Birner and Neumann, 1988.

<sup>e</sup> Dose = 0.4 mmol/kg body weight.

<sup>f</sup> Samples analyzed quantified by GC-MS with electron impact ionization and selective ion monitoring.

**TABLE 3. 3,4-DCA IN THE URINE AND ERYTHROCYTES OF DIURON-EXPOSED WORKERS<sup>a</sup>**

<i>3,4-DICHLOROANILINE (free amine)</i>		
	URINE ( $\mu\text{g/g creatinine}$ )	ERYTHROCYTES <sup>b</sup> ( $\mu\text{g/L blood}$ )
Normal Values	<10	<10
Exposed <sup>c</sup> :		
Fast Acetylators (60%)	<10 - 40	<10 - 10
Slow Acetylators (40%)	40 - 230	20 - 70

<sup>a</sup> Data from (23), Lewalter and Korallus, 1986. Tox Lett 33:153-165.

<sup>b</sup> Recommended safe level = 100  $\mu\text{g}$  3,4-DCA adducts/L whole blood.

<sup>c</sup> n=5

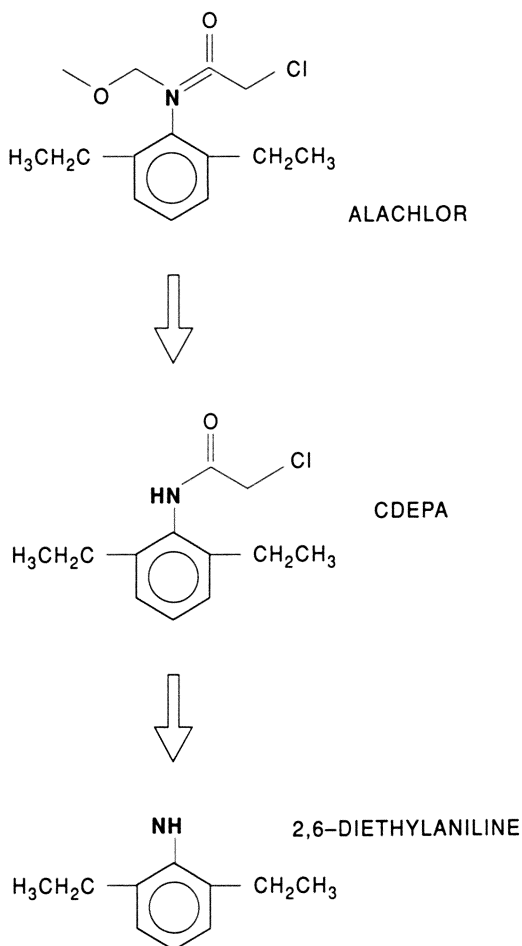


*Figure 6. Metabolism of the chloroacetanilide herbicide Alachlor to mono- and di-N-dealkylated metabolites.*

probably form methyl adducts with Hb (27). Such adducts should be measurable using the modified Edman procedure for the analysis of N-terminal valine adducts of Hb. However, they would be of little practical use for biomonitoring exposure to alachlor due to the presence of high background levels of methyl adducts of endogenous origin (28-30).

### Heterocyclic Pesticides

For the most part, the adducts reportedly formed by the heterocyclic pesticides (e.g., most triazines and triazoles) are poorly characterized. Those formed by Cyanatrin (31) and Simetryn (32) are perhaps the most well-characterized to date. Unfortunately, however, they are also the least applicable to biomonitoring in humans (33). These S-alkylthio-S-triazine herbicides are activated by S-oxygenation (34) to protein binding species in the rat. The S-oxides of both compounds bind with unusual avidity to a highly reactive thiol group (the  $\beta$ -125 cysteine) that is present in rat, guinea pig and chicken Hb, but absent in human, dog, cow, sheep, and pig Hb. Similar reactions have been observed with the thiocarbamate herbicides Molinate and Eptam (31).

The triazine herbicide Atrazine and/or its metabolites appear to bind to erythrocytes in female rats (35), but the type of binding was not reported. The two mono-N-dealkylated derivatives of atrazine have been identified as metabolites in rats (Figure 7). Each possesses a free amino group through which it could conceivably form hydrolyzable adducts with the  $\beta$ -93 cysteine of Hb. If, however, aminotriazines are capable of forming such adducts, the latter have yet to be described in the literature.

In Germany, it has been determined that a large number of pesticides, including most of the heterocyclic compounds listed in Table 1, form so-called erythrocyte protein conjugates or erythrocyte adducts (23). Although it is possible, perhaps even likely, that these adducts are associated with Hb, the limited details reported in this study are insufficient to either support or contradict such a conclusion. No specific information was found on the erythrocyte adducts reportedly formed by the triazine fungicide Anilazine, the carbamate insecticide Carbofuran, the benzimidazole fungicide Fuberidazole, the triazinone herbicide Metamitron, or the antiparasitical triazole Azocyclotin. However, the erythrocyte adducts formed by three other heterocyclic pesticides, Amitrole, Bitertanol, and Triadimefon, have been the subject of biomonitoring studies in humans (23).

Amitrole or 3-amino-1H-1,2,4-triazole is a nonselective, postemergence, translocated triazole herbicide that has been listed as a carcinogen by EPA (36). Lewalter and Korallus (23) have measured free Amitrole released from erythrocytes of exposed workers in German factories. Such measurements could indicate the formation of hydrolyzable adducts of Amitrole in exposed humans. However, in the absence of a description of the methods used, it is unclear how much of the

American Chemical  
Society Library

1155 16th St. N. W.

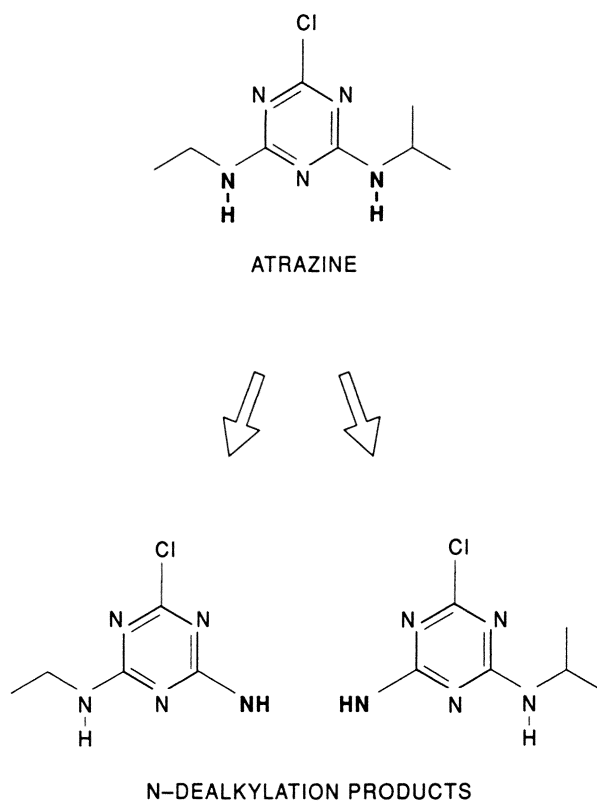


**Figure 7.** Metabolism of the triazine herbicide Atrazine to mono-N-dealkylated metabolites.

analyte may have been derived from non-covalently bound parent compound. The half-life of the Amitrole from erythrocytes was much longer than that in either blood or urine. A comparison of the daily levels of urinary Amitrole (which correlated well with amitrole air concentrations) with levels of erythrocyte conjugates determined weekly suggested that formation of Amitrole-erythrocyte adducts closely followed a dose-response relationship and provided comparable exposure control with much less sensitivity to sampling time (23). The authors indicated that, in their experience, no adverse health effects were observed even after many years of exposure, if the concentration of Amitrole adducts in erythrocytes was kept below 100  $\mu\text{g/l}$  of whole blood.

The triazole fungicides Bitertanol and Triadimefon undergo O-dealkylation to yield 4-phenylphenol and p-chlorophenol, respectively (Figure 8), metabolites that can, in practice, be detected in the blood and urine of exposed humans. According to Lewalter and Korallus (23), these same phenolic metabolites may also be released (method not specified) from erythrocytes isolated from exposed workers. The authors compared the levels of these analytes in the urine and erythrocytes of exposed workers (Table 4) and interpreted the results as reflecting interindividual differences in erythrocyte conjugate concentrations. However, it is not possible to assess the validity of this conclusion in the absence of any details regarding methodology. This omission is particularly unfortunate since the Lewalter and Korallus paper remains the primary source of information for more than a dozen pesticides reported to form Hb-adducts or erythrocyte conjugates in exposed humans. Perhaps the limited information that was provided will suffice to arouse curiosity and stimulate further adduct research on these and other pesticides.

### Miscellaneous Pesticides

Dichlorvos or 2,2-dichlorovinyl dimethyl phosphate is a direct-acting, organophosphorus insecticide that may also be formed *in vivo* as a metabolite of the schistosomiasis drug metrifonate (37-38). Apparent binding of radiolabeled Dichlorvos is some 30 times greater in protein than in DNA (39). While most protein binding is due to dimethylphosphorylation or transalkylation from neighboring phosphorylated residues, direct methylation of both Hb and DNA (Figure 9) has been demonstrated *in vivo* (38). It is also possible that dichloroacetaldehyde, a mutagenic metabolite of Dichlorvos, forms adducts with DNA and Hb. The erythrocyte adducts reportedly formed by Demeton-S-Methyl, Omethoate, Methiocarb, and Phoxim (23) have not yet been characterized. The structures of the first three compounds suggests that they, like Dichlorvos, might alkylate Hb via both methylation and phosphorylation mechanisms. Similarly, one might speculate that Phoxim both ethylates and phosphorylates proteins.

Until recently, ethylene dibromide (EDB) was widely used as a pesticide, soil fumigant, and lead scavenger in gasoline. The first two uses have been banned by

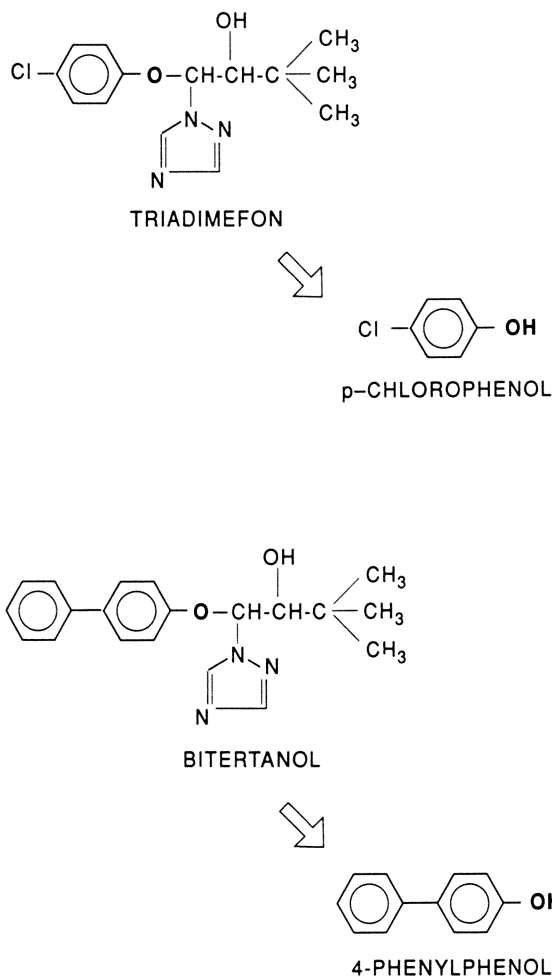


**Figure 8.** Metabolism of the fungicides Triadimefon and Bitertanol to their major metabolites, *p*-chlorophenol and 4-phenylphenol.

**TABLE 4. 4-PHENYLPHENOL AND p-CHLOROPHENOL IN URINE AND ERYTHROCYTES OF WORKERS EXPOSED TO THE FUNGICIDES BITERTANOL OR TRIADIMEFON<sup>a</sup>**

	<i>URINE</i> ( $\mu\text{g/g creatinine}$ )	<i>ERYTHROCYTES<sup>b</sup></i> ( $\mu\text{g/L blood}$ )
<i>4-PHENYLPHENOL</i>		
Normal Values	<10	<10
Exposed Workers:		
Subject #1	130	<10
Subject #2	300	<10
Subject #3	430	40
<i>p-CHLOROPHENOL</i>		
Normal Values	<10	<10
Exposed Workers:		
Subject #1	250	<10
Subject #2	650	70
Subject #3	730	<10
Subject #4	810	70

<sup>a</sup> Data from (23), Lewalter and Korallus, 1986.

<sup>b</sup> Recommended safe level = 100  $\mu\text{g}$  RBC adduct/L whole blood.

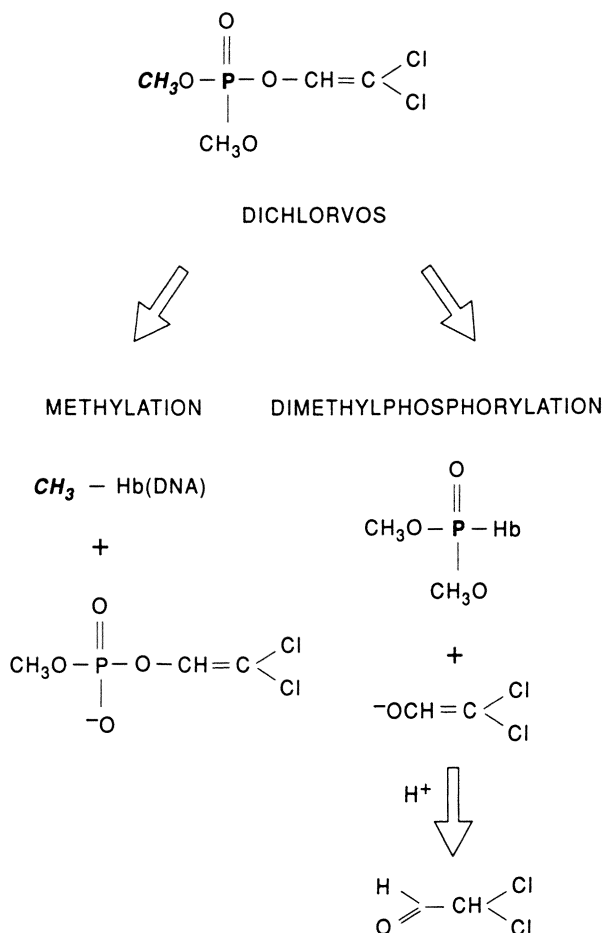


*Figure 9. Alkylation of hemoglobin by Dichlorvos via both phosphorylation and methylation mechanisms, and methylation of DNA.*

the EPA, and the use of leaded gas is declining. The formation of EDB adducts in rat serum albumin has been demonstrated both *in vitro* and *in vivo* (40). Although no EDB-Hb adducts have been identified as yet, the Hb adducts of a related 1,2-dihaloethane has (41-42). By analogy with ethylene dichloride, one would expect EDB to introduce 2-oxoethyl groups at cysteine and histidine residues of Hb. The herbicide monochloroacetic acid (43) and the insecticide trichloroacetonitrile (44) form uncharacterized adducts with serum albumin and Hb, respectively.

Unidentified erythrocyte conjugates are reportedly formed by the carbamate insecticide Propoxur, the phenolic fungicide *p*-nitrophenol, the pyrethroid insecticide Fenfluthrin, the organometallic dithiocarbamate fungicide Propineb, and the sulfamide fungicide Tolyfluanid (23). Propoxur is the only one of these pesticides for which any additional information was available. Propoxur is hydrolyzed *in vivo* to 2-isopropoxyphenol (Figure 10) which is then excreted in the urine. The same phenolic metabolite has also been detected in erythrocytes of Propoxur-exposed workers in Germany (23). Levels of 2-isopropoxyphenol in erythrocytes correlated somewhat better with the inhibition of erythrocyte acetylcholinesterase activity than did levels of the metabolite in urine (Table 5). The authors recommended 100  $\mu$ g 2-isopropoxyphenol per liter of whole blood as indicating a safe level of exposure to propoxur. Their longer life span would make Hb adducts more useful than either plasma pseudocholinesterase or urinary metabolites for monitoring chronic exposure to organophosphates. However, the data presented in Table 5 do not support replacing the standard erythrocyte AChE assay for recent OP exposure.

Although naphthalene is still used in the manufacture of various dyes and other synthetic compounds, its use as a moth repellent and insecticide has declined since the introduction of chlorinated compounds such as *p*-dichlorobenzene.  $^{14}$ C-labeled naphthalene has been reported to bind to Hb in rats (5). However, naphthalene exhibits direct hemolytic effects *in vivo* that would probably negate any potential value of naphthalene-Hb adducts as biomarkers of exposure.

Pentachlorophenol (PCP) is widely used as a fungicide, molluscicide, herbicide, and wood preservative. Due to its persistence and the extent and mode of its use, PCP is ubiquitous in the environment and may be detected in the bodily fluids and fat of nonoccupationally exposed people. Urinary levels of PCP may reflect exposure over several weeks rather than the usual 24 to 48 hr (45). The primary microsomal oxidative metabolites of PCP in man, i.e., the benzoquinone or the semiquinone forms of 1,4- and 1,2-tetrachlorohydroquinone, are capable of binding covalently to proteins (46). However, the resulting *in vivo* products, if any, have not yet been described in the literature.

## Summary

A consideration of the kinetics of formation and elimination of known Hb adducts suggests that the latter have significant potential as dosimeters of exposure to environmental contaminants that yield electrophiles *in vivo*. Measurements of

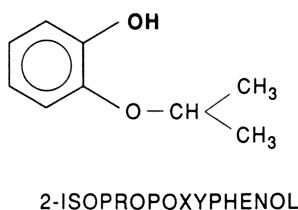
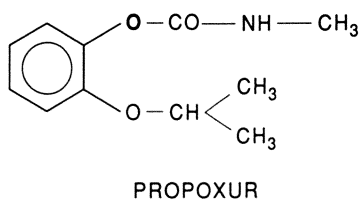


*Figure 10. Ester hydrolysis of the carbamate insecticide Propoxur to the major metabolite 2-isopropoxyphenol.*

**TABLE 5. COMPARISON OF ERYTHROCYTE CHOLINESTERASE INHIBITION AND 2-ISOPROPOXYPHENOL LEVELS IN URINE AND ERYTHROCYTES OF PROPOXUR-EXPOSED WORKERS<sup>a</sup>**

	<i>2-ISOPROPOXYPHENOL</i>		
	<i>ERYTHROCYTE AChE<sup>b</sup></i> (% decrease)	<i>URINE</i> (mg/g creatinine)	<i>ERYTHROCYTES</i> (μg/L blood)
Normal Values:	± 2	<0.1	<10
Exposed:			
Chronic (n=5)	0 - 5	0.2 - 0.9	<10 - 40
Acute (n=2)	18 - 24	1.3 - 2.4	80

<sup>a</sup> Data from (23) Lewalter and Korallus, 1986.

<sup>b</sup> Substrate used in this assay was acetylthiocholine. All subjects exhibiting decreased erythrocyte acetylcholinesterase were slow acetylators.

parent compounds or metabolites in blood or urine typically reflect only those exposures that have occurred within the last day or two. By contrast, steady state levels of hemoglobin adducts can reflect exposure over the previous 4 months. They may also have some potential as surrogate biomarkers of DNA damage. Hemoglobin adducts have been used experimentally to monitor human exposure to a number of chemicals, including aromatic amines. A number of N-aryl pesticides may be converted *in vivo* to aromatic amines by the action of acylamidases present in many mammalian tissues. These pesticide metabolites may then form acid/base-labile sulfinamide adducts with the  $\beta$ -93 cysteine of Hb. Such adducts have been detected in rats exposed orally to various arylamine-based pesticides, and may also be present in humans exposed to these pesticides via residues in food. Numerous other pesticides may also be expected to form adducts with hemoglobin. However, additional research is needed to characterize the adducts formed and determine their potential for use in monitoring pesticide exposure in humans. For a more comprehensive review of chemicals (including non-pesticides) that form adducts with either Hb or serum albumin, see Schnell, F. C. *Rev. Environ. Toxicol.* 1993, Vol. 5 (in press).

## Notice

The information in this chapter has been funded by the United States Environmental Protection Agency under Contract No. 68-CO-0049 with Lockheed Environmental Systems and Technologies. It has been subjected to Agency review and approved for publication.

## Literature Cited

1. Perera, F. P. *Mutat. Res.* **1988**, 205, 255-269.
2. Skipper, P. L.; Tannenbaum, S. R. *Carcinogenesis* **1990**, 11, 507-518.
3. Harris, J. W.; Kellermeyer, R. W. *The Red Cell: Production, Metabolism, Destruction: Normal & Abnormal*; Harvard University Press: Cambridge, MA, 1970.
4. Dickerson, R. E.; Geis, I. *Hemoglobin: Structure, Function, Evolution, and Pathology*; The Benjamin/Cummings Publishing Company Inc.: Menlo Park, CA, 1983.
5. Pereira, M. A.; Chang, L. W. *Chem. Biol. Interact.* **1981**, 33, 301-305.
6. Green, L. C.; Skipper, P. L.; Turesky, R. J.; Bryant, S. M.; Tannenbaum, S. R. *Cancer Res.* **1984**, 44, 4254-4259.
7. Neumann, H.-G. In *Monitoring Human Exposure to Carcinogenic and Mutagenic Agents*; Berlin, A.; Draper, M.; Hemminki, K.; Vanio, H., Eds.; IARC Scientific Publications; International Agency for Research on Cancer: Lyon, France, 1984, Vol. 59, pp. 115-126.
8. Waynforth, H. B. *Experimental and Surgical Technique in the Rat*; Academic Press: New York, 1980.

9. Skipper, P. L.; Bryant, M. S.; Tannenbaum, S. R.; Grooper, J. D. *J. Occup. Med.* **1986**, *28*, 643-646.
10. Bryant, M. S.; Skipper, P. L.; Tannenbaum, S. R.; Maclure, M. *Cancer Res.* **1987**, *47*, 602-608.
11. Tannenbaum, S. R.; Bryant, M. S.; Skipper, P. L.; Maclure, M. In *Mechanisms of Tobacco Carcinogenesis*; Hoffman, D.; Harris, C. C., Eds.; Banbury Report No. 23; Cold Spring Harbor Laboratory, NY, 1986, pp. 63-75.
12. Neumann, H.-G. In *Detection Methods for DNA-Damaging Agents in Man: Applications in Cancer Epidemiology and Prevention*; Bartsch, H.; Hemminki, K.; O'Neill, I. K., Eds.; IARC Scientific Publications; International Agency for Research on Cancer, Lyon, France, 1988, Vol. 89; pp. 157-165.
13. Maclure, M.; Katz, R. B.; Bryant, M. S.; Skipper, P. L.; Tannenbaum, S. R. *Am. J. Pub. Health* **1989**, *79*, 1381-1384.
14. Meerman, J. H. N.; Van Dorn, A. B. D.; Mulder, G. J. *Cancer Res.* **1980**, *40*, 3772-3779.
15. Pereira, M. A.; Lin, L.-H. C.; Chang, L. W. *Toxicol. Appl. Pharmacol.* **1981**, *60*, 472-479.
16. Anson, M. L.; Mirsky, E. J. *Gen. Physiol.* **1930**, *13*, 477-481.
17. Jain, N. C. *Schalm's Veterinary Hematology*, 4<sup>th</sup> Edition; Lea & Febiger: Philadelphia, PA, 1986, pp. 549 and 947.
18. Schreibner, G.; Urban, J.; Zahringer, J.; Reutter, W.; Frosch, U. *J. Biol. Chem.* **1971**, *246*, 4531-4538.
19. Birner, G.; Neumann, H. G. *Arch. Toxicol.* **1988**, *62*, 110-115.
20. Sabbioni, G.; Neumann, H.-G. *Carcinogenesis* **1990**, *11*, 111-115.
21. McMillan, D. C.; Freeman, J. P.; Hinson, J. A. *Toxicol. Appl. Pharmacol.* **1990**, *103*, 90-101.
22. McMillan D. C.; McRae, T.A.; Hinson, J.A. *Toxicol. Appl. Pharmacol.* **1990**, *105*, 503-507.
23. Lewalter, J.; Korallus, U. *Toxicol. Lett.* **1986**, *33*, 153-165.
24. Neumann, H.-G. *Int. Arch. Occup. Environ. Health* **1988**, *60*, 151-155.
25. Feng, P. C.; Wilson, A. G.; McClanahan, R. H.; Patanella, J. E.; Wratten, S.J. *Drug Metab. Dispos.* **1990**, *18*, 373-377.
26. Brown, M. A.; Kimmel, E. C.; Casida, J. E. *Life Sci.* **1989**, *43*, 2087-2094.
27. Kautiainen, A.; Tornqvist, M.; Svensson, K.; Osterman-Golkar, S. *Carcinogenesis* **1989**, *10*, 2123-2130.
28. Bailey, E.; Connors, T. A.; Farmer, P. B.; Gorf, S. M.; Rickard, J. *Cancer Res.* **1981**, *41*, 2514-1517.
29. Farmer, P. B. In *Indicators of Genotoxic Exposure*; Bridges, B. A.; Butterworth, B. E.; Weinstein, I. B., Eds.; Banbury Report No. 13; Cold Spring Harbor Laboratory, N.Y., 1982, pp. 169-175.
30. Törnqvist, M.; Osterman-Golkar, S.; Kautiainen, A.; Naslund, M.; Calleman, C.J.; Ehrenberg, L. *Mutat. Res.* **1988**, *204*, 521-529.
31. Crawford, M. J.; Hutson, D. H.; Stoydin, G. *Xenobiotica* **1980**, *10*, 169-185.
32. Hughes, G. D.; DeJong, C.; Fisher, R. W.; Winterhalter, K. H.; Wilson, K. J. *Biochem. J.* **1981**, *199*, 61-67.

33. Hamboeck, H.; Fisher, R. W.; Di Iorio, E. E.; Winterhalter, K. H. *Mol. Pharmacol.* **1981**, *20*, 579-584.
34. Crawford, M. J.; Hutson, D. H. *Xenobiotica* **1980**, *10*, 187-192.
35. U.S. Environmental Protection Agency. Office of Drinking Water Health Advisories. In *Drinking Water Health Advisory. Pesticides*; Lewis Publishers Inc.: Michigan, OH., **1989**, pg. 43-67.
36. National Toxicology Program. In *Sixth Annual Report on Carcinogens. Summary*; National Institute of Environmental Health Sciences, Research Triangle Park, NC, 1991, pp. 93-95.
37. Segerbäck, D. *Hereditas* **1981**, *94*, 73-76.
38. Segerbäck, D.; Ehrenberg, L. *Acta Pharmacol. Toxicol.* **1981**, *49*, 56-66.
39. Lawley, P. D.; Shah, S. A.; Orr, D. J. *Chem. Biol. Interact.* **1974**, *8*, 171-181.
40. Kaphalia, B. S.; Ansari, A. *Toxicol. Lett.* **1992**, *62*, 221-230.
41. Svensson, K.; Osterman-Golkar, S. In *The Role of Cyclic Nucleic Acid Adducts in Carcinogenesis and Mutagenesis*; Singer, B.; Bartsch, H., Eds.; IARC Scientific Publications; International Agency for Research on Cancer, Lyon, France, 1986, Vol. 70, pp. 269-279.
42. Guengerich, F. P.; Peterson, L. A.; Cmarik, J. L.; Koga, N.; Inskeep, P. B. *Environ. Health Perspect.* **1987**, *76*, 15-18.
43. Kaphalia, B. S.; Bhat, H. K.; Khan, M. F.; Ansari, G.A. *Toxicol. Ind. Health* **1992**, *8*, 53-61.
44. Lin, E. L.; Reddy, T. V.; Daniel, F. B. *Cancer Lett.* **1992**, *62*, 1-9.
45. Uhl, S.; Schmid, P.; Schlatter, C. *Arch. Toxicol.* **1986**, *58*, 182-186.
46. Van Ommen, B.; Adang, A.; Muller, F.; Van Bladeren, P.J. *Chem. Biol. Interact.* **1986**, *60*, 1-11.

RECEIVED May 10, 1993

## Chapter 10

# Immunoassay for *p*-Nitrophenol in Urine

Kim R. Rogers and J. M. Van Emon

Environmental Monitoring Systems Laboratory, U.S. Environmental  
Protection Agency, Las Vegas, NV 89193-3478

Urinary excretion of nitrophenol metabolites is an important index of human exposure to organophosphate pesticides. In particular, *p*-nitrophenol, a major urinary metabolite of parathion, can be used as a biomarker of human exposure. Immunoassay methods have been recently described for detection of *p*-nitrophenol (Q. X. Li et al., *J. Agric. Food Chem.*, 1991, 39, 1685-1692). In the present paper, the effects of a urine matrix on the detection of *p*-nitrophenol are reported using both fluorescence and absorbance-based ELISAs. A competition format using the enzyme-amplified catalysis of 4-nitrophenyl phosphate or 4-methylumbelliferyl phosphate was used to report the analyte concentration. The presence of urine during the antibody-analyte interaction inhibited product formation in the final step of the assay and shifted the inhibition curves to the right, increasing the apparent  $I_{50}$  values for *p*-nitrophenol. The various urine samples collected from volunteers, not occupationally exposed to parathion, varied in their ability to inhibit color formation and increase  $I_{50}$  values.

Environmental and biological monitoring are two key elements in the determination of human exposure to environmental pollutants for risk assessment and enforcement through monitoring. Certain questions, however, concerning total absorption, metabolism and excretion required to determine dose estimates can only be answered by observation of biological parameters. A number of innovative biological markers for human exposure to pollutants have been reported such as DNA alterations, protein adducts and changes to enzymatic and immunological systems (1). Nevertheless, measurement of pollutants and their metabolites in blood and urine continues to dominate human biological monitoring efforts.

This chapter not subject to U.S. copyright  
Published 1994 American Chemical Society

A number of obvious advantages and limitations exist for detection of metabolites in urine as compared to whole blood, plasma or tissue. The major advantage to the use of urine is that compliance to requests for monitoring of potentially exposed individuals is more easily accomplished using this medium. Limitations include; a short collection window typically between 8 and 48 hr, uncertainties in the total integrated excretion and for field screening applications the variability in matrix.

There has been a long standing interest in the use of urinary metabolites as biomarkers of acute human exposure to the organophosphorus insecticides (2). Major urinary metabolites of parathion include alkyl phosphates and *p*-nitrophenol. Although these compounds can be measured by laboratory-based methods such as gas chromatography (GC), analyses using these methods are typically expensive and time consuming.

The time and expense involved in classical analysis of *p*-nitrophenol in urine is primarily due to the extensive sample preparation and derivitization required (3). Polarographic methods for *p*-nitrophenol in urine have been reported which require no sample preparation, however, these methods suffer from low sensitivities (i.e., 500 mM detection limits) (4).

The need for fast, sensitive and cost-effective analytical methods to measure metabolites in biological fluids is rapidly growing. Analysis of samples in minutes rather than days can be critical for decisions concerning acute exposures in the general population, field worker re-entry intervals, spray drift and medical diagnosis of accidental poisonings. Consequently, efforts to develop field assay formats which are simple, fast and cost-effective and which reduce sample handling and turnaround time may facilitate the implementation of a greater number of important studies using the limited resources available. A variety of immunoassays which meet these requirements have been developed and are currently used in the clinical area. As the number of commercially available antibodies directed toward pesticides and their metabolites increases, immunoassay may also become a powerful analytical tool in assessment of human exposure to toxic pollutants.

One of the reasons why immunoassay is attractive for development of field screening methods is that in many cases environmental or physiological matrices can be analyzed with little sample preparation other than dilution (5). This, however, depends to some extent on the antibody, analyte and assay format. The following experiments were performed to explore the matrix effects of urine on a competitive ELISA for *p*-nitrophenol using the herein described reagents and format.

## Methods

**Chemicals and Instrumentation.** Anti-rabbit IgG alkaline phosphatase conjugate, *p*-nitro-phenol, 4-nitrophenyl phosphate and 4-methylumbelliferyl phosphate were obtained from Sigma Chemical Co., Saint Louis, MO. Urine samples were collected from non-occupationally exposed volunteers and stored at 4°C until assayed within 48 hr. Enzyme-linked immunosorbant assays (ELISAs) were performed in 96 well microtiter plates (Nunc, MaxiSorp, Roskilde, Denmark; or Dynatech, MicroFLUOR, Chantilly, Virginia) and read using either a Vmax absorbance plate reader (Molecular

Devices Corp., Menlo Park, CA) using the dual wavelength mode (405-650 nm) or a Pandex Fluorescence Concentration Analyzer (Baxter Healthcare Corp., Mundelein, IL) at excitation and emission maxima of 400 nm and 450 nm, respectively.

**Preparation of Antiserum and Coating Antigen.** Antiserum and coating antigen were developed under an EPA cooperative agreement with UC Davis, Department of Entomology (Davis, CA 95616) and prepared as previously reported (6). The antiserum was obtained from rabbit 1812 immunized with a 2-hydroxy-5-nitrobenzyl bromide conjugate of bovine serum albumin. The coating antigen was an ovalbumin conjugate of 4-nitrophenylacetic acid (C-OVA) (6). As previously reported (6), the antiserum showed negligible cross-reactivity for the protein carrier of the coating antigen.

**Competitive Immunoassay Procedure.** Microtiter plates were coated with C-OVA at 2  $\mu\text{g/mL}$  (100  $\mu\text{L/well}$ ) in 0.1 M sodium bicarbonate buffer (pH 9.6). Plates were sealed and incubated at 4°C overnight. The plates were then washed 3 times with phosphate buffered saline (pH 7.4) (PBST) containing sodium phosphate 10 mM, NaCl 100 mM, Tween 20 (0.05%) and  $\text{NaN}_3$  (0.02%) using an automated plate washer (Skatron, Lier, Norway). The antiserum at a 1:1000 dilution into PBST was then mixed with PBST containing *p*-nitrophenol and urine (as specified in Results). This reaction mixture (50  $\mu\text{L/well}$ ) was immediately transferred to the antigen-coated plate. After a 1 hr incubation at room temperature, the plate was washed 3 times with PBST followed by addition of 50  $\mu\text{L/well}$  of goat anti-rabbit IgG conjugated to alkaline phosphatase diluted 1:1000 with PBST. After a 1 hr incubation at room temperature, the plate was washed and 100  $\mu\text{L}$  of either a 1mg/mL solution of 4-nitrophenyl phosphate in 10% diethanolamine buffer (pH 9.8) or a 50  $\mu\text{M}$  solution of 4-methylumbelliferyl phosphate in 100 mM bicarbonate buffer (pH 9.2) containing 1 mM magnesium chloride was added to each well. The plates were incubated (30-60 min) and read using either a Vmax or a Pandex plate reader for absorbance or fluorescence measurements, respectively. Curves were analyzed and  $I_{50}$  values (i.e. concentration of inhibitor yielding 50% inhibition) determined using a four parameter logistic curve-fitting program with either Softmax or Sigma Plot software.

## Results and Discussion

Addition of urine to the initial incubation step (primary antibody Ab 1812 with *p*-nitrophenol) resulted in an inhibition of product formation in the final step of this assay (Figure 1). Because the plate was washed after the initial incubation, the inhibition of color formation as a result of the urine matrix was most likely due to a decrease in the binding of primary antibody to the antigen-coated wells. Levels of *p*-nitrophenol, from sources other than parathion, typically found in a non-occupationally exposed population are between 12 and 26 ppb (3) and may have contributed in part to this inhibition. Furthermore, since *p*-nitrophenol derived from parathion is excreted in humans as glucuronide and sulfate conjugates (7) and cross-reactivities of this serum with these conjugates would be expected to be quite low, the observed matrix effects were most likely not due to parathion exposures by the study participants. Furthermore, as evidenced by persistent inhibition of color formation at high *p*-nitrophenol concentrations, a *p*-nitrophenol-independent component was observed.

Ab 1812 shows relatively low cross-reactivity with substituted nitrobenzenes

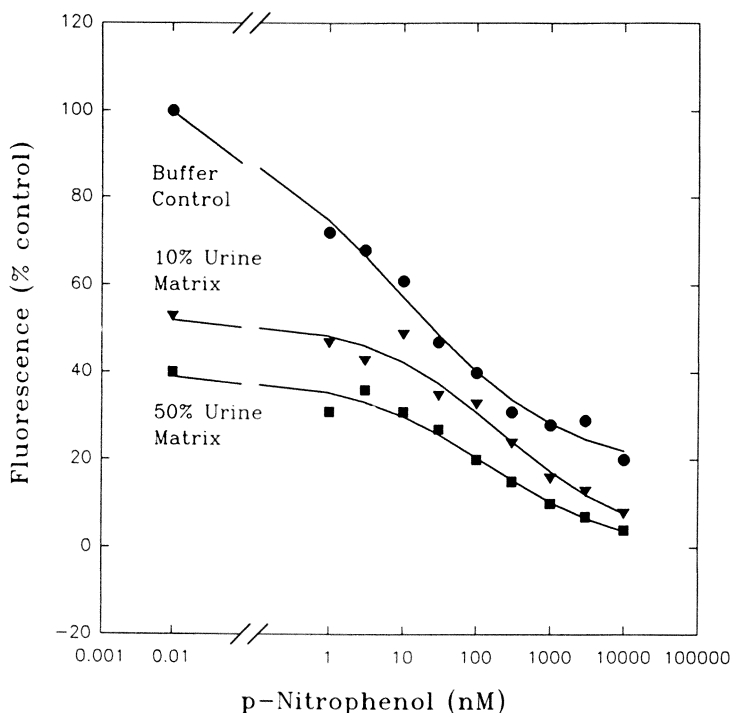


Figure 1. Effect of Urine on Competition ELISA for *p*-Nitrophenol. Fluorescence data were compared to the control which contained no urine and no *p*-nitrophenol. *p*-Nitrophenol, antiserum and urine (final concentration specified in figure) were incubated in the antigen-coated wells. The substrate for the alkaline phosphatase was 4-methylumbelliferyl phosphate. These data are averages of two plates of triplicate wells for each analyte concentration. The %CVs for the Buffer Control, 10% Urine Matrix and 50% urine Matrix were 5.2, 6.2 and 5.6, respectively.

(6), however, cross-reactivity of these compounds may become significant at concentrations in the high ppb range. The various urine samples appeared dramatically different in color intensity and presence or absence of precipitates after storage at 4°C for 24 hr. These urine samples also showed considerable variation in their effects on inhibition of product formation (Figure 2). Certain samples inhibited color formation more at 5% than others at 25%. The pH values of the buffered urine ranged from 6.0 to 7.2 and showed no correlation with the degree of inhibition of color formation. Similar results were observed in both the absorbance-based and fluorescence-based assays (Figure 3).

In addition to inhibiting product formation, the urine matrix shifted the inhibition curves to the right, consequently shifting  $I_{50}$  values to higher concentrations (Table I). These values increased in a concentration-dependent manner and were similar for both fluorescence and absorbance based assays. Variations in the shift in  $I_{50}$  values were also observed for different urine samples (Table II). At a 10% urine concentration, the  $I_{50}$  values varied by up to a factor of 4 among urine samples.

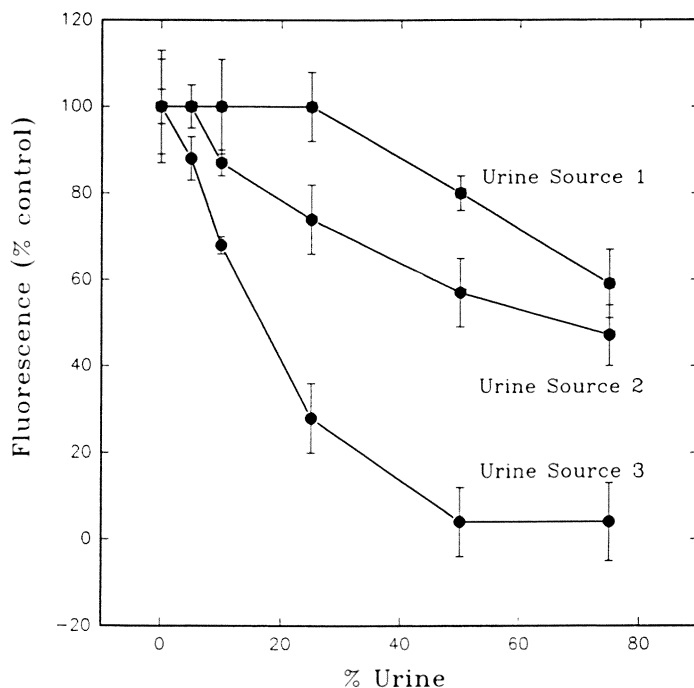


Figure 2. Effect of Various Urine Samples on the ELISA Using 4-Methylumbelliferyl Phosphate as the Enzyme Substrate. Data sets for each urine sample were compared to the control (containing no urine) for each set. Antiserum and urine (as specified) were incubated in the antigen-coated wells. These data are averages of two plates of triplicate wells for each analyte concentration. The symbols and bars represent means and %CV (n=6).

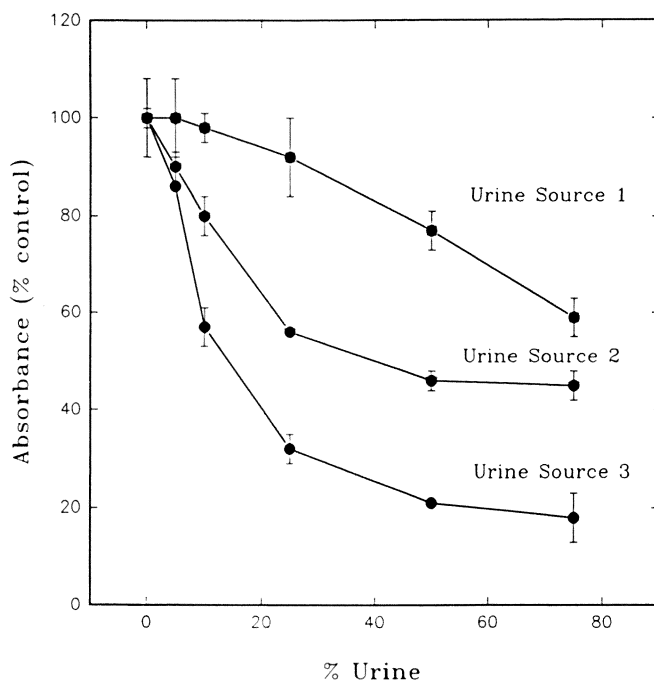


Figure 3. Effect of Various Urine Samples on the ELISA Using 4-Nitrophenyl Phosphate as the Substrate. Antiserum and urine (as specified) were incubated in the antigen-coated wells. Data sets for each urine sample were compared to the control (containing no urine) for each set. The initial absorbance differences (i.e., 405nm - 650nm) for curves 1-3 ranged from 0.130 to 0.095. These data are averages of two plates of triplicate wells for each analyte concentration. The symbols and bars represent means and %CV (n=6).

Table I. Effect of Urine Concentration on Assay Sensitivity<sup>a</sup>

Enzyme Substrate	Urine Concentration (%)	I <sub>50</sub> (ppm)
4-NP-P <sup>b</sup>	0	4
	10	8
	50	24
4-MUB-P <sup>c</sup>	0	7
	10	17
	50	43

<sup>a</sup>Experiments were performed using a single urine sample (see source 2 Table II). These data are averages of two plates of triplicate wells for each analyte concentration.

<sup>b</sup>4-nitrophenol phosphate

<sup>c</sup>4-methylumbelliferyl phosphate

**Table II. Effect of Urine Sample on Assay Sensitivity<sup>a</sup>**

Urine Source	I <sub>50</sub> (ppb)
Buffer Control	7
Sample 1	13
Sample 2	17
Sample 3	9
Sample 4	25
Sample 5	13
Sample 6	30

<sup>a</sup>10% Urine matrix; enzyme substrate was 4-methylumbelliferyl phosphate. These data are averages of two plates of triplicate wells for each analyte concentration.

In field versions of a number of immunoassays for environmental samples, the variability of matrix effects is minimized by dilution of the sample, typically from 100 to 1000 times (1 to 0.1%, respectively). Although the sensitivity of the assay is decreased, many field applications do not require the very low detection limits afforded by immunoassays run with pristine laboratory standards. For the herein reported assay the variability in the matrix effect of the urine is significantly reduced at urine concentrations below 5% (Figures 2, 3). Further, at a 1% urine concentration, this assay would have a detection limit of about 0.1 ppm. This value is well within the range expected from occupational exposures to parathion which result in average urinary *p*-nitrophenol levels of 2.5, 0.26 and 0.11 ppm for commercial applicators, field workers and near-field residents, respectively (8). Consequently, this assay shows potential for development as a field screening assay for occupational exposures to parathion.

Our continued efforts using these immunochemicals will focus primarily on simple, fast and cost-effective procedures for extraction of *p*-nitrophenol from urine samples of parathion-exposed individuals. Other efforts will focus on laboratory-based immunochemical assay methods for detection of this and related metabolites.

### Notice

The research described in this report has been supported by the United States Environmental Protection Agency under Cooperative Agreement No. CR-819047-01-0 with the University of California, Davis. It has been subjected to Agency review and approved for publication.

### Acknowledgments

The authors would like to thank Daliah Zoderu for her skilled technical assistance.

**Literature Cited**

1. *Biomarkers: Biochemical, Physiological and Histochemical Markers of Anthropogenic Stress*; Huggett, R. J.; Kimerle, R. A.; Mehrle, P. M.; Bergman, H. L., Eds.; SETAC Special Publications Series; Lewis Publishers: Ann Arbor, MI, 1992.
2. Weisskopf, C. P.; Seiber, J. N. In *Biological Monitoring for Pesticide Exposure*; Wang, R. G. M., Franklin, C. A., Honeycutt, R. C.; Reinert, J. C., Eds.; ACS Symposium Series; American Chemical Society, Washington, D.C., 1989, vol 382; pp 206-214.
3. Kirby, K. W.; Keiser, J. E.; Groene, J.; Slach, E. F. *J. Agric. Food Chem.* 1979, 27, 757-759.
4. Zietek, M. *Microchim. Acta.* 1979, 2, 75-83.
5. Van Emon, J. M.; Lopez-Avila, V. *Anal. Chem.* 1992, 64, 79A-88A.
6. Li, Q. X.; Zhao, M. S.; Gee, S. J.; Kurth, M. J.; Seiber, J. N.; Hammock, B. D. *J. Agric. Food Chem.* 1991, 39, 1685-1692.
7. Quebbelmann, A. J.; Anders, M. W. *J. Pharmacol. Exp. Ther.* 1973, 184, 695-708.
8. Arterberry, J. D.; Durham, W. F.; Elliott, J. W.; Wolfe, H. R. *Archives Env. Health.* 1961, 3, 112-121.

RECEIVED April 22, 1993

## Chapter 11

# Isolation of Pesticide-Binding Protein from Rat Blood

G. L. Larsen<sup>1</sup>, K. L. Davison<sup>1</sup>, J. E. Bakke<sup>1</sup>, and N. M. Bass<sup>2</sup>

<sup>1</sup>Biosciences Research Laboratory, Agricultural Research Service, U.S.  
Department of Agriculture, Fargo, ND 58105

<sup>2</sup>University of California School of Medicine, San Francisco, CA 94143

Rats were given a single oral dose of the herbicide propachlor-[1-<sup>14</sup>C] ( $8 \times 10^6$  d.p.m., 10.3mg). The plasma, erythrocyte cytosol and erythrocyte ghosts (collected 90 min after dosing) contained 41%, 15%, and 28%, respectively, of the <sup>14</sup>C in the blood (0.5% of the <sup>14</sup>C dose). Plasma, erythrocyte cytosol, and erythrocyte ghost were found to contain protein(s) 13.4 to 13.9 kDa (MW) which were associated with the <sup>14</sup>C (2.4% of <sup>14</sup>C in plasma; 51% of <sup>14</sup>C in erythrocyte cytosol and 65% of <sup>14</sup>C in erythrocyte ghosts). This <sup>14</sup>C associated with protein was extractable with methanol and was tentatively characterized by t.l.c. to be the cysteine conjugate (11%), the mercapturic acid conjugate (18%), S-oxide of the mercapturic acid conjugate (18%) and propachlor (25%). MW of the native 13.4-13.9 kDa protein(s) was found to be 43.5 kDa. Immunoblot or binding studies of the 13.4-13.9 kDa protein(s) showed no evidence that this protein(s) was liver or heart fatty-acid-binding-protein (FABP) or transthyretin.

Our laboratories have been involved in determining the biochemical and physiological processes involved in the disposition of glutathione conjugates of xenobiotics *in vivo*. During a study using propachlor metabolism in rats as a model (Davison and Larsen, *Xenobiotica*, in press) it was found that <sup>14</sup>C labelled metabolites were distributed between the plasma and erythrocytes, and that <sup>14</sup>C in the erythrocytes was associated with protein while <sup>14</sup>C in the plasma was not. We describe here the characterization of this erythrocyte protein and speculate that it may be involved in the transport and metabolism of metabolites in the erythrocyte.

## Materials and Methods

**Chemicals.** 2-Chloro-*N*-isopropyl [1-<sup>14</sup>C] acetanilide (<sup>14</sup>C-propachlor, 2.73 mCi/mM) was prepared as previously described (1).

**Animals.** Four male Sprague-Dawley rats (350-400g) were anaesthetized with sodium pentobarbital given intraperitoneally. A ventral midline incision was made, 3.6  $\mu\text{Ci}$  of  $^{14}\text{C}$  propachlor dissolved in 0.3 ml of ethanol was injected directly into the stomach and the incision closed. Ninety minutes later the rats were exsanguinated by withdrawal of blood from the abdominal aorta. A similar experiment was conducted except that the bile ducts were cannulated on a second set of four rats, each given 3.8  $\mu\text{Ci}$  of  $^{14}\text{C}$ -propachlor.

**Polyacrylamide Electrophoresis and Immunoblot Analysis.** The method for sodium dodecyl sulfate polyacrylamide gel electrophoresis (SDS-PAGE), using 13% acrylamide is that of Mazel (2). SDS-PAGE was run under reduced conditions and the following proteins were used as standard globular proteins for estimation of molecular weight (MW): trypsin inhibitor (21,500), carbonic anhydrase (31,000), ovalbumin (42,700), bovine albumin (66,200), and phosphorylase B (97,000). SDS-PAGE gels were stained with Coomassie blue. Protein samples were electrophoretically transferred to a sheet of nitrocellulose (Schleicher and Schuell, Keene, NH) by the method of Towbin and Gordon (3). Western blots of separated proteins were blocked by incubation for two hours in Tris-saline-Tween buffer (0.15 M Tris, 0.5 M NaCl, 0.05% Tween 20, pH 7.5) and then incubated for two hours at room temperature with liver or heart fatty-acid-binding-protein (FABP), albumin or transthyretin antibody (1:800 dil in Tris-saline-tween buffer). The Western blots were washed three times with Tris-saline-tween buffer (5 min each) and then incubated with the same buffer containing goat anti-rabbit horseradish peroxidase conjugate antibody (Bio-Rad, 1:3000 dil) for one hour at room temperature. The Western blots were washed twice with Tris-saline-tween buffer (5 min each), once with Tris-saline-tween buffer (0.15 M Tris and 0.5 M NaCl, pH 7.5), and then incubated in substrate solution (25 ml Tris-saline buffer plus 12.5  $\mu\text{l}$  30%  $\text{H}_2\text{O}_2$  and 5 ml of 3 mg/ml solution of 4-chloro-1-naphthol).

**Protein Purification.** Blood (34 ml) was separated into plasma, erythrocyte cytosol and erythrocyte ghosts. Plasma (15 ml) was isolated as the supernatant after a 1,600xg centrifugation. Erythrocytes (1,600xg pellet) were suspended in 15 ml of 0.15 M NaCl and centrifuged at 1,600xg. The supernatant (wash) was removed, assayed for  $^{14}\text{C}$  and discarded. Erythrocytes were lysed on resuspension of the 1,600xg pellet in 20 ml of distilled water and centrifuged at 10,000xg for 30 min. The supernatant was removed and recentrifuged at 10,000xg for 30 min. The resulting supernatant was then centrifuged at 100,000xg for 1 hour and this supernatant (erythrocyte cytosol) was saved for further analysis.

The two 10,000xg pellets were resuspended in water, combined and centrifuged at 10,000xg for 30 min. The resulting pellet (erythrocyte ghosts) was suspended and homogenized in two to three parts (w/v) of distilled water in a Potter-Elvehjem homogenizer with a Teflon pestle and saved for further analysis.

Samples of plasma, erythrocyte cytosol and erythrocyte ghosts were each applied to a G-75 Sephadex column (5x100 cm, G-75) that was equilibrated and eluted with 5 mM  $\text{K}^+ \text{PO}_4$  (pH 7.2, buffer A). Individual fractions which

contained protein that eluted from the G-75 with buffer A (see Figure 1) were subjected to SDS-PAGE. Eluting volumes that contained albumin or 10,000-15,000 Da MW proteins were individually combined and freeze-dried.

**Gel Filtration Determination of MW.** A non-denatured MW of the 13,400-13,900 Da protein (from SDS-PAGE analysis) was determined using a Sephacryl S-200 HR column (2.2x85 cm, S-200) eluted with 50 mM  $K^+PO_4$  buffer (pH 7.2) calibrated with bovine serum albumin (67,000), ovalbumin (43,000), chymotrypsin A (25,000), and ribonuclease (13,700). All procedures were carried out at 5° C or in an ice bath. Protein concentrations were determined by the method of Bradford (4) with  $\gamma$ -globulin as a protein standard. Radioactivity was determined by liquid scintillation counting.

**Fatty Acid Binding Protein (FABP), rabbit anti (FABP IgG), Retinal Binding Protein (RBP), Transthyretin (TTR) and rabbit anti (TTR).** FABP from rat liver (L-FABP), and heart (H-FABP) were prepared as described previously (5-6). Monospecific antibodies to FABP were produced in rabbits as described previously (6-7). Authentic human RBP, human TTR and monospecific rabbit anti TTR IgG were gifts from Dr. William Blaner, Columbia University, New York, NY. Rabbit anti rat albumin was obtained from Organon Teknika Corporation, West Chester, PA.

**Delipidation.** Protein fraction (5 ml) were delipidated by addition of 50  $\mu$ l of 50 mM ethylenediaminetetraacetic acid and 10 ml of *n*-butanol/diisopropyl ether (40:60). The resulting solution was allowed to mix on a rocking table mixer for 1 hour at 27° C. The organic layer was removed and residual diisopropyl ether in the aqueous phase was removed under vacuum.

**Binding Assays.** The FABP binding assays were conducted by the method of Glatz and Veerkamp (8). Assays consisted of 0.3 ml of 10 mM  $K^+PO_4$  pH 7.2; 0.3 ml of [ $^{14}C$ ]-oleic acid (10,000-40,000 dpm; Amersham, Arlington Heights, IL; 52 mCi/mM) and 0.3 ml of protein sample. This mixture was mixed on a vortex mixer and incubated at 27°C for 3 hours. After incubation, 0.25 ml of a 60% solution of hydroxyalkoxypropyl dextran, Type VI (lipidex, Sigma Chemical Co. St. Louis, Mo, USA) in 10 mM  $K^+PO_4$  (pH 7.2) was added, mixed on a vortex mixer and centrifuged (14,000 kg, 2 min). A 0.2 ml aliquot of supernatant was removed for assay of radioactivity. All assays were conducted in triplicate in the absence of protein (nonspecific binding) or lipidex (total amount of ligand present). Binding of [ $^{14}C$ ]-propachlor or [ $^{14}C$ ]-propachlor metabolites to protein was determined by co-chromatography of [ $^{14}C$ ] and protein on Sephadex G-75 and Sepacryl S-200, by equilibrium dialysis (D-0405 Dialysis Tubing, Sigma Chem. Co., St. Louis, MO) against 800 ml of Buffer A twice, and by extraction of freeze-dried [ $^{14}C$ ]-protein with methanol.

**Characterization of the Ligand.** A portion of the radioactive-protein complex isolated from plasma, erythrocyte cytosol or erythrocyte ghosts was freeze-dried

and homogenized in methanol. The methanol extract was centrifuged (10,000xg, 20 min) and the resulting pellet was rehomogenized in methanol and centrifuged (10,000xg, 20 min). The first and second methanol extracts were combined, taken to dryness, redissolved in distilled water, and chromatographed by t.l.c. [0.5 mm silica gel using the following solvent systems: ethylacetate-water-formic acid-xylene; 35:2:2:1 by volume (solvent 1) and *n*-butanol-water acetic acid; 12:5:3 by volume (solvent 2)].

## RESULTS

Table I summarizes the distribution of radioactivity in the blood after fractionation into plasma, erythrocyte cytosol and erythrocyte ghosts from rats dosed with  $^{14}\text{C}$  propachlor. The plasma, erythrocyte cytosol and erythrocyte ghosts contained 41%, 15%, and 28%, respectively, of the  $^{14}\text{C}$  in the blood. These three fractions were chromatographed on the G-75 column and the protein and  $^{14}\text{C}$  elution patterns are shown in Figure 1. MW of proteins in various eluting volumes were determined using SDS-PAGE (Figure 2). The plasma was found to contain a number of proteins >67,000 Da in an initial protein peak (475-560 ml, Figure 1A). A second plasma protein peak (560-750 ml, Figure 1A) contained a single 66 kDa protein which was characterized to be serum albumin by its cochromatography with bovine serum albumin on SDS-PAGE (Figure 2, Gel A) and its cross reactivity with rabbit antibodies to rat serum albumin in a Western blot analysis (Figure 4, Blot 1). A third protein eluted after the serum albumin (750-900 ml, Figure 1) which was shown to contain a doublet protein band at 13.4-13.9 kDa. These 13.4-13.9 kDa protein(s) are thought to be related proteins with apparent MWs of 13.4 and 13.9 kDa as determined by comparing their migration rates with the standards on SDS-PAGE (Figure 2). This doublet is believed to be the result of proteolytic modification of/or differences in ligand content in the binding protein. Association of  $^{14}\text{C}$ -propachlor metabolites with blood proteins was shown by cochromatography of  $^{14}\text{C}$  with the proteins eluted from the G-75 column. The high MW proteins, albumin and the 13.4-13.9 kDa protein(s) associated with 4.6%, 5.9% and 2.4% of the plasma  $^{14}\text{C}$ , respectively, while 86.5% of the  $^{14}\text{C}$  remained unassociated with proteins (1350-1750 ml, Figure 1).

$^{14}\text{C}$  in the erythrocyte ghosts coeluted with a protein peak eluting from G-75 at 600-900 ml, tailing off to 2000 ml (Figure 1B). SDS-PAGE analysis of this 600-900 ml eluting volumes showed only the 13.4-13.9 kDa protein(s) [data not shown but the SDS-PAGE identical to that shown in Figure 2B for erythrocyte cytosol].

The majority of the protein in the erythrocyte cytosol (Figure 1C) coeluted with  $^{14}\text{C}$  between 600-950 ml, although some  $^{14}\text{C}$  remained unassociated with protein and eluted between 1350-1900 ml from the G-75 column. SDS-PAGE showed only protein(s) of MW 13.4-13.9 kDa in the protein 600-950 ml fraction. The  $^{14}\text{C}$  associated with the 13.4-13.9 kDa protein(s) represented 51.3% of the  $^{14}\text{C}$  in the erythrocyte cytosol.

Table II shows that  $^{14}\text{C}$ -propachlor metabolites were associated with the 13.4-13.9 kDa protein(s) because, when these  $^{14}\text{C}$ -protein(s) obtained from plasma,

TABLE I. FRACTIONATION OF RAT BLOOD FROM RATS  
GIVEN  $^{14}\text{C}$  PROPACHLOR VIA STOMACH

Fraction	$^{14}\text{C}(\text{dpm})$	% of $^{14}\text{C}$ in blood	Fate
Whole blood	153,700		
Plasma			
1,600xg sup	51,900	33.8	to G-75 column discarded
Erythrocyte wash (1,600xg sup)	10,800	7.0	
Erythrocytes	96,600	62.8	
Erythrocyte cytosol			
10,000xg sup	25,000	16.6	to 100,000xg to G-75 column
100,000xg sup	22,900	14.9	
Erythrocyte ghosts			
10,000xg pellet	44,200	28.8	washed discarded
10,000xg pellet (washed)	1,500	1.0	
resuspend 10,000xg (pellet)	42,700	27.9	to G-75 column

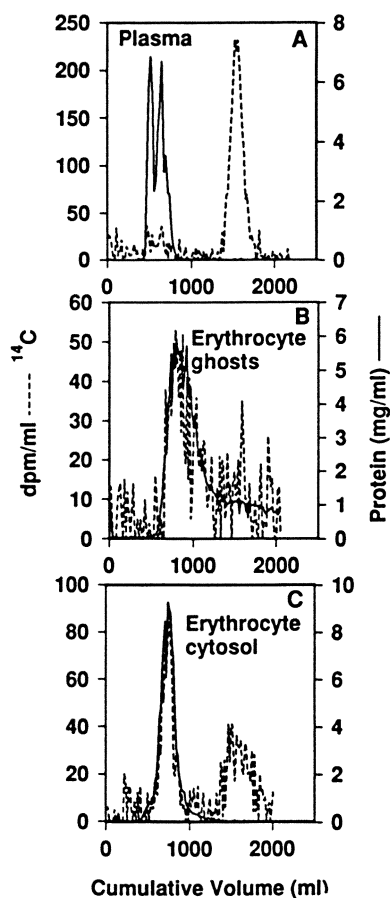


Figure 1. Elution patterns upon chromatography of (A) plasma, (B) erythrocyte ghosts and (C) erythrocyte cytosol from a Sephadex G-75 column. Fractions were assayed for protein ——— and radioactivity ----- as described in Materials and Methods section.

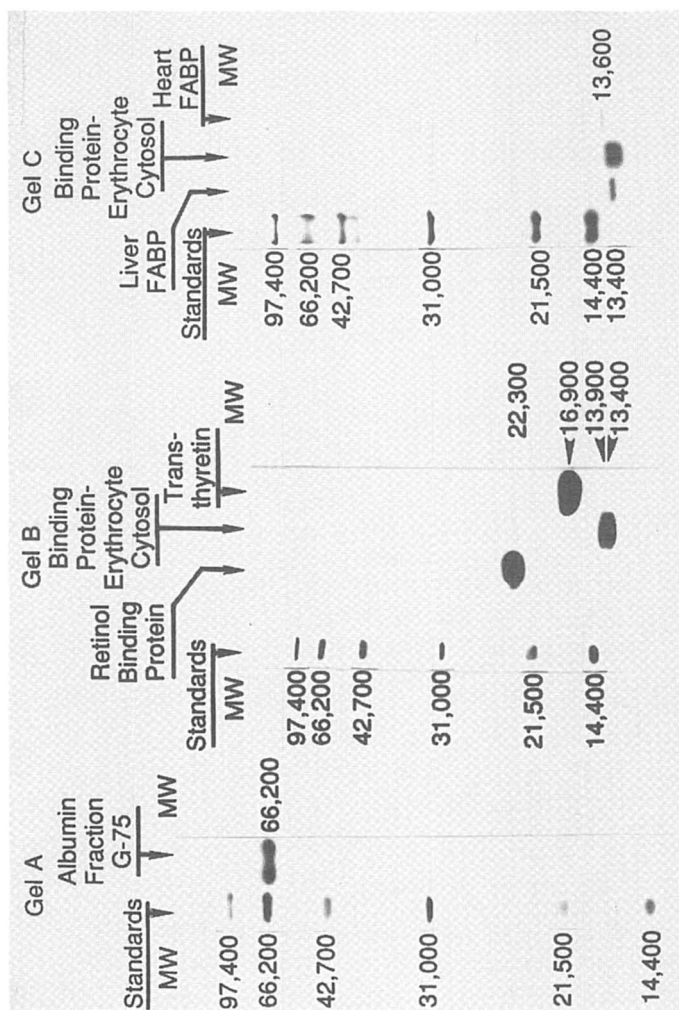


Figure 2. Electrophoresis (SDS-PAGE) of protein-propachlor metabolite complex from plasma [G-75 (560-750 ml); 5 µg; Gel A], erythrocyte cytosol [G-75 (750-900 ml); 10 µg; Gel B; 5 µg; Gel C] and authentic human retinal binding protein, human transthyretin, rat liver FABP and rat heart FABP. Photograph of SDS-PAGE stained for protein with Coomassie blue is shown. MW=molecular weight.

TABLE II. STABILITY OF <sup>14</sup>C PROPACHLOR METABOLITES/13.4-13.9 KDa PROTEIN(S) COMPLEX TO DIALYSIS

	Plasma		Erythrocyte cytosol		Erythrocyte ghosts	
	<sup>14</sup> C (DPM)	Protein (mg)	<sup>14</sup> C (DPM)	Protein (mg)	<sup>14</sup> C (DPM)	Protein (mg)
Sample Before Dialysis	430	284	13,300	630	3,220	904
1st Dialysis wash	0	0	0	45	464	18
2nd Dialysis wash	0	0	396	45	392	50
sample after dialysis *	609	330	16,500	657	4,570	928

\* Increases observed in <sup>14</sup>C and protein on dialysis are believed to result from loss of quenching agents on dialysis or manipulative errors occurring in radioactivity or protein assays or both.

erythrocyte cytosol and erythrocyte ghosts were subjected to dialysis, the  $^{14}\text{C}$ -propachlor metabolites remained associated with the 13.4-13.9 kDa protein(s). Furthermore, chromatography on a S-200 column gave a single peak of protein which cochromatographed with  $^{14}\text{C}$  (Figure 3).

Comparison of the elution volume profiles from the S-200 column of the  $^{14}\text{C}$ -protein (13.4-13.9 kDa) complex (306 ml) from erythrocyte cytosol with those of globular protein standards gave an estimate of 43.5 kDa for the MW of the native protein indicating that the native protein may consist of a trimer of 13.4-13.9 kDa subunits. These MW data suggested that the 13.4-13.9 kDa protein(s) might be retinol binding protein or transthyretin; however, the 13.4-13.9 kDa protein(s) did not co-chromatography with authentic retinol binding protein or transthyretin on SDS-PAGE (Figure 2, Gel B).

When Western blots of the 13.4-13.9 kDa protein(s) were probed with rabbit antibodies to liver or heart FABP or transthyretin, cross reactivity was not observed. Cross reactivity was observed between authentic liver or heart FABP and transthyretin and their respective rabbit antibodies (Figure 4, Blots 2, 3, and 4).

Binding studies were conducted with  $^{14}\text{C}$ -oleic acid to determine if the 13.4-13.9 kDa proteins have FABP capacity. Binding was not observed with proteins which had not previously undergone delipidization with a solution of butanol/diisopropyl ether. However, after delipidation these proteins bound  $^{14}\text{C}$ -oleic acid only in low molar ratios as shown in Table III which indicates nonspecific binding, not characteristic of FABP. These results indicate that they may be a specific erythrocyte binding protein(s).

The cysteine conjugate of propachlor was the major unbound metabolite in systemic blood (Davison and Larsen, *Xenobiotica*, in press). The radioactivity associated with the 13.4-13.9 kDa protein(s) from a sample of freeze-dried erythrocyte cytosol was extracted with methanol and characterized by t.l.c. Virtually all of the  $^{14}\text{C}$  extracted with methanol (>98%) which shows this bonding is noncovalent. T.l.c. of the radioactivity in the methanol extract gave four peaks. These peaks cochromatographed with propachlor [solvent 1,  $R_f=0.94$ ; solvent 2,  $R_f=0.98$ ; (25.4% of the  $^{14}\text{C}$  associated with the 13.4-13.9 kDa protein(s))], the *S*-oxide of the mercapturate [solvent 1,  $R_f=0.28$ ; solvent 2,  $R_f=0.60$ ; (18.4%)], the mercapturate [solvent 1,  $R_f=0.76$ ; solvent 2,  $R_f=0.74$ ; (17.7%)] and the cysteine conjugate [solvent 1,  $R_f=0.18$ ;  $R_f=0.69$ ; (10.8%)].

## DISCUSSION

Binding of  $^{14}\text{C}$ -propachlor and its mercapturic acid pathway metabolites to this low MW erythrocyte protein is significant because this protein might bind other xenobiotics and their MAP metabolites. Further glutathione conjugation with subsequent mercapturic acid pathway metabolite formation represents a major metabolic pathway for the metabolism of numerous electrophilic xenobiotics. We considered whether this 13.4-13.9 kDa propachlor-binding protein (PBP) isolated from erythrocytes might be related to the 14.0-15.0 kDa fatty acid-binding protein (FABP) family. The erythrocyte PBP is similar in size to these proteins which are

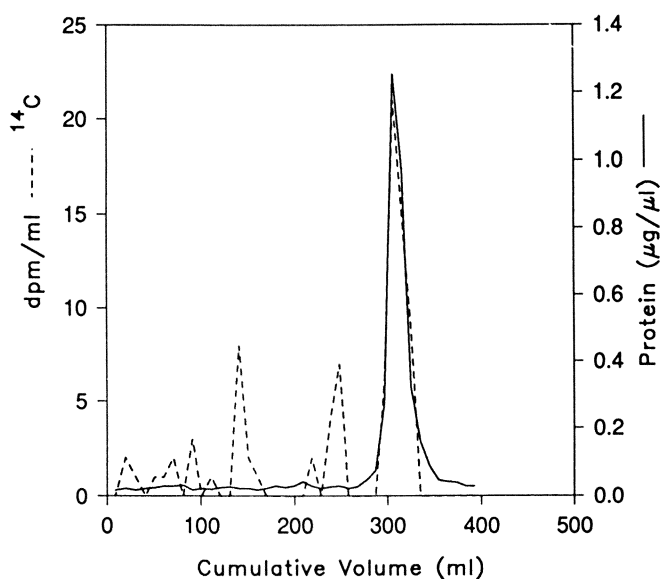


Figure 3. Elution pattern upon chromatography on a Sephacryl S-200 column of the erythrocyte cytosol fraction [13.4-13.9 kDa protein(s)] which eluted from Sephadex G-75 (750-900ml). Fractions were assayed for protein — and radioactivity ----- as described in Materials and Methods section.

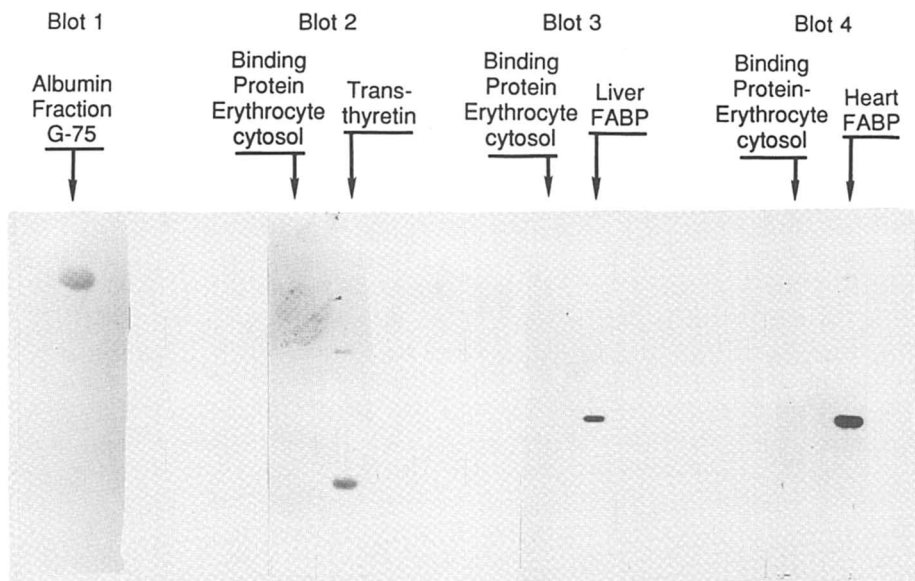


Figure 4. Immunoblots (2.5 $\mu$ g, blots 1-4) of protein-propachlor metabolite complex [erythrocyte cytosol from G-75 (750-900 ml)], plasma albumin [G-75 (560-750 ml)], human transthyretin, rat liver FABP and rat heart FABP. Aliquots from samples were separated on SDS-PAGE (figure 2), transferred to nitrocellulose sheets. The blots were incubated with the following rabbit antibodies: blot 1 with anti-rat albumin, blot 2 with anti-rat transthyretin, blot 3 with anti-liver FABP and blot 4 with anti-heart FABP. Bound antibody on the Western immunoblots were visualized following incubation of the blots with goat anti-rabbit horseradish peroxidase conjugate antibody developed with 4-chloronaphthol and hydrogen peroxide.

abundantly expressed in a variety of tissues and bind, in addition to fatty acids, a relatively broad range of xenobiotics and organic anions (7-10). However, the erythrocyte PBP displayed negligible fatty acid binding with oleic acid in the binding assay, and also showed no immunological cross-reactivity with liver-FABP or heart muscle-FABP. A relationship between erythrocyte PBP and the FABP family of proteins therefore appears unlikely on the basis of the data at hand, although definitive exclusion of this possibility must await primary structural analysis of PBP. While the natural function of the erythrocyte PBP is not known at this time, it may be involved in the uptake, intracellular transport, storage and metabolism of xenobiotics and their mercapturic acid conjugates within the erythrocyte. These processes may also be responsible for the transport of metabolites of xenobiotics from organ to organ via the blood, resulting in specific metabolism and/or accumulation of xenobiotic metabolites in a particular tissue.

Table III. Binding Assay for Delipidated Erythrocyte Cytosolic 13.4-13.9 kDa Protein(s)

	available bound <sup>14</sup> C-oleic acid		13.4-13.9 kDa protein(s)	binding molar ratio
	(dpm)	(nmole)	(nmole)	oleic acid
				13.4-13.9 kDa protein(s)
Exp. 1	481 ± 134	11.3	280	1/24
Exp. 2	249 ± 65	5.8	87	1/14.9
Exp. 3	76 ± 17	1.8	87	1/48

Mention of trademark or proprietary product does not constitute a guarantee or warranty of the product by the U.S. Department of Agriculture and does not imply its approval to the exclusion of other products that may also be suitable.

#### Acknowledgments.

The authors acknowledge the technical assistance of Barbara Magelky, Joyce Wold and Kristin McDonald.

#### Literature Cited

1. Pekas, J.C.; Larsen, G.L.; Feil, V.J. *J. Toxicol. Environ. Health.* 1979, 5, pp. 653-662.
2. Mazel, J.V. Jr. *J. Biol. Chem.* 1971, 246, pp.179-246.
3. Towbin, H.; Gordon, J. *J. Immun. Meth.* 1984, 72, pp.313-340.
4. Bradford, M.H. *Anal. Biochem.* 1976, 72, pp.248-254.
5. Ochner, R.K.; Manning J.A.; Kane, J.P. *J. Biol. Chem.* 1982, 257, pp.7872-7878.
6. Bass, N.M.; Manning N.A. *Biochem. Biophys. Res. Commun.* 1986, 137, pp.929-935.
7. Bass, N.M. *Chem. & Phys. of Lipids.* 1985, 38, pp.95-114.
8. Glatz, J.F.C.; Veerkamp, J.H. *J. Biochem. Biophys. Meth.* 1983, 8, 57-61.
9. Bass, N.M. *International Review of Cyto.* 1988, 111, pp.143-184.
10. Glatz, J.F.C.; Veerkamp, J.H. *Inter. J. Biochem.* 1985, 17, pp.13-22.

RECEIVED September 17, 1993

## Chapter 12

# Body Burden and Nonoccupational Exposure Assessment

John A. Santolucito

Harry Reid Center for Environmental Studies, University of Nevada, Las Vegas, NV 89154-4009

When assessing human exposures to pesticides or other toxicants, ambient monitoring is often supplemented with measurements of the toxicant's concentration in a tissue or body fluid in order to more accurately estimate exposure to internal targets. Tissue analysis is routinely carried out despite the uncertainty of the quantitative relationship between the amount of toxicant in a tissue and the intensity/duration of the human exposure. Classical toxicological studies, using experimental animals, do not substantially contribute to identifying and characterizing the uncertainties associated with human exposure assessments. There is a need to replace or supplement tissue burden determinations with measurements that will make more tangible contributions to quantitative exposure assessments. To fill this need, major emphasis is being placed on (1) the development of physiologically based pharmacokinetic models for simulating internal exposures, and (2) measuring, directly or indirectly, target tissue exposures. This paper examines the relationship of tissue or body burden to internal exposure for an organophosphate pesticide (EPN), a metal (Pb), and a volatile organic compound (benzene), and considers alternative approaches to more cost-effective exposure assessment in the general population.

The determination of a body burden to assess exposure of small organisms to environmental chemicals is a relatively straightforward task. Since the sample analyzed is the entire body, the amount of parent compound or metabolite present is the true body burden. For larger animals and humans, a true body burden can only be obtained by analyzing samples of each tissue/fluid compartment, estimating the mass of each tissue compartment, and summing the

0097-6156/94/0542-0178\$06.00/0  
© 1994 American Chemical Society

derived tissue burdens. While this approach is feasible at autopsy, biological monitoring of living humans is usually restricted to tissues that can be sampled using noninvasive methods.

The amount of toxicant present in less accessible tissues or in the whole body can theoretically be estimated from the amount present in the sampled tissue provided the pharmacokinetic and pharmacodynamic behavior of the toxicant and the approximate exposure scenario are known (1). In this approach, the tissue analyzed becomes a surrogate for the target tissue or whole body. In practice, attention is usually directed toward estimating a target tissue concentration rather than a body burden despite the uncertainty over which may be a better biomarker of exposure.

Body burdens may reflect total exposure, as well as health risk, more accurately than a surrogate measure for bioaccumulating toxicants because both stored toxicant and that entering from ongoing exposure contribute to the target tissue dose. And in the event current exposure ceases, stored toxicant can impact target tissues until depleted. On the other hand, a surrogate measure may adequately assess current exposures to non-accumulating pollutants.

### Body Burden vs. Tissue Burden

An attempt is made here to elucidate the relationships between body burden, tissue burden, and exposure by examining the results of published studies. Studies were targeted in which experimental animals were repeatedly or chronically exposed to toxicant and analyses performed on all or most of the major tissue compartments. Though these criteria were not fully met, the studies used contained data sets complete enough to reconstruct an approximate body burden. Together, the three studies presented address the organophosphate pesticide EPN and two widely dispersed environmental chemicals, lead (bioaccumulating) and benzene (non-bioaccumulating).

**Study 1: EPN (O-Ethyl O-4-Nitrophenylphosphonothioate).** In a study reported by Abou-Donia et al. (2), hens weighing 1.5 kg were administered a single oral dose of 10 mg/kg of uniformly phenyl-labeled [ $^{14}\text{C}$ ] EPN ( $\text{LD}_{50}$ ) and sacrificed at 0.5, 2, 4, 8, and 12 days after dosing. Tissue radioactivity (dpm/g, representing parent compound and metabolites combined) was reported for spinal cord, sciatic nerve, brain, lung, heart, RBC, plasma, liver, bile, kidney, muscle, adipose tissue, and skin. Though the data are not reproduced here, the highest concentration of  $^{14}\text{C}$  attained during the 12-day period was reported for liver followed by bile, kidney, adipose tissue, and muscle. Of the nervous tissues reported, brain contained the highest concentration of  $^{14}\text{C}$ , except on day 0.5 when sciatic nerve was highest, and spinal cord contained the lowest amount. The total body burden at day 12 was about 14% of the peak level seen at day 0.5. During the 12-day period of this study, approximately 90% of the measured body burden of EPN was contained in the liver, muscle, fat, and skin.

For this exercise, the reported tissue radioactivities were multiplied by the estimated tissue weights to obtain tissue burdens. The percentages of body weight used to estimate each tissue weight for *Gallus gallus* were: brain, 0.3;

spinal cord, 0.3; peripheral nervous system, 0.01; lungs, 0.6; RBC, 3.1; plasma, 4.7; heart, 0.6; liver, 2.2; kidneys, 0.6; muscle, 45.0; fat, 5.0; skin, 5.0; feathers, 3.7; skeleton, 5.0; and GI tract, 20 (*Bradley, personal communication, and 3-5*).

Relative tissue burdens, i.e., tissue burdens expressed as a percent of the body burden, are shown in Table I for each time interval. The radioactivity levels reported for sciatic nerve were considered representative of peripheral nerve tissue for this exercise and were used to estimate the tissue burden of the peripheral nervous system (PNS).

Table I. Tissue Burdens of EPN (Expressed as Percent of Body Burden)

	Days After Single Oral Dose of EPN				
Tissue	0.5	2	4	8	12
	Relative Tissue Burden				
Brain	0.12	0.41	0.48	0.43	0.22
Sp. Cord	0.09	0.12	0.11	0.12	0.19
PNS <sup>1</sup>	6.01	9.72	9.43	3.20	7.02
Lung	0.58	.73	0.57	0.20	.27
RBC	0.26	1.45	1.30	0.83	1.09
Plasma	0.63	2.87	2.88	0.53	0.33
Whole Blood	0.09	4.31	4.22	1.35	1.42
Heart	0.09	0.54	0.37	0.19	0.20
Liver	5.68	25.50	32.20	12.14	7.46
Kidneys	0.92	4.30	3.61	4.31	8.04
Muscle	80.72	49.96	43.97	59.52	63.67
Fat	6.24	8.82	9.01	13.49	8.89
Skin	4.67	5.29	5.50	8.24	9.65
Feathers	EPN content considered negligible				
Skeleton	EPN content considered negligible				
GI Tract	Tissue was not analyzed				

<sup>1</sup> ×10<sup>-5</sup>

Relative tissue burdens for plasma, brain, liver, and fat decreased between days 8 and 12 and either increased or remained about the same for the remaining tissues (Table I). Thus, plasma EPN may be a satisfactory surrogate for brain, liver, and fat tissue burdens. However, of the nervous tissues analyzed, brain is the least susceptible to EPN-induced delayed neurotoxicity.

Tissues with the least variable relative burdens of EPN over the 12-day observation period are those whose EPN burdens fluctuated in closest agreement with body burden and may be better surrogate markers of body burden than tissues with greater variability. Tissues in Table I with lowest coefficients of variation (CV) include: muscle, 24%; fat, 29%; spinal cord, 30%; skin, 32%; and PNS, 38%, none of which are readily available for routine monitoring. Admittedly, the short duration of the study is not representative of steady-state conditions seen with prolonged chronic exposure. Further, the extent to which the results obtained in this study, and the conclusions drawn from them, are applicable to humans is not known.

**Study 2: Lead.** In this study, mice were administered a single intraperitoneal injection of 50  $\mu\text{g}$   $^{210}\text{Pb}$ , and the uptake in various tissues, as well as whole bodies, was plotted as a function of time. The data reported (6), were used to reconstruct the tissue burdens of lead shown in Table II. The mass of each tissue type, as percent of body weight, was obtained from compilations of morphological/anatomical measurements of laboratory mice (3,4,7).

In addition to whole-body lead uptake, values were reported by Kumar for blood cells, plasma, liver, kidneys, pancreas, lungs, stomach, intestine, heart, thigh muscle, spleen, and femur (6). The lead content of tissues not analyzed was approximated as follows: the measured lead concentration of skeletal muscle was also used for abdominal fat based on a study of human accident fatalities showing these tissues to be among the lowest in lead concentration (8); the measured lead concentration of lung was applied to skin since both tissues are high in collagen; 150% of the measured lead concentration in mouse femur was applied to brain based on a study by P'an and Kennedy (9) showing the uptake of lead by rat brain to be about 50% higher than for bone one week after an injected dose; the measured lead concentration of the stomach was applied to the cecum because they are of similar composition; and for the same reason the measured lead concentration of spleen was applied to seminal glands, testes, and lymph nodes/thymus.

The measured femur lead concentration was applied to the entire skeleton even though the literature confirms that lead concentration as well as lead kinetics varies between bones (10,11).

Between 2 and 10 days post-injection, liver, erythrocyte, intestine, stomach, and cecum lead burdens decreased 70-80%; muscle, skin, kidney, pancreas, and lung decreased 50-60%; seminal gland, testis, lymphatic tissue, and spleen decreased 30-40%; abdominal fat, skeleton, and brain either remained the same or increased slightly. The plasma lead burden was very low at both 2 and 10 days post-injection.

Examination of Table II shows good agreement between the lead body burden obtained by summing the individual tissue burdens (34.04  $\mu\text{g}$ ) and that

**Table II. Reconstruction of lead body burden in mice**

Tissue	% of B.W.	Tissue Wt. <sup>1</sup> (gm)	Percent of dose <sup>2</sup> /gm of tissue (Tissue burden, $\mu\text{g}$ )	
			2 Days	10 Days
Skeletal Muscle	44.0	11.0	0.10 (0.55)	0.05 (0.28)
Skin	16.0	4.0	0.40 (0.80)	0.20 (0.40)
Abdominal Fat	10.0	2.5	0.10 (0.20)	0.05 (0.25)
Skeleton	8.2	2.1	22.00 (22.6)	23.00 (23.6)
Plasma	4.6	1.2	0.07 <sup>3</sup> (0.04)	<0.05 (NC) <sup>4</sup>
Liver	4.3	1.1	2.00 (1.1)	0.30 (0.17)
Erythrocytes	3.2	0.8	0.80 <sup>3</sup> (0.32)	0.25 <sup>3</sup> (0.10)
Intestine	2.3	0.6	0.80 (0.24)	0.20 (0.06)
Kidneys	1.5	0.4	4.60 (0.92)	1.80 (0.36)
Brain	1.4	0.4	33.00 (6.6)	34.50 (6.90)
Pancreas	0.7	0.2	1.70 (0.17)	0.60 (0.06)
Seminal Glands	0.7	0.2	1.30 (0.13)	0.80 (0.08)
Testes	0.7	0.2	1.30 (0.13)	0.8 (0.08)
Heart	0.4	0.1	<0.05 (NC) <sup>4</sup>	<0.05 (NC) <sup>4</sup>
Lung	0.4	0.1	0.40 (0.02)	0.20 (0.01)
Lymph tissue <sup>5</sup>	0.3	0.1	1.30 (0.07)	0.8 (0.04)
Stomach	0.3	0.1	0.80 (0.04)	0.25 (0.01)
Cecum	0.2	0.1	0.80 (0.04)	0.25 (0.01)
Spleen	0.2	0.1	1.30 (0.07)	0.90 (0.05)
$\Sigma^6$	99.4	25.3	(34.04)	(32.46)
Whole Body <sup>7</sup>	100.0	25.0	2.40 (30.00)	1.50 (18.75)

<sup>1</sup> Calculated for 25 gm mouse<sup>2</sup> Single intraperitoneal injection of 50  $\mu\text{g}$  lead as lead nitrate<sup>3</sup> per ml of tissue<sup>4</sup> Not Calculable<sup>5</sup> Lymph nodes + thymus gland<sup>6</sup> Sums of column entries<sup>7</sup> Whole body counts reported by Kumar (6)

determined by whole-body counting (30.00  $\mu\text{g}$ ) on day 2, but not day 10 (32.46  $\mu\text{g}$  vs. 18.75  $\mu\text{g}$ ) (6). Depending upon which value is used, the body burden decreased either 4.6% or 37.5% between days 2 and 10.

Thus, between days 2 and 10, seminal gland, testes, lymphatic tissue, and spleen, none of which are suitable for routine monitoring, reflected the change in lead body burden more accurately than other tissues analyzed.

Of greater relevance to markers of lead exposure in the general population are the results reported by P'an and Kennedy (9) for rats receiving repeated injections of lead acetate for six months. Two groups of animals were intraperitoneally administered 10 and 20 mg/lead acetate/kg, respectively, at intervals of 1, 2, 4, 8, 12, 16, 20, and 24 weeks. Twenty-four hours after each treatment, 8 rats were randomly selected from each treatment group and placed in metabolism cages for a 24-hour urine and feces collection. Following this collection period, saliva and blood were obtained under ether anesthesia before the animals were sacrificed. Lead analyses were performed on femur, kidney, brain, whole blood, plasma, plasma filtrate, liver, salivary glands, testes, urine, saliva, fur, and feces (Table III).

**Table III. Lead concentration of selected tissues following repeated injections of lead acetate in rats**

Dose <sup>1</sup>	10			20		
Week of Sacrifice	6	12	24	6	12	24
	Lead Concentration			Lead Concentration		
Femur <sup>2</sup>	200	270	590	250	350	692
Brain <sup>2</sup>	1.1	2.1	3.3	1.6	2.6	3.9
Kidney <sup>2</sup>	100	150	228	150	360	649
Blood <sup>3</sup>	60	75	79	90	101	149
Liver <sup>2</sup>	3.2	4.6	7.4	6.9	12.1	20.7
Fur <sup>2</sup>	6.3	25	34	9.7	34	37
Urine <sup>4</sup>	.2	.1	.3	.2	.2	.3
Feces <sup>2</sup>	24	106	54	41	121	133

<sup>1</sup> mg PbAc/kg administered on weeks 1, 2, 4, 8, 12, 16, 20, and 24

<sup>2</sup>  $\mu\text{g/g}$

<sup>3</sup>  $\mu\text{g}/100\text{ml}$

<sup>4</sup>  $\mu\text{g}/\text{mg}$  creatinine

In this study, the small number of tissue types analyzed precluded reconstructing a meaningful lead body burden. Nevertheless, several relationships of interest can be seen. The lead concentration in salivary gland, saliva, testes, and urine remained fairly constant during the approximately 6-month treatment period at both dose levels. These tissues were not good surrogate measures of duration of exposure, dose level, or other tissue burdens (only urine is shown in Table III). Blood lead was not a very sensitive indicator of duration or intensity of exposure. Of the remaining tissues, bone, fur, and brain reflected uniform increases with duration of treatment at both dose levels, but showed little difference between dose levels. Both liver and kidney reflected the difference between duration of exposure and dose rates much better than did other tissues. In both treatment groups, fecal lead correlated highly with bone, fur, and brain lead. Liver and urine lead began to rise only after 12 weeks of treatment. Of the tissues studied, fur offers the greatest potential for convenient repeated sampling and could serve as a surrogate for brain lead level; neither distinguished differences between doses very well.

**Study 3: Benzene.** An early paper by Schrenk et al. (12) examined benzene concentrations in the major tissue compartments of dogs following different exposure regimes to benzene vapor. It was found that blood benzene levels of continuously exposed dogs reached a plateau in about two hours, and this equilibrium level correlated with the concentration of benzene in the air. In this study, each 100 ppm benzene vapor in air resulted in an equilibrium blood concentration of 0.21 mg/100 ml. Thus, during a continuous exposure of at least two hours, benzene exposure rate could be assessed from the concentration of benzene in the blood.

In the same study, other dogs were exposed to benzene vapor for several hours per day for prolonged periods and their tissues analyzed for benzene content (12). Using these data together with body composition data reported by Andersen (13), benzene body burdens were reconstructed for this exercise.

The results for two dogs, each receiving a different amount of exposure, are presented in Table IV. Because the data available were incomplete, certain assumptions and omissions had to be made. For example, bone tissue was not analyzed; therefore, bone benzene burdens could not be approximated (12). Benzene concentrations were reported for brain, heart, kidneys, liver, lung, and pancreas separately. Together, they account for an estimated 8.6 % of the dogs' body weight. A weighted mean benzene concentration was calculated for this group of six organs using the fractional contribution of each to the 8.6% of body weight. This weighted mean appears in Table IV as the benzene concentration for OST (other soft tissue). Since the concentrations of benzene in skin and GI tract were not reported by Schrenk (12), they were assigned the benzene concentration calculated for OST. Accordingly, their percentages of B.W. are included in the OST percent of B.W. column, and their approximated tissue burdens are included in the OST tissue burden columns.

Benzene burdens of tissues rich in hemo-myoglobins (skeletal muscle, blood, and heart) appear to remain constant or decrease slightly between days 38 and 192 (benzene concentrations reported for heart at 38 and 192 days were

7.3 and 6.2 mg/100 g, respectively) (12). Whether tissue compartments had reached a steady state at 192 days could not be determined. However, in another trial, the tissue concentrations of benzene in one dog carried to 272 days were not higher than those exposed for 192 days (12).

**Table IV. Reconstruction of benzene body burden in dogs**

Air Conc. (ppm)		800		800	
Daily Exposure (hr)		8		8	
Exp. Duration (days)		38		192	
Tissue	Per- cent of B.W.	Tissue Conc. mg per 100 gm	Tissue Burden <sup>1</sup> mg	Tissue Conc. mg per 100 gm	Tissue Burden <sup>1</sup> mg
Blood	8.0	1.4	10.1	1.3	9.4
Skeletal Muscle	46.0	4.5	186.3	3.0	124.2
OST <sup>2</sup>	30.6 <sup>3</sup>	3.0 <sup>4</sup>	82.6	4.0 <sup>4</sup>	110.2
Fat	7.0	18.6	117.2	25.7	161.9
Bone <sup>5</sup>	9.0				
<b>TOTAL =</b>	<b>100.6</b>		<b>396.2</b>		<b>405.7</b>

<sup>1</sup> Tissue burdens are calculated for 9 kg dog.

<sup>2</sup> Other Soft Tissues.

<sup>3</sup> Includes: analyzed organs, 8.6% B.W.; Skin, 17% B.W.; GI tract, 5.0% B.W.

<sup>4</sup> Determined by summing the products of each tissue's fractional contribution to the 8.6% of B.W. times that tissue's benzene concentration.

<sup>5</sup> Bone represents about 9% of body weight and is included only to document total body composition.

Under the prolonged exposure conditions in this study, blood benzene burden remained approximately the same for the two exposure durations, as did body burden. Thus, blood benzene burden was a useful surrogate measure of body burden but not of total exposure. On the other hand, benzene levels in fat or OST showed a slight increase at the higher exposure level and may potentially be considered as insensitive surrogate measures of total exposure but even poorer measures of body burden. However, these tissues are not readily available for long-term monitoring studies.

## Inferences Drawn

The studies presented above demonstrate the need for a better understanding of the relationships between pesticide exposures and the resulting tissue/body burdens. The most conspicuous deficiencies were associated with interpreting the relationship between blood toxicant level and exposure. For example, plasma EPN levels (but not whole blood) reflected EPN levels in the brain tissue of chicken, but not in the more critical peripheral nervous tissue (2); though blood lead reflected both the dosage and the duration of repeated lead injections in rats, it was an insensitive indicator of either (9); and blood benzene levels of dogs did not reflect the fivefold difference in duration of exposure (12). Keeping in mind that animal studies are conducted under rigidly controlled conditions while investigations of population exposures are not, human studies would be expected to reflect even greater inconsistencies. Uncertainties notwithstanding, surrogate body burden measurements are frequently made when assessing exposures in the general population.

The most compelling reasons for doing so are (1) the large body burden database already in existence, for both experimental animals and humans, represents a valuable resource deserving of better utilization and continued expansion; (2) methodologies already developed for sampling and analysis of a number of pesticides and other toxicants can usually be adapted for use with other pollutants of concern with minor modification; (3) the information obtained is useful for identifying patterns of exposure over time (trend) and space (hot spots); (4) when the pharmacodynamics and pharmacokinetics of a pollutant are fully understood, body burden measurements can be used as inputs to mathematical models that will yield accurate exposure assessments; and (5) body burden measurements, or their surrogates, can contribute significantly to risk assessments. The extent to which each of these expectations has been realized is discussed briefly below.

## Existing General Population Body Burden Databases

EPA's National Human Monitoring Program (NHMP) was established in 1967 to determine and assess changes in detectability and concentrations of pesticide residues in the general population. Its main component is the National Human Adipose Tissue Survey (NHATS), although a National Blood Network is also planned. Initially directed toward pesticides, the NHATS was later expanded to include other environmental chemicals as well (14).

Other data bases include the National Center for Health Statistics' National Health and Nutrition Examination Surveys (NHANES) which determine blood levels of selected environmental chemicals in cooperation with other programs, and EPA's Total Exposure Assessment Methodology (TEAM) study which measures personal exposures of selected populations to selected airborne pollutants. Of these, NHANES is the only program that uses a population-based sample and only NHATS provides regularly repeated observations with sufficient frequency to detect reasonably current changes. In addition to these ongoing programs, numerous animal and human studies have

been carried out to define the relationship between an exposure and a surrogate measure of body burden.

In general, useful correlations are found between exposure and concentration of parent compound (or its metabolites) in (1) exhaled air, for many volatile compounds (VOC's in blood can potentially equilibrate with alveolar air so that exhaled air can proxy for blood as a biological matrix); (2) fat, for fat-soluble compounds; (3) bone, for some inorganics; and (4) urine, for water-soluble parent compounds and/or their metabolites. However, for human exposure monitoring, practicality limits the number of biological matrices available for sampling to those which the subject is willing to share; usually blood, urine, saliva, sweat, and breath.

Surrogate measures of body burden have been used most successfully for monitoring occupational exposures. In contrast to general population exposures, samples can be obtained on a regular schedule and in known relationship to time and duration of chemical exposures in the workplace. Thus, correlations can be established between exposure histories, body burden measurements, and associated signs/symptoms. Such correlations are difficult to establish in the nonoccupational setting.

The chemicals in Table V are those for which surrogate measures of body burden are frequently used as markers of internal exposure, primarily in occupationally exposed populations.

### Sampling and Analysis

With reference to exposure monitoring, analytical methods research has usually been directed first to the detection of toxicants in air, water, and food and later to biological samples. Analytical methods, using traditional instrumental analyses, are sufficiently well developed for biological monitoring programs in the workplace for about 70 chemicals (20). Not all of these methods are suitable, however, for detecting the low levels usually encountered in the general population. In addition, the hazardous chemicals potentially of concern number in the thousands. Thus, a substantial need remains for analytical methods which are cost-effective and have the specificity and sensitivity required for exposure assessments in the general population.

### Trend and Distribution Analysis

The data collected by NHMP has documented widespread pesticide exposures in the general population (14). It has also shown that reduced use of PCBs, DDT, and dieldrin resulted in lower tissue concentrations of those compounds. Despite the demonstrated success of NHMP for trend identification, few uses have been made of the data base for this purpose (14).

Single or sporadic studies, such as NHANES, are not expected to identify trends in a timely manner, but have been able to provide information on the presence and regional distribution of selected pesticides (14).

**Table V. Environmental Chemicals and Commonly Used Surrogate Measures of Body Burden**

Chemical	Toxic <sup>1</sup> Agent	Target <sup>2</sup>	Biological <sup>3</sup> Monitor	Ref.
Antimony	P	entr; s; ns	antimony; ur	15,16
Arsenic	P	entr; s; c; ns	arsenic; ur	16,17
Benzene	P	cns	benzene; bl, br	16,18
Benzene	M	hem	phenol; ur	15
Cadmium	P	entr; k	cadmium; ur, bl	15,17
Carbaryl	P	ns	1-naphthol; ur	16
CCl <sub>4</sub> <sup>4</sup>	P	ns; l; k	CCl <sub>4</sub> <sup>4</sup> ; br	16
Chlordane	P	ns; l; k	oxychlordane; bl	16
Chlordecon	P	ns, l	chlordecon; bl	16
Cobalt	P	s; p; c	cobalt; ur	15,17
Cresol	P	ns; p; l; k	cresol; ur	16
Cyanide	P	ns	thiocyanate; ur	15-17
Diazinon	M	ns	org. phosph.; ur	16
Dieldrin	P	ns	dieldrin; bl, fat	16
2,4-D <sup>4</sup>	P	ns; l; k	2,4-D conjug.; ur	16
Dioxins	P	s; f	dioxin; bl, fat	15,16
Diquat	P	entr; ns	diquat; ur	16
DDT <sup>4</sup>	P	ns; r	DDT; bl, fat	16,19
DDT	M		DDA; ur, bl	16,19
DDT	M		DDD; ur, bl	16,19
DDT	M		DDE; ur, bl	16,19
DMF <sup>4</sup>	P	l; k; ns	DMF; br	16
DMF	M		MF; ur	16
DNOC <sup>4</sup>	P	s; ns	DNOC; bl	16
Endrin	P	ns	endrin; bl	16
Ethylbenzene	P	entr; ns	mandelic acid; ur	16

Table V. Continued

Chemical	Toxic <sup>1</sup> Agent	Target <sup>2</sup>	Biological <sup>3</sup> Monitor	Ref.
Hexachloro- benzene	P	s	hexachlorobenzene; bl	16
2-Hexanone	M	ns	2-hexanone; bl, br	16
Lindane	P	ns; hem	lindane; bl	16
Malathion	M	ns	org. phosph.; ur	16
MEK <sup>4</sup>	P	ns; entr	MEK; bl, br, ur	15
Nitrobenzene	M	hem; ns	methemoglobin; bl	16
Nitrobenzene	M		p-nitrophenol; ur	16
Paraquat	P	p; k	paraquat; ur	16
Parathion	P	ns	parathion; bl, ur	16
Parathion	M		p-nitrophenol; ur	16
Pentachlorophenol	P	s; ns	pentachlorophenol; bl, ur	16
Perchlorethylene	P	s; ns; l; k	perchlorethylene; br	16
Styrene	P	entr; ns	styrene; bl	15
Styrene	M	l	mandelic acid; ur	16
Trichlorethylene	M	l; k; ns	trichlorethylene; br	16
2,4,5-T <sup>4</sup>	P	ns; s	2,4,5-T; bl, ur	16
Toluene	P	ns	toluene; bl, br	16
Toluene	M		hippuric acid; ur	15
Vinylchloride	P	bone; ns; l	vinylchloride; br	16
Phenols	P	entr; ns; l; k	phenol; ur	15
Lead, Inorg.	P	hem; ns; k	aminolevulinic acid; ur	15-17
Lead, alkyl	P	ns	lead; ur	16
Mercury, Inorg.	P	k	mercury; ur	15-17
Mercury, alkyl	P	ns; f	alkyl mercury; bl	15,16

*Continued on next page*

Table V. Continued

Chemical	Toxic <sup>1</sup> Agent	Target <sup>2</sup>	Biological <sup>3</sup> Monitor	Ref.
Selenium	P	entr; s	selenium; ur	15,16
Tin, alkyl	P	ns	alkyl tin; feces	16
Hydrazine	P	s; l; p; hem; k	hydrazine; bl	15
PC/PB-biphenyls	P	s; ns	PC/PB- biphenyl; bl, fat	16

<sup>1</sup> P=parent compound; M=metabolite.

<sup>2</sup> c=cardiovascular; entr=eye, nose, throat, resp. tract; f=fetus;  
hem=hematopoietic sys.; k=kidney; l=liver; ns=nervous sys.; p=lung;  
r=reproductive sys.; s=skin.

<sup>3</sup> bl=blood; br=exhaled air; ur=urine.

<sup>4</sup> CCl<sub>4</sub>=Carbon tetrachloride; 2,4-D=2,4 dichlorophenoxyacetic acid;  
DMF=Dimethylformamide; DDT= Dichlorodiphenyl-trichloroethane;  
MEK=Methyl Ethyl Ketone; 2,4,5-T=Trichlorophenoxyacetic acid.

### Exposure Assessment

Biomarkers of exposure can be either bioindicators which reflect only the presence or absence of a pollutant, e.g., residues of toxic chemicals in human tissues (21), or biomonitors which provide for regular surveillance and quantification of the exposure. Tissue levels have not yet proven to be reliable biomonitors of pesticide exposure in the general population. The development of exposure assessment methodology usually emphasizes improving the accuracy and precision of the analytical methods used to measure tissue levels of toxicant at the expense of the more difficult task of gaining an understanding of the biological system. A consequence is that tissue concentrations of environmental chemicals can be estimated with far greater accuracy and precision than can their pharmacodynamic (PD) and pharmacokinetic (PK) behaviors, and the analytical chemical 'signal' becomes buried in biological 'noise'.

The development of holistic PK models for estimating doses to human target tissues from surrogate body burden measures represents a significant effort. Target tissue dose depends upon the exposure rate and the kinetics of pollutant uptake, intake, internal distribution, and elimination. While external exposure rates can be derived from environmental monitoring data applicable to both humans and animals, the development and verification of PK models are derived mainly from data obtained from animal experiments. Thus, the model must be able to extrapolate PK data between species. The amount of physiological, biochemical, and behavioral data needed, in addition to tissue burden data, for successful extrapolation between species is not known. Nor is it known, with respect to humans, whether the additional data must be obtained in conjunction with the tissue sampling or whether they can be acquired at another time.

At present, PK models suitable for assessing human exposures from body burden data are not available. However, rapid progress is being made toward incorporating physiologically based parameters into the modeling effort. Pharmacokinetic non-linearities occur between different doses and between different species. Physiologically based pharmacokinetic models are accurate tools for taking these non-linearities into account (22). As a result, more realistic and usable physiologically based pharmacokinetic (PBPK) models soon may become available.

### Risk Assessment

Neither detection nor determination of concentration of a toxicant in tissues of individuals or the general population has satisfactorily provided a quantitative estimate of risk to human health. A major difficulty is the large variation in susceptibility to toxicant insult of the general population (23). For example, people living downstream from a defunct DDT plant in Triana, Alabama, were chronically exposed to DDT in their diets for many years and had several times the national geometric mean for DDT (and related chemicals) in their serum. However, a survey of the health status of 499 of them (out of approx. 600), indicated that the total DDT body burdens were not associated with specific

illness or ill health (24). Admittedly, the limited number of epidemiological studies to date suggest that DDT is relatively nontoxic in humans. However, even for the more toxic pesticide kepone, the variability of blood kepone levels precluded a quantitative risk assessment when comparisons were made between workers with and without overt signs of toxicity from kepone exposure (25). Some chemicals are cleared from the body or degraded in the body so rapidly that they cannot be detected in tissues with conventional analytical methods, even a few hours after exposure. Examples are benzidine, aflatoxin, vinyl chloride, and formaldehyde. Therefore, failure to detect a chemical in human tissues does not mean that potentially toxic exposure to it has not occurred (14).

The extent to which a human population is susceptible to a toxic stressor depends not only upon the intensity and duration of exposure but also upon the rate of uptake, intake, metabolism, storage, excretion, abundance of target macromolecules at the cellular level, and potential for adaptation to the toxicant. These processes are in turn regulated and/or modified by the genetic makeup of the individuals, their health status, and variable numbers of host (lifestyle) factors (26).

## Discussion

Surrogate measures of human body burden repeated with some regularity over time, such as the NHMP, have proven effective in revealing trends of pesticide exposure (27). Similarly, single determinations in selected subpopulations have disclosed geographic gradients of exposure. Surrogate measures that quantitatively reflect exposure have been described for a few volatile (e.g., benzene) or gaseous (e.g., carbon monoxide) environmental pollutants at present.

No reports were found which quantitatively relate tissue toxicant level with the degree of health risk in the general population. However, examples to the contrary are readily found for toxicant measured in nontarget tissue, e.g., DDT in blood (24, 25) or a presumptive target tissue, e.g., chlorinated hydrocarbons and PCBs in bone marrow of children (28).

As a result, three main approaches have evolved toward achieving the capability to quantitatively assess exposure and health risk. First, the development of holistic, PBPK models for pollutants, or pollutant classes, of concern. In traditional kinetic analysis, empirical compartments are inferred from fitting a model to the data obtained experimentally. In PBPK models compartments are, to the extent possible, characterized beforehand based on the physical structure of the organism and are defined realistically with respect to pertinent biological or physicochemical parameters (29). If the relevant biological structure and chemical-specific parameters are correctly described, e.g., the tissues involved, blood flows, reaction pathways, tissue solubilities of toxicant, specific binding proteins, etc., then the physiologically based model will accurately simulate the uptake, intake, tissue distribution, metabolism, and excretion of pollutants under different exposure scenarios.

Species differences in PK and PD behaviors for a given toxicant are due to quantitative and/or qualitative species differences in biological structure and/or metabolic pathways. To the extent that these differences are adequately

described in a physiologically based model, the model will also simulate actual interspecies differences in the toxicant's PK and PD behavior. In other words, PBPK models can be powerful tools for interspecies extrapolation provided the biological processes are understood and pertinent parameter values can be accurately measured (29).

For each pollutant of concern, input data to the model must be derived from human and animal experiments. Stringent design of animal experiments (e.g., randomization) ensures that relatively simple methods of data analysis will discriminate between exposure groups and that probabilistic statements made about these differences will be valid. However, most human population exposure assessments cannot be carried out within the design constraints of a randomized controlled trial. For this reason, the standard mathematical models based upon animal experiments can lead to biased or imprecise results. Population PK/PD has been proposed as a way to exploit less stringent observational data for which standard models and analyses do not work (30).

A second approach to quantitative exposure assessment is to develop functional biomarkers of internal exposure. These include changes in molecular, genetic, biochemical, immunologic, physiological, or behavioral status. They offer the potential of relating more directly to risk assessment than do tissue pollutant concentrations. Functional biomarkers can be extremely sensitive but usually lack pollutant specificity. For example, alterations in behavior were measured in rats dosed with the insecticide carbaryl at a time when tissue levels of parent compound or metabolite(s) were undetectable using conventional analytical methods (31). Even with the advent of analytical methods having the required sensitivity, the behavioral changes seen were not specific to carbaryl. Similarly, cholinesterase inhibition is not peculiar to a particular pesticide or chemical class of pesticides (32), nor is the alteration in erythrocyte protoporphyrin profile unique to lead exposure (33). The nonspecific nature of functional biomarkers limits their usefulness in human exposure assessments at present.

Yet to be explored are biomarkers that combine elements of both tissue burden and functional biomarkers. A reactive toxicant molecule initiates its action by binding to critical macromolecules on or in cells. Therefore, determining the level of toxicant, or its metabolite, bound to the critical macromolecule may be both sensitive (measures an incipient functional change) and specific (measures the pollutant concentration at a critical molecular site). These markers may also support health risk assessments more directly than would tissue concentration measurements. Analytical methods utilizing immunoassay and biosensor methodologies, alone or in combination, can potentially measure macromolecular-bound toxicant with high sensitivity and specificity (34,35).

The third approach to quantitative exposure assessment is development of indirect indicators (used as predictors of body burden, critical tissue concentration, or macromolecular-bound toxicant) which are more cost-effectively obtained than body burden data. Considerable progress has been made toward this end first using selected physico-chemical properties and, more recently, computer-aided molecular prediction (CAMP) methods. While these

methods are useful for suggesting possible metabolic and kinetic behaviors of toxicants, they are characteristics of the toxicant and do not totally replace animal experimentation (36). Thus, there is a need for a predictor which includes characteristics of the biological system.

## Conclusions

The quantitative exposure assessment methods discussed above are not sufficiently developed for routine application in human population studies. In the meantime, there is a need for indicators of internal exposure which can be used to cost-effectively screen large numbers of chemicals in the same way the LD<sub>50</sub> is used to screen for acute toxicity.

The method of statistical moments (37) has been extensively used in the pharmaceutical industry. The method is based on the knowledge that movement of the individual molecules through the body is governed by probability, since all will not be metabolized or excreted at the same time. The time course of the plasma concentration following a single dose (i.e., transfer function) can be regarded as a statistical distribution curve. It is an individual characteristic and implies the complete kinetics of a compound or metabolite in the body. Analysis of the distribution curve can be made by the use of the method of statistical moments: the area under the curve (AUC), the mean residence time of the intact molecules (MRT), and the variance of the MRT are the zero, first, and second moments, respectively. The MRT can be defined as the mean time for intact molecules to transit through the body; it involves a composite of all kinetic processes. In contrast with the  $t_{1/2}$ , the MRT of a chemical or metabolite depends upon the whole concentration/time profile (37). And as pointed out by Yamaoka *et al.* (37), analysis of the distribution curve (a transfer function) can be made without knowing the kinetics of the toxicant. The method of statistical moments may satisfy the need for a biologically based characteristic to be used for development of predictors of body burden, critical tissue concentration, or macromolecular-bound toxicant. It has been suggested that an indirect indicator, e.g., a 'black box' transfer function, may be feasible in the short term and provide very usable exposure assessments while the more accurate holistic model is under development (38).

A systematic determination of the transfer functions of pesticides in experimental animals has not yet been reported. However, many studies have been reported in which periodic determinations were made of plasma or blood pesticide levels following administration of a single dose. The method of statistical moments applied to these data could provide an initial evaluation of the transfer function as an indirect indicator of 'internal' exposure.

In addition, transfer functions could be determined for compounds representative of the major chemical classes of pesticides in humans and in commonly used experimental animal species. Comparisons among these would provide a systematic basis for extrapolating toxicological data between species. The animal experiments required to determine transfer functions are straightforward, and computer programs are available for calculating the statistical moments (39). In combination with CAMP and other physico-chemical

based predictors of body burden, the transfer function should enhance the predictability of internal exposure.

### Acknowledgments

The information in this chapter has been funded by the U.S. Environmental Protection Agency under Cooperative Agreement No. CR 817495-01-0 with the Harry Reid Center for Environmental Studies, University of Nevada-Las Vegas. It has been subjected to Agency review and approved for publication.

### Literature Cited

1. O'Flaherty, E.J. *Toxicants and Drugs: Kinetics and Dynamics*; John Wiley & Sons: New York, NY, 1981; pp 81-172.
2. Abou-Donia, M.B.; Reichert, B.L.; Ashry, M.A. *Toxicol. Appl. Pharmacol.* 1983, 70, 18.
3. *Handbook of Biological Data*; Spector, W.S., Ed; W.B. Saunders Company: Philadelphia, PA, 1956. p. 584.
4. *Biological Handbook: Growth, Including Reproduction, Morphology, and Development*; Altman, P.L.; Ditmer, D.S., Eds.; Federation of American Societies for Experimental Biology: Washington, DC, 1962. p. 608.
5. *Form and Function in Birds*; King, A.S.; McLelland, J., Eds.; Academic Press, Inc.: New York, NY, 1979; Vol. 1. p. 459.
6. Kumar, S.; Mehta, D.; Singh, S.; Garg, M.L.; Mangal, P.C.; Trehan, P.N. *Indian J. Exp. Biol.* 1988, 26, 860.
7. Crispens, Jr., C.G. *Handbook on the Laboratory Mouse*; Charles C. Thomas: Springfield, IL, 1975. p.267.
8. Quartermann, J. In *Trace Elements in Human and Animal Nutrition*; Mertz, W., Ed.; 5th Edition; Academic Press, Inc.: New York, NY, 1986; Vol. 2; pp 281-317.
9. P'an, A.Y.S.; Kennedy, C. *Environ. Res.* 1989, 48, 238.
10. Denton, J.E.; Potter, G.D.; Santolucito, J.A. *Environ. Res.* 1980, 23, 264.
11. Erkkila, J.; Armstrong, R.; Riihimaki, V.; Chettle, D.R.; Paakkari, A.; Scott, M.; Somervaille, L.; Starck, J.; Kock, B.; Aitio, A. *Br. J. Ind. Med.* 1992, 49, 631.
12. Schrenk, H.H.; Yant, W.P.; Pearce, S.J.; Patty, F.A.; Sayers, R.R. *J. Ind. Hyg. Toxicol.* 1941, 23, 20.
13. Andersen, A.C. *The Beagle As An Experimental Dog*; The Iowa University Press: Ames, IA, 1970. p.616.
14. *Monitoring Human Tissues for Toxic Substances*; Report of the National Research Council's Committee on National Monitoring of Human Tissues; National Academy Press: Washington, DC, 1991. p. 211.
15. *Analyses of Hazardous Substances in Biological Materials*; Anger, J.; Schaller, K.H., Eds. VCH Publishers: New York, 1988; p. 252.
16. Baselt, R. C. *Biological Monitoring Methods For Industrial Chemicals*; PSG Publishing Co., Inc.: Littleton, MA, 1988.

17. *Biological Monitoring of Toxic Metals*; Clarkson, T.W.; Friberg, L.; Nordberg, G.F.; Sager, P.R., Eds. Plenum Press: New York, NY, 1988, p. 686.
18. Sato, A.; Nakajima, T.; Fujiwara, Y.; Murayama, N. *British J. Ind. Med.* **1975**, 32, 321.
19. *Toxicological Profile for DDT, DDE, and DDD*. Agency for Toxic Substances and Disease Registry; ATSDR/TP-89/08, 1989.
20. Wogen, G.N.; Gorelick, N.J. *Environ. Health Perspec.* **1985**, 62, 5.
21. Kutz, F.W.; Cook, B.T.; Carterpokras, O.D.; Brody, D.; Murphy, R.S. *J. Toxicol. Environ. Health.* **1992**, 37, 277.
22. Blancato, J.N. *Ann. Inst. Super. Sanità.* **1991**, 27, 601.
23. Kimbrough, R.D. *Environ. Health Perspect.* **1983**, 48, 77.
24. Kreis, K.; Zack, M.M.; Kimbrough, R.D.; Needham, L.L.; Smrek, A.L.; Jones, B.T. *J. Am. Med. Assoc.* **1981**, 245, 1926.
25. Cannon, S.B.; Veazey, J.M., Jr.; Jackson, R.S.; Burse, V.W.; Hays, C.; Straul, W.E.; Landrigan, P.J.; Liddle, J.A. *Am. J. Epidemiol.* **1978**, 107, 529.
26. *Determining Risks To Health, Federal Policy and Practice*. U.S. Department of Health and Human Services, Task Force on Health Risk Assessment; Auburn House Publishing Company: Dover, MA, 1986. p. 410.
27. Kutz, F.; Yobs, A.; Strassman, S.; et al. *Pest. Monit. J.* **1977**, 11, 61.
28. Scheele, J.; Teufel, M.; Niessen, K.H. *Europ. J. Pediatr.* **1992**, 151, 802.
29. Conolly, R.B.; Andersen, M.E. *Ann. Rev. Toxicol.* **1991**, 31, 503.
30. Sheiner, L.B.; Ludden, T.M. *Ann. Rev. Pharmacol. Toxicol.* **1992**, 32, 185.
31. Sideroff, S.I.; Santolucito, J.A. *Physiol. Behav.* **1972**, 9, 459.
32. *Pesticide Fact Handbook*; U.S. Environmental Protection Agency; Noyes Data Corporation: Park Ridge, NJ, 1988. p.827.
33. *Biological Monitoring of Toxic Metals*; Clarkson, T.W.; Friberg, L.; Nordberg, G.R.; Sager, P.R., Eds. Plenum Press: New York, NY, 1988. p. 686.
34. Schultz, J.S. *Ann. N.Y. Acad. Sci.* **1987**, 506, 406.
35. Parce, W.J. In *Proceedings of the 156th National Meeting AAAS*; Compiled by Games, M.D.; American Association for the Advancement of Science: Washington, DC, 1990, pp 35.
36. Saleh, M.A. In *Pesticide Transformation Products, Fate and Significance in the Environment*; Somasundaram, L.; Coats, J.R., Eds.; ACS Symposium Series 459; Washington, DC, 1991, pp 148-159.
37. Yamaoka, K.; Nakagawa, T.; Uno, T. *J. Pharmacokin. Biopharm.* **1978**, 6, 547.
38. Opdam, J.J.G. In *Health Surveillance Of Individual Workers Exposed To Chemical Agents*; Notten, W.R.F.; Herber, R.F.M.; Hunter, W.J.; Monster, A.C.; Zielhuis, R.L., Eds.; Springer-Verlag: Berlin, Heidelberg, New York, 1988, pp 31-38.
39. Efthymiopoulos, C.; Piemont, E.; Jung, L. (Bibliographic Citation): *Trends Pharmacol. Sci.* **1989**, 10, 480.

RECEIVED May 10, 1993

## Chapter 13

### **Chronic Organophosphorus Exposure Biomarkers in the Detection of Immune Dysfunction and the Development of Lymphomas**

David S. Newcombe<sup>1,2,4</sup>, Ali M. Saboori<sup>1</sup>, and Ahmed H. Esa<sup>3,5</sup>

<sup>1</sup>Department of Environmental Health Sciences, <sup>2</sup>Department of Medicine,  
and <sup>3</sup>Department of Oncology, Johns Hopkins Medical Institutions,  
Baltimore, MD 21205

The health effects of chronic organophosphate (OP) exposures are incompletely understood, but evidence in animals and man suggests an association between organophosphate exposure, immune dysfunction, and the occurrence of hematopoietic tumors, especially lymphomas. Epidemiological studies have shown an excess of these tumors in populations exposed to OPs, and immune dysfunctions have also been associated with the development of lymphomas in animals and man. Despite the predisposition to lymphomas in humans with immune dysfunction and the increased risk of lymphoma in OP-exposed populations, links between organophosphates and the immune system have not been defined. Evaluation of *in vitro* human natural killer (NK) cell and cytotoxic T lymphocyte (CTL) activities in the presence of OPs shows that the cytotoxic functions of these cells are significantly inhibited by some organophosphate compounds. Such functional OP-induced changes may represent sensitive biomarkers of chronic organophosphate exposure and effect when integrated with duration and intensity of exposure. In turn, possible linkages to the development of hematopoietic tumors in some human hosts through the suppression of immune surveillance mechanisms may be uncovered in this process.

<sup>4</sup>Current address: Bedford VA Hospital, 200 Springs Road, Bedford, MA 01730

<sup>5</sup>Current address: Department of Immunology, Pasteur Institute, 25 rue du docteur Roux, 75724 Paris, France

Acute organophosphorus exposures and their health effects have been extensively investigated and characterized (1), but chronic exposures to this same class of chemicals have been incompletely evaluated even though there is evidence relating OP exposures to the development of hematopoietic tumors. Since organophosphates are not generally identified as definite human carcinogens, the association between OP exposure and tumorigenesis may represent either a yet to be defined carcinogenic effect or may occur by an indirect mechanism that places the host at risk for the development of cancer.

In this paper, the evidence supporting the potential for chronic OP exposure to promote the development of serious human health effects such as lymphomas is first reviewed. Then, the mechanisms by which this class of chemicals causes suppression of the human immune surveillance system is described. Biomarkers of exposure and effect are defined for the recognition and possible prevention of immune dysfunctions and their serious health effects in humans exposed to organophosphates.

### **Epidemiological Studies of Organophosphate Exposed Populations**

**Lymphomas in Farmers.** The initial impetus for our laboratory to examine the mechanisms by which significant health effects might be associated with chronic organophosphorus exposures arose from published epidemiological studies (2-6). A large number of studies determined that farmers succumb more frequently to lymphomas or hematopoietic tumors than would be expected in healthy non-farming populations (2-6). Such data have been documented not only for farmers residing in the United States, but also for those in other countries (3,6). An excess of lymphomas has been most recently reported in Italian farmers (7). There have been no epidemiological data supporting a specific chemical compound or group of compounds as contributors to this increment in lymphatic cancers in farming populations, but pesticides have been prominently suggested as possible etiologic factors. The reasons for the excess of lymphomas observed in some farming populations and not others has remained elusive. To date it is not known whether such factors represent differences in host responses to chemicals, the use of different chemicals, or the habits of farming groups in their use and application of chemicals.

**Lymphomas in Grain Mill Workers.** Investigations of grain mill workers who also have been determined to have more lymphomas than would be expected in normal populations have

provided additional data as to the possible causative agents for the excess tumors in these workers. Studies performed by epidemiologists from the National Cancer Institute have reported that the workers who acquire these tumors in excess have been exposed to pesticides (8), and the latter substances have been postulated to be prime candidates as the cause for the development of such tumors in exposed hosts. Further, only janitors cleaning around grain storage silos and those working directly in the silos that have been treated with pesticides to prevent rodents and other animals from damaging the grain stores show an increased risk for the development of lymphomas (9). Malathion, an organophosphorus pesticide, was one of the several chemicals identified by workers exposed to pesticide-treated grain (9).

**Lymphomas in Resin Workers and Automobile Manufacturers.** Finally, two additional population groups, resin workers and automobile manufacturers, have also been shown to have an excess of lymphomas (10). It is clear that resin workers in the course of their work may be exposed to organophosphorus chemicals used either as flame retardants, stabilizers, or plasticisers. However, such workers have not been evaluated for their exposures to specific chemicals that may be lymphomagenic. Automobile manufacturers may also be exposed to plastic components in addition to a number of other substances that could contribute to the increased expression of lymphomas in this group. Nonetheless, one should recognize that about 30 to 40 percent of the components in an automobile are made of plastic, and some automobile workers may be involved in the molding of these plastic parts. Such a group could well be at risk from exposure to molten plastics containing organophosphorus agents.

### **Organophosphorus-induced Immune Dysfunction**

The determination that organophosphorus compounds are potent inhibitors of *in vivo* and *in vitro* monocyte esterase activity (11-16), an enzyme known to be an essential component of the cytotoxic effects of monocytes and other immune cells, was a key link between impaired immune functions and organophosphorus exposures. Perhaps the earliest clue to an organophosphorus-induced defect in monocyte esterase activity comes from the work of Lee and Waters (15). These investigators determined that a variety of organophosphorus pesticides and carbamate insecticides inhibited, to a significant degree, human peripheral blood monocyte esterase activity. Such inhibition occurred in the absence of direct contact with Shell pest strips in which the chemicals were imbedded since these pesticides were volatile. The inhibitor concentrations resulting in 50 percent inhibition of the target enzyme ( $IC_{50}$ ) for the various pesticides tested by Lee and Waters have been

calculated from their published data and are shown in Table I (15) along with the LD<sub>50</sub> values given in the same paper. As can be seen from these data, the organophosphorus insecticides investigated by these workers are fairly potent inhibitors of human monocyte esterase activity. The key to the significance of this work came later when Oertel and his colleagues first showed that inhibiting monocyte esterase with bis nitrophenyl phosphate resulted in a significant suppression of the capacity of this cell to form conjugates with a target cell, the K562 erythroleukemic cell (12). Consequently, the monocyte failed to lyse these same target cells (12). Although the doses of the bis nitrophenyl phosphate in this study were relatively high and the decrement in conjugate formation and lysis was not striking, these data provided the first evidence that organophosphorus compounds could impair the monocyte's ability to carry out cytotoxic reactions against the tumor cell line, K562.

**Organophosphorus Suppression of NK Cell Activity.** Both cytotoxic T lymphocytes and natural killer cells are essential for cell-mediated immunity, the elimination of virus-infected cells, and provide immune surveillance for premalignant cells. We postulated that organophosphate-induced defects in human immune surveillance systems might provide a possible link between immune dysfunction, lymphoproliferation, and lymphomagenesis. Initial studies by our group showed that non-pesticide organophosphates used in the manufacture of plastics resulted in both *in vivo* and *in vitro* inhibition of monocyte esterases (17). Subsequently, we showed that some organophosphorus compounds suppressed NK cell activity (Fig. 1). In these studies, peripheral blood lymphocytes were isolated by standard procedures and incubated for one hour in the presence or absence of organophosphorus compounds. K562 cells were labeled for 1 hour with <sup>51</sup>Cr and graded doses of organophosphorus-treated or control peripheral blood lymphocytes were exposed to target cells for four hours. Target cell lysis was then measure by quantifying the release of radiolabeled chromium after corrections were made for nonspecific release. As can be seen in this figure, tetra-*o*-cresylpiperazinyl diphosphamidate (TCPD), triphenyl phosphate (TPP), and tertiary butyl triphenyl phosphate (TBTPP) at 20 uM concentrations significantly suppressed NK cell activity when compared to controls containing no organophosphates ( $p < 0.001$ ). Triphenyl phosphine oxide (TPPO) and triphenyl thiophosphate (TPTP) did not significantly alter NK cell activity from control values.

**Organophosphorus Suppression of CTL Function.** We have also examined the effects of OPs on cytotoxic T lymphocyte function. Allogeneic CTLs, harvested on day 7, were

Table I. Monocyte Esterase Inhibition by Insecticides

PESTICIDE	COMMON NAME	LD <sub>50</sub> (mg/kg)	IC <sub>50</sub> (M) *
PHOSPHORIC ACID, 2,2-DICHLOROETHENYL DIMETHYL ESTER	VAPONA	52-80	1.0 x 10 <sup>-9</sup>
PHOSPHORIC ACID, 2-CHLORO-1-(2,4,5- TRICHLOROPHENYL) ETHENYL DIMETHYL ESTER	RABON	1,100	4.5 x 10 <sup>-9</sup>
PHOSPHORIC ACID, 1,2-DIBROMO-2,2- DICHLOROETHYL DIMETHYL ESTER	NALED	250	9.0 x 10 <sup>-9</sup>
PHOSPHOROTHIOIC ACID, O,O-DIETHYL O-(4- NITROPHENYL) ESTER	PARATHION	2	1.3 x 10 <sup>-7</sup>
PHOSPHOROTHIOIC ACID, O,O-DIMETHYL O-(3,5,6- TRICHLORO-2-PYRIDYL) ESTER	DURSBAN	941	5.2 x 10 <sup>-5</sup>
PHENOL, 2-(1-METHYLETHOXY)- METHYL CARBAMATE	BAYGON	83	6.7 x 10 <sup>-7</sup>
1-NAPHTHALENOL, METHYL CARBAMATE	CARBARYL	250	5.5 x 10 <sup>-4</sup>

\*Data derived from reference 15, copyright 1977. Insecticides were diluted in saline (0.9%)-EDTA (0.5%), and esterase activity was determined after a 15 minute incubation in the presence or absence of insecticide using an assay designed for the Hemalog D cell counter.

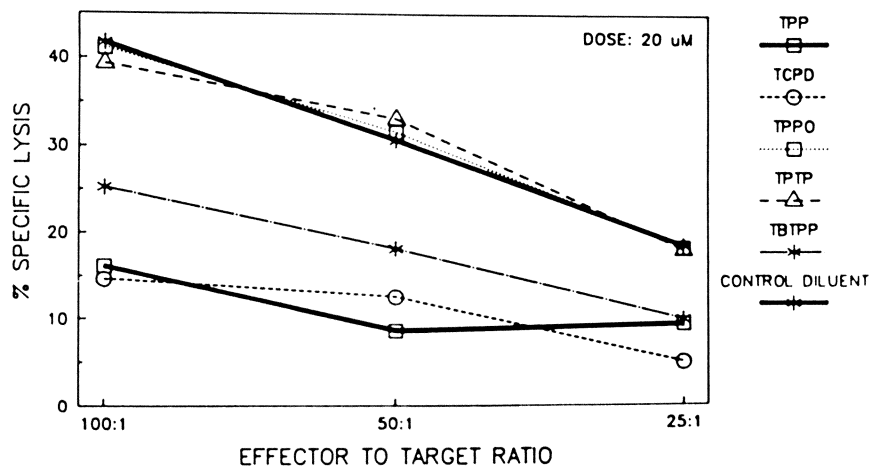


Figure 1. The Effect of Organophosphorus Compounds on Natural Killer Cell Activity

exposed to various OP compounds for 1 hour and then examined for their ability to lyse PHA-blasts from the stimulating cells in short-term <sup>51</sup>chromium release assays. The mean percent lysis inhibition  $\pm$  one standard deviation for five separate experiments in which each compound was compared with diluent control is shown in Table II. The effector to target ratio was 30:1. Each organophosphorus treatment (10  $\mu$ M for 60 minutes) significantly impaired the cytotoxic capacity of CTLs. Triphenyl thiophosphate had the weakest effect, only inhibiting this killing process by approximately 40 percent as compared to diluent treated controls, whereas tetra-o-cresylpiperazinyl diphosphoridate, triphenyl phosphate, and triphenyl phosphine oxide all inhibited cell lysis by 50 percent or greater when compared to appropriate controls. Thus, our studies and those of other investigators have shown organophosphorus-induced abnormalities in human cytotoxic T lymphocyte, natural killer cell, and cytotoxic monocyte functions that regulate human immune surveillance.

### **Immune Dysfunctions and Lymphomas**

Recent studies by the hematology group at the Belfast Hospital have provided some striking findings with regard to human monocyte esterase and the development of lymphomas (18,19). Their studies on a woman with a lymphoma documented the absence of monocyte esterase in her family and described an autosomal dominant inheritance of this immune cell enzyme deficiency (20). Subsequently, they evaluated the frequency of monocyte esterase deficiencies in hospitalized patients with malignancies, in normal healthy blood donors, and in patients hospitalized for non-malignant diseases (18).

The data from their publications is reproduced in Table III. It shows that monocyte esterase deficiency was almost four times more frequent with malignancies than in normal individuals. Further, monocyte esterase deficiency occurred twice as often in those with malignancies as compared with patients hospitalized for non-malignant disease.

**Esterase Deficiencies and Hematopoietic Tumors.** When those with malignancies were characterized further, reticuloendothelial malignancies were found to be significantly increased in patients expressing a deficiency in their monocyte esterase and included patients with Hodgkin's disease, non-Hodgkin lymphoma, and B cell chronic lymphatic leukemia (18). These data clearly suggested a relationship between lymphoma/leukemia and monocyte esterase deficiencies. Although the effects of therapeutic drugs as a cause for the monocyte esterase deficiency were excluded in these hospitalized patients, no occupational

**Table II. Organophosphorus Inhibition of Cytotoxic T cells in an Allogeneic Mixed Lymphocyte Reaction**

ORGANOPHOSPHORUS AGENT	LYSIS INHIBITION (%)
TRIPHENYLPHOSPHINE OXIDE	89±7
TRIPHENYL PHOSPHATE	76±5
TETRA-O-CRESYLPIPERAZINYL DIPHOSPHORIDATE	50±6
TRIPHENYL THIOPHOSPHATE	38±6

**Table III. Monocyte Esterase Deficiency**

SUBJECTS	NUMBER OF SUBJECTS	MONOCYTE ESTERASE DEFICIENT SUBJECTS
HEALTHY BLOOD DONORS	474	4 (0.8%)
MALIGNANT NEOPLASIA	808	32 (3.9%)
NONMALIGNANT DISEASE	3172	54 (1.7%)

Only subjects with greater than 73% esterase negative monocytes were classified as monocyte esterase deficient. Reprinted with permission from reference 18, copyright 1990.

histories were reported and previous chemical exposures with the exception of therapeutic drugs were not defined for this large population of patients. It is of interest to note that cancer of the stomach was also significantly increased in patients with monocyte esterase deficiencies although not to the degree observed with the lymphoma/leukemia group (18). An increase in cancer of the stomach has also been reported in patients with ataxia telangiectasia (21), a disorder associated with a striking increase in the frequency of lymphomas. These investigators also showed that monocytes expressing esterase deficiency were much less efficient in their capacity to lyse K562 cells when compared to monocytes with no esterase deficiency (19). Such studies supported the concept that defective monocyte cytotoxicity could play a significant role in the increased frequency of lymphomas observed in monocyte esterase deficient patients.

#### **Organophosphorus Inhibition of Monocyte Esterase Activity.**

In our laboratory, investigations examined the inhibition of human monocyte esterase (carboxylesterase) purified to homogeneity and determined the inhibitor constants ( $K_i$ ) for triphenyl phosphate and tetraphenyl resorcinol diphosphate to be in the range of  $10^{-9}$  to  $10^{-10}$  M (22). We also determined that the interaction between these compounds and monocyte esterase did not result in covalent binding of the inhibitor to the enzyme (22). Such data suggest that at least some organophosphorus compounds are reversible inhibitors of monocyte esterase and may bind to these enzymes through hydrophobic rather than covalent bonds. How this reversible inhibition leads to the development of lymphomas remains to be defined.

#### **Oncogenic Viruses and Organophosphorus-induced Mutations**

Since tumor development is preceded by an initiation and promotion step, several factors appear to be essential for the generation of lymphomas in man. Epstein-Barr virus (EBV) infection is associated with both malignant and non-malignant lymphoproliferative disorders (23). African Burkitt's lymphoma was the first tumor shown to be associated with EBV, and subsequently other types of Hodgkin's and non-Hodgkin lymphoma have been shown to be associated with this same virus (24).

**Immunodeficiency and Lymphomas.** Immunocompromised patients are also prone to clonal B cell expansions and malignant lymphomas. NK cell-deficient patients and immunocompromised patients are often prone to repeated viral infections, including those with EBV (25). The NK cell-deficient  $bg^+/bg^+$  mouse is also more likely to develop lymphomas than its normal counterpart (26). Patients with congenital immune deficiencies have an increased frequency

of lymphomas, and the cells isolated from such individuals almost always contain EBV genomes (27). These facts all suggest that EBV infections are closely related to the expression of lymphomas.

**Immune Deficiencies and Epstein-Barr Virus Infections.** Since NK cells, CTLs as well as cytotoxic monocytes can recognize virus-altered cells and destroy them, a deficiency in the functions of these cells could result in an increased risk of EBV-mediated B cell immortalization and virus-altered lymphoproliferation. Further, reactivation of a latent EBV infection could cause unregulated B cell proliferation, thus increasing the risk of mutations leading to carcinogenesis. Therefore, chronic organophosphorus exposures causing an impairment in esterase-dependent immune surveillance systems may facilitate oncogenic virus infection, an increase in the frequency of lymphocyte mutations, and the subsequent development of lymphomas.

**Organophosphorus-induced Chromosomal Aberrations.** Several *in vitro* studies have also shown organophosphorus-induced mutations in human peripheral blood lymphocytes and human lymphoid cell lines of B-cell origin (28). Those investigations have documented an increase in sister chromatid exchanges and stable chromosomal mutations such as translocations in these cells when they were exposed *in vitro* to a variety of organophosphorus insecticides (28). Similar chromosomal changes have frequently been observed in patients with acute organophosphorus intoxications (29-34). Until very recently no attempt has been made to characterize these chromosomal aberrations further. It has now been determined that farm populations including farmers exposed to pesticides in the production of grain, dairy farmers, and organic farmers have chromosomal mutations in antigen-receptor genes identical to those mutations observed in individuals with the autosomal recessive immunodeficiency disease, ataxia telangiectasia (35).

**Ataxia Telangiectasis, Lymphoma, and Pesticide Exposure.** It is well known that about 15 percent of individuals with ataxia telangiectasia die from cancer and frequently the tumors observed in this group are leukemias and lymphomas (21,36). The lymphomas observed with this heritable disease include both T and B cell type lymphomas. In fact, whites with this disorder have a frequency of cancer sixty-fold greater than normal individuals, and in blacks, there is a one hundred and eighty-fold excess of cancer. Such frequencies approximate the rate at which the hybrid antigen-receptor gene forms in the peripheral blood lymphocytes of patients with ataxia telangiectasia. Mutations from translocation of T cell receptor genes to the immunoglobulin heavy chain genes in such individuals

are frequently associated with lymphomas. There is a strong implication that the variable-(diversity)-joining recombinase is associated with or contributes to the transformations seen in both ataxia telangiectasia and agricultural workers. Nonetheless, there is a difference between the frequency of lymphoid malignancies in these two populations since ataxia telangiectasia patients have a much higher propensity to develop these tumors than do agricultural workers. In fact, the latter group may require some additional steps to trigger tumorigenesis.

The frequency of such mutations has been shown to be significantly greater in workers with high exposures than in those with low exposures to pesticides (35). In fact, the low exposure group did not manifest chromosomal changes significantly different from controls. Another indication that such mutations are related to pesticide exposure has been derived from evaluations of the chromosomal aberrations observed in peripheral blood lymphocyte chromosomes recovered prior to exposure, during exposure, and post-exposure (35). In the small number of agricultural workers (n=5) studied in this manner, the frequency of hybrid antigen-receptor genes in their peripheral blood lymphocytes has been determined to be higher during pesticide application times than before or after pesticide use. Furthermore, this increase has been shown to be significantly greater than controls, but samples evaluated from the pre-exposure and post-exposure periods did not differ significantly from controls. Such data also suggest that chromosomal aberrations associated with pesticide exposure are transient and decrease when exposure is discontinued, but the disappearance of these mutations is a significant parameter that needs further documentation in a larger population group.

Recent studies have developed a method for screening small amounts (0.2 ml) of peripheral blood for a marker of genomic instability that has been found in excess in populations with inherited or acquired chromosomal damage from environmental genotoxins (37). Genomic instability of this type is often associated with lymphomagenesis.

**Immune Function Biomarkers in Organophosphate-exposed Populations.** The foregoing data serve to emphasize the need to evaluate the status of both cell-mediated immunity and chromosomal integrity in individuals who are chronically exposed to organophosphates. Although changes in both these parameters have clearly been associated with in vivo and in vitro organophosphate exposures, the natural history of such chemically-induced alterations is essential to our understanding of the role they might play in the development of lymphomas. If a definitive role can be defined for these organophosphorus-induced alterations in

chromosomal structure, immune function, and the subsequent development of lymphomas, then immune function biomarkers with their specificity and sensitivity defined would provide a means for the early detection and prevention of these harmful effects.

**Immune Cells as Markers of Organophosphorus Exposure.** Both chromosomal aberrations and cell-mediated immunity can be readily assessed using peripheral blood samples from populations at risk with appropriate protocols and schedules. In addition to the data showing the in vitro organophosphate-induced defects in natural killer cell and cytotoxic T lymphocyte activities, we have compared the inhibitor constants ( $K_i$  values) obtained from the human enzymes, monocyte carboxylesterase and plasma butyrylcholinesterase. Preliminary data show that the monocyte carboxylesterase enzyme preparations have lower  $K_i$  values than those determined for plasma butyrylcholinesterase under the same conditions (Table IV). These data suggest that immune cell esterases may be a more sensitive marker of organophosphate exposure than plasma butyrylcholinesterase, a standard biomarker frequently used to detect organophosphate exposures.

**Specificity and Sensitivity of Immune Cell Esterases.** Although both the data on mononuclear cell esterases presented here and the studies of others reviewed in this paper provide substantive evidence that an association exists between organophosphate exposure, immune cell dysfunctions, and lymphomagenesis, several additional issues must be addressed before these immune cell biomarkers of effect can be accepted for screening purposes. The genes for both human monocyte carboxylesterase and mouse cytotoxic T lymphocyte have been cloned (38-43). Both enzymes are known to contain a serine molecule at their active sites (38-43). However, a complete panel of serine reactive compounds has not been examined to assess the specificity of the organophosphate inhibition of these enzymes. It is essential to identify other classes of chemicals that may inhibit these enzymes so that false positive test results can be excluded. Even though most, if not all, organophosphates are likely to be inhibitors of these immune cell esterases, their avidity for the active sites of these enzymes will vary. Such variances may limit the usefulness of these biomarkers since compounds with low inhibitory capacity are not likely to impair function to a significant degree. Since the concentrations of some industrial organophosphorus compounds resulting in 50 percent inhibition of monocyte esterase have been shown to be in the range of 1-20  $\mu$ M (44), workers exposed to the same chemicals who show decreased monocyte esterase activity may have circulating in vivo concentrations at or greater than the in vitro

Table IV. Human Monocyte Carboxylesterase and Plasma Butyrylcholinesterase: Comparative Inhibitor Constants

COMPOUNDS	CHOLINESTERASE $K_i$ (M)	CARBOXYLESTERASE $K_i$ (M)	DIFFERENCE
TRIPHENYL PHOSPHATE	$2.0 \times 10^{-5}$	$8.0 \times 10^{-9}$	2500
DIPHENYLMETHYL PHOSPHATE	$5.0 \times 10^{-5}$	$1.8 \times 10^{-7}$	277
TRIPHENYL PHOSPHITE	$8.0 \times 10^{-6}$	$4.8 \times 10^{-8}$	166
TRICYCLOHEXYL PHOSPHATE	$7.8 \times 10^{-5}$	$4.8 \times 10^{-7}$	164
TRIETHYL PHOSPHITE	N.I.*	$2.0 \times 10^{-6}$	-
TRIBUTYL PHOSPHITE	N.I.	$3.4 \times 10^{-6}$	-

All assays for enzyme activity were performed with alpha-naphthyl butyrate as the substrate using the ultraviolet spectrophotometric method as described in reference 22.

\*N.I.= not inhibited.

inhibitory range. For screening purposes, inhibitory concentrations must be determined for each chemical and in vivo concentrations of the toxic chemical measured as well.

Further, some organophosphates may react covalently with the active sites of both these enzymes as has been shown for diisopropylfluorophosphate (22,45). Such covalent reactants may be important to identify since the killing functions mediated by covalently inhibited esterases will be completely impaired as long as significant exposures continue and enzyme turnover is unable to replace organophosphorus-inhibited enzyme with new, active enzyme.

In addition to the incomplete knowledge about the specificity of these tests of cell-mediated immunity and the mode of inhibitor binding, the sensitivity of these biomarkers must be determined by measuring monocyte and lymphocyte cytotoxic responses using human cells exposed under standard conditions to organophosphates in vivo and in vitro. Presently, there are no known methods to assess in vivo cytotoxic reactions in the human, so cells from exposed individuals must be obtained and assayed in vitro. Finally, to derive data as to the validity of these potential biomarkers of exposure and effect, large control and organophosphate-exposed population groups must be studied in a prospective manner.

## Conclusions

Epidemiological studies have identified occupational groups at risk for lymphomas, and organophosphates represent work-related exposures that may contribute to the pathogenesis of such lymphomas. Immune dysfunctions including ataxia telangiectasia, acquired hypogammaglobulinemia, beige (natural killer deficient) mice, acquired immunodeficiency syndrome, Chediak-Higashi syndrome, common variable immunodeficiency disease, iatrogenic immunosuppression, Klinefelter's syndrome, rheumatoid arthritis, systemic lupus erythematosus, Swiss-type agammaglobulinemia, Sjogren's syndrome, Wiscott-Aldrich syndrome, and x-linked lymphoproliferative syndrome are also associated with an increased frequency of hematopoietic tumors in animals and man suggesting that altered immune defense functions could represent a key event linking chemical exposures and the occurrence of lymphomas. There is also evidence that chromosomal translocations and virus infections (EBV) are often observed in some types of lymphomas. Recent studies have clearly shown an increased frequency of chromosomal mutations similar to those observed in the immune disorder, ataxia telangiectasia, and patients with this disease are also at increased risk for the development of lymphomas.

Our group and others have documented an

organophosphate-induced inhibition of monocyte esterase and cytotoxic T lymphocyte esterase (17,46-48) which results in a decrease in the capacity of such cells to kill target cells. Human natural killer cell activity is also significantly reduced in the presence of organophosphates (17), and NK cell deficiencies are also associated with lymphoma development (26,49,50). *In vivo* these same immune surveillance cells are utilized to destroy virus-infected and transformed cells that may be the precursors of malignant lymphomas. Similarly, the absence of monocyte esterase has been shown to be associated with an increased frequency of hematopoietic tumors. Although the mechanistic pathway leading to the production of these tumors remains to be mapped, assays of esterase-dependent immune function biomarkers and the delineation of chromosomal aberrations in organophosphate exposed individuals coupled with prospective clinical evaluations could serve to document the longevity of such chemical-induced immune dysfunctions, to identify specific risk factors for lymphomas, and to design methods for the early recognition and prevention of such tumors. Clearly, any analysis of pesticide-induced cellular changes in exposed populations must be accompanied by information about the type, magnitude, and duration of pesticide exposure. Further, the permanence of any observed cellular changes should be related to the characteristics of the exposure.

**Acknowledgments:** The authors wish to thank Ms. Julie Connely and Nancy Hopa for their technical assistance. This work was supported in part by a grant from G.E. Plastics to DSN and NIH grant #A124682 to AHE.

### Literature Cited

1. Gallo, M.A.; Lawryk, N.J. In Handbook of Pesticide Toxicology; Hayes, W.J., Jr. and Laws, E.R., Eds.; Academic Press, Inc., San Diego, California, 1991, Vol. 2; pp. 917-1123.
2. Blair, A.; Malke, H. et al. Scand. J. Work Environ. Health **1985**, *11*, pp. 397-407.
3. Giles, G.G.; Lickess, J.N. et al. J. Natl. Cancer Inst., **1981**, *72*, pp. 1233-1240.
4. LaVecchia, C.; Negri, E. et al. Br. J. Cancer, **1989**, *60*, pp. 385-388.
5. Burmeister, L.F. J. Natl. Cancer Inst., **1981**, *66*, pp. 461-464.
6. Pearce, N.E.; Smith, A.H.; Fisher, D.O. Amer. J. Epidemiol., **1985**, *121*, pp. 225-237.
7. Pasqualetti, P.; Casale, R. et al. Amer. J. Hematol., **1991**, *38*, pp. 147-149.
8. Alavanja, M.C.R.; Rush, G.A. et al. J. Natl. Cancer Inst., **1987**, *78*, pp. 247-252.

9. Alavanja, M.C.R.; Blair, A.; Masters, M.N. J. Natl. Cancer Inst., **1990**, 82, pp. 840-848.
10. Hall, N.E.L.; Rosenman, K.D. Amer. J. Ind. Med., **1991**, 19, pp. 145-159.
11. Emmett, E.A.; Lewis, P.G. et al. J. Occup. Med., **1985**, 27, pp. 904-914.
12. Oertel, J.; Hagner, G. et al. Br. J. Haematol., **1985**, 61, pp. 717-726.
13. Oemichen, M.; Pedal, M. et al. Forensic Sci. Int., **1984**, 25, pp. 181-189.
14. Mandel, J.S.; Berlinger, N.J. et al. Amer. J. Ind. Med., **1989**, 15, pp. 207-212.
15. Lee, M.J.; Waters, H.C., III Blood, **1977**, 50, pp. 947-951.
16. Talcott, R.E.; Mallipudi, N.M. et al. Toxicol. Appl. Pharmacol., **1979**, 49, pp. 107-112.
17. Newcombe, D.S.; Esa, A.H. In Clinical Immunotoxicology; Newcombe, D.S.; Rose, N.R.; Bloom, J.C., Eds.; Raven Press, New York City, New York, 1992; pp. 349-363.
18. Markey, G.M.; McCormick, J.A. et al. J. Clin. Pathol., **1990**, 43, pp. 282-286.
19. McCormick, J.A.; Markey, G.M. et al. Br. J. Haematol., **1991**, 77, pp. 287-290.
20. Markey, G.M.; Alexander, H.D. et al. Br. J. Haematol., **1986**, 63, pp. 359-362.
21. Hecht, F.; Hecht, B.K. Cancer Genet. Cytogenet., **1990**, 46, pp. 9-19.
22. Saboori, A.M.; Newcombe, D.S. J. Biol. Chem., **1990**, 265, pp. 19792-19799.
23. Okano, M.; Thiele, G.M. et al. Clin. Microbiol. Rev., **1988**, 1, pp. 300-312.
24. Harris, N.L. Amer. J. Clin. Pathol., **1992**, 98, pp. 278-281.
25. Biron, C.A.; Byron, K.S.; Sullivan, J.L. N. Engl. J. Med., **1989**, 320, pp. 1731-1735.
26. Biemer, J.J. Ann. Clin. Lab. Sci., **1990**, 20, pp. 175-191.
27. Ambinder, R.F. Hematol. Oncol. Clin. North Am., **1990**, 4, pp. 821-823.
28. Sobti, R.C.; Krishan, A.; Pfaffenberger, C.D. Mutat. Res., **1982**, 102, pp. 89-102.
29. Yoder, J.; Watson, W.; Benson, W.W. Mutat. Res., **1973**, 21, pp. 335-340.
30. van Boa, T.; Szabo, I. et al. Hum. Genet., **1974**, 24, pp. 33-57.
31. Ruzicka, P.; Czeizel, A. et al. Mutat. Res., **1973**, 21, pp. 187-188.
32. Dulout, F.N.; Pastori, M.C. et al. Mutat. Res., **1985**, 143, pp. 237-244.
33. Kiraly, J.; Szentesi, I. et al. Arch. Environ. Contam. Toxicol., **1979**, 8, pp. 309-319.
34. Gaill, M.H.; Pluda, J.M. et al. J. Natl. Cancer Inst., **1991**, 83, pp. 695-701.

35. Lipkowitz, S.; Garry, V.F.; Kirsch, I.R. Proc. Natl. Acad. Sci. USA, **1992**, *89*, pp. 5301-5305.
36. Morrell, D.; Cromartie, E.; Swift, M. J. Natl. Cancer Inst., **1986**, *77*, pp. 89-92.
37. Fishbein, W.N.; Kirsch, I.R. FASEB J., **1993**, *7*, p.A1130.
38. Zschunke, F.; Salmassi, A. et al. Blood, **1991**, *78*, pp. 506-512.
39. Trapani, J.A.; Klein, J.L. et al. Proc. Natl. Acad. Med. USA, **1988**, *85*, pp. 6924-6928.
40. Gerschenfeld, H.K.; Weissman, I.L. Science, **1986**, *232*, pp. 854-858.
41. Brunet, J.F.; Dossetto, M. et al. Nature, **1986**, *322*, pp. 268-270.
42. Lobe, C.G.; Finley, B.B. et al. Science, **1986**, *232*, pp. 858-862.
43. Lobe, C.G.; Havele, C.; Bleakley, R.C. Proc. Natl. Acad. Sci. USA, **1986**, *83*, pp. 1448-1452.
44. Esa, A.H.; Warr, G.A.; Newcombe, D.S. Clin. Immunol. Immunopathol., **1988**, *49*, pp. 41-52.
45. Pasternack, M.S.; Verret, C.R. et al. Nature, **1986**, *322*, pp. 740-743.
46. Rogers, K.E.; Grayson, M.H.; Ware, C.F. J. Immunol., **1988**, *40*, pp. 564-570.
47. Roder, J.C.; Kiessling, R. et al. J. Immunol., **1978**, *121*, pp. 2509-2517.
48. Roder, J.C.; Karre, K.; Kiessling, R. Prog. Allergy, **1981**, *28*, pp. 66-159.
49. Roder, J.C.; Haliotis, T. et al. Nature, **1980**, *284*, pp. 553-555.
50. Sullivan, J.L.; Byron, K.S. et al. Science, **1980**, *210*, pp. 543-545.

RECEIVED August 13, 1993

## Chapter 14

# **Validation of a Pharmacokinetic Model To Predict Exposure of Ground Boom Mixer–Loader–Applicators to Chlorophenoxyacetic Acid Herbicides Comparison to Conventional Approaches**

**D. G. Baugher**

**Orius Associates Inc., 615 North Market Street, P.O. Box 4187,  
Frederick, MD 21705–4187**

The pharmacokinetics (PK) of human absorption and urinary excretion of the chlorophenoxyacetic acid herbicides 2,4-D and MCPA were determined from 2 clinical studies and 1 occupational exposure monitoring study. A quantitative model based on the MCPA clinical study of percutaneous absorption after a single exposure was cascaded to predict absorption and urinary excretion after multiple exposures to different amounts of active ingredient. Excretions predicted by the MCPA clinical model were validated by comparison to observed dermal exposures and urinary excretions in a second occupational exposure study of ground boom mixer/loader/applicators working barehanded. A regression of 81 comparisons of predicted *versus* measured daily urinary excretions resulting from 26 different applications of 2,4-D by 6 different workers yielded an excellent fit of the model to the data: intercept near zero ( $0.025 \mu\text{g/kg BW/day}$ ); slope near 1.0 (1.009); and,  $r^2 = 0.65$  ( $r = 0.80$ ). The validated PK model was calibrated with linearized and corporeally regionalized percutaneous absorption rates from the 2 clinical studies. Absorbed daily doses observed in the second field study and predicted by the PK model were compared to exposures estimated by the current convention of multiplying dermal exposure times the percent percutaneous absorption. The current convention was not validated by the PK model or observed exposures: absorbed doses were substantially under-estimated or overestimated, depending on the conventions used. The PK model provided the best estimates of daily absorbed dose after occupational exposure.

The structurally similar chlorophenoxyacetic acid herbicides (CPAH), 2,4-Dichlorophenoxyacetic acid (2,4-D) and 2-Methyl-4-chlorophenoxyacetic acid (MCPA), are used worldwide in ground boom application equipment. Estimates

0097–6156/94/0542–0214\$06.00/0  
© 1994 American Chemical Society

of occupational exposure to CPAH have been based on passive dermal dosimetry (classical "patch" monitoring), biological monitoring (urinary excretion), combined passive dermal dosimetry and biological monitoring, or surrogate data from mixer/loader/applicator monitoring studies with other pesticides. As is typical, the estimated rates of exposure from the different types of monitoring studies have varied widely. And, although the absorption, distribution, and excretion of CPAH have been extensively studied in humans and other mammals, it has been generally concluded that the results from passive dosimetry, biological monitoring, and human metabolism studies could not be quantitatively correlated. However, with the recent availability of more powerful graphics and curve-fitting programs for personal computers, key studies could be re-evaluated from a pharmacokinetic (PK) point of view, with the goal of developing a quantitative model for estimating both dermal exposure and absorbed dose. The following stepwise process was used to develop and validate a predictive model: absorption and excretion in urine were qualitatively and quantitatively evaluated after oral, intravenous, and dermal administration of CPAH to humans; a PK model of percutaneous absorption and excretion was developed; the PK model was validated with results from passive dermal dosimetry and urinary monitoring of ground boom mixer/loader/applicators using CPAH; the PK model was calibrated; and, the calibrated PK model was used to predict daily and seasonal exposures for a typical use scenario.

The appropriateness of conventional approaches to estimating absorbed doses and of clinical study designs were also quantitatively evaluated.

### Pharmacokinetics of MCPA and 2,4-D in Humans

In man and other mammals, absorbed CPAH are protein-bound in plasma and excreted as parent compound in urine. Although there are species-specific differences in the rates of excretion, residues do not accumulate in tissues (1). It is generally accepted that urinary excretion of CPAH represents absorption of an administered or occupationally acquired dose.

Since agricultural occupational exposure to CPAH is primarily dermal, 2 clinical studies and 1 field study were used to quantitatively assess the pharmacokinetics of percutaneous absorption and/or urinary excretion of MCPA and 2,4-D in humans. In the first clinical study, 5 volunteers had a 10 cm<sup>2</sup> soft paper pad applied to the skin of the thigh (2). The pad was soaked with 10 mL of 10% MCPA salt in water prepared from a 75% liquid formulation (= 1.0 g MCPA/-pad). After 2 hr the pad was removed and the application site was thoroughly washed with soap and water.

In the second clinical study of several pesticides (3), radiolabelled 2,4-D in acetone was applied to the skin of the ventral forearm at a concentration of 4 µg/cm<sup>2</sup> in 6 subjects. The application site was not occluded, and after 24 hr the site was washed. Urinary excretion of the topical dose was adjusted for incomplete urinary excretion of an intravenous dose of the same magnitude into the antecubital vein of the ventral forearm. In the case of 2,4-D, excretion of the intravenous dose was 100% and no adjustment was necessary.

The third study (4) was a biomonitoring study with 2,4-D applied to wheat in

the northern United States in 1980. Ground crews provided 7 consecutive 24-hr urine samples following a single 2,4-D application. No attempt was made to alter work habits or clothing--the subjects were free-living. From each worker's reported excretion ( $\mu\text{g}$  excreted/kg BW/day) presented in Table V in Reference 4, the mean percent of the total (seasonal excretion) excreted per day was calculated for 7 applicators, 7 mixer/loaders, and 9 mixer/loader/applicators. For mixer/loader/applicators, the daily geometric means were also calculated. Hereafter, this study will be referred to as the "Northern US" study.

The time-course of urinary excretion was graphed from the cited data. After inspection of the graphs, and fitting curves with TableCurve Curve Fitting Software, Version 3.11, Jandel Scientific, it was concluded that excretion was incomplete at the end of the sampling intervals. Therefore, the excretion curves were extrapolated to nearly complete elimination at 10 days from the curve-fitting parameters in Table I: the "predicted total excreted" was the sum of 10 days excretion predicted by the curve-fitting equations. From the predicted 10-day total excretion, the observed percent of the predicted total excreted during each day was calculated and shown in Table I. The predicted daily percent excretion was graphed as shown in Figure 1.

**Table I. Observed and Predicted Human Urinary Excretion of MCPA and 2,4-D After a Single Dermal Exposure\***

OBSERVED PERCENT OF PREDICTED TOTAL EXCRETED:						
	Clinical Studies:		Field Studies, 2,4-D		M/L/A:	
Day	MCPA	2,4-D	M/L	A	Mean	Geo. Mean
0	0.0	0.0	0.0	0.0	0.0	0.0
1	17.3	8.2	0.1	0.1	1.4	1.1
2	30.8	25.7	23.8	24.8	17.3	14.2
3	24.0	31.0	24.7	26.6	19.1	18.4
4	11.3	16.2	24.3	24.2	21.1	19.9
5	6.0	10.2	12.3	10.2	22.2	20.3
6	4.5		10.5	6.9	12.6	10.7
7	3.0		4.3	7.3	7.7	7.3

Curve-fitting  $r^2$ :

0.99      0.98      0.96      0.95      0.90      0.95

Curve-fitting Parameters:

a=	0.3715	0.2720	-1.2808	-0.4072	-9.8440	-1.4082
b=	31.4118	30.5556	28.9019	29.5441	31.9818	22.7615
c=	1.8684	2.5601	2.8312	2.7579	3.2271	3.6719
d=	0.5556	1.1677	0.5140	-0.4767	0.7897	1.9046

\* M/L = Mixer/Loader; A = Applicator; M/L/A = Mixer/Loader/Applicator. Recalculated from References 2, 3, and 4.

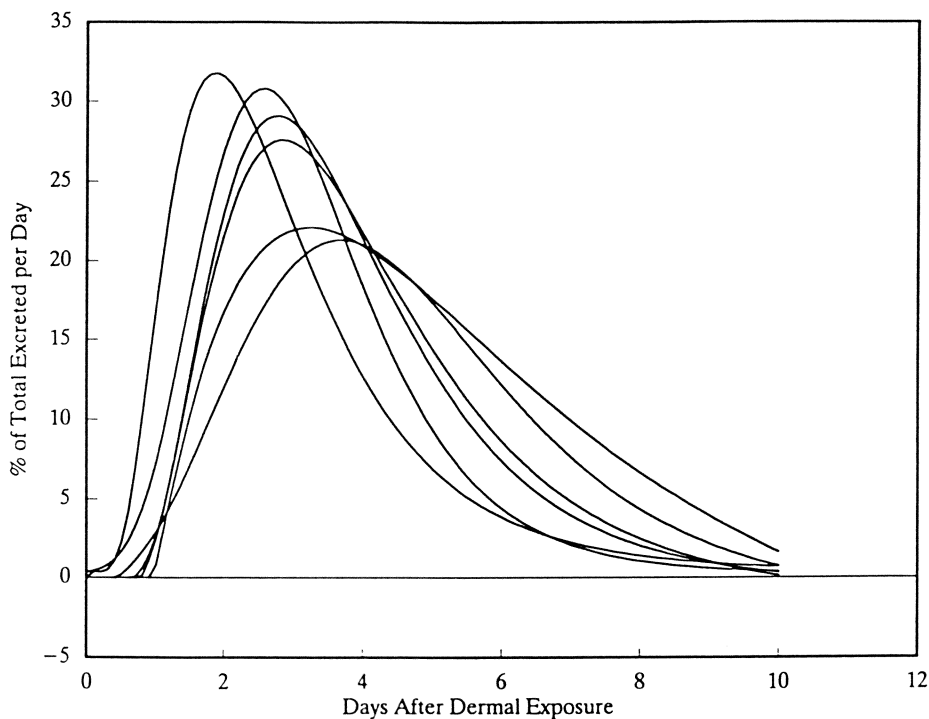


Figure 1. Human urinary excretion of dermal doses of MCPA or 2,4-D: percent of total excreted by day calculated from curve-fitting parameters in Table I. Peaks, in descending order: MCPA, clinic; 2,4-D, clinic; 2,4-D, mixer/loaders, applicators, mixer/loader/applicators, and geometric mean mixer/loader/applicators.

The curve-fitting equations for the parameters in Table I, where  $x$  = days postexposure and  $y$  = daily percent of total excreted, were:

MCPA and Field Studies:

$$y = a + b \exp(-0.5(\ln(x/c)/d)^2)$$

2,4-D, Clinical Study:

$$y = a + b \exp(-(x-c)/d) - (((x-c)/d) + 1)$$

Although some of the equations predicted small negative numbers or were not solvable at time zero, this was handled in a very practical manner. Time zero was pre-exposure, therefore all time zero predictions were constrained to be zero, as would be expected when no exposure had occurred.

As shown in Figure 1, the shapes of the urinary excretion curves were different. The differences in phase and magnitude of the excretions were probably related to the different durations and routes of dosing: 2 hr on a patch on the skin of the thigh for MCPA compared to 24 hr on the forearm skin for 2,4-D in clinical trials compared to unknown durations and multiple routes in free-living subjects occupationally exposed to 2,4-D. The differences may also reflect the diluents and perhaps minor differences in the structure/activity of each substance.

From data presented in the *Reference 2*, the kinetics of absorption into plasma after oral and dermal administration were also evaluated. Likewise, where possible, subsequent urinary excretion was also evaluated. In general, the shapes of the plasma concentration *versus* time curves were similar to the urinary excretion *versus* time curves, with peak urinary excretion occurring approximately 24 hr after peak plasma concentrations were measured. From this observation, it was concluded that urinary excretion was a good biological marker of absorption of MCPA and 2,4-D and that the PK of urinary excretion was representative of the PK of absorption into plasma.

### The Pharmacokinetic Model for Multiple Dermal Exposures.

Farmworkers are often serially exposed to the same agrochemicals over a growing season. The greatest potential for absorption and accumulation of an agrochemical would occur when serial daily applications are made over part of the growing season. For MCPA and 2,4-D, the following hypothetical use scenario based on current U.S. Environmental Protection Agency (USEPA) exposure assessment conventions was used to construct an additive PK model of excretion. Assume that a ground boom mixer/loader/applicator treats an average of 50 ha/day at a rate of 0.5 kg active ingredient (AI)/ha; that the rate of dermal exposure is 30  $\mu\text{g/kg}$  bodyweight (BW)/kg AI handled; and, that 0.72% of the dermal dose is absorbed (see *Modelling Exposures* section for basis). By current USEPA conventions, the "point estimate" total exposure for the day would be:

$$50 \text{ ha/day} \times 0.5 \text{ kg AI/ha/day} \times 30 \mu\text{g/kg BW/kg AI} \times 0.72\% \text{ absorp.} = 5.40 \mu\text{g/kg BW}$$

The daily total exposure would be absorbed and excreted in urine over a period of 10 days, with each day's fractional excretion predicted by the excretion curve equations above. By cascading the model, and adding the daily contributions to exposure and excretion, daily and seasonal absorbed and excreted doses may be predicted. In Table II, the model was cascaded with the MCPA curve-fitting equations for 6 consecutive daily applications and the use rates in the above example. One use rate, treated ha/day, was varied by  $\pm 50\%$  to reflect variation in daily work productivity. Absorption and excretion were considered to be complete 10 days after the last application.

**Table II. Modelled Urinary Excretion of MCPA After Dermal Exposure of Ground Boom Mixer/Loader/Applicators\***

Kg AI:	12.5	25.0	37.5	12.5	25.0	37.5	
Dermal:	375	750	1,125	375	750	1,125	
Absorbed:	2.7	5.4	8.1	2.7	5.1	8.1	
Work Day:	0	1	2	3	4	5	

Day:	Excreted $\mu\text{g/kg BW}$ :						Total:
0	0						
1	0.46	0					0.46
2	0.85	0.92	0				1.77
3	0.60	1.70	1.38	0			3.69
4	0.34	1.20	2.56	0.46	0		4.56
5	0.19	0.68	1.80	0.85	0.92	0	4.45
6	0.10	0.37	1.03	0.60	1.70	1.38	5.19
7	0.06	0.21	0.56	0.34	1.20	2.56	4.93
8	0.04	0.12	0.31	0.19	0.68	1.80	3.14
9	0.03	0.08	0.18	0.10	0.37	1.03	1.79
10	0.02	0.05	0.11	0.06	0.21	0.56	1.01
11	0	0.04	0.08	0.04	0.12	0.31	0.59
12		0	0.06	0.03	0.08	0.18	0.34
13			0	0.02	0.05	0.11	0.18
14				0	0.04	0.08	0.12
15					0	0.06	0.06
16						0	0
Total:							32.40
Min.:							0.46
Max.:							5.19
Mean:							1.08
S.D.:							1.72

\* Dermal =  $\mu\text{g/kg BW}$  @ 30  $\mu\text{g/kg BW/kg AI}$

Absorbed = Dermal  $\mu\text{g/kg BW}$  x 0.72% percutaneous absorption.

Daily urinary excretion can be modelled for virtually any combination of rates of use, rates of dermal exposure, rates of percutaneous absorption, days of application, and days postapplication. In the example in Table II, and in the following discussions, programs written in LOTUS 123 Release 3.1+ were used to cascade the model for different scenarios based on actual reported occupational conditions. Since the models based on the MCPA and geometric mean 2,4-D mixer/loader/applicator curve-fitting parameters yielded better predictions with better  $r^2$  than the other models, all of the following work was based on those 2 models.

### Validation of the Pharmacokinetic Models

If certain major assumptions are true, then the PK models derived above should predict the time and magnitude of urinary excretion of CPAH by occupationally exposed people. The assumptions include, but are not limited to: (A) the kinetics of percutaneous absorption and subsequent urinary excretion of the wide range of dermal doses acquired occupationally are the same as for the doses administered clinically or acquired occupationally in the 2,4-D field study (= linearity and nonsaturated over the dose range); (B) repeated exposures result in additive absorption and excretion; (C) oral and inhalation exposure are minor compared to the dermal route; and, (D) the time of each occupational dermal exposure, the magnitude of each repeated dermal exposure, the percutaneous absorption from each, and the daily urinary excretion of CPAH are known.

Ideally, the assumptions of linearity and additivity would be tested clinically before being validated in the workplace. Such studies have not been published for MCPA or 2,4-D. Therefore validation of the model was dependent upon occupational monitoring studies.

Two reports of occupational monitoring studies provided sufficient information to attempt validation of the PK models. In addition to the Northern US biomonitoring study described above, a combined passive dosimetry and biomonitoring study was used.

**Passive Dosimetry and Biomonitoring of Ground Boom Mixer/Loader/-Applicators.** Two companion publications of the results of a large occupational monitoring study provided sufficient information to attempt validation of the PK models: kg AI handled/day;  $\mu\text{g}$  dermal exposure/day; workers' kg BW; total  $\mu\text{g}$  urinary excretion; and, graphically represented  $\mu\text{g}$  urinary excretion for each day of the application season and several days after the last application (5 and 6).

*Reference 5* was a combined biomonitoring and passive dosimetry study with 2,4-D applied by tractor-drawn ground sprayers with rear-mounted booms in 1981 and 1982 in Saskatchewan, Canada. Eight farmers applied liquid formulations of the dimethylamine salt of 2,4-D to their own fields at rates of 315 to 630 g acid equivalent (AE = AI)/ha in spray volumes of 45 to 123 L/ha. During the application season, the farmers mixed/loaded/sprayed 2 to 7 times over 1 to 17 days, treating 16 to 194 ha per spray operation and handling 6.7 to 88.3 kg AI per spray operation which lasted 55 to 870 min. The workers wore standardized sets of laundered clothing consisting of cotton work pants, a short-sleeved cotton

T-shirt, and a long-sleeved heavyweight cotton coverall. Composite 24-hr urine samples were collected preexposure and then continuously during the spray operations and through 7 days postapplication: total excretion was reported. Dermal dosimeters were placed underneath the clothing on the chest, upper arms, wrists, knees, and ankles. Potential dermal exposures were extrapolated from the dosimeters based on the workers' bodyweights and calculated body surface areas. Exposure of the hands was measured by 750-mL rinses with 1% NaHCO<sub>3</sub> solution. All exposures were standardized by the authors to mass of 2,4-D AI/kg BW/kg AI handled. From the data presented in *References 5 and 6* (primarily Table 5 in 5), the following rates of exposure were calculated for the barehanded mixer/loader/applicators in Table III. Three outliers identified by the study authors were excluded: F(81) dermal exposure excursion on head patch; C(82) wearing chemical resistant gloves; and, C(81) exposed before the monitoring.

**Table III. Measured Dermal Exposure and Urinary Excretion of 2,4-D by Ground Boom Mixer/Loader/Applicators in Canada, 1981-82\***

Worker, Kg BW	Hr/ Exposure (Exposures)	Total µg/kg BW/kg AI: Dermal	Urinary as % of Dermal
A(82), 84	1.88 (4)	102.0	1.49%
B(81), 84	1.90 (3)	60.1	0.49
B(82), 84	4.50 (2)	49.3	0.49
D(82), 88	4.45 (4)	89.9	0.26
E(81), 68	2.82 (7)	71.3	0.17
G(82), 82	6.25 (6)	186.0	0.39
Mean: 82	3.63 (4)	93.1	0.55
S.D.: 7	1.73 (2)	49.4	0.49
Geo. Mean:	3.29	84.4	0.43
G.S.D:	1.65	1.59	2.09

\* Recalculated from *References 5 and 6*.

The mean exposure on the hands was  $78.5 \pm 16.5\%$  of the total dermal exposure. Potential inhalation exposure was considered trivial:  $<0.5\%$  of the dermal dose in 7 of 9 cases; and, a maximum of 1.6% of dermal dose. Exposure by the oral route could not be measured, but would probably consist only of the nonrespirable fraction of the potential inhalation exposure estimated from air sampling.

In the companion reference (6), the authors graphically presented the daily urinary excretion of each subject, along with the kg AI handled on each day.

Each worker's daily excretion was numerically estimated from the graphs and standardized to  $\mu\text{g/kg BW/day}$ .

Hereafter these reports will be referred to as the "Canadian" study.

**Validation of the Pharmacokinetic Models with the Occupational Monitoring Data.** Urinary excretions predicted by the cascaded MCPA clinical PK model and the 2,4-D field study PK model were compared to observed urinary excretions after multiple exposures in the Canadian field study and single exposures in the Northern US field study. The model was cascaded with the individual use rates (kg AI handled) and individual absorption rates (or total urinary excretion, Northern US study) for each of the mixer/loader/applicators and the predicted daily urinary excretions were compared to the observed daily excretions. Since the sampling regimen did not go through 10 days after the last application, comparisons were made only when measured excretion results were reported.

In all, there were 81 comparisons of predicted and measured urinary excretion resulting from 26 different applications of 2,4-D by 6 different workers in the Canadian study. One observation was an obvious outlier (Subject G, Observation 5 in *Reference 5*) and was deleted from statistical analyses of the results.

In the Northern US study, there were 61 comparisons of predicted and measured urinary excretion resulting from single applications of 2,4-D by 9 different workers. Again, 1 observation was an obvious outlier (Worker 20, Day 6, Table V in *Reference 4*) and was deleted from statistical analyses of the results.

If a model nearly perfectly describes the monitoring data, then a linear regression of predicted excretion versus observed excretion would have an intercept of zero, a slope of 1.0, and  $r^2 > 0.99$ . Likewise, the model would predict the mean and maximum excretions--values useful for risk assessments.

As shown in Table IV, the cascaded MCPA clinical PK model fit the observed daily excretion of 2,4-D in the Canadian field study very well: the intercept was near zero; the slope was essentially 1.0; and, the  $r^2$  of 0.65 ( $r = 0.80$ ) was considered quite acceptable for these types of data, especially since the residuals of predicted versus observed values appeared to be random. Because the data spanned 4 orders of magnitude, the log-log graphic representation is shown in Figure 2 ( $y = -0.066 + 0.957x$ ,  $r^2 = 0.68$ ). Likewise, the predicted maximum, mean, and geometric mean were similar to the observed values. The MCPA clinical PK model did not fit the Northern US field study data: the intercept was substantially greater than zero; the slope of 0.259 was substantially less than 1.0; and, the  $r^2$  was only 0.07. However, the predicted maximum, mean, and geometric mean were similar to the observed values: the model predicted the magnitude but not the kinetics of exposure and excretion.

The cascaded 2,4-D field PK model did not fit the observed daily excretion of 2,4-D in the Canadian field study as well as the MCPA model: the intercept was greater than zero; the slope was less than 1.0; and, the  $r^2$  of 0.47 ( $r = 0.69$ ) was considered marginally acceptable for these types of data, although the residuals of predicted versus observed values appeared to be random. The predicted maximum, mean, and geometric mean were similar to the observed values. The 2,4-D field PK model fit the Northern US field study data much better than the MCPA clinical PK model: although the intercept was greater

**Table IV. Statistical Summary of Predicted versus  
Observed Urinary Excretion of 2,4-D by Ground  
Boom Mixer/Loader/Applicators**

---

**DATA SET: CANADIAN FIELD STUDY**

**Daily Urinary Excretion-- $\mu\text{g/kg BW}$ :**

	<u>Observed</u>	<u>Predicted</u>	<u>Predicted</u>
Maximum:	12.72	13.19	12.90
Mean:	1.61	1.65	1.66
S.D.:	2.03	2.55	2.43
Geo. Mean:	0.85	0.74	0.78
G.S.D.:	3.24	3.92	3.73

**Regression Parameters--Predicted Excretion vs. Observed:**

No. of Observations:	81	
Degrees of Freedom:	79	
Intercept:	0.025	0.329
Std. Error of Y Est.	1.540	1.794
X Coefficient:	1.009	0.823
Std. Error of Coef.:	0.084	0.098
r-squared:	0.65	0.47

---

**DATA SET: NORTHERN US FIELD STUDY**

**Daily Urinary Excretion-- $\mu\text{g/kg BW}$ :**

	<u>Observed</u>	<u>Predicted</u>	<u>Predicted</u>
Maximum:	10.40	10.95	7.30
Mean:	2.61	2.51	2.39
S.D.:	2.39	2.36	1.75
Geo. Mean:	1.27	1.50	1.66
G.S.D.:	5.20	3.06	2.65

**Regression Parameters--Predicted Excretion vs. Observed:**

No. of Observations:	61	
Degrees of Freedom:	59	
Intercept:	1.833	0.753
Std. Error of Y Est.	2.314	0.918
X Coefficient:	0.259	0.627
Std. Error of Coef.:	0.124	0.049
r-squared:	0.07	0.73

---

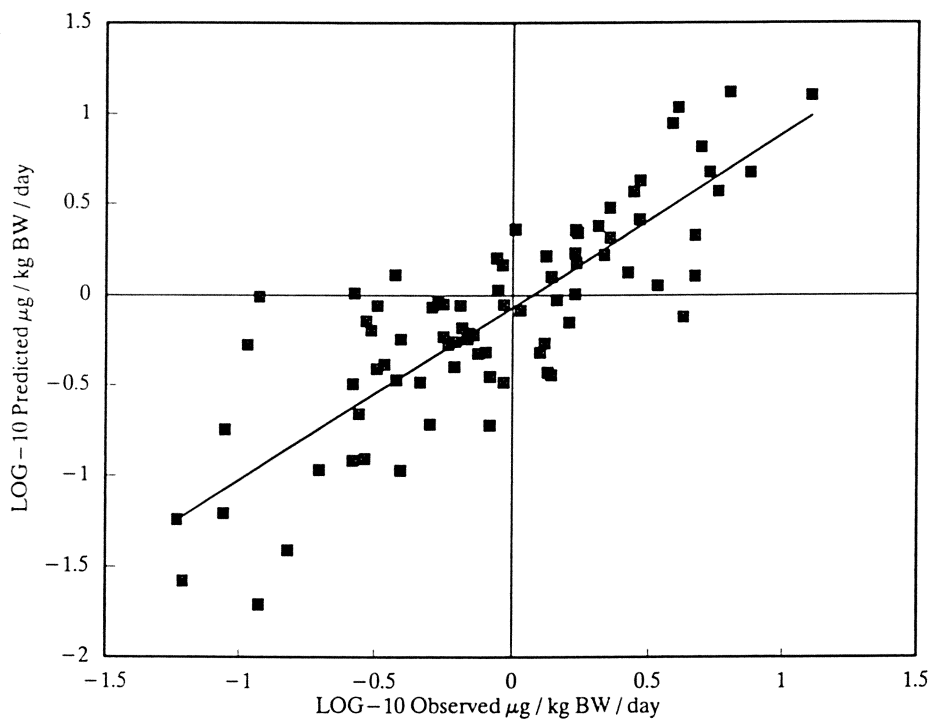


Figure 2. Daily urinary excretion predicted by the MCPA clinical model *versus* observed season-long daily urinary excretion of 2,4-D by Canadian mixer/loader/applicators.

than zero and the slope of 0.627 was less than 1.0, the  $r^2$  was 0.73 ( $r = 0.85$ ). Again, the predicted mean and geometric mean were similar to the observed values, but the predicted maximum was meaningfully less than the observed maximum: 7.3 versus 10.4  $\mu\text{g/kg BW/day}$ .

That the MCPA clinical PK model did not fit the Northern US field study was not surprising. The free-living mixer/loader/applicators in 1980 probably wore contaminated clothing during part of the postexposure monitoring and certainly did not thoroughly wash after 2 hr of exposure, a significant element of the underlying clinical PK study.

That the MCPA clinical PK model fit the multiexposure data from the Canadian field study was surprising until the conditions of the study were reconsidered. In the Canadian study, most of the dermal residue was removed by handwashing immediately after exposure (mean time = 3.6 hr); and, the provision of freshly laundered clothing prevented prolonged or repeated exposures from contaminated clothing. Compared to the Northern US field study, the Canadian study could be considered a "clinical" field study. Importantly, the practices in the 1981-1982 Canadian field study were representative of the practices now required by mid-1990's labels on the CPAH: washing after occupational exposure and laundering clothing after use in addition to the wearing of chemical resistant gloves. The Canadian field study was therefore considered relevant to today's issues in exposure assessment.

The 2,4-D field PK model did not fit the Northern US field study from which it was derived as well as expected. That was because the PK model was derived from geometric means and compared to individual observations which had a high variance. However, since the work practices represented in the 1980 study of free-living mixer/loader/applicators should not be relevant to today's work practices, this model and field study will not be used in the following analyses.

### Calibration of the Pharmacokinetic Model.

In the above comparison of predicted and observed urinary excretion of CPAH, the total occupational excretion was known and the clinical model described the kinetics. In order for the model to be more useful for occupational exposure assessment, the magnitude of absorption must be known in addition to the kinetics. By current convention, the magnitude of dermal exposure to pesticides is estimated from individual monitoring studies using passive dermal dosimetry or from collections of passive dermal dosimetry studies, such as the recently released Pesticide Handlers Exposure Database (PHED)(7). The rate of dermal exposure is normalized to  $\mu\text{g/kg BW/kg AI}$  handled for risk assessments. Percutaneous absorption of the dermal dose is typically estimated from total percutaneous absorption *in vivo* in the rat (8), or, when such studies exist, *in vivo* in the human. *In vitro* absorption studies with rat, rabbit, and human cadaver skin are also used to estimate human occupational percutaneous absorption. The percutaneous absorption studies typically do not account for the route or duration of occupational exposure.

Since urinary excretion of the CPAH represents total absorbed dose, the MCPA clinical PK model with its excellent fit to the Canadian field study data

provided an ideal empirical test of the current theoretical practice: applying a percutaneous absorption rate to a rate of dermal exposure to estimate absorbed occupational doses of a substance.

Theoretically, if the true mean or geometric mean rate of dermal exposure ( $\mu\text{g/kg BW/kg AI}$ ) is multiplied by the true mean or geometric mean rate of percutaneous absorption and the kg AI handled during each application, and used as inputs to the PK model, then the cascaded MCPA clinical PK model will yield an intercept of zero and a slope of 1.0 with the Canadian field study data, as above. The model, which accurately predicted absorbed doses, was used to test the robustness of current conventions for estimating occupational exposures in the following examples. Any combination of dermal exposure and percutaneous absorption which resulted in a slope near 1.0 could be considered sound. When the slope was greater than 1.0, exposures were overestimated by the conventions. When the slope was less than 1.0, exposures were underestimated by the conventions. To make comparisons less complicated, all regressions of predicted versus observed urinary excretions were constrained to have an intercept of zero. This condition was nearly true in identical unconstrained regressions except when slopes were substantially greater or lesser than 1.0. For the illustrative purposes, the values below were editorially rounded.

**Example A.** The 24-hr percutaneous absorption rate of 2,4-D in the human clinical study was 6%. When applied to the measured mean and geometric mean dermal exposure rates of 65 and 50  $\mu\text{g/kg BW/kg AI}$  in the Canadian field study, the slopes were  $>8$ . Assuming that the rate of absorption in the clinical study was linear over time, and could be reduced to 0.9% to simulate the observed mean 3.6-hr exposure, then the corresponding slopes would be  $>1.4$ --again substantial overestimates of exposure. When the 24-hr percutaneous absorption rate was applied to other rates of dermal exposure (e.g., 20 to 27 [ $=30$ ]  $\mu\text{g/kg BW/kg AI}$  from the PHED and Orius Associates Inc. unpublished databases for barehanded ground boom mixer/loader/applicators), the slopes were  $>3.6$ --overestimates. When the 3.6-hr absorption rate was used, 1 prediction was an underestimate (slope = 0.56 for 20  $\mu\text{g/kg BW/kg AI}$ ) and 1 prediction was reasonably robust (slope = 0.84 for 30  $\mu\text{g/kg BW/kg AI}$  cell). That 1 estimate was robust was considered fortuitous, as the surrogate rate of dermal exposure was less than one-half the observed mean rate of dermal exposure in the field study.

**Example B.** The 2-hr percutaneous absorption rate of MCPA in the human clinical study was 0.2%. When applied to the measured mean and geometric mean dermal exposure rates of 65 and 50  $\mu\text{g/kg BW/kg AI}$  in the Canadian field study, the slopes were  $<0.45$ , substantial underestimates. When applied to the lesser rates of dermal exposure from the PHED and Orius Associates Inc. databases, exposures were even more substantially underestimated. Assuming that the rate of absorption in the clinical study was linear over time, and could be increased by 1.8X to 0.36% to simulate the mean 3.6-hr exposure, then the corresponding slopes for the mean and geometric mean dermal exposures were  $\leq 0.75$ --approaching 1.0 but nevertheless underestimates.

When applied to surrogate rates of dermal exposure of 20 to 30  $\mu\text{g/kg BW/kg AI}$ , the slopes ranged from 0.35 to 0.45--again substantial underestimates.

**Discussion of Examples.** The potential rates of dermal exposure ranged from geometric means of 20-30  $\mu\text{g/kg BW/kg AI}$  in PHED and Orius Associates surrogates to a geometric mean of 50 and a mean of 65  $\mu\text{g/kg BW/kg AI}$  in the Canadian field study. The differences were considered to be meaningful and to be related both to the changing work practices over the last decade and to the products studied in the respective databases. Specifically, the Orius (and probably PHED) database relied on studies with products known or expected to be highly toxic by the monitored workers: MCPA and 2,4-D were considered to be not very toxic in 1980-1982. The mean and geometric mean from the Canadian study were similar, and there was no reason to believe that the dosimetry in that study was flawed. However, that rate of exposure may not be representative of exposures of trained and certified applicators in the mid-1990's.

Examples A and B directly illustrate a conventional wisdom: the results from passive dermal dosimetry and biomonitoring studies are difficult to correlate, are seldom corroborative of each other, and often cannot be reconciled with clinical studies of percutaneous absorption. More importantly, the examples show that the conventional practice of applying a single percutaneous absorption rate to a single rate of exposure is not valid for occupational exposure assessment when the percutaneous absorption rate fails to account for routes of exposure, durations of exposure, and kinetics of absorption.

**Partitioning of Exposures.** In other studies of human percutaneous absorption, the rate was different depending upon the body region exposed (9). For example, absorption by the palm of the hand was 0.83X that of the forearm for hydrocortisone, 0.85X for malathion, and 0.96X to 2X for parathion (by the palm compared to the arm). Likewise, many studies have shown that the magnitude of absorption can be linear over time. Using these observations as assumptions, the mean exposures in the Canadian field study were partitioned into "hand exposure" and "body exposure" and the relevant clinical absorption data were linearly extrapolated to the mean time period of exposure in an attempt to match magnitudes of exposure with the kinetics of exposure. There were insufficient data in the referenced studies to do more detailed partitioning (see *Reference 10* for an example).

Direct application of 2,4-D to the forearm skin was considered representative of exposure of the hands. Prorating the 6% absorption after 24 hr residence on the skin (0.25%/hr) to the mean 3.6 hr duration of the exposure periods in the Canadian field study yielded a percutaneous absorption rate of 0.9% for the hands. Adjusting that rate by 0.8 for the regional difference of palm to forearm yielded an effective percutaneous absorption rate of 0.72% for the hands. Applying that rate to the mean exposure of the hands (78.5% x 65.4  $\mu\text{g/kg BW/kg AI}$ ) yielded an absorbed exposure rate for the hands of 0.369  $\mu\text{g/kg BW/kg AI}$  handled.

Exposure of the rest of the body, mostly clothed, was considered to be represented by the test of the saturated patch application of MCPA to the thigh.

Prorating the 0.2% absorption after 2 hr in contact with the skin (0.1%/hr) to the 3.6 hr duration of the exposure periods in the Canadian field study yielded a percutaneous absorption rate of 0.36% for the body excluding the hands. There was insufficient information to estimate an adjustment factor for the thigh to other body regions, therefore a factor of 1.0 was assumed. Applying the linearly extrapolated rate of absorption to the mean exposure of the body ( $21.5 \times 65.4 \mu\text{g/kg BW/kg AI}$ ) yielded an absorbed exposure rate for the body of  $0.051 \mu\text{g/kg BW/kg AI}$  handled.

The sum of the absorbed doses from the hands and body, as calculated above from the extrapolated rate functions from clinical studies, was  $0.42 \mu\text{g/kg BW/kg AI}$  handled ( $0.369 + 0.051$ ). This was remarkably close to the total calculated from the field study:  $0.36 \mu\text{g/kg BW/kg AI}$  ( $65.4 \mu\text{g/kg BW/kg AI}$  mean dermal  $\times 0.55\%$  mean absorption, see Table III). Reasonably assuming that the hands of farmworkers are more calloused and resistant to chemicals than the hands of university employees in clinical studies, and that some of the residues on farmworkers' hands would be sloughed off during work, a palm to forearm percutaneous absorption ratio of approximately 0.7 (reasonably reduced from 0.8) would yield hand exposure of  $0.323 \mu\text{g/kg BW/kg AI}$  and a whole-body sum of  $0.374$ --within 4% of the observed magnitude of excretion and in concordance with the predicted and observed kinetics of absorption and excretion (based on partitioned rates of exposure: slope =  $1.16 @ a = 0$ ; slope =  $0.96 @ a = 0.797$ ).

**Modelling Exposures.** Based on the validated MCPA clinical PK model, and partitioning of the exposures and magnitudes of the rates of absorption between the hands and the remainder of the body as above, exposure scenarios can be modelled as in the example in Table II. The only modification required for the example in Table II is partitioning of the single rate of dermal exposure and single rate of percutaneous absorption into manual and corporeal rates. The example single rates of  $30 \mu\text{g/kg BW/kg AI}$  and  $0.72\%$  percutaneous absorption are the weighted averages of the partitioned rates. More precisely, the header to Table II would show the following elements for use in calculating exposures for an 8-hr workday with a lunch break at midday, with washing of the hands at midday and changing of clothing at the end of the work day:

Kg AI/day:	25
Dermal $\mu\text{g/kg BW/kg AI}$ :	30
% on hands:	80%
Hr on hands:	4
Absorption rate, %/hr, hands:	0.25%
Absorption factor, regional:	0.7
Absorbed $\mu\text{g/kg BW}$ , hands:	4.2
% on body:	20%
Hr on body:	8
Absorption rate, %/hr, body:	0.1%
Absorption factor:	1.0
Absorbed $\mu\text{g/kg BW}$ , body:	1.2
Total $\mu\text{g/kg BW}$ absorbed, hands+body:	5.4

Each column header in Table II would be expanded as shown here, although the

calculated results would not change. In this example the rate of dermal exposure was derived from the PHED and Orius databases and rounded up to 30 from 20-27: the CPAH probably are not handled as carefully as the more toxic pesticides in the underlying databases.

By current conventions, the point estimate of daily absorbed exposure to 25 kg AI would be  $5.4 \mu\text{g/kg BW/day}$ . In contrast, as shown by column 3 of the PK model in Table II, the maximum daily absorbed dose would be  $1.7 \mu\text{g/kg BW/day}$  and the mean daily absorbed dose over the 10 days of absorption and excretion would be  $0.54 \mu\text{g/kg BW/day}$ . The maximum, mean, and area under the time curve from the PK model provide more realistic estimates of exposure than the conventional approach for ground boom barehanded mixer/loader/-applicators. Other scenarios of exposure may be modelled and compared to the conventional approach simply by altering the input data: the resulting comparisons are generally the same as in the above example.

## Conclusions

Because the chlorophenoxyacetic acid herbicides MCPA and 2,4-D are quantitatively excreted in urine after percutaneous (or other) absorption, studies with the CPAH were used to model the kinetics of dermal absorption and excretion in clinical and occupational settings. From a series of independent clinical and field studies, a valid model of the kinetics of dermal absorption in clinical studies was found to be applicable to occupational exposures of ground boom mixer/loader/-applicators practicing currently labelled hygienic standards of washing and wearing freshly laundered clothing. Linear extrapolations of magnitudes of percutaneous absorptions from studies which simulated routes of exposure but not durations of exposure were found to be valid. Although true in this case, linear extrapolations may or may not be true as a general rule. Therefore, it is recommended that clinical studies of the magnitude and kinetics of percutaneous absorption be designed to represent routes and durations of relevant occupational exposures.

The application of a single percutaneous absorption rate from clinical studies to a single rate of dermal exposure from occupational exposure studies, as is the current conventional practice, was found to be invalid. Except in fortuitous cases, the current conventional practice is expected to be generally invalid and will yield erroneous estimates of absorbed doses.

Since a model could be validated and calibrated with independent clinical and occupational monitoring studies with MCPA and 2,4-D, similar models should be developed for other substances with appropriately designed clinical and occupational pharmacokinetic studies.

## Literature Cited

1. Arnold, E.K.; Beasley, R. *Vet. Hum. Toxicol.* **1989**, *31*(2), 121-125.
2. Kolmodin-Hedman, B.; Hoglund, S.; Swensson, A.; Akerblom, M. *Arch. Toxicol.* **1983**, *54*, 267-273.

3. Feldmann, R.J.; Maibach, H.I. *Toxicol. and Appl. Pharmacol.* **1974**, *28*, 126-132.
4. Nash, R.G.; Kearney, P.C.; Maitlen, J.C.; Sell, C.R.; Fertig, S.N. In *Pesticide Residues and Exposure*; Plimmer, J.R., Ed. *ACS Symposium Series 182*; American Chemical Society: Washington, D.C., **1982**; 119-132.
5. Grover, R.; Cessna, A.J.; Muir, N.I.; Riedel, D.; Franklin, C.A.; Yoshida, K. *Arch. Environ. Contam. Toxicol.* **1986**, *15*, 677-686.
6. Grover, R.; Franklin, C.A.; Muir, N.I.; Cessna, A.J.; Riedel, D. *TOXLett.* **1986**, *1638S*, 73-83.
7. Versar Inc. *PHED: The Pesticide Handlers Exposure Database*. Prepared for: The PHED Task Force representing Health and Welfare Canada, the U. S. Environmental Protection Agency, and The National Agricultural Chemicals Association; Versar Inc., Springfield, VA, **1992**.
8. Zendzian, R.P. *Guideline for Studying Dermal Absorption of Pesticides: Background Document*. Health Effects Division, Office of Pesticide Programs, USEPA, Washington, D.C.; February **1991**.
9. Wester, R.C.; Maibach, H.I. In *Percutaneous Absorption: Mechanisms--Methodology--Drug Delivery*; Bronaugh, R.L.; Maibach, H.I., Ed's.; *Second Edition, Revised and Expanded*; Marcel Dekker, Inc.: New York, NY, **1989**, 111-119.
10. Guy, R.H.; Maibach, H.I. In *Percutaneous Absorption: Mechanisms--Methodology--Drug Delivery*; Bronaugh, R.L.; Maibach, H.I., Ed's.; *Second Edition, Revised and Expanded*; Marcel Dekker, Inc.: New York, NY, **1989**, 391-396.

RECEIVED May 13, 1993

## Chapter 15

# Dermal Absorption and Disposition of Formulations of Malathion in Sprague–Dawley Rats and Humans

Curtis C. Dary<sup>1</sup>, Jerry N. Blancato<sup>1</sup>, Mark Castles<sup>2</sup>, Vijayapal Reddy<sup>2</sup>,  
Michael Cannon<sup>2</sup>, Mahmoud A. Saleh<sup>3</sup>, and Gordon G. Cash<sup>4</sup>

<sup>1</sup>Exposure Assessment Research Division, Environmental Monitoring  
Systems Laboratory, U.S. Environmental Protection Agency, Las  
Vegas, NV 89109

<sup>2</sup>Department of Life Sciences, Midwest Research Institute, Kansas  
City, MO 64110

<sup>3</sup>Environmental Chemistry and Toxicology Laboratory, Department  
of Chemistry, Texas Southern University, Houston, TX 77004

<sup>4</sup>Office of Pesticides and Toxic Substances, Chemical Management  
Division, U.S. Environmental Protection Agency, Washington, DC 20460

Dermal absorption of neat malathion, a 50% emulsifiable concentrate (50% EC), and a 1% and 10% aqueous mixture of the 50% EC formulation was examined in human volunteers. The absorption and elimination profiles of [<sup>14</sup>C]-malathion equivalents in the urine of the human were compared with the rat. Constants of absorption and elimination were calculated. Distribution of [<sup>14</sup>C]-malathion equivalents in selected tissues were examined in the rat. The 50% EC formulation was absorbed as readily as the neat malathion. The absorption of the organic based formulations was influenced by the increase in the surface area of the site of application. The total cumulative absorption was concentration dependent. The rate of absorption of the neat malathion, the 50% EC formulation, and 10% aqueous mixture was less than the rate of elimination resulting in a depletion of the body burden. The rate of absorption and elimination of the 1% aqueous mixture were coincident. The elimination of malathion was efficient and independent of surface area, concentration, and formulation. The disposition of malathion favored organs of metabolism and elimination, liver and kidney. A substantial portion of the dose remained at the site of application. The results suggest that acute human toxicity could occur from handling the concentrate when a substantial portion of the exposed skin is contaminated. Acute toxicity from contact with surfaces treated with the aqueous mixtures would be unlikely. Repeated exposure, however, could burden organs of metabolism and elimination, skin, liver and kidney.

Human exposure to insecticides used in the residential non-occupational market-place may occur during mixing the concentrate by the untrained consumer or from contact with treated surfaces upon re-entry in treated microenvironments. The rate

of dermal absorption, disposition, and elimination of a contacted dose would greatly impact on the analysis of risk (1). Without such information, understanding the human activities that relate to the rate of contact and transfer of residues are not as meaningful (2-5). Dislodgeable residues, even if contacted and entirely transferred to the skin, may not be appreciably absorbed and when absorbed may be readily and efficiently eliminated (5-7). Understanding bioavailability of selected pesticides could greatly reduce the need and the associated cost of environmental monitoring (4).

The elimination half-times and cumulative percent of the dermal dose of certain pesticides excreted indicate a great deal of variation in the rate of clearance (1,8). The percent of the dermal dose varies from 0.18% for diquat and 0.50% for aldrin to as much as 12.5% and 15.9% for azinphos-methyl (Guthion) and propoxur (Baygon) respectively (1). These results suggest that no more than 15% of a dermal dose of a given pesticide is absorbed and eliminated in urine. However, intravenous and intraperitoneal doses are efficiently eliminated in urine (8-9). The human studies protocol using the indirect method of adjustment for incomplete metabolism (8-9) does not account for evaporative and mechanical loss and retention of the dose at the skin surface and the epidermis (10).

This study was designed to determine the rates of absorption and elimination of malathion as an organic concentrate and aqueous mixture when applied to the ventral forearms of human volunteers. The additional aim was to account for the dermal dose on the surface of the skin and epidermis of the human. When additional information on the disposition of malathion in tissues appeared compelling, a limited dermal absorption study was conducted in the rat. The overall purpose of the study was to compare the absorption kinetics of the organic based concentrates that impact on mixer/loader activities and contact and transfer of surface (wet) aqueous mixtures that might result from exposure upon re-entry.

## Methods

**Human Exposure Study.** Twelve healthy men and women ages 21 to 35 years were selected to participate in this study. The subjects were briefed on the goals, procedures, risks and benefits of participation. Each subject received a physical examination. The subjects were reported to have no history of acute or chronic disease or disability or previous exposure to malathion within the last six months. The subjects were admitted to the study upon receiving their written informed consent. Recruitment, selection and testing complied with U.S. EPA Order 1000.17, "Policy and Procedures for Protection of Human Subjects in Biomedical and Behavioral Research".

**Experimental Design.** The subjects were divided into two groups of six. Each subject within a group would receive a nominal dose of a particular dosing solution of [ $^{14}\text{C}$ ]-malathion applied to a 4.6cm<sup>2</sup> area of the ventral forearm (Table I). After completing the exposure and urine collection period for the first application, the subjects were allowed to rest for two weeks prior to the application of the second dosing solution. Pre-dose urine was examined for residual radioactivity prior to dosing. Thus individuals in group A that received neat malathion in the first application received the 1.0% aqueous mixture in the second application as members of group C. Individuals in group B receiving the concentrated commercial formulation in the first application received the 10.0% aqueous mixture in the second application as members of group D.

**Test and Control Articles.** [ $^{14}\text{C}$ ]-Malathion(31.1 $\mu\text{Ci}/\text{mg}$ ) was obtained from Sigma Chemical Company, St. Louis, Missouri. The radiochemical purity was confirmed as 98.3% by reverse phase HPLC with a Perkin-Elmer

**Table I. Experimental Design and Dosing Solutions**

Groups	Dosing Solution	Number of Subjects	Dose Levels		
			Nominal <sup>14</sup> C (μCi)	Malathion (mg)	Malathion (mg/cm <sup>2</sup> )
A	Neat <sup>a</sup>	6	7.24	24.6	5.4
B	50% EC <sup>b</sup>	6	7.25	25.7	5.6
C	1% mixture <sup>c</sup>	6	2.45	157.1 (μg)	34.2 μg/cm <sup>2</sup>
D	10% mixture <sup>d</sup>	6	5.70	5.5	1.2

a Mixture of radiolabeled and nonradiolabeled malathion (neat).

b Mixture of radiolabeled malathion with undiluted commercial product (EC Malathion 50).

c Mixture of radiolabeled malathion with 1% diluted commercial product (1% malathion) in tap water.

d Mixture of radiolabeled malathion with 10% diluted commercial product (5% malathion) in tap water.

LC55B variable wavelength detector at 230 nm and a Radiomatic Flo-One Hewlett-Packard radiochemical detector. The system was equipped with a Spherisorb ODS-2 reverse-phase C<sub>18</sub> column (150 mm x 4.6 mm, ID 5 µm). A C<sub>18</sub> guard column (Brownlee, 15 mm x 3.8 mm, ID) was placed ahead of the analytical column. The mobil phase (0.2% trifluoroacetic acid in water [A] / 0.1% trifluoroacetic acid in acetonitrile [B]) was delivered at 1.0 mL/min with a Perkin-Elmer Model 250 binary pump.

The HPLC/radiochemical column eluent was collected and diluted with scintillation cocktail for liquid scintillation counting (LSC) on a Packard Tricard Model 4530. Standards were prepared from aliquots of the sample solution used for chromatographic analysis. The radiochemical purity was determined as the percentage of the malathion peak to the total radioactivity. Column recovery was determined as the percentage of radioactivity eluted from the column as compared to the direct measurement of 100 µL of the standard by LSC.

The non-labeled malathion was obtained from Chem Service Inc., West Chester, Pennsylvania. The commercial product, Ortho Malathion 50, containing 50% malathion by weight was purchased over the counter from a department store in the Kansas City area.

**Dose Preparation.** The dosing solutions were prepared separately three to four hours before dosing. The [<sup>14</sup>C]-malathion in toluene was reduced to near dryness and resuspended in non-labeled malathion to yield a predetermined amount of radioactivity for each dosing solution (Table I). Before dose application, aliquots of the dosing solution were counted to determine final radioactive content.

**Dose Application.** Baseline urine samples were collected prior to dosing. In preparation to dosing, each subject's arm was washed once with soap and water and allowed to air dry. A 4.6 cm<sup>2</sup> test area was outlined with a graphite pencil on the ventral forearm. The dose was applied within the test area from the lure tip of a glass Hamilton Gas-Tight microliter syringe. The weight of the loaded syringe was obtained prior to application and again following the delivery of the dose to determine the final weight of the dose delivered. The final dose administered was adjusted for loss of dosing solution due to running of the neat and concentrated commercial formulation (Table II).

The application site was observed for four hours after application for spreading of the test substance beyond the test area. The area of application was adjusted to reflect spreading of the neat and commercial formulation (Table II). At the conclusion of the four hour period of observation, the test area was covered with an occlusive patch.

**Sample Collection.** Collection intervals were based on the time from dose application. Urine was collected at four hour intervals up to 12 hours post application (Table II). After 12 hours of exposure, urine was collected and pooled at 12 hour intervals. The site was examined after 24 hours and gently washed two times with soap and water and rinsed three times to remove only the residual amount of the applied dose and not any of the material that had penetrated the integument. The gauze sponges used to clean the site and the occlusive patches and contaminated bench paper were extracted in methanol to obtain residual site concentrations.

**Radiochemical Analysis.** Aliquots of urine (2.0g) were prepared in duplicate for LSC. The well mixed samples were prepared in 10 mL Ultima Gold® (Packard, Downers Grove, Illinois) scintillation cocktail. The vials were kept at 8°C for 24 hours prior to LSC for 10 minutes on a Packard, Model 2000CA liquid scintillation spectrophotometer. Counts per minute (CPM) were corrected for

**Table II. Cumulative Percent of the Applied Dose of [<sup>14</sup>C]-Malathion Recovered in the Urine of Human Volunteers at Selected Time Intervals Following Exposure to Neat Malathion, the 50% EC Formulation, and 1% and 10% Aqueous Mixtures**

Percent Cumulative Concentration													
Neat Malathion (Group A)													
Sub.	Surface Area (cm <sup>2</sup> )	Dose(mg)	Site(mg) <sup>†</sup>	Pre	0-4	4-8	8-12	12-24	24-36	36-48	48-60	60-72	Hours
A1	66.50	23.60	17.50	0.00	0.02	0.06	3.92	15.46	17.96	18.02	18.29	18.36	
A2	27.10	24.90	20.90	0.00	0.01	0.17	0.72	1.78	2.36	2.41	2.44	2.45	
A3	75.20	23.30	18.80	0.00	0.03	0.82	1.62	7.88	9.22	9.39	9.46	9.53	
A4	11.70	23.70	13.90	0.00	0.04	0.21*	1.39	3.67	4.70	4.98	5.04	5.05	
A5	24.60	10.50	7.85	0.00	0.02	0.44	0.85	2.57	3.07	3.10	3.10	3.10	
A6	29.00	23.20	11.80	0.00	0.05	0.22*	1.32*	4.83	5.38	5.55	5.60	5.62	
50% EC Formulation (Group B)													
Sub.	Surface Area (cm <sup>2</sup> )	Dose(mg)	Site(mg) <sup>†</sup>	Pre	0-4	4-8	8-12	12-24	24-36	36-48	48-60	60-72	Hours
B1	20.20	26.70	17.10	0.01	0.04	0.14	0.34	1.71	2.24	2.30	2.32	2.33	
B2	17.00	20.40	16.00	0.00	0.01	0.06	0.80	2.94	4.06	4.20	4.23	4.24	
B3	15.60	24.40	16.60	0.00	0.02	0.44	2.60	6.13	7.07	7.16	7.20	7.23	
B4	24.00	13.60	8.73	0.00	0.07	0.51*	2.26	7.71	8.86	8.96	9.00	9.01	
B5	56.70	21.90	15.50	0.01	0.03	0.37	1.67	7.09	8.71	8.97	9.01	9.04	
B6	36.80	19.80	12.10	0.00	0.03	0.03*	0.84	1.31	2.42	2.52	2.55	2.57	

<sup>†</sup> Concentration removed from site by wiping and rinsing

\* Interpolated value

*Continued on next page*

Table II. Continued

1% Aqueous Mixture (Group C)				Percent Cumulative Amount									
Sub.	Surface Area (cm <sup>2</sup> )	Dose(mg)	Site(mg) <sup>†</sup>	Pre	0-4	4-8	8-12	12-24	24-36	36-48	48-60	60-72	Hours
C1	4.6	0.11	0.10	0.01	0.64	3.12	7.15	14.68	16.38	16.58	16.74	16.86	
C2	4.6	0.14	0.02	0.00	0.42	1.43	5.65	16.01	19.11	19.39	19.54	19.59	
C3	4.6	0.17	0.05	0.01	0.45	1.20	2.74	6.46	8.85	9.01	9.25	9.40	
C4	4.6	0.12	0.00	0.01	0.45	0.45*	20.95	27.82	28.12	28.29	28.53	28.60	
C5	4.6	0.16	0.05	0.00	0.25	0.25*	4.92	9.47	10.30	10.36	10.46	10.57	
C6	4.6	0.15	0.06	0.00	0.61	0.99	1.52	10.46	11.48	11.65	11.89	11.93	
10% Aqueous Mixture (Group D)													
Sub.	Surface Area (cm <sup>2</sup> )	Dose(mg)	Site(mg) <sup>†</sup>	Pre	0-4	4-8	8-12	12-24	24-36	36-48	48-60	60-72	Hours
D1	4.6	5.48	3.40	0.00	0.06	0.16	0.49	1.88	2.42	3.03	3.10	3.13	
D2	4.6	5.50	5.12	0.00	0.10	0.72*	1.28	5.02	7.10	7.42	7.46	7.48	
D3	4.6	5.43	4.56	0.00	0.12	0.39*	1.00*	2.95	4.08	4.36	4.38	4.40	
D4	4.6	5.46	4.09	0.00	0.09	0.41*	1.34	2.71	3.84	4.64	4.73	4.76	
D5	4.6	5.38	3.67	0.00	0.10	0.47	0.80	3.05	5.00	5.20	5.25	5.27	
D6	4.6	3.98	3.46	0.00	0.07	1.01*	3.32	8.17	10.45	10.94	10.98	10.99	

\* Interpolated value

† Concentration removed from site by wiping and rinsing

background automatically. CPM were converted to disintegrations per minute (DPM) by the external standard method. The efficiency curve was derived from a set of commercially prepared standards. Duplicate samples that differed by more than 10% of the mean were sampled again in duplicate.

**Metabolite Identification.** Pre-application and post-application (12-24 hour) urine samples from subjects A1 and B5 were characterized for metabolites. The post-application samples were lyophilized and reconstituted in water/acetonitrile(90%/10%). The reconstituted samples were filtered through a 0.45  $\mu\text{m}$  Acrodisc-CR (Gelman, Ann Arbor, Michigan) syringe-tip filtration system. The radiochromatographic HPLC system was the same as that used to determine radiochemical purity. A linear gradient was initiated from 100% [A] to 100% [B] in 50 minutes following 5 minutes at initial conditions. Aliquots (100  $\mu\text{L}$ ) were injected and the chromatographic eluant was collected in 100 0.5 minute fractions using a FOXY model fraction collector (ISCO, Lincoln, Nebraska).

Multiple injections of each sample were made and the chromatographic eluent from each injection was overlaid with prior collections such that the effective volume of urine injected was approximately 2.0 mL. The collected fractions were mixed with 5 mL Scintiverse LC(Fisher Scientific) scintillation cocktail and the radioactivity determined (10 minute counts) by LSC on a Packard Model 4530 liquid scintillation spectrophotometer.

Metabolites were identified by Gas-Chromatography with flame photometric detection (GC/FPD) and confirmed by Gas-Chromatography/Mass Spectrometry (GC/MS). The pre-application and post-application samples (12-24 hours) from subject B5 were lyophilized and reconstituted in 4.0 mL deionized water. The reconstituted urine was acidified (1.0 mL, 1 N HCl) and extracted with two 7.0 mL portions of diethyl ether. The ether extracts were combined, mixed, and divided into two equal portions. One portion was treated with ethereal diazomethane and the other was treated with diazoethane. Following a reaction time of 30 minutes at room temperature, the ether extracts were evaporated to near dryness and reconstituted in acetonitrile (1.0 mL).

Analysis was performed using a Hewlett Packard 5890 gas chromatograph equipped with a 30 meter DB-1 Megabore capillary column (J&W Scientific, Folsom, California) and an on-column splitless (45 s) injection system. The injector temperature was 250°C. Helium was used as the carrier gas at a flow rate of 5.0 mL/min. The column temperature was held at 50°C for 5 minutes and then programmed to 220°C at a rate of 10°C/min. The detector was operated in the phosphorus mode at a temperature of 260°C.

Identification of metabolites by GC/FPD was confirmed by GC/MS in full scan mode (40 to 400 amu, 70 eV) using a Finnigan 4000 quadrapole mass spectrometer interfaced with a Hewlett-Packard Model 5890A gas chromatograph and an INCOS 2400 data system. Separations were accomplished with a 30 meter DB-5 capillary column (J&W Scientific, Folsom, California) and a splitless (45 s) injection system. The injector temperature was 270°C. Helium was used as the carrier gas at a flow rate of 5.0 mL/min. The column temperature was held at 50°C for 5 minutes and then programmed to 250°C at a rate of 10°C/min.

Samples were compared with standard solutions of the dicarboxylic (DCA) and monocarboxylic (MCA) acid esters of malathion. Analytical standards of malathion, MCA (85% alpha and 15% beta), DCA, and maloxon were generously provided by American Cyanamid (Princeton, New Jersey). Reconstructed ion current chromatograms (RIC) and mass spectra were obtained for the diazoethane

and diazomethane ether extracts. MCA and DCA, prepared as methylated derivatives, were used as reference standards.

**Dermal Absorption in the Rat.** Adult male albino rats (*Rattus norvegicus* L.) Sprague Dawley strain were obtained from Bantin and Kingman Inc. Laboratories. The average weight at treatment was 180 grams. The animals were kept individually in well aerated cages under hygienic conditions with standard diet. The animals were allowed to acclimate for one week in their cages prior to the experiment. The experiment was conducted according to strict adherence to the "Guide for the Care and Use of Laboratory Animals" (NIH Publication No. 85-23), the Animal Welfare Act (Public Law 89-544, as amended by Public Law 91-579 and Public Law 94-279) and the standard operating procedures concerning care and use of laboratory animals of Texas Southern University.

**Experimental Design.** Three rats were randomly assigned to each of three groups according to sample collection and time of sacrifice. A total of nine rats were exposed to neat malathion and nine to the concentrated commercial formulation. Three rats were prepared as untreated controls. Urine and feces were collected from three rats in group 1, 24 hours after dose application. Excreta were collected from rats in group 2, 24, 48 and 72 hours after dosing. Collection of excreta in group 3 was extended for seven days post application. Animals in group 1 were sacrificed after 24 hours. Animals in groups 2 and 3 were sacrificed on days three and seven respectively. At the time of sacrifice the following tissues were collected: blood, liver, kidney, small intestine, large intestine and skin at the site of application. The animals were sacrificed by decapitation.

**Test and Control Articles.** Neat malathion (purity 94.6%) was obtained from American Cyanamid Co., Princeton, New Jersey. The commercial product, a 50% emulsifiable concentrate (E.C.) of malathion was obtained from Southern Mill Creek Products, Inc., Houston, Texas. [ $^{14}\text{C}$ ]-malathion (14.2 mCi/mmol) was purchased from Sigma Chemical Company, St. Louis, Missouri. NCS tissue solubilizer was purchased from Amersham Searle, Arlington Heights, Illinois.

**Dose Preparation.** The dose was selected as 10% of the dermal  $\text{LD}_{50}$ , a nominal concentration of 73.8 mg malathion per animal of the neat and the 50% E.C. formulation. The dosing solutions were spiked with 1.0  $\mu\text{Ci}$  [ $^{14}\text{C}$ ]-malathion. The concentration of [ $^{14}\text{C}$ ]-malathion in the dosing solution was confirmed by a standard curve of expected and observed DPM per volume of dosing solution. Before dose application, aliquots of the dosing solutions were counted to determine final radioactive content.

**Dose Application.** Twenty four hours before dosing, a 6.452  $\text{cm}^2$  area on the back was shaved with care not to abrade the integument. The shaved area was washed with acetone. A nominal dose of 11.4  $\text{mg}/\text{cm}^2$  (410 $\text{mg}/\text{kg}$ ) was applied within the marked area from the lure tip of a glass microliter Hamilton syringe. The amount delivered in an appropriate volume of 500  $\mu\text{L}$  to the site was determined as the difference between the weight of the loaded syringe and the empty syringe after application. The site of application was occluded with an adhesive patch.

**Sample Collection.** Urine and feces were collected on ice from metabolism cages and stored frozen until analysis. Metabolism cages were rinsed with aqueous ethanol after each collection. After collection of the final urine and fecal specimens, the animals were sacrificed by decapitation. Blood was heparinized and stored briefly before analysis. Tissues were weighed and stored frozen.

**Radiochemical Analysis.** Radioactivity was measured by LSC using a Wallac 1409 liquid scintillation spectrophotometer. Aliquots (100  $\mu$ L) of the urine samples were well mixed and prepared directly for LSC. Blood, feces, and tissues were processed according to the procedure of Muan and Nafstad (11) with modifications. To each sample, 30 mL methanol was added and homogenized and digested in NCS tissue solubilizer for 24 hours. The clear digest (100  $\mu$ L) was prepared for LSC. All samples were prepared in triplicate by weight and counted in duplicate cycles. The counting efficiency was determined by the external standard method.

**Data Reduction and Statistical Analysis.** Repeated measures analysis of variance (rm-ANOVA) was used to test the interaction of the main effects, the repeated measurements of [ $^{14}$ C]-malathion equivalents in urine, with the subjects within groups (12). The repeated measures were sorted by ranks. The rm-ANOVA was performed on the ranked data (13). This transformation was made because of the violation of the sphericity assumption. The rm-ANOVA on ranked data was justified over angular and logarithmic transformations because of the stabilization of the variance over the number of zero events.

Multiple linear regression was used to obtain regression statistics for the curvilinear absorption profiles (14). The multiple regression model was used as the first iteration of the curvilinear regression. The multiple linear regression analysis did not constrain the minima at the origin.

Linear regression analysis was used to obtain absorption and elimination rate constants (14). Multiple linear regression was used to determine relationships between predictor and response variables (14). Cluster analysis was used to identify closely related cases (14). The clusters were formed in a stepwise fashion from independent variables and a single response variable. Single variable clusters were legitimized by examining the clustered values against the 95% confidence intervals for the clustered values.

## Results.

**Human Exposure Study.** Concentrations of  $^{14}$ C equivalents of malathion in urine increased to a maximum at 24 hours after exposure (Figure 1). The greatest concentration of  $^{14}$ C equivalents of malathion was recovered in urine of volunteers exposed to neat malathion (Figure 1). The main effect for the ranks of the repeated measures of  $^{14}$ C-equivalents in urine collected within selected time intervals was found to be significant ( $F_{8,160}=148.14$ ,  $p<0.001$ ). As expected, the ranks of the totals differed between measurements. More substantively, a significant group/time interaction ( $F_{1,20}=30.49$ ,  $p<0.001$ ) was found which indicated that the pattern of excretion for subjects within the groups was dependent on whether they were exposed to an organic based formulation or an aqueous mixture. This significant interaction was attributed to a significant difference between groups ( $F_{3,20}=45.07$ ,  $p<0.001$ ). Tests on the differences between group means (Newman-Keuls procedure) revealed significant differences between group C and groups A, B, and

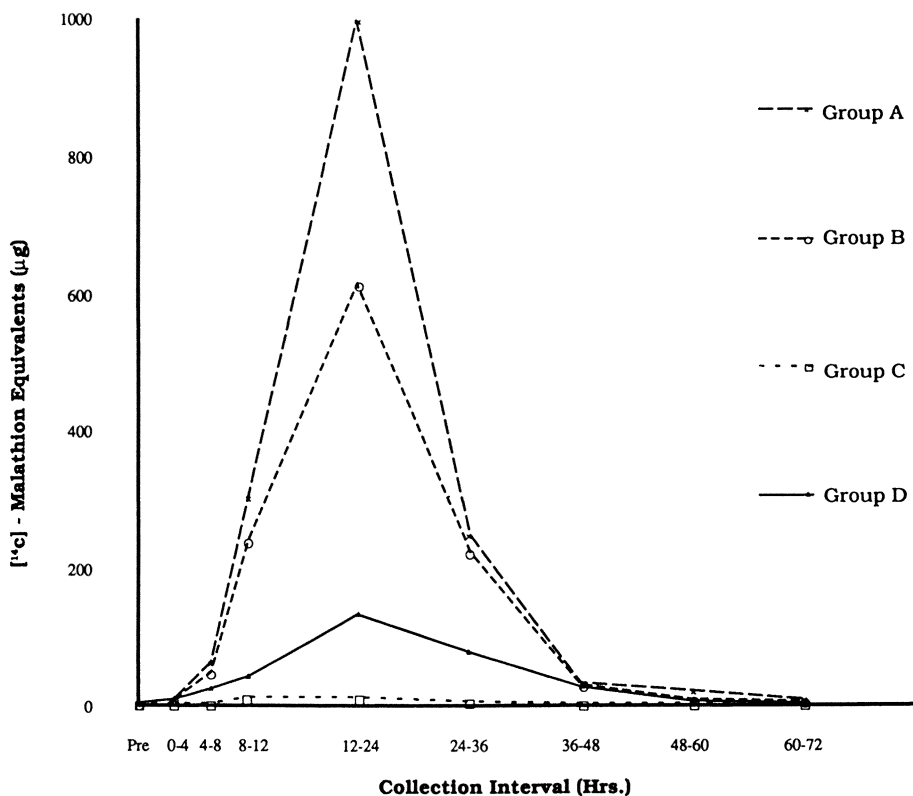


**Figure 1. Elimination Profile of  $[^{14}\text{C}]$ -Malathion Equivalents in Urine of Human Volunteers Exposed to Neat Malathion (Group A), the 50% EC Formulation (Group B), and the 1% (Group C) and 10% (Group D) Aqueous Mixtures.**

D. Significant differences were observed between group A and groups B and D. Groups B and D were not significantly different.

These differences between group means are graphically portrayed as the cumulative amount of malathion at each time interval (Figure 2). When normalized as percent of the applied dose, the mean of group C was found to be significantly different from groups A, B, and D (Figure 3). The results suggest that lower concentrations of malathion are more rapidly and readily absorbed than higher concentrations. More precisely, establishment of steady state relative to concentration was more rapidly achieved with the 1% aqueous mixture. The total amount absorbed was dose dependent while the rate of absorption was controlled by factors that influence the attainment of steady state.

Another factor that might influence attainment of steady state and ultimately the rate of absorption is surface area of exposure. An unplanned outcome of this study was the increase in the surface area of the application site due to spreading of the neat and 50% emulsifiable concentrate on the forearms of volunteers in groups A and B. The 4.6 cm<sup>2</sup> area of the site of application increased to 11.7 cm<sup>2</sup> on the forearm of subject A4 to as much as 75.0 cm<sup>2</sup> on the forearm of subject A3 (Table II). This increase in surface area afforded an opportunity to study surface area effects.

Normalizing the cumulative percent of malathion recovered as given in figure 3 to the surface area of exposure resulted in significant differences between group C and groups A and B, and significant differences between group D and groups A, B and C (Figure 4). The significant differences between group C and groups A and B were attributed to dose. The group D differences were attributed to surface area. The influences of surface area and dose on the rate of absorption and cumulative absorption can be more readily gleaned from plots of cumulative amount recovered among subjects within groups. The total amount of neat malathion absorbed was greatest for those subjects with larger surface areas of exposure, subjects A1 and A3 (Figure 5). The cumulative totals for the subjects exposed to neat malathion in group A were found to be significantly different. The cumulative total for subject A5 was significantly less than for subjects A3, A1, A4, and A6 at the 1.0% level of significance and for subject A2 at the 5.0% level.

Normalizing the cumulative absorption to dose and surface area of exposure resulted in a reordering of absorption profiles for subjects in group A (Figure 6). Following this normalization, the cumulative totals for subjects A3 and A5, and A5 and A6 were found to be not significantly different. The profiles for the subjects were significantly different as indicated by the time-subject interaction ( $F_{9,40}=77.22$ ,  $p<.001$ ). The surface area of exposure and the dose applied to the site influenced the rate of the "apparent" absorption profile and the total cumulative recovery in urine.

The rate of "apparent" absorption may be seen as the shaded portion of the absorption profile (Figure 5). The term "apparent" is used to distinguish between events that contribute to dermal penetration and events underlying the appearance of drug in the urine for the *in vivo* situation where plasma concentrations are not in evidence. The apparent rate of absorption was taken from the regression on cumulative amount of [<sup>14</sup>C]-malathion equivalents in urine as a function of time with the regression constrained at  $t=0$  and 24 hours (Figure 7). The "apparent" rates of absorption were used to gain statistical inferences between groups and among subjects as a model independent form of analysis.

For subject A1, the apparent rate of absorption was extremely rapid compared to other subjects in group A (Table III). The curvilinear regression coefficients for the six subjects in group A were significantly different

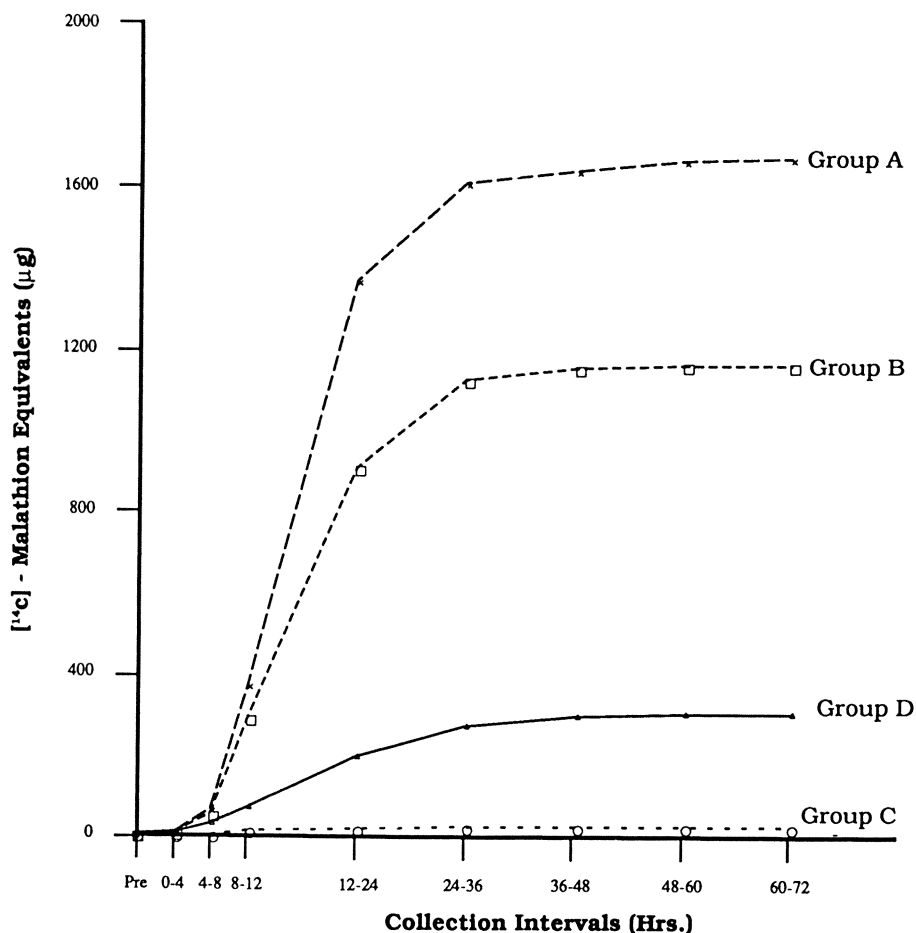


**Figure 2. Cumulative Elimination  $[^{14}\text{C}]$ -Malathion Equivalents in urine of Human Volunteers Exposed to Neat Malathion (Group A), the 50% EC Formulation (Group B), and the 1% (Group C) and 10% (Group D) Aqueous Mixtures.**

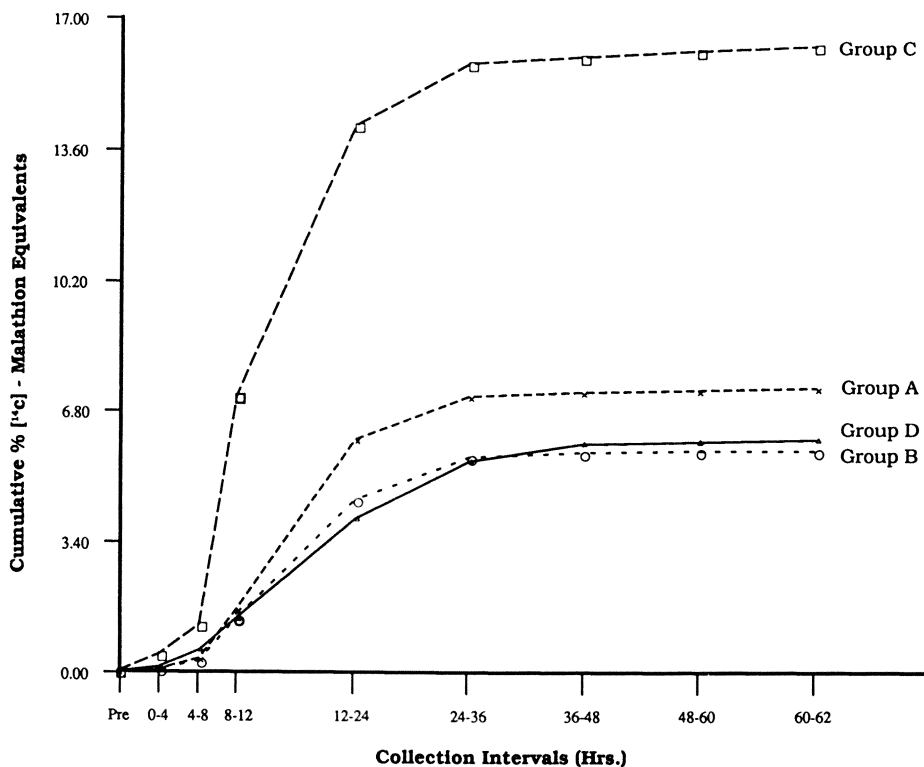


**Figure 3. Cumulative Percent Elimination of the Applied Dose of [ $^{14}\text{C}$ ]-Malathion Equivalents in the urine of Human Volunteers Exposed to Neat Malathion (Group A), the 50% EC Formulation (Group B), and the 1% (Group C) and 10% Aqueous Mixtures.**

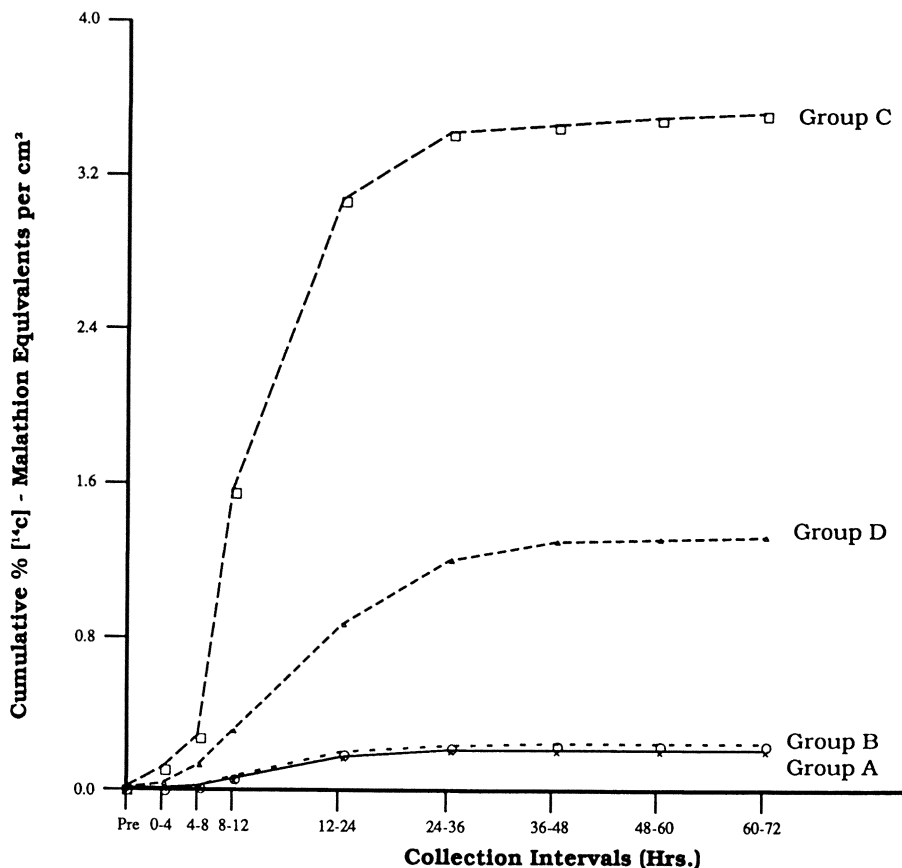


**Figure 4. Cumulative Percent Elimination of the Applied Dose Of  $[^{14}\text{C}]$ -Malathion Normalized to the Surface Area ( $\text{cm}^2$ ) of Exposure.**

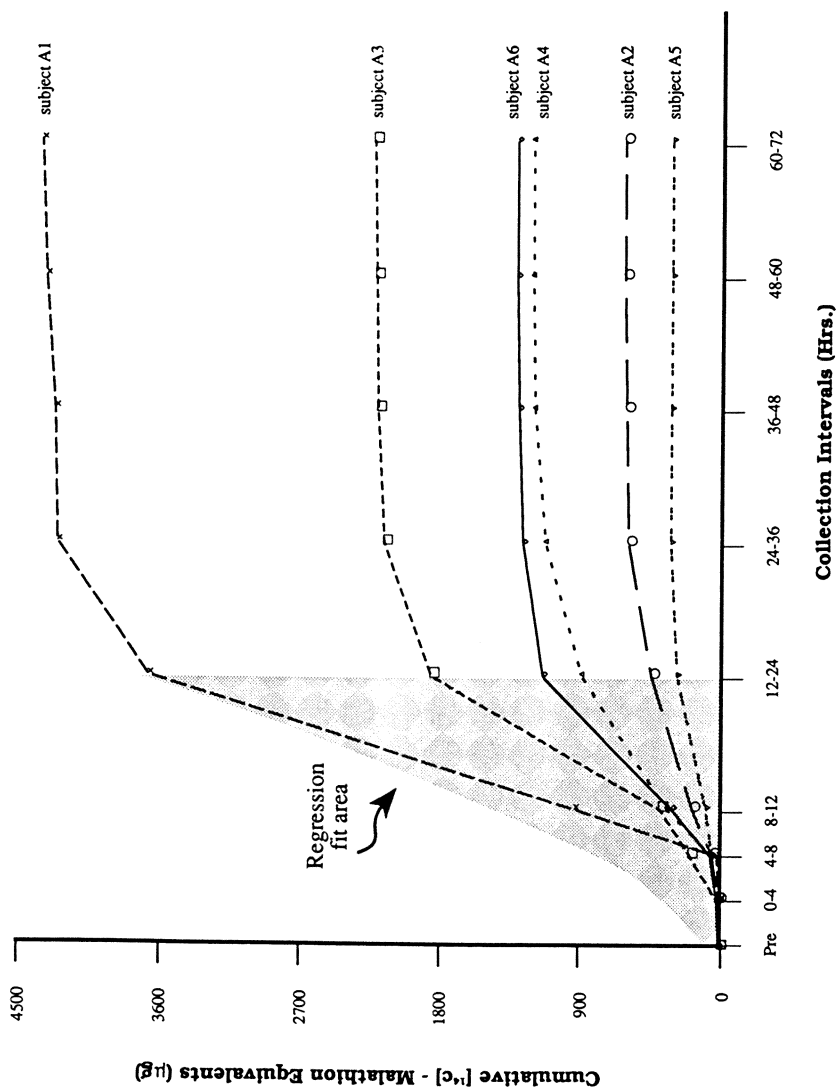


**Figure 5. Cumulative Absorption of [14C]-Malathion in Subjects Exposed to Neat Malathion in Group A.**

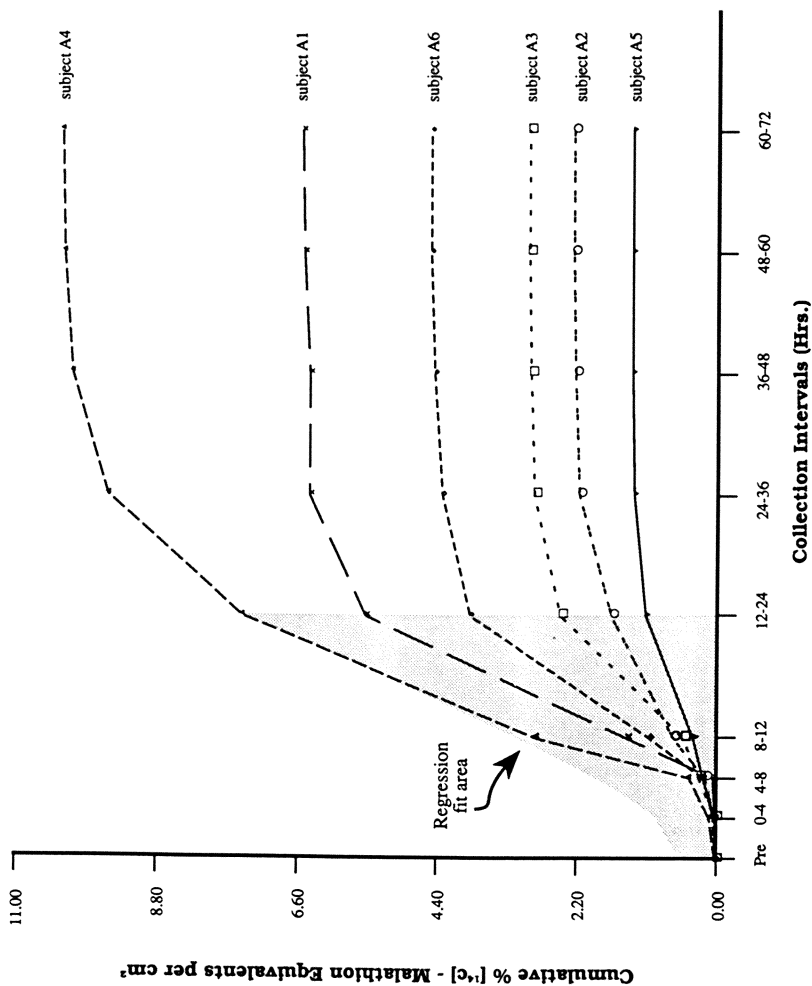


**Figure 6. Cumulative Percent Absorption of [14C]-Malathion in subjects Exposed to neat Malathion after Normalization for Surface Area.**

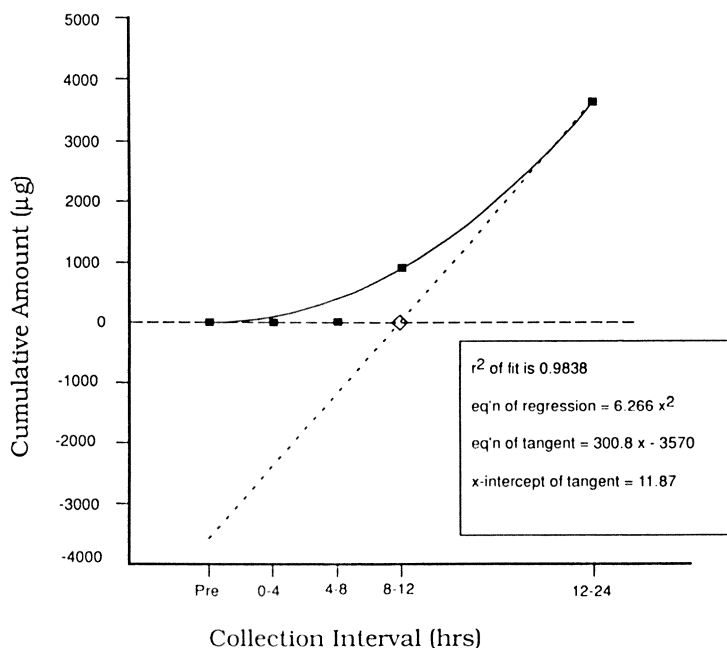


**Figure 7. Apparent Rate of Absorption ( $\mu\text{g/hr}$ ) as the Tangent of the Curvilinear Regression on Cumulative Amount of Malathion Recovered in Urine as a Function of time and the Associated Intercept to Predict the Apparent Lag Time.**

American Chemical  
Society Library  
1155 16th St. N. W.  
Washington, D. C. 20036

Table III. Summary of Kinetic Parameters to predict absorption and Elimination of Malathion in the Human System

group	subject	concentration mg/cm <sup>2</sup>	cumulative % of applied dose	quadratic slope <sup>†</sup> µg/hr	lag time <sup>†</sup> (hours)	absorption rate const k <sub>a</sub> (hr <sup>-1</sup> )	absorption half-time (hours)	elimination rate constant k <sub>e</sub> (hr <sup>-1</sup> )	elimination half-time (hours)	k <sub>a</sub> /k <sub>e</sub> ratio
A	A1	0.35	18.4	6.63	11.9	0.012	55.6	0.099	7.00	7.94
	A2	0.92	2.45	0.80	12.4	0.007	95.0	0.098	7.06	13.5
	A3	0.31	9.53	3.15	11.9	0.009	77.5	0.094	7.40	10.5
	A4	2.03	5.05	1.55	12.3	0.022	31.2	0.101	6.86	4.54
	A5	0.43	3.10	0.48	12.3	0.012	57.2	0.129	5.38	10.6
	A6	0.80	5.62	1.94	12.0	0.028	24.6	0.097	7.10	3.46
		0.81±0.65	7.35±5.94	2.42±2.26	12.1±0.2	0.015±0.008	56.8±26.8	0.103±0.013	6.80±0.72	8.42±3.85
group	subject	concentration mg/cm <sup>2</sup>	cumulative % of applied dose	quadratic slope <sup>†</sup> µg/hr	lag time <sup>†</sup> (hours)	absorption rate const k <sub>a</sub> (hr <sup>-1</sup> )	absorption half-time (hours)	elimination rate constant k <sub>e</sub> (hr <sup>-1</sup> )	elimination half-time (hours)	k <sub>a</sub> /k <sub>e</sub> ratio
B	B1	1.32	2.32	0.78	11.8	0.019	37.3	0.106	6.56	5.69
	B2	1.20	4.24	1.04	11.9	0.010	68.5	0.103	6.74	10.2
	B3	1.56	7.23	2.69	12.4	0.016	43.2	0.106	6.53	6.61
	B4	0.57	9.01	1.83	12.1	0.018	37.5	0.117	5.90	6.35
	B5	0.39	9.04	2.67	11.9	0.014	48.1	0.104	6.66	7.23
	B6	0.54	2.57	0.49	12.9	0.021	33.8	0.088	7.88	4.29
		0.93±0.49	5.74±3.09	1.58±0.96	12.2±0.4	0.016 ±0.004	44.7±12.7	0.104±0.009	6.71±0.64	6.72±1.96

† slope of the curvilinear regression  
† tangent of the line through the x intercept

Table III. Continued

group	subject	concentration mg/cm <sup>2</sup>	cumulative % of applied dose	quadratic slope <sup>†</sup> μg/hr	lag time <sup>‡</sup> (hours)	absorption rate const k <sub>a</sub> (hr <sup>-1</sup> )	absorption half-time (hours)	elimination rate constant k <sub>e</sub> (hr <sup>-1</sup> )	elimination half-time (hours)	k <sub>a</sub> /k <sub>e</sub> ratio
C	C1	0.023	17.5	0.03	12.7	0.004	187.4	0.089	7.74	24.2
	C2	0.031	19.2	0.04	12.3	0.091	7.59	0.111	6.25	1.21
	C3	0.036	9.68	0.02	12.5	0.051	13.5	0.075	9.28	1.45
	C4	0.027	28.1	0.06	13.2	0.154	4.49	0.106	6.56	0.68
	C5	0.034	10.7	0.03	12.6	0.047	14.7	0.087	8.01	1.84
	C6	0.033	11.8	0.03	11.7	0.037	18.5	0.097	7.17	2.59
		0.031±0.005	16.2±7.0	0.035±0.014	12.5±0.5	0.064±0.052	41.0±1.9	0.094±0.0132	7.50±1.10	5.33±9.27
group	subject	concentration mg/cm <sup>2</sup>	cumulative % of applied dose	quadratic slope <sup>†</sup> μg/hr	lag time <sup>‡</sup> (hours)	absorption rate const k <sub>a</sub> (hr <sup>-1</sup> )	absorption half-time (hours)	elimination rate constant k <sub>e</sub> (hr <sup>-1</sup> )	elimination half-time (hours)	k <sub>a</sub> /k <sub>e</sub> ratio
D	D1	1.19	3.13	0.18	12.0	0.020	34.8	0.079	8.72	4.00
	D2	1.20	7.48	0.48	12.1	0.003	232.3	0.107	6.50	35.7
	D3	1.18	4.40	0.28	12.3	0.007	95.3	0.095	7.31	13.0
	D4	1.19	4.76	0.27	12.7	0.012	57.6	0.084	8.28	6.95
	D5	1.17	5.27	0.29	12.1	0.016	43.5	0.097	7.11	6.12
	D6	0.865	11.0	0.59	12.4	0.006	118.8	0.130	5.32	22.3
		1.13±0.13	6.00±2.82	0.35±0.15	12.3±0.3	0.011±0.007	97.0±73.6	0.0987±0.0183	7.21±1.23	14.7±12.3

‡ slope of the curvilinear regression  
† tangent of the line through the x intercept

( $F_{5,12}=126.69$ ,  $p < 0.001$ ). Between subjects, the slopes for subjects A6 (1.94  $\mu\text{g/hr}$ ) and A4 (1.55  $\mu\text{g/hr}$ ) were not significantly different ( $t_6=2.027$ ,  $p < 0.10$ ). The apparent rates of absorption of neat malathion were significantly different for all subjects except subjects A6 and A4 in group A.

The apparent rates of absorption for subjects treated with 50% EC formulation in group B were significantly different ( $F_{5,12}=54.16$ ,  $p < 0.001$ ) as indicated by the curvilinear regression coefficients (Table III). A pairwise examination of the slopes revealed, that the slopes for subjects B1 (0.93  $\mu\text{g/hr}$ ), B2 (1.16  $\mu\text{g/hr}$ ), and B3 (1.71  $\mu\text{g/hr}$ ) were not significantly different. Likewise, the slopes of subjects B3 and B4 (1.78  $\mu\text{g/hr}$ ) could be grouped.

The apparent rates of absorption for the subjects in group B were taken from the shaded portion of the absorption profile (Figure 8). As previously observed for subjects in group A, the absorption profiles for subjects in group B were significantly different as indicated by the time-subject interaction ( $F_{8,40}=31.88$ ,  $p < 0.001$ ). This significant interaction was attributed to the repeated measurements (between collection intervals) as observed for group A and not between subjects ( $F_{5,40}=2.07$ ,  $p < 0.10$ ). The cumulative total absorption was not significantly different between subjects in group B. Moreover, the cumulative absorption totals between subjects in groups A and B were not significantly different. This finding together with the significant (group X subject X repeated measures) interaction pointed to an influence on the rate of absorption and elimination for subjects in groups A and B.

To explain the apparent rate of absorption in terms of surface area of exposure and concentration at the site (external dose), the curvilinear slopes for the subjects in groups A and B (Table III) were plotted and analyzed by multiple linear regression. The stepwise multiple regression (F-to-enter 3.84, F-to-remove 2.71) produced a significant correlation ( $r = .6660$ ,  $F_{1,10}=7.973$ ,  $p < 0.018$ ) with slope and surface area. External dose and the possible internal dose (the difference between external dose and the concentration removed at the site by washing-site wash) were not allowed to enter. The apparent rate of absorption may be partially explained by surface area. However, less than 45% of the variability in the regression could be explained by surface area. The plot of the curvilinear slope and surface area revealed a cluster of cases (subjects) with surface areas and slopes less than 40cm<sup>2</sup> and 3.0  $\mu\text{g/hr}$  respectively; subjects A1, A3, and B5 were distinct outliers (Figure 9).

With surface area and curvilinear slope as the grouping variables, nearest neighbor cluster analysis revealed a common cluster for subjects in groups C and D as expected and a single cluster for subjects A2, A4, A5, B1 and B2. Subjects A1, A3, and B5 formed clusters at the extremes. The addition of external dose to the analysis produced two distinct clusters for groups C and D and a single cluster for all subjects in groups A and B except subjects A1, A3, and B5. The apparent rate of absorption was greatest for those subjects where the surface area of exposure was greatest.

Increased surface area did not influence the "apparent" lag-time which was taken as the tangent intercept of the curvilinear regression line (Figure 7). The "apparent" lag-times for the subjects (Table III) were not significantly different between groups ( $F_{3,20}=1.29$ ,  $p < 0.30$ ). The mean "apparent" lag-time for the groups was  $12.3 \pm 0.4$  hours. This index may be seen as the time required to reach steady-state in the system and not for the establishment of steady-state flux across the membrane (15). For the in vitro system where the thickness of the membrane is known, steady state flux is achieved 2.7 times later than the lag-time (15). For the

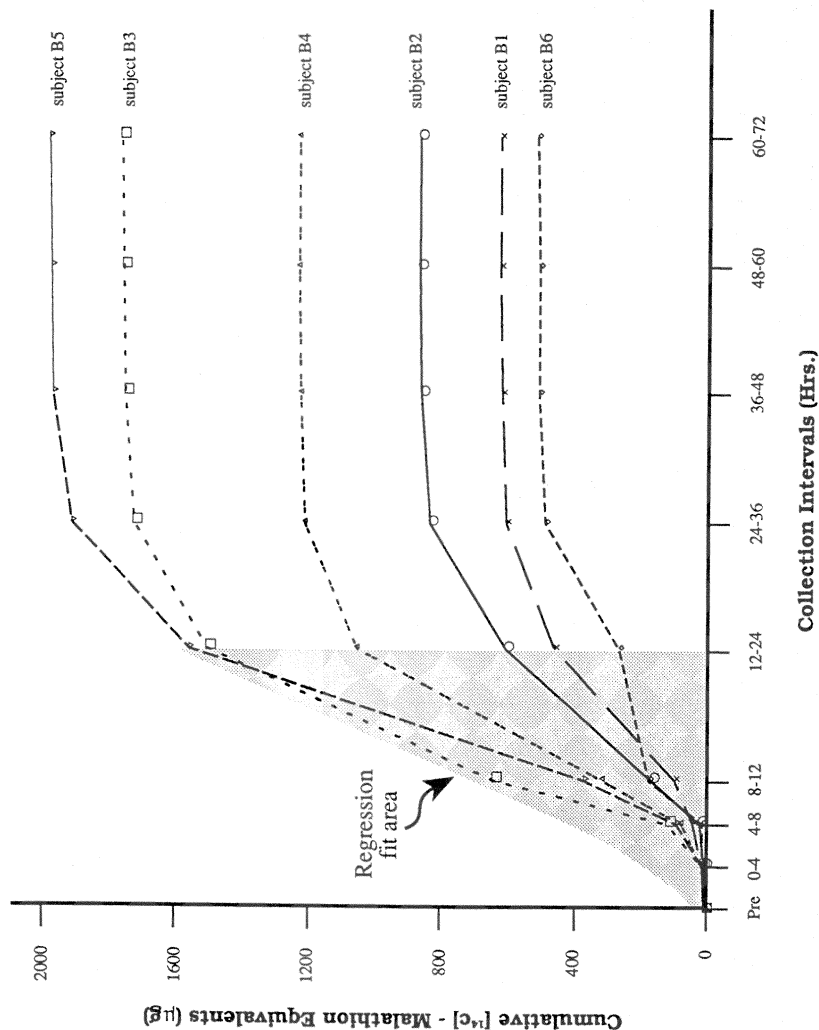


**Figure 8. Cumulative Absorption of  $[^{14}\text{C}]$ -Malathion in Subjects Exposed to the 50% EC Formulation in Group B.**

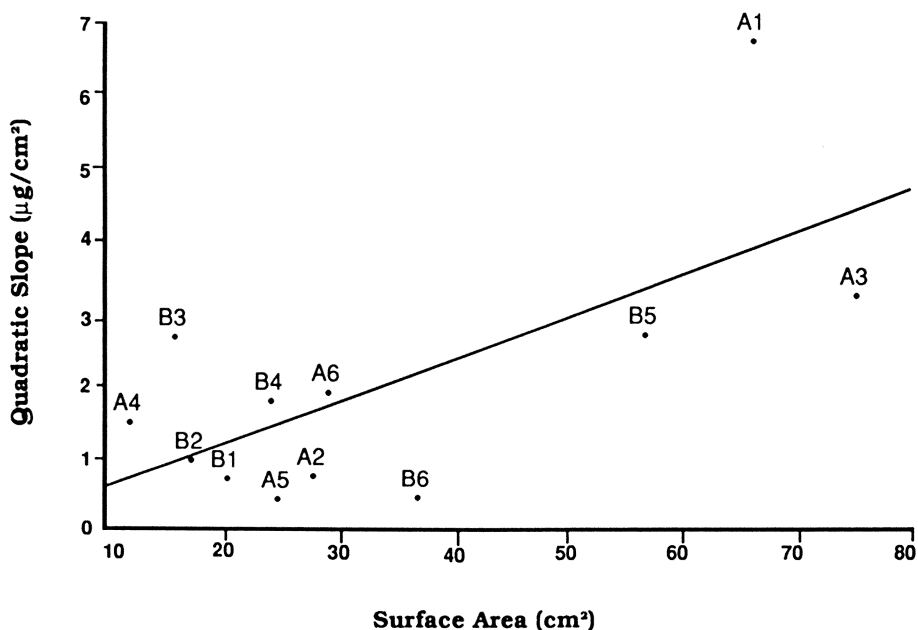


**Figure 9. Linear Regression to Explain Quadratic Slope of the Cumulative Absorption Profiles for Subjects in Groups A and B in Terms of Surface Area of Exposure.**

in vivo situation, the "apparent" lag-time may represent the balance point between circulating concentrations and the front of the elimination profile.

The apparent lag-time was not dose or surface area dependent. In keeping with the appearance of measurable urinary concentrations, the rates of elimination among subjects were not significantly different between groups ( $F_{3,20}=0.66$ ,  $p<0.58$ ); the rate of elimination was not dose or surface area dependent (Table III). However, the slope of subject A5 ( $-0.05596$ ) was significantly less than slopes of other subjects in group A ( $F_{5,36}=3.25$ ,  $p<0.05$ ). This subject had a final dose of 10.5mg compared to the expected 24.6mg per subject in group A. The elimination rate constant,  $k_e=0.1287 \text{ hr}^{-1}$ , was outside the 95% confidence interval ( $0.0896<\mu<0.1165$ ) for subjects in group A. The elimination half-time was as well outside the 95% confidence interval ( $6.05<\mu<7.55$ ) for subjects in group A.

The group A mean elimination rate constant ( $k_e=0.1030\pm0.0128$ ) indicated that approximately 10.3% of the [ $^{14}\text{C}$ ]-malathion equivalents were excreted per hour (Table III). An average of  $6.80\pm.72$  hours would be required to eliminate half of the absorbed concentration. The mean group  $k_e$  for groups C and D were slightly but not significantly less than groups A and B (Table III). Subjects in group C eliminated an average of 9.40% per hour while subjects in group D averaged 9.87% per hour. Correspondingly, the mean half-times for groups C ( $7.50\pm1.10$  hrs) and D ( $7.20\pm1.23$  hrs) were more protracted than groups A and B ( $6.71\pm0.64$  hrs).

The mean apparent lag-time ( $12.3\pm0.4$  hrs) and mean elimination rate constant ( $k_e=0.0999\pm0.0135 \text{ hr}^{-1}$ ) and corresponding mean elimination half-time ( $T_{\text{elim}}/2=7.05\pm0.95$  hrs) for the groups suggested the attainment of circulating concentrations after 12 hours of exposure with 10 percent of the body burden eliminated per hour to reach 50% in seven hours. Moreover, elimination as expected was not external dose or surface area dependent and followed first order kinetics.

The major urinary metabolites were identified as the mono- and dicarboxylic acids of malathion by radiochromatographic analysis. The predominant metabolite was the monocarboxylic acid (MCA) which represented approximately 29% and 36% of the radioequivalents excreted in the urine of subjects B5 and A1 respectively. The dicarboxylic acid (DCA) represented 23% (subject B5) and 27% (subject A1). The parent malathion represented 8% (subject B5) and 2% (subject A1). Other trace  $^{14}\text{C}$ -equivalents were tentatively identified as maloxon and desmethyl-malathion. The GC/FPD profiles obtained for the ethylated and methylated urine samples supported the identification of MCA and DCA as the predominant urinary metabolites. The isomeric configuration of the major urinary metabolite was identified as the beta isomer of MCA. The alpha isomer was identified at much lower concentrations.

The apparent rate of absorption and the total amount absorbed were dependent on surface area. The absorption profiles were significantly different between groups and between subjects within groups. The mean percent rate of absorption taken from the absorption profiles for subjects in group C ( $2.60\pm1.29\%/hr$ ) were significantly different ( $F_{3,20}=6.48$ ,  $p<0.003$ ) than subjects in groups A ( $1.07\pm.92\%/hr$ ), B ( $0.79\pm.49\%/hr$ ) and D ( $0.71\pm.42\%/hr$ ). Approximately 2.6 percent of the 1% dose of malathion applied to the ventral forearms of subjects in group C was absorbed per hour compared to 1.07% for subjects in group A treated with neat malathion, 0.79% for the 50% EC formulation (group B), and 0.71% for the 10% mixture (group D).

This statistical treatment of absorption was in agreement with the classical approach (16) as obtained by the relation:

$$\ln M/M_0 = -k_a t$$

where  $M$  is the amount of malathion remaining at the site at 24 hours,  $M_0$  is the amount initially applied to the site and  $k_a$  is the rate constant for absorption (Table III). The mean absorption rate constant for subjects in group C ( $0.0642 \pm 0.0523 \text{ hr}^{-1}$ ) was significantly different ( $F_{3,20}=5.32$ ,  $p < 0.007$ ) than the means of groups A ( $0.0152 \pm 0.0082 \text{ hr}^{-1}$ ), B ( $0.0164 \pm 0.0037 \text{ hr}^{-1}$ ), and D ( $0.0107 \pm 0.0065 \text{ hr}^{-1}$ ). For subjects treated with the 1% aqueous mixture of malathion in group C, approximately 6.42% of the external concentration was absorbed per hour.

As previously observed (Figure 3), the mean relative rate of absorption was rapid for the subjects exposed to the 1% aqueous mixture as compared to the 10% mixture (1.07%/hr), the 50% concentrate (1.64%/hr) and neat malathion (1.52%/hr). However, the mean total recovery of [ $^{14}\text{C}$ ]-malathion equivalents in urine of subjects treated with neat malathion in groups A ( $1.66 \pm 1.46 \text{ mg}$ ) was significantly different ( $F_{3,20}=5.51$ ,  $p < 0.01$ ) than the means for the 10% mixture, group D ( $0.30 \pm 0.10 \text{ mg}$ ) and the 1% mixture, group C ( $21.8 \pm 7.4 \text{ }\mu\text{g}$ ). The mean total recovery for group B ( $1.16 \pm 0.61 \text{ mg}$ ) was not significantly different than the group A mean. After adjusting for the applied dose, however, the mean cumulative percent of the applied dose of group C ( $16.2 \pm 7.0\%$ ) was significantly different ( $F_{3,20}=5.77$ ,  $p < 0.005$ ) than the means for groups A, B and C (Table III). The 1.0% aqueous mixture appeared to be more readily and efficiently absorbed than the other formulations with greater concentrations of malathion.

The relative rate of absorption of the 1% aqueous material was significantly more rapid than any of the other materials yet the rate of elimination was not significantly different (Table III). For certain subjects exposed to the 1% material in group C (C2, C3, C4, and C5), the rate of absorption was nearly equal to the rate of elimination as indicated by the  $k_e/k_a$  ratio (Table III). However, in like manner, other subjects in group C demonstrated a far slower rate of absorption compared to elimination ( $k_e/k_a \geq 10$ ). Subjects in groups A and B demonstrated consistently but not significantly ( $F_{3,20}=1.61$ ,  $p < 0.22$ ) slower rates of absorption relative to rates of elimination than subjects in groups C.

A substantial amount of the external concentration remained unaccounted for as part of the site wash and that recovered in urine (Table II). This material might have become associated with the stratum corneum or absorbed and distributed into other tissues and organs. To understand the disposition of the applied dose a dermal absorption study was conducted in the rat.

**Dermal Absorption Study in the Rat.** The distribution of [ $^{14}\text{C}$ ]-malathion equivalents in selected tissues of the rat may be viewed in Figure 10. The percent of the applied dose (73.8 mg) declined rapidly leaving  $19.5 \pm 0.7\%$  of the neat and  $12.5 \pm 0.2\%$  of the 50% EC formulation in the excised skin at 24 hours. The amounts in skin were significantly different between days ( $F_{4,12}=2612.29$ ,  $p < 0.001$ ) when the animals were sacrificed and the tissue excised. The total amount in skin was not significantly different ( $F_{1,12}=0.041$ ,  $p < 0.50$ ) between formulations (Table IV). The 50% EC malathion appeared to be retained in the skin longer than the neat formulation. The rate constant for absorption of the neat malathion

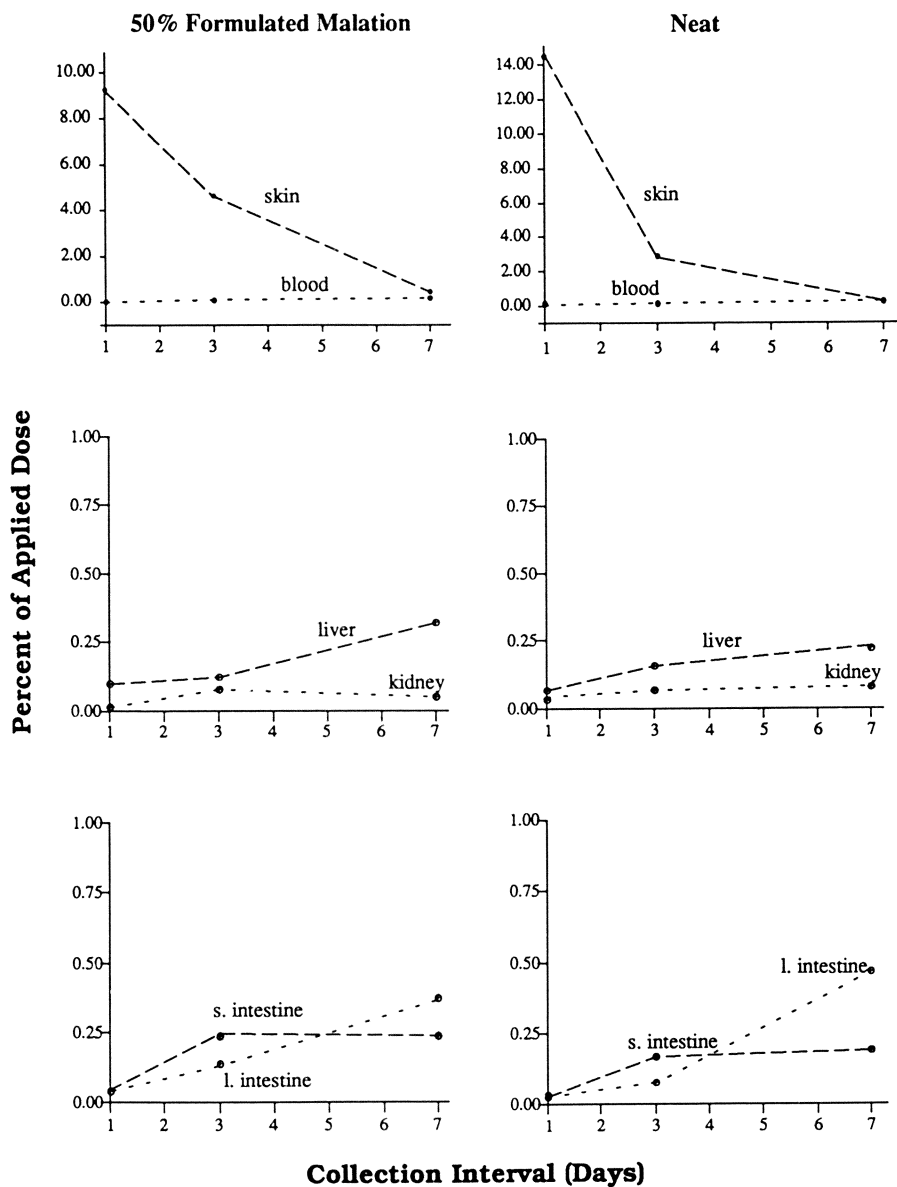


**Figure 10. Cumulative Percent of the Applied Dose of  $[^{14}\text{C}]$ -Malathion in Selected Tissues of Rats Treated with Neat Malathion and the 50% EC Formulation.**

Table IV. Disposition of [<sup>14</sup>C]Malathion Equivalents as Percent of the Applied Dose in Blood, Tissues, and Excreta of the Rat

Neat Malathion							
Selected Tissues				Excreta			
Day	Blood	Skin	Liver	Kidney	S.Intestine	L. Intestine	Feces
1	0.201±0.14	19.5±0.7	0.09±0.03	0.05±0.01	0.04±0.01	0.04±0.01	8.58±1.05
2	NA	NA	NA	NA	NA	NA	3.21±0.11
3	0.14±0.10	3.98±0.07	0.22±0.05	0.03±0.01	0.08±0.01	0.10±0.04	0.98±0.08
4	NA	NA	NA	NA	NA	NA	2.42±0.26
5	NA	NA	NA	NA	NA	NA	2.34±0.17
6	NA	NA	NA	NA	NA	NA	4.47±0.16
7	0.30±0.08	0.29±0.01	0.30±0.01	0.11±0.00	0.26±0.01	0.64±0.06	4.45±0.02
50% EC Formulation							
Selected Tissues				Excreta			
Day	Blood	Skin	Liver	Kidney	S.Intestine	L. Intestine	Feces
1	0.06±0.01	12.5±0.2	0.13±0.06	0.02±0.01	0.05±0.00	0.05±0.00	11.5±1.0
2	NA	NA	NA	NA	NA	NA	7.27±0.11
3	0.13±0.11	6.27±0.03	0.17±0.02	0.04±0.01	0.11±0.01	0.19±0.01	3.33±0.03
4	NA	NA	NA	NA	NA	NA	1.27±0.11
5	NA	NA	NA	NA	NA	NA	0.88±0.02
6	NA	NA	NA	NA	NA	NA	0.88±0.04
7	0.26±0.03	0.65±0.01	0.44±0.01	0.07±0.01	0.03±0.02	0.51±0.01	0.55±0.01

( $k_a=0.0289 \text{ hr}^{-1}$ ) as determined from the slope of the log-linear regression ( $b=0.6945$ ,  $r^2=0.9967$ ) over the seven day period of exposure was significantly greater ( $t_{14}=4.307$ ,  $p<0.01$ ) than the rate constant for 50% EC formulation ( $b=0.5033$ ,  $r^2=0.9882$ ,  $k_a=0.0210 \text{ day}^{-1}$ ).

By this means of analysis, the remaining neat malathion was absorbed at the rate of 2.89% per hour and the 50% EC malathion at the rate of 2.10% per hour over the seven day period of exposure. The absorption half-time for the neat malathion was nearly 24 hours ( $T_{\text{absorp}1/2}=23.9 \text{ hrs}$ ). The absorption half-time for the 50% EC formulation was more protracted ( $T_{\text{absorp}1/2}=33.0 \text{ hrs}$ ). The rates of absorption of the neat and 50% EC formulation in the rat were more rapid but not inconsistent with those for the human,  $k_a=0.0152 \text{ hr}^{-1}$  and  $k_a=0.0164 \text{ hr}^{-1}$  for the neat and 50% EC formulation respectively.

The amount of malathion entering the vascular compartment after one, three and seven days of exposure (Figure 10) did not differ between days ( $F_{4,12}=1.13$ ,  $p<0.25$ ) and formulations ( $F_{1,12}=1.97$ ,  $p<0.25$ ). Conceivably, blood amounts had reached a minimum after 24 hours of exposure. Amounts of malathion in selected tissues were similarly near limits of detection and acceptance (Figure 10). Concentrations of [ $^{14}\text{C}$ ]-malathion equivalents in brain, heart, and lung were below the twice background level of detection and acceptance. While the mean percent of the applied dose of malathion in blood declined over the sampling time points, the mean percent in the selected tissues increased (Figure 10). Significant increases were observed among sampling time points (days) in liver ( $F_{4,12}=45.6$ ,  $p<0.01$ ), kidney ( $F_{4,12}=131.8$ ,  $p<0.001$ ), small intestine ( $F_{4,12}=340.1$ ,  $p<0.001$ ), and large intestine ( $F_{4,12}=224.5$ ,  $p<0.001$ ). Mean percent accumulated in the tissues was not significantly different between formulations.

No more than an average of 2.0% of the applied dose of the 50% EC formulation and the neat malathion were recovered at any collection period in the selected tissues, liver, kidney, and small and large intestine. The circulating concentrations remained at less than 0.3% of the applied dose of neat malathion and the 50% EC formulation at each collection period (Table IV). A cumulative total of 25.7% of the applied dose of the 50% EC formulation and 26.5% of the neat malathion were recovered in the urine excreted over the seven day period (Figure 11). Cumulative recovery of the 50% EC formulation (0.92%) and the neat malathion (1.80%) in feces represented less than 2.0% of the applied dose (Figure 11).

These observations suggest that more than 80% of applied dose of neat malathion and the 50% EC formulation was either lost through evaporation or absorbed and distributed in the carcass within the first 24 hours. From figure 11, it can be seen that  $8.58\pm1.05\%$  of the neat malathion and  $11.5\pm1.0\%$  of the 50% EC formulation were excreted at 24 hours suggesting that 60% of the absorbed dose remained in the system. The excretion rate constant for the neat malathion ( $k_e=0.00447 \text{ hr}^{-1}$ ) would predict that 10.7% of the absorbed dose would be excreted in 24 hours (Figure 11). The excretion half-time was determined as 6.46 days. Excretion of neat malathion appeared to be incomplete.

The excretion of the 50% EC formulation was more rapid than the neat malathion (Figure 11). The excretion rate constant ( $k_e=0.0118 \text{ hr}^{-1}$ ) would predict that 28.1% of the absorbed dose would be excreted in the first 24 hours and half of the absorbed dose would be excreted in 2.45 days. However, this prediction like that for the neat malathion was inconsistent with the cumulative recovery in urine. The excretion of the 50% EC formulation appeared to be complete.

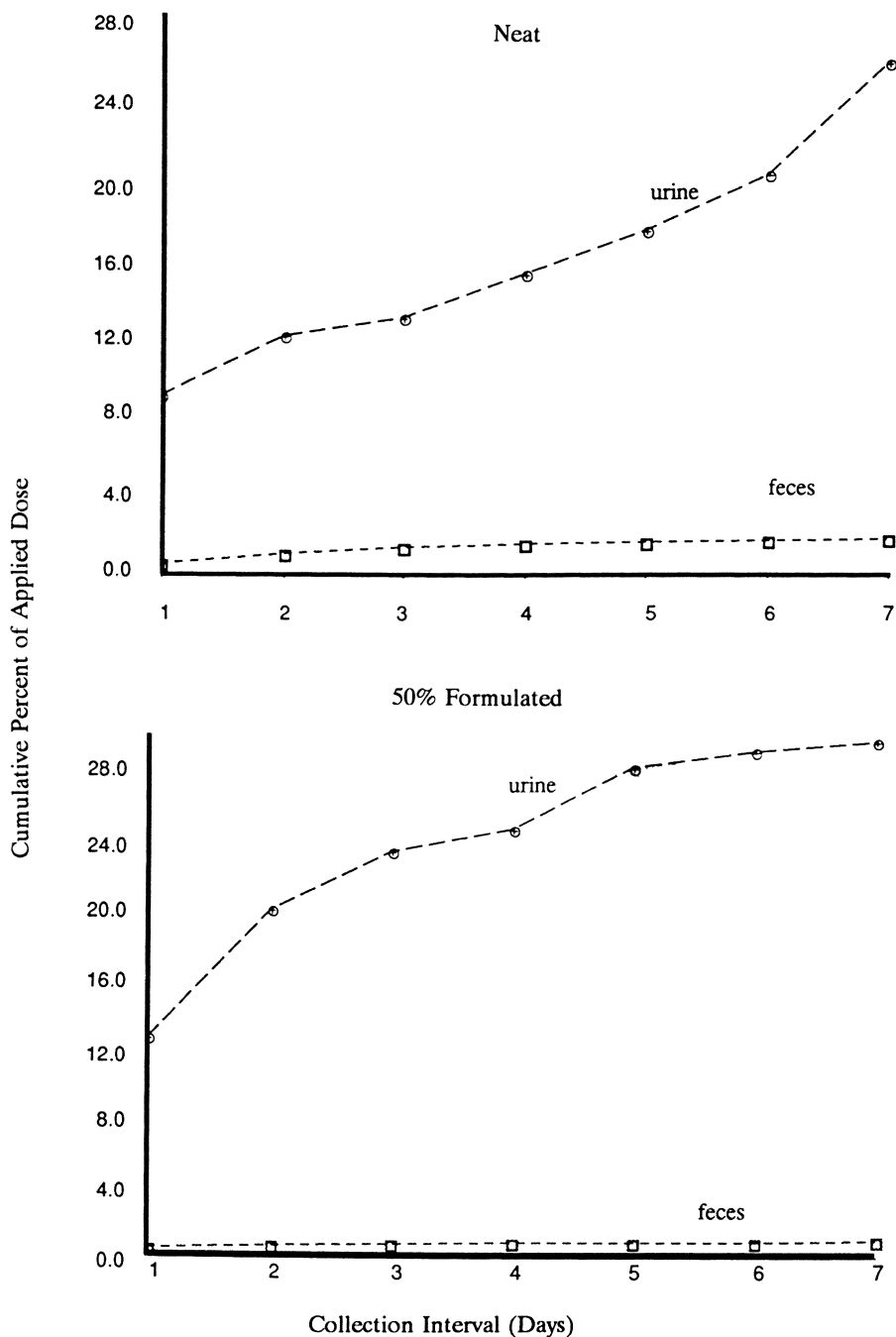


**Figure 11. Percent of the Applied Dose of [ $^{14}\text{C}$ ]-Malathion in Urine and Feces of Rats Exposed to Neat Malathion and the 50% EC Formulation.**

This accounting summary points out that approximately 70% of the applied dose of the formulations remained unaccounted for in the excreta and in the selected tissues. It also points out the importance of incorporating material balance as part of a dermal absorption protocol. We may assume that the remaining 70% of the applied dose may be accounted for in the carcass or through loss due to evaporation.

## Discussion.

In a study aimed at determining skin penetration and distribution of selected insecticides including malathion, Reifenrath et. al. (10) observed a significant loss by evaporation of [ $^{14}\text{C}$ ]-malathion ( $4.0\text{ }\mu\text{g}/\text{cm}^2$ ) applied topically to excised pig skin in vitro after increasing the air flow over the skin surface for 48 hours. The rate of evaporative loss increased from 24 percent of the applied dose at 60 mL air/min to 74% at 600 mL air/min. However, at the air flow rate of 60 mL/min, 31% of the applied dose remained associated with the skin surface and the epidermis while 21% penetrated into the receiving fluid.

These results demonstrate, as pointed out by Reifenrath et. al. (10) the importance of controlling experimental conditions that influence surface loss and penetration. In the human study reported herein, the site of application was occluded after a four hour period of observation for skin irritation. The occlusive patch was removed after 24 hours of exposure. An average of  $29.5\pm 13.0\%$  of the applied dose was found in the occlusive patches used to cover the application sites of subjects exposed to neat malathion in group A. This average percent of the applied dose which was unavailable for absorption was not significantly different than those of groups B ( $32.2\pm 6.2\%$ ) and D ( $21.8\pm 11.9\%$ ). The mean percent of the applied dose found in the patches of subjects in group C ( $65.4\pm 31.3\%$ ) was significantly greater than groups A, B, and D ( $F_{3,20}=6.75$ ,  $p<0.0025$ ).

The percent of the applied dose recovered in the occlusive patches may represent evaporative and mechanical loss. On average this loss was greatest for subjects treated with the 1.0% aqueous mixture. Loss of the dose applied to the rats would be expected to have occurred as it did for the humans. Reifenrath et. al. (10) observed a 48% evaporative loss of parathion ( $4.0\mu\text{g}/\text{cm}^2$  in ethanol) in the absence of a flow of air over the skin surface over 24 hours. At the same time, the skin surface and the epidermal layer retained 78% of the applied dose which declined steadily to 26% after 24 hours. Four percent of the applied dose penetrated the excised skin to enter the receiving fluid while seven percent remained in the dermis; approximately 18% of the applied dose remained unaccounted for (10).

By accounting for percent of the recovered dose of dermally applied [ $^{14}\text{C}$ ]-carbaryl and [ $^{14}\text{C}$ ]-parathion in the carcass as well as urine, feces, blood and liver, Shah and Guthrie (9) were able to account for more than 95% of the carbaryl and nearly 99% of the parathion. After four hours of exposure, approximately 25.7% of the carbaryl and 5.77% of the parathion were found in the carcass. The proportion of the dose of both insecticides declined in the carcass to less than 2.0% after 120 hours as the cumulative recovery in the feces and urine increased. As was observed for malathion in this study, the proportion of the applied dose of carbaryl and parathion in blood remained below 0.10%; the proportion in liver less than 0.6%.

Shah and Guthrie (9) observed that the direct measurement of radio-equivalents in blood, tissues and excreta correlated with the method of indirect excretion analysis of Feldman and Maibach (8) where the recovery of the dermal dose in urine is adjusted for incomplete elimination in the system by a paired

analysis of recovery of an intravenous dose. By this method, Feldman and Maibach (8) determined that  $8.2 \pm 2.7\%$  of a dermal dose of [ $^{14}\text{C}$ ]-malathion ( $4.0 \mu\text{g}/\text{cm}^2$  in acetone) applied to the ventral forearm of human volunteers was eliminated in a five day period. The elimination went to near completion. They did not derive elimination rate constants or elimination half-times from the dermal data. The elimination half-time for the intravenous administration of malathion was given as three hours. The elimination went to completion and  $90.2 \pm 9.7\%$  of the dose was recovered in the urine.

Using the data of Feldman and Maibach (8), Fisher et. al. (1) determined a peak excretion rate of  $0.073 \text{ hr}^{-1}$  for the dermal application of malathion by their method of deconvolution. The peak excretion rate of the i.v. dosing was  $14\%$  per hour. The time required to reach the peak ranged from 2 to 3 hours ( $T_{\text{elim } 1/2} = 9.49$  hours). Peak excretion of the dermal application was not given but could be estimated as between four and eight hours. The total cumulative percent absorbed was estimated as  $6.53\%$  of the applied dose. The body burden over the 120 hour period of exposure was estimated as  $0.67\%$  of the dose. The peak body burden was  $2.2\%$  at eight hours.

The results of the human study reported here for the absorption of malathion appear to be consistent with Feldman and Maibach (8) and Fisher et. al. (1). The mean percent recovery of the neat malathion ( $7.35 \pm 5.93\%$ ), the 50% EC formulation ( $5.74 \pm 3.09\%$ ) and the 10% aqueous mixture ( $6.00 \pm 2.82\%$ ) were in near agreement with the estimates reported by Fisher et. al. (1). The mean recovery of the 1.0% aqueous ( $16.2 \pm 7.0\%$ ) mixture was significantly different than the other formulations. The 1.0% aqueous mixture was more readily absorbed on the basis of the percent of dose and efficiently excreted than the other formulations (Table III). From the point of view of exposure assessment, absorption of a 1.0% mixture of an active ingredient (mean concentration of  $31.0 \pm 5.0 \mu\text{g}/\text{cm}^2$ ) at the rate of  $6.4\%$  per hour would likely represent less of a health risk than exposure to a concentrated formulation absorbed at the relative rate of  $1.6\%$  per hour as observed for the 50% EC formulation.

However, as has been observed from this study both for the human and the rat treated with malathion as well as the work of Reifenrath et. al. (10), Shah and Guthrie (9) and Feldman and Maibach (8), a substantial portion of the dermal dose of the insecticide formulation remained outside of the system. For the work of Feldman and Maibach (8), more than 90% of the applied dose of [ $^{14}\text{C}$ ]-malathion remained external to the human system. Knaak et. al. (17) predicted the retention (half-time) time of [ $^{14}\text{C}$ ]-parathion ( $40 \mu\text{g}/\text{cm}^2$ ) on the skin of the rat to be from 24.3 to 28.6 hours. Parathion was absorbed at the rate of  $0.5 \mu\text{g}/\text{hr} \cdot \text{cm}^2$  which may be interpreted as a relative absorption rate of  $1.25\%$  per hour. Knaak et. al. (17) predicted the plasma half-time to be 28.5-39.5 hour. The skin retention half-time (40 hours) and plasma half-time (67 hours) for [ $^{14}\text{C}$ ]-carbaryl was more protracted.

The intravenous dose of malathion is rapidly and efficiently eliminated in the human system (8) and the rat (11). Clearance of malathion is equally efficient by the oral route (18-19). Uptake in the tissues favored organs of metabolism and elimination. The intravenous dose of malathion is rapidly (within 1 minute after administration) distributed to the kidney and liver of the rat (11). After accounting for concentrations in the stomach, the oral dose of malathion is distributed in liver and kidney (18) although the proportions may differ between studies (19). In human forensic cases ( $n=6$ ) where the apparent suicide was caused by ingestion of a single lethal bolus of malathion, highest concentrations were recovered in kidney, blood, spleen and liver (20). From this study, a dermal dose of neat malathion and

50% EC formulation may be expected to be distributed to the liver and kidney (Table IV).

In an exposure scenario where the consumer contacts residues of the organic based pesticide concentrate on the surface of the container or splashes the concentrate or aqueous mixture on the skin (probably the hands), approximately 80% of the dose may become associated with the skin surface and the epidermis in the first 15 minutes to an hour after exposure (10). Evidence from this study indicates that  $70.5 \pm 13.0\%$  of the neat malathion and  $67.8 \pm 6.2\%$  of the 50% EC formulation can be removed from the site of application through washing. The removal of the organic based formulations was not significantly different than the removal of the 10% aqueous material ( $78.2 \pm 11.9\%$ ). However, removal of the 1.0% aqueous material ( $34.5 \pm 31.3\%$ ) was significantly different than the other formulations ( $F_{3,20}=6.75$ ,  $p < 0.003$ ). Thus washing the site within one hour after exposure could reduce the external dose of an organic based pesticide concentrate or aqueous mixture on the skin surface and the epidermis by 70 percent. The remaining 10% of the dose would be absorbed.

In the event that the site could not be washed, approximately 40% of the external dose might be lost through evaporation (10). Air flow over the site (600 mL/min) could reduce the residual concentration by 70 percent (10). The residual 30 to 40 percent of the external concentration of malathion might be absorbed at the rate of 1-6% per hour (Table III). The rate of absorption would be compound and formulation dependent (8,10) exacerbated by dose and surface area exposed (Table III). Reifenrath et. al. (10) observed nearly a tenfold greater recovery of ethanol based [ $^{14}\text{C}$ ]-parathion in urine of female Yorkshire pigs compared to neat [ $^{14}\text{C}$ ]-parathion. The choice of vehicle has been established as a means to enhance percutaneous absorption of topically applied drugs in a variety of animal models and man (21,22). Pesticides are manufactured in a variety of formulations containing a diluent (vehicles) and wetting agents. Ingredients are listed on the label. Malathion as a 50% emulsifiable concentrate (50% EC) would contain a certain percentage of an organic solvent and inert ingredients. The product is sold in a reusable container from which aliquots are drawn to prepare an aqueous mixture. Exposure may be expected to occur through repeated handling of the container and through sloppy methods of mixing and loading the sprayer.

With malathion because of its relatively low mammalian toxicity (20) compared to other organophosphorus insecticides (23) untoward effects from a single dermal exposure would be minimal unless the concentrate covered a substantial portion of the skin surface. Repeated exposure might, however, lead to injury to certain organs including the skin from repeated contact and the burden exerted on organs of elimination, primarily the kidney (21). Study of injury to these tissue may require an examination of clinical chemistries (liver enzyme profiles) in addition to histo-pathology (25).

## Conclusion.

When assessing exposure to pesticides used by the untrained consumer, consideration should be given to the rate of absorption and rate of elimination of the concentrated product and the aqueous mixture. We observed that the undiluted product, a 50% emulsifiable concentrate of malathion, is as readily absorbed by the skin of human volunteers and the shaved unabrased skin of the rat as neat malathion. The rate of absorption of neat malathion and the 50% EC formulation was dependent on surface area of exposure which increased through spreading beyond the treated area

on the ventral forearms of human volunteers. The absorption profiles of the 1.0% and 10% aqueous mixtures were significantly different than the neat malathion.

Absorption of the aqueous mixtures was concentration dependent. The relative rate of absorption was greater for the 1.0% aqueous mixture although the absolute rate of absorption and total amount of malathion absorbed was greatest for the neat malathion, the 50% EC formulation and the 10% aqueous mixture. Absorption of malathion was therefore concentration dependent. Elimination of the absorbed dose primarily through the urine, however, was not concentration dependent. Distribution of the neat malathion and the 50% EC formulation in tissues of the rat indicated retention of as much as 17% of the applied dose in the skin after 24 hours. Accumulation in the tissues favored organs of metabolism and excretion, primarily the kidney and liver.

Human exposure to malathion would likely occur through handling and spillage of the concentrate or aqueous mixture or from contact with treated surfaces. Washing the exposed site would remove approximately 70% of the concentrate from the skin surface and epidermis. An unwashed site would retain better than 80% of the dose for up to an hour after exposure. After 24 hours, 30 to 40 percent of the dose would be lost through evaporation. Circulating concentrations would be established within 12 hours after exposure. Ten percent of the residual concentration would be absorbed with nearly 90% eliminated in the urine. The slow rate of absorption and efficient rate of elimination would reduce the risk of acute toxicity for all exposures except where the concentrated formulation comes in contact with substantial portions of unprotected skin. However, repeated exposure from contact with treated surfaces could burden organs of metabolism and elimination.

A dermal absorption protocol where the purpose is exposure assessment should be based on material balance with direct measurement of tissue concentrations in the rat. Absorption profiles should be set to collect urine and feces during the early (alpha) phase (0-24 hours) after dosing and until the concentrations fall to limits of detection (twice background) up to five days (beta phase). Tissues should be harvested at the close of the study to minimize the number of animals for sacrifice. The site of application should be excised or cleared of residual concentrations. Examination of blood should include clinical chemistries where a base line may be established prior to dosing. From this approach, absorption profiles should be examined statistically. Absorption constants ( $k_a$ ) and elimination constants ( $k_e$ ) should be estimated. Concentrations in tissues and organs should be examined in relation to the chemicals effect on metabolism and elimination.

## Acknowledgments

The authors appreciate the expert technical assistance of Mr. Peter Banka, Mr. Joseph W. Gifford and Ms. Natalie Faught in the preparation of this manuscript. In the rush of meeting deadlines and tending to business, we could not have performed as well without their aid and feel so grateful to them.

## Literature Cited

1. Fisher, H.L.; Most, B.; Hall, L.L. *Journal of Applied Toxicology*, 1985, **5**, 164-177.

2. Ross, J.; Thongsinthusak, T.; Fong, H.R.; Margetich, S.; Krieger, R. Chemosphere, 1990, **20**, 349-360.
3. Roberts, J.W.; Camann, D.E. Bulletin of Environmental Contamination & Toxicology, 1989, **43**, 717-724.
4. Fenske, R.A.; Black, K.G.; Elkner, K.P.; Lee, C.; Methner, M.M.; Soto, R. American Journal of Public Health, 1990, **80**, 689-693.
5. Berteau, P.E.; Knaak, J.B.; Mengle, D.C. In: Biological Monitoring for Pesticide Exposure; Wang, R.G.M.; Franklin, C.A.; Honeycutt, R.C., Reinert, J.C. ACS Symposium Series 382; Washington, D.C., 1989.
6. Fenske, R.A.; Curry, P.B.; Wandelmaier, F.; Ritter, L. Journal of Exposure Analysis and Environmental Epidemiology, 1991, **1**, 11-30.
7. Wright, C.G.; Jackson, M.D. Bulletin of Environmental Contamination & Toxicology, 1975, **13**, 123-128.
8. Feldman, R.J.; Maibach, H.I. Toxicol. Appl. Pharmacol., 1974, **28**, 126-132.
9. Shah, P.V.; Guthrie, F.E. The Journal of Investigative Dermatology, 1983, **80**, 291-293.
10. Reifenrath, W.G.; Hawkins, G.S.; Kurtz, M.S. Journal of Pharmaceutical Sciences, 1991, **80**, 526-532.
11. Maun, B.; Nafstad, I. J. Agric. Food Chem., 1989, **37**, 210-213.
12. Winer, B.J.; Brown, D.R.; Michels, K.M. Statistical Principles in Experimental Design, McGraw-Hill: New York, 1991.
13. SAS/STAT User's Guide, Release 6.03 Edition, SAS Institute Inc.: Cary, NC, 1988, 1028 pp.
14. SPSS for Windows™: Advanced Statistics, Release 5, SPSS Inc., 1992.
15. Barry, B.W. Dermatological Formulations, Mercel Dekker, Inc.: New York, Basel, 1983.
16. Goldstein, A.; Aronow, L.; Sumner, M.K., Principals of Drug Action: The Basis of Pharmacology, John Wiley & Sons: New York, 1974.
17. Knaak, J.; Iwata, I.; Maddy, K.T. In: The Risk Assessment of Environmental and Human Health Hazards: A Textbook of Case Studies; Paustenbach, D.J., Ed., John Wiley & Sons, New York, 1989.
18. Bourke, J.B.; Broderick, E.J.; Hackler, L.R.; Lippold, P.C., J. Agr. Food Chem., 1968, **16**, 585-589.
19. Lechner, D.W.; Abdel-Rahman, M.S., Journal of Toxicology and Environmental Health, 1986, **18**, 241-256.
20. Jadhav, R.K.; Sharma, V.K.; Rao, G.J.; Saraf, A.K.; Chandra, H. Forensic Science International, 1992, **52**, 223-229.
21. Wester, R.C.; Noonan, P.K.; Maibach, H.I. Arch. Dermatol. Res., 1980, **267**, 229-235.
22. Wester, R.C.; Maibach, H.I.; Bucks, D.A.; Guy, R.H. Toxicology and Applied Pharmacology, 1983, **68**, 116-119.
23. Eto, M. Organophosphorus Pesticides: Organic and Biological Chemistry, CRC Press: Cleveland, 1974.
24. Imamura, T.; Hasegawa, L. Toxicology and Applied Pharmacology, 1984, **72**, 476-483.
25. Syed, M.A.; Arshad, J.H.; Mat, S. J. Environ. Sci. Health, 1992, **27**, 347-354.

RECEIVED September 17, 1993

## Chapter 16

# Physiologically Based Pharmacokinetic Models Examples of Their Use in Exposure and Risk Assessment

Jerry N. Blancato<sup>1</sup> and Mahmoud A. Saleh<sup>2</sup>

<sup>1</sup>Office of Research and Development, Environmental Monitoring Systems Laboratory, U.S. Environmental Protection Agency, Las Vegas, NV 89193

<sup>2</sup>Environmental Chemistry and Toxicology Laboratory, Department of Chemistry, Texas Southern University, Houston, TX 77004

Pharmacokinetics describes the time course disposition of a xenobiotic, its biotransformed products, and its interactive products within the body. It includes a description of the compounds's absorption across the portals of entry, transport and distribution throughout the body, biotransformation by metabolic processes, interaction with biomolecules, and eventual elimination from the body.

Pharmacokinetic (PK) analyses or assessments can be used in two very general ways. First, they can be applied for forward analysis. Such PK analyses use exposure data to calculate biologically meaningful measures of dose. Second, they can be applied for reconstructive dose assessment. In this case, data on measured biomarkers or tissue concentrations of a compound and/or its metabolites are used to calculate total dose of a xenobiotic received by an organism. This paper will focus on general concepts of model structure, examples of their use and examples of the use of models for analysis of biomarker data.

Pharmacokinetics is the study and description of the processing of chemical compounds by living organisms. The movement of compounds throughout the body is a kinetic rather than static process. Foreign molecules and endogenous biomolecules exhibit, like all other molecules in the universe, continuous motion. Thus, the representation of the interaction of xenobiotics and biologic tissues as a static process is an inaccurate oversimplification. It is easy to imagine foreign invaders cross membranes, floating in the blood, attaching themselves as free riding passengers onto the surfaces of cells, organelles, and receptors. They may readily embrace and interact with the very enzymes and molecules that maintain life itself.

0097-6156/94/0542-0264\$06.00/0  
© 1994 American Chemical Society

More specifically, pharmacokinetics describes the time course disposition of a xenobiotic, its biotransformed products, and its interactive products within the body. It includes a description of the compound's absorption across the portals of entry, transport and distribution throughout the body, biotransformation by metabolic processes, interaction with biomolecules, and eventual elimination from the body.

There are two general ways to use pharmacokinetic (PK) analyses. First, they can be used for forward analysis. For forward analysis the risk assessor uses exposure data to calculate meaningful measures of dose. Second, the assessor can apply PK analysis to reconstruct dose from biomarkers of exposure. There are several ways to do such analyses but pharmacokinetic models are the emerging technique of choice. These models include a series of mass balance equations that describe the total disposition of the xenobiotic within the body. These models are formulated in as a complex or simple fashion as the data allow or demand and then set up and solved on computers.

Two types of models can be used. Classical models have been traditionally used in clinical situations to help optimize therapeutic doses. These depend on rate constants describing the transfer of xenobiotics usually between one and two arbitrary compartments. Although simple mathematical manipulation shows the rate constants to be meaningfully related to actual physiologic and thermodynamic parameters, the utility of the classical models tend to be better suited for descriptive rather than predictive purposes. While useful for optimizing therapeutic doses, they do not lend themselves easily for interspecies extrapolations of dose. Because these classical models tend to describe the body as one or two compartments, many physiologic and metabolic process are implicitly lumped together. As stated, the intercompartmental rate constants for transfer can be mathematically shown to have physiologic meaning. However, because of this implicit lumping, the models only fit the actual data when the rate constants are adjusted from their theoretical mathematically derived values. As a result, their actual value can no longer be exactly predicted from actual physiologic and thermodynamic properties. When clinical or environmental conditions and the exposed species change, the rate constants must be readjusted to fit the new data. New data sets are needed for each perturbation of the environmental and exposure conditions.

The second type, termed physiologically based pharmacokinetic (PBPK) models tend to be a more direct and accurate description of the actual anatomy and physiology and represent many of the body's actual organs and tissues. These models lend themselves to being better predictors of target level dose within and between species. These models have parameters that are actual physiologic constants such as blood flows, organ volumes, and metabolic rates. Although curve fitting routines are sometimes used to find values for constants that are chemical and experiment specific, values of many of the constants such as blood flow are learned from known biological data, allometric extrapolation, or independent experiments. As such, the models can be adjusted to predict for different species and for widely different exposure regimens. Frequently, the models are formulated in conjunction with experimental data for the chemical of interest. Based on these

data, other experiments, other biological data, and sometimes allometric scaling, the model can be reformulated to apply to humans exposed under various scenarios of interest. It is because of this flexibility that physiologic models are being increasingly used in exposure and risk assessments. Many physiologic processes are non-linear and the characteristics of these non-linear processes may differ between dose levels and between species. Basically the physiologic models enable the risk assessor to account, quantitatively, for differences in pharmacokinetics that occur between different species, dose levels, and exposure regimens.

The risk assessor often extrapolates from high dose animal experiments to low dose human exposure conditions. Understanding and quantifying the pharmacokinetic non-linearities can greatly reduce some uncertainties associated with this extrapolation process. It is important to note that differences in incidence of pathology between species and even individuals is probably due to more than just pharmacokinetic differences. Different organisms have different repair mechanisms, immuno-surveillance, cell numbers, and sensitivities. However quantifying pharmacokinetic differences reduces at least some of the uncertainties that exist with most assessments.

## MODEL REPRESENTATION

Figure 1 shows a typical diagrammatic representation of a physiologically based pharmacokinetic (PBPK) model which describes disposition into several body organs. Foreign substances such as pesticides and other agricultural chemicals can be introduced into the body through the respiratory system, gastrointestinal system, and the skin. Each of these portals of entry has its own unique properties and is described accordingly. The foreign substance is delivered to each of the body's organs via the arterial blood flow. This, of course, is analogous to the delivery of oxygen. Blood leaving each organ enters the venous blood and returns to the heart where it is pumped to the lungs. Here exchange occurs with alveolar air that is a mixture of pulmonary air and environmental air. It is this environmental air that may contain the foreign substances. At this point such substances may cross the pulmonary membranes into the blood to enter the arterial blood and thus to the various organs inside the body. It should also be noted that the pulmonary membrane is a possible route of elimination to the environment, especially for volatile compounds, which are in the blood. This would be analogous to the elimination process for carbon dioxide.

Although the physical and chemical nature of the substances may differ as do the exact micro-physiologic processes, similar access to the body can be gained through transmembrane passage at the other portals of entry. It should be noted however that for the case of the skin, the foreign substance enters venous blood and must be circulated through the right side of the heart and the lungs before entering the arterial portion of the circulation. Only after passing into the arterial blood does it become available for transcapillary passage into the body's organs and tissues. Thus it is possible that some materials, depending upon their physical properties, may be partially eliminated from the body before becoming available

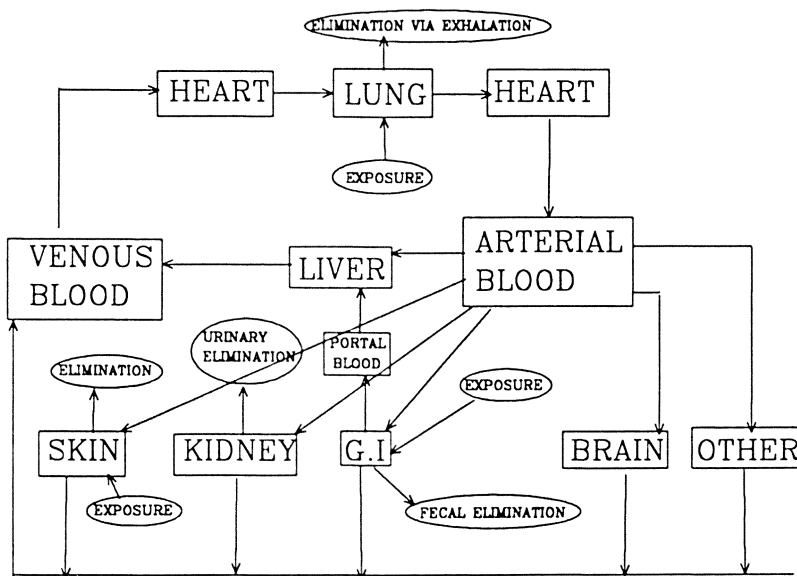


Figure 1: Diagrammatic representation of organ level physiologically based pharmacokinetic model

to the arterial circulation. Similarly for the gastrointestinal system, absorbed substances enter the venous circulation. In this case however, they must first pass through the liver via the portal vein, before entering the general systemic venous flow leading to the heart, lungs, and arterial blood. As result, biotransformation of the xenobiotic to more or less active products may occur to some extent even before the substance has become first available to the other organs via the arterial circulation. This is known as the "first pass effect" described in the pharmacology literature.

Each of the body's organs can extract some chemical from the blood with each pass of blood. Obviously, the concentration of a chemical in an organ is the difference between the concentration of the entering arterial blood and the exiting venous blood. This typical model depicts each organ as a homogeneous collection of tissues, with the chemical quickly passing into the organ and achieving equilibrium within all elements of the organ. The two assumptions inherent in this description are the perfusion limited and well-stirred assumptions. Perfusion limitation simply means that the rate limiting step (or slowest) of the process is delivery by the blood flow. That is, the passage of the chemical across the membranes into the organ is rapid compared to the perfusion rate of the blood. The well stirred assumption implies that the chemical distributes homogeneously within an organ. While these assumptions generally result in adequate models, alternate structures can be described if biologic information so warrants. Such models are described elsewhere (1-2)..

Any physiologic process affecting the chemical, such as biotransformation, can be accounted for in any of these models. Further, if the toxic chemical of interest is a product of such biotransformation it can also be incorporated into the model.

## MATHEMATICAL DESCRIPTION

Mathematically, these models consist of mass balance equations that account for all of the mass of the substance or substances of interest. In the typical physiologic models, as depicted here, the equations are ordinary differential equations. Many have no obvious analytic solutions and are solved by numerical methods.

The following equation is an example of one description at one portal of entry, the skin:

$$\frac{dC_s}{dt} = \frac{PA(C_{su} - C_s/R_{su}) + Q_s(C_{art} - C_s/R_s)}{V_s} \quad (1)$$

$V_s$ : Volume of dermal portion of skin in area of absorption

$dC_s/dt$ : Rate of change of concentration of chemical in dermis in area of absorption

$P$ : Permeation coefficient for substance across skin in cm/time

- A: Area of absorption on skin in (CM<sup>2</sup>)  
 C<sub>su</sub>: Concentration of substance of surface of skin  
 C<sub>s</sub>: Concentration of substance in dermis at area of absorption  
 C<sub>art</sub>: Concentration of substance in arterial blood  
 R<sub>su</sub>: Partition coefficient between skin surface and exposure medium  
 R<sub>s</sub>: Partition coefficient between skin and blood

The integral of the above equation over time results in the instantaneous concentration. The left side of Equation 1 is the rate of change of the concentration within the skin. The first term in the numerator of the right side describes the diffusion of the chemical from the skin surface into the dermis of the skin. This term actually describes the transport process at the environment to body interface. The second term in the numerator of the right side of Equation 1 describes the removal of the substance from the dermis by the circulating blood. This term describes the movement of the chemical from the interface (skin) to the rest of the body via the blood stream. Hence, it represents the "exposure" component for the internal body organs. This equation assumes no loss of substance to the atmosphere. If such loss occurs suitable terms would be added to the system of equations. It should also be noted that the permeation coefficient is usually a steady-state parameter. That is, it is derived from in-vitro experiments under steady-state conditions. Suitable corrections can be made for the dynamic nature of the transport process for the non steady-state conditions usually occurring in-vivo. One might expect that for some substances the permeation rate changes with time and might, for example, result in a lag time during the early exposure phase.

A typical description for entry via the lungs, at least for chemicals which reach rapid equilibrium between alveolar air and blood and for which no storage is assumed to occur in the lungs, follows (3-5):

$$Q_{Alv}C_{inh}dt + Q_tC_{ven}dt = Q_{alv}C_{alv}dt + Q_tC_{art}dt \quad (2)$$

(Ref: 5)

- Q<sub>alv</sub>: Alveolar ventilation flow  
 C<sub>inh</sub>: Concentration of chemical in inhaled air  
 dt: time interval  
 Q<sub>t</sub>: Total Blood Flow; C<sub>art</sub>: Concentration of chemical in arterial blood  
 C<sub>ven</sub>: Concentration of chemical in venous blood; C<sub>alv</sub>: Concentration of chemical in alveolar air

Basically this equation describes the conservation of mass within the lung. The left side of equation 2 represents the amount of chemical entering the lung from both the inhalation of contaminated environmental air and from the systemic venous return of blood from the body's organs. The right side of equation 2 represents the amount of chemical leaving the lung by exhalation and by the circulating arterial blood that carries the chemical to the rest of the body. Equilibrium between alveolar air and pulmonary blood is assumed and described according to:

$$G = \frac{C_{art}}{C_{alv}} \quad (3)$$

With the relationship described in equation 3 and with algebraic manipulation equation 2 can be transformed to:

$$C_{art} = \frac{(Q_{alv}C_{inh} + Q_t C_{ven})}{(Q_t + \frac{Q_a}{G})} \quad (4)$$

It should be noted that with this description it is assumed that alveolar ventilation is continuous rather than cyclic. The lungs are depicted as a large mixing tank into which environmentally contaminated air and material from the blood is mixed with existing pulmonary air. This continuous ventilation assumption is not necessarily physiologically accurate, but for many chemicals under typical exposure conditions the error introduced is relatively minor. For other cases, such as when concentration in the inhaled air is low or for chemicals that do not readily pass into the blood, the lung can be described in more exact and physiologic terms. In such cases the lungs can be subdivided into various dead space compartments and the ventilation described according to various oscillating patterns (6).

Gastrointestinal absorption is also described by mass balance equations. There are varying descriptions based on physiology and the characteristics of the particular exposure situation (7-8).

As previously discussed, a typical organ level representation assumes rapid equilibrium between tissue and the venous outflow blood from that tissue and that the organ is well stirred. The mathematical description for an organ under these assumptions is:

$$\frac{dC_i}{dt} = \frac{Q_i (C_{art} - C_{vi})}{V_i} \quad (5)$$

$V_i$ : Volume of organ, i

$C_i$ : Concentration of chemical in organ, i

t: time

$Q_i$ : Blood flow to organ, i

$C_{art}$ : Concentration of chemical in arterial blood

$C_{vi}$ : Concentration of chemical in venous blood leaving organ, i

Equation 5 means that the rate of change of concentration of a chemical in organ *i* (left side of equation), is equal to the difference between the concentration in the incoming arterial blood and the outflowing venous blood of organ *i* (right side of equation). The equilibrium assumption is represented by:

$$\frac{C_i}{C_{vi}} = R_i \quad (6)$$

which when transformed and substituted equation 5 results in:

$$\frac{dC_i}{dt} = \frac{Q_i (C_{art} - \frac{C_i}{R_i})}{V_i} \quad (7)$$

These organ specific equations, with their limiting assumptions already described, are derived from equations that describe the transport processes within the various organ subcompartments. In such more detailed descriptions the organs are divided into three separate regions. Chemical is depicted as passing first into the organ's blood volume as a result of some of the blood flow being shunted from the main arteries into the local capillaries. The flow through the capillaries is much slower than the main arterial flow. As capillaries fill more and more open and receive the toxin containing blood from the main arterial supply. The blood in the open capillaries can be thought of as a supply pool for the tissues of the organ. Toxin then diffuses from this capillary blood compartment into the extracellular fluid of the organ. Toxin next diffuses from this extracellular compartment across the cell membranes and into the intracellular compartment. Often, the diffusion across the capillary membrane is assumed to be very rapid and the three subcompartments are lumped into one "organ" compartment. Equations 5, 6, and 7 describe such a lumped organ. A more explicit description of the mathematical derivation of Equations 5 and 7 from these more physiologically accurate representations can be found elsewhere (2, 9).

## MODEL SOLUTION

Given the advanced computer hardware and software now available numerical integration is often the method of choice for solution of such PBPK models. Traditionally the integration was performed by using a variety of approaches such as the trapezoidal or Newton's methods. With today's more advanced computational methods a variety of more sophisticated approaches are employed. They simultaneously solve the differential equation (dy/dt) at various increments of the independent variable (dt). A record of the solved values of the change in the

dependent variable ( $dy$ ) is maintained, and the area under the curve of dependent variable ( $dy$ ) with respect to the independent variable ( $dt$ ) is the solution for the value of the dependent variable ( $y$ ). The key for success is to have the solution program choose an appropriate increment or step size ( $dt$ ) for the independent variable ( $t$ ). Making the step too large results in inaccurate results while making it too small is inefficient and time consuming.

The commonly used numerical integrators can be placed into two general categories. As their name implies, the fixed step integrators have a predetermined step size throughout the process. For many equations the only way to assure accuracy is to have the solver take very small steps at the cost of computational efficiency. Variable step integrators have a changing step size throughout the course of the integration. Step size changes according to the results of sequential solutions steps. The step size is set in relation to the calculated eigenvalues. Thus, small step sizes are taken when calculating for a rapidly changing component and larger steps when a rapidly changing component is nonexistent or insignificant. This makes these methods suited for solving stiff ordinary differential equations.

Stiff conditions can be described by specific mathematical characteristics, such as certain eigenvalues. One practical example of stiff conditions is if one variable's value is changing rapidly while another is changing slowly with respect to the independent variable. Conditions may also be stiff if within one equation the dependent variable changes very rapidly at one value of the independent variable and changes slowly at another value of the independent variable.

The most widely noted method employed to solve stiff differential equations is that of Gear (10). There are others such as the Lawrence Livermore Solver of Ordinary Differential Equations (LSODE) (11) that somewhat modify Gear's approach. Typically the various methods are now found in libraries that can be called upon as subroutines in Fortran or other computational language programs.

In recent years specialized simulation languages have been developed. These often incorporate a translator and compiler into one package. They also contain their own libraries with various mathematical capabilities including various differential equation solvers and statistical routines. Often, these allow for laboratory or monitored data to be used with the model for parameter estimation and optimization. Most also include routines for sophisticated graphical output of results. Examples of such languages include Simusolv and Adapt that are Fortran based and ScopeFit based in C-language.

Future developments will most probably evolve along two fronts. One will continue to depend upon numerical solutions. Improvements can be expected in the mathematical approximation techniques, parameter estimation routines (including the ability to easily take population variances into account), and uncertainty analysis. As model structures become more complex more powerful computational capabilities will be necessary. In some case super computers will be the hardware of choice. The second major approach will be to make new strides in developing more exact and efficient alternatives to numerical solution techniques. Quasi-analytical solutions using re-cursive techniques may be possible for some models

or for at least models under certain environmental conditions. It would be expected that these methods will lend themselves to parallel computing approaches.

## EXAMPLE

**Example 1 Toxification from Metabolism** An illustrative PBPK model, depicted in Figure 2, pictures the body as consisting of several compartments. Metabolism occurs in the liver and other vessel rich compartments. This model is similar to one developed by Hattis and Wasson (12) for butadiene. The model is being used here for hypothetical chemicals in the mixture. As described, PBPK models use physiologic and thermodynamic parameters. Organ volumes, blood flows, and metabolic rate constants are determined and become part of the model. Additional parameters, such as partition coefficients, are thermodynamic and may also be chemical specific. For actual use, appropriate thermodynamic and biochemical parameters must be determined for each of the chemicals. Realistic values for blood flows to and volumes of each organ were used. The partition coefficients and metabolic rate constants were arbitrarily chosen for illustrative purposes. This model was solved by using SIMUSOLV (Licensed to EPA by the Dow Chemical and Mitchell and Gauthier Companies and housed on one of EPA's VAX 8650 computers at the National Computing Center in Research Triangle Park, North Carolina)

For the purposes of illustration the following assumptions were made:

- 1: The mixture contains three potentially toxic chemicals that might occur in a mixture of pesticides, herbicides and other agricultural chemicals
- 2: The pharmacokinetics of each chemical are independent of the other
- 3: The metabolic pathways for each are saturable at different levels and exhibit different rates
- 4: Each has its own characteristic chemical and physical properties and thus partitions differently into the blood and the various tissues
- 5: The risk of each is directly related to the amount of chemical biotransformed by internal metabolic pathways
- 6: The risk resulting from each chemical is equal on a molar basis
- 7: Exposure is via inhalation only

Any or all these assumptions can be changed depending upon the actual chemicals in an exposure scenario. These were chosen for the purposes of illustration.

The following are the characteristics of the chemicals in this hypothetical mixture:

- |                 |   |
|-----------------|---|
| Component One   | not readily absorbed but efficiently metabolized once absorbed.                                     |
| Component Two   | not readily absorbed or metabolized, but that which is absorbed readily dissolves in fatty tissues. |
| Component Three | readily absorbed and efficiently metabolized.   |

Two exposure scenarios were compared. People could either be exposed for 30 days continuously or for two eight-hour bursts during the 30-day period. The total concentration  $\times$  time of exposure was the same. For this example the

concentration for each chemical was equal to 0.00089 mmoles/Liter for the continuous exposure and to 0.04 mmoles/Liter for the intermittent exposure. Both resulted in 0.02 (mmole/L)\*(day) over the 30-day period. Figures 3 through 5 show the results of one simulation. The exposure was simulated to occur over 30 days or 720 hours. The simulation was continued for 30 days beyond the exposure period (for a total of 60 days or 1440 hours). Exposure was either continuous or intermittent. The intermittent exposure simulated, as discussed previously, two eight-hour periods occurring on the first and fifteenth day of the exposure window.

Figure 3 shows that for component one, the intermittent exposure regimen results in a greater effective dose, as measured by the amount of material metabolized, over the 30-day exposure window. Note from the plateau on both profiles that once exposure has ceased no further metabolism occurred.

Figure 4, showing the profile for component 2, suggests that the continuous exposure results in greater effective dose than intermittent. Remember that this component is only poorly absorbed and metabolized. Thus, comparatively little material enters the body and is metabolized in the short eight hour exposure bursts of the intermittent scenario. Also, some toxic endpoints exhibit threshold behavior (as some noncancer endpoints do). Assume for discussion that this threshold is reached at eight mmoles of metabolite formed. Then, in this intermittent exposure scenario, the amount of toxin formed through metabolism would not exceed this threshold while it would for the continuous exposure.

Figure 5 shows the profile for component three. The results here are similar to those for component one. However the difference between the two exposure patterns is greater than for component one. For component three the intermittent exposure pattern results in a greater increase in the effective dose than it does for component one. This occurs because of greater metabolic capability for this compound than for the others. Also, note that the amount metabolized under either exposure condition is greater than for the other two components. This is due to the greater metabolic capability and to the more efficient absorption for this compound.

Table 1 summarizes the findings for the amount metabolized of the three components. Inspection of this Table reveals that for components one and three the intermittent exposure scenario results in slightly more effective doses (and presumably greater risk from that component) than the continuous exposure. For component two, on the other hand, the opposite is true. There is a fivefold reduction in effective dose produced (under the assumptions used here) for the intermittent exposure scenario compared to the continuous exposure scenario.

The last row of the table shows the results of adding the effective doses of all three components. Under most practical circumstances this would not be appropriate. To determine risk estimates, dose response functions for each component would be used and estimates of risk for each component would thus be derived. Then the two scenarios would be compared. However it should be recalled that here it was assumed for simplicity that each of the components produced equal risk on a molar basis; the effective doses have been added to arrive at some estimate of total effective dose. From this it can be observed that in this case the intermittent scenario produces more effective doses than the continuous.

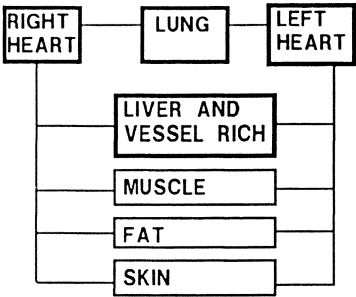


Figure 2: Physiologically based pharmacokinetic model used for this illustration

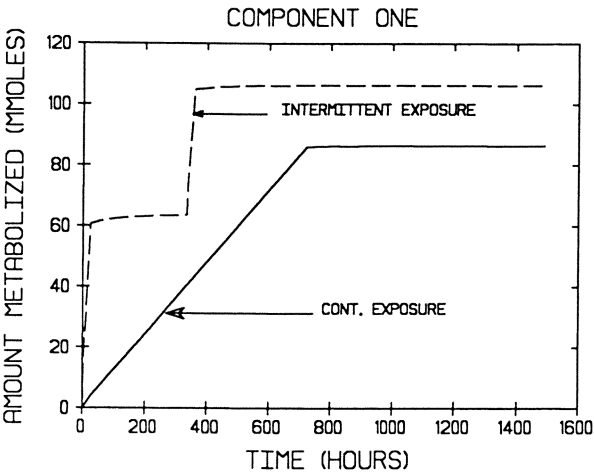


Figure 3: Model results for the amount metabolized after exposures to component one in the hypothetical mixture

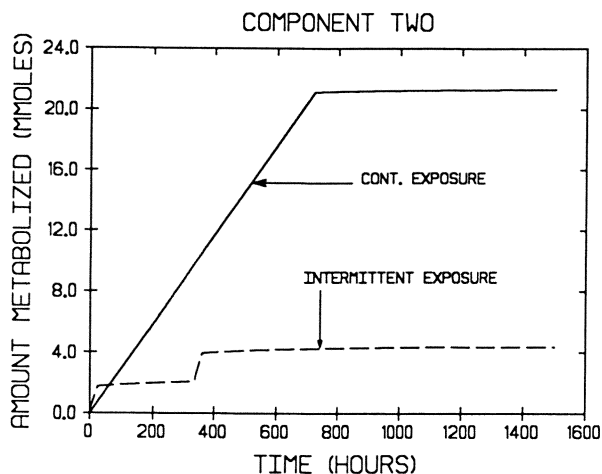


Figure 4: Model results for the amount metabolized after exposures to component two in the hypothetical mixture

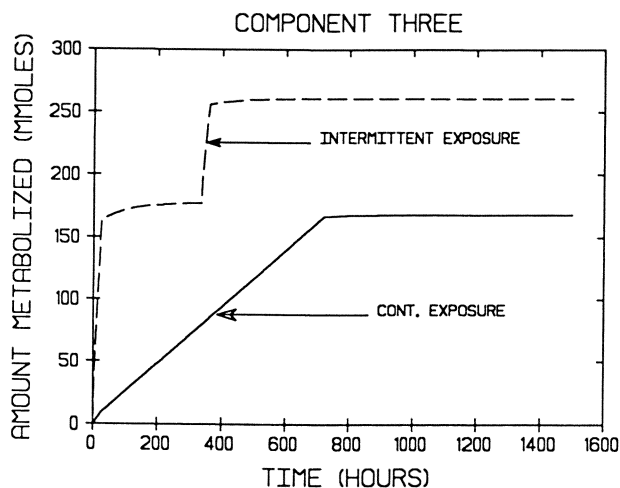


Figure 5: Model results for the amount metabolized after exposures to component three in the hypothetical mixture

**Example 2 - Biomarker** In some cases because of the paucity of data regarding parameters or the nature of the distribution of the compound within the body a simpler representation of the body is warranted. This may prove to be especially true when biomarker data in the form of body burden or urinary metabolites are used for exposure analysis. Given the mathematical complexity involved in reverse calculation (calculating exposure from internal biomarkers) and the complex physiology often involved, complex, albeit representative models, may not always be practical. In fact, they may often result in models which cannot be used because of lack of knowledge regarding key parameters. In other cases they may be overparametrized and one has little confidence in the resultant calculations. Thus, depending upon the nature of the toxin and the information desired more compact lumped models can sometimes be used. The second model depicted here is such an example. The body is described as having three pertinent compartments, the blood, the fat, and the remainder of the body called "the body." This model, which might apply for substances, such as the large organochlorine molecules, which have a significant tendency to partition in the fat. A simple model used here assumes such partitioning into fat, steady-state intakes (as might be expected to have occurred with some pesticides such as DDT), and linear elimination kinetics. With these assumptions the following equations describe the model:

$$\frac{dC_{bo}}{dt} = \frac{Q_{bo} \left( C_B - \frac{C_{bo}}{R_{bo}} \right) - K(C_{bo}) + D}{V_{bo}} \quad (8)$$

$$\frac{dC_F}{dt} = \frac{Q_F \left( C_B - \frac{C_F}{R_F} \right)}{V_F} \quad (9)$$

$$\frac{dC_B}{dt} = \frac{Q_F \left( \frac{C_F}{R_F} \right) + Q_{Bo} \left( \frac{C_{bo}}{R_{bo}} \right) - C_B (Q_F + Q_{bo})}{V_B} \quad (10)$$

- $C_{Bo}$ : Concentration of toxin in body compartment
- $Q_{Bo}$ : Blood flow to body compartment
- $C_B$ : Concentration of toxin in blood
- $K$ : Clearance of toxin from body
- $D$ : Dosing term or function of toxin into body
- $V_{Bo}$ : Volume of body compartment
- $C_F$ : Concentration of toxin in fat
- $Q_F$ : Blood flow to fat
- $R_{Bo}$ : Partition coefficient between body compartment and blood
- $R_F$ : Partition coefficient between fat and blood
- $V_F$ : Volume of fat
- $V_B$ : Volume of blood

The clearance term  $K$ , in Equation 8 is, for this case, written as a first order elimination rate. Clearance can also follow other types of kinetics including such mixed-order types as Michaelis-Menten. The  $K$  term would be replaced by an appropriate expression for those cases. Likewise the  $D$ , or dosing term, in Equation 8 can be replaced by different expressions, depending upon the nature of the dosing and absorption processes. In this example, for the sake of simplicity, clearance has been assumed to be a first order-process and dosing to be a simple zero-order process.

The model is used here to determine daily dose from blood lipid or adipose tissue data. Several assumptions are made for this example. First, the compound is fat soluble and the partitioning between fat and blood is known and is constant along the concentration range of interest. Second, the elimination kinetics are first order and the dosing kinetics are zero order. Third, the compound partitions similarly in the remaining tissues of the body (other than fat and blood). Fourth, the biological half-life of this compound is in the order of several years. Fifth, the dosing is at some steady-state, that is, the dosing of this compound can be modeled as occurring consistently over the exposure period. Such dosing might result from the wide contamination of many common food products eaten on a regular basis. The model can be modified to account for alterations in any of these assumptions. This particular set of assumptions is chosen for this example mainly for the sake of brevity. It should also be noted that the structure of this model simply tracks the parent compound rather than any metabolite. It is used here for analysis of biomonitoring data rather than for target dose assessment.

The model can be applied to determine dose under the above assumptions from biomonitored data. Values for the partition coefficients are determined in the laboratory or taken from published literature sources. The value for the clearance term ( $K$ ) is determined from monitoring data. For many compounds half-lives are known as are body burden levels (including adipose or blood lipid levels). The initial conditions of the model are then set to those body burden levels and the dosing term or function is set to zero. The value of  $K$  is then optimized to result in a half-life which agrees with the published or monitored data. Appropriate analyses can also be incorporated to account for population variance in the parameters.

Levels in blood or fat tissues are considered as the biomarker. Monitoring adipose tissue levels is inconvenient, however blood lipid levels for many compounds correspond well with levels in adipose tissues (Schecter 1991). Concentrations in whole blood can also be used, however these are often too low for measurement. Figure 6 shows the concentration profile in the fat (CF) and the body (CBO) of the pesticide "X" after a daily dose of 0.5 ng/kg body weight/day. It should be noted that the model is written to account for growth of the individual from birth to the 20<sup>th</sup> year (3.2 kg at birth growing to 77 kg at age 20 and remaining at 77 kg until age 70).

Under the assumptions outlined above the model is used to optimize dose against monitored levels in either the whole blood, blood lipid, or adipose tissue. Table 2 summarizes the results for such optimizations at various monitored

Table 1. Amount Metabolized as a Result of Different Exposure Conditions

COMPONENT	CONTINUOUS EXPOSURE -- AMOUNT METABOLIZED	INTERMITTENT EXPOSURE -- AMOUNT METABOLIZED	RATION OF INTERMITTENT TO CONTINUOUS -- AMOUNT METABOLIZED
ONE	86.39	106.13	1.19
TWO	21.28	4.36	0.20
THREE	168.29	260.84	1.55
SUM OF 1, 2, 3	275.96	368.33	1.33

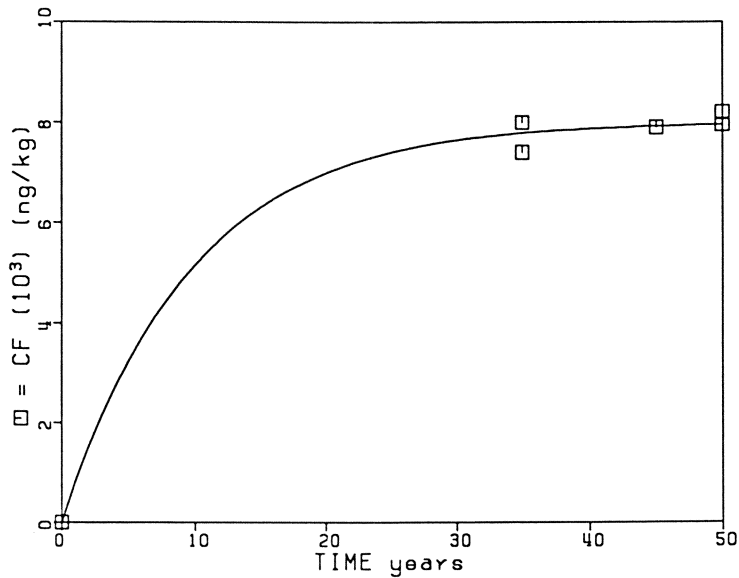


Figure 6: Model fit to steady-state data for determination of daily intake

concentrations in the blood lipid or adipose tissue for pesticide "X." The adipose tissue concentrations were assumed to be monitored at steady-state levels (plateau region on Figure 6).

As an alternative, monitoring can be repeated at various time points. The monitoring strategy should be carefully designed to assure that several points are taken along the steep non steady-state portion of the curve. Monitoring along the steady-state portion of the curve need only be repeated to assure that steady-state is being maintained. The model is then optimized in reference to the monitored data to estimate daily dose. Figure 7 shows the results of such an analysis for pesticide "X", where the biological half-life was set at a value slightly greater than 6 years. The optimized daily intake from these "data" was 0.55 ng/kg/d. This value is similar to that obtained from the case where only steady-state data were available (see Figure 6). A second optimization scenario was performed with several more data points added, and with the half-life varying between 4 and 7 years. The results are shown in Figure 8. In this case the resultant daily intake was 0.82 ng/kg/d. and the optimal half-life was slightly greater than 4 years. Close inspection of Figure 8 reveals that the fit to data in the early phase is improved when more data are collected and used. The fit to the plateau (steady-state) levels was most probably improved by allowing the half-life to vary to as short as > 4 years (compared to > 6 year value used in Figures 6 and 7). This type of analysis has revealed that given a half-life of > 6 years the current model overpredicts the steady-state fat levels. Further analysis were performed varying other key parameters (partition coefficients and compartment volumes). Results showed little or no improvement in the fit. In fact, any improved fit to steady-state levels came at the expense reduced agreement for the rising phase. From this rather simple analysis it is quickly realized that the model is very sensitive to the elimination rate (derived from the half-life). Thus, in an actual monitoring situation studies would be designed for its accurate determination.

With results such as these how is one to determine the actual daily intake? If the half-life is clearly and confidently determined as being in the 6 year range, one must assume that the daily intake is nearly equal to 0.55 ng/kg/d. That the model slightly ill-fits the data (Figure 7) indicates that elimination might be better described some type of mixed kinetics such as the Michaelis Menten form. More probable however, is that half-life determinations vary somewhat and the 4 to 6 year range chosen here (with the shorter value resulting in the fit observed in Figure 8) is not unreasonable. Thus, one might conclude that the average daily dose for the data set monitored is between 0.55 and 0.82 ng/kg/d.

## SUMMARY AND CONCLUSION

PBPK models are useful for examining the impact that different exposure scenarios have on the amount of effective (presumably the toxic dose) which is available to critical organs and tissues. This approach can be used even for mixtures of two or more agricultural chemicals that can separately cause toxicity. With proper knowledge of metabolism and other physiologic processes for a particular chemical,

Table 2. Adipose Tissue Concentration after Three Different Daily Doses

Adipose tissue or blood lipid concentration (ng/g)	Daily dose (ng/kg/d)
4.0	0.25
8.0	0.50
11.0	0.68

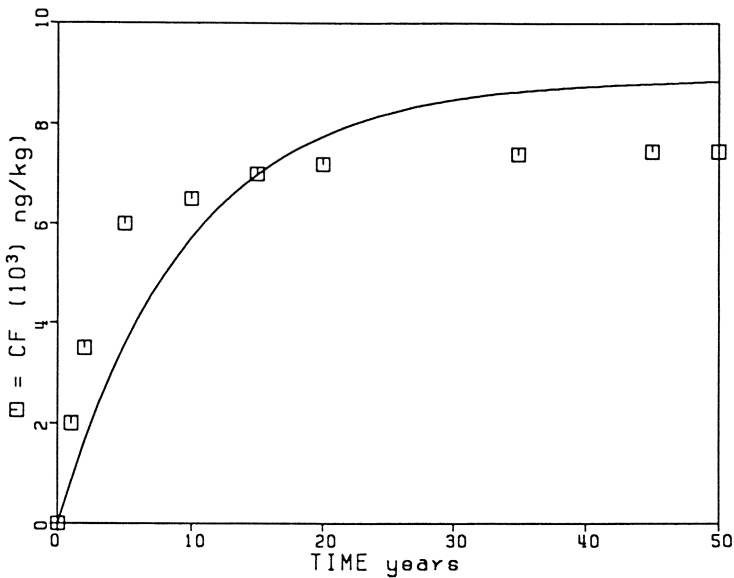


Figure 7: Model fit to non and steady-state data for determination of daily intake, fixed half-life

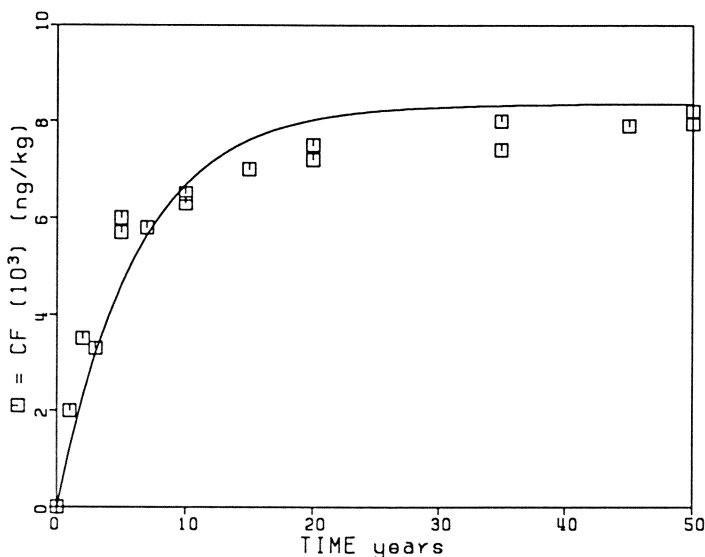


Figure 8: Model fit to non and steady-state data for determination of daily intake, varying half-life

pharmacokinetic interactions between the components of the mixture can also be accounted for by these types of models.

The demonstrations presented in this chapter were deliberately simplified for the sake of brevity. One example demonstrated the use of PBPK models to determine target level dose, an important function for helping perform rational risk assessments. The second example demonstrated the use of lower resolution model (only three compartments) to estimate daily intake (total body dose) from biomonitoring data. Due to the nature of such problems unique solutions may not always result, particularly when numerical solution techniques are employed. Analytic or quasi-analytic solutions which are generally more exact may have to be employed for this purpose. The reader is referred to the Chapter by Brown in this volume for greater detail on such solution techniques.

Computers and advanced computational techniques offer the ability to solve models that are highly descriptive of the complex biologic process within the body. Thus, it is hoped that more rational and reliable estimates of dose and eventually risk may be made.

**Acknowledgment:** The information in this document has been funded wholly by the United States Environmental Protection Agency. It has been subject to Agency review and approved for publication.

## Literature Cited

- 1)     Blancato JN, Bischoff KB; Presented at the North American Symposium of the International Society for the Study of Xenobiotics. Key Biscayne, FL, November, 1985
- 2)     Blancato JN, Bischoff KB in *Health Risk Assessments: dermal and inhalation exposure and absorption of toxicants*; Wang, RGM; Knaak, JB; Maibach, HI eds CRC Press, Boca Raton, FL, 1992
- 3)     Ramsey JC, Andersen ME; *Tox and Appl Pharm*, **1984** 73:159-175
- 4)     Chen CW, Blancato JN in *Pharmacokinetics in Risk Assessment: Drinking Water and Health*, National Academy Press, Washington, DC, 1987
- 5)     Travis CC, Craig PH, Bowers JC *Atmospheric Environment*, **1991** 25A(8): 1643-1647
- 6)     Bernards, J, MS Thesis, University of Delaware, Newark DE 1986
- 7)     Corley RA, Medrala FA, Smith DA, Staats, JL, Gargas, RB, Conolly, RB, Andersen ME Reitz RA *Tox and Appl Pharm*, **1990** 103: 512-527
- 8)     Blancato, JN in *Proceedings of the EPA/W&WMA Specialty Conference: Total Exposure Assessment Methodology*, November 27 - 30, 1989, 1990
- 9)     Gerlowski LE, Jain R J. *Pharm. Sci.* **1983** 72(10): 1103-1127
- 10)     Gear, CW Numerical Initial Value Problems in Ordinary Differential Equations; Prentice-Hall, Englewood Cliffs, NJ, 1971
- 11)     Hindmarsh AS *ACM Signum Newsletter*, **1980** 15: 10-11
- 12)     Hattis D; Wasson J A *Pharmacokinetic/Mechanism-Based Analysis of the Carcinogenic Risk of Butadiene* National Institute of Occupational Safety and Health, CTPID 87-3, 1987

RECEIVED August 19, 1993

## Chapter 17

# Prediction of Anticholinesterase Activity and Urinary Metabolites of Isofenphos

## Use of a Percutaneous Physiologically Based Pharmacokinetic–Physiologically Based Pharmacodynamic Model

J. B. Knaak<sup>1,2</sup>, M. A. Al-Bayati<sup>3</sup>, O. G. Raabe<sup>2,3</sup>, and Jerry N. Blancato<sup>4</sup>

<sup>1</sup>Occidental Chemical Corporation, 360 Rainbow Boulevard South, Niagara Falls, NY 14302–0728

<sup>2</sup>Department of Biochemistry and Toxicology and <sup>3</sup>Institute of Toxicology and Environmental Health, University of California, Davis, CA 95616

<sup>4</sup>Exposure Assessment Research Division, Environmental Monitoring Systems Laboratory, U.S. Environmental Protection Agency, P.O. Box 93478, Las Vegas, NV 89193–3478

An isofenphos percutaneous PBPK/PBPD model was developed to predict metabolite concentrations in tissues and the inhibition of tissue esterases. Rat  $V_{\max}$  and  $K_m$  values for the metabolism of isofenphos to des N-isopropyl isofenphos, isofenphos-oxon, and des N-isopropyl isofenphos oxon (DNIO) by liver microsomal P-450 enzymes were used in the PBPK portion of the model along with estimated partition coefficients for isofenphos and metabolites between liver, fat, brain, kidney, skin, vessel rich group, vessel poor group, and blood. In the PBPD portion of the model, the bimolecular rate constants for the phosphorylation of brain and blood acetylcholinesterase (AChE), and liver, blood, and brain carboxylesterases and butyrylcholinesterases by DNIO were used to predict their inhibition. Model mass balance data provided summary information on the relationship between topically applied isofenphos and exposure biomarkers such as urinary monoethylphosphate, 2-hydroxy hippuric acid, and inhibited blood enzymes.

Isofenphos, 1-methylethyl 2-[[ethoxy[(1-methylethyl)-amino]phosphinothioyl]oxy]benzoate, was developed and sold by Mobay Chemical Corp., Kansas City, Mo. as a 3% granular formulation under the tradename Oftanol for turf insect (white grubs, cinch bugs, sod webworms) and termite control. Isofenphos is metabolized to des N-isopropyl isofenphos oxon (DNIO), an inhibitor of acetylcholinesterase (AChE) and neurotoxic esterase (NTE)(1). Knaak et al.(2) studied the percutaneous absorption of isofenphos in the rat because the use of Oftanol on turf grass resulted in small quantities being transferred to the skin of individuals in contact with treated turf and soil(3).

0097–6156/94/0542–0284\$06.00/0  
© 1994 American Chemical Society

This paper describes work performed in the development of a physiologically based pharmacokinetic/pharmacodynamic (PBPK/PBPD) model relating the percutaneous absorption and metabolism of isofenphos in the rat to inhibition of acetylcholinesterase (AChE), butyrylcholinesterase (BuChE), and carboxylesterase (CaE) in blood, brain, and liver, for the purpose of predicting urinary metabolites and anticholinesterase activity in exposed workers when the model is completed and validated.

## DEVELOPMENT OF A PBPK/PBPD MODEL FOR ISOFENPHOS

**Model.** The percutaneous PBPK/PBPD dosimetry model given in Figure 1 consists of tissue compartments, total cardiac flow, and those to fat, liver, brain, kidney, vessel rich group, and vessel poor group. Concentrations,  $C$ , are those in the arterial blood, venous blood, and in the venous blood leaving the tissues. The venous blood concentrations are dependent on the chemical concentrations in the tissues, and the tissue/blood partition coefficients. Removal of isofenphos and metabolites from the liver is described kinetically by  $V_{\max}$ , and the Michaelis constant,  $K_m$ , while the inhibition of tissue CaE, BuChE and AChE by DNIO is described by bimolecular rate constants. SimuSolv/ACSL (Dow Chemical/Mitchell and Gauthier Associates, Inc.) on a DEC VAX/VMS system was used to run the model.

**Physiological Parameters.** Physiological parameters compiled by Arms and Travis and published by EPA were used (4).

### Time Course Data, Skin Permeability, and Metabolism in the rat.

Pharmacokinetic data on the percutaneous absorption of  $^{14}\text{C}$ -ring labeled isofenphos was obtained from the study of Knaak et al.(2). On day one of treatment, 1120 ug ( $3.2 \times 10^6$  pmoles) of ring labeled isofenphos dissolved in 0.2 ml of acetone was topically applied to 12  $\text{cm}^2$  of clipped skin. Time-course recovery data was obtained for  $^{14}\text{C}$ -isofenphos equivalents in urine, feces, carcass, skin, plasma, liver, heart, kidney, fat, GI tract, and brain. The skin permeability constant,  $K_p$ , was estimated to be  $0.0066 \text{ cm hr}^{-1}$ .

Ring labeled isofenphos (IF) was metabolized by the rat and excreted in urine primarily as 2-hydroxy hippuric acid (glycine conjugate of 2-hydroxy benzoic acid) along with small amounts of three intact organophosphorus compounds believed to be carboxylic acids of isofenphos (IF), des N-isopropyl isofenphos (DNI), isofenphos oxon (IO), and des N-isopropyl isofenphos oxon (DNIO) or their glycine conjugates (2). Figure 2 gives the chromatographic profiles of urinary metabolites from orally administered  $^{14}\text{C}$ -ring and  $^3\text{H}$ -ethyl labeled isofenphos on a 250 x 10 mm SynChropak AX100 weak anion exchange column, using 0.5M Tris/HCL buffer, pH 8.0, as the eluting solvent. The radiolabeled metabolites were detected using a Radiomatic Flo-One/Beta detector. Monoethylphosphate, O-ethylthiophosphate, and 2-hydroxy hippuric acid chromatographed as shown in Figure 2.

**Enzymes and Metabolic Pathway.** Isolated rat liver P-450 enzymes fortified with NADPH metabolized IF to IO, DNI, and DNIO as shown in Figure 3 (5). DNI and DNIO are believed to be hydrolyzed by A-esterases to isopropyl salicylate, O-ethyl aminophosphate, and O-ethyl aminothiophosphate or decarboxylated to give O-ethyl O-2-carboxylic acid phenyl phosphoramidothioate (DNIA) and O-ethyl O-2-carboxylic acid phenyl phosphoramidate (DNIOA). Isopropyl salicylate was decarboxylated to give 2-hydroxy benzoic acid. The free carboxylic acids are believed to be conjugated with glycine prior to elimination. The metabolic pathway shown in Figure 3 was used to develop the PBPK/PBPD model.

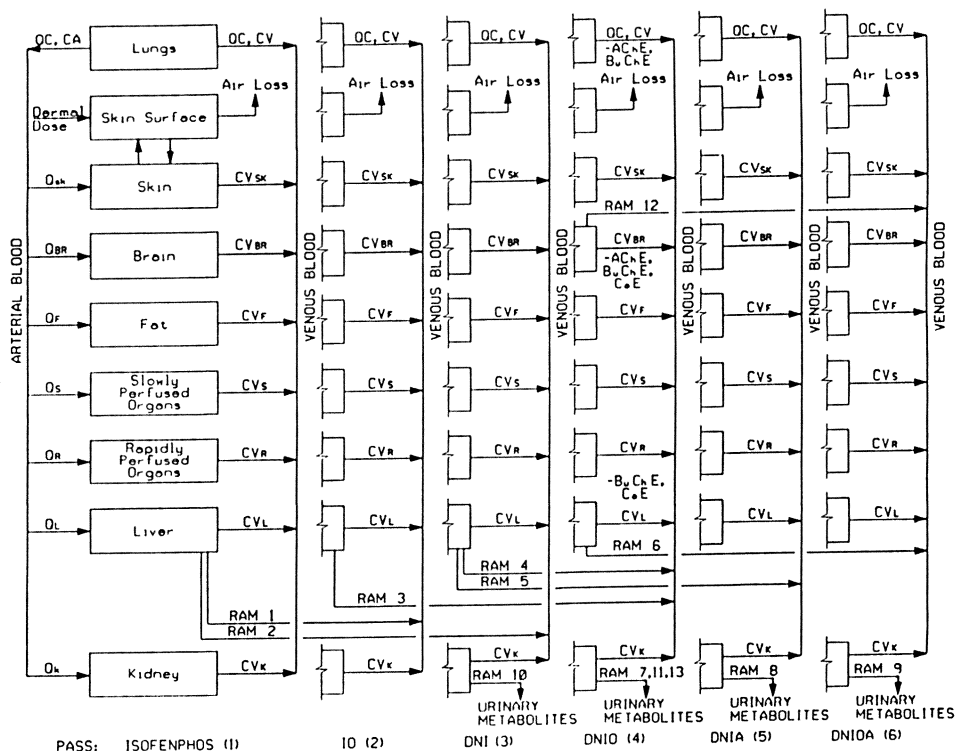


**Figure 1. Percutaneous absorption: Physiologically based pharmacokinetic model. Pass 1, IF to DNI and IO; Pass 2, IO to DNIO; Pass 3, DNI to DNIO, DNIA, O-ethylaminothiophosphate and isopropyl salicylate; Pass 4, DNIO to DNIOA, O-ethylaminothiophosphate, and isopropyl salicylate; phosphorylation of AChE, BuChE, and CaE by DNIO; Pass 5, DNIA to DNIG; Pass 6, DNIOA to DNIOG.**

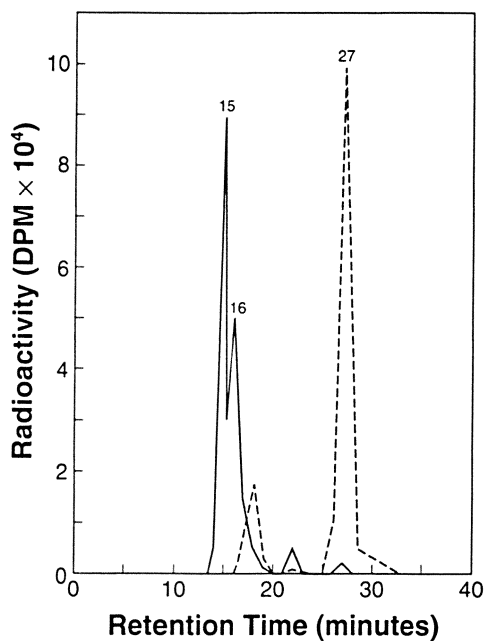
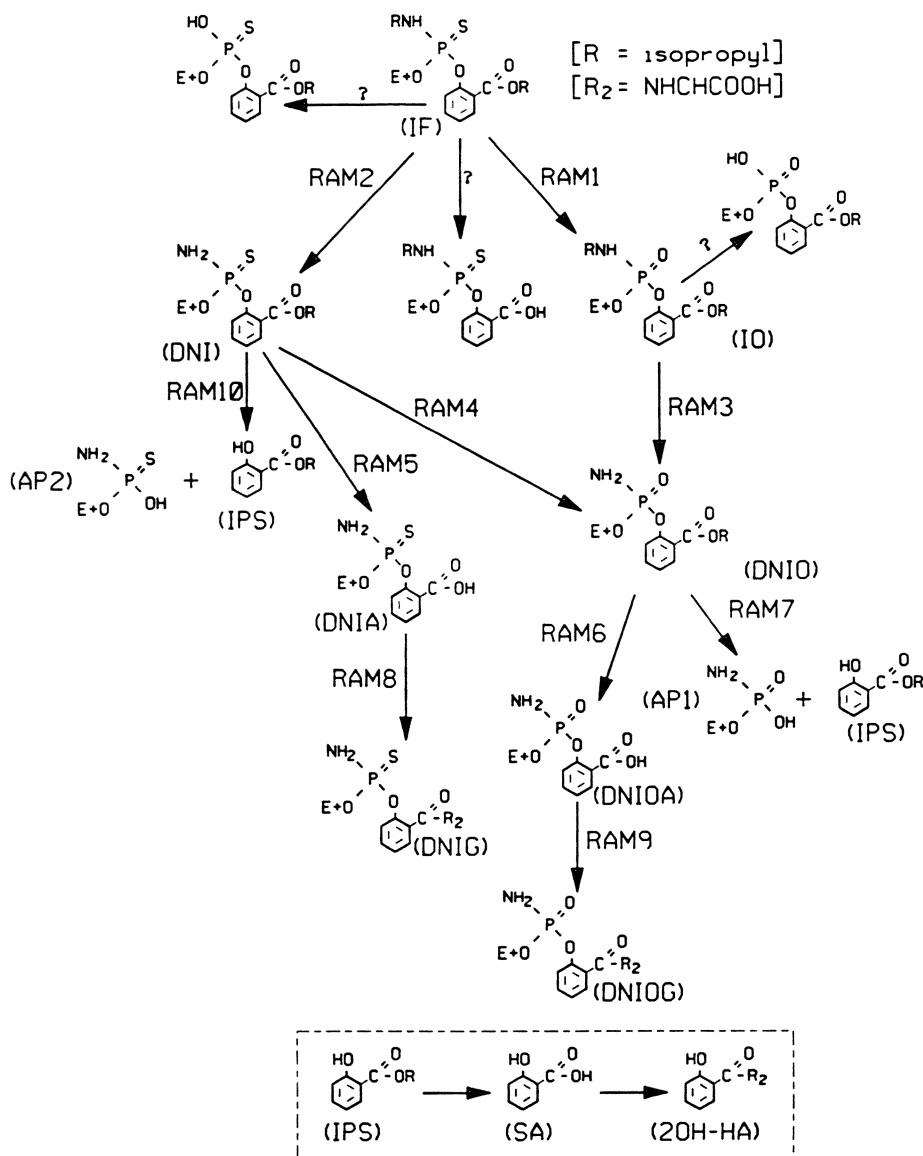


Figure 2. Ion Exchange Chromatography of Rat Urinary Metabolites of  $^3\text{H}$ -ethyl and  $^{14}\text{C}$ -ring labeled Isofenphos. dashed line,  $^{14}\text{C}$ -ring labeled metabolites; solid line,  $^3\text{H}$ -ethyl labeled metabolites; standards: 15 min., monoethylphosphate; 16 min., O-ethylthiophosphate; 27 min., 2-hydroxy hippuric acid.



**Figure 3.** Metabolism of Isufenphos by the Rat. IF, isufenphos; IO, isufenphos oxon; DNI, des N-isopropyl isufenphos; DNIO, des N-isopropyl isufenphos oxon; IPS, isopropyl salicylate; AP1, O-ethylaminophosphate; AP2, O-ethylaminophosphate; DNIA, O-ethyl O-2-carboxylic acid phenyl phosphoramidate; DNIOA, O-ethyl O-2-carboxylic acid phenyl phosphoramidate; DNIG, glycine conjugate of DNIA; DNIOG, glycine conjugate of DNIOA

Knaak et al. (6) recently indicated that DNI and DNIO appeared to be deaminated prior to being hydrolyzed by A-esterases to monoethyl phosphate and O-ethylthiophosphate because authentic samples of these alkyl phosphates co-chromatographed with H<sup>3</sup>-ethyl labeled urinary metabolites on a 250 x 10 mm SynChropak AX100 anion exchange column as shown in Figure 2. According to Ueji and Tomizawa (7) IF was metabolized by a rat microsomal-NADPH system to DNI, IO, the alkyl phosphates of IF, IO, desisopropylamino isofenphos (O-ethyl O-2-isopropylcarbonyl phenyl hydrogen phosphorothioate), and desisopropylamino isofenphos oxon (O-ethyl O-2-isopropylcarbonyl phenyl hydrogen phosphate). An unidentified metabolite believed to be formed from IO was reported by these authors. This unknown metabolite may have been DNIO. Desisopropylamino isofenphos oxon was also identified as a metabolite of IO in the hen by investigators at Mobay Chemical. The work by Ueji and Tomizawa (7) and by the Mobay Chemical investigators lends support to deamination as a metabolic pathway for IF.

**Partition Coefficients.** Tissue/blood partition coefficients for isofenphos and metabolites were estimated based on their octanol/water partition coefficients and are listed below in Table I (2).

**Table I. Estimated Partition Coefficients used in the Model**

<i>Chemical</i> <sup>a</sup>	<i>L/B</i> <sup>b</sup>	<i>F/B</i>	<i>K/B</i>	<i>Br/B</i>	<i>A/Sk</i>	<i>Sk/B</i>
IF	15.0	70.0	10.0	3.5	1.6	2.0
IO	2.0	5.0	2.0	2.0		
DNI	2.0	5.0	2.0	1.0		
DNIO	1.2	2.0	1.2	1.0		
DNIA	1.2	2.0	1.2	1.0		
DNIOA	1.2	2.0	1.2	1.0		

<sup>a</sup>IF, isofenphos; IO, isofenphos oxon; DNI, des N-isopropyl isofenphos; DNIO, des N-isopropyl isofenphos oxon; DNIA, O-ethyl O-2-carboxylic acid phenyl phosphoroamidothioate; DNIOA, O-ethyl O-2-carboxylic acid phenyl phosphoramidate.

<sup>b</sup>L/B, Liver/Blood; F/B, Fat/Blood; K/B, Kidney/Blood; Br/B, Brain/Blood; A/Sk, Air/Skin; Sk/B, Skin/Blood

**Metabolic Enzyme Kinetics.** In *vitro* P-450 V<sub>max</sub> and K<sub>m</sub> values for the conversion of IF to DNI and IO and the conversion of DNI and IO to DNIO are given in Tables II and III (5). These P-450 values were reduced to the velocities given in Table V during modeling to fit *in vivo* percutaneous elimination data. For modeling purposes, hydrolysis of DNI by A-esterases and CaE was assumed to occur only in the liver and to be saturable according to Michaelis-Menten kinetics, while the hydrolysis of DNIO by these enzymes was assumed to be saturable according to Michaelis-Menten kinetics and to occur only in liver, blood, and brain. The velocities for liver CaE and A-esterases were estimated by fitting the model to elimination data from the percutaneous study. The addition of the reactions involving the phosphorylation of CaE, AChE, and BuChE necessitated the addition of brain CaE and A-esterases and blood A-esterases to the model to reduce the concentration of DNIO in these tissues.

**Table II. Rate of Isofenphos Conversion to Metabolites by Liver P-450 Enzymes<sup>a</sup>**

Species	Units	Desulfuration Isofenphos to Isofenphos Oxon		Dealkylation Isofenphos to des N- Isopropyl Isofenphos	
		$V_{max}^b$	$K_m^c$	$V_{max}$	$K_m^c$
Rat	1)	66 ± 2.9	14.1 ± 1.8	17.2 ± 0.39	9.9 ± 0.77
	2)	3,690		962	
	3)	137,220		35,775	
	4)	62.9		16.4	

<sup>a</sup>1.3 nmol of cytochrome P-450/10ml volume was incubated with isofenphos<sup>b</sup>Units 1) nmol hr<sup>-1</sup> per 130 nmol of microsomal P-4502) nmol hr<sup>-1</sup> per gram of liver3) nmol hr<sup>-1</sup> per kg of body weight4) nmol hr<sup>-1</sup> per mg microsomal protein<sup>c</sup> $K_m$  umol L<sup>-1</sup> isofenphos

NOTE: Data taken from ref. 5.

**Table III. Rate of Conversion of Isofenphos Oxon & des N-Isopropyl Isofenphos to des N-Isopropyl Isofenphos Oxon by Liver P-450 Enzymes<sup>a</sup>**

Species	Units	Desulfuration des N-isopropyl Isofenphos to des N-isopropyl Isofenphos Oxon		Dealkylation Isofenphos Oxon to des N- Isopropyl Isofenphos Oxon	
		$V_{max}^b$	$K_m^c$	$V_{max}$	$K_m^c$
Rat	1)	12 ± 0.4	7.9 ± 1.1	34.9 ± 1.8	9.5 ± 2.1
	2)	675		1,952	
	3)	25,105		75,590	
	4)	11.5		33.2	

<sup>a</sup>1.3 nmol of cytochrome P-450/10ml volume was incubated with isofenphos oxon and des N-isopropyl isofenphos.<sup>b</sup>Units 1) nmol hr<sup>-1</sup> per 130 nmol of microsomal P-4502) nmol hr<sup>-1</sup> per gram of liver3) nmol hr<sup>-1</sup> per kg of body weight4) nmol hr<sup>-1</sup> per mg microsomal protein<sup>c</sup> $K_m$  umol L<sup>-1</sup> isofenphos oxon or des N-isopropyl isofenphos

NOTE: Data taken from ref. 5.

**Table IV. Rate of Inhibition of AChE, BuChE, and CaE by Des N-Isopropyl Isofenphos Oxon based on  $K_i$  values from paraoxon/DFP<sup>a</sup>**

Enz/source	Enz Conc <sup>b</sup>	$K_i^c$	DNIO Conc <sup>d</sup>	Inhibition Rate <sup>e</sup>
CaE/Liver	455.0x10 <sup>5</sup>	1.1x10 <sup>-6</sup>	100	5.0x10 <sup>3</sup>
BuChE/Blood	4.8x10 <sup>3</sup>	3.0x10 <sup>-5</sup>	100	14.4
AChE/Brain	37.8x10 <sup>3</sup>	1.5x10 <sup>-5</sup>	100	56.7

<sup>a</sup>Ref 9,10<sup>b</sup>Ref 8, pmol L<sup>-1</sup><sup>c</sup>(pmol L<sup>-1</sup>)<sup>-1</sup>hr<sup>-1</sup><sup>d</sup>pmol L<sup>-1</sup>, value of 100 selected for normalizing Inhibition Rates<sup>e</sup>pmol L<sup>-1</sup> hr<sup>-1</sup>

**Phosphorylation of AChE, BuChE, and CaE.** The AChE, BuChE, and CaE concentrations in blood, liver, and brain given in Table IV were obtained from Maxwell et al. (8). The *in vitro* paraoxon and DFP bimolecular rate constants,  $k_j$ , for the inhibition of AChE, BuChE, and CaE given in Table IV were obtained from Wang and Murphy (9) and Gearhart et al. (10) and used as initial values for estimating the inhibition of these enzymes by DNIO in the model.

**Mass Balance Equations.** The PBPK/PBPD dosimetry model in Figure 1 and the metabolic pathway shown in Figure 3 for liver were used to write a set of mass balance equations describing the rate of change of the concentration of each metabolite in each tissue through time. The volumes of the tissues, cardiac output, blood flow rates through tissues, tissue/blood partition coefficients, and metabolism were considered in the model. Mass balance equations for the metabolism of DNIO in blood and brain were also included in the model along with equations for the inhibition of AChE, BuChE, and CaE by DNIO based on those developed by Gearhart et al. (10) for DFP. The mass balance equations for percutaneous absorption and loss to air were published earlier by Knaak et al. (2,6) for IF, while the equations for tissue/blood exchange, and metabolism were reported by Ramsey and Andersen (11). The mass balance equations for DNIO in the brain were written using the equations for tissue/blood, metabolism, and inhibition.

#### Mass Balance for percutaneous absorption

$$\begin{aligned} dA_{\text{surf}}/dt &= K_p \cdot A \cdot (C_{\text{sk}}/P_{\text{a/sk}} - C_{\text{surf}}) - K_a A_{\text{surf}}, \text{ pmol hr}^{-1} \\ C_{\text{surf}} &= A_{\text{surf}}/V_{\text{sk}}, \text{ pmol cm}^{-3} \\ C_{\text{sk}} &= A_{\text{sk}}/V_{\text{sk}}, \text{ pmol cm}^{-3} \\ dA_{\text{air}}/dt &= K_a \cdot A_{\text{surf}}, \text{ pmol hr}^{-1} \\ dA_{\text{sk}}/dt &= K_p \cdot A \cdot (C_{\text{surf}} - C_{\text{sk}}/P_{\text{a/sk}}) + Q_{\text{sk}} \cdot (CA_1 - C_{\text{sk}}/P_{\text{sk/b}}) \end{aligned}$$

where:

$A_{\text{surf}}$  = Amount of isofenphos on skin surface, pmol (applied dose)  
 $C_{\text{surf}}$  = Concentration on skin surface, pmol cm<sup>-3</sup>  
 $V_{\text{surf}}$  = Area \* depth, cm<sup>3</sup>  
 $K_p$  = permeability constant, cm hr<sup>-1</sup>  
 $A_{\text{sk}}$  = Amount in skin, pmol  
 $C_{\text{sk}}$  = Concentration within skin, pmol cm<sup>-3</sup>  
 $V_{\text{sk}}$  = Volume of skin, cm<sup>3</sup>  
 $A_{\text{air}}$  = Amount in air, pmol  
 $K_a$  = rate of loss to air, hr<sup>-1</sup>  
 $P_{\text{a/sk}}$  = partition coefficient, air/skin  
 $P_{\text{sk/b}}$  = partition coefficient, skin/blood  
 $CA_1$  = Concentration of isofenphos in arterial blood, pmol cm<sup>-3</sup>

#### Mass Balance for Tissue/Blood Exchange

$$\begin{aligned} Q_i CA_i dt &= dA_i = Q_i CV_i dt, \text{ pmol hr}^{-1} \\ dA_i/dt &= Q_i (CA - CV_i), \text{ pmol hr}^{-1} \\ CV_i &= A_i/(V_i \cdot P_i), \text{ pmol L}^{-1} \\ C_i &= A_i/V_i, \text{ pmol L}^{-1} \end{aligned}$$

where:

$Q_i$  = Blood flow to tissue i, L hr<sup>-1</sup>

$CA_i$  = Concentration of isofenphos/metabolites in arterial blood entering tissue  $i$ ,  $\text{pmol L}^{-1}$

$CV_i$  = Concentration of isofenphos/metabolites in venous blood leaving tissue  $i$ ,  $\text{pmol L}^{-1}$

$A_i$  = Amount of isofenphos/metabolites in tissue  $i$ ,  $\text{pmol}$

$C_i$  = Concentration of isofenphos/metabolites in tissue  $i$ ,  $\text{pmol L}^{-1}$

$P_i$  = Tissue  $i$  blood/tissue partition coefficient for parent/metabolites

$V_i$  = Volume of tissue  $i$ ,  $L$

### Mass Balance Equation for Metabolism

$$dA_m/dt = V_{\max} * CV_l / (K_m + CV_l), \text{ pmol hr}^{-1}$$

$$dA_l/dt = Q_l(CA - CV_l) - dA_m/dt, \text{ pmol hr}^{-1}$$

where:

$A_m$  = Amount metabolized in liver,  $\text{pmol}$

$V_{\max}$  = Michaelis Menten rate constant,  $\text{pmol hr}^{-1}$  per kg of body weight

$K_m$  = Substrate Concentration, at half maximum velocity,  $\text{pmol L}^{-1}$

$CV_l = A_l / (V_l * P_l)$ , Concentration in venous blood leaving liver,  $\text{pmol L}^{-1}$

$A_l$  = Amount in liver,  $\text{pmol}$

$V_l$  = Volume of liver,  $L$

$P_l$  = liver/blood partition coefficient

$Q_l$  = Blood flow to liver,  $L \text{ hr}^{-1}$

$CA$  = Concentration in arterial blood,  $\text{pmol L}^{-1}$

### Inhibition of AChE, BuChE, and CaE in the Brain

$$dAABr/dt = (K_{AChE2} * C_{AEBR} * C_{Br4} * V_{Br}), \text{ pmol hr}^{-1}$$

$$dABBr/dt = (K_{BChE2} * C_{BEBR} * C_{Br4} * V_{Br}), \text{ pmol hr}^{-1}$$

$$dACBr/dt = (K_{CaE2} * C_{CEBR} * C_{Br4} * V_{Br}), \text{ pmol hr}^{-1}$$

where:

$V_{Br}$  = Volume of brain,  $L$

$AABR$  = Inhibited AChE,  $\text{pmol}$

$BEBR$  = Inhibited BuChE,  $\text{pmol}$

$ACBr$  = Inhibited CaE in brain,  $\text{pmol}$

$K_{AChE2}$  = AChE bimolecular inhibition rate constant,  $(\text{pmol L}^{-1})^{-1} \text{ hr}^{-1}$

$K_{BChE2}$  = BuChE bimolecular inhibition rate constant,  $(\text{pmol L}^{-1})^{-1} \text{ hr}^{-1}$

$K_{CaE2}$  = CaE bimolecular inhibition rate constant,  $(\text{pmol L}^{-1})^{-1} \text{ hr}^{-1}$

$C_{AEBR}$  = Free AChE in brain,  $\text{pmol L}^{-1}$

$C_{BEBR}$  = Free BuChE in brain,  $\text{pmol L}^{-1}$

$C_{CEBR}$  = Free CaE in brain,  $\text{pmol L}^{-1}$

$C_{Br4}$  = Concentration of DNIO in the brain,  $\text{pmol L}^{-1}$

### Mass Balance Equation for DNIO in the Brain

$$dC_{Br4}/dt = Q_{Br} * (CA_4 - CV_{Br4})$$

$-(V_{\max 11R} * CV_{Br4}) / (K_{m11} + CV_{Br4})$ , hydrolysis by A-esterase

$-K_{AChE2} * C_{AEBR} * C_{Br4} * V_{Br}$ , inhibition of AChE

$-K_{CaE2} * C_{CEBR} * C_{Br4} * V_{Br}$ , inhibition of CaE

$-K_{BChE2} * C_{BEBR} * C_{Br4} * V_{Br}$ , inhibition of BaChE,  $\text{pmol hr}^{-1}$

where:

$Q_{Br}$  = Blood flow to brain,  $L\ hr^{-1}$

$CA_4$  = DNIO concentration in arterial blood entering brain,  $pmol\ L^{-1}$

$CV_{Br4}$  = DNIO concentration in venous blood leaving brain,  $pmol\ L^{-1}$

$V_{max11R}$  = Michaelis Menten brain hydrolysis rate constant for DNIO,  $pmol\ hr^{-1}$

$K_{m11}$ , DNIO concentration at half maximum velocity,  $pmol\ L^{-1}$

In Figure 1, six passes through blood, liver, brain and other tissues were required to model the fate of IF: pass 1), isofenphos was metabolized by liver to IO (RAM1) and DNI (RAM2); pass 2), IO was metabolized by liver to DNIO (RAM3); pass 3), DNI was metabolized by liver to DNIO (RAM4), DNIA (RAM5), O-ethylaminothiophosphate and isopropyl salicylate (RAM 10); pass 4), DNIO was metabolized by liver and brain to DNIOA (RAM6, RAM12), and two hydrolysis products (O-ethyl aminophosphate and isopropyl salicylate (RAM7, RAM11, RAM13)) by liver, blood and brain; DNIO phosphorylated CaE, and BuChE in liver, blood, and brain, and AChE in blood and brain; pass 5), DNIA was conjugated with glycine to form DNIG (RAM8); and in pass 6), DNIOA was conjugated with glycine to form DNI OG (RAM9). The alkyl phosphates (RAM7,10,11,13) were eliminated along with DNIG (RAM8) and DNI OG (RAM9). Isopropyl salicylate (RAM7,10,11,13) was hydrolyzed, and conjugated with glycine prior to being eliminated as shown at the bottom of Figure 2. These metabolic reactions were considered to occur simultaneously and were not written into the model as separate steps.

## PERCUTANEOUS MODEL OUTPUT

**Metabolism.** In the model, the P-450  $V_{max}$  values ( $nmol\ hr^{-1}$  per kg of b.w.) listed in Tables II and III over predicted the rate of metabolism of IF in the percutaneous ( $1120\ ug/12\ cm^2; 3.2 \times 10^6\ pmoles\ cm^{-3}$ ) study based on  $^{14}C$ -isofenphos equivalents in tissue, urine and feces. However, good fit was obtained using the enzyme velocities listed in Table VI. These values were obtained by reducing the velocities of the reactions ( $V_{max}$  values  $\times 0.26$ , etc.) until a fit was obtained. The *in vitro*  $K_m$  values given in Tables II and III were used and are listed in Table V.

The constants for the hydrolytic enzymes, A-esterases and CaE, were obtained by modeling and are sufficient in size to reproduce the *in vivo* elimination curves.

Figure 4 gives the percentages of the percutaneous dose ( $3.2 \times 10^6\ pmoles/12cm^2$ ) retained on skin (PASFC), eliminated in urine and feces (PAUFE), and lost to air (PAX), for the  $^{14}C$ -ring labeled IF study and the model (2). The fate of topically applied IF is given in Table VI for the percutaneous  $^{14}C$ -ring labeled IF study and the model. Ninety seven percent of the applied dose was recovered in the *in vivo* study, and 100% by the model. In the percutaneous study, 38% of the applied dose was metabolized to 2-hydroxy hippuric acid and eliminated in urine, while the model predicted the metabolism of 33.9% to 2-hydroxy hippuric acid.

Table V. Enzyme Velocities used in the Model

Enzyme(s)	Metabolism	Velocity	K <sub>m</sub>
<b>P-450<sup>a</sup></b>			
Liver	IF to IO	36.15x10 <sup>6</sup>	14.1x10 <sup>6</sup>
Liver	IF to DNI	10.1x10 <sup>6</sup>	12.5x10 <sup>6</sup>
Liver	IO to DNIO	15.9x10 <sup>6</sup>	9.5x10 <sup>6</sup>
Liver	DNI to DNIO	5.48x10 <sup>6</sup>	7.9x10 <sup>6</sup>
<b>A-esterases<sup>b</sup></b>			
Liver	DNIO to Ring/AP <sup>c</sup>	2.2x10 <sup>6</sup>	8.0x10 <sup>6</sup>
Blood	DNIO to Ring/AP	1.0x10 <sup>6</sup>	1.0x10 <sup>6</sup>
Brain	DNIO to Ring/AP	1.0x10 <sup>6</sup>	1.0x10 <sup>6</sup>
Liver	DNI to Ring/AP	5.55x10 <sup>6</sup>	1.7x10 <sup>6</sup>
<b>CaE<sup>b</sup></b>			
Liver	DNIO to DNIOA	1.0x10 <sup>6</sup>	1.0x10 <sup>6</sup>
Brain	DNIO to DNIOA	1.0x10 <sup>6</sup>	1.0x10 <sup>6</sup>
Liver	DNI to DNIA	1.0x10 <sup>6</sup>	1.0x10 <sup>6</sup>

<sup>a</sup>pmoles hr<sup>-1</sup> per kg of b.w.; values = 0.26, 0.282, 0.210, and 0.218x V<sub>max</sub> from Tables II and III; K<sub>m</sub>, pmol L<sup>-1</sup> from Tables II and III

<sup>b</sup>V, pmol hr<sup>-1</sup> per kg of b.w.; K<sub>m</sub>, pmol L<sup>-1</sup>; estimated values

<sup>c</sup>Ring = isopropyl salicylate; AP = alkyl phosphate

Table VI. Fate of Topically Applied Isufenphos

	In Vivo <sup>a</sup>	Model <sup>a</sup>
Loss to Air, <sup>14</sup> C-ring	35.0	44.0
Retained on skin, <sup>14</sup> C-ring	15.2	10.0
Urine and Feces, <sup>14</sup> C-ring	43.1	45.0
Carcass, <sup>14</sup> C-ring	4.0	1.0
Total	97.3	100.0
Excreted in Urine as:		
2 Hydroxy hippuric acid	38.0	33.9
Alkyl phosphates <sup>b</sup>	--	16.7
Alkyl phosphates retained by tissues in the form of phosphorylated enzymes <sup>c</sup>		
		17.2

<sup>a</sup>percentage of applied dose (3.2 x 10<sup>6</sup> pmoles; 1120 ug) using <sup>14</sup>C-ring labeled isufenphos

<sup>b</sup>percentage in urine estimated by model, a percutaneous study was not conducted with <sup>3</sup>H-ethyl labeled isufenphos

<sup>c</sup>percentage used in the phosphorylation of AChE, BuChE, and CaE in liver, blood, and brain estimated by model

**Phosphorylation of AChE, BuChE, and CaE.** The use of the *in vitro* derived paraoxon/DFP bimolecular rate constants (Table IV) for AChE and BuChE in the percutaneous PBPK/PBPD model resulted in the phosphorylation of over 100% of tissue AChE and BuChE within hours after the application of the dose, while in the percutaneous absorption study topically applied isfenphos (1120 ug/ 12.0 cm<sup>2</sup>; 3.2x10<sup>6</sup> pmoles cm<sup>-2</sup>) inhibited less than 30% of blood AChE activity over the course of 72 hrs.

The model, therefore, was used to estimate the size of the *in vivo* bimolecular rate constants for DNIO using several blood BuChE and AChE *in vivo* inhibition data points obtained in the dermal study and the *in vitro* paraoxon/DFP bimolecular rate constants as initial values. The values are given in Table VII. The percentages of AChE/BuChE/CaE phosphorylated over the course of the study using these  $k_i$  values are shown graphically in Figures 5, 6, and 7 for liver, blood and brain, respectively. Figure 8 gives the concentrations of DNIO in brain, blood, and liver predicted by the model. According to the model, 35.9% of topically applied IF was converted to DNIO and 50% of the DNIO phosphorylated liver CaE and BuChE, with less than 1% of the DNIO reacting with blood and brain enzymes.

**Table VII. Rate of Inhibition of AChE, BuChE, and CaE by Des N-Isopropyl Isfenphos Oxon based on  $K_i$  values estimated from Model**

Enz/source	Enz Conc <sup>a</sup>	$K_i^b$	DNIO Conc <sup>c</sup>	Inhibition Rate <sup>d</sup>
BuChE/Liver	8.22x10 <sup>3</sup>	5x10 <sup>-7</sup>	100	0.411
CaE/Liver	455.0x10 <sup>5</sup>	1x10 <sup>-6</sup>	100	4.55x10 <sup>3</sup>
AChE/Blood	1.1x10 <sup>3</sup>	8x10 <sup>-7</sup>	100	0.09
BuChE/Blood	4.8x10 <sup>3</sup>	1x10 <sup>-6</sup>	100	0.48
AChE/Brain	37.8x10 <sup>3</sup>	5x10 <sup>-6</sup>	100	18.9
BuChE/Brain	12.7x10 <sup>3</sup>	4x10 <sup>-6</sup>	100	5.1
CaE/Brain	549.8x10 <sup>3</sup>	1x10 <sup>-6</sup>	100	54.9

<sup>a</sup>Ref 8, pmol L<sup>-1</sup>

<sup>b</sup>(pmol L<sup>-1</sup>)<sup>-1</sup>hr<sup>-1</sup>

<sup>c</sup>pmol L<sup>-1</sup>, value of 100 selected for normalizing Inhibition Rates

<sup>d</sup>pmol L<sup>-1</sup> hr<sup>-1</sup>

## DISCUSSION

<sup>14</sup>C-Ring labeled isfenphos and equivalents in tissues and excreta from topically treated rats along with *in vitro* rat P-450 V<sub>max</sub> and K<sub>m</sub> data developed by Knaak et al. (2,5) were used to develop the percutaneous model. The bimolecular rate constants involving the phosphorylation of CaE, AChE, and BuChE were estimated by the model using *in vitro* literature values for paraoxon/DFP as the initial values. The hydrolytic rate constants for the A-esterases and CaE were estimated using the model and *in vivo* elimination data. The model clearly demonstrates the importance of A-esterases in the detoxification of DNIO in the rat. Recent studies in our laboratory involving the metabolism of IF in the guinea pig and dog indicate that A-esterases are less important, as CaE in these animals are more active in hydrolyzing the carboxyl esters of IF, DNI and DNIO. *In vitro* studies with human liver suggest that CaE plays an important role in the metabolism of IF in humans.

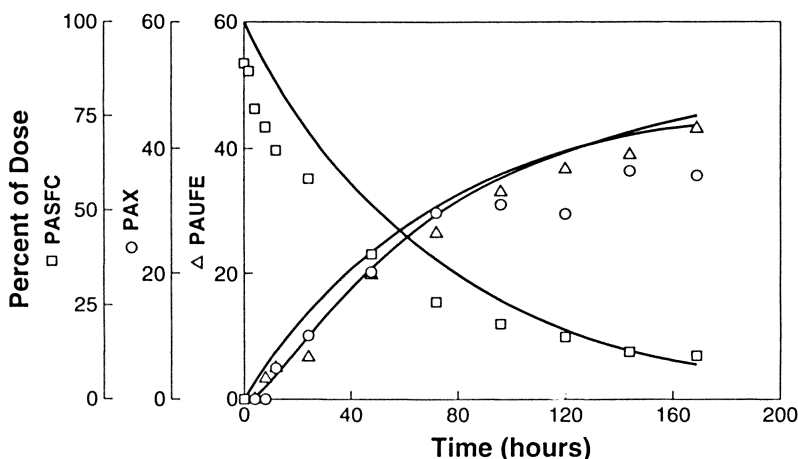


Figure 4. Physiologically based pharmacokinetic Model: retention of [ $^{14}\text{C}$ ]-ring Isufenphos on skin, loss to air, elimination in urine and feces. Solid line, model output; square, circle, and triangle, percutaneous study; PASFC, % of dose retained on skin; PAX, % of dose lost to air; PAUFE, % of dose eliminated in urine and feces.

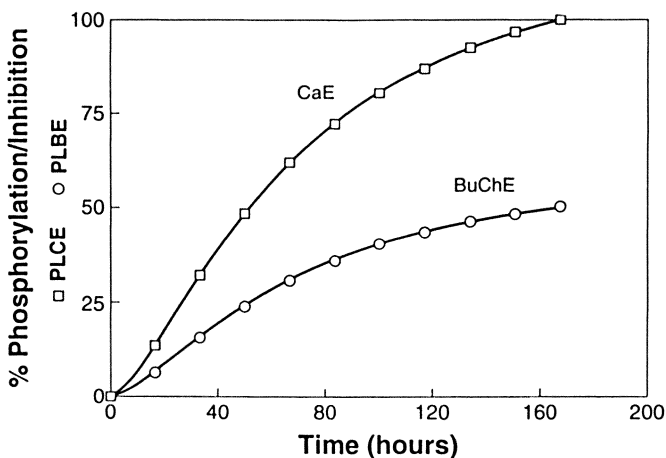


Figure 5. Physiologically based pharmacokinetic Model: Phosphorylation of liver BuChE and CaE by des N-Isopropyl Isufenphos Oxon (DNIO). Solid lines, squares, and circles, model output; PLCE, % of liver CaE phosphorylated; PLBE, % of liver BuChE phosphorylated.

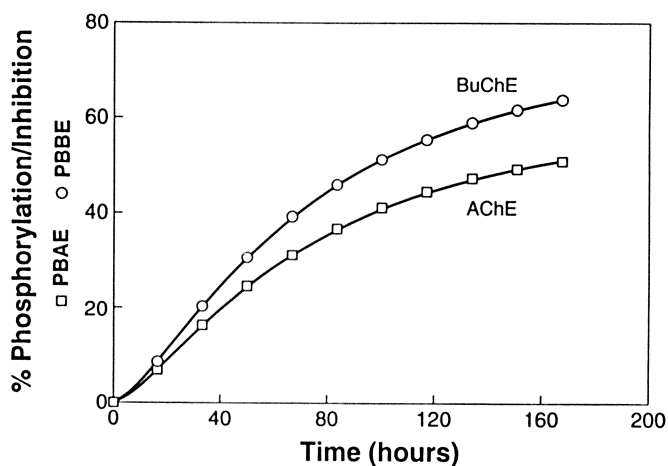


Figure 6. Physiologically based pharmacokinetic Model: Phosphorylation of Blood AChE and BuChE by des N-Isopropyl Isofenphos Oxon (DNIO). Solid lines, squares, and circles, model output; PBAE, % blood AChE phosphorylated; PBBE, % of blood BuChE phosphorylated.

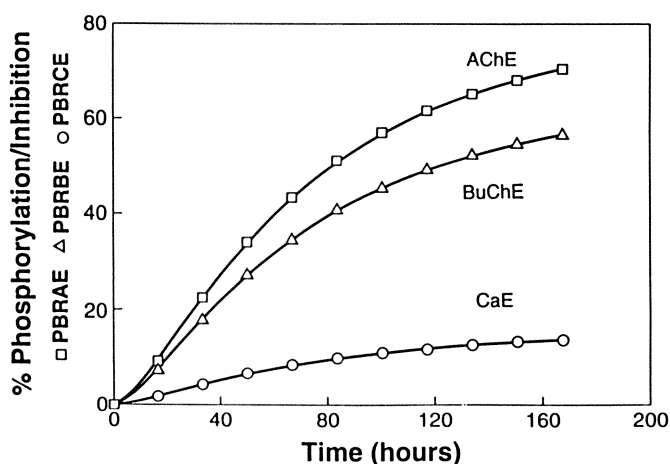


Figure 7. Physiologically based pharmacokinetic Model: Phosphorylation of Brain AChE, BuChE, and CaE by des N-Isopropyl Isofenphos Oxon (DNIO). Solid lines, circles, squares, and triangles, model output; PBAE, % of brain AChE phosphorylated; PBRBE, % of brain BuChE phosphorylated; PBRCE, % of brain CaE phosphorylated.

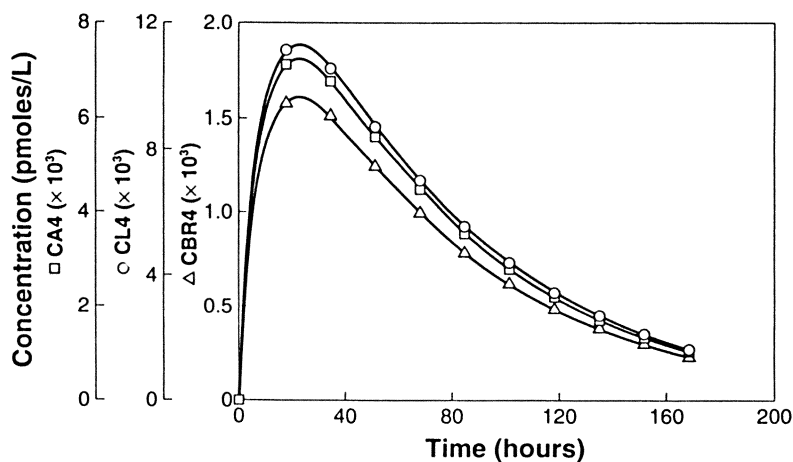


Figure 8. Physiologically based pharmacokinetic Model: Concentration of DNIO in blood (CA4), brain (CBR4), and liver (CL4). Solid lines, circles, squares, and triangles, model output; pmoles/L.

Methods are currently being worked on for directly analyzing DNI, IO, and DNIO in blood and other tissues. The existence of a separate metabolic pathway for IF involving the one-step removal of an isopropyl amino group from either IF or IO is also being investigated. The formation of desisopropylamino isufenphos and desisopropylamino isufenphos oxon would support the presence of monoethylphosphate and ethylthiophosphate in urine. At the present time no information is available to indicate whether or not deamination occurs in one step by removal of the isopropylamino group or stepwise starting with the removal of the isopropyl group via DNI and DNIO. This issue needs to be resolved because loss of the isopropylamino group from IO would significantly reduce the toxicity of IF by decreasing the amount of IO available for metabolism to DNIO.

The alkyl phosphates present in urine are good biomarkers of exposure to IF. A gas chromatographic procedure is currently being worked on to assist in the positive identification of these two metabolites and the development of a method for monitoring urine from exposed workers. The ring metabolite, 2-hydroxy hippuric acid, may be used as a biomarker provided workers use a pain killer other than aspirin (acetylsalicylate).

Blood/tissue partition coefficients are currently being developed. Paraoxon is required to prevent the decarboxylation of IF, IO, DNI, and DNIO by CaE during the equilibration period.

Blood cholinesterase activity is a good biomarker of acute and chronic exposure to IF. According to the model, DNIO formed by liver P-450 enzymes rapidly phosphorylates liver CaE and BuChE, partitions into blood, phosphorylates blood AChE and BuChE, and partitions out of blood into brain tissue to phosphorylate AChE, BuChE, and CaE. The  $k_i$  values estimated by the model in Table VII are tentative values and will be replaced by *in vitro* values when they become available. Current plans are to include IO as an enzyme inhibitor in the model. An *in vivo* enzyme inhibition-time course study will be required to validate the model.

In the model, *in vitro* derived bimolecular rate constants,  $k_i$ , for the phosphorylation of AChE, BuChE, and CaE by paraoxon/DFP and *in vitro* derived  $V_{\max}$  values for the metabolism of isufenphos to IO, DNI, and DNIO over predicted reaction rates occurring *in vivo*. This was anticipated for  $V_{\max}$  values, because the dose rate to the liver was insufficient to saturate P-450 enzymes resulting in a metabolic rate,  $v$ , less than  $V_{\max}$  (nmol hr<sup>-1</sup> per kg of body weight). In the case of the bimolecular rate constants for paraoxon and DFP, where  $k_i = k_p/K_d$ , the overall potency of these OPs is made up of two factors, the affinity term ( $K_d$ , uM<sup>-1</sup>) and a phosphorylation term ( $k_p$ , min<sup>-1</sup>). The  $K_d$  and  $k_p$  values for paraoxon and DFP are believed to be similar to DNIO. A concentration of 10<sup>-6</sup>M results in 50% of the enzyme being rapidly converted to an enzyme inhibitor complex prior to phosphorylation. Under *in vivo* conditions, much less inhibitor (DNIO, 10<sup>-12</sup>M) is present, less enzyme inhibitor complex is formed, and the overall reaction requires a longer period of time (12).

A sensitivity analysis was not performed on model parameters. However, in the fitting process  $K_p$  (skin permeability),  $V_{\max}$  and  $K_m$  values,  $k_i$  (bimolecular rate constant) values, enzyme concentrations, and cardiac output were identified as sensitive parameters. An analysis will be performed when the work on partition

coefficients, metabolic pathway, and other parameters has been completed and the values added to the model. Human  $V_{\max}$ ,  $K_m$  values are currently available for predicting the fate of IF in man (5).

## CONCLUSIONS

A PBPK/PBPD model is a powerful tool for estimating and testing the effects of experimental values such as skin permeability constants, evaporation rates,  $V_{\max}$ ,  $K_m$  and  $k_i$  on tissue concentrations, enzyme inhibition and elimination rates. A properly validated model may be used to extrapolate from one route of exposure to another and from animals to man. The effect of dose rate and metabolic rate on the fate of administered chemicals can be easily determined. Biomarkers may be used to validate PBPK/PBPD models and estimate exposure.

## ACKNOWLEDGMENTS

We thank D. Uyeminami and F. Gielow, University of California for their assistance in developing the biological data and Melvin Andersen, Duke University, for assistance in PBPK modeling. This project was sponsored by the United States Environmental Protection Agency under Cooperative Agreement No. CR-816332 with the University of California, Davis.

## LITERATURE CITED

1. Wilson, B.W.; Hooper, M.; Chow, E.; Higgins, R.J.; and Knaak, J.B. *Bull. Environ. Contam. Toxicol.*, 1984, 33(4), 386.
2. Knaak, J.B.; Al-Bayati, M.A.; Raabe, O.G.; and Blancato, J.N. In "Prediction of Percutaneous Penetration: Methods, Measurements, Modelling"; Scott, R.C.; Guy, R.H.; and Hadgraft, J., Eds., IBC Technical Service Ltd. London, 1990; pp. 1-18.
3. California Department of Food and Agriculture, Unpublished report, 1982 (DFA-isofenphos Japanese beetle).
4. Arms, A.D.; and Travis, C.C., Reference Physiological Parameters in Pharmacokinetic Modeling, Report No. EPA/600/6-88/004, National Technical Information Service, Springfield, VA 22161.
5. Knaak, J.B.; Al-Bayati, M.A.; Raabe, O.G.; and Blancato, J.N., *Toxicol. Appl. Pharmacol.*, 1993, 120, 106.
6. Knaak, J.B.; Al-Bayati, M.A.; Raabe, O.G., In "Health Risk Assessment through Dermal and Inhalation Exposure and Absorption of Toxicants"; Wang, R.G.; Knaak, J.B.; and Maibach, H.I., Eds., CRC Press, Boca Raton, FL, 1992, Chapter 1.
7. Ueji, M.; and Tomizawa, C., *J. Pesticide Sci.*, 1985, 10, 691.
8. Maxwell, D.M.; Lenz, D.E.; Groff, W.A.; Kaminski; and Froehlich, H.L., *Toxicol. Appl. Pharmacol.*, 1987, 88, 66.
9. Wang, C.; and Murphy, S.D., *Toxicol. Appl. Pharmacol.*, 1982, 66, 409.
10. Gearhart, J.M.; Jepson, G.W.; Clewell, H.J. II; Andersen, M.E.; and Conolly, R.B., *Toxicol. Appl. Pharmacol.*, 1990, 106, 295.
11. Ramsey, J.C.; and Andersen, M.E. *Toxicol. Appl. Pharmacol.*, 1984, 73, 159.
12. Main, A.R., In "Essays in Toxicology", Hayes, W.L., Ed., Academic Press, NY, 1973; pp 59-105.

RECEIVED August 26, 1993

## Chapter 18

# Analytic Solution of a Linear Physiologically Based Pharmacokinetic Model Prototype Useful in Risk Assessment

Robert N. Brown

Exposure Assessment Research Division, Environmental Monitoring  
Systems Laboratory, U.S. Environmental Protection Agency, P.O. Box  
93478, Las Vegas, NV 89193-3478

Explicit analytic solutions of physiologically based pharmacokinetic (PBPK) models yield important qualitative as well as quantitative information about chemical exposure and risk in the human body beyond that provided by general purpose numerical simulation software for such models and may provide convenient replacements for unwieldy or inaccurate simulation tools in some applications. Biologically based risk assessments for chronic toxicity typically utilize integrated concentration, i.e., area under the concentration curve (AUC), for the internal exposure or dose metric in dose-response risk models. Simple matrix based algebraic formulas for target organ AUCs are developed for bolus dose inputs and steady-state infusions for a progression of 1,2,3 and 4 compartment linear PBPK models, paralleling but enhancing analogous algebraic methods for classical compartmental drug models. Interspecies scaling formulas are derived for potential extrapolation of dose from small animals to humans. Comparative dose formulas are given for the relative impact of bolus dose administration by two exposure routes, formulas that may be useful in developing optimal drug efficacy or pesticide useage strategies.

Physiologically based pharmacokinetic (PBPK) risk assessment models of toxic compound exposure, internal dose and health effect are typically solved with numerical simulation packages using general purpose ordinary differential equation (ODE) discretization methods, such as SimuSolv's Gear algorithm [5], used by Anderson, et al., for their analysis of methylene chloride toxicity [2]. On the other hand, first integral analytic solutions of general linear matrix ODE systems are well known ([7], [8]) and should provide accurate time dependent analytic concentration formulas for PBPK models. In this paper, however, our interests focus on longer term quantitative risk

This chapter not subject to U.S. copyright  
Published 1994 American Chemical Society

assessment (QRA) applications (e.g., intermediate term drug effects or long latency cancer effects) from chronic exposure to toxic compounds such as agricultural pesticides or fumigants. Thus, our goal will be to adapt classical first and second integral matrix ODE solutions for internal organ dose to second integral area under the concentration curve (AUC) dose measures and to steady-state concentration levels for small linear PBPK models. This will generalize AUC results for nonphysiological classical compartmental models [6]. System based analytic AUC formulas for classical compartmental drug models have occasionally appeared in the literature, but their systematic exploitation in the PBPK context appears to be insufficiently explored [9] for many risk assessment purposes. This general lack of interest in analytic PBPK solution development may be due to the fact that: (1) PBPK models are considered more complex than classical compartmental models; (2) PBPK model forms have not been well standardized in matrix terms; (3) the formalistic equivalence between PBPK and classical models is poorly understood; and (4) the second integral analytic solution of PBPK models involves a seemingly unwieldy and computationally inefficient inversion of the system matrix. In addition, the ready availability of general purpose numerical simulation packages for nonanalytic number crunching of integral solutions has tended to discourage the search for, and utilization of, analytic methods for PBPK models, even linear models.

However, general purpose numerical software tools yield relatively little conceptual understanding of biological toxicity processes (due to lack of analytic expressions) result in computationally intensive sensitivity analyses (Monte Carlo analyses) and may be computationally inaccurate or inefficient under some conditions (from use of finite difference approximations or small step sizes).

One goal of this paper shall be to address these misperceptions regarding the presumed obsolescence of analytic solutions given the availability of general purpose numerical simulators. It will present, apparently for the first time in a generic PBPK context, simple analytic solutions for a sequence of small dimensional ( $n \leq 4$ ) prototypical PBPK models that may be useful in representative QRA applications. Representative applications include (1) identification of sensitive system parameters, (2) inverse reconstruction of exposure inputs from internal system biomarkers or physiological outputs, (3) extrapolation of dose from small animals to humans, and (4) comparison of target organ dose by different routes of toxicant administration.

A broader goal is to begin the use of analytic solution methods to motivate more efficient model formulation, validation, manipulation and estimation procedures for PBPK models than is currently available using nonanalytic numerical simulation approaches alone. Furthermore, linear analytic solution methods may motivate development of both more powerful analytic and numerical algorithms for understanding and applying nonlinear PBPK models. Nonlinear QRA applications might include analytic extrapolation of internal dose from high-to-low exposures and extrapolation of internal dose from

continuous to bolus dose exposures – trivial problems in the linear, but not nonlinear, model case.

The analysis of PBPK models may be simplified through the use of factored matrix formulations. Although not necessary for system solution, factored matrices help standardize model form, clarify biological parameter and state variable interrelationships and simplify solution methods. To motivate greater use of factored matrix PBPK models for QRA, it will be helpful to clarify the relation between PBPK and classical compartmental models.

### 1-Compartment Classical and PBPK Model

The classical 1-compartment pharmacokinetic model is given by [6]

$$\frac{dA_1}{dt} = -k_1 A_1 + i_{A_1}(t) \quad (1)$$

where  $A_1$  is the amount of toxicant in the well-stirred main compartment,  $k_1$  is the elimination rate to the outside and  $i_{A_1}(t)$  is the temporal input function into the main compartment and may be a continuous function or bolus dose. Use of amounts simplifies mass balancing of inputs and outputs, but the biologically convenient concentration form is given by

$$\frac{dA_1}{V_1 dt} = -k_1 \frac{A_1}{V_1} + \frac{i_{A_1}}{V_1} \Leftrightarrow C_1'(t) = -k_1 C_1 + i_1 \quad (2)$$

where  $V_1$  is compartment volume,  $C_1$  is concentration and  $i_1(t) = i_{A_1}(t)/V_1$  is concentration input rate in units of mass/volume-time rather than the previous bolus dose input rate,  $i_{A_1}(t)$ , which was in units of mass/time. The standard ([6], [7], [8]) first integral solution of (2) is given by

$$C_1(t) = \int_0^t e^{-k_1(t-s)} i_1(s) ds \quad (3)$$

for the arbitrary input  $i_1(s)$ , and reduces to

$$C_1(t) = C_{10} e^{-k_1 t} \quad (4)$$

for bolus dose input  $C_1(0) = C_{10}$  at time zero. The bolus AUC is given by

$$AUC_1 \equiv \lim_{t \rightarrow \infty} \frac{C_{10} e^{-k_1 t}}{-k_1} \Big|_0^t \rightarrow \frac{C_{10}}{k_1} = k_1^{-1} C_{10}. \quad (5)$$

For the inverse problem of reconstructing a bolus dose input from internal dose measurements, one can invert either the first integral expression at fixed time  $t$  or the second integral expression at time infinity, obtaining

$$C_{10} = e^{k_1 t} C_1(t) = k_1 (AUC_1). \quad (6)$$

The choice of inversion formula for specific risk assessment applications will depend upon whether biomeasurements reflect instantaneous internal body concentrations or cumulative concentrations.

Under constant infusion input, (2) yields a steady-state concentration of

$$0 = -k_1 C_{1,ss} + i_1 \Rightarrow C_{1,ss} = k_1^{-1} i_1 \quad (7)$$

which is equivalent to the above bolus dose AUC formula (5) after changing bolus dose input units (e.g., mg/kg) to infusion rate units (e.g., mg/kg-hr). Note that kinetic rate units for  $k_1$  (e.g., hr<sup>-1</sup>) remain unchanged.

Analogously, a 1-compartment pseudo PBPK model might be given by

$$\begin{aligned} C'_1 &= -\frac{Q_1 C_1}{V_1 R_1} - k_{1e} C_1 + i_1 = -\frac{Q_1}{V_1 R_1} \left( 1 + \frac{k_{1e}}{\frac{Q_1}{V_1 R_1}} \right) C_1 + i_1 \\ &= -k_{1b} (1 + \epsilon_{11}) C_1 + i_1 = -k_{1b} \hat{1}_{11} C_1 + i_1 = -k_1 C_1 + i_1 \end{aligned} \quad (8)$$

where  $Q_1$  represents blood flow,  $R_1$  the partition coefficient (ratio of internal concentration to outgoing concentration),  $k_{1b}$  the primary (bloodflow) pollutant elimination rate ( $\frac{Q_1}{V_1 R_1}$ ),  $k_{1e}$  the secondary (nonbloodflow) elimination rate,  $\epsilon_{11} \equiv k_{1e}/k_{1b}$  can be thought of as the relative importance of secondary to primary elimination and  $\hat{1}_{11} \equiv (1 + \epsilon_{11})$  the relative magnitude of total elimination to primary elimination. Since  $k_1 \equiv k_{1b} \hat{1}_{11}$  represents the total elimination rate from the compartment, the 1-compartment PBPK model (8) appears formalistically equivalent to the 1-compartment classical model (2). It is a pseudo model since the circulating bloodflow input is missing from the model. The difference between the classical and physiological model is that the knowledge of the composite  $k_1$  in the classical model is insufficient to well determine  $k_{1b}$  (much less  $Q_1, V_1$  or  $R_1$ ) and  $k_{1e}$  separately in the PBPK model. Thus, the greater biological realism of PBPK models is accompanied by increased parameter estimation instability - in the absence of auxiliary internal biomarker measurements or judicious choice of otherwise unidentifiable parameters.

## 2-Compartment Model

A natural extension to a 2-compartment PBPK model might be given by

$$\begin{aligned} C'_1 &= \frac{A'_1}{V'_1} = -\left( \frac{Q_1 C_1}{V_1 R_1} + k_{1e} C_1 \right) + \frac{Q_2 C_2}{V_1 R_2} + i_1 \\ C'_2 &= \frac{A'_2}{V'_2} = \frac{Q_2 C_1}{V_2 R_1} - \left( \frac{Q_2 C_2}{V_2 R_2} + k_{2e} C_2 \right) + i_2, \end{aligned} \quad (9)$$

or, in factored matrix form, by

$$\begin{pmatrix} C'_1 \\ C'_2 \end{pmatrix} = - \begin{pmatrix} \frac{Q_1}{V_1} & 0 \\ 0 & \frac{Q_2}{V_2} \end{pmatrix} \begin{pmatrix} \hat{1}_{11} & -1_{12} \\ -1_{21} & \hat{1}_{22} \end{pmatrix} \begin{pmatrix} R_1^{-1} & 0 \\ 0 & R_2^{-1} \end{pmatrix} \begin{pmatrix} C_1 \\ C_2 \end{pmatrix} + \begin{pmatrix} i_1 \\ i_2 \end{pmatrix}, \quad (10)$$

where indices (1,2) denote main (e.g., blood) and peripheral compartments (all other organ compartments lumped together in the 2-compartment case);  $(i_1, i_2)^T$  is the system column input vector;  $Q_1$  is the total blood flow and  $Q_2$  is the bloodflow to compartment 2 which, in the 2-compartment model case

only, equals the total bloodflow to all other organs and thus  $Q_1 = Q_2$ ;  $V_1$  and  $V_2$  are the corresponding compartment volumes;  $R_1$  and  $R_2$  the corresponding partition coefficients ( $R_1 = 1$  typically). Also,  $k_{ib} = \frac{Q_i}{V_i R_i}$  and  $k_{ie}$  are the  $i^{\text{th}}$  compartment bloodflow and secondary elimination rate constants ( $i$  is a compartment index here, not the system input above),  $\hat{1}_{11} \equiv 1 + \epsilon_{ii} \equiv 1 + k_{ie}/k_{ib}$  relative total/bloodflow elimination rates;  $1_{12}$  and  $1_{21}$  are off diagonal unity elements indicating organ bloodflow interconnections.

The PBPK matrix form (10) simplifies to

$$C' = -QV^{-1}SR^{-1}C + i \quad (11)$$

or, in classical compartmental model form, to

$$C' \equiv -KC + i \quad (12)$$

after collapsing the physiological matrices into one product matrix.  $C$  denotes the vector of concentrations for compartments 1 and 2,  $C'$  the vector of concentration time derivatives,  $i$  the vector of inputs,  $Q$  the 2-dimensional diagonal matrix of blood flows,  $V^{-1}$  the diagonal matrix of inverse compartmental volumes,  $R^{-1}$  the diagonal matrix of inverse partition coefficients,  $S$  the unitless structural matrix whose  $j^{\text{th}}$  column off diagonal components indicate the relative magnitude of input rates ( $1_{12}, 1_{21}$ ) from the other compartment to the  $j^{\text{th}}$  compartment's diagonal relative elimination rate ( $\hat{1}_{11}, \hat{1}_{22}$ ), and  $K = QV^{-1}SR^{-1}$  the 2-dimensional classical compartment composite transfer rate matrix. Again, simply knowing the composite  $k_{ij}$  ( $i, j = 1, 2$ ) components of  $K$  does not uniquely well-define the individual physiological components of  $Q$ ,  $V^{-1}$ ,  $R^{-1}$  or  $S$ .

One might speculate that it is necessary to know about 3/4 of the components  $Q_i$ ,  $V_i$ ,  $R_i$  and  $k_{ie}$  to reduce PBPK model fitting complexity to that of classical compartmental model fitting? Fitting classical matrix models is difficult enough and typically requires internal biomarker data (i.e., organ exposure or dose) to identify model parameters and state variables.

The standard solution ([7], [8]) to the linear ODE system (12) is given by a matrix exponential integral analogous to the scalar case (3), namely

$$C(t) = \int_0^t e^{-K(t-s)} i(s) ds \quad (13)$$

for continuous input and by

$$C = e^{-Kt} C_0, \quad (14)$$

for bolus dose input, where  $C_0 = \begin{pmatrix} C_{10} & C_{20} \end{pmatrix}^T$  is the vector of initial concentrations. The area under the concentration curve is similarly given by

$$\begin{aligned} AUC &= -K^{-1} \left( e^{-Kt} \Big|_0^\infty \right) C_0 = K^{-1} C_0 = \left( QV^{-1}SR^{-1} \right)^{-1} C_0 \\ &= RS^{-1}VQ^{-1}C_0 = RS^{-1}Q^{-1}A_0. \end{aligned} \quad (15)$$

Broken down into its AUC components, one has

$$\begin{aligned}
 \begin{pmatrix} AUC_1 \\ AUC_2 \end{pmatrix} &= \begin{pmatrix} R_1 & 0 \\ 0 & R_2 \end{pmatrix} \left[ |S|^{-1} \begin{pmatrix} \check{S}_{11} & \check{S}_{12} \\ \check{S}_{21} & \check{S}_{22} \end{pmatrix} \right] \begin{pmatrix} Q_1^{-1} & 0 \\ 0 & Q_2^{-1} \end{pmatrix} \begin{pmatrix} A_{10} \\ A_{20} \end{pmatrix} \\
 &= \begin{pmatrix} R_1 & 0 \\ 0 & R_2 \end{pmatrix} |S|^{-1} \begin{pmatrix} \hat{1}_{22} & 1_{12} \\ 1_{21} & \hat{1}_{11} \end{pmatrix} \begin{pmatrix} Q_1^{-1} A_{10} \\ Q_2^{-1} A_{20} \end{pmatrix} \\
 &= |S|^{-1} \begin{pmatrix} R_1 \left( \hat{1}_{22} Q_1^{-1} A_{10} + 1_{12} Q_2^{-1} A_{20} \right) \\ R_2 \left( 1_{21} Q_1^{-1} A_{10} + \hat{1}_{11} Q_2^{-1} A_{20} \right) \end{pmatrix} \\
 &= \begin{pmatrix} R_1 & 0 \\ 0 & R_2 \end{pmatrix} |S|^{-1} \begin{pmatrix} \hat{1}_{22} & 1_{12} \\ 1_{21} & \hat{1}_{11} \end{pmatrix} \begin{pmatrix} Q_1^{-1} A_{10} \\ Q_2^{-1} A_{20} \end{pmatrix} \\
 &= |S|^{-1} \begin{pmatrix} R_1 \left( \hat{1}_{22} Q_1^{-1} A_{10} + 1_{12} Q_2^{-1} A_{20} \right) \\ R_2 \left( 1_{21} Q_1^{-1} A_{10} + \hat{1}_{11} Q_2^{-1} A_{20} \right) \end{pmatrix}
 \end{aligned} \tag{16}$$

where  $|S| \equiv \det(S)$  and  $\check{S}$  is the adjoint matrix of transposed cofactors given by

$$\check{S}_{ij} = (-1)^{i+j} \det(S(\{j\}', \{i\}')) = (-1)^{i+j} M_{ji} = C_{ji}$$

where  $M_{ji} = \det(S(\{j\}', \{i\}'))$  is the  $ji^{\text{th}}$  minor of  $S$  – the determinant of  $S$  with  $j^{\text{th}}$  row and  $i^{\text{th}}$  column deleted [8] and  $S^{-1} \equiv (S^{-1})_{i,j=1,2} = |S|^{-1} \check{S}$ ,  $|S| = (\hat{1}_{11}\hat{1}_{22} - 1_{12}1_{21}) = (\epsilon_{1e} + \epsilon_{2e} + \epsilon_{1e}\epsilon_{2e})$ . Note that all AUC components are nonnegative since  $|S| > 0$  and  $\check{S} \geq 0$ . Nonnegativity results if some compartment has systemic elimination (e.g., a metabolic or urinary elimination that is not input for another modeled compartment) such that some  $\hat{1}_{ii} > 1$ . If  $\det(S) = 0$ , then row sums of  $S$  are zero and solutions blow up.

Analogous to scalar results for an infusion reinterpreted as a periodic bolus dose input, the linear system steady-state is given by

$$C_{ss} = K^{-1}i = K^{-1}t^{-1}C_0 = RS^{-1}Q^{-1}t^{-1}A_0. \tag{17}$$

Thus system infusion internal doses equal those from equivalent bolus inputs.

### 3-Compartment Model

An extension to a higher resolution 3-compartment PBPK model is given by

$$\begin{aligned}
 C_1' &= -\left(\frac{Q_1C_1}{V_1R_1} + k_{1e}C_1\right) + \frac{Q_2C_2}{V_1R_2} + \frac{Q_3C_3}{V_1R_3} + i_1 \\
 C_2' &= \left(\frac{Q_2C_1}{V_2R_1}\right) - \left(\frac{Q_2C_2}{V_2R_2} + k_{2e}C_2\right) + i_2 \\
 C_3' &= \left(\frac{Q_3C_1}{V_3R_1}\right) - \left(\frac{Q_3C_3}{V_3R_3} + k_{3e}C_3\right) + i_3
 \end{aligned} \tag{18}$$

or, in factored matrix form, by

$$C' \equiv \begin{pmatrix} C_1' \\ C_2' \\ C_3' \end{pmatrix} = -QV^{-1}SR^{-1} \begin{pmatrix} C_1 \\ C_2 \\ C_3 \end{pmatrix} C + \begin{pmatrix} i_1 \\ i_2 \\ i_3 \end{pmatrix} = -KC + i \tag{19}$$

where

$$QV^{-1} = \begin{pmatrix} \frac{Q_1}{V_1} & 0 & 0 \\ 0 & \frac{Q_2}{V_2} & 0 \\ 0 & 0 & \frac{Q_3}{V_3} \end{pmatrix}, R^{-1} = \begin{pmatrix} R_1^{-1} & 0 & 0 \\ 0 & R_2^{-1} & 0 \\ 0 & 0 & R_3^{-1} \end{pmatrix}, \quad (20)$$

$$S = \begin{pmatrix} \hat{1}_{11} & -q_{12} & -q_{13} \\ -1_{21} & \hat{1}_{22} & 0 \\ -1_{31} & 0 & \hat{1}_{33} \end{pmatrix}, C = \begin{pmatrix} C_1 \\ C_2 \\ C_3 \end{pmatrix}, i = \begin{pmatrix} i_1 \\ i_2 \\ i_3 \end{pmatrix}$$

where  $q_{12} \equiv Q_2/Q_1$ ,  $q_{13} = Q_3/Q_1$ ,  $q_{12} + q_{13} = 1$ ,  $K = QV^{-1}SR^{-1}$  and all solution vectors ( $C$ ,  $AUC$  and  $C_{ss}$ ) are also natural 3-dimensional extensions of their 2-compartment PBPK analogues. The structural inverse is given by

$$S^{-1} = (S^{-1})_{i,j=1,2,3} = |S|^{-1} \begin{pmatrix} \check{S}_{11} & \check{S}_{12} & \check{S}_{13} \\ \check{S}_{21} & \check{S}_{22} & \check{S}_{23} \\ \check{S}_{31} & \check{S}_{32} & \check{S}_{33} \end{pmatrix} \quad (21)$$

$$= |S|^{-1} \begin{pmatrix} \hat{1}_{22}\hat{1}_{33} & q_{12}\hat{1}_{33} & q_{13}\hat{1}_{22} \\ 1_{21}\hat{1}_{33} & (\hat{1}_{11}\hat{1}_{33} - q_{13}1_{31}) & 1_{21}q_{13} \\ 1_{31}\hat{1}_{22} & 1_{31}q_{12} & (\hat{1}_{11}\hat{1}_{22} - q_{12}1_{21}) \end{pmatrix}$$

with  $\det(S) = |S| = \hat{1}_{11}\hat{1}_{22}\hat{1}_{33} - q_{12}1_{21}\hat{1}_{33} - q_{13}1_{31}\hat{1}_{22}$ . AUC is given by

$$\begin{pmatrix} AUC_1 \\ AUC_2 \\ AUC_3 \end{pmatrix} = |S|^{-1} \begin{pmatrix} R_1 \left( \check{S}_{11}Q_1^{-1}A_{10} + \check{S}_{12}Q_2^{-1}A_{20} + \check{S}_{13}Q_3^{-1}A_{30} \right) \\ R_2 \left( \check{S}_{21}Q_1^{-1}A_{10} + \check{S}_{22}Q_2^{-1}A_{20} + \check{S}_{23}Q_3^{-1}A_{30} \right) \\ R_3 \left( \check{S}_{31}Q_1^{-1}A_{10} + \check{S}_{32}Q_2^{-1}A_{20} + \check{S}_{33}Q_3^{-1}A_{30} \right) \end{pmatrix}$$

$$= |S|^{-1} \begin{pmatrix} R_1 \left( \hat{1}_{22}\hat{1}_{33}Q_1^{-1}A_{10} + q_{12}\hat{1}_{33}Q_2^{-1}A_{20} + q_{13}\hat{1}_{22}Q_3^{-1}A_{30} \right) \\ R_2 \left( 1_{21}\hat{1}_{33}Q_1^{-1}A_{10} + (\hat{1}_{11}\hat{1}_{33} - q_{13}1_{31})Q_2^{-1}A_{20} + 1_{21}q_{13}Q_3^{-1}A_{30} \right) \\ R_3 \left( 1_{31}\hat{1}_{22}Q_1^{-1}A_{10} + 1_{31}q_{12}Q_2^{-1}A_{20} + (\hat{1}_{11}\hat{1}_{22} - q_{12}1_{21})Q_3^{-1}A_{30} \right) \end{pmatrix} \quad (22)$$

and all AUC components are nonnegative as before since  $|S| > 0$  for net degradative systems ( $\hat{1}_{ii} > 1$  for some  $i$ ) and  $0 < q_{1i} < 1$ ,  $i = 2, 3$ .

**Uniqueness of 3-Compartment PBPK Models.** Use of 1 or 2 compartment PBPK models may be sufficient for some applications purposes where internal physiology is of little importance. Indeed, modeller's typically lump as many organs as possible into composite organs to simplify the models as far as possible without adversely affecting the analysis' goals (Occam's razor principle). On the other hand, use of 3 or greater compartments may be critical for many risk assessment tasks.

A unique matrix structural aspect of the 3 compartment PBPK model above comes from the fact that it is the smallest dimensioned refinement with less than 100% blood flow to peripheral organs (i.e.,  $0 < q_{1i} < 1$ ,  $i = 2, 3$ ). Such fractional flows impart to PBPK models an important qualitative physiological distinction and potential advantage over nonphysiological compartmental models for understanding and controlling human exposure and risk.

Typically, compartments 1, 2 and 3 represent composite blood, liver and slowly perfused (fat and muscle combined) compartments. Other physiological organs are lumped together with one of the 3 primary composite organs for specific analysis purposes. For some QRA purposes, a 3-compartment fractional flow PBPK model may offer significant biological improvements over a more classical 2-compartment PBPK model.

#### 4-Compartment Model

Most models may be extended into higher dimensions in many ways. A simple extension of (18) above would involve splitting the third (or second) compartment into two subcompartments for potentially greater biological resolution. Thus, the mass balance equations might be given by

$$\begin{aligned} C_1' &= -\left(\frac{Q_1 C_1}{V_1 R_1} + k_{1e} C_1\right) + \frac{Q_2 C_2}{V_1 R_2} + \frac{Q_3 C_3}{V_1 R_3} + \frac{Q_4 C_4}{V_1 R_4} + i_1 \\ C_2' &= \left(\frac{Q_2 C_1}{V_2 R_1}\right) - \left(\frac{Q_2 C_2}{V_2 R_2} + k_{2e} C_2\right) + i_2 \\ C_3' &= \left(\frac{Q_3 C_1}{V_3 R_1}\right) - \left(\frac{Q_3 C_3}{V_3 R_3} + k_{3e} C_3\right) + i_3 \\ C_4' &= \left(\frac{Q_4 C_1}{V_4 R_1}\right) - \left(\frac{Q_4 C_4}{V_4 R_4} + k_{4e} C_4\right) + i_4 \end{aligned} \quad (23)$$

or, in factored matrix form, by

$$C' = \begin{pmatrix} C_1' \\ C_2' \\ C_3' \\ C_4' \end{pmatrix} = -QV^{-1}SR^{-1} \begin{pmatrix} C_1 \\ C_2 \\ C_3 \\ C_4 \end{pmatrix} + \begin{pmatrix} i_1 \\ i_2 \\ i_3 \\ i_4 \end{pmatrix} = -KC + i, \quad (24)$$

where

$$\begin{aligned} QV^{-1} &= \begin{pmatrix} \frac{Q_1}{V_1} & 0 & 0 & 0 \\ 0 & \frac{Q_2}{V_2} & 0 & 0 \\ 0 & 0 & \frac{Q_3}{V_3} & 0 \\ 0 & 0 & 0 & \frac{Q_4}{V_4} \end{pmatrix}, R^{-1} = \begin{pmatrix} R_1^{-1} & 0 & 0 & 0 \\ 0 & R_2^{-1} & 0 & 0 \\ 0 & 0 & R_3^{-1} & 0 \\ 0 & 0 & 0 & R_4^{-1} \end{pmatrix}, \\ S &= \begin{pmatrix} \hat{1}_{11} & -q_{12} & -q_{13} & -q_{14} \\ -1_{21} & \hat{1}_{22} & 0 & 0 \\ -1_{31} & 0 & \hat{1}_{33} & 0 \\ -1_{41} & 0 & 0 & \hat{1}_{44} \end{pmatrix} \end{aligned} \quad (25)$$

where  $q_{12} \equiv Q_2/Q_1$ ,  $q_{13} = Q_3/Q_1$ ,  $q_{14} = Q_4/Q_1$  such that  $q_{12} + q_{13} + q_{14} = 1$ . All vectors and matrices are indexed as in the 3 compartment case, but for 4 dimensions. The inverse structural matrix  $(S^{-1})_{i,j=1,2,3,4}$  is given by

$$S^{-1} = |S|^{-1} \begin{pmatrix} \check{S}_{11} & \check{S}_{12} & \check{S}_{13} & \check{S}_{14} \\ \check{S}_{21} & \check{S}_{22} & \check{S}_{23} & \check{S}_{24} \\ \check{S}_{31} & \check{S}_{32} & \check{S}_{33} & \check{S}_{34} \\ \check{S}_{41} & \check{S}_{42} & \check{S}_{43} & \check{S}_{44} \end{pmatrix} =$$

$$\begin{pmatrix} \hat{l}_{22}\hat{l}_{33}\hat{l}_{44} & \begin{pmatrix} q_{12}\hat{l}_{33}\hat{l}_{44} \\ \hat{l}_{11}\hat{l}_{33}\hat{l}_{44} \\ -q_{14}\hat{l}_{41}\hat{l}_{33} \\ -q_{13}\hat{l}_{31}\hat{l}_{44} \end{pmatrix} & q_{13}\hat{l}_{22}\hat{l}_{44} & q_{14}\hat{l}_{22}\hat{l}_{33} \\ \hat{l}_{21}\hat{l}_{33}\hat{l}_{44} & \begin{pmatrix} -q_{12}\hat{l}_{41}\hat{l}_{33} \\ -q_{13}\hat{l}_{31}\hat{l}_{44} \end{pmatrix} & \hat{l}_{21}q_{13}\hat{l}_{44} & \hat{l}_{21}q_{14}\hat{l}_{33} \\ \hat{l}_{31}\hat{l}_{22}\hat{l}_{44} & \hat{l}_{31}q_{12}\hat{l}_{44} & \begin{pmatrix} \hat{l}_{11}\hat{l}_{22}\hat{l}_{44} \\ -q_{12}\hat{l}_{21}\hat{l}_{44} \\ -q_{14}\hat{l}_{41}\hat{l}_{22} \end{pmatrix} & \hat{l}_{31}q_{14}\hat{l}_{22} \\ \hat{l}_{41}\hat{l}_{22}\hat{l}_{33} & \hat{l}_{41}q_{12}\hat{l}_{33} & \hat{l}_{41}q_{13}\hat{l}_{22} & \begin{pmatrix} \hat{l}_{11}\hat{l}_{22}\hat{l}_{33} \\ -q_{12}\hat{l}_{21}\hat{l}_{33} \\ -q_{13}\hat{l}_{31}\hat{l}_{22} \end{pmatrix} \end{pmatrix} \quad |S| \quad (26)$$

where  $|S| = \hat{l}_{11}\hat{l}_{22}\hat{l}_{33}\hat{l}_{44} - q_{12}\hat{l}_{21}\hat{l}_{33}\hat{l}_{44} - q_{13}\hat{l}_{31}\hat{l}_{22}\hat{l}_{44} - q_{14}\hat{l}_{41}\hat{l}_{22}\hat{l}_{33}$ . Thus, the AUC components are given by

$$\begin{pmatrix} AUC_1 \\ AUC_2 \\ AUC_3 \\ AUC_4 \end{pmatrix} = \begin{pmatrix} R_1 \left( \frac{(\hat{s}_{11}Q_1^{-1}A_{10} + \hat{s}_{12}Q_2^{-1}A_{20} + \hat{s}_{13}Q_3^{-1}A_{30} + \hat{s}_{14}Q_4^{-1}A_{40})}{|S|} \right) \\ R_2 \left( \frac{(\hat{s}_{21}Q_1^{-1}A_{10} + \hat{s}_{22}Q_2^{-1}A_{20} + \hat{s}_{23}Q_3^{-1}A_{30} + \hat{s}_{24}Q_4^{-1}A_{40})}{|S|} \right) \\ R_3 \left( \frac{(\hat{s}_{31}Q_1^{-1}A_{10} + \hat{s}_{32}Q_2^{-1}A_{20} + \hat{s}_{33}Q_3^{-1}A_{30} + \hat{s}_{34}Q_4^{-1}A_{40})}{|S|} \right) \\ R_4 \left( \frac{(\hat{s}_{41}Q_1^{-1}A_{10} + \hat{s}_{42}Q_2^{-1}A_{20} + \hat{s}_{43}Q_3^{-1}A_{30} + \hat{s}_{44}Q_4^{-1}A_{40})}{|S|} \right) \end{pmatrix} \quad (27)$$

$$= \begin{pmatrix} \frac{R_1 \left( \left( \hat{l}_{22}\hat{l}_{33}\hat{l}_{44} \right) Q_1^{-1}A_{10} + q_{12}\hat{l}_{33}\hat{l}_{44}Q_2^{-1}A_{20} + q_{13}\hat{l}_{22}\hat{l}_{44}Q_3^{-1}A_{30} + q_{14}\hat{l}_{22}\hat{l}_{33}Q_4^{-1}A_{40} \right)}{|S|} \\ R_2 \left( \hat{l}_{21}\hat{l}_{33}\hat{l}_{44}Q_1^{-1}A_{10} + \begin{pmatrix} \hat{l}_{11}\hat{l}_{33}\hat{l}_{44} \\ -q_{13}\hat{l}_{31}\hat{l}_{44} \\ -q_{14}\hat{l}_{41}\hat{l}_{33} \end{pmatrix} Q_2^{-1}A_{20} + \hat{l}_{21}q_{13}\hat{l}_{44}Q_3^{-1}A_{30} + \hat{l}_{21}q_{14}\hat{l}_{33}Q_4^{-1}A_{40} \right) \\ R_3 \left( \hat{l}_{31}\hat{l}_{22}\hat{l}_{44}Q_1^{-1}A_{10} + \hat{l}_{31}q_{12}\hat{l}_{44}Q_2^{-1}A_{20} + \begin{pmatrix} \hat{l}_{11}\hat{l}_{22}\hat{l}_{44} \\ -q_{12}\hat{l}_{21}\hat{l}_{44} \\ -q_{14}\hat{l}_{41}\hat{l}_{22} \end{pmatrix} Q_3^{-1}A_{30} + \hat{l}_{31}q_{14}\hat{l}_{22}Q_4^{-1}A_{40} \right) \\ R_4 \left( \hat{l}_{41}\hat{l}_{22}\hat{l}_{33}Q_1^{-1}A_{10} + \hat{l}_{41}q_{12}\hat{l}_{33}Q_2^{-1}A_{20} + \hat{l}_{41}q_{13}\hat{l}_{22}Q_3^{-1}A_{30} + \begin{pmatrix} \hat{l}_{11}\hat{l}_{22}\hat{l}_{33} \\ -q_{12}\hat{l}_{21}\hat{l}_{33} \\ -q_{13}\hat{l}_{31}\hat{l}_{22} \end{pmatrix} Q_4^{-1}A_{40} \right) \end{pmatrix} \quad |S|$$

with all AUC components nonnegative since  $|S| > 0$  for degradative systems.

### Risk Assessment Uses

Analytic AUC or  $C_{ss}$  formulas are useful for elegantly clarifying the relative role and sensitivity of model parameters in QRA applications such as (1) intermittent exposure variation and interpolation, (2) high-to-low-dose extrapolation, (3) route-to-route extrapolation, (4) intraspecies variation and

interspecies scaling, (5) inverse reconstruction of exposure from dose, and (6) model expansion or collapse.

With respect to intermittent exposure variation and interpolation, equations (15, 17) show that both the integrated concentration (AUC) and steady-state concentration ( $C_{ss}$ ) vectors are proportional, as a matrix function, to the vector of bolus dose ( $C_0$ ) or constant infusion inputs. This inherent additivity property (linear superposition principle) for linear systems also implies that administration of a given amount of toxicant as one bolus dose, several bolus doses or continuously over time will yield the same systemic or target organ AUC dose. With respect to high-to-low-dose extrapolations, linear equations imply that internal dose measures are proportional to administered dose. Thus a 10-fold reduction in administered dose implies a 10-fold reduction in target organ dose. Therefore, for simple intermittent exposure variation and high-to-low-dose extrapolation applications, use of target organ dose, under linear system conditions, seems to provide no advantage over use of administered dose and knowledge of physiological model parameters is unnecessary. For such cases, use of a 1-compartment risk model (i.e., the standard linear proportional model) for administered dose should be sufficient. Under more typical nonlinear conditions, however, physiological parameters are required since output is no longer proportional to input.

On the other hand, for the inverse reconstruction of exposure from internal dose or the collapse or expansion of the model to reduce model bias or uncertainty, knowledge of PBPK parameters may be critical to biological understanding, computational solution and regulatory application.

More importantly, for interspecies comparison of target organ dose (e.g., mouse-to-man extrapolation) or intraspecies comparisons (e.g., child-to-adult or slow-to-fast metabolizer), knowledge of PBPK parameters is necessary. With respect to comparing target organ dose by different routes of exposure (inhalation, ingestion, dermal), knowledge of PBPK parameters is clearly critical. For example, agricultural pesticides are absorbed by three routes under typical usage conditions. Interspecies scaling and route-to-route extrapolation applications are explored below.

**Single Input/Single Output (SISO) Formulas Revisited.** The AUC dose metric for target organs is useful for studying many intermediate term drug efficacy effects and is generally preferred for long latency cancer health effects where short-term temporal exposure variations might be time averaged to approximate longer term effects. Thus, AUC formulas provide the focus for the QRA applications below.

The 4-compartment model output (27) reflects AUC output additivity for simultaneous but independent system inputs. The  $i^{th}$  compartment dose output from a  $j^{th}$  compartment bolus dose input is given by

$$AUC_{ij} = R_i (S^{-1})_{ij} Q_j^{-1} A_{j0}, \quad (28)$$

in amount form, and, in concentration form, by

$$AUC_{ij} = R_i (S^{-1})_{ij} Q_j^{-1} V_j C_{j0} = \frac{R_i}{R_j} (S^{-1})_{ij} \left( \frac{C_{j0}}{\frac{Q_j}{V_j R_j}} \right) = \frac{R_i}{R_j} (S^{-1})_{ij} \left( \frac{C_{j0}}{k_{jb}} \right). \quad (29)$$

The concentration form is perhaps most useful for showing PBPK generalizations of 1-compartment classical results ( $AUC = C_0/k$ ), for interspecies scaling applications and for comparing target organ doses by two routes of physiological absorption (e.g., inhalation and dermal) from a common environmental media concentration (e.g., ppm in the air). The coefficient of  $C_{j0}$ ,  $\tilde{k}_j^{-1} \equiv ((R_i R_j^{-1} (S^{-1})_{ij} k_{jb}^{-1}))$ , represents a PBPK generalization of the classical total inverse elimination rate, or mean residence time, of toxicant in compartment  $j$ .

The amount forms, however, provide simpler comparative target organ risk formulas for given bolus dose inputs, primarily because they ignore physiological absorption factors. Because we are interested here in the feasibility of development of simple analytic formulas, we will emphasize the amount forms in the construction of comparative dose formulas below.

Manipulation of (27, 29) shows that the 16 SISO 4-compartment AUC dose formulas appear to reduce to 5 conditions:

$$AUC_{ij} = \frac{R_i}{R_j} \left( \frac{q_{1j}}{\hat{1}_{ii} \left( 1 - \frac{q_{12}}{\hat{1}_{11}} \frac{\hat{1}_{21}}{\hat{1}_{22}} - \frac{q_{13}}{\hat{1}_{11}} \frac{\hat{1}_{31}}{\hat{1}_{33}} - \frac{q_{14}}{\hat{1}_{11}} \frac{\hat{1}_{41}}{\hat{1}_{44}} \right)} \right) \left( \frac{C_{j0}}{k_j} \right), i = 1, i \neq j \quad (30)$$

$$AUC_{ij} = \frac{R_i}{R_j} \left( \frac{1_{i1}}{\hat{1}_{ii} \left( 1 - \frac{q_{12}}{\hat{1}_{11}} \frac{\hat{1}_{21}}{\hat{1}_{22}} - \frac{q_{13}}{\hat{1}_{11}} \frac{\hat{1}_{31}}{\hat{1}_{33}} - \frac{q_{14}}{\hat{1}_{11}} \frac{\hat{1}_{41}}{\hat{1}_{44}} \right)} \right) \left( \frac{C_{j0}}{k_j} \right), i \neq j, j = 1 \quad (31)$$

$$AUC_{ij} = \frac{R_i}{R_j} \left( \frac{1_{i1} q_{1j}}{\hat{1}_{ii} \hat{1}_{11} \left( 1 - \frac{q_{12}}{\hat{1}_{11}} \frac{\hat{1}_{21}}{\hat{1}_{22}} - \frac{q_{13}}{\hat{1}_{11}} \frac{\hat{1}_{31}}{\hat{1}_{33}} - \frac{q_{14}}{\hat{1}_{11}} \frac{\hat{1}_{41}}{\hat{1}_{44}} \right)} \right) \left( \frac{C_{j0}}{k_j} \right), i \neq j; i, j \neq 1 \quad (32)$$

$$AUC_{ij} = \left( \frac{1}{\left( 1 - \frac{q_{12}}{\hat{1}_{11}} \frac{\hat{1}_{21}}{\hat{1}_{22}} - \frac{q_{13}}{\hat{1}_{11}} \frac{\hat{1}_{31}}{\hat{1}_{33}} - \frac{q_{14}}{\hat{1}_{11}} \frac{\hat{1}_{41}}{\hat{1}_{44}} \right)} \right) \left( \frac{C_{j0}}{k_j} \right), i = j = 1 \quad (33)$$

$$AUC_{ij} = \left( \frac{\left( 1 - \frac{q_{12}}{\hat{1}_{11}} \frac{\hat{1}_{21}}{\hat{1}_{22}} - \frac{q_{13}}{\hat{1}_{11}} \frac{\hat{1}_{31}}{\hat{1}_{33}} - \frac{q_{14}}{\hat{1}_{11}} \frac{\hat{1}_{41}}{\hat{1}_{44}} \right)}{\left( 1 - \frac{q_{12}}{\hat{1}_{11}} \frac{\hat{1}_{21}}{\hat{1}_{22}} - \frac{q_{13}}{\hat{1}_{11}} \frac{\hat{1}_{31}}{\hat{1}_{33}} - \frac{q_{14}}{\hat{1}_{11}} \frac{\hat{1}_{41}}{\hat{1}_{44}} \right)} \right) \left( \frac{C_{j0}}{k_j} \right), i = j \neq 1; j_1, j_2 \neq j \quad (34)$$

There are many ways to represent AUC dose. The relative dose representations above emphasize product ratios and sums of physiologically related parameters (e.g.,  $\frac{R_i}{R_j}$ ,  $\frac{1_{i1}}{\hat{1}_{ii}}$ ,  $\frac{q_{1j}}{\hat{1}_{11}}$ ,  $\frac{1}{\left( 1 - \frac{q_{12}}{\hat{1}_{11}} \frac{\hat{1}_{21}}{\hat{1}_{22}} - \frac{q_{13}}{\hat{1}_{11}} \frac{\hat{1}_{31}}{\hat{1}_{33}} - \frac{q_{14}}{\hat{1}_{11}} \frac{\hat{1}_{41}}{\hat{1}_{44}} \right)}$ ,  $\left( \frac{C_{j0}}{k_j} \right)$ ) and are relatively natural and informative extensions of 1-compartment model AUC formula (i.e.,  $\frac{C_{j0}}{k_j}$ ) and are useful for specific exposure, risk or efficacy assessment applications (e.g., interspecies toxicity scaling below).

The formula for the 3-compartment model is identical to the 4-compartment model formula after dropping reference to the omitted 4th compartment. Likewise, 1 and 2-compartment model formulations are identical after dropping reference to the omitted compartments. Similarly, these formula should extend in a reasonable natural fashion to larger dimensioned PBPK models (extensions will be presented elsewhere).

**Interspecies Scaling Formulas.** From (5,8) the 1-compartment AUC,

$$AUC = \frac{C_0}{k_1} = \frac{\frac{A_{10}}{V_{10}}}{k_{1b}(1 + \epsilon_1)} = \frac{\frac{A_{10}}{V_{10}}}{\frac{Q_1}{V_1 R_1} \left(1 + \frac{k_{1e}}{\frac{Q_1}{V_1 R_1}}\right)}, \quad (35)$$

can be rewritten, for interspecies scaling purposes, proportionally as

$$AUC \propto \frac{\frac{W^b}{W^1}}{\frac{W^b}{W^1} \left(1 + \frac{W^{\beta-1}}{\frac{W^b}{W^1}}\right)} = \frac{W^{b-1}}{W^{b-1} \left(1 + \frac{W^{\beta-1}}{W^{b-1}}\right)} \approx \begin{pmatrix} W^0 & \text{if } k_{1e} \ll k_{1b} \\ W^{b-\beta} & \text{if } k_{1e} \gg k_{1b} \end{pmatrix}, \quad (36)$$

where  $W$  refers to the body weight of the animal,  $b$  refers to the scaling constant for the compartment's basal metabolism related "primary" physiological uptake processes for amounts or volumes,  $b - 1$  refers to the scaling constant for the equivalent concentration uptake processes, and  $\beta - 1$  refers to the compartment's concentration scaling constant for secondary elimination processes, if any. Typically, the primary basal metabolism concentration uptake scale constant is about  $(b - 1) = -.25$  and the secondary elimination constant is also about  $(\beta - 1) = -.25$  (if it is also basal metabolism correlated). However, the secondary elimination constant may be closer to  $(\beta - 1) = 0$  for some subcellular elimination processes such as metabolic clearances processes largely independent of animal body weight and spontaneous thermodynamic elimination processes associated with reactive metabolite clearance [11]. Indeed, empirical curve fits suggest that  $b = .73$  is an appropriate overall interspecies scaling constant for many composite uptake and elimination processes dominated by basal metabolism energy needs [10].

If AUC is independent of body weight (i.e.,  $\propto W^0$ ), then this is typically referred to as overall basal metabolism scaling. If AUC is proportional to  $W^{-.25}$ , then this is typically referred to as overall bodyweight scaling. This terminology may be a misleading oversimplification since AUC scaling is proportional to the ratio of composite uptake to composite elimination processes, implying that the overall scaling constant is the difference of uptake and elimination scale constants  $((b - \beta) = (b - 1) - (\beta - 1))$ .

The often cited basal metabolism scaling constant ( $b \approx .75$ ) might be thought of as the observed surface area to volume scaling constant for commonly measured animal shapes rather than that for homogeneous spheres ( $b=2/3$ ). Commonly estimated scale constants may reflect values greater than  $2/3$  as the composite result of two separate scaling phenomena: the

scaling of small pudgy animals (e.g., mice, rats, hamsters) to large pudgy animals (e.g., minipigs) and the scaling of pudgy animals to spindle-shaped animals (e.g., monkeys and humans).

To extend this scaling formula to larger PBPK models, consider the 4-compartment AUC formula (32), which can be reformulated as

$$\begin{aligned}
 AUC_{ij} &\propto \left( \frac{1_{i1} q_{1j}}{1_{ii} 1_{11}} \frac{1}{\left( 1 - \frac{q_{12} 1_{21}}{1_{11} 1_{22}} - \frac{q_{13} 1_{31}}{1_{11} 1_{33}} - \frac{q_{14} 1_{41}}{1_{11} 1_{44}} \right)} \right) \left( \frac{C_{j0}}{k_j} \right), i \neq j; i, j \neq 1, \\
 &\propto \left( \frac{\left( \frac{W^{b_j-1}}{W^{b_j-1} \left( 1 + \frac{W^{\beta_j-1}}{W^{b_j-1}} \right)} \right)}{\left( 1 + \frac{W^{\beta_i-1}}{W^{b_i-1}} \right) \left( 1 + \frac{W^{\beta_1-1}}{W^{b_1-1}} \right) \left( 1 - \frac{q_{12} 1_{21}}{W_{11} W_{22}} - \frac{q_{13} 1_{31}}{W_{11} W_{33}} - \frac{q_{14} 1_{41}}{W_{11} W_{44}} \right)} \right) \\
 &\approx \propto \left( \frac{1}{\hat{W}_{ii} \hat{W}_{11}} \right) \left( \frac{1}{\hat{W}_{jj}} \right) = \hat{W}_{ii}^{-1} \hat{W}_{11}^{-1} \hat{W}_{jj}^{-1} \approx \propto W^{0=\sum_{k=1,i,j} (b_k - \beta_k)},
 \end{aligned} \quad (37)$$

where the term  $(0 = \sum_{k=1,i,j} (b_k - \beta_k))$  represents a plausible range for the composite sum of three scaling constant differences for the compartments  $(1, i, j)$ ,  $\hat{W}_{ii} = \left( 1 + \frac{W^{\beta_i-1}}{W^{b_i-1}} \right) \approx \propto W^0$  ( $i = 1, i, j$ ) if primary elimination,  $k_{ib} = \frac{Q_i}{V_i R_i}$ , dominates secondary elimination  $k_{ie}$  (i.e.,  $\hat{1}_{ii} = (1 + \frac{k_{ie}}{k_{ib}}) \rightarrow 1$ ). However,  $\hat{W}_{ii} \approx \propto W^{.25}$  where secondary elimination dominates (i.e.,  $\hat{1}_{ii} \rightarrow \infty$ ) and scales as bodyweight ( $\beta_i - 1 = 0$ ). Significantly, the long denominator term,  $\left( 1 - \frac{q_{12} 1_{21}}{W_{11} W_{22}} - \frac{q_{13} 1_{31}}{W_{11} W_{33}} - \frac{q_{14} 1_{41}}{W_{11} W_{44}} \right)$ , appears to have smaller relative effect upon the overall composite scaling constant than the isolated  $\hat{W}_{ii}$  terms, at least when this long term is bounded away from zero (e.g., when liver flow is large and the liver has dominant secondary metabolism). However, as it approaches zero, the corrective effect of this long term increasingly counteracts the scaling effect of the separate product factors,  $(\hat{W}_{ii}^{-1} \hat{W}_{11}^{-1} \hat{W}_{jj}^{-1})$ . This second order effect should be looked at more carefully in specific scaling situations. The individual  $(b_k - \beta_k)$  terms can theoretically be positive or negative, but positive differences would seem, intuitively, to predominate where secondary elimination is spontaneous (e.g., for reactive metabolites) or metabolic but proportional to cellular volume (i.e., independent of cellular basal metabolism energy needs).

To highlight the potential magnitude of effect upon the scaling constant, it may be illustrative to consider a somewhat extreme "double-teamed" case where the target organ and main compartments both eliminate toxicity by bodyweight scaled processes ( $\beta_i - 1 = \beta_1 - 1 = 0$ ) dominated, say, by secondary spontaneous metabolic elimination pathways, but uptake and other elimination processes scale as basal metabolism ( $\beta_j - 1 = b_1 - 1 = b_i - 1 = b_j - 1 = -.25$ ). In this case, the long denominator term (1-...) is near unity and has minimal corrective impact. Then (38) below suggests  $AUC_{ij} \propto W^{-.5}$ , which would imply that large animals are at far less risk than small animals

– less than bodyweight scaling ( $AUC \propto W^{-.25}$ ) and much less than basal metabolism scaling ( $AUC \propto W^0$ ) would imply. On the other hand, empirical evidence for human drugs with respect to noncancer health endpoints suggests the use of more conservative (i.e., more protective) human scaling closer to basal metabolism scaling [4]. Furthermore, empirical evidence for cancer endpoints ([1], [4]) suggests scaling constants between bodyweight scaling ( $b = 1.0$ ) and spherical surface area scaling ( $b = 2/3$ ). For comparison, overall interspecies scaling constants traditionally used by United States regulatory agencies for cancer risk range from surface area scaling ( $b = 2/3$ ) typically used by the Environmental Protection Agency and Consumer Product Safety Commission, to body weight scaling ( $b = 1.0$ ) used by the Food and Drug Administration and Occupational Safety and Health Administration [4].

When input and target compartments coincide, (33, 34) imply that

$$AUC_{ii} \approx \hat{W}_{ii}^{-1} \propto W^{0 \equiv (b_i - \beta_i)}, \quad (38)$$

where the term  $0 \equiv (b_i - \beta_i)$  denotes a plausible range of scale constants.

**Comparative Risk (CR) Route-to-route Dose Extrapolation.** One of the most important theoretical and practical uses of analytic PBPK formulas is to compare the relative impact upon target organ dose from two different routes of toxic compound exposure or bolus dose administration. To clarify the discussion of the comparative dose formulas below, it will be helpful to consider plausible physiological interpretations of each of the four compartments. In particular, it may be helpful to assume that: (1) the first compartment represents the arterial blood compartment, possibly lumped together with the venous blood, kidney, lung or some other rapidly perfused organs, (2) the second compartment represents the lumped liver, gall bladder and perhaps some other rapidly perfused compartments not lumped with the main blood compartment, (3) the third compartment represents the fat compartment and (4) the fourth compartment represents other lumped slowly perfused organs (e.g., muscle, bone and skin). Depending upon the toxic compound and risk application, appropriate organ lumpings can vary.

Representative comparative dose formulas are given below for several cases of potential bolus dose input into two different compartments of the 4-compartmental model above. While most of these results may be intuitively understood by researchers utilizing classical compartmental modeling tools, the comparative PBPK formulas below appear to provide more complete quantitative and qualitative tools for internal dose description, biological understanding and risk assessment manipulation.

First, for the case of peripheral fat compartment comparative risk (CR) from liver and blood bolus dose toxicant inputs (e.g., by ingestion into liver and inhalation into blood), CR is given by equation (27) as

$$CR_{32/31}^{(4)} \equiv \frac{AUC_{32}}{AUC_{31}} = \frac{(S^{-1})_{32} Q_2^{-1} A_{20}}{(S^{-1})_{31} Q_1^{-1} A_{10}} = \frac{A_{20}}{\hat{1} A}. \quad (39)$$

Thus for equal bolus dose inputs, comparative risk is  $\leq 1$  ( $A_{20} = A_{10}$ ). In particular,  $CR=1$  when liver secondary elimination is zero (i.e.,  $\hat{1}_{22} = 1$ ), but  $CR \rightarrow 0$  as secondary elimination increasingly dominates primary elimination (as  $\hat{1}_{22} \rightarrow \infty$ ). This represents a simple mathematical description of the liver's biologically critical role as a first pass effect in protecting peripheral organs from environmental insults via ingestion relative to insults by inhalation and shows that only target organ and input compartment parameters effect relative risk in linear models. However, this is not true for absolute AUC where the noncancelling  $\det(S)$  reflects contributions from all compartments. Note that comparative risk can be easily computed when bolus inputs are not equal, but some insights may be easier with equal inputs.

By symmetry to the above case,  $CR_{42/41}^{(4)} = (AUC_{42}/AUC_{41}) = A_{20}/A_{10}\hat{1}_{22}$ . Also by symmetry,  $CR_{43/41}^{(4)} = A_{30}/A_{10}\hat{1}_{33}$ , which is unity for equal inputs ( $A_{30} \doteq A_{10}$ ) when fat secondary elimination is zero ( $\hat{1}_{33} = 1$ ).

Second, the liver compartment CR for liver and blood inputs is given by

$$CR_{22/21}^{(4)} = \frac{AUC_{22}}{AUC_{21}} = \frac{(S^{-1})_{22} Q_2^{-1} A_{20}}{(S^{-1})_{21} Q_1^{-1} A_{10}} = \frac{\hat{1}_{11}}{q_{12}\hat{1}_{21}} \left( 1 - \frac{q_{13}\hat{1}_{31}}{\hat{1}_{11}\hat{1}_{33}} - \frac{q_{14}\hat{1}_{41}}{\hat{1}_{11}\hat{1}_{44}} \right) \frac{A_{20}}{A_{10}} \quad (40)$$

If secondary elimination occurs only in the liver ( $\hat{1}_{22} \neq 1$ ,  $\hat{1}_{11} = \hat{1}_{33} = \hat{1}_{44} = 1$ ), then  $CR=1$  (if  $A_{20} = A_{10}$ ), since the parenthetical term then equals  $q_{12}$ . But  $CR \rightarrow q_{12}^{-1}\hat{1}_{11} \rightarrow \infty$  as secondary elimination in the blood increases (i.e., as  $\hat{1}_{11} \rightarrow \infty$ ) via kidney elimination or lung and blood metabolism. Thus, (39,40) show that the relative importance to CR of liver and blood inputs may reverse as the target organ changes from the noninput fat compartment to the input liver compartment,

Third, blood compartment CR for liver and blood inputs is given by

$$CR_{12/11}^{(4)} = \frac{AUC_{12}}{AUC_{11}} = \frac{(S^{-1})_{12} Q_2^{-1} A_{20}}{(S^{-1})_{11} Q_1^{-1} A_{10}} = \frac{q_{12} Q_2^{-1} \hat{A}_{20}}{\hat{1}_{22} Q_1^{-1} A_{10}} = \frac{A_{20}}{\hat{1}_{22} A_{10}}, \quad (41)$$

equaling  $CR_{32/31}^{(4)}$ , and thus also reflects the liver's first pass relative effect.

By symmetry,  $CR_{13/11}^{(4)} = A_{30}/(\hat{1}_{33}A_{10})$  and  $CR_{14/11}^{(4)} = A_{40}/(\hat{1}_{44}A_{10})$ .

Fourth, the muscle compartment CR for liver and fat inputs is given by

$$CR_{42/43}^{(4)} = \frac{AUC_{42}}{AUC_{43}} = \frac{(S^{-1})_{42} Q_2^{-1} A_{20}}{(S^{-1})_{43} Q_3^{-1} A_{30}} = \frac{1_{41} q_{12} \hat{1}_{33} Q_2^{-1} A_{20}}{1_{41} q_{13} \hat{1}_{22} Q_3^{-1} A_{30}} = \frac{\hat{1}_{33} A_{20}}{\hat{1}_{22} A_{30}}, \quad (42)$$

implying  $CR \rightarrow 0$  as liver secondary elimination increases faster (as  $\hat{1}_{22} \rightarrow \infty$ ) than fat. However,  $CR \rightarrow \infty$  if fat secondary elimination increases faster (as  $\hat{1}_{33} \rightarrow \infty$ ) than liver. Also,  $CR=1$  if  $A_{20} = A_{30}$  and liver and fat secondary elimination are both zero. By symmetry,  $CR_{23/24}^{(4)} = (\hat{1}_{44}A_{30})/(\hat{1}_{33}A_{40})$ .

Fifth, blood compartment CR for liver and fat inputs is given by

$$CR_{12/13}^{(4)} = \frac{AUC_{12}}{AUC_{13}} = \frac{(S^{-1})_{12} Q_2^{-1} A_{20}}{(S^{-1})_{13} Q^{-1} A_{30}} = \frac{q_{12} \hat{1}_{33} \hat{1}_{44} Q_2^{-1} A_{20}}{q \hat{1} \hat{1} Q^{-1} A} = \frac{\hat{1}_{33} A_{20}}{\hat{1} A} \quad (43)$$

which surprisingly equals  $CR_{42/43}^{(4)}$  above. Thus, changing the target organ from the peripheral (muscle) compartment to the main (blood) compartment does not change comparative risk relative to two other peripheral compartment inputs (i.e., liver and fat)! Also, by symmetry,  $CR_{13/14}^{(4)} = (AUC_{13}/AUC_{14}) = (\hat{1}_{44}A_{30})/(\hat{1}_{33}A_{40})$ , which tends toward unity for equal bolus dose inputs ( $A_{30}=A_{40}$ ) since fat and muscle secondary elimination is typically zero. However,  $CR \rightarrow 0$  as fat secondary elimination increases faster (as  $\hat{1}_{33} \rightarrow \infty$ ) than muscle, but  $CR \rightarrow \infty$  if the reverse relationship holds.

Sixth, the liver compartment CR for liver and fat inputs is given by

$$CR_{22/23}^{(4)} = \frac{AUC_{22}}{AUC_{23}} = \frac{(S^{-1})_{22} Q_2^{-1} A_{20}}{(S^{-1})_{23} Q_3^{-1} A_{30}} = \frac{\hat{1}_{11} \hat{1}_{33}}{1_{21} q_{12}} \left( 1 - \frac{q_{13} 1_{31}}{\hat{1}_{11} \hat{1}_{33}} - \frac{q_{14} 1_{41}}{\hat{1}_{11} \hat{1}_{44}} \right) \frac{A_{20}}{A_{30}}, \quad (44)$$

which mimics  $CR_{22/21}^{(4)}$  above (40), but increases faster as secondary blood and fat elimination increase together ( $CR \rightarrow q_{12}^{-1} \hat{1}_{11} \hat{1}_{33} \rightarrow \infty$  as  $\hat{1}_{11}, \hat{1}_{33} \rightarrow \infty$ ).

Similar comparisons have been attempted elsewhere for more complex models using general purpose numerical simulation tools [3].

## Discussion and Future Directions

Simple 1,2,3 and 4-compartment linear PBPK dose models have been reformulated in factored matrix ODE form in order to elucidate their essential structure and to simplify their analytic solution to forms potentially more useful for quantitative risk assessment (QRA) and experimental design (ED) applications. Theoretical applications to interspecies scaling of internal organ AUC dose and to comparative target organ dose or risk from two routes of bolus dose administration have been theoretically explored. Practical applications might include development of optimal drug delivery strategies for humans or prioritization of pesticide exposure control strategies for farmworkers. Such simple linear exposure models suffer many potential biological weaknesses surrounding the following issues: (1) relative absorption rates for the major routes of administration, (2) organ lumping strategies (i.e., model expansion and collapse), (3) complex compartmental interconnections and feedbacks, (4) well-stirred compartment assumptions, (5) poorly specified physiochemical activation or deactivation metabolism parameters, (6) cellular and subcellular exposure pharmacodynamics, and (7) nonlinear parameters. The simple models analyzed and solved above shall hopefully provide fundamental motivation and component building blocks for development of similar, but extended, analytic solutions, quasianalytic approximations or general numerical algorithms for more complex linear and nonlinear PBPK models that would be of practical use in risk analysis, especially QRA and ED applications. Such issues will be explored elsewhere.

## References

- [1] Allen, B.C.; Crump, K.C.; Shipp, A.M. *Risk Anal.* 1988, *8*, 531-544.
- [2] Anderson, M.E.; Clewell III, H.J.; Gargas, M.L.; Smith, F.A.; Reitz, R.H. *Toxicol. Appl. Pharmacol.* 1987, *87*, 185-205.
- [3] Blancato, J.E. *Proceedings of the International Water Disinfection Conference, Aug 31-Sept. 3, 1992*; Int. Life Sci. Instit.: Washington, DC, in press.
- [4] United States Environmental Protection Agency. *Federal Register, Part V, June 5, 1992*
- [5] Gear, C.W. *Numerical Initial Value Problems in Ordinary Differential Equations*; Prentice-Hall: Englewood Cliffs, NJ, 1971; pp.1-253.
- [6] Gibaldi, M.; Perrier, D. *Pharmacokinetics, 2nd Ed.*; Marcel Dekker: New York, NY, 1982; pp 1-494.
- [7] Hirsch, M.W., Smale, S. *Differential Equations, Dynamical Systems, and Linear Algebra*; Academic Press: New York, NY, 1974; pp 1-358.
- [8] Kreyszig, E. *Advanced Engineering Mathematics, 7th Ed.*; John, Wiley: New York, NY, 1992; pp 1-1294.
- [9] Nakashima, E.; Benet, L.Z. *J. Pharmacokin. Biopharm.* 1989, *17*, 673-685.
- [10] Travis, C.C.; White, R.K. *Risk Anal.* 1988, *8*, 119-125.
- [11] Travis, C.C. *Risk Anal.* 1990, *10*, 317-321.

RECEIVED May 19, 1993

## Author Index

- |                                    |                               |
|------------------------------------|-------------------------------|
| Abou-Donia, Mohamed B., 125        | Fernando, John C., 51         |
| Al-Bayati, M. A., 284              | Jett, David A., 51            |
| Anis, Nabil A., 114                | Johnson, Deadre J., 125       |
| Bakke, J. E., 166                  | Knaak, J. B., 284             |
| Bass, N. M., 166                   | Lack, Leon, 125               |
| Baugher, D. G., 214                | Larsen, G. L., 166            |
| Blancato, Jerry N., 76,231,264,284 | Matsumura, Fumio, 37          |
| Blankenship, Alan, 37              | Nauman, C. H., 1              |
| Brown, Robert N., 301              | Newcombe, David S., 197       |
| Cannon, Michael, 231               | Raabe, O. G., 284             |
| Cash, Gordon G., 65,231            | Reddy, Vijayapal, 231         |
| Castles, Mark, 231                 | Rogers, Kim R., 114,158       |
| Dary, Curtis C., 1,231             | Saboori, Ali M., 197          |
| Davison, K. L., 166                | Saleh, Mahmoud A., 76,231,264 |
| DeVito, Stephen C., 22             | Santolucito, J. A., 1,178     |
| Eldefrawi, Amira T., 51            | Schnell, Frank C., 133        |
| Eldefrawi, Mohyee E., 114          | Thompson, Roy, 114            |
| Emon, J. M. Van, 158               | Valdes, J. J., 114            |
| Esa, Ahmed H., 197                 | Wallace, Cecil, Jr., 76       |
| Famini, George R., 22              | Wilson, Leland Y., 22         |

## Affiliation Index

- |  |  |
|--|--|
| Agricultural Research Service, 166                   | U.S. Army Research Development and Engineering Center, 114               |
| Duke University Medical Center, 125                  | U.S. Department of Agriculture, 166                                      |
| Johns Hopkins Medical Institutions, 197              | U.S. Environmental Protection Agency, 1,22,65,76,114,158,231,264,284,301 |
| La Sierra University, 22                             | University of California, Davis, 37,284                                  |
| Lockheed Environmental Systems and Technologies, 133 | University of California, San Francisco, 166                             |
| Midwest Research Institute, 231                      | University of Maryland, 51,114   |
| Orius Associates Inc., 214                           | University of Nevada, 1,178  |
| Texas Southern University, 76,231,264                |  |
| U.S. Army Chemical Research, 22                      |  |

## Subject Index

### A

Acetylcholinesterase, use as biosensor, 115

echothiophate inhibition, 118–120*r*

edrophonium inhibition, 118,119*f*

Acetylcholinesterase—*Continued*

fluorescence, 116,118

inhibition for fiber-optic biosensors and colorimetric assay, 120*r*

instrument, 116,117*f*

substrate specificity, 118*r*

## Author Index

- |                                    |                               |
|------------------------------------|-------------------------------|
| Abou-Donia, Mohamed B., 125        | Fernando, John C., 51         |
| Al-Bayati, M. A., 284              | Jett, David A., 51            |
| Anis, Nabil A., 114                | Johnson, Deadre J., 125       |
| Bakke, J. E., 166                  | Knaak, J. B., 284             |
| Bass, N. M., 166                   | Lack, Leon, 125               |
| Baugher, D. G., 214                | Larsen, G. L., 166            |
| Blancato, Jerry N., 76,231,264,284 | Matsumura, Fumio, 37          |
| Blankenship, Alan, 37              | Nauman, C. H., 1              |
| Brown, Robert N., 301              | Newcombe, David S., 197       |
| Cannon, Michael, 231               | Raabe, O. G., 284             |
| Cash, Gordon G., 65,231            | Reddy, Vijayapal, 231         |
| Castles, Mark, 231                 | Rogers, Kim R., 114,158       |
| Dary, Curtis C., 1,231             | Saboori, Ali M., 197          |
| Davison, K. L., 166                | Saleh, Mahmoud A., 76,231,264 |
| DeVito, Stephen C., 22             | Santolucito, J. A., 1,178     |
| Eldefrawi, Amira T., 51            | Schnell, Frank C., 133        |
| Eldefrawi, Mohyee E., 114          | Thompson, Roy, 114            |
| Emon, J. M. Van, 158               | Valdes, J. J., 114            |
| Esa, Ahmed H., 197                 | Wallace, Cecil, Jr., 76       |
| Famini, George R., 22              | Wilson, Leland Y., 22         |

## Affiliation Index

- |  |  |
|--|--|
| Agricultural Research Service, 166                   | U.S. Army Research Development and Engineering Center, 114               |
| Duke University Medical Center, 125                  | U.S. Department of Agriculture, 166                                      |
| Johns Hopkins Medical Institutions, 197              | U.S. Environmental Protection Agency, 1,22,65,76,114,158,231,264,284,301 |
| La Sierra University, 22                             | University of California, Davis, 37,284                                  |
| Lockheed Environmental Systems and Technologies, 133 | University of California, San Francisco, 166                             |
| Midwest Research Institute, 231                      | University of Maryland, 51,114   |
| Orius Associates Inc., 214                           | University of Nevada, 1,178  |
| Texas Southern University, 76,231,264                |  |
| U.S. Army Chemical Research, 22                      |  |

## Subject Index

### A

Acetylcholinesterase, use as biosensor, 115

echothiophate inhibition, 118–120*r*

edrophonium inhibition, 118,119*f*

Acetylcholinesterase—*Continued*

fluorescence, 116,118

inhibition for fiber-optic biosensors and colorimetric assay, 120*r*

instrument, 116,117*f*

substrate specificity, 118*r*

- Acetylcholinesterase—*Continued*  
total internal reflection fluorescence vs.  
acetylcholinesterase activity, 116,117f
- Alachlor  
biomonitoring, 13–14  
metabolism to hemoglobin adducts,  
144,146f,147
- Amitrole, detection by using hemoglobin  
adducts, 147,149
- Anagen phase of hair growth, 131
- Analyte selection, biomonitoring, 5*t*,7
- Analytic solution of linear physiologically  
based pharmacokinetic model for risk  
assessment  
comparative risk route-to-route dose  
extrapolation, 314–316  
experimental objectives, 302,303  
four-compartment model, 308–309  
future directions, 316  
interspecies scaling formulas, 312–314  
one-compartment model, 303–304  
risk assessment uses, 309–316  
single input–single output formulas,  
310–312  
three-compartment model, 306–308  
two-compartment model, 304–306
- Analytical methods, biomonitoring, 5*t*,7–8
- Anticholinesterase(s), detection by using  
acetylcholinesterase biosensor, 116–120
- Anticholinesterase activity, prediction by  
using isofenphos percutaneous physio-  
logically based pharmacokinetic–  
pharmacodynamic model, 284–300
- Applications, pesticides, 3
- Arylamine-based pesticides, detection by  
using hemoglobin adducts, 138–147
- Ataxia telangiectasis, relationship to  
lymphoma and pesticide exposure,  
205–206
- Atrazine, detection by using hemoglobin  
adducts, 147,148f
- B**
- Benzene, body burden vs. tissue burden  
exposure assessment, 184,185*t*
- Bicycloorthocarboxylates, computer-aided  
molecular modeling for development of  
biomarkers for human exposure to  
pesticides, 76–112
- Bicycphosphates, computer-aided  
molecular modeling for development of  
biomarkers for human exposure to  
pesticides, 76–112
- Bioavailability of compound, importance of  
data, 2
- Biochemical parameters, changes induced by  
exposure to dioxin-type chemicals, 37–48
- Bioindicators, description, 191
- Biological matrix, biomonitoring, 5*t*,6
- Biological monitoring, determination of  
human exposure to environmental  
pollutants, 158
- Biomarkers  
body burden exposure assessment, 193  
human exposure to insecticides  
computer-aided molecular modeling for  
development, 76–112  
previous studies, 76–77  
immune dysfunction and lymphoma  
detection after chronic organophosphorus  
exposure  
cytotoxic T lymphocyte function  
suppression by organophosphorus,  
200,202,203*t*  
future work, 210  
immune cell(s), 207,208*t*  
immune cell esterase, specificity and  
sensitivity, 207,209  
immune dysfunction–organophosphorus  
exposure relationship, 199–201*t*  
immune function, 206–207  
lymphomas in farmers, 198  
lymphomas in grain mill workers, 198–199  
lymphomas in resin workers and auto-  
mobile manufacturers, 199  
monocyte esterase activity inhibition by  
organophosphorus, 204  
monocyte esterase deficiency vs. malignan-  
cies, 202–204  
natural killer cell activity suppression by  
organophosphorus, 200,201*f*  
oncogenic viruses vs. organophosphorus  
exposure, 204–209
- Biomonitor(s), description, 191
- Biomonitoring  
analysis of data by using pharmacokinetic  
modeling approaches, 3  
analyte selection, 5*t*,7  
analytical methods, 5*t*,7–8

**Biomonitoring—Continued**

- applications, 2–3,14
  - biological matrix, 5*t*,6
  - definition, 2
  - general considerations, 5*t*–8
  - importance of bioavailability data, 2
  - methods, 8–14
  - sample collection, 5*t*,6
  - sample handling, 5*t*,7
- Biosensor(s)**, 114–115
- Biosensor for cholinesterase detection**
- acetylcholine effect on fluorescence, 120,121*f*,123
  - comparison to Ellman spectrophotometric method, 122*f*,123
  - paraoxon effect on fluorescence, 120,121*f*,123
  - pH effect on total internal reflection fluorescence, 120,121*f*
  - whole blood effect on fluorescence, 120,121*f*

**Bitertanol**, detection by using hemoglobin adducts, 149–151*t*

**Blood**, rat, isolation of pesticide binding protein, 166–177

**Blood cells**, occurrence of muscarinic receptors, 62–63

**Body burden**, determination of exposure to toxicants, 178–194

**Body burden exposure assessment**

- analytical methods, 187
- approaches, 178–179,192–194
- comparison to tissue burden, 179–186
- distribution analysis, 187
- exposure assessment, 191
- general population databases, 186–190*t*
- exposure–body burden relationship, 186
- risk assessment, 191–192
- sampling, 187
- trend identification, 187

**C**

**Calibration of pharmacokinetic models of pesticide exposure**

- examples, 226–227
- modeling of exposures, 228–229
- partitioning of exposures, 227–228
- procedure, 225–226

**Catagen phase of hair growth**, 131

**Chloracne**, description, 38

**Chlorinated insecticides**, computer-aided molecular modeling for development of biomarkers for human exposure to pesticides, 76–112

**(Chlorophenoxy)acetic acid herbicides**, exposure monitoring methods, 214–215

**Chloropropham**, detection by using hemoglobin adducts, 140,141*f*,145*t*

**Cholinesterase(s)**, detection by using biosensor, 120–123

**Cholinesterase depression**, description, 13

**Chromosomal aberrations**, role of organophosphorus, 205

**Chronic organophosphorus exposure**, use of biomarkers in immune dysfunction detection and lymphoma development, 198–210

**Classical pharmacokinetic models**, 265

**Classification**, pesticides, 3,4*t*

**Comparative molecular field analysis**, 81

**Computer-aided molecular modeling** for development of biomarkers for human exposure to pesticides

**bicycloorthocarboxylates and bicyclophosphates**, physicochemical properties and biological activities, 81–84*t*

**chlorinated insecticides**

physicochemical properties and biological activities, 81,85*t*

structures, 77,79*f*

**comparative molecular field analytical procedure**, 81

**conformational analytical procedure**, 80

**dipole moment calculation procedure**, 80

**energy**, 81–86

**energy minimization procedure**, 80

**experimental description**, 77

**low-energy conformations of hexachlorohexane isomers**, 81,86*f*

**molecular alignment procedure**, 80

**molecular surface area calculation procedure**, 80

**molecular volume calculation procedure**, 80

**orientation**, 81–86

**structure**, 81–86

**structure–activity relationship**,

predictivity, 81,87–112

**quantitative determination procedure**, 81

- Computer-aided molecular modeling for development of biomarkers for human exposure to pesticides—*Continued*  
SYBYL molecular modeling procedure, 77,80  
total strain calculation procedure, 80  
trioxabicyclo[2.2.2]octane-based structures, 77–79f  
*c-ras* expression, indicator of dioxin-type chemical actions, 47  
Cyanide release from nitriles, biochemical basis, 22–24  
Cytochrome P-450 mediated acute nitrile toxicity modeling using theoretical linear solvation energy relationships  
advantages, 33  
biochemical basis of cyanide release from nitriles, 22–24  
descriptor calculation procedure, 26–27  
experimental procedure, 26  
 $\alpha$ -hydrogen atom abstraction effect, 30–33  
hydrophobicity effect, 30–32  
linear solvation energy relationship model, 24–25  
mouse acute toxicity data, 27–30f  
theoretical linear solvation energy relationship model, 25–26  
validity, 30–33  
volume effect, 33  
Cytotoxic T lymphocytes, function  
suppression by organophosphorus, 200,202,203t
- D**
- 2,4-D [(Dichlorophenoxy)acetic acid]  
exposure monitoring methods, 214–215  
ground boom application equipment, 214  
multiple dermal exposure model, 218–229  
pharmacokinetics, 215–218  
Dermal absorption and disposition of malathion in rats and humans  
absorption and elimination in humans, predictive kinetic parameters, 241,248–250  
apparent rate of absorption vs. time, 241,247f  
application rate vs. elimination, 241–243f  
applied dose, distribution in rats, 254–259  
Dermal absorption and disposition of malathion in rats and humans—*Continued*  
data reduction procedure, 239  
determination methods, 259–261  
dose application  
human exposure study, 234–237  
rat dermal absorption studies, 238  
elimination profile in humans, 239–241  
experimental condition effect, 259  
experimental design  
human exposure study, 232,233t  
rat dermal absorption studies, 238  
metabolite identification procedure for human exposure study, 237,238  
radiochemical analytical procedure  
human exposure study, 234,237  
rat dermal absorption studies, 239  
sample collection  
human exposure study, 234  
rat dermal absorption studies, 239  
statistical analytical procedure, 239  
statistical treatment of adsorption for humans, 253–254  
subject effect in humans, 250,251f  
surface area vs. elimination, 241,244–246f,250,252f,253  
test and control articles  
human exposure study, 232,234  
rat dermal absorption studies, 238  
washing effect, 261  
3,4-Dichloroaniline, measurement in urine and erythrocytes of diuron-exposed workers, 144,145t  
Dichlorvos, detection by using hemoglobin adducts, 149,151f  
Diethylaniline-yielding metabolites, biomonitoring, 14  
Dioxin-type chemicals  
*c-ras* expression as indicator of actions, 47  
epidermal growth factor receptors as indicator of actions, 46–47  
glucose transporter proteins as indicator of actions, 47–48  
hyperkeratinization of epithelial cells as indicator of actions, 39–46  
toxicity assessment, previous studies, 38–39  
Diuron, detection using hemoglobin adducts, 140,143f,145t  
DNA adducts, potential as biomarkers, 134

## E

- Environmental exposure to pesticides, sources, 2–3
- Environmental monitoring, determination of human exposure to environmental pollutants, 158
- Enzyme biosensors, examples, 115
- Epidermal growth factor receptors, indications of dioxin-type chemical action, 46–47
- Epithelial cells, hyperkeratinization as indicator of dioxin-type chemical actions, 39
- Epstein–Barr virus infections, relationship to immunodeficiencies, 205
- O*-Ethyl *O*-4-nitrophenyl phosphonothioate, body burden vs. tissue burden exposure assessment, 179–181
- Ethylene dibromide, detection using hemoglobin adducts, 149,153
- Exposure assessment
  - body burden determination, 178–194
  - physiologically based pharmacokinetic models, 264–282
- Exposure to pesticides, biomonitoring, 2–14

## F

- Fiber-optic evanescent fluorosensor instrument, description, 116,117*f*
- First-pass effect, description, 266,268
- Forward analysis, description, 265

## G

- Glucose oxidase, use as biosensor, 115
- Glucose transporter proteins, indicator of dioxin-type chemical actions, 47–48
- Ground boom mixer–loader–applicators, pharmacokinetic model of exposure to (chlorophenoxy)acetic acid herbicides, 214–229

## H

## Hair

- biological marker for 2,5-hexanedione precursors
  - colors developed by Ehrlich's reagent, 128,129*f*

## Hair

- biological marker for 2,5-hexanedione precursors—*Continued*
  - detection period, 128,131
  - experimental procedure, 127
  - pigmentation effect, 131
  - rat hair analytical procedure, 127–128
  - vibrissae from treated animal, 128,130*f*
- foreign substance incorporation, 125
- use as biomarker, 125–126
- Halogenated aromatic hydrocarbons, toxic chemicals, 37–38
- Hemoglobin adduct formation, 134,136
- Hemoglobin adducts of pesticides
  - adduct formation, kinetics, 136
  - alachlor detection, 144,146*f*,147
  - amitrole detection, 147,149
  - aromatic amine formation from arylamine-based pesticides, 138,140–147
  - arylamine–hemoglobin adduct formation, mechanism, 138,139*f*
  - atrazine detection, 147,148*f*
  - binding, measures, 136
  - bitertanol detection, 149–151*t*
  - 3,4-dichloroaniline detection, 144,145*t*
  - dichlorvos detection, 149,151*f*
  - ethylene dibromide detection, 149,153
  - pentachlorophenol detection, 153
  - pesticides forming adducts, 136,137*t*
  - propoxur detection, 153,154*f*,*t*
  - triadimefon detection, 149–151*t*
- Herbicides, biomonitoring methods, 13–14
- Heterocyclic pesticides, detection by using hemoglobin adducts, 147–151
- n*-Hexane, use of hair as biological marker, 126
- 2,5-Hexanedione
  - hair as biological marker for precursors, 126–132
  - neurotoxicity, 126
- Human(s), dermal absorption and disposition of malathion, 231–261
- Human exposure
  - insecticides, sources, 231–232
  - pesticides, computer-aided molecular modeling for development of biomarkers, 76–112
  - pollutants, influencing factors, 133–134

Hyperkeratinization of epithelial cells  
dioxin-type chemical actions, indicators,  
39–48  
XB cells, description, 39–40

## I

Immune cell(s), biomarkers of organophos-  
phorus exposure, 207,208*t*  
Immune cell esterases, specificity and  
sensitivity as biomarkers of organophos-  
phorus exposure, 207,209  
Immune dysfunction, role of organophos-  
phorus, 199–210  
Immune function, biomarkers and organo-  
phosphorus exposure, 206–207  
Immunoassay(s), advantages for field  
screening of biological fluid  
metabolites, 159  
Immunoassay for *p*-nitrophenol in urine  
antiserum preparation, 160  
coating antigen preparation, 160  
competitive immunoassay procedure, 160  
cross-reactivity with substituted  
nitrobenzenes, 160–162*f*  
experimental materials, 159  
future work, 164  
instrumentation, 159–160  
urine concentration vs. assay sensitivity,  
161,163*t*  
urine effect from urine addition to initial  
incubation step, 160,161*f*  
urine sample effect, 161–163*f*  
urine sample vs. assay sensitivity,  
161,164*t*  
Immunodeficiency  
relationship to Epstein–Barr virus  
infections, 205  
relationship to lymphomas, 204–205  
Immunosensors, specificity, 115  
Indirect indicators, body burden exposure  
assessment, 193–194  
Insecticides, regulation of muscarinic  
receptors as biomarker of exposure, 51–63  
Isofenphos  
development and metabolism, 284  
prediction of anticholinesterase activity  
and urinary metabolites, 284–300

Isofenphos percutaneous physiologically  
based pharmacokinetic–pharmacodynamic  
model  
development, 285–293  
enzymes, 285,288*f*  
experimental description, 284–285  
inhibition of cholinesterase in brain, 292  
mass balance equations  
des-*n*-isopropylisofenphosoxon in brain,  
292–293  
metabolism, 292  
percutaneous absorption, 291  
tissue–blood exchange, 291–292  
metabolic enzyme kinetics,  
289,290*t*,294*t*  
metabolic pathway, 285,288*f*,289  
metabolism, 285,287*f*,293,294*t*,296*f*  
model, 285,286*f*  
partition coefficients, 289*t*  
phosphorylation of cholinesterases,  
290–291,295–298*f*  
physiological parameters, 285  
sensitivity analysis, 299–300  
skin permeability, 285  
time course data, 285

## L

Lead, body burden vs. tissue burden  
exposure assessment, 181–184  
Linear solvation energy relationships,  
model, 24–25  
Linuron, detection by using hemoglobin  
adducts, 140,143*f*,145*t*  
Lymphomas  
factors required for generation, 204  
relationship to ataxia telangiectasis and  
pesticide exposure, 205–206  
relationship to immunodeficiencies,  
204–205

## M

Malathion, dermal absorption and disposi-  
tion in rats and humans, 231–261  
Metabolites in biological fluids, need for  
improved analytical measurement  
methods, 159

- Methyl *n*-butyl ketone, use of hair as biological marker, 126
- (2-Methyl-4-chlorophenoxy)acetic acid (MCPA)  
exposure monitoring methods, 214–215  
ground boom application equipment, 214  
multiple dermal exposure model, 218–229  
pharmacokinetics, 215–218
- 1-Methylethyl 2-({ethoxy[(1-methylethyl)-amino]phosphinothioyl}oxy)benzoate,  
*See* Isofenphos
- Molecular biological parameters, changes induced by exposure to dioxin-type chemicals, 37–48
- Molecular connectivity index(es), methodology, 65
- Molecular connectivity index–toxicity relationship for organic nitriles  
compounds examined, 67*t*  
correlations with two principal components, 72*f*, 73  
methodology, 65–67  
observations used in regression analyses, 68, 70*t*  
observed and predicted values of –log of lethal dose, 74, 75*t*  
principal component loadings, 68, 71*t*, 72  
regression analyses, 68, 69*t*  
terminology, 65  
univariate correlation of transformed variables, 73, 74*f*
- Molecular modeling for development of biomarkers for human exposure to pesticides, computer aided, *See* Computer-aided molecular modeling for development of biomarkers for human exposure to pesticides
- Monocyte esterase  
activity inhibition by organophosphorus, 204  
deficiency vs. hematopoietic tumor formation, 202–204  
inhibition of activity, 199–201*t*
- Monuron, detection by using hemoglobin adducts, 140, 142*f*
- Muscarinic receptors  
description, 52–53  
occurrence in blood cells, 62–63  
organophosphates, direct action, 53–56  
relationship to second messenger systems and cell membrane, 53, 54*f*
- Muscarinic receptors—*Continued*  
schematic representation, 53, 54*f*  
subchronic parathion effect, 56–62
- N
- Natural killer cells, activity suppression by organophosphorus, 200, 201*f*
- Neurotransmitter receptors, 51–52
- Nitriles  
cyanide release, 22–23  
industrial applications, 22  
structure–toxicity relationships, 23–24  
toxicity  
mechanism-based model, 24  
modeling using theoretical linear solvation energy relationships, 25–33
- p*-Nitrophenol in urine  
disadvantages of classical analysis, 159  
immunoassay, 159–164
- O
- Occupational exposure to pesticides, 2
- Optical immunosensors, examples, 115–116
- Organic nitriles, correlations of molecular connectivity indices with toxicities, 65–75
- Organochlorines  
biomonitoring methods, 8, 13  
occurrence, 8, 12*t*
- Organophosphate(s), direct actions on muscarinic receptors, 53–56
- Organophosphate-exposed populations, epidemiological studies, 198–199
- Organophosphorus anticholinesterase pesticides, biosensor for monitoring blood cholinesterases as biomarker of exposure, 114–123
- Organophosphorus compounds, biomonitoring methods, 13
- Organophosphorus exposure  
acute exposures and health effects, 198  
chronic, use of biomarkers in immune dysfunction detection and lymphoma development, 198–210
- P
- Parathion, subchronic exposure effect on muscarinic receptors, 56–62

- Pentachlorophenol, detection by using hemoglobin adducts, 153
- Perfusion limitation, description, 268
- Pesticide(s)
- analytical methods, 3
  - applications, 3
  - classification, 3,4*t*
  - computer-aided molecular modeling for development of biomarkers for human exposure to pesticides, 76–112
  - detection by using hemoglobin adducts, 133–154
  - environmental exposure–biologically effective dose–health effect relationship, 134,135*f*
  - organophosphorus anticholinesterase, biosensor for monitoring blood cholinesterases as biomarker of exposure, 114–123
- Pesticide binding protein, isolation from rat blood
- binding assay, 168,174,176,177*t*
  - chemicals, 166
  - delipidation procedure, 168
  - electrophoresis, 169,172*f*
  - elution patterns
    - Sephacryl S–200 column, 174,175*f*
    - Sephadex G–75 column, 169,171*f*
  - gel filtration determination of molecular weight, 168
  - immunoblot
    - analytical procedure, 167
    - protein–pesticide complex, 174,176*f*
  - ligand characterization procedure, 168–169
  - material preparation, 168
  - metabolite–protein complex, stability to dialysis, 169,173*t*,174
  - polyacrylamide gel electrophoretic analytical procedure, 167
  - protein purification procedure, 167–168
  - radioactivity distribution after fractionation, 169,170*t*
- Pesticide exposure
- biomonitoring, 2–14
  - relationship to ataxia telangiectasia,205–206
- Pharmacokinetic analyses, 265
- Pharmacokinetic model of exposure of ground boom mixer–loader–applicators to (chlorophenoxy)acetic acid herbicides—*Continued*
- development process, 215
  - multiple dermal exposure model, 218–220
  - pharmacokinetics of 2,4-D and MCPA, 215–218
  - validation, 220–225
- Pharmacokinetic modeling, applications, 3
- Pharmacokinetics
- analyses, 265
  - definition and description, 264–265
  - models, 265–266
- Physiologically based pharmacokinetic models
- assumptions, 268
  - biomarker example, 277–282
  - body burden exposure assessment, 192–193
  - description, 265–266
  - diagrammatic representation, 266,267*f*
  - first-pass effect, 266,268
  - mathematical description, 268–271
  - solution method, 271–272
  - toxification from metabolism example, 273–276,279
  - use in exposure and risk assessments, 266
- Physiologically based pharmacokinetic–pharmacodynamic model, prediction of anticholinesterase activity and urinary metabolites of isofenphos, 284–300
- Physiologically based pharmacokinetic risk assessment models
- analytic solution, 302–316
  - differential equation discretization methods for solution, 301
- Pollutant, factors affecting human exposure, 133–134
- Principal component analyses, molecular connectivity index–toxicity relationship for organic nitriles, 68,71–74
- Propham, detection by using hemoglobin adducts, 140,141*f*,145*t*
- Propoxur, detection by using hemoglobin adducts, 153,154*f*,*t*
- Protein adducts, potential as biomarkers, 134
- Protein isolation from rat blood, pesticide binding, *See* Pesticide binding protein, isolation from rat blood

- R**
- Rat, dermal absorption and disposition of malathion, 231–261
- Rat blood, isolation of pesticide binding protein, 166–177
- Receptor biosensors, example, 115
- Risk assessment, use of physiologically based pharmacokinetic models, 264–282
- S**
- Sample collection, biomonitoring, 5*t*,6
- Sample handling, biomonitoring, 5*t*,7
- SCOUT, description, 66–67
- T**
- 2,3,7,8-Tetrachlorodibenzo-*p*-dioxin (TCDD) equivalent, description, 38
- Theoretical linear solvation energy relationships, 25–26
- Tissue burden, comparison to body burden, 179
- Toxicity from nitriles, 24–33
- Toxicity–molecular connectivity index relationship for organic nitriles, *See* Molecular connectivity index–toxicity relationship for organic nitriles
- Triadimefon, detection by using hemoglobin adducts, 149–151*t*
- Triazine herbicides, biomonitoring, 13
- U**
- Urinary metabolites of isofenphos, prediction by using percutaneous physiologically based pharmacokinetic–pharmacodynamic model, 284–300
- Urine**
- advantages and limitations for use in metabolite detection, 159
- immunoassay for *p*-nitrophenol, 159–164
- V**
- Valence molecular connectivity indexes, 65
- Validation of pharmacokinetic models of pesticide exposure
- occupational monitoring data, 222–225
- passive dosimetry and biomonitoring, 220–222
- W**
- Wasting syndrome, description, 48
- X**
- XB cell(s), description, 39–40
- XB cell hyperkeratinization assay
- cell culture preparation, 40
- chemical addition to cell cultures, procedure, 40
- dose–response relationship, 41–43*f*
- experimental materials, 40
- quantitation procedure, 40–41
- reliability and specificity, 41,46
- staining procedure, 40
- TCDD equivalent concentrations, calculation, 41
- toxic vs. nontoxic congener response, 41,44–45*f*
- use as indicators, 39

*Production: Meg Marshall*  
*Indexing: Deborah H. Steiner*  
*Acquisition: Anne Wilson*

*Printed and bound by Maple Press, York, PA*